# DEVELOPMENT OF NOVEL BIOSORBENTS IN REMOVING HEAVY METALS FROM AQUEOUS SOLUTION

*A*
***Thesis Submitted***
in Fulfilment of the Requirement
for the degree of

**DOCTOR OF PHILOSOPHY**
**IN**
**ENVIRONMENTAL ENGINEERING**

By
**Md Anwar Hossain**

**Under the Guidance of**
**Prof. Dr. Huu Hao NGO**

**School of Civil and Environmental Engineering**
**Faculty of Engineering and Information Technology**
**University of Technology, Sydney (UTS)**
**Sydney, Australia**
**December, 2013**

# Certificate

I certify that this thesis has not already been submitted for any degree and is not being submitted as part of candidature for any other degree.

I also certify that the thesis has been written by me and any help that I have received in preparing this thesis, and all sources used, have been acknowledged in this thesis.

Signature of Candidate

Production Note:
Signature removed prior to publication.

…… …….

(Md Anwar Hossain)

**I dedicated this work to my beloved parents**

***Md Akbar Ali***
***Mosa. Ruhila Khatun***

# Acknowledgement

It was not simple and easy task, but both nerve-racking and enjoyable during my doctoral research at Centre for Technology in Water and Wastewater (CTWW), University of Technology, Sydney (UTS), Australia. It would not have been feasible and possible to achieve this doctoral research without the help and support of the people around me and therefore they need a special mention and thanks here.

I would like to appreciate the people for their help and support during my research. My first thanks and gratitude goes to my principal supervisor Prof. Dr. Huu Hao **NGO**. He was a source of continuous inspiration, motivation, stimulation and strength throughout my research. I would like to show my deep gratitude to my co-supervisors Dr Wenshan **GUO**, Dr. T. V. **Nguyen** and Prof. Dr. S. **Vigneswaran** for their constant help and support.

My thanks also go to lab technical officer of the environmental laboratory Md Abu Jahir and Technical officer of MEP, Mr. Harj Sandhu for their valuable effort in the environmental laboratory with appropriate instructions and methods. It is a pleasure to thank Mr. Rami Hadad, lab manager and David Hooper for their help and support. I would also like to thank my colleagues and mates Wen, Thanh, Zuthi, Hang, Zhou, Bandita, Lijuan, Santonu and Luo, I had a wonderful time with these guys.

I would like to show my gratitude to IPRS and UTS-SP authorities for the financial support to conduct this research and for living allowances to stay my family in Australia. I owe my thanks to the academic and technical support of the University of Technology, Sydney and its staff, especially Ms. Phyllis for all my academic support. Above all, I would like to thank my wife-Kabita, my children, Kabbyo and Kathon for their personal support and great patience at all times. My family was always with me during the accomplishment of this doctoral research. Thanks very much every one.

Finally, I would like to forward all my appreciation to almighty ALLAH who guided those people who supported and helped me through my research.

# Table of Contents

# List of Tables

# Lists of Figures

# Acronyms and symbols

| | | |
|---|---|---|
| GG | : | Garden grass |
| CW | : | Cabbage waste |
| BP | : | Banana peel |
| ML | : | Maple leaves |
| POFS | : | Palm oil fruit shells |
| FTIR | : | Fourier-transform infrared spectroscopy |
| XRD | : | X-ray diffraction |
| SEM | : | Scanning electron microscopy |
| AAS | : | Atomic absorption spectroscopy |
| BDST | : | Bed Depth Service Time |
| TEMP | : | Temperature |
| TIME | : | Contact time |
| BET | : | Brunauer, Emmer and Teller model |
| US EPA | : | United States Environmental Protection Agency |
| Cd | : | Cadmium |
| Cu | : | Copper |
| Pb | : | Lead |
| Zn | : | Zinc |
| min | : | Minute |
| ml | : | Millilitre (0.001 litre) |
| mm | : | Millimetre (0.001 metre) |
| l | : | Litre |
| MW | : | Molecular weight |
| A | : | Cross-section area of the media sample |
| $C_0$ | : | Initial metal concentration |
| $C_e$ | : | Final metal (or residual/equilibrium) concentration |
| m | : | Dry weight of biomass (dose) |
| $q_e$ | : | Equilibrium uptake of metal |
| $q_m$ | : | Maximum metal uptake or maximum adsorption capacity |
| V | : | Volume of liquid |
| $K_L$ | : | Langmuir constant (empirical constant) |
| $K_F$ | : | Freundlich capacity factor |
| n | : | Freundlich intensity parameter (dimensionless) |
| $K_{RP}$ | : | Redlich-Peterson isotherm constant |
| $\alpha_{RP}$ | : | Redlich-Peterson isotherm constant |
| $\beta$ | : | Redlich-Peterson isotherm exponent |
| $A_{KC}$ | : | Koble-Corrigan parameter |

| | | |
|---|---|---|
| BKC | : | Koble-Corrigan parameter |
| p | : | Koble-Corrigan parameter |
| $K_T$ | : | Temkin isotherm constant |
| A | : | specific surface area |
| $B_1$ | : | Temkin constant in relation to heat of sorption |
| $b_T$ | : | Toth parameter |
| $\beta_R$ | : | Radke-Prausnitz isotherm exponent |
| $\alpha_R$ | : | Radke-Prausnitz model constants |
| $r_R$ | : | Radke-Prausnitz model constants |
| $b_K$ | : | Khan model constant |
| $a_K$ | : | Khan model exponent |
| S | : | Temperature dependent Unilan model constants |
| d | : | Temperature dependent Unilan model constants |
| $K_{FH}$ | : | Flory-Huggins model's equilibrium constant |
| $n_{FH}$ | : | Flory-Huggins model's exponent |
| $B_{DR}$ | : | Dubinin-Radushkevich constant related to sorption energy |
| ε | : | Dubinin-Radushkevich polanyi potential |
| $K_s$ | : | Sips isotherm constants |
| $\alpha_s$ | : | Sips isotherm constants |
| β | : | Sips isotherm exponent |
| $k_1$ | : | First-order rate constants |
| $k_2$ | : | Second-order rate constants |
| $k_p$ | : | Intraparticle diffusion rate constant |
| $K_{AV}$ | : | Avrami kinetic constant |
| $n_{AV}$ | : | Fractionary constant for Avrami kinetic |
| $C_s$ | : | The concentration at the solid/liquid interface |
| D | : | The axial diffusion coefficient |
| $\beta_a$ | : | The kinetic coefficient of the external mass transfer |
| $C_{break}$ | : | The outlet concentration at breakthrough |
| $t_{break}$ | : | The time at breakthrough |
| τ | : | Time required for 50% adsorbate breakthrough |
| $K_T$ | : | Thomas rate constant |
| θ | : | The volumetric flow rate |
| ΔG° | : | Gibbs free energy |
| ΔH° | : | Enthalpy change |
| ΔS° | : | Entropy change |

# List of Publications

## Publications and presentations as the outcomes from this study:

1. **Hossain, M.A.**, H.H. Ngo, W.S. Guo, T.V. Nguyen. "***Palm oil fruit shells as biosorbent for copper removal from water and wastewater: Experiments and sorption models***" Bioresource Technology 113 (2012) 97–101.

2. **Hossain, M.A.**, H.H. Ngo, W.S. Guo, T. Setiadi. "***Adsorption and desorption of copper(II) ions onto garden grass***". Bioresource Technology 121 (2012) 386–395.

3. **Hossain, M. A.**, H. H. Ngo, W. S. Guo and T. V. Nguyen. "***Biosorption of Cu(II) From Water by Banana Peel Based Biosorbent: Experiments and Models of Adsorption and Desorption***" Journal of Water Sustainability, Volume 2, Issue 1, March 2012, 87–104.

4. **Hossain, M. A.**, H. H. Ngo, W. S. Guo, T. V. Nguyen and S. Vigneswaran, "***Performance of cabbage and cauliflower wastes for heavy metals removal***". Journal of Desalination and Water Treatment- Science and Engineering (2013) 1–17.
5. **Hossain, M. A.**, H. Hao Ngo, W. S. Guo **"*Introductory of Microsoft Excel SOLVER function-spreadsheet method for isotherm and kinetics modelling of metals biosorption in water and wastewater*"** Journal of Water Sustainability Journal of Water Sustainability, Vol.3(4), 2013, 223–237.
6. **Hossain, M. A.**, H. Hao Ngo, W. S. Guo, J. Zhang and S. Liang. "***A laboratory study using maple leaves as a biosorbent for lead removal from aqueous solutions*"*.*** Water Quality Research Journal of Canada (Accepted and in press).
7. **Hossain, M. A.**, H. H. Ngo, W. S. Guo, L. D. Nghiem, F. I. Hai, S. Vigneswaran, T. V. Nguyen, "***Competitive adsorption of metals on cabbage waste from multi-metal solutions*"*,*** Bioresource Technology, (Accepted and in press).

## Conference papers:

1. ***Feasibility study of palm oil fruit shells as biosorbent for copper removal from water and wastewater***, International Conference on Challenges in Environmental Science & Engineering (4th CESE 2011, Tainan, Taiwan).

2. ***Comparison study on the performance of cabbage and cauliflower for heavy metals removal***, International Conference on Challenges in Environmental Science & Engineering (5th CESE 2012, Melbourne, Australia).

# Abstract

The contamination of water by toxic heavy metals including lead, cadmium, copper and zinc is a global problem. The release of these metals into the environment has become a serious health problem due to its toxicity. Progressively stricter discharge regulations on heavy metals have accelerated the search for highly efficient but economically feasible or alternative treatment methods for its removal. The use of low-cost and bio-waste or agro-waste as biosorbents for dissolved metal ions removals has shown potential to provide economic solutions to this environmental setback.

Garden grass (GG), cabbage waste (CW), banana peels (BP), maple leaves (ML) and palm oil fruit shells (POFS) have been identified as potentially low cost and efficient biosorbent for the removal of toxic heavy metals from aqueous solution. Very simple methods were used to prepare these biosorbents. The collected GG, CW, BP, ML and POFS were washed, cut into pieces, dried in oven at 105°C, grounded into powder and used for experiments.

The biosorbents were characterized by SEM, XRD, FTIR and BET tests. Surprisingly, all biosorbents showed that the surfaces of biosorbents' particles are porous, heterogeneous structures, with uneven, asymmetric steps and pores which contained high internal spaces and posed higher specific surface area. The BET surface areas are 21.28, 1.027, 22.59, 10.94 and 39.76 $m^2/g$ for GG, CW, BP, ML and POFS, respectively. These biosorbents possesses many hydroxyl, carbonyl and phenyl functional groups (by FTIR test) and therefore, all these biosorbents are good contenders for water treatment and purification utilizations.

Biosorption of all four metals [Pb(II), Cd(II), Cu(II) and Zn(II)] by GG, CW, BP, ML and POFS was found to be dependent on experimental conditions. The optimum biosorption were noted at pH 6-6.5, shaking speed of 120 rpm, initial concentration of 10 mg/l, dose of 5g/l, contact time of 2 h and particle sizes < 75µm. The increase of temperature negatively affected the metals biosorption and at room temperature the metals biosorption process is spontaneous and exothermic in nature. The acid medium (0.1N $H_2SO_4$) was found be a better eluent for regeneration of exhausted biosorbents and it could be reused 5-7 times with minor deviation of efficiency except CW.

The efficient metal removing ability of biosorbents in both batch experiments and continuous flow fixed bed column bioreactors used to produce a biosorbent based metals removal system. It suggests that these novel biosorbents could lead to the development of a viable and cost-effective technology for metals removal from water and wastewaters. The prepared biosorbents were evaluated for the adsorption of Pb(II), Cd(II), Cu(II) and Zn(II) ions from single and multimetals aqueous solution by the batch method. The biosorption data were evaluated by equilibrium isotherms models. GG isotherm data posed better fitness with Langmuir, Freundlich and SIPS models as the $R^2$ lies between 0.991 and 0.999. Three-parameter models (Redlich-Peterson, Koble-Corrigan and SIPS) and two-parameter models (Langmuir and Freundlich) showed good fitness ($R^2$: 0.991-1.0) with equilibrium adsorption data from CW. The biosorption data from BP are evaluated by Langmuir, SIPS, Redlich-Peterson, Radke-Prausnitz, and Brouers-Sotolongo and results showed a good fitness as the $R^2$ were between 0.998 to 1. Among the models three-parameter models such as Sips, Redlich-Peterson and Unilan showed good fitness with isotherm data from ML as the $R^2$ are 0.988-1.00. Likewise the equilibrium data from POFS posed proper agreement with three parameter models for biosorption of Cu(II). Significantly low RMSE and $\chi^2$ values are found from all the used models which also signify the models fitness.

The maximum Pb(II) adsorption capacities ($q_m$) are 54.205, 61.267, 120.096 and 50.267 mg/g for GG, CW, BP and ML respectively; whereas it were 41.66, 22.123, 50.459 and 39.599 mg/g for Cd(II) biosorption. Among the biosorbents GG, ML and POFS showed good biosorption capacities for Cu(II) ion and the values are 58.34, 34.534 and 59.502 mg/g. The Zn(II) adsorption capacities are moderate and the magnitude of capacities are 57.53, 12.236, 51.896 and 29.94 mg/g for GG, CW, BP and ML respectively. A strong antagonisms were found among the metals ions [Pb(II), Cd(II), Cu(II) and Zn(II) ions] in the multimetals adsorption systems though Pb(II) and Cd(II) ions dominated. Surprisingly, the maximum reduction in capacities were also found for Pb(II) and Cd(II). The equilibrium and kinetics data for desorption were also evaluated the by isotherm models and kinetics models. Some data from GG and ML showed good agreement with models but most of the data did not pose appropriate fitness.

The kinetics of metal removal by all biosorbents was extremely fast, reaching equilibrium in about 15-60 minutes which is showed the practical potentiality. The both

pseudo-first-order and pseudo-second-order models was found to be the best fit ($R^2$: 0.991-1.00) to describe the biosorption mechanism of Pb(II), Cd(II), Cu(II) and Zn(II) ions onto the biosorbents. This is implies that the adsorption mechanisms are both physisorption and chemisorption. As reaction constant, $k_2$ and $n_{AV}$ (from order and Avrami equation) values were greater than 1 suggested that biosorption reaction is more than one order. Intraparticle diffusion also involved for biosorption process. Along with this, Elovich and Fraction power models also posed good fitness with kinetics data.

The metal removing capacity of CW was also tested in continuous flow fixed-bed column bioreactors for artificial wastewater. The removal capacities were 15.72, 62.23, 68.23 and 70.71 times higher than that obtained in a batch system for Pb(II), Cd(II), Cu(II) and Zn(II) ions. The appropriate service times to breakthrough and metals ions concentration were 5-10 h and 10 mg/l, respectively. The design of a continuous fixed bed column treatment system with CW biosorbent for Pb(II), Cd(II), Cu(II) and Zn(II) laden wastewater can be reached using the BDST, Yoon-Nelson and Clark breakthrough models.

Elucidate the biosorption mechanisms is one of the aims for biosorption of metals. Fitness of pseudo-first-order and pseudo-second-order models suggested the biosorption are both physisorption and chemisorption. FTIR tests showed the functional groups which responsible ions exchange. Isotherm data fitted more with three-parameter models which signifies the adsorption onto heterogeneous surface. It is also found from SEM and XRD data. Thus, it could not be ascertained from the results which single mechanism involved for metals biosorption. However, it could presume that combination of all mechanisms with complexation are responsible for Pb(II), Cd(II), Cu(II) and Zn(II) ions and therefore, high biosorption capacities were found.


**Faculty of Engineering and Information Technology**
**University of Technology, Sydney (UTS)**

# Chapter 1

# Introduction

# 1. Background

Water, a precious resource sustains all forms of life on the earth. The accessibility of clean water to the human population is of supreme significance in the recent world. A report by UN disclosed that nearly one billion people do not have access to the safe drinking water in third world country (GLAAS, 2012). Though the drinking water access is gradually increasing but the scenario is not appreciable till today. As the world population increases, water consumption also increases. It predicted that more than half of the world population will be facing water-based vulnerability or a water crisis by 2025 (Rijsberman, 2006; Swain, 2001). There are several causes of the water crisis and these include: (i) limited access to safe drinking water due to pollution of water resources, (ii) ground water over pumping for irrigation, and (iii) regional conflicts over common water resources etc. The deficiency of clean water also negatively impacts on biodiversity and aquatic life on the earth. In the recent global context, water pollution is a key crisis for safe drinking water and has even been recommended to be the leading cause of death and disease worldwide (WWDR4, 2012). There are now regulations in the developed world that is governing the disposal of industrial waste water which contains toxic heavy metals/chemicals. However, the real scenario in the developing or third world counties is catastrophic. Sensible people round the globe are also being begged for responsible and sustainable use of water for present and future generations, and therefore, a lot of technological improvements are occurred to recycle/treat the industrial waste water and/or polluted water before it is discharged into natural water.

## 1.1 Heavy metals pollution in water and health risk

Wastewaters with various heavy metals are discharged annually by a number of industries. Heavy metals like lead, cadmium, zinc and copper contamination in wastewater is mainly come from manmade sources like battery, electronics, paper and pulp industries, metal fabrication and mining activities, smelting, electrolysing, drug manufacturing, paint preparation, alloy manufacturing, galvanizing, printing, dyeing, paper making, ceramics manufacturing and inorganic dyestuff preparation (Liu et al., 2008; Sari et al., 2007). Untreated and uncontrolled discharge of metal containing wastewaters into the natural environment could be toxic to humans, animals, plants, and to urban ecosystems (Ahmad et al., 2010; Pamukoglu and Kargi, 2006). Low level of heavy metals could be acted as toxic (Kusvuran et al., 2012), and absorbed to the body of living organisms (Gavrilescu, 2004). Cu(II), Pb(II), Cd(II) and Zn(II) are the metals

using for essential activities and some uses for nutrients needed by the body in trace amounts. However, an increase in the intake of Cu(II) can cause health problems such as gastrointestinal disturbance, liver and kidney failure, Wilson's disease and insomnia to human, while high Cd(II) intake can lead to birth defects, kidney damage, renal disorder, Itai-Itai disease, hepatic damage, cancer, and hypertension (Han et al., 2009; Igwe and Abia, 2007; Kurniawan et al., 2006a; Kurniawan et al., 2006b). On the other hand, Pb(II) has no essential function to the human body but has several unwanted effects like encephalopathy, seizures and mental retardation, kidney damage, and disruption of the nervous system, reduces haemoglobin production (Igwe and Abia, 2007; Qaiser et al., 2007). Similarly, Zn(II) has little uses for plants but not for human and it could create some severe effects such as depression, lethargy, neurologic signs such as seizures and ataxia, and increased thirst (Kurniawan et al., 2006a; Kurniawan et al., 2006b). In addition, the presence of heavy metals at higher levels in surface and groundwater ecosystem also inhibits the growth aqueous organism and stops any beneficial use of the water bodies. These metal ions, and their supplementary complexes, could accumulate in the body of fishes and other aquatic organisms, and finally could reach to the human body by bio-accumulation, bio-concentration and bio-magnification through the drink and food chains (Hong et al., 2006; Hu et al., 2007). Removal of heavy metal ions from wastewater is now a subject of major concern for both industry and environmental protection agencies here at home and abroad. Hence, it is crucial to control the level of heavy metals in wastewaters before its disposal into the nature.

## 1.2 Removal of heavy metals from water

A wide range of techniques such as membrane separation, chemical coagulation, extraction, ion-exchange, electro deposition, and chemical precipitation and electrochemical techniques have been employed to sanitise water and wastewater from heavy metals. Nevertheless, these techniques require the use of expensive chemicals, and prove as costly and incompetent, especially in removing lower concentration of heavy metals (Popuri et al., 2009; Xiangliang et al., 2005). Additional disadvantage is the production of metals contained sludge, which requires further treatment to dispose (Rhazi et al., 2002). Besides these, adsorption process is widely used to remove heavy metals from water and it is already proved the effectiveness of removing contaminants from wastewater with high solute loadings and even at dilute concentrations (<100

mg/l)(Popuri et al., 2009; Rhazi et al., 2002). Among the adsorbents, activated carbon is commonly used as a commercial adsorbent for removing heavy metal from wastewater. However, this is still an expensive and high-tech produced material. For this reason, many researchers emphasis for finding and identifying an inexpensive alternative adsorbent.

## 1.3 Biosorption of heavy metals

A search for a low-cost and easily available adsorbent has led to the investigation of materials of biological origin as potential metal biosorbents. In recent years, a significant number of studies on the removal of heavy metals from aqueous solutions by non-live, inactive biomass have been conducted worldwide. This approach of wastewater remediation is defined as biosorption, and the non-live biomass used in this approach is defined as biosorbent.

Removal of heavy metals by biosorption is a relatively new and developing technology in the field of water decontamination (Schiewer and Volesky, 2000). Absorbent materials (biosorbents), derived from a suitable agro-biomass, can be used for the effective removal and recovery of heavy metallic ions from wastewater streams (Raize et al., 2004). Extensive studies have been commenced in recent years with the aims of finding alternative and economically feasible biosorbents for wastewater and water treatment. At a large scale, economic sorbents can be defined as materials which are abundant in nature or can be found as a by-product or waste from agro-industry, nature and industry, cheap and effective and which normally do not require pre-processing. Recent studies on the removal of heavy metals using numerous types of biomass/biomaterials are reported in literature. Several mechanisms involve for biosorption of metals that differ qualitatively and quantitatively from species to species, origin, and processing procedure of biomass/biomaterials (Volesky and Holan, 1995). Some biosorbents show high heavy metal binding capacity, and the biological material is abundant and obtained inexpensively from the natural environment. Biomass/biomaterials comprise with several chemical or functional groups such as acetamido, amino, amido, sulfhydryl, sulfate, and carboxyl which could attract and sequester the metals from solution (Gardea-Torresdey et al., 1990; Schiewer and Volesky, 2000; Volesky and Holan, 1995). Mainly ionic interactions and exchanges;

formation of complexes between metal cations and ligands contained in the structure of the cell wall biopolymers, and precipitation on the cell wall matrix of biosorbent are the followed complex mechanisms of biosorption of metals (Schiewer and Volesky, 2000). Pearson's concept of hard and soft acid and base theory (HSAB) and by Irving-Williams series could be used to explain the binding characteristics of metallic cations during biosorption (Schiewer and Volesky, 2000). Consequently, biosorbents are now being considered as an alternative to ion exchangers or other metal extraction and concentration operations in metal recovery. As such, the study of biosorption is of great importance from an environmental point of view. There are biomass types of various kinds, such as leaves, wood or agricultural residues, waste crustacean biomass-anything renewable that grow, including microbes. Biosorbent is generally ranked in categories of bacterial, fungi, algae, industrial wastes, agricultural wastes, natural residues, and other biomaterials. The main advantages of biosorption are that it is either abundant or wastes from other sectors. Distinctive capabilities of certain types of biomass which adsorb and immobilize heavy metals can be more or less selective. These advantages have made biosorption an alternative cost-effective way for the treatment of metal bearing wastewaters.

## 1.4 Aims and objectives

The main aim of this study was to prepare biosorbents, perform characterisation and evaluate their efficacy as adsorbents for the removal of heavy metals [Pb(II), Cd(II), Cu(II) and Zn(II)] ions from aqueous solution.

In meeting the above goal, the following specific objectives are to be apprehended:

- To investigate the characteristics of biosorbent such as surface morphology, specific surface area, functional groups and elemental mapping;
- To characterize of various biosorption process parameters (i.e. pH, equilibrium time, initial metal ion, particle sizes, temperature, doses, shaking speed and biosorbent concentration) for determining optimum operational conditions for maximum uptake of heavy metal ions by newly developed biosorbents;
- To investigate on various treatments to find more appropriate metal desorbing agent for the elution of toxic metal from metal-laden biosorbent system.

- To evaluate the adsorption and desorption properties of the biosorbents by carrying out batch adsorption and desorption experiments using heavy metals [Pb(II), Cd(II), Cu(II) and Zn(II)] as model pollutants;
- To determine the adsorption and desorption capacity of each biosorbents by applying some commonly used adsorption isotherms and kinetic models through non-linear modelling;
- To carry out of competitive biosorption studies of heavy metals mixed together onto selected biosorbents;
- To investigate on the metals biosorption potential of cabbage waste biosorbent in column bioreactors in continuous flow mode and to determine the optimum operational conditions (column bed height, flow rate and biosorbent quantity) using single and mixed metal solutions.

It is expected that this research would strengthen the information available on use of agro-waste and bio-waste as biosorbents for removal of heavy metals from water by providing more specific characteristics of biosorbent, and enhance the understanding of adsorption and desorption behaviour.

## 1.5 Research hypotheses and outline of thesis

In this study, agro-wastes and bio-wastes [garden grass (GG), cabbage waste (CW), banana peel (BP), maple leaves (ML) and palm oil fruits shells (POFS)] that are abandoned in nature or discarded by people were prepared to biosorbents with the aim of achieving materials with enhanced adsorption properties for the removal of toxic heavy metals from aqueous solution.

This thesis has three main sections and consists of a total of ten chapters. The first section is made up of Chapters 1 and 2 which deal with the introduction and literature review. Chapter 1 contains a general introduction to the thesis. The aims and objectives of this study are also presented including the hypotheses and outline of the thesis. Chapter 2 reviews the valuable information from the previous related to the heavy metals pollution and its impact on environment and human, conventional heavy metals removal and its constraints, biosorption, its influential factors and advantages over other methods, and biosorbents and their characteristics, availability and recent developed

biosorbents with previous work on their use as adsorbents. This chapter also incorporate the isotherm, kinetics and column adsorption models for evaluating the metals biosorption process.

The second section consists of Chapters 3, 4, 5, 6, 7 and 8 which present the experimental work carried out to achieve the objectives of this thesis. This section focuses on the preparation of the biosorbents from selected bio-waste and agro-waste (GG, CW, BP, ML and POFS). Chapter 3 presents the details of the chemical reagents used in this study as well as the collection information. A general description of the preparation methods and characterisation techniques of biosorbents [Fourier transform infrared spectroscopy (FTIR), X-ray diffraction (XRD) analysis, scanning electron microscopy (SEM) and Brunauer-Emmet-Teller (BET)] are presented in the Chapter 3. The detailed experimental procedures are also explained with all biosorbents for removal of Pb(II), Cd(II), Cu(II) and Zn(II) ions from water in single and multimetals systems. In connection to process design for dynamic heavy metals removal, a column reactor was constructed and details experimental procedure was explained.

The chapters 4, 5, 6, 7 and 8 which cover the evaluation of the prepared biosorbents for their adsorption of heavy metals from aqueous solution in single and multimetals systems. The procedures for the adsorption of heavy metals are reported in each chapter with referring to the section of Chapter 3. The evaluation and discussion of characterisation results are incorporated in the first section of 'Results and Discussion' section of each chapters. To get optimum operating conditions for high removal of heavy metals, experimental conditions such as pH, doses, initial metals concentrations, contact time, shaking speed, temperature and particle size of biosorbents are evaluated in the second section of 'Results and Discussion' section of each chapters. The regeneration capability and successive uses of biosorbent are also evaluated in the each chapter. The isotherms and kinetics data from the adsorption and desorption experiments are assessed and discussed in the third section of each chapters. In the last section of each chapter the multimetals adsorption data are discussed with fitted models. The adsorption results are discussed in relation to the available information for other biosorbents in literature.

The third section of the thesis consists of Chapters 9 and 10. Chapter 9 covers the evaluation of adsorption capability of heavy metals by CW in a dynamic system. The procedures for the adsorption of heavy metals are reported in Chapter 3 while adsorption data from the column experiments and its evaluation are presented in this chapter. Chapter 10 gives a general conclusion of the research and recommendations for future work.


**Faculty of Engineering and Information Technology**
**University of Technology, Sydney (UTS)**

# Chapter 2

# Literature Review

## 2.1 Background

Environmental pollution has become a prime concern for industrial and developing countries from the middle of last century. Massive human and industrial growth has changes the pristine condition of the environment towards a worse condition. The need to supply the basic needs for humans a massive development in the industrial sector as well as the modern agriculture sector has impacted on the world. These sectors have become sources of pollutants for nature. The pollutants coming from different sources as wastes are gaseous, liquid and solid form. These wastes are been released to the air, discharged to water or buried into landfill which causes further problems to the environment and living creatures.

Heavy metals are abundantly present in nature and are also added to water by human-activities such as battery production, electronics, paper and pulp industries, metal fabrication and mining activities, smelting, electrolyzing, drug manufacturing, paint preparation, alloy manufacturing, galvanizing, printing, dyeing, paper making, ceramics manufacturing and inorganic dyestuff preparation (Liu et al., 2008; Sari et al., 2007). The presence of potentially toxic heavy metals in the environment is of very much concern, primarily due to their non-biodegradability and persistence in the environment (Volesky, 1999b). High concentrations of heavy metals in water supplies are undesirable as they may have potentially adverse effects on the health of organisms, the suitability of water for various purposes, the longevity of water and sewer networks, and the aesthetic of the environment (Demirbas, 2008; Vieira and Volesky, 2010). Some metals are known to be able to become concentrated in food chains through bioaccumulation, notably mercury and cadmium (Burger and Gochfeld, 2004). Some metals are harmless and traces are required as nutrients for balanced growth; for example, cobalt, copper, iron, selenium, and zinc are considered nutrients needed for balanced growth. High dosage of heavy metals may cause toxicity that is acute, chronic, synergistic, or mutagenic/teratogenic (Burger and Gochfeld, 2004). The presence of heavy metals at higher levels in surface and groundwater ecosystems also inhibits the growth of aqueous organisms and stops any beneficial use of the water bodies. These metal ions, and their supplementary complexes, could accumulate in the body of fishes and other aquatic organisms, and finally could reach to the human body by bio-accumulation, bio-concentration and bio-magnification through the drink and food chains (Hong et al., 2006; Hu et al., 2007).

## 2.2 Heavy metals: sources, toxicity and environmental fates

### 2.2.1 Sources of heavy metals

Heavy metals enter the environment through natural and anthropogenic activities. For instance, the weathering of rocks naturally produces heavy metals. On the other hand, the burning of petroleum and non-ferrous metalworking contribute to the emissions of heavy metals in the atmosphere. It is estimated that an average of 332,350 tons of lead(II), 35,370 tons of copper(II) and 131,880 tons of zinc(II) are emitted in the atmosphere each year. Furthermore, the main causes of water pollution are household waste, iron and steel production, metal smelters, metal plating or finishing operations, mining and fertilizer applications. The anthropogenic median annual inputs of lead, copper, nickel and zinc into aquatic systems were reported to be 138,000 t, 112,000 t, 113,000 t and 226,000 t, respectively (Nriagu et al., 2004). The two principal sources of heavy metals in soils are the disposal of ash residues from coal combustion and general disposal of commercial products on land. It is estimated the average annual worldwide emissions into the soils to be 796,000 t for lead; 954,000 t for copper; 325,000 t for nickel and 1,372,000 t for zinc) (Nriagu et al., 2004).

Heavy metal pollution is one of the most important environmental problems today. Various industries produce and discharge wastes containing different heavy metals into the environment, such as mining and smelting of metalliferous ores, surface finishing industry, energy and fuel production, fertilizer and pesticide industry and application, metallurgy, iron and steel, electroplating, electrolysis, electro-osmosis, leatherworking, photography, electric appliance manufacturing, metal surface treating, aerospace and atomic energy installation etc (Wang and Chen, 2009). Among these, the following four appear as the main priority targets, particularly in the industrialized world (Volesky, 2007):

- acid mine drainage (AMD)-associated with mining operations,
- electroplating industry waste solutions (growth industry),
- coal-based power generation (throughput of enormous quantities of coal),
- Nuclear power generation (uranium mining/processing and special waste generation).

Three kinds of heavy metals are of concern, including toxic metals (such as Hg, Cr, Pb, Zn, Cu, Ni, Cd, As, Co, Sn, etc.), precious metals (such as Pd, Pt, Ag, Au, Ru etc.) and

radionuclides (such as U, Th, Ra, Am, etc.) (USEPA, 2002; Wang and Chen, 2009). Global production of lead from mines has reduced from 3.6 million tonnes in 1975 to 3.1 million tonnes in 2004, while global refined lead production has amplified from 4.7 million tonnes to 7.1 million tonnes, because the recycled lead has added to the supply (USEPA, 2002). Lead production is not much by developing countries compared to the production by other developed countries like China, Australia, USA and Canada. They produce about 76% of the world production. Table 4 shows lead production through different countries including developing ones where, the production via recycling of previously used lead is higher for developed countries (60-70% of their lead production) than developing countries (<30%).

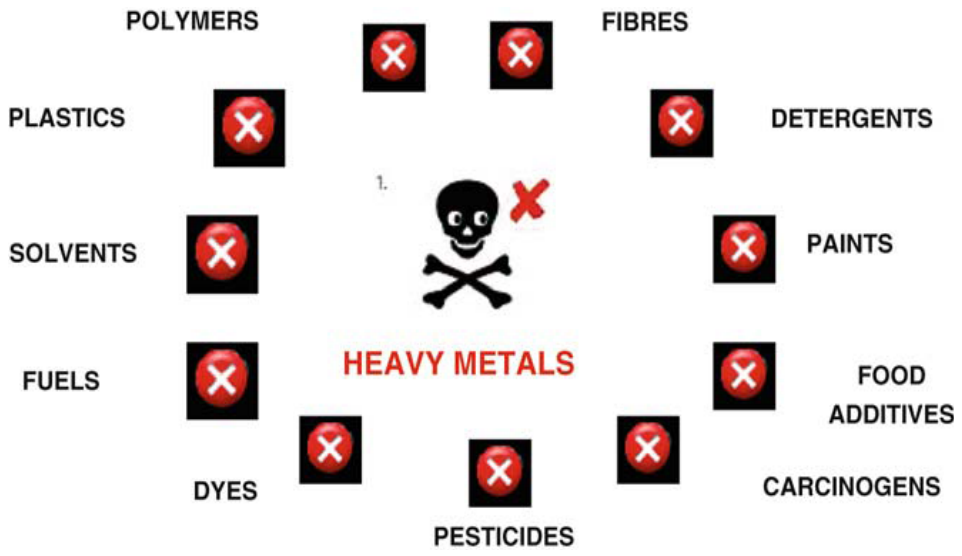


**Figure 2.1** Heavy metals pollution: A prize tag of modern society
(Adopted from Srivastava and Goyal, 2010)

### 2.2.2 Heavy metals in industrial wastewater

Contamination of water by toxic heavy metals through the discharge of industrial wastewater is a worldwide environmental problem. Rapid industrialization has seriously contributed to the release of toxic heavy metals to water streams. Industrial wastewater streams containing heavy metals are produced from different industries. Electroplating and metal surface treatment processes generate significant quantities of wastewaters containing heavy metals (such as cadmium, zinc, lead, chromium, nickel, copper, vanadium, platinum, silver, and titanium) from a variety of applications. Mining, electroplating, metal processing, textile, battery manufacturing, tanneries, petroleum refining, paint manufacture, pesticides, pigment manufacture, printing and photographic

industries (Liu et al., 2010) are the main sources of heavy metal ion contamination. Metals such as lead, cadmium, copper, arsenic, nickel, chromium, zinc and mercury have been recognized as hazardous heavy metals. Unlike organic wastes, heavy metals are non-biodegradable and can be accumulated in living tissues, causing various diseases and disorders; therefore they must be removed before discharge. Other sources for the metal wastes include: the wood processing industry where a chromated copper-arsenate wood treatment produces wastes containing arsenic inorganic pigment manufacturing producing pigments that contain chromium compounds and cadmium sulphide; petroleum refining which generates conversion catalysts contaminated with nickel, vanadium, and chromium; and photographic operations producing film with high concentrations of silver and ferrocyanide. All of these generators produce a large quantity of wastewaters, residues, and sludges that can be categorized as hazardous wastes requiring extensive waste treatment (Sörme and Lagerkvist, 2002).

### 2.2.3 Heavy metals in domestic wastewater

Heavy metals may enter domestic wastewater due to discharge from households and industries. The waste effluent from households contains much organic and inorganic waste. For example, detergents contain trace-levels of metals such as iron, magnesium, chromium, copper, and strontium. Heavy metals can be adsorbed onto biological solids (large, small, and colloidal) due to higher affinities between metals and solids. There is an increasing awareness that urban runoff causes a serious metal problem (Raskin et al., 1997). Street dust (from the air), dirt, and various solids, together with various chemicals applied (e.g., pest control), have contributed significantly to the problem. Another domestic source of heavy metal contaminants is landfill. Landfill is an engineered measure for solid waste storage. Solid waste often has heavy metals existing in solid and liquid forms. For a longer period of time, anaerobic reactions occur in the site, which leads to low pH, “pushing” the metals to the geo-environment when the lining (landfill liner) is not effective. Waste-activated sludge may be used as a nutrient source for plant growth due to its good values of carbon, potassium, pathogen, and phosphorus (Bhogal et al., 2003). However, the metal content in the “fertilizer” (sludge) is normally quite high. When it is applied, the metals could enter the surface water and groundwater (Chang et al., 1987).

Sewage sludge also contains high heavy metal concentrations, which produce harmful unwanted environmental impact such as phyto and microbial toxicity, food chain and groundwater contamination (Bhogal et al., 2003; Boller, 1997; Chang et al., 1987). In low concentrations, several heavy metals such as Fe, Mn, Zn, Cu, Ni and Mo are essential micronutrients for plants (Raskin et al., 1997). When sewage sludge is used as a soil conditioner, toxic metals can limit the application rate. Literature data show that more than 50% of the sludge is inadequate for use in agricultural areas due to their metal contents. The remediation of soils contaminated with toxic metals is a challenging task because metals do not degrade with time. It is therefore critical to know the physical and chemical properties of biosolids applied to land, particularly their elemental contents both in terms of total concentrations and the extractable metals at pH 7, which have potentially negative biological effects. Total metal concentration represents a good indicator of the degree and extent of contamination but in most cases, limited information on the mobility and availability of heavy metals.

### 2.2.4 Forms and fate of heavy metals in the aquatic environment

Many hidden processes can change the physico-chemical forms or speciation of the heavy metals and can have a great influence on the stability of metals in aquatic environments. The processes involved are oxidation/reduction, adsorption/desorption, precipitation/dissolution and aggregation/disaggregation (Li et al., 2009).

#### 2.2.4.1 Cadmium

Since cadmium is present in the $Cd^{+2}$ oxidation states in oxygenated surface waters, redox reactions are not common for this element (Arain et al., 2008; USEPA, 2002). Cadmium can form complexes with hydroxide, carbonate, chloride, sulfate and humic material. However, uncomplexed cadmium is the dominant species below pH = 6.9 (Jamali et al., 2009; McBride, 1995).

#### 2.2.4.2 Copper

Copper occurs in four oxidation states: 0, +1, +2 and +3, but most commonly as $Cu^{+1}$ (cuprous), and $Cu^{+2}$ (cupric). Cuprous copper ($Cu^{+1}$) is unstable in aerated aqueous solutions, and is normally oxidized to cupric copper ($Cu^{+2}$) (Arain et al., 2008). Divalent copper salts are very soluble in water. Copper is generally more soluble in acidic waters, and precipitates as $Cu(OH)_2$ at pH values above 6.5 (Li et al., 2009; USEPA, 2002). In the presence of excess cupric ion in alkaline waters, carbonates, hydroxides, oxides and

sulphides form precipitates. In the presence of soluble organic matter, sorption of copper may be relatively ineffective (Jamali et al., 2009; McBride, 1995).

#### 2.2.4.3 Lead

Lead exists in several oxidation states: 0, +1,+2 and +4. However, the divalent form $Pb^{2+}$ is the stable ionic species in most natural environments (USEPA, 2002). Precipitation and sorption are the principal mechanisms controlling the distribution of lead in the aquatic environment. In the presence of inorganic ligands, lead can precipitate as a number of compounds including $PbSO_4$, $PbCO_3$, $Pb(OH)_2$, PbS, and $Pb_3(PO_4)_2$(Jamali et al., 2009). At $5 \leq pH \leq 7$, most of the lead is precipitated and adsorbed as sparingly soluble hydroxides (Arain et al., 2008). At $7 \leq pH \leq 9$, $PbCO_3$ is the major species (USEPA, 2002). Below about pH 5-6, the formation of cationic species prevents the formation of hydroxides (Arain et al., 2008; McBride, 1995).

#### 2.2.4.4 Zinc

The chemistry of zinc is quite similar to that of cadmium. In aqueous solutions, zinc exists in the +2 oxidation state (McBride, 1995). Sorption of zinc by hydrous metal oxides, clay minerals and organic materials, is common in aquatic systems. In the presence of dissolved solids, zinc is transported in solution as hydrated cations or complex species. In the presence of suspended solids, sorption of zinc may occur (McBride, 1995). However, at pH 6.2-8.0, the predominant species is the free cation (Jamali et al., 2009; Li et al., 2009).

### 2.2.5 Toxicity

Metals can be divided into two groups: those that are essential for survival, such as iron and calcium, and those that are nonessential or toxic, such as cadmium and lead. These toxic metals, unlike some organic substances, are not metabolically degradable and their accumulation in living tissues can cause death or serious health threats. Furthermore, these metals, dissolved in wastewaters and discharged into surface waters, will be concentrated as they travel up the food chain (Castro-González and Méndez-Armenta, 2008; Lussier et al., 1985). Eventually, extremely poisonous levels of toxin can migrate to the immediate environment of the public. Metals that seep into ground waters will contaminate drinking water wells and harm the consumers of that water. Pollution from man-made sources can easily create local conditions of elevated metal presence, which could lead to disastrous effects on animals and humans. Actually, man's exploitation of

the world's mineral resources and his technological activities tend to unearth, dislodge, and disperse chemicals and particularly metallic elements, which have recently been brought into the environment in unprecedented quantities and concentrations and at extreme rates (Jortner, 2008; Mansour and Gad, 2010; Oehme, 1978).

Heavy metals in dosages higher than critical values can cause a series of health problems. The toxicity may damage or reduce mental and central nervous functions, lower energy levels, and damage blood composition, lungs, kidneys, liver, and other vital organs (Lussier et al., 1985). Long-term exposure of toxic heavy metals may cause various cancers, Parkinson's disease, muscular dystrophy, multiple sclerosis, and neurological degenerative processes (e.g., Alzheimer's disease). One can see that toxicity is affected by many factors (Oehme, 1978; ul Islam et al., 2007). Heavy metals express their toxicity to human beings, which may result from the following mechanisms:

i. Heavy metals (divalent or higher) can easily form precipitates with anionic substances ($CO_3^{-2}$, $SO_4^{-2}$, and $PO_4^{-3}$). The precipitates (solids) may stay in the human body.

ii. Heavy metals can be adsorbed onto organic functional groups in various tissues of the human body, which may change their biological activities (e.g., enzymes). This may also "force" the essential metals to detach from enzymes and be replaced by harmful heavy metals (e.g., Cu versus Zn).

iii. Some heavy metals may cause redox reactions, "forcing" the basic elements (e.g., carbon) to change their chemistry. For example, hexavalent chromium $CrO_4^{-2}$ can cause oxidation of carbon in tissues of the human body. The carbon may be oxidized, and thus its chemistry may be changed. As such, hexavalent chromium is much more toxic than trivalent chromium.

#### 2.2.5.1 Effect of lead

Generally lead can be accumulated and adsorbed by the body through inhalation, ingestion, skin contact (occupational exposure), or transfer via the placenta. Adults can absorb 10% of ingested lead into their body (Ochiai, 1987; ul Islam et al., 2007; Zhang et al., 2013). Young children can absorb from 40% to 53% of lead ingested from food and the adsorbed lead can enters either a "rapid turnover" biological pool with distribution to the soft tissues (blood, liver, lung, spleen, kidney, and bone marrow) or a

“slow turnover” pool with distribution mainly to the skeleton (Lussier et al., 1985; USEPA, 1987). 80-95% and 73% of the total adsorbed lead accumulate in adults and in children skeleton respectively (Jortner, 2008; Påhlsson, 1989). It is stated that the biological half-life of lead is approximately 16-40 days in blood and about 17-27 years in bones (Holland, 1979; Mansour and Gad, 2010; Oehme, 1978).

Contemporary results revealed that earthenware glazed surfaces and pigments of older paints can causes lead poisoning to children. Like most of the heavy metals inorganic lead is a general metabolic poison and enzyme inhibitor. Organic lead is even more poisonous than inorganic lead (Niu et al., 2009). The previously discovered symptoms of lead poisoning are physical like abnormal excitement, depression, lack of tolerance and irritability. Young children are particularly affected and can suffer mental retardation and semi-permanent brain damage. Inorganic lead very dangerous effects as has the ability to replace bone calcium, remain there long time and make the bone susceptible to breaking (Khlifi and Hamza-Chaffai, 2010; Niu et al., 2009). The lead content in blood is the usual indicator of the degree of inorganic lead poisoning in humans. Different authorities suggest safety levels in the range of 0.2-0.8 pap (Port Augusta Prison-unit used for safety level indication) (ul Islam et al., 2007).

Lead can be accumulated in the human body and cause general poisoning, with fetuses, infants, children up to six years of age, and pregnant women (because of their fetuses) being most susceptible to adverse health effects. It has severe effects on the central nervous system of humans and as a result a human can show dullness, restlessness, irritability, poor attention span, headaches, muscle tremor, hallucinations, and loss of memory (ATSDR, 1990; Zhang et al., 2013). If the blood lead level goes to 50-80 μg/l, adults may show the signs of tiredness, sleeplessness, irritability, headaches, joint pain, and gastrointestinal symptoms (ATSDR, 1990). After one or two years of exposure, muscle weakness, gastrointestinal symptoms, lower scores on psychometric tests, disturbances in mood, and symptoms of peripheral neuropathy were observed in occupationally exposed populations at blood lead levels of 40-60 μg/l (Baker et al., 1984).

Renal failure has long been associated with lead poisoning if the blood level is over 40 μg/l and there has been a long time exposure. Lead has a significant effect on general

intelligence ratings (Jortner, 2008; Zhang et al., 2013). Lead toxicity can affect both the central and peripheral nervous systems causing subencephalopathic neurological and behavioral effects in adults and electrophysiological evidence of both central and peripheral effects on the nervous system in children with blood lead levels well below 30 µg/l (IARC, 1982). The carcinogenicity of lead in humans has been investigated in several epidemiological studies of occupationally exposed workers (IARC, 1982).

Lead can enter (drinking) water through corrosion of pipes. This is more likely to happen when the water is slightly acidic. That is why public water treatment systems are now required to carry out pH-adjustments in water that will serve drinking purposes. As far as we know, lead fulfils no essential function in the human body, it can merely do harm after uptake from food, air or water. Lead can cause several unwanted effects (Giaccio et al., 2012), such as:

- Disruption of the biosynthesis of haemoglobin and anaemia
- A rise in blood pressure
- Kidney damage
- Miscarriages and subtle abortions
- Disruption of nervous systems
- Brain damage
- Declined fertility of men through sperm damage
- Diminished learning abilities of children
- Behavioural disruptions of children, such as aggression, impulsive behavior and hyperactivity
- Lead can enter a foetus through the placenta of the mother. Because of this it can cause serious damage to the nervous system and the brains of unborn children.

#### 2.2.5.2 Effect of cadmium

Cadmium, lead and mercury are the “Big Three” toxic categories of heavy metals because of their acute toxicity to humans and the environment. Stomach irritation, vomiting and diarrhoea may happen instantly after taking heavily contaminated food and drinking water (Gallego et al., 2012; Ochiai, 1987; Påhlsson, 1989; USEPA, 1987; Zhang et al., 2012b). The acute oral lethal dose of cadmium for humans has to be several hundred milligrams (Li and Zhou, 2012; Lussier et al., 1985). Cadmium has

been established as a very toxic heavy metal. It is stated that 15-30 mg of cadmium from acidic foodstuffs can resulted in acute gastroenteritis. Melting or pouring of cadmium metal can cause acute poisoning in humans (Jortner, 2008; ul Islam et al., 2007; WHO, 1974). Fatalities have been found from a 5h exposure to 8 $mg/m^3$ of Cd and acute pneumonitis resulted from inhalation of concentrations between 0.5 and 2.5 $mg/m^3$ for 3 days (Holland, 1979; Marion and Denizeau, 1983; Oehme, 1978; Zhang et al., 2012b).

The acute poisoning of Cd may cause pulmonary edema, headaches, nausea, vomiting, chills, weakness, and diarrhoea (Graeme and Pollack Jr, 1998; Zhang et al., 2012a). Osteomalacia (softening of the bone) is a disease of bones originated from acute cadmium poisoning and elderly women who have had many children can be affected more than others (Holland, 1979; Li et al., 2014). This disease is known as “Itai-Itai” in Japan. The symptoms shown by the affected peoples are lumbar pain, myalgia, and spontaneous fractures with skeletal deformation. It is accompanied by the classical renal effects of proteinuria, and often glucosuria, and aminoaciduria (Mansour and Gad, 2010; Niu et al., 2009; Qu et al., 2013).

Cadmium can accumulate in the kidneys and liver of humans. Chronic cadmium poisoning produces proteinuria and formation of kidney stones, lung and prostate cancer. There is evidence of a link between cadmium and hypertension (Ebau et al., 2012; Malik, 2004). Chronic exposure to airborne cadmium results in a number of toxic effects; the two main symptoms are lung emphysema and proteinuria (WHO, 1974). The World Health Organization (WHO) has recommended that the provisional permissible intake of cadmium not exceed 0.4-0.5 mg per week (WHO, 1974).

The general public may be exposed to cadmium poisoning with mass smoking in public places along with the smoker. This is an important single source of cadmium exposure. A study has reported that about 10% of cadmium is inhaled through smoking cigarettes. The lungs are much more effective than the gut in absorbing cadmium and cigarette smoking is very effective way for absorbing it (Díaz et al., 2006; Malik, 2004). Smokers can have cadmium concentrations 4-5 times higher in the blood and 2-3 times higher in the kidneys than non-smokers. There seems to be little chance to exposure to cadmium from passive smoking as the cigarettes contains higher cadmium (Díaz et al., 2006). It

was revealed that no significant effect on blood cadmium concentrations could be detected in children exposed to environmental tobacco smoke (Hogan et al., 2010).

Human uptake of cadmium takes place mainly through food. Foodstuffs that are rich in cadmium can greatly increase the cadmium concentration in human bodies. Examples are liver, mushrooms, shellfish, mussels, cocoa powder and dried seaweed (Lafuente, 2013; Zhang et al., 2012a). An exposure to significantly higher cadmium levels occurs when people smoke. Tobacco smoke transports cadmium into the lungs. Blood will transport it through the rest of the body where it can increase effects by potentiating cadmium that is already present from cadmium-rich food (Gallego et al., 2012; Ige and Akhigbe, 2013).

Other high exposures can occur with people who live near hazardous waste sites or factories that release cadmium into the air and with people that work in the metal refinery industry. When people breathe in cadmium it can severely damage the lungs (Bucio et al., 1995). This may even cause death. Cadmium is first transported to the liver through the blood (Baker et al., 2003; Fowler, 2009). There, it is bonded to proteins to form complexes that are transported to the kidneys (Marion and Denizeau, 1983). Cadmium accumulates in the kidneys, where it damages filtering mechanisms. This causes the excretion of essential proteins and sugars from the body and further kidney damage. It takes a very long time before cadmium that has accumulated in kidneys is excreted from a human body (Fowler, 2009). Other health effects that can be caused by cadmium are:

- Diarrhoea, stomach pains and severe vomiting
- Bone fracture
- Reproductive failure and possibly even infertility
- Damage to the central nervous system
- Damage to the immune system
- Psychological disorders
- Possibly DNA damage or cancer development

#### 2.2.5.3 Effect of copper

Among the heavy metals Copper is the major available type of heavy metal in the aquatic environment. Copper entering the blood system may generate reactive free

oxygen species and damage the protein, lipids and DNA (Brewer, 2010; Holland and White, 1988; USEPA, 1987). Excess copper compound in the body may have effects on aging, schizophrenia, mental illness, Indian childhood cirrhosis, Wilson's and Alzheimer's diseases (Brewer, 2007; Faller, 2009; Hureau and Faller, 2009). Excessive copper in the marine system has been found to damage marine life (Van Genderen et al., 2005) and damage the gills, liver, kidneys, the nervous system and changing sexual life of fishes (Flemming and Trevors, 1989; Jortner, 2008; Li et al., 2014; Ochiai, 1987).

Copper can be found in many kinds of food, in drinking water and in air. Because of that significant quantities of copper can be absorbed each day by eating, drinking and breathing. The absorption of copper is necessary, because copper is a trace element that is essential for human health (Li et al., 2014; Påhlsson, 1989). Although humans can handle proportionally large concentrations of copper, too much copper can still cause significant health problems. Copper concentrations in air are usually quite low, so that exposure to copper through breathing is negligible. However people that live near smelters that process copper ore into metal do experience this kind of exposure. People that live in houses that still have copper plumbing are exposed to higher levels of copper than most people, because copper is released into their drinking water through corrosion of pipes. Occupational exposure to copper often occurs. In the work place environment copper contagion can lead to a flu-like condition known as metal fever (Flemming and Trevors, 1989; Zhang et al., 2012b). This condition will pass after two days and is caused by over sensitivity.

Long-term exposure to copper can cause irritation of the nose, mouth and eyes and it causes headaches, stomachaches, dizziness, vomiting and diarrhoea (Holland and White, 1988; Påhlsson, 1989). Intentionally high uptakes of copper may cause liver and kidney damage and even death. Whether copper is carcinogenic has not been determined yet (Shaligram and Campbell, 2013). There are scientific articles that indicate a link between long-term exposure to high concentrations of copper and a decline in intelligence with young adolescents. Whether this should be of concern is a topic for further investigation. Industrial exposure to copper fumes, dusts, or mists may result in metal fume fever with atrophic changes in nasal mucous membranes (Babaei et al., 2012). Chronic copper poisoning characterized by a hepatic cirrhosis, brain damage, demyelination, renal disease, and copper deposition in the cornea, resulted in Wilson's disease.

There are environmental effects of copper. When copper ends up in soil it strongly attaches to organic matter and minerals. As a result, it does not travel very far after release and it hardly ever enters groundwater. In surface water copper can travel great distances, either suspended on sludge particles or as free ions. Copper does not break down in the environment and because of that it can accumulate in plants and animals when it is found in soils (Hu et al., 2013). Copper can interrupt the activity in soils, as it negatively influences the activity of microorganisms and earthworms (Holland and White, 1988). The decomposition of organic matter may seriously slow down because of this. When the soils of farmland are polluted with copper, animals will absorb concentrations that are damaging to their health (Shaligram and Campbell, 2013). Mainly sheep suffer a great deal from copper poisoning, because the effects of copper are manifesting at fairly low concentrations.

#### 2.2.5.4 Effect of zinc

Zinc toxicosis is not a common problem for man and animals. Zinc poisoning occurs in humans from acid foods or beverages stored in galvanized containers. Animals may get zinc poisoning from ingesting or exposure to galvanized metal objects, certain paints and fertilizers, zinc-containing coins etc (Ochiai, 1987; Påhlsson, 1989; Poulson et al., 1997; Zhang et al., 2012b). Several factors such as water hardness, salinity, temperature, and the presence of other contaminants influence zinc toxicity in aquatic environments. This modification in zinc toxicity is the result of an effect on zinc availability and on sorption or binding of available zinc to biological tissues (Nriagu, 2011). The effect of water hardness on zinc toxicity is by far the most studied factor (Giaccio et al., 2012; Holland and White, 1988; Li et al., 2014).

Clinical manifestations of zinc deficiency in animals include growth retardation, testicular atrophy, skin changes, and poor appetite. Zinc is ubiquitous in the environment and its deficiency in humans and animals may be considered an unlikely problem. Nevertheless, zinc deficiency and related problems in humans, animals, birds, and plants have been reported in the literature (Gaetke and Chow, 2003; Holland and White, 1988; Nriagu, 2011).

Zinc is a trace element that is essential for human health. When people absorb too little zinc they can experience a loss of appetite, decreased sense of taste and smell, slow wound healing and skin sores (Heng et al., 2010). Zinc-shortages can even cause birth

defects. Although humans can handle proportionally large concentrations of zinc, too much zinc can still cause eminent health problems, such as stomach cramps, skin irritations, vomiting, nausea and anaemia (Nriagu, 2011). Very high levels of zinc can damage the pancreas and disturb the protein metabolism, and cause arteriosclerosis. Extensive exposure to zinc chloride can cause respiratory disorders (Heng et al., 2010).

In the work place environment zinc contagion can lead to a flu-like condition known as metal fever. This condition will pass after two days and is caused by over sensitivity. Zinc can be a danger to unborn and newborn children (Johnson et al., 2011). When their mothers have absorbed large concentrations of zinc the children may be exposed to it through blood or milk of their mothers (Heng et al., 2010). The world's zinc production is still rising. This basically means that more and more zinc ends up in the environment. Water is polluted with zinc, due to the presence of large quantities of zinc in the wastewater of industrial plants. This wastewater is not purified satisfactorily. One of the consequences is that rivers are depositing zinc-polluted sludge on their banks. Zinc may also increase the acidity of waters. Some fish can accumulate zinc in their bodies, when they live in zinc-contaminated waterways (Wu et al., 2013). When zinc enters the bodies of these fish it is able to bio magnify up the food chain (Tate Jr et al., 1999).

**Table 2.1** The maximum contaminant level (MCL) standards for the most hazardous heavy metals (**WHO:** adapted from Babel and Kurniawan, 2003)

| SL | Heavy metal | MCL (mg/l) | Toxicities |
|---|---|---|---|
| 1. | Cu(II) | 0.25 | Liver damage, Wilson disease, insomnia |
| 2. | Pb(II) | 0.006 | Damage the fetal brain, diseases of the kidneys, circulatory system, and nervous system |
| 3. | Zn(II) | 0.80 | Depression, lethargy, neurological signs and increased thirst |
| 4. | Cd(II) | 0.01 | Kidney damage, renal disorder, human carcinogen |

Zinc is an essential element, with a human daily requirement of 10 to 20 mg (Lester et al., 1986). Zinc tends to be less toxic than other heavy metals. However, some symptoms of zinc toxicity are vomiting, dehydration, electrolyte imbalance, stomach pain, nausea, lethargy, dizziness, and muscular incardination. Last, the role of zinc as a carcinogen or carcinogen is unclear (Lester et al., 1986).

### 2.2.6 Heavy metal pollution scenario

Heavy metal pollution is a problem in developed countries which are associated with areas of intensive industries. Nowadays, roadways and automobiles are the largest sources of heavy metals. Zinc, copper, and lead are three of the most common heavy

metals released from road travel among the 90 total metals from road runoff. Lead concentrations have been decreasing since using leaded gasoline was discouraged. Small amounts of many other metals like nickel and cadmium are also found in road runoff and exhaust. Automobiles are adding about half of the zinc and copper contribution to the environment from urbanization. Tire wears releases zinc while brakes release copper (Li et al., 2014; ul Islam et al., 2007). Motor oil is also another pathway by which metals enter the environment.

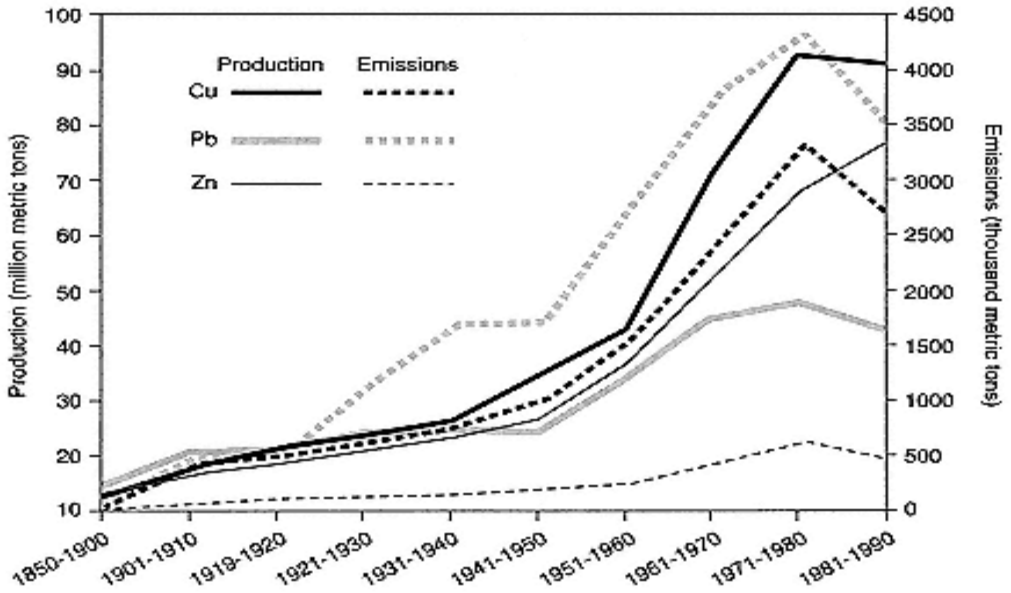


**Figure 2.2** Global scenario of heavy metal pollution from the ancient time (adapted from Nriagu, 1996)

The common metals in road runoff are lead, zinc, iron, copper, cadmium, chromium, nickel and aluminum. Among the metals, lead is coming to water runoff from leaded gasoline, tire wear, lubricating oil and grease and bearing wear. Zinc is being added to surface water from tire wear, motor oil, grease, brake emissions and corrosion of galvanized parts. Bearing wear, engine parts and brake emissions are major source of copper addition in surface water. The toxic cadmium may enter surface water and groundwater from the tire wear, fuel burning and batteries (Hsu et al., 2006).

Heavy metals from automobiles become bound to the surfaces of road dust or particulates. The bound metals will either become dissolved or be swept off the roadway with the dust by runoff and the metals will enter into soil and surface water. These metals can be transported by several processes from soil and aquatic environments.

These processes are governed by the chemical nature of metals, soil and sediment particles, and the pH of the surrounding environment (Nriagu, 1990; Nriagu, 1996).

Most heavy metals are cations, meaning they carry a positive charge. Zinc and copper, for instance, both carry a $2^+$ charge. Soil particles and loose dust also carry charges. Most clay minerals have a net negative charge. Soil organic matter tends to have a variety of charged sites on their surfaces, some positive and some negative. The negative charges of these various soil particles tend to attract and bind the metal cations and prevent them from becoming soluble and dissolved in water. The soluble form of metals is thought to be more dangerous because it is easily transported and more readily available to plants and animals. By contrast, soil bound metals tend to stay in place (Goldberg et al., 1977; Järup, 2003).

Metal behavior in the aquatic (streams, lakes and rivers) environment is surprisingly similar to that outside a water body. Streambed sediments exhibit the same binding characteristics found in the normal soil environment. As a result, many heavy metals tend to be sequestered at the bottom of water bodies. Some of these metals will dissolve. The aquatic environment is more susceptible to the harmful effects of heavy metal pollution because aquatic organisms are in close and prolonged contact with the soluble metals. pH tends to be a master variable in this whole process. pH is a measure of the concentration of hydrogen ($H^+$) ions dissolved in water. $H^+$ is the ion that causes acidity; however, it is also a cation. As a cation it is attracted to the negative charges of the soil and sediment particles. In acid conditions, there are enough $H^+$ ions in the water to occupy many of the negatively charged surfaces of clay and organic matter. Little room is left to bind metals, and as a result, more metals remain in the soluble phase (Nriagu, 1990).

#### 2.2.6.1 Heavy metal pollution in Australia

Australia has been actively involved in research on causes, effects and remediation of pollution created by heavy metals. This country is also suffering from serious heavy metal pollution like other countries in world. The major associated sources are mining activities and the metal processing industry. On the other hand there have also been examples of localized pollution by electroplating wastes, metal-based pigments and a number of other industrial wastes which cause localised heavy metals pollution. After taking several steps by Government departments, a considerable set of results has been

obtained in the study of heavy metals. Most of the steps were limited simply to the measurement of concentrations in waters, sediments and biota, leaving considerable gaps in the understanding of the processes influencing the behaviour of heavy metals in the environment and of their effects on Australian biota.

**Table 2.2** Heavy metal contents of representative gold mine tailings in Australia (Caspers, 1981)

| Heavy metals | Total contents(mg/kg) | Threshold levels(mg/kg) |
|---|---|---|
| Arsenic | 1,120 | 20 |
| Chromium | 55 | 50 |
| Copper | 156 | 60 |
| Manganese | 2,000 | 500 |
| Lead | 353 | 300 |
| Strontium | 335 | NA |
| Zinc | 283 | 200 |

*NA not available.

Natural processes, such as weathering and volcanic activity, also are continually adding heavy metals to the Australian environment (Caspers, 1981; Caspers, 1985; Salomons and Förstner, 1984). In addition, human activities are adding a significant amount of heavy metals to the environment especially the aquatic environment. The amounts of heavy metals contribution in the global environment from anthropogenic sources have exceeded those from natural resources. This is particularly so in the case of lead, copper and zinc. A proportion of heavy metals have stopped mobilization by buildings and rubbish dumps. Regardless of this, the amount eventually discharged into the atmosphere or the aquatic environment can be large. Heavy metals sources are point and non-point sources. Point sources are those in which the pollution can be easily identified as coming from a particular factory or treatment works. Non-point sources are more diffuse; examples would include heavy metals in rainfall, urban runoff and agricultural runoff. Most of the Australian examples where heavy metals pollution occurred have been localized and created from one-point sources. Little has been done in Australia to assess the importance of anthropogenic emissions of heavy metals to the atmosphere and a data suggest that anthropogenic sources exceed natural sources in the case of cadmium and lead addition.

**Table 2.3** Australian heavy metals found in different water bodies (Caspers, 1981)

| System | Name of the water body | Location in Australia | Metals found |
|---|---|---|---|
| Streams | Yarra river | Victoria | Cd, Cu, Pb, Zn |
| | Magela creek | Northern Territory | Cd,Cu,Zn |
| | South creek | NSW | Cd,Cu,Pb,Zn |
| Lakes | East Basin Lake | Victoria | Cd, Cu, Pb, Zn |
| | Lake Tarli Karng | Victoria | Cd, Cu, Pb, Zn |
| | Tarago reservoir | Victoria | Cd,Cu,Pb,Zn |
| | Albert Park Lake | Victoria | Cd |
| | Woronora reservoir | NSW | Cd,Cu,Pb,Zn |
| | Magela Creek billabongs | Northern Territory | Cu |
| Estuaries | Derwent estuary | Tasmania | Zn |
| | Yarra estuary | Victoria | Cd,Cu,Pb,Zn |
| | Georges R. estuary | NSW | Cd, Cu, Pb, Cr |
| | Corio bay | Victoria | Cd, Cu, Zn |
| Coastal waters | Bass Strait | Victoria | Cd,Cu,Zn |
| | South Eastern Australia | | Cd,Cu,Pb,Zn |
| | Northwest shelf | | Cd, Cu, Zn, Ni |

The Australian Academy of Science (Stark, 1998) has provided information that lead is the only significant atmospheric heavy metal emission in Australia and estimated that 7000 to 8000 tonnes of lead are emitted annually to the Australian atmosphere, with motor cars contributing over 5000 tonnes annually. A remarkable work has also been done on lead pollution from the largest lead smelter at Port Pirie, South Australia and it has found that atmospheric emission was the largest source of lead to the environment in Australia (Ward and Young, 2002). Large quantities of heavy metals can be added to the atmosphere by wind-blown dust and it is severe in Tasmania due to fine contaminated dust from a zinc producing company. It was a significant source of zinc to the Derwent estuary and residential areas of Hobart around Risdon (Bloom and Ayling, 1977).

A detail of heavy metals found in different water bodies in Australia is presented in Table 2.3. Mining activities and ore processing systems have resulted in serious heavy metal pollution in a number of areas in Australia such as the King River in Tasmania (Cu, Zn, Pb and Cd); South Esk River, Tasmania (Zn and Cd); Derwent River estuary, Tasmania (Zn, Cd and Hg); Captains Flat and Molongolo River in New South Wales

(Zn, Cu, Cd, Pb and As); Rum Jungle and Finniss River in the Northern Territory (Cu and Zn)(Bloom and Ayling, 1977; Stark, 1998).

Also there are a very huge number of probable industrial sources of heavy metals in Australia, most of the industries in different States discharge effluents to a stream or the sewer under state's license. As a result of the pollution there are two major implications to be noticed. First, significantly more attention is paid to the adequate treatment of wastes and to in-plant management. Second, researching toxic compounds containing heavy metals from the many uses has led to the result that some compounds have been totally banned (e.g. phenyl-mercury compounds used as slimicides in the paper industry), and others have been strictly restricted in use. Sludges and sewage effluents from industries and treatment plants are also indicated a potentially huge source of adding heavy metals to the environment. The major proportion of the sewage and sludge disposal in Australia is to estuarine and coastal marine waters (Stark, 1998). A recent study of urban storm-water quality in major catchments of Australia has shown in Table 2.3.

## 2.3 Technologies for removal of heavy metals from wastewater

Heavy metal removal has become a burning issue in the industrialized as well as in the developing world where industrial use and discharging of heavy metal is gradually increasing. The adverse and toxic effect of heavy metal on aquatic life and the environment is well established. Humans are not free from this pollution because the toxic metals are entering into the human body through the complex and diverse food chain (Liu et al., 2007). In these circumstances sustainable heavy metals removal is a serious research concern among researchers and technologists (Al-Rub, 2006). The commonly used methods for removing metal ions from aqueous streams include physical, chemical and biological methods used separately or inclusively based on need. The available methods are chemical precipitation, lime coagulation, ion exchange, reverse osmosis and solvent extraction (Areco et al., 2012). The process description of each method is presented below (Table 2.4).

**Table 2.4** Comparison of the effectiveness of removal of heavy metals using various techniques

| Method | Metal | Initial conc. (mmol/l) | Maximum removal (%) | Operating parameters | References |
|---|---|---|---|---|---|
| Adsorption by activated carbon | Cu(II)<br>Zn(II)<br>Cr(VI) | 0.580<br>0.410<br>0.180 | 99.93<br>80.00<br>72.00 | Types of modifying agents, initial concentration of modifying agents | (Monser and Adhoum, 2002) |
| Adsorption by natural zeolite | Co(II)<br>Cu(II)<br>Zn(II)<br>Mn(II) | 1.700-6.800<br>1.600-6.400<br>1.500-6.000<br>1.800-7.200 | 77.96<br>66.10<br>45.96<br>19.84 | Initial metal concentration | (Erdem et al., 2004) |
| Biosurfactant | Cu(II)<br>Cd(II)<br>Pb(II) | 20.000<br>10.000<br>80.000 | 81.13<br>71.17<br>89.95 | Initial solution pH, collector to heavy metals ratio, and the ionic strength (NaCl) | (Yuan et al., 2008) |
| Chelation in supercritical fluid | Cu(II) | 1.600-16.000 | 63.00 | Initial metal concentration, temperature, pressure, and chelating agent concentration | (Murphy et al., 2009) |
| High gradient magnetic separation | Cd(II)<br>Cu(II)<br>Ni(II)<br>Zn(II) | n.a<br>n.a<br>n.a<br>n.a | 99.90 | Initial solution pH, concentration of ferric Ion (Fe3+), and magnetic field strength | (Anand et al., 1985) |
| Ion exchange | Cu(II)<br>Ni(II) | 4.730-18.900 | n.a<br>n.a | Initial pH value, metal concentrations, and volumetric flow rate | (Lin et al., 2008) |
| Ultrafiltration | Cd(II)<br>Cu(II)<br>Co(II)<br>Zn(II) | 1.000 | Higher than 95% for single metal, and removal decrease with the presence of other metals | Anionic surfactant initial concentration and the effect of the presence other metals | (Kim et al., 2008) |

n.a: not available.

Based upon the metal binding capacities of various biological materials, biosorption can separate heavy metals from wastewater (Vilar et al., 2007). Lately, biosorption has emerged as a cost-effective and efficient alternative for application to low strength wastewaters (Pavasant et al., 2006). Biosorption is a term used here to describe the removal of heavy metals using a passive binding process with nonliving microorganisms including bacteria, fungi, and yeasts (Parvathi and Nagendran, 2007), and other biomass types that are capable of efficiently collecting heavy metals. Obviously, some of the advantages biosorption has over conventional treatment methods include low cost, high efficiency for dilute concentration solutions, an aminimal amount of chemical and/or biological sludge, no additional nutrients required

and the possibility of biosorbent regeneration and metal recovery (Vilar et al., 2007a). The sorption of heavy metals onto these biomaterials is attributed to their constituents, which are mainly proteins, carbohydrates and phenolic compounds, since they contain functional groups such as carboxylates, hydroxyls and amines, which are able to attach to the metal ions (Choi and Yun, 2006).

### 2.3.1 Physical methods and processes

Physical and chemical processes are processes which include the processes of chemical precipitation, coagulation-flocculation, oxidation, ion exchange, adsorption and membrane processes. Heavy metals are widely used in industrial activities and are often found in industrial and municipal waste streams. A number of heavy metal ions, such as Cd, Hg, and Pb have been reported to have toxic and/or carcinogenic effects on human health (Pamukoglu and Kargi, 2007). Thus, heavy metal removal is an important concern in landfill leachate treatment. As previously discussed, biological leachate treatment cannot effectively treat and remove all organic and inorganic compounds, particularly heavy metal ions. Many physical-chemical treatment processes can be very costly, because large quantities of chemicals are required. As such, the use of low-cost natural adsorbents would be beneficial for the removal of heavy metals from landfill leachate (Pamukoglu and Kargi, 2006).

A wide range of physical and chemical processes is available for the removal of Cr (VI) from wastewater, such as electro-chemical precipitation, ultrafiltration, ion exchange and reverse osmosis (Sekar et al., 2004; Yurlova et al., 2002). A major drawback with precipitation is sludge production. Ion exchange is considered a better alternative technique for such a purpose. However, it is not economically appealing because of high operational cost. Adsorption using commercial activated carbon (CAC) can remove heavy metals from wastewater, such as Cd (Turgut, 2003); Cu (Monser and Adhoum, 2002). However, CAC remains an expensive material for heavy metal removal.

#### 2.3.1.1 Evaporators

Evaporators are chief and easy methods which are used to concentrate and recover valuable plating chemicals and metals (Gregory, 1993). Evaporation is the use of an energy source to vaporize a liquid form from a solution, slurry, or sludge. In electroplating, non-volatile metal salts are concentrated in the evaporating water and can

be reused. Recovery is accomplished by boiling sufficient water from the collected rinse stream to allow the concentrate to be returned to the plating bath. Many of the evaporators in use also permit the recovery of the condensed steam for recycle as rinse water. Four types of evaporators are used throughout the elctroplating industry (Baek et al., 2005; USEPA, 1979) (i) Rising film evaporators; (ii) Flash evaporators using waste heat; (iii) submerged tube evaporators; (iv) Atmospheric evaporators. Both capital and operational costs for evaporative recovery systems are high. Chemical and water reuse values must offset these costs for evaporative recovery to become economically feasible (USEPA, 1987). Evaporation is an easy, maintenance-free, reliable and commonly applicable process (Peters et al., 1985). The main disadvantages are high-energy consumption and undesirable constituents in the recycled bath.

#### 2.3.1.2 Precipitation

Precipitation is the most common method for removing toxic heavy metals up to parts per million (ppm) levels from water. Since some metal salts are insoluble in water are precipitated when the correct anion is added. Although the process is cost effective its efficiency is affected by low pH and the presence of other salts (ions). The process requires addition of other chemicals, which finally leads to the generation of a high water content sludge, the disposal of which is cost intensive (Gray and Schrefler, 2001). Precipitation with lime, bi-sulphide or ion exchange lacks specificity and is ineffective in removal of the metal ions at low concentration (Charerntanyarak, 1999; USEPA, 1990a).

Precipitation is a chemical process in which soluble chemicals are removed from solution by the addition of a reagent with which they react to form a (solid) precipitate. This precipitate can then be removed by standard flocculation, sedimentation, and/or filtration processes (Cushnie, 1985; Kurniawan et al., 2006). Most heavy metals can be precipitated from water as hydroxides with the addition of a caustic (e.g., sodium hydroxide or lime). Alternatively, sodium sulphide or ferric sulphide may be added to precipitate metals as sulphides. The sulphide process is effective for certain metals, such as mercury, which do not precipitate as hydroxides. Precipitation processes produce a sludge that may have to be managed as hazardous waste due to the presence of concentrated heavy metals. Disposal costs for these sludge may therefore be significant. Lime and caustic soda are common sources of hydroxide ($OH^-$) ions. $OH^-$ ions combine

with ions of some metals to form insoluble metal hydroxides (precipitation) (Abrego, 1997; Srivastava and Majumder, 2008). Precipitated metals settle out and thus are removed from the water; adsorption, using activated carbon, improves this separation process. Iron is one of many metals which is commonly removed in this way.

#### 2.3.1.3 Cementation

Cementation is another type of precipitation method using an electrochemical mechanism in which a metal having a higher oxidation potential passes into solution e.g. oxidation of metallic iron, Fe(0) to Fe(II) to replace a metal having a lower oxidation potential. Copper is most frequently separated by cementation along with noble metals such as Ag, Au and Pb as well as As, Cd, Ga, Pb, Sb and Sn which can be recovered in this manner (Case, 1974; Dean et al., 1972). In this method a metal is displaced from solution by a metal higher in the electromotive series. It offers an attractive possibility for treating any wastewater containing reducible metallic ions. In practice, a considerable spread in the electromotive force between metals is necessary to ensure adequate cementation capability. Due to its low cost and ready availability, scrap iron is the metal used often. Cementation is especially suitable for small wastewater flow because a long contact time is required. Some common examples of cementation in wastewater treatment include the precipitation of copper from printed etching solutions and the reduction of Cr (VI) in chromium plating and chromate-inhibited cooling water discharges (Brown et al., 2000; Case, 1974). Removal and recovery of lead ions by cementation on an iron sphere packed bed has been reported (Angelidis et al., 1989; Kadirvelu and Namasivayam, 2000).

#### 2.3.1.4 Ion-exchange

In this process, metal ions from dilute solutions are exchanged with ions held by electrostatic forces on the exchange resin. Ion exchange processes involve the displacement of a given ion from an insoluble exchange material by other ionic species in solution (Dean et al., 1972; Kurniawan et al., 2006). The most common use of this process is in domestic water softening. Prior to ion exchange, the leachate needs to be clarified by coagulation /flocculation/precipitation to remove suspended solids and non-aqueous liquids. Ion exchange is generally not recommended for any leachate containing over 2500 mg/l of dissolved solids (Dabrowski et al., 2004; Gold et al., 1987). The disadvantages include high cost and partial removal of certain ions. It

is a method used successfully in the industry for the removal of heavy metals from effluents. Though it is relatively expensive as compared to the other methods, it has the ability to achieve ppb levels of clean up while handling a relatively large volume. An ion exchanger is a solid capable of exchanging either cations or anions from the surrounding materials. Commonly used matrices for ion exchange are synthetic organic ion exchange resins. The disadvantage of this method is that it cannot handle concentrated metal solution as the matrix gets easily fouled by organics and other solids in the wastewater. Moreover ion exchange is non-selective and is highly sensitive to pH of the solution (Brower et al., 1997; Dabrowski et al., 2004).

A major drawback with precipitation is sludge production. Ion exchange is considered a better alternative technique for such a purpose. However, it is not economically appealing because of high operational cost. Adsorption using commercial activated carbon (CAC) can remove heavy metals from wastewater, such as Cd (Caeiro et al., 2005); Cu (Monser and Adhoum, 2002). However, CAC remains an expensive material for heavy metal removal. It requires pre-treatment process to reduce suspended solid concentration in solution to prevent fouling or channelling. However, apart from their cost, which can be prohibitive especially to smaller processing plants, resins are vulnerable to oxidation by chemicals, are affected by the presence of magnesium or calcium ions in solution, and are prone to fouling by precipitates and organics (Kaewsarn, 2002; Monser and Adhoum, 2002; Tiravanti et al., 1997).

#### 2.3.1.5 Membrane process

The use of membrane technology for valuable metal removal is gaining considerable attention in many industries. Ultrafiltration can be used to remove water from wastewater containing emulsified oil, and exclude the metal particles. However, ultrafiltration membranes need to be cleaned and back-flushed regularly to operate efficiently and replaced periodically (Alvarez‐Vazquez et al., 2004; Harland, 1994; Robinson et al., 2004). Reverse osmosis (RO) may be applied in plating processes removing sodium chloride. RO system requires high-quality feed for efficient operation, thus wastewater must be treated to remove solids prior to RO treatment. Application of membrane technology to metal-bearing waste streams has several major drawbacks. Apart from the expense, membranes are also unable to resist certain types of chemicals and pH values and are prone to deterioration in the presence of microorganisms.

Membrane fouling, compaction, scaling, limited life of membranes, dissolution of the membrane by oxidized agents, solvents and other organic compounds, and applicability only to feed streams with low concentrations of metal ions are major limitations associated with the use of membrane technologies (Kitagawa et al., 1977; Ramalho, 1977).

Membrane processes usually consist of microfiltration, ultrafiltration, nanofiltration and reverse osmosis. The basis of these processes is that higher molecular weight organics cannot pass through when pressured wastewater is forced through the membrane (Belfort, 1984). Reverse osmosis systems are the most widely used membrane process for leachate treatment (Radjenović et al., 2008). The drawback of membrane processes is that the membranes are susceptible to fouling due to the formation of biological slimes. Their construction and operation are very costly compared to traditional biological treatment processes (Radjenović et al., 2008).

#### 2.3.1.6 Reverse osmosis

It is a process in which heavy metals are separated by a semi-permeable membrane at a pressure greater than osmotic pressure caused by the dissolved solids in wastewater (Cruver and Nusbaum, 1974; Sourirajan, 1970; Van Hoof et al., 1999). The disadvantage of this method is that it is expensive. Reverse osmosis and electro-dialysis involves the use of semi-permeable membranes for the recovery of metal ions from dilute wastewater. In electro-dialysis, selective membranes (alternation of cation and anion membranes) are fitted between the electrodes in electrolytic cells, and under continuous electrical current the associated ion migrates, allowing the recovery of metals (Fritzmann et al., 2007).

#### 2.3.1.7 Electrodialysis

Electrolytic metal recovery is one of a number of technologies capable of removing metals from wastewater. In this process, the ionic components (heavy metals) are separated through the use of semi-permeable ion selective membranes (Marder et al., 2004; Strathmann, 1992). Application of an electrical potential between the two electrodes causes a migration of cations and anions towards respective electrodes. Because of the alternate spacing of cation and anion permeable membranes, cells of concentrated and dilute salts are formed. The disadvantage is the formation of metal hydroxides, which clog the membrane. Electrolytic industrial processes for metals

include the production of metals themselves from their compounds, which is called the electrowinning of metals; the electrolytic purification of metals; and the deposition or electroplating of metals on conducting surfaces (Mohammadi et al., 2005; Mohammadi et al., 2004). In all three types of electrolytic process, the reactions are reduction of ions of the metal in solution in some carefully selected electrolyte. This process is a highly energydependent and labor-intensive process. Electrodialysis is a process that efficiently maintains a low metal ion concentration in the anodizing bath solution by transporting metal ions from the bath solution through a selective membrane into a capture media using an electrical current to induce flow (Chao and Liang, 2008). In the electrodialysis process, ionic components of a solution are separated through the use of semipermeable ion-selective membranes (Sadrzadeh et al., 2007). However, this process involves moderately high capital cost, increases in the number of possible exposures with regard to the handling of hazardous waste, and must be able to locate a company that will recover and reclaim metals from the sludge (Jakobsen et al., 2004).

#### 2.3.1.8 Ultrafiltration

Ultrafiltration is a pressure-driven technique for separating dissolved molecules/metals in solution on the basis of size which means that molecules larger than the membrane pore size rating will be retained at the surface of the membrane (Cañizares et al., 2002; Saifuddin M and Kumaran, 2005). They are pressure driven membrane operations that use porous membranes for the removal of heavy metals. The accumulation of retained molecules may form a concentrated gel layer. The impact of gel-layer formation is that it can significantly alter the performance characteristics of the membrane (Chaufer and Deratani, 1988). This is commonly called concentration polarization. The main disadvantage of this process is the generation of sludge.

#### 2.3.1.9 Flocculation and coagulation

The coagulation-flocculation processes facilitate the removal of suspended solids, colloidal particles. It is used in the final stage of solids-liquids separation. Coagulation is the destabilization of colloidal particles brought about by the addition of a chemical reagent called a coagulant. Flocculation is the agglomeration of destabilized particles into microfloc and after into bulky floccules that can be settled called floc (Charerntanyarak, 1999; Golob et al., 2005). The addition of another reagent called a flocculant or a flocculant aid may promote the formation of the floc. Flocculation is the slow stirring or gentle agitation to aggregate the destabilized particles and form a rapid

settling floc. This technique has been known to be capable of removing heavy metals from solution. The EPA investigated the use of lime softening and coagulation (using ferric sulfate or alum) for removal of heavy metals as $Pb^{2+}$, $Cd^{2+}$, $Cr^{3+}$, $Cr^{6+}$, etc (Amuda and Amoo, 2007; USEPA, 1979).

#### 2.3.1.10 Flotation

Flotation is considered a well-established unit operation in the field of mineral and environmental technology. It also has been practiced for the separation of biological materials, such as algae from drinking water sources, mainly due to their small size and density (Rubio et al., 2002). Flotation, following metal biosorption, was proved to be a useful and effective separation method of metal-loaded biomass, producing efficient removals, usually over 95% (Mavrov et al., 2003). The main critical parameters are solution pH and ionic strength. The different techniques, such as foam or bubble fractionation, foam separation or froth flotation, were examined for the separation of metal-loaded baker's yeast *Saccharomyces cerevisiae* (Zouboulis et al., 2001).

### 2.3.2 Chemical methods and processes

#### 2.3.2.1 Chemical precipitation

Precipitation of metals is achieved by the addition of coagulants such as alum, lime, iron salts and other organic polymers. The large amount of sludge containing toxic compounds produced during the process is the main disadvantage (Kurniawan et al., 2006). The most commonly used inorganic chemicals in chemical precipitation include aluminium chloride, calcium hydroxide (lime) and ferric chloride (Tchobanoglous and Burton, 2003). The most widely used process for removal of heavy metals from solution is chemical precipitation. The conventional process of heavy metal removal from industrial wastewater involves chemical precipitation of metals usually by lime, followed by settling of the metal precipitates in a pond and/or a clarifier. The most commonly used precipitation technique is hydroxide treatment due to its relative simplicity, low cost of precipitant, and ease of automatic pH control. Hydroxide precipitates tend to resolubilize if the solution pH is changed, but the removal of mixed metal wastes may not be effective because the minimum solubilities for different metals occur at different pH condition (Charerntanyarak, 1999). Carbonate precipitation and sulphide precipitation has also been used for the treatment of metal containing waste water. Generally, precipitation has been widely used for its simplicity, but has two drawbacks: it usually results in a net increase in the total dissolved solids of

the wastewater being treated, and a large amount of sludge requiring treatment, which, in turn, may contain toxic compounds that may be difficult to treat (Matlock et al., 2002).

#### 2.3.2.2 Hydroxide precipitation

Heavy metals can be precipitated in the form of their hydroxides using lime or sodium hydroxide and it is widely used (Khraisheh et al., 2004). Due to low cost and ease of controlling pH, lime is used for precipitation purposes. The unused lime also serves as an adsorbent for the removal of metal ions. The efficiency of removal of metals depends on the factors of pH, ease of hydrolysis of the metal ion, nature of the oxidation state, presence of complex forming ions, standing time, degree of agitation and settling and filtering and characteristics of the precipitate (Chen, 2004; Kinniburgh et al., 1976). The restrictions of this method are the optimum pH for hydroxide formation may lead to problems in the treatment of effluents containing multi metal ions. The metal hydroxide solubility at a fixed pH is a drawback of the hydroxide precipitation (Namasivayam and Ranganathan, 1995a).

#### 2.3.2.3 Carbonate precipitation

Carbonate precipitation of metals is done by calcium or sodium carbonate. The use of this method is very limited. Some literature reported an enhanced result for Cd (II) and Pb (II) removal from electroplating effluents using carbonate precipitation (Lake et al., 1984; Patterson et al., 1977). Some metals (lead, cadmium, nickel) form insoluble carbonates that can be used in carbonate precipitation. Some wastewaters already contain enough carbonates to allow precipitation to occur. Alternatively, inorganic carbonates (e.g., $Na_2CO_3$) can be added. Carbonate precipitation takes place only if carbonate ions ($CO_3^{-2}$) are present. Free carbonate ions are present only if the pH is high. A caustic is often added to raise the pH. High pH's also promote the precipitation of the metals as hydroxides. Hence, carbonate precipitation is often a co-precipitation (Armenante, 2012).

#### 2.3.2.4 Sulphide precipitation:

Normally most of the heavy metals form stable sulphides. This property can be used as an excellent method of metal removal called sulphide precipation. Sulphide precipitation is most useful when used as a refining step after conventional hydroxide precipitation or when very higher removals are required for multi-metals system

(Kaksonen et al., 2003). Metal sulfides are typically very insoluble. Therefore metals can be precipitated by adding sulfide ions ($S^{-2}$). Metal sulfides have much lower solubilities than the corresponding metal hydroxides, thus allowing lower residual metal concentrations in the treated wastewater (Armenante, 2012; Kaksonen et al., 2003).

#### 2.3.2.5 Chemical reduction

Chemical reduction/oxidation (Redox) reactions are the chemical processes which convert hazardous contaminants to nonhazardous or less toxic compounds. It makes the compounds more stable, less mobile and inert. Electrons transfer from one compound to another this is the key process for this method and consequently one reactant is oxidized (loses electrons) and one is reduced (gains electrons) (Kurniawan et al., 2006). The most commonly used oxidizing agents for treatment of hazardous contaminants are ozone, hydrogen peroxide, hypochlorites, chlorine, and chlorine dioxide (Fu and Wang, 2011). The factors that may limit the applicability and effectiveness of the process include incomplete oxidation or formation of intermediate contaminants, the process is not cost-effective for high contaminant concentrations and oil and grease in the media need prior removal to optimize process efficiency (Monser and Adhoum, 2002). It is a full-scale, well-established technology used for disinfection of drinking water and wastewater. Previously it was a common treatment method for cyanide (oxidation) and chromium (reduction of Cr (VI) to Cr (III) prior to precipitation) wastes. Nowadays an enhanced system is being used more frequently to treat hazardous wastes in soils (Igwe and Abia, 2006; USEPA, 1990b).

#### 2.3.2.6 Xanthate process

The biosorbents which contains sulfur-bearing groups have a high affinity to heavy metals compared to lighter metals examples of sulfur-bearing groups are sulfides, thiols, dithiocarbamates, dithiophosphates and xanthates. Xanthates are most widely used because they are cheap and easy to prepare and are highly insoluble (Bailey et al., 1999; Flynn et al., 1980). The xanthates are prepared with reaction between an organic hydroxyl-containing substrate and carbon disulfide. Heavy metal removal by xanthate takes place by an ion exchange reaction which is much similar to hydroxide precipitation. There has been an examination of solidification of both cellulose and starch xanthate sludges (Bricka and Hill, 1989). Xanthated sawdust was used for adsorption of Cd, Mn, Co, Ni, Ag, Zn, Hg and Pb (Flynn et al., 1980). The adsorption

capacity for Cd was 0.28 ± 0.38 meq/g (15.7±21.4 mg Cd/g) but the adsorption capacity ranged from 0.3 to 0.4 meq/g for Zn, Pb, Mn, Co, Ni, Ag and Hg. The particle size and porosity of the xanthate are the controlling parameters for adsorption of metals (Fu and Wang, 2011). The removal capacity of xanthate also decreased with time due to de-composition and air oxidation of sulfur-containing species. It is also quite selective for heavy metals and high concentrations of light metals decrease the heavy metal capacity significantly.

#### 2.3.2.7 Solvent extraction

Solvent extraction (SX) is an emerging technology for metals recovery purposes. It includes the process of separation, purification and recovery techniques. Normally uranium, copper, nickel, cobalt and rare earths are extracted from solutions or ores. This method uses an organic solution containing a special reagent (extractant) to transport selected metals from one aqueous solution to another, so that metals are separated, purified and recovered (Dean et al., 1972; Yun et al., 1993).

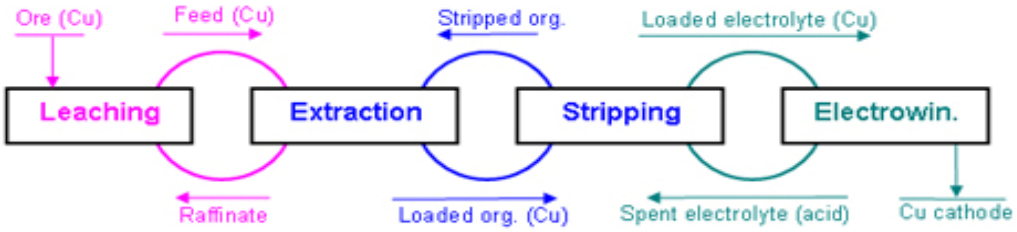


**Figure 2.3** A schematic showing a typical solvent extraction process for copper.

There are normally four steps for this method. Initially the intended metal ore is made soluble in aqueous solution (Leaching). This solution is mixed with a selected organic solution and it extracts the targeted metals. This step is called extraction. Later the extracted metal is stripped by using an acid solution (stripping). Lastly the metal is deposited onto a cathode and pure metals are obtained. This step is known is electrowin (Bang Mo, 1984). The following flow diagram will show the steps of copper recovery and removal processes (Fig.2.2).

#### 2.3.2.8 Electrodeposition

Electrodeposition is the process of deposition of one metal upon another metal. Normally it is used in electroplating industries. Electroplating is achieved by passing an electrical current through a solution containing dissolved metal ions and the metal objects to be plated (Sciban et al., 3007). Contaminated wastewaters produce from

metals processing industries contain different metals. These metals can be removed from wastewater by using the electrodeposition technology. This is also a metal recovery process from wastewater (Ajmal et al., 2000; Algarra et al., 2005).

### 2.3.3 Biological methods

In the late 20$^{th}$ century to meet the challenge of heavy metal removal from water and wastewater in aspect of toxicity to man and the environment different technologies have evolved. Apart from the conventional removal processes, biological techniques have been developed. Phytoremediation and bio-filtration using bacteria have recently been identified as two main biological treatment techniques for removing heavy metals from contaminated water in an eco-friendly way (Murugesan et al., 2009; Singh et al., 2009).

Heavy metals are removed from sewage by biological processes along with physical and chemical treatment processes. This process includes sedimentation with suspended solids and activated sludge flocs, co-precipitation by organic compounds and chemical precipitation. Heavy metals removal from wastewater depends on applied technology, type and concentration, oxidation state of metals, composition and pH of wastewater, type of microorganisms and mechanism of metal removal (Al-Rub, 2006; Zou et al., 2006). Living microorganisms can bind heavy metals actively in intracellular accumulation, extracellular precipitation and chemical transformations catalyzed by these microorganisms, such as oxidation, reduction, methylation, demethylation. Passively the heavy metals can be bound by extracellular complexation of metal, by substances excreted by cells and biosorption, binding of heavy metals to active groups of chemical compounds of cell walls and membranes (Macaskie et al., 1996; Tobin et al., 1990).

#### 2.3.3.1 Phytoremediation

Phytoremediation is an emerging technology in heavy metals removal from water and wastewater. It uses plants and their associated rhizospheric microorganisms to remove various heavy metals from contaminated soils, sludge, sediment, groundwater, and surface water through contaminant removal, degradation, stabilization, or containment of the contaminant (Padmavathiamma and Li, 2009). It uses living plants for in situ and ex situ remediation of contaminated sites. Phytoremediation not only removes heavy metals but also remediate various contaminants, including pesticides, solvents, explosives, petroleum hydrocarbons, polycyclic aromatic hydrocarbons, and landfill

leachate. It is also applicable to point and nonpoint source hazardous waste control (Padmavathiamma and Li, 2009). Phytoremediation is the best applicable method for taking contamination of organic, nutrient, or metal pollutants. It is an emerging technology and can be used because of its cost effectiveness, aesthetic advantages, and longterm applicability (Jabeen et al., 2009). Initially, hyper-accumulator plants are of prime intererest for researcher for metals removal because they are capable of accumulating potentially toxic metals in their body at a significant level (Chehregani et al., 2009). These plants have strong ability to sequester metals and have greater internal requirements for specific metals. Some species have mobilizing ability of metals from less soluble soil fractions in comparison with non hyperaccumulating species. For examples a species of Thlaspi (*Brassicaceae*) can accumulate more than 3% Zn, 0.5% Pb, and 0.1% Cd in their shoots (Manousaki and Kalogerakis, 2009). The mechnisms involved for phytoremediation are phytotransformation, rhizosphere, bioremediation, phytostabilization, phytoextraction and rhizofiltration (Karami and Shamsuddin, 2010).

#### 2.3.3.2 Microremediation

Water bodies are full of different bacteria and waste matter. Heavy metals present in the waste matter can cause hazardous and toxicity to aquatic organisms (Volesky and Holan, 1995c). Heavy metals which cause toxicity are lead, cadmium, chromium, zinc, mercury, uranium, selenium, arsenic, silver, gold, and nickel (Ahalya et al., 2006). Toxicity originated from heavy metal pollution in the aquatic system has become a serious threat to the environment because it is non-biodegradable and persistent. Metals can be mobilized from one trophic level to an other and enter the food chain as a consequence of leaching from waste dumps, polluted soils and water. In time the metals concentration increases in all level of the food chain and transfer to the higher levels of the food chain, phenomenon known as bio-magnification (Alluri et al., 2007a).

Microremediation is one of the forms of biosorption. The so-called biosorption can be defined as the non-directed physicochemical interaction between metal species and microbial cells (McHale and McHale, 1994). It is a natural and biological method for environmental control. It is used as an alternative to conventional contaminated water treatment facilities by the different water treatment organisation from all over the world. This method has several advantages over conventional treatment methods like low

costs, highly efficient, low sludge production, no requirement of additional nutrients, and regeneration of biosorbent with possibility of metal recovery.

The biosorption process includes two phases like a solid phase (sorbent or biosorbent; usually a biological material) and a liquid phase (solvent, normally water) containing a dissolved species to be sorbed (sorbate, a metal ion). Different mechanisms are involved for attraction and binding of metal on sorbent (Romera et al., 2008). The process continues until equilibrium is attained. Mechanisms involved in biosorption can be classified as cell metabolism which is metabolism dependent and non- metabolism dependent which is extra cellular accumulation/precipitation, cell surface sorption/precipitation and intra cellular accumulation. The adsorbed ions are transported across the membrane in a similar mechanism as metabolically important ions such as potassium, magnesium, and sodium. These mechanisms encompass (i) physical adsorption e.g., electrostatic interaction has been demonstrated to be responsible for copper biosorption by bacterium *Zooglea ramigera* and alga *Chorella vulgaris* (Aksu and Gonen, 2006), (ii) ion exchange e.g., biosorption of copper by fungi *Ganoderma lucidium* and *Asperigillus niger* (Muraleedharan et al., 1991*)*, (iii) complexation e.g., biosorption of copper by *C. vulgaris* and *Z. ramigera* takes place through both adsorption and formation of co-ordinate bonds between metals and amino or carboxyl groups of cell walls (Aksu and Balibek, 2007). Different biosorption mechanisms mentioned above can take place simultaneously.

The sources of biomass are a considerable factor while choosing the biomass for metal biosorption. Biomass can come from different sources like activated sludge or fermentation waste from industries like those of food, dairy and starch. In addition, different organisms like bacteria, yeast, fungi and algae etc coming from their natural habitats are good sources of biomass. Fast growing organisms like crab shells, seaweeds, prawn shells etc can be used as biosorbents (Volesky, 2007). Distant from the microbial sources even agricultural products such as wool, rice, straw, coconut husks, peat moss, exhausted coffee (Dakiky et al., 2002), waste tea (Ahluwalia and Goyal, 2005), walnut skin, coconut fibre, cork biomass (Chubar et al., 2003), seeds of *Ocimumbasilicum* (Melo and D'Souza, 2004), defatted rice bran, rice hulls, soybean hulls and cotton seed hulls (Khan et al., 2004), wheat bran, hardwood (*Dalbergia sissoo*) sawdust, pea pod, cotton and mustard seed cakes, (Saeed et al., 2009) have also

proven to be good biomass sources. However, sea weeds, molds, yeasts, bacteria have been tested for metal biosorption with encouraging results (Vieira and Volesky, 2010).

#### 2.3.3.3 Heavy metals biosorption by microorganisms

A huge number of microorganism groups such as bacteria, fungi, yeasts, cyanobacteria and algae etc have been reported in literature for adsorption of heavy metals. The function of various microorganisms for removal and recovery of heavy metals has been well reviewed and documented (Ahalya et al., 2003; Zouboulis et al., 2004). Most of the studies reported in literatures have been carried out with living microorganisms for metals sorption. Heavy metal removal and recovery is not reasonable for all metals and situation using living microorganisms due to certain inherent disadvantages. For instance, industrial effluents which contain toxic metals and medium is acidic and these conditions are destructive for growth and maintenance of an active microbial population. There are several advantages for non-living biomass over microbial biomass as a biosorbent and they are as follows:

- Nonliving biomass is growth independent and not subject to toxicity limitation of living cells.
- Industrial wastes can be used as biomass like wastes from the fermentation industry which will be a cheap source of biomass.
- The physiological condition is not governed for adsorption like microbial cells.
- Nonliving biomass acts as an ion exchanger and the adsorption process is very rapid. The metal uptake is efficient even with a high loading of metals.
- Non-living biomass are not limited to those conducive for the growth of cells. Hence, a wider range of operating conditions such as pH, temperature and metal concentrations can be used for biosorption.
- Metals can be desorbed readily from biomass and then recovered. If the value and the amount of metal recovered are insignificant and if the biomass is plentiful, the metal loaded biomass can be incinerated, eliminating further treatment.

Biosorption takes place through the processes of ionic, chemical and physical adsorption. A variety of ligands located on the fungal cell walls like carboxyl, amine, hydroxyl, phosphate and sulphydryl group atc are involved for metal adsorption. Metal ions could be adsorbed by complexing with negatively charged reactions sites on the

cell surface. Different micro-organisms and fungal biomass produce a high percentage of cell wall material, which shows outstanding metals adsorption properties (Clements et al., 2010; Vieira and Volesky, 2010). Numerous fungi and yeast species have shown an excellent metal biosorption, particularly the genera *Rhizopus*, *Aspergillus*, *Streptoverticullum* and *Sacchromyces* (Gadd, 2004; Kosolapov et al., 2004).

Precipitation of oxide or sulphide of metals is the most common method for removing toxic heavy metals from water. Since some metal salts are insoluble in water, microorganism could react and get precipitated. Microorganisms can remove a number of metals and metalloids from the environment or waste streams by reducing them to a lower redox state (Lovley, 1995). Many of the organisms that catalyze such reactions use the metals or metalloids as terminal electron acceptors in anaerobic respiration. Such microorganisms, known as dissimilatory metal-reducing bacteria, are phylogenetically and physiologically (Lonergan et al., 1996) diverse (Lonergan et al., 1996); however, most share the ability to use Fe3+ and So as terminal electron acceptors (Lonergan et al., 1996). Several recently described Cr(VI) reducing bacteria have displayed desirable characteristics for in situ chromium remediation in that they are resistant to Cr(VI) toxicity and can reduce Cr(VI) aerobically (Campos et al., 1995). The microbial reduction of Cr(VI) to Cr(III) has been one of the most widely studied forms of metal bioremediation (Lovley, 1995; Wang and Shen, 1995). A wide diversity of heterotrophic organisms are known to carry out this reaction which, depending upon the organism, can take place an-aerobically or aerobically (Wang and Shen, 1995). A cyano-bacterium capable of Cr(VI) reduction has also been described (Garnham and Green, 1995). In common with Geobacter species, one such organism, Pyrobaculum islandicum, also reduced toxic metals including U(VI), Tc(VII), Cr(VI) and Co(III). Possible roles in the formation of uranium deposits and magnetite in hydrothermal environments were highlighted.

The way microbes interact with metals depends in part on whether the organisms are prokaryotic or eukaryotic (Ehrlich, 1997). Both types of microbes have the ability to bind metal ions present in the external environment at the cell surface or to transport them into the cell for various intracellular functions. On the other hand, only the prokaryotes (*eubacteria* and *archaea*) include organisms that are able to oxidize Mn(II),

Fe(II), Co(II), Cu(I), $AsO^{2-}$, Se° and $SeO_3^{2-}$ or reduce Mn(IV), Fe(III), Co(III), $AsO_4^{2-}$, $SeO_4^{2-}$ and $SeO_3^{2-}$, on a large scale and conserve energy in these reactions. Some microbes may reduce metal ions such as $Hg^{2+}$ or $Ag^{+}$ to Hg° and Ag°, respectively, but do not conserve energy from these reactions (Ehrlich, 1997; Summers and Sugarman, 1974). Some prokaryotes and eukaryotes may form metabolic products-such as acids or ligands-that dissolve base metals contained in minerals like Fe, Cu, Zn, Ni, Co, and others. Others may form anions that precipitate dissolved metal ions. Some prokaryotes may methylate a number of metal and metalloid compounds, producing corresponding volatile metal derivatives (Ehrlich, 1997; Summers and Sugarman, 1974).

## 2.4 Biosorption and biosorbents

### 2.4.1 Introduction

Sorption is a process in which a substance is taken into and retained in another substance. Sorption encompasses both absorption and adsorption processes, while desorption is the reverse process. Absorption is a physical or chemical phenomenon. Absorption is a condition in which something takes in another substance. There are two phenomena in the absorption process which are not related. The first phenomenon is when atoms, molecules, or ions enter into some bulk phase-gas, liquid or solid material. For instance, a sponge absorbs water when it is dry. The second phenomenon refers to the process by which the energy of a photon is taken up by another entity, for example, by an atom whose valence electrons make transition between two electronic energy levels.

Adsorption has been defined in several ways. Adsorption concerns itself with the concentration, as a result of surface forces existing on a solid, of gases, vapors, liquids or solutes (i.e. solids dissolved in a solvent, dispersed materials and colloids) (Areco et al., 2012). Adsorption is a surface phenomenon in which molecules or atoms of one phase are accumulated on the other phase. The material getting adsorbed is known as the adsorbate and the material on which adsorbate is adsorbed is known as the adsorbent. Generally the adsorbent is a solid material and is porous. Sometimes confusion arises between adsorption and absorption. The adsorption as described earlier is the accumulation of adsorbate on the surface of the adsorbent and it may be with or without chemical reaction. On the other hand in absorption adsorbate molecules penetrate the adsorbent structure thus producing a solid solution. Hence a general term

'sorption' may be used when a gas, vapor or liquid is taken up by a solid (Areco et al., 2012). Today adsorption has found a significant place in physical, chemical and biological sciences. Various kinds of adsorption processes are detailed elsewhere (Amankwah and Yen, 2003; Munagapati et al., 2010).

On the other hand, adsorption is a member of the family of the removal/separation techniques like stripping and extraction, but it is not a filtration technique (Bayramoglu et al., 2003). Adsorption is similar to filtration, but refers to a surface rather than a volume: adsorption is a process that occurs when a gas or liquid solute accumulates on the surface of a solid or, more rarely, a liquid (adsorbent), forming a molecular or atomic film (the adsorbate). It is different from absorption, in which a substance diffuses into a liquid or solid to form a solution (Volesky and Holan, 1995c).

Adsorption may be defined as the sticking/adhesion of atoms, ions, biomolecules or molecules of gas, liquid, or dissolved solids to a surface of adsorbent. A film of the adsorbate (the molecules or atoms being accumulated) is created on the surface of the adsorbent by the adsorption process (Wang and Chen, 2006b). The adsorption process is different from absorption. In the absorption process a fluid permeates to a liquid or is dissolved by solid. The term sorption includes both adsorption and absorption processes. Desorption is the reverse of adsorption. It is a surface phenomenon (Das et al., 2008).

### 2.4.2 Biosorbents

A material having the capacity or tendency to adsorb other substances or materials is known as an adsorbent. Biosorbents are materials from a biological origin which can adsorb some things especially pollutants. This biological origin product is of prime interest for the environmental scientist for environment friendly cleansing. Adsorption, ion exchange, and chromatography are sorption processes in which certain adsorbates are selectively transferred from one phase to an other phase. Strong biosorbents behaviour of certain micro-organisms towards metallic ions is a function of the chemical make-up of the microbial cells. This type of biosorbents consists of dead and metabolically inactive cells (Friis and Myers-Keith, 1986).

Some types of biosorbents would be broad range, binding and collecting the majority of heavy metals with no specific activity, while others are specific for certain metals. Some

laboratories have used easily available biomass whereas others have isolated specific strains of microorganisms and some have also processed the existing raw biomass to a certain degree to improve their biosorption properties.

Recent biosorption experiments have focused attention on waste materials, which are by-products or waste materials from large-scale industrial operations. For example the waste mycelia available from fermentation processes, olive mill solid residues (Pagnanelli et al., 2002), activated sludge from sewage treatment plants (Zouboulis et al., 1997), biosolids (Norton et al., 2004), aquatic macrophytes (Keskinkan et al., 2004).

Another inexpensive source of biomass where it is available in copious quantities is in oceans as seaweeds, representing many different types of marine macro-algae. However most of the contributions studying the uptake of toxic metals by live marine and to a lesser extent freshwater algae focused on the toxicological aspects, metal accumulation, and pollution indicators by live, metabolically active biomass. Focus on the technological aspects of metal removal by non-living algal biomass has been rare.

Although abundant natural materials of cellulosic nature have been suggested as biosorbents, very little work has been actually done in that respect. The mechanism of biosorption is complex, mainly ion exchange, chelation, adsorption by physical forces, entrapment in inter and intra-fibrillar capillaries and spaces of the structural polysaccharide network as a result of the concentration gradient and diffusion through cell walls and membranes (Argun et al., 2005; Bayramoglu and Arica, 2008; Kara, 2009; Lucaci and Duta, 2009; Ozer et al., 2004).

There are several chemical groups that would attract and sequester the metals in biomass: acetamido groups of chitin, structural polysaccharides of fungi, amino and phosphate groups in nucleic acids, amido, amino, sulphhydryl and carboxyl groups in proteins, hydroxyls in polysaccharide and mainly carboxyls and sulphates in polysaccharides of marine algae that belong to the divisions Phaeophyta, Rhodophyta and Chlorophyta (Caramalau et al., 2009; Chu et al., 2004; Jeon and Park, 2005; Ren et al., 2008; Solener et al., 2008). However, it does not necessarily mean that the presence of some functional group guarantees biosorption, perhaps due to steric, conformational or other barriers.

### 2.4.3 Importance of biosorbents in water treatment

The search for new technologies involving the removal of toxic metals from wastewaters has directed attention to biosorption, based on metal binding capacities of various biological materials. Biosorption can be defined as the ability of biological materials to accumulate heavy metals from wastewater through metabolically mediated or physico-chemical pathways of uptake (Mahvi, 2008). Algae, bacteria and fungi and yeasts have proven to be potential metal biosorbents (Volesky and Holan, 1995c). The major advantages of biosorption over conventional treatment methods include (Plazinski and Rudzinski, 2010):

- Low cost;
- High efficiency;
- Minimisation of chemical and lor biological sludge;
- No additional nutrient requirement;
- Regeneration of biosorbents;
- Possibility of metal recovery.

The biosorption process involves a solid phase (sorbent or biosorbent; biological material) and a liquid phase (solvent, normally water) containing a dissolved species to be sorbed (sorbates, metal ions). Due to the higher affinity of the sorbent for the sorbates species, the latter is attracted and bound there by different mechanisms. The process continues until equilibrium is established between the amount of solid-bound sorbates species and its portion remaining in the solution (Igwe et al., 2008; Tarley and Arruda, 2004; Volesky, 1999b; Volesky and Holan, 1995b). The degree of sorbent affinity for the sorbates determines its distribution between the solid and liquid phases.

### 2.4.4 Advantages and disadvantages of biosorption

The technological, environmental and biological importance of adsorption can never be in doubt. Its practical applications in industry and environmental protection are of paramount importance. To use biosorbents for metal removal from water and wastewater has some profound advantages over other methods of metal removal. As, Hg and Pb, are examples of heavy metals which present in different types of industrial effluents responsible for environmental pollution. Their removal is traditionally made by chemical precipitation, ion-exchange and other methods. However, this is expensive

and it is not completely feasible to reduce their concentrations to the levels as low as required by the environmental legislation. Biosorption is a process in which solids of natural origin are employed for binding the heavy metal. It is a promising alternative method to treat industrial effluents, mainly because of its low cost and high metal binding capacity (Igwe et al., 2008).

Biosorption is a property of certain types of inactive, non-living microbial biomass to bind and concentrate heavy metals from even very dilute aqueous solution. Biomass exhibits this property, acting just as a chemical substance, as an ion exchanger of biological origin. It is particularly the cell wall structure of certain algae, fungi and bacteria, which was found responsible for this phenomenon (Volesky, 1999b). Until now, research in the area of biosorption suggests it an ideal alternative for decontamination of metal containing effluents. Advantages and disadvantages of biosorption by non-living biomass are as follows(Michalak and Chojnacka, 2010; Mosavi et al., 2010; Mouni et al., 2010; Muhamad et al., 2010; Munagapati et al., 2010; Nadeem et al., 2010):

#### 2.4.4.1 Advantages

- Growth-independent, non-living biomass is not subject to toxicity limitation of cells. No requirement of costly nutrients required for the growth of cells in feed solutions. Therefore, the problems of disposal of surplus nutrients or metabolic products are not present.
- Biomass can be procured from the existing fermentation industries, which is essentially a waste after fermentation.
- The process is not governed by the physiological constraint of living microbial cells.
- Because the non-living biomass behaves as an ion exchanger; the process is very rapid and takes place between few minutes to few an hours. Metal loading on biomass is often very high, leading to very efficient metal uptake.
- Because cells are non-living, processing conditions are not restricted to those conducive for the growth of cells. In other words, a wider range of operating conditions such as pH, temperature and metal concentration is possible. No aseptic conditions are required for this process.

- Metal can be desorbed readily and then recovered if the value and amount of metal recovered are significant and if the biomass is plentiful, metal-loaded biomass can be incinerated, thereby eliminating further treatment.

#### 2.4.4.2 Disadvantages

- Early saturation can be problem i.e. when metal interactive sites are occupied, metal desorption is necessary prior to further use, irrespective of the metal value.
- The potential for biological process improvement (e.g. through genetic engineering of cells) is limited because cells are not metabolizing. Because production of the adsorptive agent occurs during pre-growth, there is no biological control over the characteristics of the biosorbent. This will be particularly true if waste biomass from a fermentation unit is being utilized.
- There is no potential for biologically altering the metal valency state for example less soluble forms or even for degradation of organo-metallic complexes.

### 2.4.5 Characteristics of biosorbents

There are several key characteristics which controls the adsorption ability of adsorbents. The characteristics are the physiochemical characteristics of adsorbents materials. Specific surface area, pore volume, ash content, particle sizes, pH, charge/polarity and surface functional groups are properties of adsorbents.

#### 2.4.5.1 Specific surface area

The solid adsorbents are often characterised by their specific surface area ($a_s$) and pore size distribution ($A_S$). The value of $A_s$ refers to unit mass (m) of adsorbent (Tóth 1981):

$$a_s = \frac{A_s}{m} \qquad (2.1)$$

The pore size distribution provides information on the size and amount of pores present in the solid adsorbent: Macropores are pores with widths exceeding about 50 nm. Mesopores are pores with widths between 2 nm and 50 nm. Micropores are pores with not exceeding about 2 nm (Tóth, 2000).

A large specific surface area is preferable for providing large adsorption capacity, but the creation of a large internal surface area in a limited volume inevitably gives rise to large numbers of small sized pores between adsorption surfaces. The size of the micropores determines the accessibility of adsorbate molecules to the internal adsorption surface, so the pore size of the micropores is another important property for

characterizing adsorptivity of adsorbents. In particular materials such as zeolite and carbon molecular sieves can be specificially engineered with precise pore size distributions and hence tuned for a particular separation (Marczewski, 2007).

The average thickness of the adsorbate is often expressed with the names mono and multilayer adsorption. In monolayer adsorption, all the adsorbed molecules are in contact with the surface of the adsorbent. In multilayer adsorption, the adsorption space accommodates more than one layer of molecules so that not all adsorbed molecules are in direct contact with the molecules of the adsorbent (Tóth 2000).

Coverage is a measure of the extent of adsorption of a species onto a surface, usually denoted by the lower case Greek "theta", θ. Exposure is a measure of the amount of gas which as surface has seen; more specifically, it is the product of the pressure and time of exposure (normal unit is the Langmuir, where 1 L = $10^{-6}$ Torrs) (Gereli et al., 2006).

**2.4.5.2 Pore volume**

The pore volume and its distribution in the adsorbents are the important properties of adsorbents. Pore Volume Distributions can be determined by either gas adsorption porosimetry (typically N2, Ar or CO2) or mercury intrusion porosimetry. Gas porosimetry measures pores from 3.5°A to about 4000°A in diameter. Mercury porosimetry is applicable to pores from 30°A up to 900μm in diameter. The pores remain in the adsorbent either as micropores or mesopores. The pore size ranged from 200 to 800°A are defined as micropores and from 20 to 90°A are defined as mesopores. The physical characteristics, i.e., micropore area and pore volume distribution, may have a greater effect on the adsorption capacity of adsorbents than the surface oxygenated functional groups (Dias and do Carmo, 2006; Diaz et al., 2005).

**2.4.5.3 Ash content**

Ash content also is an important property of an adsorbent. Activated carbon is made from pitch and coal, yielding almost pure carbon, which leaves only a small amount of ash in the fibres. The ash content is different for different minerals and derivatives and it has significanant impact on adsorption (Jianqiu et al., 2010; Zhong et al., 2012).

**2.4.5.4 Particle sizes**

Surface area of a particle is a function of the particle's size. Increase in particle size decreases metal adsorption while increase in pore size increases the metal adsorption.

This may be due to availability of more surface area for adsorption in case of small size particles (Kumar et al., 2010). The removal efficiency and sorption capacity increases with the decrease of the particle size. This indicates that the smaller the sorbent particle size, then for a given mass, more surface area is made available and therefore the number of sites increases (Ho et al., 2002b). The rate constant (k) of kinetic adsorption by the clay adsorbent decreased with increasing particle size (Tsai et al., 2003). The solid phase diffusion coefficient estimated from batch reactor analysis, is found to be invariant with particle diameter (Kahraman et al., 2008).

#### 2.4.5.5 pH

The value of the pH necessary to affect a net zero charge on a solid surface in the absence of specific sorption is called the point of zero charge (pHPZC). Adsorption capacities of adsorbents are strongly dependent on initial solution pH. Initial solution pH affects the magnitude of negative charge on adsorbents surface and the adsorption capacities (Abate and Masini, 2005; Abdel-Ghani and Elchaghaby, 2007; Ho et al., 1994). The adsorption capacity of an adsorbent increases with increases in solution pH. Low adsorption capacities observed for metal ions in an acidic medium may be due to hydrogen ions strongly competing with adsorbate for negatively charged sites on the adsorbent. As solution pH increases, the hydrogen ion concentration of the solution is reduced thereby reducing the competition for binding sites by hydrogen ions. It is also known that at specific pH range, functional groups such as carboxylic acids with pKa value around 3.5 (Abate and Masini, 2005; Abdel-Ghani and Elchaghaby, 2007) will be in the ionized form, increasing the magnitude of negative charge on the adsorbent's surface.

#### 2.4.5.6 Charge/polarity

Surface polarity corresponds to affinity with polar substances such as water or alcohols. Polar adsorbents are thus called “hydrophilic” and aluminosilicates such as zeolites, porous alumina, silica gel or silica-alumina are examples of adsorbents of this type. On the other hand, nonpolar adsorbents are generally “hydrophobic”. Carbonaceous adsorbents, polymer adsorbents and silicates are typical nonpolar adsorbents. These adsorbents have more affinity with oil or hydrocarbons than water (Ho et al., 2002d; Marczewski, 2007).

#### 2.4.5.7 Surface functional groups

There are several' functional groups in the adsorbents which are surface oxygenated groups or none oxygenated. Carbonyl, phenolic and lactone were the major surface oxygen functional groups for adsorbents of biological origin. The carbonyl group was also the major oxygen functional group of adsorbent (Arpa et al., 2000; Barriada et al., 2009; Ben Hamissa et al., 2010; Boota et al., 2009). Based on the oxygen surface functional groups, the surface of activated carbon fibres was less polar than that of activated carbon and of sludge adsorbent. Since adsorption is a surface phenomenon, the rate and extent of adsorption are functions of the specific surface area of the adsorbent used, i.e., the portion of the total surface area that is available for adsorption. In fact, the amount of adsorption per unit weight of fly ash depends on its composition, texture and porosity (Kara et al., 2007).

FTIR (Fourier transform infrared spectroscopy) technique was used to examine the surface groups of the adsorbent and to identify those groups responsible for adsorption. Adsorption in the IR region takes place because of rotational and vibrational movements of the molecular groups and chemical band of a molecule. The IR spectra of the samples were recorded on a spectrophotometer using a pellet (pressed-disk) technique (Boota et al., 2009).

### 2.4.6 Mechanism of metal biosorption

There are two phases involved in the biosorption processes. One is a solid phase (sorbent or biosorbents: biological material) and other is a liquid phase (solvent: normally water) which contain a dissolved species to be sorbed (sorbate: metal ions). The sorbate and sorbent is attracted and bound to each other by different mechanisms due to their higher affinity. This process continues until equilibrium is reached between the amount of solid bound sorbate species and its portion remaining in the solution. The degree of sorbent affinity for the sorbates determines its distribution between the solid and liquid phases. The following are the mechanisms which are involved in the adsorption process:

#### 2.4.6.1 Physisorption

Physisorption or physical sorption is a type of adsorption, in which the adsorption adheres to the surface only through weak intermolecular interactions (van der Waals)

(Ren et al., 2008; Sing et al., 1982). This process does not engage a significant modification in the electronic orbital patterns of the species involved. The synonym of physical adsorption is van der Waals adsorption, but its use is not recommended. It is characterised by low ambient temperature (always under the critical temperature of the adsorbate) and low enthalpy ($\Delta H<20$ kJ/mol). In physisorption, adsorption takes place in multilayer. The process requires low activation energy and the energy state of adsorbate is not altered. Physisorption is a reversible process (Chakravarty et al., 2010; Horsfall and Spiff, 2005a; Vieira et al., 2010b). The following are the characteristics of physisorption which helps to recognise the physisorption:

i. physisorption is a general phenomenon and happens in any solid/fluid system, even though certain specific molecular associations may take place, arising from particular geometrical or electronic properties of the adsorbent and/or adsorptive;
ii. a small change may be visible in the electronic states of adsorbent and adsorbate;
iii. the chemical nature of the liquid may not be changed by adsorption and subsequent desorption as the adsorbed species are chemically identical with those in the liquid phase;
iv. the changes in energy between the adsorbate and the adsorbent is same in magnitude, but it is greater than the energy of condensation of the adsorption;
v. activation energy is not a first step in physical adsorption during a gas phase adsorption. Slow, temperature dependent equilibration may be attained in rate-determining adsorption processes;
vi. in this process equilibrium is attained between the adsorbate and the fluid phase.
vii. ions/molecules from the gas phase may be adsorbed in excess of those in direct contact with the surface under appropriate conditions of pressure and temperature.

#### 2.4.6.2 Chemisorption

Chemisorption or chemical adsorption is the type of adsorption where same valence forces of the same charged materials form a chemical compounds. Chemisorption is a type of adsorption whereby a molecule adheres to a surface through the formation of a chemical bond, as opposed to the Van der Waals forces which cause physisorption. It is characterised by high temperatures and high enthalpy ($50$ KJ/mol $< \Delta H <$ 800 kJ/mol) (Volesky, 1999b). The strength of the interaction is stronger than pure physical

adsorption, and more likely there is a chemical (covalent) bond between adsorbate and surface. Bond strength of around 80 kJ/mol is often taken to be indicative of a true chemical interaction (Vieira et al., 2010b). In chemisorption, adsorption takes place only in a monolayer. The process has high activation energy and there is an increase in electron density in the adsorbent-adsorbate interface. Chemisorption is reversible only at high temperature. The following are the characteristics of chemisorption which helps to identify it:

i. chemical specificity is the characteristics phenomena of chemisorptions;
ii. electronic state of the compound will be changed during this process which may be measurable by suitable physical mean;
iii. the original species cannot be recovered by surface dissociation or reaction; it depends on chemical nature of compound; in this sense chemisorption may not be reversible;
iv. the energy changes in this process will be same in order of magnitude as exothermic or endothermic and changes may range from very small to very large;
v. activation energy is the prime step in chemisorptions process;
vi. in chemisorptions process a true equilibrium may be attained slowly or in practice not at all where the activation energy is large (activated adsorption);
vii. while the adsorbed ions are tied to the surface of adsorbent by valence bonds, adsorption sites are occupied by ions and only monolayer of adsorption is formed.

#### 2.4.6.3 Biosorption

Biosorption is a specific example of adsorption which has gained increasing attention over the last few years. The term 'biosorption' is now generally accepted as referring to passive or physico-chemical attachment of the sorbates to a biomass, thus excluding metabolic or active-uptake processes (Volesky, 1999a). Biosorption is essentially the binding of chemical species to biopolymers and the existence of this phenomenon has been reported for many different plant- and animal-derived materials (Simmons et al., 1995). It is defined as the removal of metal or metalloid species, compounds and particulates from water and wastewater by the materials originated from biological material (Volesky, 1999b). This ability of biological material to uptake metals from the surrounding environment is a widely recognized phenomenon that has a number of

important implications. Biosorption could be used in the area of wastewater treatment, especially since conventional physical and chemical means of removing soluble metal waste are generally expensive when the contaminant concentrations are in the range 10-100 ppm (Vieira and Volesky, 2010; Volesky and Holan, 1995a; Zouboulis et al., 2008). There appears to be a great potential in exploiting the intrinsic capability of abundant natural materials or agro-wastes or certain waste products from industrial operations as inexpensive biosorbents to "clean up" wastewaters. Recent studies on metals biosorption (Plazinski, 2012; Prakash Williams et al., 2012; Puyen et al., 2012; Ramakul et al., 2012; Remenárová et al., 2012; Rodrigues et al., 2012; Tunali Akar et al., 2012b; Zuo et al., 2012) have highlighted the advanced removals/recovery of metals which have demonstrated the potential use of biosorption by biomaterials from different types of solutions.

#### 2.4.6.4 Biosorption mechanism

It is stated that there are two types of binding that can occur in biological and biologically derived materials, depending on whether the biomass is living or dead (Drake and Rayson, 1996). Passive binding occurs in both living and nonliving cells and this involves very rapid, reversible, physical adsorption and/or ion exchange with cell surface (Lin and Rayson, 1998). A much slower, irreversible, metal uptake characterizes the active binding, typical of living cells, as a result of metabolic activity and this process is often termed bioaccumulation (Martinez-Garcia et al., 2006). Bioaccumulation includes “all processes responsible for the uptake of metal ions by living cells” and thus includes biosorption mechanisms, together with intracellular accumulation and bio-precipitation mechanisms (Eccles, 1995; Gupta and Keegan, 1998; Vinodhini and Narayanan, 2008). Therefore, the mechanism by which the biological material removes the metal ion from solution depends on whether it is living (metabolism dependent) or dead (non-metabolism dependent) (Ngah and Hanafiah, 2008). The complex mechanisms involved in the biosorption of metal ions in some cases are still not very well understood (Iqbal et al., 2009b; Pagnanelli et al., 2000; Plazinski and Rudzinski, 2010; Schiewer and Volesky, 2000; Tarley and Arruda, 2004). However, the metal-binding mechanisms postulated are as follows:

**(i)Transport across cell membrane**

The heavy metal’s ions can cross the microbial cell membranes along with the metabolically important ions such as potassium, magnesium and sodium. The toxic

metals' ions which are same charge and ionic radius associated with essential ions may confuse the bacterial metabolism system and it is not associated with metabolic activity (Stein, 1986). Fundamentally biosorption process by living microorganisms includes two distinct steps, which are first, a metabolism dependent intracellular uptake, whereby metal ions are transported across the cell membrane and second, metabolism independent binding where the metals are bound to the cell walls (Foulkes, 2000; Simkiss and Taylor, 1995).

**(ii)Physical adsorption**

Physical adsorption is the adsorption mediated by the help of van der Waals' forces. It is reported that copper, cadmium, zinc, uranium and cobalt sorption by dead cells/biomasses of algae, fungi and yeasts takes place through electrostatic interactions between the metal ions in solutions and cell walls of microbial cells (Kuyucak and Volesky, 1988; Rowsell and Yaghi, 2006; Vidali et al., 1991). Copper biosorption by bacterium *Zoogloea ramigera* and alga *Chiarella vulgaris* occurs with the interactions of electrostatic forces, and also for chromium biosorption by fungi *Ganoderma lucidum* and *Aspergillus niger* (Aksu and Kutsal, 1991).

**(iii)Ion exchange**

There have been some indications that ion exchange plays an important role in metal sorption by algal biomass (Kuyucak and Volesky, 1989). For marine algae, the active molecular entities involved are believed to be carboxyl and sulphate groups (Davis et al., 2003). Functional groups in marine algae like carboxyl groups of alginic acid and the carboxyl and sulfate groups of fucoidan are responsible for ions exchange. Polysaccharides which are contained in biosorbents cells can be exchanged with the bivalent metal ions (Treen-Sears et al., 1984). For example, $K^+$, $Na^+$, $Ca^{2+}$, and $Mg^{2+}$ from biosorbents can be exchanged with counter ions such as $Co^{2+}$, $Cu^{2+}$, $Cd^{2+}$ and $Zn^{2+}$ resulting in the biosorptive uptake of heavy metals (Kuyucak and Volesky, 1988; Schiewer and Volesky, 1995). Similarly copper biosorption by fungi *Ganoderma lucidium* (Muraleedharan and Venkobachar, 1990) and *Aspergillus niger* was by ion exchange (Brower et al., 1997).

**(iv)Complexation**

Complex formation is the key process for metal removal from a solution. In this removal process, complexes are formed between the active groups of cell surface and

metal ions (Treen-Sears et al., 1984). It is reported that biosorption of copper occurs through both adsorption and formation of coordination bonds between metals and amino and carboxyl groups of cell wall polysaccharides by C. *vulgaris* and Z. *ramigera* (Kapoor and Viraraghavan, 1995). Calcium, magnesium, cadmium, zinc, copper and mercury accumulation by *Pseudomonas syringae* occurs by the mechanism of complexation. Metallo-organic molecules are formed by the chelating of the toxic metal with the organic molecules. Microorganisms produce an organic acid (e.g., citric, oxalic, gluonic, fumaric, lactic and malic acids) which acts as a chelating agent (Han et al., 2006). The organic acid also helps in the solubilisation of metal compounds and leaching them from their surfaces. Metals may be biosorbed or complexed by carboxyl groups found in microbial polysaccharides and other polymers (Wang and Chen, 2006a).

**(v)Precipitation**

Precipitation may be occurred by the action of cellular metabolism or independently. In the case of cellular metabolism, the active defence system of the microorganisms produce compounds to resist the toxic metals which help the precipitation process and subsequently metal is removed (Chen et al., 2000; Schneider et al., 2001). In the case of precipitation not dependent on the cellular metabolism, the metal is removed as a consequence of the chemical interaction between the metal and the cell surface (Öztürk et al., 2004). All mechanisms can take place simultaneously.

The investigation of the metal removal efficiency by the microbial biomass is necessary for the industrial use of biosorption, as it gives information about the equilibrium of the process which is necessary for the design of the equipment.

The following factors affect the biosorption process:

- Temperature is an influential parameter for biosorption. The favourable temperature for biosorption is 20-35$^{o}$C (Kaewsarn, 2002).
- pH also is a most important parameter for biosorption: it affects the solubility of the metals, the activity of the functional groups in the biomass and the competition of metallic ions (Friis and Myers-Keith, 1986; Solisio et al., 2000).
- Biomass load in the system seems to influence the specific metal uptake; for lower biomass load there is an increase in the specific metal uptake (Fourest and Roux,

1992b; Gong et al., 2005). On the other hand an increase in biomass load leads to interference between the binding sites (Gadd, 2000).

- Shortage of metal concentration in an aqueous system may lead to a decrease in the uptake of metal (Fourest and Roux 1992). Therefore this factor should be considered in any application of microbial biomass as biosorbents.
- The presence of multi ions in a wastewater treatment system may affect the biosorption process; the removal of one metal ion may be influenced by the presence of other metal ions. For example: cobalt uptake by different microorganisms seemed to be completely inhibited by the presence of uranium, lead, mercury and copper (Ahalya et al., 2003).

**(vi) Binding sites for agro based biosorbents**

The removal of metal ions from aqueous streams using agricultural materials is based upon metal biosorption (Volesky and Holan, 1995b). The process of biosorption involves a solid phase (sorbent) and a liquid phase (solvent) containing a dissolved species to be sorbed. Due to high affinity of the sorbent for the metal ion species, the latter is attracted and bound by a rather complex process affected by several mechanisms involving chemisorption, complexation, adsorption on surface and pores, ion exchange, chelation, adsorption by physical forces, entrapment in inter and intra-fibrillar capillaries and spaces of the structural polysaccharides network as a result of the concentration gradient and diffusion through cell wall and membrane (Basso and Cukierman, 2008; Chojnacka et al., 2005; Muraleedharan and Venkobachar, 1994; Qaiser et al., 2007) (Figure 2:3).

Agricultural waste materials are usually composed of lignin and cellulose as the main constituents. Other components are hemicellulose, extractives, lipids, proteins, simple sugars, starches, water, hydrocarbons, ash and many more compounds that contain a variety of functional groups present in the binding process. Cellulose is a crystalline homo-polymer of glucose with $\beta_1 \rightarrow 4$ glycosidic linkage and intra-molecular and intermolecular hydrogen bonds (Demirbas, 2009; Demirbas, 2008; Demirbas, 2000). Hemicellulose is a heteropolymer of mainly xylose with $\beta_1 \rightarrow 4$ glycosidic linkage with other substances of acetyl feruoyl and glycouronyl groups (Garg et al., 2008; Garg et al., 2007). Lignin is a three dimensional polymer of aromatic compounds covalently linked with xylans in hardwoods and galactoglucomannans in softwoods (Alluri et al., 2007b;

Garg et al., 2007). The functional groups present in biomass molecules are acetamido groups, carbonyl, phenolic, structural polysaccharides, amido, amino, sulphydryl carboxyl groups, alcohols and esters (Beveridge and Murray, 1980; Gupta and Rastogi, 2008). These groups have the affinity for metal complexation. Some biosorbents are non-selective and bind to a wide range of heavy metals with no specific priority, whereas others are specific for certain types of metals depending upon their chemical composition. The presence of various functional groups and their complexation with heavy metals during the biosorption process has been reported by different research workers using spectroscopic techniques (Ahluwalia and Goyal, 2007; Alluri et al., 2007b; Dos Santos et al., 2010; Tarley and Arruda, 2004).

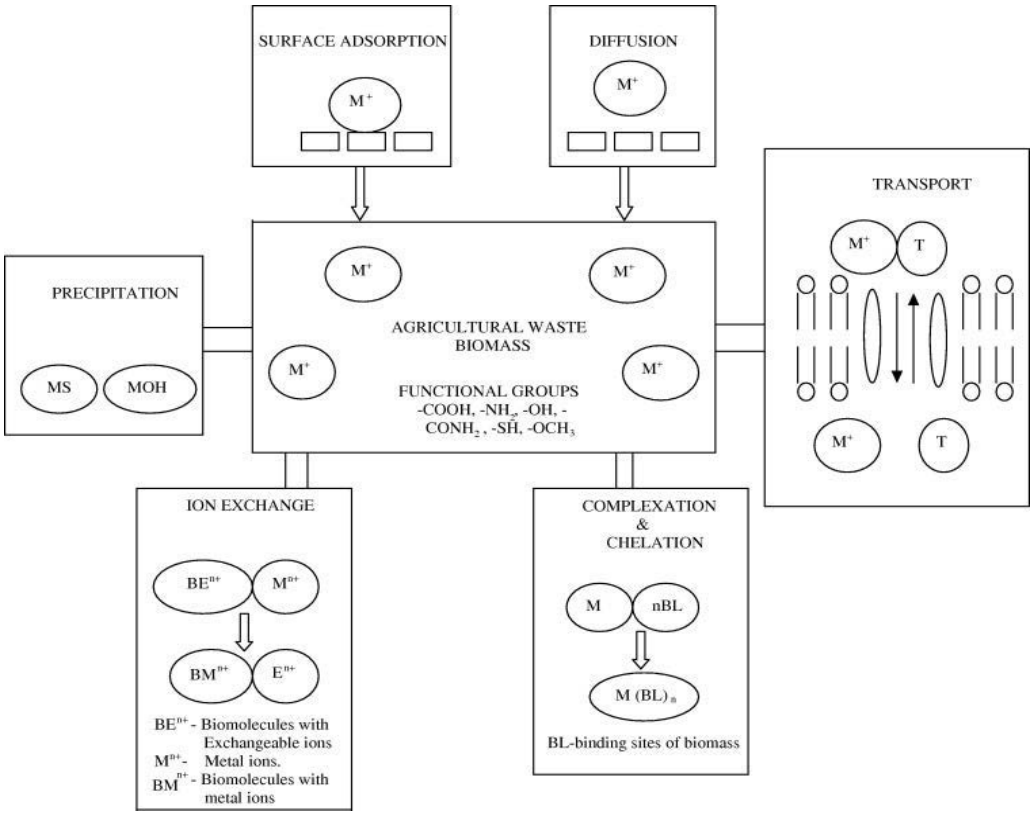


**Figure 2.4** Plausible mechanism of biosorption (adapted from Sud et al., 2008)

Biosorption has been associated with to different types of chemical groups such as hydroxyl, carbonyl, carboxyl, sulfhydrl, thioether, sulfonate, amine, imine, amide, imidazole, phosphonate, and phosphodiester groups present in the macromolecule in the cell wall of various microorganisms (Giguere et al., 1987; Gupta et al., 2001; Zeroual et al., 2003). The importance of any given group for biosorption of a certain metal by a certain biomass depends on factors such as: the number of sites in the biosorbent

materials, the accessibility of the sites, the chemical state of the sites, availability, and affinity between site and metal (Meneghetti et al., 2010; Vieira et al., 2010a; Vieira and Volesky, 2010). Freshwater algae contain carboxylate, sulfate, and amino groups that may be responsible for metal binding (Yu et al., 1999). The polysaccharides from green freshwater alga have the chelating ability of metals and their carboxyl groups would be negatively charged and could bind metal ions (Vieira and Volesky, 2010; Yu et al., 1999). Cell modifications of biosorbent pose both enhanced and decreased results for metal adsorption by amine and carboxyl groups (Ahluwalia and Goyal, 2007; Bailey et al., 1999).

### 2.4.7 Factors affecting biosorption

The adsorption process is a complicated phenomenon. It is obvious that the sorption performance is correlated to the number of binding sites, which is related to the chemical composition of the chosen biosorbent (Vieira and Volesky, 2010). However, the amount of metal that can be bound depends on several factors. Actually the efficiency or adsorption capacity depends on the following factors: (i) Nature of adsorbate (ii) Nature of adsorbent (iii) Specific area of the adsorbent (iv) pH (v) Pressure (vi) Temperature (vii) Activation of the adsorbent (viii) Enthalpy of adsorption (ix) contact time. The influence of these particular factors on the sorption mechanism will be described in the following section.

#### 2.4.7.1 Nature of adsorbate

The physiochemical natures of adsorbates have significant effects on both capacity and rate of the adsorption. Physical adsorption is non-specific in nature, so every metals is adsorbed on the surface of any solid to a lesser or greater extent (Çetinkaya Dönmez et al., 1999). However, easily ionized materials are adsorbed to a greater extent whereas low ionized materials are adsorbed to a lesser extent (Davis et al., 2003). pH is the controlling factor for ionization.

#### 2.4.7.2 Nature of biosorbent

Physisorption is a general phenomenon which does not depend on the nature of adsorbent (solid). Chemisorption is specific and depends on the nature of both adsorbent and adsorbate (Naiya et al., 2009). For example, nickel, platinum and iron readily adsorb hydrogen; silica gel adsorbs moisture and tungsten adsorbs oxygen. The common adsorbents are biosorbents, carbon, activated carbon, metal oxides, silica gel,

alumina and clay. Each adsorbent has its own characteristics and functional groups are the main metal binding factors.

#### 2.4.7.3 Specific area of the adsorbent

Specific area means the surface area available for adsorption of 1 gram of adsorbent. The amount of adsorption depends on the surface area of the solid. The more the surface area the more will be the biosorption (Vilar et al., 2007b). Hence, capacity of the porous or powder form of the adsorbent adsorbs more than the block of the same material, viz (Pierotti and Rouquerol, 1985). The iron powder adsorbs more than the iron block. The pores of a porous adsorbent must be so large that the molecules of the adsorbate ions can enter through them (Peigney et al., 2001).

#### 2.4.7.4 pH of water

pH is an influencing criteria for the adsorption process. The solubility of adsorbates like metals depend on pH. On the other hand the activation of binding sites also depends on pH. For instance, hydrogen and hydroxide ions are adsorbed quite strongly; the adsorption of other ions is influenced by the pH of the solution. In general, adsorption of a typical organic pollutant from water is increased with decreasing pH. Metal adsorption largely depends on the nature of the species solution i.e pH. At lower pH, $H^+$ competes with metals for the exchange sites in the system thereby partially releasing the latter. The heavy metals are completely released under circumstances of extreme acidic conditions (Annadurai et al., 2003). As it was anticipated, at lower pH, more protons are available, thereby decreasing electrostatic attraction between cationic adsorbate and positively charged sites of adsorbent. This case may be the reason for the decrease of adsorption below pH 7.5. When the pH value of the solution was increased, the surfaces of the adsorbent become negatively charged. In addition to this, the concentration of OH-ion also increased with the increase of pH and no exchangeable anions on the outer surface of the adsorbent will remain at higher pH values (Namasivayam et al., 2007; Ozcan et al., 2005; Yu et al., 2001).

#### 2.4.7.5 Pressure

The pressure is a deciding factor for the state of adsorbent and adsorbate. As the pressure increases in the adsorption system the temperature will increase and the activity of adsorption may increase (Kratochvil et al., 1995). The amount of metals adsorbed at a given temperature increases initially with increase in pressure and it is true

for both physisorption and chemisorption (Zu et al., 2006). The amount of metal adsorbed almost becomes constant at high pressure. In chemisorption, at high pressure the adsorbed layer is monolayer; in physisorption it is multilayer (Volesky, 1999a).

#### 2.4.7.6 Temperature

Temperature is such type of property of adsorption process which excites the metals and binding sites of adsorbents for being adsorbed (Özer and Özer, 2003). Physisorption is quite fast at low temperatures, whereas chemisorption occurs at high temperature. In general both types of adsorption decrease with increase temperature since the processes are exothermic (Gereli et al., 2006). Generally, sorption mechanisms are exothermic, that is to say the equilibrium constant decreases with increasing temperature. However, the binding of Cu and release of light metals were believed to be endothermic (Haug and Smidsrod, 1970). The positive entropy change was assumed to result from a larger ordering effect of $Cu^{2+}$ (than $Ca^{2+}$) upon the water in the hydration sphere. Overall, the temperature is believed to have a smaller effect on the biosorption than the other factors (Tsezos et al., 1995).

#### 2.4.7.7 Activation of the adsorbent

The adsorption process solely depends on the activation of the outer surface of adsorbents and adsorbate. Activation is done by using some activation agents in the adsorption process. Normally some acidic or alkaline solution or salt is used for activation. After adding activation agent the ionizing strength and pH of the system changes and either adsorbent or adsorbate or both become activated (Aksu, 2001). As a result of this the adsorption capacity become faster and increase adsorption capacity.

#### 2.4.7.8 Enthalpy of adsorption.

Temperature has a direct affect on the adsorption process. In the temperature aided adsorption process the thermodynamic parameters like enthalpy change (ΔH) and entropy change (ΔS) were obtained from the Van't Hoff equation.

$$\log K_c = \frac{\Delta S^o}{2.303R} - \frac{\Delta H^o}{2.303RT} \qquad (2.2)$$

where, ΔS◦ and ΔH◦ were calculated from the slope and intercept of linear plots of log *K*c vs. 1/*T*. Equilibrium constant (*K*c) was calculated from the following relationship (Namasivayam and Ranganathan, 1995b).

$$K_c = \frac{C_{Ae}}{C_e} \quad (2.3)$$

where, $C_{Ae}$ and $C_e$ are the equilibrium concentrations of metal (mg/l) on sorbent and in solution, respectively.

Free energy change *(*$\Delta G^\circ$*)* was calculated from the relation:

$$\Delta G^o = -RT \ln K_c \quad (2.4)$$

where, T(K) is the absolute temperature, *R* (J/K.mol) gas constant, $\Delta G^\circ$ is the standard free energy change.

The positive and negative values of $\Delta H^\circ$ for metals adsorption indicate that the process will be either endothermic or exothermic in nature respectively. Temperature might have an effect on the increasing adsorption capacity which happened due to change in the pore size and enhanced rate of intra-particle diffusion (Benhammou et al., 2005). The free energy change ($\Delta G^\circ$) of the process decreases with increase in temperature, which indicates that the process is spontaneous and spontaneity increases with increase in temperature. The positive value of entropy change ($\Delta S^\circ$) shows the increase in randomness at the solid/solution interface during the sorption of Cu(II) and Cd(II). Increased adsorption with temperature is due to an increase in the number of adsorption sites generated due to the breaking of some internal bonds near the edge of the active surface sites of adsorbent (Panday et al., 1986).

**2.4.7.9 Co-ions**

The presence of other ions (co-ions) can affect the sorption of metal ions (primary ion) to the biomass and it is called competitive adsorption (Mishra et al., 1998). In reality, wastewater is a mixture of different metals and competition among the co-ions are common. This interaction can be synergistic, antagonistic or non-interactive, and cannot be predicted on the basis of single metal studies (Ting and Teo, 1994; Tsezos et al., 1996). During biosorption on biosorbents, metal ions often compete with each other for surface binding sites (Kolodynska and Hubicki, 2008; Satiroglu et al., 1998). For example, mutual inhibition was observed during the sorption of $Cd^{2+}$, $Cu^{2+}$ and $Zn^{2+}$ on brown algae *Ascophyllum nodosum* (Leusch et al., 1995*)*, $Zn^{2+}$ being the weakest bound ion and $Cu^{2+}$ the most strongly bound ion (Chong and Volesky, 1995). Similarly, $Pb^{2+}$, $Cd^{2+}$ and $Cu^{2+}$ sorption on the fungus *Aspergillus niger* was found to be lower when the metal ions were present in a mixture than when they were present individually in the solution (Kapoor and Viraraghavan, 1997). In addition, another study showed the

influence of $Cd^{2+}$, $Cu^{2+}$, $Co^{2+}$ and $Ni^{2+}$ on Pb(II) and Zn(II) sorption by *Streptovercillium cinnamoneum* and *Penicillium chrysogenum* (Puranik and Paknikar, 1999). Mutual inhibition was observed in binary systems containing $Zn^{2+}$, whereas systems including lead displayed unequal inhibition. Furthermore recent studies have shown that light metals such as $Na^{+}$, $Ca^{2+}$, $Mg^{2+}$, and $K^{+}$ competed with heavy metals for ionic sorption sites and diminished heavy metal sorption (Matheickal and Yu, 1999; Saha et al., 2001). However the inhibition of the metal ion binding to microbial biomass by $Na^{+}$, and $K^{+}$ was shown to be lower than the uranium or radium binding inhibition by heavy metals such as $Zn^{2+}$, $Cu^{2+}$and $Fe^{2+}$(Tsezos and Georgousis, 1997). The binding strength to the biomass depends on metal chemistry (including parameters such as the charge, the ionic radius, the Pauling electronegativity), affinity for binding sites, and the type of metal binding (electrostatic or covalent) (Fourest and Roux, 1992b; Veglio and Beolchini, 1997).

#### 2.4.7.10 Initial metal concentration

The initial concentration of metal solution strongly influences the biosorption of metals ions (Fourest and Roux, 1992a). As long as the binding sites are not saturated, the higher the initial concentration of the metal ion, the larger the metal uptake (Reddad et al., 2002). However, it is apparent that increasing the amount of the available metal results in decreasing the fraction of metal bound (Blanco et al., 1999). The relationship between variable initial metal concentrations and metal uptake, at a fixed temperature and fixed biomass concentration is commonly represented by sorption isotherms (Astier et al., 2012; Çolak et al., 2011; Feng et al., 2011; Jiuzhou et al., 2012; Tunali Akar et al., 2012a).

#### 2.4.7.11 Biomass concentration

It is commonly reported in the literature that the amount of metal bound per biomass decreases as the biomass concentration increases. With metals biosorption at favourable pH, the increase of biomass concentration causes a diminution of the maximum specific metal uptake due probably to cell aggregation phenomena, whereas at acidic pH values the previous trend is inverted perhaps because of the effect of partial hydrolysis of the bacterial cell wall constituents. For instance, this trend has been observed for the biosorption of Ni, Cd and Zn on mycelial wastes of *Rhizopus arrhizus* (Fourest and Roux, 1992b), the biosorption of $Cu^{2+}$, $Fe^{2+}$, $Ni^{2+}$ and $Zn^{2+}$ on immobilized *Phormidium laminosum* (Blanco et al., 1999) biomass, the biosorption of $Cu^{2+}$, $Ni^{2+}$and $Cr^{6+}$on dried

algae (Aksu and Dönmez, 2003). Contributing factors that have been suggested for such biomass concentration dependency include electrostatic interactions between cells (de Rome and Gadd, 1987; Lodeiro et al., 2006), interference between binding sites, and reduced mixing (Akhtar et al., 2003; Gadd, 1988; Gadd, 2009) at high cell densities.

#### 2.4.7.12 Contact time

As reported in the literature, the metal sorption is often rapid, and usually complete in less than one hour. For metabolism independent uptake by algae, sorption is generally achieved in 5-10 minutes (Gadd, 1988). Binding of metal ions to aquatic particulates is considered to be a fast chemical reaction, with an equilibrium time depending only on the mass transfer resistance (Waite et al., 1994). To establish an appropriate contact time between the biosorbents and metallic ions solution, adsorption capacities of metal ion need to be measured as a function of time. Normally the removal is higher in the beginning and gradually drops with time. That is probably due to the larger surface area of the biosorbents being available at the beginning for the adsorption of metals. As the surface adsorption sites become exhausted, the uptake rate is controlled by the rate at which the adsorbate is transported from the exterior to the interior sites of the adsorbent particles (McKay, 1982; Yang et al., 2009).

### 2.4.8 Application of agro-wastes in removal of heavy metals from wastewater

There are several different options currently available for the removal of heavy metals from wastewaters. Regardless of the availability of numerous methods for the treatment of heavy metals from water and wastewater, adsorption is constantly viewed as a highly effective technique for this purpose, especially in low metal concentration solutions. Some recent research on removal of heavy metal by adsorption using naturally occurring and low cost adsorbents represented mainly by agricultural by-products and natural fibres is explained here. Agricultural by-products and natural fibres are mostly composed of lignin and cellulose, as well as other polar functional group-containing compounds, which include alcohols, aldehydes, ketones, carboxylates, phenols and ethers. These groups are able to bind heavy metals through replacement of hydrogen ions with metal ions in solution or by donation of an electron pair from these groups to form complexes with metal ions in solution (Ofomaja and Ho, 2007).

Biological materials/biomaterials include bacterial or fungi biomass, agricultural waste biomass and wood biomass. There are many reports in the literature on the use of bacteria and fungi biomass for the removal of a wide range of pollutants from contaminated water. The use of bacteria and fungi biomass for adsorption purposes is attractive and very promising judging from the relatively high adsorption capacities reported (Kahraman et al., 2005). However, the need for special media and attention in the culturing of these microbes adds to the total cost of the biosorbent, and it means that the adsorbent may not be readily available. Agricultural waste, wood and tree leaves biomass have attracted greater attention because of their wide availability, low cost and the fact that there is no need for special growth media like bacteria and fungi. The biomaterials are also known as 'Lignocellulosic' biomass that can be easily collected, harvested and used for biosorption purposes with simple modification. The following section below looks biomaterials application as a biosorbent for the removal of heavy metals from aqueous solution.

#### 2.4.8.1. Process design

The process of metal recovery using biosorbents is basically a solid-liquid contact process consisting of the metal uptake (sequestering) cycle and the metal desorption (elution) cycle. The metal-laden solution can contact the solid sorbent phase in many different types of process configurations such as upflow and downflow reactors, rotating biological contactors, trickle filters, fixed packed-bed contactor, and fluidized-bed contactor. Downflow contactors should theoretically be the most cost-effective process, since they do not require power other than from gravity to transfer water. However, in this type of process, the operator does not have a total control over the effluent retention times within the reactor. Another disadvantage of this system is the possible compaction of the bed with subsequent backflow of the waste stream. On the other hand, optimization of the contact process is possible by arranging the contact beds, columns or mixing vessels in series or parallel (Volesky, 1994).

#### 2.4.8.2. Regeneration of the biomass

The metal laden biosorbent can be incinerated and/or stored in landfill, reducing the volume of the initial heavy metal contaminated matrix (in comparison with wastewater). However, the active agent is preferably regenerated through a desorbing cycle using relatively inexpensive acid such as sulphuric acid (Tsezos, 2007; Tsezos, 2009). It is

also reported that some biosorbent like garden grass could be used for five cycles after desorption (Hossain et al., 2012). Thus, the purpose of desorption is not only to resolubilize biomass-bound metals in a more concentrated form, but also to recover metals if they are economically significant.

#### 2.4.8.3 Suitability of the biosorption technology for an industrial use

Compared to conventional heavy metals removal systems the main advantages of biosorption are:

- The process is rapid (most of the sorption described in the literature is achieved within one hour) (Ho and McKay, 1998a).
- The removal of metals is selective and efficient, even at low concentration. For instance, biosorbents and ion exchange resins (Duolite GT-73 and IRC-718) were compared for the removal of heavy metals from plating factory wastewater (Brower et al., 1997).
- The system can operate over a broad pH range (3 to 9), and temperature range (4 to 90 C°) (Vieira and Volesky, 2010; Volesky, 1994).
- The technology offers low capital investment and operation costs (using cheap raw biomass, and including waste products from other industries, such as fermentation or pharmaceutical by-product).
- The volume of chemical sludge to be disposed of is eliminated or minimized.
- The material has particle size, shape and mechanical strength suitable for use under continuous flow conditions (Ho et al., 2002b).
- The regeneration of the biosorbent is metal - selective and economically feasible (Ho and McKay, 1999).

#### 2.4.8.4 Recent uses for biomaterials for removal of heavy metals

Biosorption technology is in the developing stage. Scientists and researchers are exploring agro-based wastes as biosorbents to decontaminate water polluted with heavy metals. Here below are the accumulation of some biosorbents used for removal of Pb(II), Cu(II), Cd(II) and Zn(II) found in the literatures.

**Table 2.5** Pb(II) adsorption capacities (mg/g) by biosorbents recently reported in literature

| SL | Biosorbent | $q_m$ (mg/g) | References |
|---|---|---|---|
| 1. | Olive tree pruning | 12.286 | (Ronda et al., 2013a) |
| 2. | Almond shell | 26.546 | (Ronda et al., 2013b) |
| 3. | Dried cactus (*Opuntia ficus*) | 25.32 | (Barka et al., 2013) |
| 4. | Brown algae | 247.39 | (Moghaddam et al., 2013) |
| 5. | *Avena fatua* biomass | 211.344 | (Areco et al., 2013) |
| 6. | *Rivularia bulata* Algae | 34.30 | (Kizilkaya et al., 2013) |
| 7. | Alginate beads | 62.5 | (Subhashini et al., 2013) |
| 8. | Alga *Anabaena sphaerica* | 121.95 | (Abdel -Aty et al., 2013) |
| 9. | Chinese ephedra residue | 207.2 | (Feng and Zhang, 2013) |
| 10. | *Durvillaea antarctica* | 135.1 | (Hansen et al., 2013) |

**Table 2.6 Cu**(II) adsorption capacities (mg/g) by biosorbents recently reported in literature

| SL | Biosorbent | $q_m$ (mg/g) | References |
|---|---|---|---|
| 1. | Almond shell | 9.438 | (Ronda et al., 2013b) |
| 2. | Spirogyra sp. | 42.96 | (Guler and Sarioglu, 2013) |
| 3. | Wheat straw | 4.3 | (Gorgievski et al., 2013) |
| 4. | *Typha latifolia* root | 20.41 | (Rajaei et al., 2013) |
| 5. | *Avena fatua* biomass | 22.87 | (Areco et al., 2013) |
| 6. | *Eichhornia crassipes* | 27.7 | (Komy et al., 2013) |
| 7. | Coconut shell | 7.25 | (Acheampong et al., 2013) |
| 8. | *Ulva lactuca* | 54.01 | (Trinelli et al., 2013) |
| 9. | Soybean meal waste | 43.30 | (Witek et al., 2013) |
| 10. | *Rosa bourbonia* phyto-biomass | 7.22 | (Manzoor et al., 2013) |

**Table 2.7** Cd(II) adsorption capacities (mg/g) by biosorbents recently reported in literature

| SL | Biosorbent | $q_m$ (mg/g) | References |
|---|---|---|---|
| 1. | Dried cactus (*Opuntia ficus*) | 11.40 | (Barka et al., 2013) |
| 2. | Grapefruit peel | 10.43 | (Torab-Mostaedi et al., 2013) |
| 3. | *Avena fatua* biomass | 105.468 | (Areco et al., 2013) |
| 4. | Rivularia bulata Algae | 26.36 | (Kizilkaya et al., 2013) |
| 5. | Alga *Anabaena sphaerica* | 111.1 | (Abdel -Aty et al., 2013) |
| 6. | Agaricus bisporus | 6.98 | (Nagy et al., 2013) |
| 7. | Cabbage | 20.57 | (Hossain et al., 2013) |
| 8. | Cauliflower | 21.32 | (Hossain et al., 2013) |
| 9. | Mango peel | 68.92 | (Iqbal et al., 2009a) |
| 10. | Lemon grass | 39.53 | (Zuo et al., 2012) |

**Table 2.8** Zn(II) adsorption capacities (mg/g) by biosorbents recently reported in literature

| SL | Biosorbent | $q_m$ (mg/g) | References |
|---|---|---|---|
| 1. | Wheat straw | 3.6 | (Gorgievski et al., 2013) |
| 2. | *Typha latifolia* root | 16.67 | (Rajaei et al., 2013) |
| 3. | *Avena fatua* biomass | 23.54 | (Areco et al., 2013) |
| 4. | *Ngella sativa* seeds | 93 | (Al-Tohami et al., 2013) |
| 5. | *Undaria pinnatifida* | 100.04 | (Plaza Cazón et al., 2013) |
| 6. | Coconut shell-based activated carbon fiber | 9.43 | (Shrestha et al., 2013) |
| 7. | Corn Cob | 79.21 | (Buasri et al., 2012) |
| 8. | Lemon grass | 15.87 | (Zuo et al., 2012) |
| 9. | freshwater charophytes (*C. aculeolata*) | 6.73 | (Sooksawat et al., 2013) |
| 10. | Neem biomass | 147.08 | (Arshad et al., 2008) |

## 2.5 Modelling of biosorption

Mathematical modelling is the derived relation among the components present in a system. In the case of sorption process the components are equilibrium concentration, initial concentration, adsorbents doses, reaction/contact time, reaction rate etc. There are also some empirical models used for describing the sorption process. Modelling is the method of prediction of impact of any component on any other components as well as on the results. Nowaday, several computer simulated model is using for prediction of sorption in different biosorption process.

### 2.5.1 Adsorption theories/isotherms

Equilibrium study provides fundamental information required to evaluate the affinity or capacity of an adsorbent, which is one of the most important criteria in selecting a suitable adsorbent (Yang et al., 2010). Meanwhile, equilibrium behaviour of an adsorption system is an essential prerequisite during mathematical modelling of the adsorption kinetics. A clear review of the various equilibrium isotherms and their applications is in the literature (Al-Duri et al., 1995).

Isotherm adsorption models have been used in waste stream treatment to predict the ability of a certain adsorbent to remove a pollutant down to a specific discharge value. When a mass of adsorbent and a waste stream are in contact for a sufficiently long time, equilibrium between the amount of pollutant adsorbed and the amount remaining in solution will develop. For any system under equilibrium conditions, the amount of material adsorbed onto the media can be calculated using the mass balance of Eq.(2.5):

$$\frac{x}{m} = (C_o - C_e)\frac{v}{m} \qquad (2.5)$$

where x/m (typically expressed as mg pollutant/g media) is the mass of pollutant per mass of media, $C_o$ is the initial pollutant concentration in solution, $C_e$ is the concentration of the pollutant in solution after equilibrium has been reached, v is the volume of the solution to which the media mass is exposed, and m is the mass of the media.

#### 2.5.1.1 Langmuir model

Initially the Langmuir adsorption isotherm was developed to explain gas-solid-phase adsorption onto activated carbon and has traditionally been used to quantify and contrast the performance of different biosorbents (Langmuir, 1918). The theoretical Langmuir sorption isotherm (Langmuir, 1918) is based on the assumption that the maximum adsorption occurs when a saturated monolayer of solute molecules is present on the adsorbent surface, the energy of adsorption is constant and there is no migration of adsorbate molecules in the surface plane. In its derivation, the Langmuir isotherm refers to homogeneous adsorption, in which each molecule possesses constant enthalpies and sorption activation energy (all sites possess equal affinity for the adsorbate) (Kundu and Gupta, 2006). Graphically, it is characterized by a plateau where one molecule adsorbed and later no further adsorption can take place (Demirbas, 2008; Foo and Hameed,

2010). Moreover, this model has related rapid decrease of the intermolecular attractive forces to the rise of distance. The non-linear equation of the Langmuir isotherm model is expressed as follow ( Eqn. 2.6):

$$q_e = \frac{q_m K_L C_e}{1 + K_L C_e} \qquad (2.6)$$

where $C_e$ is the supernatant concentration at the equilibrium state of the system (mg/l), $q_m$ and $K_L$ are the Langmuir constants, representing the maximum adsorption capacity for the solid phase loading and the energy constant related to the heat of adsorption respectively.

A dimensionless constant, commonly known as the separation factor ($R_L$) defined by (Torab-Mostaedi et al., 2013) can be represented (eqn.2.7) as:

$$R_L = \frac{1}{1 + K_L C_o} \qquad (2.7)$$

where $K_L$ (l/mg) refers to the Langmuir constant and $C_o$ is denoted to the adsorbate initial concentration (mg/l). In this context, lower $R_L$ value reflects that adsorption is more favourable. In a deeper explanation, $R_L$ value indicates the adsorption nature to be either unfavourable ($R_L > 1$), linear ($R_L = 1$), favourable ($0 < R_L < 1$) or irreversible ($R_L = 0$).

#### 2.5.1.2 Freundlich model

The Freundlich adsorption isotherm (Freundlich, 1906) is the earliest isotherm which describes the mathematical relationship for non-ideal and reversible adsorption. The assumption of this model has not restricted to the formation of a monolayer. This empirical model can be applicable for multilayer adsorption with non-uniform distribution of adsorption heat and affinities over the heterogeneous surface (Febrianto et al., 2009). Previously, it was devised for the adsorption of animal charcoal. It is demonstrating that the ratio of the metals/adsorbate onto a given mass of biosorbent to the solute was not a constant at different solution concentrations (Torab-Mostaedi et al., 2013). In this point of view, the amount of adsorbate which adsorbed in the adsorbent is the summation of adsorption on all sites, with the stronger binding sites being occupied first, until the adsorption energies are exponentially decreased upon the completion of adsorption process (Gorgievski et al., 2013).

Normally, the Freundlich isotherm is widely used in heterogeneous adsorption systems especially for organic compounds or highly interactive species. The slope ranges between 0 and 1 and is a measure of the adsorption intensity or surface heterogeneity, becoming more heterogeneous as its value gets closer to zero. A value below unity implies chemisorptions process where 1/n above one is an indicative of cooperative adsorption (Buasri et al., 2012). Recently, the Freundlich isotherm has been criticized for its limitation of lacking a fundamental thermodynamic basis, not approaching the Henry's law at vanishing concentrations (Ho et al., 2002c). The general Freundlich equation is:

$$q_e = K_F C_e^{1/n} \qquad (2.8)$$

where $K_F$ and $n$ are adsorption capacity and affinity, respectively. The Langmuir and Freundlich isotherm models are only applicable to batch sorption systems where sufficient time is provided to allow equilibrium between the pollutant in solution and the pollutant adsorbed on the media to occur.

#### 2.5.1.3 Redlich-Peterson model

The Redlich-Peterson isotherm (Redlich and Peterson, 1959) is a hybrid three-parameter isotherm which combined both Langmuir and Freundlich isotherms (Witek-Krowiak, 2012). It is linearly dependent on concentration in the numerator and an exponential function in the denominator and can be used for versatile adsorption system like homogeneous or heterogeneous systems to represent adsorption equilibrium over a wide range of concentration (Buasri et al., 2012; Bulgariu and Bulgariu, 2012; Gorgievski et al., 2013). The Redlich-Peterson Model describes a three-parameter isotherm, which combines elements of the Langmuir and Freundlich isotherms in a single equation given below:

$$q_e = \frac{K_{RP} C_e}{1 + \alpha_{RP} C_e^{\beta}} \qquad (2.9)$$

where, $K_{RP}$ and $\alpha_{RP}$ are the Redlich-Peterson isotherm constant; $\beta$ the Redlich-Peterson isotherm exponent, which lies between 0 to 1. The Ce and qe have the same definition used in Langmuir and Freundlich isotherms.

#### 2.5.1.4 Koble-Corrigan model

The Koble-Corrigan isotherm (Koble and Corrigan, 1952) is a three-parameter isotherm model, which combined both Langmuir and Freundlich isotherm models for

representing the equilibrium adsorption. This model has similarity to the Sips isotherm model. The nonlinear form of the model is given by

$$q_e = \frac{A_{KC} C_e^p}{1 + B_{KC} C_e^p} \qquad (2.10)$$

where $A_{KC}$, $B_{KC}$ and p are the Koble-Corrigan parameters. This model is valid when p > 1.

#### 2.5.1.5 Sips isotherm model

The Sips isotherm (Sips, 1948) is an isotherm which is obtained from combining the Langmuir and Freundlich isotherms for predicting the heterogeneous adsorption systems (Vilar et al., 2009) and avoiding the limitation of higher adsorbate concentration related with the Freundlich isotherm model. At low adsorbate concentrations, this model reduces to the Freundlich isotherm, while at high concentrations, it determines a monolayer adsorption capacity characteristic like the Langmuir isotherm. Generally, the alteration of pH, temperature and concentration of the system controls the magnitude of parameters for the equation (Blazquez et al., 2010). Sip isotherm model equation is expressed as follows:

$$q_e = \frac{K_s C_e^{\beta_s}}{1 + \alpha_s C_e^{\beta_s}} \qquad (2.11)$$

where, $K_s$ (l/g) and $\alpha_s$ (l/mg) are the Sips isotherm constants and β is the exponent which lies between 1 and 0.

#### 2.5.1.6 Temkins' isotherm

The Temkin isotherm (Temkin and Pyzhev, 1940) is an early model which develops from the adsorption of hydrogen onto platinum electrodes within acidic solutions. This model has a factor which can explain adsorbent-adsorbate interactions. Besides the exceptionally low and large magnitude of concentrations, the model assumes that heat of adsorption by all molecules in a layer would decrease linearly rather than logarithmical with coverage (Javanbakht et al., 2011). The Temkin equation can predict the gas phase equilibrium correctly and equally complex adsorption systems including the liquid-phase adsorption isotherms are usually not appropriate to be represented (Ofomaja, 2010).

Temkins' isotherm contains a factor that explicitly takes into account the absorbing species-adsorbate interactions. The isotherm assumes that (i) the heat of adsorption of all the molecules in the layer decreases linearly with coverage due to adsorbate-adsorbate interaction, (ii) adsorption is characterized by a uniform distribution of binding energies to some maximum binding energy. The Temkin isotherm is represented by the following equation:

$$q_e = \ln(K_T C_e) \tag{2.12}$$

where,

$$B_1 = \frac{RT}{K_T} \tag{2.13}$$

as analyzed according to Eq. (2.12). A plot of $q_e$ versus ln $C_e$ enables the determination of the isotherm constants $K_T$ and $B_1$. $K_T$ is the equilibrium binding constant ($dm^3$/mol) corresponding to the maximum binding energy and $B_1$ is related to the heat of adsorption.

### 2.5.1.7 Dubinin-Radushkevich isotherm model

The Dubinin-Radushkevich isotherm (Dubinin and Radushkevich, 1947) is an empirical model which was developed for the adsorption of subcritical vapors onto micropore solids with a pore filling mechanism. This model is applied to describe the adsorption mechanism with a Gaussian energy distribution onto a heterogeneous surface (Foo and Hameed, 2010). It is often effectively fitted with range of concentrations data and high solute activities, but has insufficient asymptotic properties and does not predict Henry's law at low pressure (Allen et al., 2003). This model was applied to differentiate the physical and chemical adsorption of metal ions with their mean free energy, E and it can be calculated by relationship (Foo and Hameed, 2010). The Dubinin-Radushkevich model can be expressed as follows:

$$q_e = q_m . \exp\left[ - B_{DR} \left( RT \ln\left( 1 + \frac{1}{C_e} \right) \right)^2 \right] \tag{2.14}$$

or

$$q_e = q_m e^{-B_{DR} . \varepsilon^2} \tag{2.15}$$

where $q_m$ is the Dubinin-Radushkevich monolayer capacity (mg/g), $B_{DR}$ a constant related to sorption energy, and ε is the Polanyi potential which is related to the equilibrium concentration as follows:

$$\varepsilon = RT \ln\left(1 + \frac{1}{C_e}\right) \tag{2.16}$$

where, R is the gas constant (8.314 J/mol K) and T is the absolute temperature. The constant $B_{DR}$ gives the mean free energy, E, of sorption per molecule of the sorbate when it is transferred to the surface of the adsorbent:

$$E = \frac{1}{\sqrt{2B_{DR}}} \tag{2.17}$$

The Dubinin-Radushkevich isotherm model has unique features in that it is temperature-dependent and when adsorption data at different temperatures are plotted as a function of logarithm of amount adsorbed vs the square of potential energy, all suitable data will lay on the characteristic curve.

### 2.5.1.8 Flory-Huggins isotherm model

The Flory-Huggins isotherm model (Horsfall and Spiff, 2005b) has been derived based on the degree of surface coverage characteristics of adsorbate onto adsorbent. This model can explain the feasibility and spontaneous nature of an adsorption process. The model can be expressed as:

$$\frac{\theta}{C_o} = K_{FH}\,(1 - \theta)^n$$
$$\theta = 1 - \frac{C_e}{C_o} \tag{2.18}$$

where, θ is the degree of surface coverage, where $K_{FH}$ and $n_{FH}$ are the indication of its equilibrium constant and model exponent. The equilibrium constant, $K_{FH}$ can be used for the calculation of spontaneity free Gibbs energy by the following equation (Vijayaraghavan et al., 2009):

$$\Delta G^o = -RT \ln(K_{FH}) \tag{2.19}$$

### 2.5.1.9 Hill isotherm model

The Hill equation (Hill, 1910) was developed from the NICA (Koopal et al., 1994) model and was used to describe the binding of different species onto homogeneous surfaces. The assumption of this model is that adsorption is a cooperative phenomenon, with the ligand binding ability at one site on the macromolecule influencing different binding sites on the same macromolecule (Ringot et al., 2007). The expression of the Hill model is as follows:

$$q_e = \frac{q_m C_e^n}{K_D + C_e^n} \qquad (2.20)$$

### 2.5.1.10 Unilan equation

The Unilan equation is an empirical equation having three degrees of freedom and is often used for gas phase adsorption on a heterogeneous surface. This empirical equation assumed the applicability of the local Langmuir isotherm and uniform distribution of energy (Do Duong, 1998; Ismadji and Bhatia, 2000) and also introduced a parameter "s" to account for the heterogeneity of the system. This equation has a Henry's law limit so it can be applicable at very small adsorbate loadings (Ismadji and Bhatia, 2000). The Unilan equation has the following form:

$$q_e = \frac{q_m}{S} \ln\left[\frac{1 + d\exp(S)C_e}{1 + d\exp(-S)C_e}\right] \qquad (2.21)$$

where, s and d are temperature dependent model constants.

### 2.5.1.11 Khan isotherm model

The Khan isotherm (Khan et al., 1997) is a generalized model suggested for pure solutions, where $b_K$ and $a_K$ stands for the model constant and model exponent. At relatively high correlation coefficients and minimum chi-square values, its maximum uptake values can be well determined (Khan et al., 1996).

$$q_e = \frac{q_m b_k C_e}{(1 + b_k C_e)^{a_k}} \qquad (2.22)$$

### 2.5.1.12 Radke-Prausnitz isotherm model

The correlation of the Radke-Prausnitz isotherm is usually predicted well by the high RMSE and chi-square values. Its model exponent is represented by $\beta_R$, where $\alpha_R$ and $r_R$ are referred to as the model constants (Vijayaraghavan et al., 2006).

$$q_e = \frac{\alpha_R r_R C_e^{\beta_R}}{\alpha_R + r_R C_e^{\beta_R - 1}} \qquad (2.23)$$

### 2.5.1.13 Toth isotherm model

The Toth isotherm model (Toth, 1971), is another empirical equation developed to improve Langmuir isotherm fittings (experimental data), and is useful in describing heterogeneous adsorption systems, while satisfying both the low and high boundaries of

concentration (Vijayaraghavan et al., 2006). Its correlation presupposes an asymmetrical quasi-Gaussian energy distribution, with most of its sites has an adsorption energy lower than the peak (maximum) or mean value (Ho et al., 2002d).

$$q_e = \frac{q_m C_e}{(b_T + C_e^n)^{1/n}} \tag{2.24}$$

### 2.5.2 Sorption kinetics

There are several factors which control the sorption kinetics including (i) solute transfer from the solution to the boundary film surrounding the particle (bulk diffusion), (ii) diffusion from the film to the surface of the adsorbent (external diffusion), (iii) diffusion from the surface to the intraparticular sites (intraparticular diffusion), and (iv) solute adsorption by complexation or physicochemical sorption or ion exchange (Prasad and Saxena, 2008). Providing sufficient agitation to avoid particle and solute gradients makes it possible to ignore bulk diffusion and it can be assumed that the rate is not limited by mass transfer from the bulk liquid to the particle external surface. Diffusion from the film to the surface of the adsorbent, also called external diffusion or liquid film diffusion, might govern the sorption process.

Sorption is the process of taking/uptaking some materials into a system or material. The sorption process is time dependent which leads to the term sorption kinetics. The sorption kinetic is the best way to describe the uptake behaviour of any metals (e.g. lead, copper, cadmium, arsenic, zinc etc) by a sorbent produced from biological sources. The kinetics equation is a function of time to reach equilibrium and can be explained in the following terms (Ho et al., 2002a):

$$\gamma = \frac{q_t}{q_e} \tag{2.25}$$

where, $q_t$ is the amount of heavy metal sorbed (mg/g) on adsorbent at time t and $q_e$ is the amount of heavy metal sorbed (mg/g) on adsorbent at equilibrium.

The simplest way to describe the kinetics of metal removal can be expressed (Prasad and Saxena, 2008) as

$$P + M \underset{k_2}{\overset{k_1}{\Longleftrightarrow}} MP \tag{2.26}$$

where P represents an unoccupied active site on the adsorbent and M is a free metal ion in solution. $k_1$ and $k_2$ are the adsorption and desorption rate constants, respectively.

### 2.5.2.1 Pseudo-first-order model

Understanding the kinetics of the sorption process the different rate equation is used to fit the experimental data for any kind of sorption (Ho and McKay, 1998b). A general rate expression of pseudo first order equation takes the form:

$$\frac{dq_t}{dt} = k_1(q_e - q_t) \qquad (2.27)$$

where $k_1$ ($min^{-1}$) is the rate constant of the pseudo first-order sorption, $q_e$ (mg/g) is the amount of metal ion sorbed on the adsorbent surface at equilibrium, and $q_t$ (mg/g) is the amount of metal ion sorbed at any time $t$ (min).

Rearranging the eq(2.27):

$$\frac{dq_t}{(q_e - q_t)} = k_1 dt \qquad (2.28)$$

Integrating the eq(2.28) with the boundary condition $q_t = 0$ at $t = 0$ and simplifies the equation:

$$\ln(q_e - q_t) = \ln q_e - k_1 t \qquad (2.29)$$

The above rate expression is known as the 'Lagergren' first-order equation (Ho, 2004; Lagergren, 1898) and can also be expressed as:

$$\log(q_e - q_t) = \log q_e - k_1 \frac{t}{2.303} \qquad (2.30)$$

The value of the sorption rate ($k_1$) can be calculated from linear regression analysis or from the slope of the linear plot of experimental data in $log(q_e - q_t)$ vs $t$. The non-linear form Pseudo-First-Order Model becomes:

$$q_t = q_e - q_e e^{(-k_1 t)} \qquad (2.31)$$

### 2.5.2.2 Pseudo-second-order model

The pseudo-second-order equation is the most widely used rate equation for the sorption of a solute from a liquid phase. The experimental data can also be tested for pseudo-second-order adsorption. The commonly represented pseudo-second-order adsorption equation (Ho and Ofomaja, 2006a; Ho et al., 2000; Ho and Ofomaja, 2006b) is:

$$\frac{dq_t}{dt} = k_2(q_e - q_t)^2 \qquad (2.32)$$

where, $k_2$ is the rate constant of adsorption (l/mg. min), $q_e$ is the amount of copper ions adsorbed at equilibrium (mg/g) and $q_t$ is the amount of copper ions adsorbed at time t (mg/g). Rearranging the variables of Eq. (2.34) gives:

$$\frac{dq_t}{(q_e - q_t)^2} = k_2 dt \tag{2.33}$$

Integrating the Eq(2.35) for the boundary conditions of t = 0 to t = t and $q_t = 0$ to $q_t = q_t$ gives:

$$\frac{1}{(q_e - q_t)} = \frac{1}{q_e} + k_2 t \tag{2.34}$$

which, is the integrated rate law for a pseudo-second-order reaction. Eq.(5) can be rearranged to obtain:

$$q_t = \frac{t}{\left(\frac{1}{k_2 q_e^2}\right) + \left(\frac{t}{q_e}\right)} \tag{2.35}$$

which, has a linear form of:

$$\frac{t}{q_t} = \frac{1}{k_2 q_e^2} + \frac{1}{q_e} t \tag{2.36}$$

If the initial adsorption rate, $h = q_t/t$ when t approaches to 0, h, (mg/g min) (Ho and McKay, 2000), is:

$$h = k_2 q_e^2 \tag{2.37}$$

then Eqs. (2.35) and (2.36) become:

$$q_t = \frac{t}{\frac{1}{h} + \frac{t}{q_e}} \tag{2.38}$$

and

$$\frac{t}{q_t} = \frac{1}{h} + \frac{t}{q_e} \tag{2.39}$$

Experimentally the pseudo-second-order rate constants were determined by plotting $t/q_t$ vs. t. Although there are many factors which influence the adsorption capacity, including the initial biosorbents concentration, the reaction temperature, the solution pH value, the adsorbent particle size and dose and the nature of the biosorbents, a kinetic model is concerned only with the effect of observable parameters on the overall rate.

Linear regressions are frequently used to determine the best fitting kinetic models and the method of least-squares is used for finding parameters of the kinetic models (Ho,

2006). There are five forms of pseudo-second-order model which can be used for regression analysis to determine the different parameters. The non-linear form Pseudo-Second-Order model is:

$$q_t = \frac{k_2 q_e^2 t}{(1 + q_e k_2 t)} \qquad (2.40)$$

**2.5.2.3 Intraparticle diffusion model**

In a well mixed solution the film diffusion is negligible and the rate constant is controlled by intraparticle diffusion (Yang and Al-Duri, 2005). The intraparticle model can be derived from Fick's second law of diffusion based on two assumptions. This is a single-resistance model. The two assumptions are 'the intraparticle diffusivity $D$ is constant' and 'the uptake of sorbate by the adsorbent is small relative to the total quantity of sorbate present in the solution'. The mathematical expression of the model is:

$$q_t \approx k_p \sqrt{t} \qquad (2.41)$$

where $k_p$ (mg/g. $min^{-0.5}$) is defined as the intraparticle diffusion rate constant and is related to the intraparticle diffusivity in the following way,

$$k_p = \frac{6 q_e}{R} \sqrt{\frac{D}{\pi}} \qquad (2.42)$$

where $R$ (cm) is the radius of the particle and $q_e$ (mg/g) is the solid phase concentration at equilibrium. Equation (2.43) indicates that a plot of the average particle loading, $q_t$ (mg/g), versus the square root of time, √t, would yield a straight line passing through the origin if the adsorption process obeyed the intraparticle diffusion model. The slope of the straight line equals $k_p$, the intraparticle diffusion rate constant. The equation can be written as:

$$q_t = k_p t^{0.5+C} \qquad (2.43)$$

**2.5.2.4 Avrami kinetic model**

The equation of the Avrami kinetic model presents the Avrami exponential that is a fractionary number related to the possible changes of the adsorption mechanism that take place during the adsorption process. So the adsorption mechanism could follow multiple kinetic orders that are changed during the contact of the adsorbate with the adsorbent (Lopes et al., 2003).

$$q_t = q_e\left[1 - e^{(-t.k_{AV})^{n_{AV}}}\right] \quad (2.44)$$

Where, $K_{AV}$ is the Avrami kinetic constant and $n_{AV}$ is another constant, which is related to the adsorption mechanisms changes. The linearized form of this equation is presented in Eq. (2.44):

$$\ln(\ln(\frac{q_e}{q_e - q_t})) = n_{AV} \ln k_{AV} + n_{AV} \ln(t) \quad (2.45)$$

The $\ln(\ln(q_e/q_e - q_t))$ versus ln(t) plots (plots not shown) in relation to adsorption temperature provide the $n_{AV}$ and ln $K_{AV}$ values from the slopes and intersections values, respectively. The equation can be written as:

$$q_t = q_e(1 - e^{(-K_{AV}t)^{n_{AV}}}) \quad (2.46)$$

**2.5.2.5 Elovich kinetics model**

Elovich's equation has been widely used to describe the adsorption of gases onto solid materials; it has also been applied to describe the process of adsorption of dyes from aqueous solutions. The model describes the kinetics of the chemisorption process (Cheung et al., 2000; Chien and Clayton, 1980). Elovich kinetics model is:

$$q_t = \frac{1}{\beta}\ln(\alpha\beta) + \frac{1}{\beta}\ln(t) \quad (2.47)$$

Where, α is the Elovich coefficient representing the initial adsorption rate [mg.(g.min)$^{-1}$]; β is the Elovich coefficient related to the extent of surface coverage and activation energy for chemisorption (g.mg$^{-1}$). The parameter α represents the rate of chemisorption at zero coverage; the parameter β is related to the extent of surface coverage and to the activation energy for the adsorption (Witek-Krowiak et al., 2011).

**2.5.2.6 Fractional power model**

The power function equation which is an empirical model that describes the relation between the mass of the sorbate per unit mass of the adsorbent and time 't' is as follows (Limousin et al., 2007):

$$q_t = kt^v \quad (2.48)$$

where $q_t$ is the adsorption capacity at given time (mg/g), k (mg g$^{-1}$ min$^{-1}$) and v are adjustment parameters. When v = 0.5, the equation becomes the same as the Webber–Morris intraparticle diffusion model (Weber and Morris, 1963).

## 2.6 Column adsorption

Although batch laboratory adsorption studies provide useful data and parameters on the application of adsorbents for the removal of heavy metals or, in other cases, specific waste constituents, continuously-fed filter or column experiments are also necessary to provide practical operational information with respect to the adsorption of constituents with the use of a particular adsorbent (Suksabye et al., 2008).

A fixed bed column study is important to predict the column breakthrough or the shape of the adsorption wave front, which determine the operation life span of the bed and regeneration time. Further, in order to obtain basic engineering data for the design of the application process, it is essential to study the continuous flow system. Adsorption capacities from batch studies may not give accurate scale up information in the column operation system (Maji et al., 2007) because of several factors. Although batch laboratory adsorption studies provide useful information on the application of adsorption to the removal of specific waste constituents, continuous column studies provide the most practical application of this process in wastewater treatment. The reason for this is that the high adsorption capacities in equilibrium with the influent concentration rather than the effluent concentration can be achieved (Goel et al., 2005). In static mode adsorption studies, the same solution remains in contact with a given quantity of the adsorbent. The adsorption process continues, however, till equilibrium between the solute concentration in solution, and the solute adsorbed per unit weight of the adsorbent is reached(Maiti et al., 2008). This equilibrium established is static in nature, as it does not change further with time. In dynamic column adsorption, solution continuously enters and leaves the column, so that the complete equilibrium is never established at any stage between the solute in solution and the amount adsorbed. Equilibrium has to be continuously established each time the adsorbent meets fresh concentrations; hence, equilibrium in column mode is termed dynamic equilibrium (Han et al., 2009; Maji et al., 2007).

### 2.6.1 The Break-through Curve

The adsorption process could be very well illustrated by a break-through curve (Padmesh et al., 2005) as given in Figure 2.5 in which the abscissa is either time or volume of water treated and the ordinate is the ratio of effluent to influent concentration. Referring to Figure 2.5, in the beginning all the solute is adsorbed by the

top layers and whatever escapes is totally adsorbed by the bottom layers so the adsorption zone is concentrated at the top end and at point1 the effluent is practically solute free.

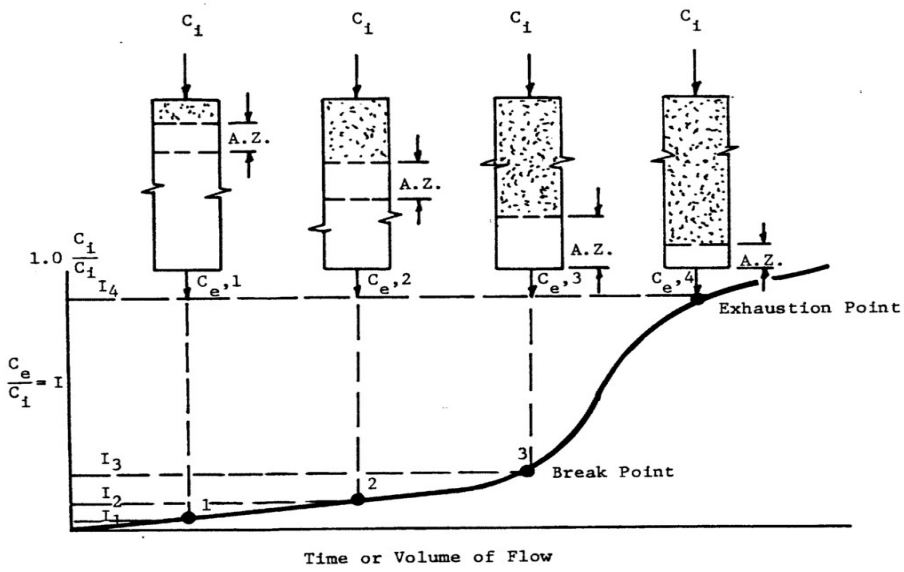


**Figure 2.5** A schematic diagram of adsorption zone in different zone and resulting break through curve (adapted from Tor et al., 2009)

At the point 2 when top layers are totally exhausted and have very little capacity to adsorb, the adsorption zone moves to the middle of the column and at point 2 more and more solute escapes in the effluent. At point 3 the adsorption zone has moved to the bottom of the column as the result of the inability of the layers above to adsorb any solute and the column is practically in equilibrium with influent water and beyond this very little adsorption will take place. This point is known as the 'break point'. At point 4 the adsorption zone tends to move out from the column and effluent solute concentration is practically the same as the influent solute concentration and at this point the column is totally exhausted. The point 4 is called the 'exhaustion point.' The total amount of solute adsorbed could be calculated by calculating the area on the left of the break-through curve (Tor et al., 2009).

### 2.6.2 Models of column studies

Fixed bed and fluidized columns of different adsorbents have been in use for long time for different adsorption processes. It is assumed that the solid is contained in a vessel of uniform cross section and that at any cross section at a given time the concentration in the solid and fluid are uniform, so that there is no loss in generality in basing all

formulas on unit cross section. Authors have not taken into account any heat effects (Orth et al., 2010; Thiele, 1946).

The performance of packed beds is described through the concept of the breakthrough curve. The breakthrough curve shows the loading behaviour of metals to be removed from solution in a fixed bed and is usually expressed in terms of adsorbed metals concentration ($C_{ad}$ = inlet metals concentration ($C_0$)-outlet metals concentration (Ce)) or normalized concentration defined as the ratio of effluent metals concentration to inlet metal concentration ($Ce/C_0$) as a function of time or volume of effluent for a given bed height (Aksu and Gönen, 2004). The area under the breakthrough curve obtained by integrating the adsorbed concentration ($C_{ad}$, g/l) versus the throughput volume (V, l) plot can be used to find the total adsorbed metal quantity (maximum column capacity). Total adsorbed metal quantity ($q_o$, mg/g) in the column for a given feed concentration and flow rate is calculated from Eq. (2.49):

$$q_o = \int_0^{V_T} \frac{(C_o - C_e)d.V}{m} \qquad (2.49)$$

where m is the mass of the adsorbent (g). The capacity value $q_o$ could be obtained by graphical integration.

### 2.6.2.1. Thomas model

Successful design of a column adsorption process requires prediction of the concentration-time profile or breakthrough curve for the effluent. The maximum adsorption capacity of a biosorbent is also needed in the design. Traditionally, the Thomas model is used to fulfill the purpose. The model has the following form (Mathialagan and Viraraghavan, 2002):

$$\frac{C_e}{C_o} = \frac{1}{1 + \exp\left[K_T\left(q_o m - C_o V\right)/\theta\right]} \qquad (2.50)$$

where, $K_T$ is the Thomas rate constant (l/(min mg)) and θ is the volumetric flow rate (l/min). The linearized form of the Thomas model is as follows:

$$\ln\left(\frac{C_o}{C_e} - 1\right) = \frac{K_T q_o m}{\theta} - \frac{K_T C_o . V}{\theta} \qquad (2.51)$$

The kinetic coefficient $K_T$ and the adsorption capacity of the bed $q_o$ can be determined from a plot of $\ln[(C_0/C_e)-1]$ against t .

#### 2.6.2.2. Yoon and Nelson model

This model is based on the assumption that the rate of decrease in the probability of adsorption for each adsorbate molecule is proportional to the probability of adsorbate adsorption and the probability of adsorbate breakthrough on the adsorbent. The Yoon and Nelson model not only is less complicated than other models, but also requires no detailed data concerning the characteristics of adsorbate, the type of adsorbent, and the physical properties of the adsorption bed.

The Yoon and Nelson equation applied to a single component system is expressed as (Aksu and Gönen, 2004):

$$\frac{C_e}{C_o} = \frac{1}{1+\exp[k(\tau - t)]} \qquad (2.52)$$

where k is the rate constant ($min^{-1}$), τ the time required for 50% adsorbate breakthrough (min) and t is the breakthrough (sampling) time (min). The linearized form of the Yoon and Nelson model is as follows:

$$t = \tau + \frac{1}{k}\ln\left(\frac{C_e}{C_o - C_e}\right) \qquad (2.53)$$

The calculation of theoretical breakthrough curves for a single-component system requires the determination of the parameters k and τ for the adsorbate of interest. These values may be determined from available experimental data.

The derivation for Eq. (2.53) was based on the definition that 50% breakthrough of the adsorption process occurs at τ. The bed should be completely saturated at 2τ accordingly. Due to the symmetrical nature of breakthrough curve, the amount of metal adsorbed by the biosorbent is one half of the total metal ions entering the adsorption column within the 2τ period. Hence, the following equation can be written (Öztürk and Kavak, 2005):

$$q_o = \frac{1}{2}C_o\theta(2\tau) = C_o\theta\tau \qquad (2.54)$$

The above equation establishes the relation among the adsorption capacity of the column ($q_o$), inlet concentration ($C_0$), liquid flow rate (θ) and the 50% breakthrough time (τ).

### 2.6.2.3. The Adams-Bohart model

The elementary equation describing the relationship between $C/C_o$ and t in a flowing system was established for the adsorption of chlorine on charcoal (Bohart and Adams, 1920). Scientists G. S. Bohart and E. Q. Adams developed the original equation for a gas–charcoal adsorption system and this overall approach can be applied successfully in the quantitative description of other systems. This model assumes that the adsorption rate is proportional to both the residual capacity of the activated carbon and the concentration of the sorbing species. This model is used for the description of the initial part of the breakthrough curve. The mass transfer rates obey the following equations:

$$\frac{\partial q}{\partial t} = -k_{AB} q C_b \tag{2.55}$$

$$\frac{\partial C_b}{\partial Z} = -\frac{k_{AB}}{U_o} q C_b \tag{2.56}$$

where, $k_{AB}$ is the kinetic constant (l/mg.min). Some assumptions are made for the solution of these differential equation systems: (i) the concentration field is considered to be low, e.g. effluent concentration $C<0.15C_o$; (ii) for $t\rightarrow\infty$, $q\rightarrow N_o$, (where $N_o$ is the saturation concentration (mg/l). When the differential equation systems are solved, the following equation is obtained with parameters $k_{AB}$ and $N_o$:

$$\ln\frac{C}{C_o} = k_{AB} C_o t - k_{AB} N_o \frac{Z}{U_o} \tag{2.57}$$

where, $C_o$ and C are the inlet and effluent phenol concentrations (mg/l), respectively. From this equation values describing the characteristic operational parameters of the column can be determined from a plot of ln $C/C_o$ against t at a given bed height and flow rate (Bohart and Adams, 1920; Diniz and Volesky, 2005; Texier et al., 2002).

### 2.6.2.4. The Wolborska model

The Wolborska model is also used for the description of adsorption dynamics using mass transfer where diffusion mechanisms are involved in the range of the low-concentration breakthrough curve (Aksu and Gönen, 2004; Wolborska, 1989). The mass transfer in the fixed bed sorption is described by the following equations:

$$\frac{\partial C_b}{\partial t} + U_o\left(\frac{\partial C_b}{\partial Z}\right) + \left(\frac{\partial q}{\partial t}\right) = D\left(\frac{\partial^2 q}{\partial^2 Z}\right) \tag{2.58}$$

$$\frac{\partial q}{\partial t} = -v\left(\frac{\partial q}{\partial Z}\right) = \beta_a\left(C_b - C_s\right) \tag{2.59}$$

where, $C_s$ is the metal ions concentration at the solid/liquid interface (mg/l); D, the axial diffusion coefficient ($cm^2$/min); v, the migration rate (cm/min); and '$\beta_a$' is the kinetic coefficient of the external mass transfer (/min). With some assumptions previously described by Wolborska: $C_s << C_b$, $v << U_o$ and axial diffusion is negligible, $D \rightarrow 0$ as $t \rightarrow 0$, the solution can be approximated to:

$$\ln \frac{C}{C_o} = \frac{\beta_a C_o}{N_o} t - \frac{\beta_a Z}{U_o} \tag{2.60}$$

$$\text{with, } \beta_a = \frac{U_o^2}{2D}\left(\sqrt{1 + \frac{4\beta_o D}{U_o^2}} - 1\right) \tag{2.61}$$

where, $\beta_o$ is the external mass transfer coefficient with a negligible axial dispersion coefficient D. Wolbraska observed that in short beds or at high flow rates of solution through the bed, the axial diffusion is negligible and $\beta_a = \beta_o$. The migration velocity of the steady-state front satisfies the relation, known as Wickes' law (Wickes, 1929):

$$v = \frac{U_o C_o}{N_o + C_o} \tag{2.62}$$

The expression of the Wolborska solution is equivalent to the Adams–Bohart relation if the coefficient $k_{AB}$ is equal to $\beta_a/N_o$. So the drawing of '$\ln C/C_o$' versus 't' would also give information on this model (Guibal et al., 1995; Wolborska, 1989).

### 2.6.2.5. The Clark model

A new simulation of breakthrough curves is devised through the Clark model (Clark, 1987). This model combines the Freundlich equation and the mass transfer concept as follows:

$$U_o \frac{dC_b}{dZ} = K(C_b - C_e) \tag{2.63}$$

where K is the mass transfer coefficient (/min). Clark resolved this system and obtained the following solution:

$$\left[\frac{C_O^{n-1}}{1 + \left[\left(\frac{C_o^{n-1}}{C_{break}^{n-1}} - 1\right) e^{rD_{break}}\right] e^{rt}}\right]^{\frac{1}{n-1}} = C \tag{2.64}$$

$$\frac{C}{C_o} = \left(\frac{1}{1 + Ae^{-rt}}\right)^{\frac{1}{n-1}} \tag{2.65}$$

with

$$A = \left( \frac{C_o^{n-1}}{C_{break}^{n-1}} - 1 \right) e^{rD_{break}} \qquad (2.66)$$

and $R(n-1) = r$ and $\mathrm{R} = \frac{\mathrm{k_{Cl}}}{\mathrm{U_O}} v$ (2.67)

Eq. (2.66) is the generalized logistic function where n, $C_{break}$ and $t_{break}$ are the Freundlich constant, the outlet concentration at breakthrough (or limit effluent concentration), and the time at breakthrough, respectively. For a particular adsorption process on a fixed bed and a chosen treatment objective, values of A and r can be determined by using Eq. (2.66) by non-linear regression analysis, enabling the prediction of the breakthrough curve according to the relationship between $C/C_o$ and t in Eq. (2.66), (Clark, 1987; Guibal et al., 1995; Tran and Roddick, 1999).

**Faculty of Engineering and Information Technology**
**University of Technology, Sydney (UTS)**

# Chapter 3

# Experimental Investigation

## 3.0 Introduction

This chapter gives the details of the materials and chemicals/reagents and an overview of the methods used for preparing the biosorbents (GG, CW, BP, ML and POFS) and stock solution of metals (Cu(II), Pb(II), Zn(II) and Cd(II)), the characterisation of biosorbents, experimental conditions, experimental procedures and data analysis. An additional description of each method used for experiments of each adsorbent is also shown in relevant sections of a chapter.

## 3.1 Biosorbents collection and preparation

### 3.1.1 Garden grass (GG)

The garden grass was collected from Oswald Street Reserve, Campsie, NSW, Australia after mowing. It was combined of three types of grasses. The names of grasses were Kikuyu grass (*Pennisetum clandestinum*), Kangaroo grass (*Themeda australis*) and weeping grass (*Microlaena stipoides*). To make it user friendly the grasses were not separated and mixed grasses were used to produce biosorbent. Inert matter was removed from GG and washed with tap water and distilled water to remove dirt. The washed GG were exposed to air for removing water from its surfaces and dried in an oven at 105$^{o}$C for 24 hours. The dried GG were grounded into powder and kept in an air-tight bottle for using in the experiments with required amounts.

### 3.1.2 Maple leaves (ML)

Maple leaves (black maple: *Acer nigrum*) were collected from a local park (Oswald street reserve, Campsie, NSW, Australia). Maple leaves were extensively washed in running tap water to remove dirt and then washed with distilled water three times, and left to air dry for some time to remove free water from the surface. The leaves were chopped into small pieces and were transferred to the oven at 105°C for 24 hours. Dried leaves were crushed, milled into powder and stored in an air-tight container for experimental uses.

### 3.1.3 Banana peels (BP)

Banana peels (*Cavendish bananas*) were collected from kitchens. Collected banana peels were cut it into small pieces (< 5 mm), washed three times with tap water and three times with distilled water to remove external dirt. Wetted banana peels were kept in air for removing the free water from the surface the oven dried for 24 hours at

105°C. The dried BP were then ground into powder and kept in an air-tight bottle prior to the experiments.

### 3.1.4 Cabbage wastes (CW)

The cabbage (*Brassica oleracea*) wastes (leaves and stems) were collected from a local fruit and vegetable market (Campsie Fruits Worlds, Campsie, NSW, Australia). Collected wastes were chopped into small pieces and washed with tap and distilled water for removing dirt. The washed wastes were air dried and transferred to an oven for drying at 105$^{o}$C. The oven dried wastes were ground into powder then kept in an air-tight bottle until used for experiments.

### 3.1.5 Palm oil fruit shells (POFS)

The palm oil (*Elaeis guineensis*) fruit shells were provided from Indonesia. Collected palm oil fruit shells were cut into small pieces (< 5 mm) and washed three times with tap water and distilled water to remove external dirt. The wetted palm oil fruit shells were kept in air for removing free water from the surface and dried in oven for 24 hours at 105°C. The dried palm oil fruit shells were ground into powder (<75 μm) and kept in air-tight bottle prior to the experiments.

## 3.2 Stock solution of metals

### 3.2.1 Copper (II) solution

A stock solution (1000 mg/l) of $Cu^{2+}$ was prepared dissolving 3.802 g of copper nitrate trihydrate ($Cu(NO_3)_2.3H_2O$) in Milli-Q water. Working solution was prepared by diluting stock solution with distilled water.

### 3.2.2 Lead (II) solution

Stock solution of $Pb^{2+}$ was prepared by dissolving 1.598g of $Pb(NO_3)_2$ in one litre of Milli-Q water to achieve a concentration of 1000 mg/l. Used water samples for all experiments were prepared by diluting the stock solution to the pre-determined concentration.

### 3.2.3 Cadmium (II) solution

The stock solution (1000 mg/l) of $Cd^{2+}$ were prepared by dissolving 2.711g of $Cd(NO_3)_2$ in milli-Q water. The working solutions were diluted from the above stock solution and were used throughout the experiment.

### 3.2.4 Zinc (II) solution

Stock solution of $Zn^{2+}$ was prepared by dissolving 4.551 g of $Zn(NO_3)_2.6H_2O$ in one litre of Milli-Q water to achieve concentration of 1000 mg/l. Water samples for all experiments were prepared by diluting the stock solution to the pre-determined concentration.

### 3.2.5 Wastewater and synthetic wastewater

The real-world wastewater was collected from AGL wastewater treatment plant in Olympic Park, Sydney. Initially the metals' content was measured. On the basis of the measured metals content in wastewater, a synthetic wastewater was prepared by mixing Pb(II), Cu(II), Zn(II) and Cd(II) solution into distilled water with the required amount and used for column tests. A stock solution of Pb(II), Cd(II), Cu(II) and Zn(II) was obtained by dissolving the exact quantity necessary of $Pb(NO_3)_2$, $Cd(NO_3)_2$, $Cu(NO_3)_2.3H_2O$ and $Zn(NO_3)_2 \cdot 6H_2O$ in Milli-Q water. The test solutions containing single Pb(II), Cd(II), Cu(II) and Zn(II) ions were prepared by diluting 1000 mg/l of stock solutions of metal ions to the desired concentrations. The ranges of concentrations of metal ions prepared from stock solutions varied between 1 mg/l and 500 mg/l.

## 3.3 Experimental procedures

### 3.3.1 Characterisation of biosorbents

This section describes the methodical techniques that were used for the characterization of adsorbents prepared. The different samples (GG, CW, BP, ML and POFS) were characterized using a number of techniques including: Fourier transform infrared spectroscopy (FTIR), X-ray diffraction (XRD) analysis, scanning electron microscopy (SEM) and Brunauer-Emmet-Teller (BET) surface area analysis.

### 3.3.1.1 SEM

The scanning electron microscope (SEM) uses a focused beam of high-energy electrons to generate a variety of signals at the surface of solid specimens. It is a type of electron microscopy that images the sample surface by scanning it with a high energy beam of electrons in a 'raster' scan pattern. The electrons interact with the atoms that make up the sample producing signals that contain information about the sample's surface topography, composition and other properties such as electrical conductivity.

SEM requires that the samples be conductive for the electron beam to scan the surface and that the electrons have a path to ground (Figure 3.1). Non-conductive solid samples are coated with a layer of conductive material (such as gold, gold/palladium alloy, platinum, tungsten or graphite). An ultra-thin layer of coating is deposited on the sample either by low vacuum sputter-coating or high vacuum evaporation.

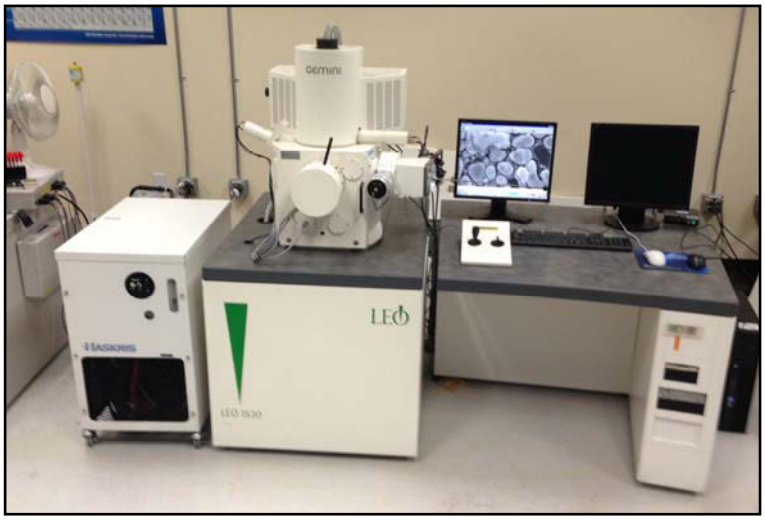


**Figure 3.1 A** typical scanning electron microscope (Gemini, JSM-35CF, UK)

The imaging mode can be based on the detection of secondary electrons or detection of back-scattered electrons. X-rays are also produced by the interaction of electrons with the sample and these can be detected in SEM instruments equipped for energy- or wavelength-dispersive X-ray spectroscopy (Goldstein et al., 2003). The surface mapping of GG, CW, BP, ML and POFS were conducted using an energy dispersive X-ray spectrometer attached to a scanning electron microscope (JEOL, JSM-35CF, UK).

### 3.3.1.2 XRD

In this method, X-rays are diffracted from the planes of a crystal (diffraction analysis). This method depends on the wave character of the X-rays and the regular spacing of the planes in a crystal. Although diffraction methods can be used for quantitative analysis, they are most widely used for qualitative identification of crystalline phases. X-ray powder diffraction analysis is a powerful method by which X-rays of a known wavelength are passed through a sample. X-ray diffraction techniques are based on the elastic scattering of X-rays from structures that have long-range order. The wave nature of the X-rays means that they are diffracted by the lattice of the crystal to give a unique pattern of peaks of 'reflections' at differing angles and of different intensity, just as light can be diffracted by a granting of suitably spaced lines. The diffracted beams from atoms in successive planes cancel unless they are in phase, and the condition for this is given by the Bragg relationship:

$$n\lambda = 2d\sin\theta \qquad (3.1)$$

where, λ is the wavelength of the X-rays, d is the distance between different planes of atoms in the crystal lattice, θ is the angle of diffraction and n is a constant. The X-ray detector moves around the sample and measures the intensity of these peaks and the position of these peaks (diffraction angle 2θ). The highest peak is defined as the 100% peak and the intensity of all the other peaks are measured as a percentage of the 100% peak. Materials that do not have long range order may also be studied by scattering methods that rely on elastic scattering of monochromatic X-rays. The X-ray techniques that can be employed include: X-ray reflectivity, wide-angle and small-angle X-ray scattering. SAXS is a small-angle scattering technique where the elastic scattering of X-rays (0.1... 0.2 nm) by a sample which has inhomogeneities in the nanometre range is recorded at very low angles (typically 0.1 - 10°). This angular range contains information about the shape and size of macromolecules, characteristic distances of partially ordered materials, pore sizes, and other data. SAXS is capable of delivering structural information of macromolecules between 5 and 25 nm, of repeat distances in partially ordered systems of up to 150 nm (Whiston, 1987). The elemental mapping of GG, CW, BP, ML and POFS was conducted using an energy dispersive X-ray spectrometer attached to a scanning electron microscope (JEOL, JSM-35CF, UK).

### 3.3.1.3 FTIR

Fourier transform infra-red (FTIR) technique is based on the excitation of molecular vibrations by light absorption. It is widely used in the determination of structure and identification of both organic and inorganic compounds. It is mainly used in the identification of functional groups present in a given sample. In infrared spectroscopy, infrared radiation is passed through a sample. Some of the infrared radiation is absorbed by the sample and some is transmitted. The resulting spectrum represents the molecular absorption and transmission, creating a molecular fingerprint of the sample. Like a fingerprint, no two unique molecular structures produce the same infrared spectrum. This makes FTIR spectroscopy useful for several types of analyses, including: identification of an unknown material, quality control of samples and the determination of amounts of components in a mixture.

The sample analysis process involves the emission of infrared radiation from a black body source. The beam of radiation passes through an aperture which controls the amount of energy presented to the sample and ultimately to the detector. The beam enters the interferometer where the 'spectral encoding' takes place. The resulting interferogram signal then exits the interferometer. The beam enters the sample compartment where it is transmitted through or reflected off the surface of the sample, depending on the type of analysis being carried out. This is where specific frequencies of energy, uniquely characteristic of the sample, are absorbed. The beam finally passes through to the detector for final measurement. The detectors used are specially designed to measure the special interferogram signal (Pavia et al., 2001). FTIR spectroscopy was employed in this study for the analysis of raw samples (GG, CW, BP, ML and POFS) as well as the analysis of the various adsorbent materials prepared in this work. Fourier Transform Infrared spectra (FTIR) of GG, CW, BP, ML and POFS were prepared by SHIMADZU FTIR 8400S (Kyoto, Japan) as KBr discs were recorded in a Perkin-Elmer Spectrum.

### 3.3.1.4 BET analysis

This technique was named after its three inventors: S. Brunauer, P. H. Emmet and E. Teller (BET). This method was devised in 1938 as they were working on ammonia catalysts. It is the first method developed to compute the specific surface area of finely

divided and porous materials. This method is useful for the analysis of surface area from pharmaceuticals, catalysts, projectile propellants, medical implants, filters, cements and adsorbents particles. The BET method is based on the adsorption of gas (normally $N_2$) on a surface. Adsorption is a consequence of surface energy change and it is minimized in the bulk when every atom or molecule is surrounded by neighbours. The amount of gas adsorbed at a given pressure allows for the determination of surface area.

In this a gas sorption experiment is done for measuring the specific area. Before that the material is heated and degassed by vacuum force or inert gas purging to remove adsorbed foreign molecules. The sample material is placed in a vacuum chamber at a constant and very low temperature (usually at -195.6 °C which is the temperature of liquid nitrogen), and subjected to a wide range of pressures, to generate adsorption and desorption isotherms. Controlled rates of an inert gas, such as nitrogen, krypton, or argon, are launched and the gas is adsorbed, or alternatively, withdrawn and desorbed. The amounts of gas molecules adsorbed or desorbed are determined by the pressure variations due to the adsorption or desorption of the gas molecules by the adsorbent material. Various amounts of gas molecules will be adsorbed or desorbed at different doses of the gas (the adsorbate). Knowing the area occupied by one adsorbate molecule, A (for example, A = 16.2 $Å^2$ for nitrogen), and using an adsorption model, the total surface area of the material can be determined (Mahboub et al., 2006).

A theory of physical adsorption of gas molecules on a solid surface (Brunauer et al., 1938) is considered as the basis for the analysis technique of specific surface area of a material. The technique is known as BET surface area measurement which is taken from the first initials of their family names of Stephen Brunauer, Paul Hugh Emmett, and Edward Teller.

An extended form of Langmuir theory is used for BET specific surface measurement. It is a theory for monolayer molecular adsorption to multilayer adsorption with the following hypotheses: (i) gas molecules physically adsorb on a solid in layers infinitely; (ii) there is no interaction between each adsorption layer; and (iii) the

Langmuir theory can be applied to each layer. The resulting BET equation is expressed by (1):

$$\frac{1}{v\left[\left(\frac{p_o}{p}\right)-1\right]}=\frac{c-1}{v_m c}\left(\frac{p}{p_o}\right)+\frac{1}{v_m c} \qquad (3.2)$$

where, p and $p_0$ are the equilibrium and the saturation pressure of adsorbates at the temperature of adsorption, v is the adsorbed gas quantity (for example, in volume units), and $v_m$ is the monolayer adsorbed gas quantity. c is the BET constant, which is expressed by (2):

$$c=\exp\left(\frac{E_1-E_L}{RT}\right) \qquad (3.3)$$

$E_1$ is the heat of adsorption for the first layer, and $E_L$ is that for the second and higher layers and is equal to the heat of liquefaction.

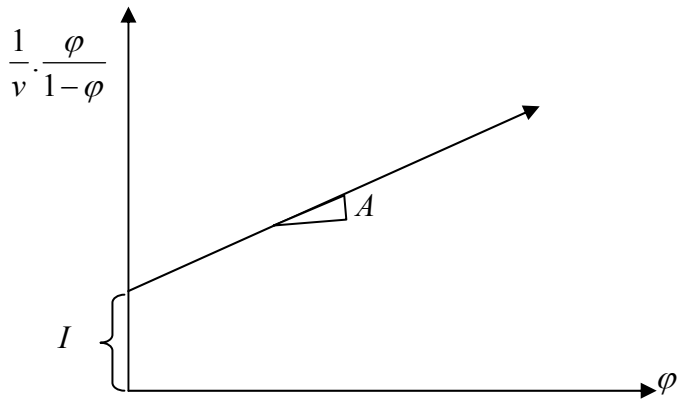


**Figure 3.2** Adsorption isotherm plot for BET surface area calculation

Equation (3.2) is an adsorption isotherm equation and can be plotted as a straight line with '$1/v[(p_o/p)-1]$' on the Y-axis and '$\varphi = p/p_o$' on the X-axis according to experimental results. This plot is called a BET plot. The linear relationship of this equation is maintained only in the range of $0.05<p/p_o<0.35$ The value of the slope A and the Y-intercept I of the line are used to calculate the monolayer adsorbed gas quantity $v_m$ and the BET constant c. The following equations can be used:

$$v_m=\frac{1}{A+I} \qquad (3.4)$$

$$c = 1 + \frac{A}{I} \tag{3.5}$$

The BET method is widely used in surface science for the calculation of surface areas of solids by physical adsorption of gas molecules. A total surface area $S_{total}$ and a specific surface area S are evaluated by the following equations:

$$S_{BET,total} = \frac{(v_m N_s)}{V} \tag{3.6}$$

where, $v_m$ is in units of volume which are also the units of the molar volume of the adsorbate gas,

$$S_{BET} = \frac{S_{total}}{m} \tag{3.7}$$

where,

$N_s$ = Avogadro's number,

A = adsorption cross section of the adsorbing species,

$v_m$ = molar volume of adsorbate gas

m = mass of adsorbent (in g)

$N_A$ is Avogadro's number and A is the area occupied by the adsorbed species. The specific surface area that can be determined by gas sorption ranges from 0.01 to over 2000 $m^2/g$. Determination of pore volume and pore size distribution of porous materials can be made from the $N_2$ gas adsorption/desorption isotherm using an assessment model, suitable for the shape and structure of the pores. The range of pore sizes that can be measured using gas sorption is from a few Ångstroms up to about half a micron (Sing et al., 1982). The BET surface areas of biosorbents (GG, CW, BP, ML and POFS) were determined from $N_2$ adsorption isotherm by Nano Porosity System (Micrometrics ASAP 2020, Mirae SI, Korea).

## 3.3.2 Experimental conditions

### 3.3.2.1 Effect of pH

The optimum pH for adsorption for adsorption of Cu(II), Pb(II), Zn(II) and Cd(II) by the biosorbents (GG, CW, BP, ML and POFS) were determined experimentally. Metals (Cu(II), Pb(II), Zn(II) and Cd(II)) solutions with the concentration of 10 mg/l were prepared in distilled water from the stock solutions. Samples of 100 ml from

these solutions were poured into 8 Erlenmeyer flasks. The initial pH of the samples was adjusted to various values in the range of 1.18 to 8.0 and each sample was adjusted using either 0.1N $H_2SO_4$ or NaOH solution. Subsequently, 0.5 g of biosorbents (GG, CW, BP, ML and POFS) was added to each flask. Equilibrium condition for heavy metal adsorption was obtained after 2-8 hours of agitation at room temperature and 120 rpm. Samples were taken after filtering the samples by Whatman™ filter (GF/C-47mm ϕ circle, GE Healthcare, Buckinghamshire, UK) after equilibrium was achieved and heavy metal concentrations were analysed by using atomic adsorption spectrometer. A step by step methodology of this study is shown in Figure 3.3. The optimum pH for each metal's adsorption was adopted from maximum metal adsorption by the biosorbents for the next experiments.

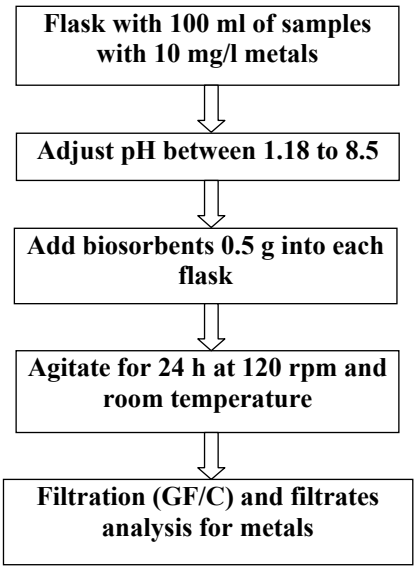


**Figure 3.3** Flow diagram of experimental setup for optimisation of pH

### 3.3.2.2 Effect of biosorbents doses

To investigate the effect of biosorbent doses, 100 ml of water samples at pH 6-6.5 with 10 mg/l of initial metals [Cu(II), Pb(II), Zn(II) and Cd(II)] concentration were stirred in a 250 ml Erlenmeyer. Doses of specified biosorbent (GG, CW, BP, ML and POFS) (between 0.01g-1g per 100 ml water) were added to each Erlenmeyer and shaken at 120 rpm for 2-8 hours. At the end of the shaking period, the Erlenmeyers were removed from the shaker and the contents allowed to settle for 5 minutes and then filtered through Whatman™ filter paper. The filtrates were then separately analysed

for residual concentrations of specific metal (Cu(II), Pb(II), Zn(II) and Cd(II)) according to standard methods as specified in the manual of spectrophotometer operation (AAS, Analytic Jena ). The optimum biosorbent doses were accepted in this study for the next experiment.

### 3.3.2.3 Effect of stirring rate

Studies on the effect of stirring rate on the adsorption of metals' ions (Cu(II), Pb(II), Zn(II) and Cd(II)) onto biosorbents (GG, CW, BP, ML and POFS) were conducted by varying speeds of 30-200 rpm (Figure 3.4) at the optimum adsorbent doses of 0.5g per 100 ml of water at room temperature for 2-8 hours. The other test conditions remained same as in the effect of adsorbent dose. After filtering, the water samples were analysed in term of metals. The optimum stirring rate was adopted in this study.

### 3.3.2.4 Effect of contact time

The effect of contact time (2-8 hours) on adsorption of metals (Cu(II), Pb(II), Zn(II) and Cd(II)) onto biosorbents (GG, CW, BP, ML and POFS) were studied at the optimum stirring rate, initial metals concentration (10-100 mg/l) and adsorbent dose. The experimental procedure was the same as in the effect of adsorbent dose except that the beakers were removed from the batch apparatus in the course of the experiment at specified intervals (between 2-8 hours) and analysed for residual concentrations of metals. The optimum contact time was implemented in this study for the next experiments.

### 3.3.2.5 Effect of initial metal concentrations

The effect of initial metal concentration (Cu(II), Pb(II), Zn(II) and Cd(II)) on adsorption onto biosorbents (GG, CW, BP, ML and POFS) were examined with optimum pH, doses and contact time for 1-10 mg/l metals concentration in 100 ml water. After filtering the water samples were analysed for residual concentrations of metals. The optimum concentrations of metals were taken on in this study during other experiments.

### 3.3.2.6 Effect of particles sizes

The grounded powder of used biosorbents (GG, CW, BP, ML and POFS) were graded with standard sieves to six particles sizes (600, 420, 300, 150, 75 and < 75 μm).

Biosorbents (0.5g) from each graded size were added to six Erlenmeyer with 100 ml water with optimum metals' concentration, pH, stirring speed and contact time. The residual concentrations of metals in the water samples were analysed after filtration by AAS.

#### 3.3.2.7 Effect of temperatures

To determine the thermodynamic feasibility and the thermal effects on the adsorption, temperature variation experiments were conducted at 30, 40, 50 and 70°C, with an initial metals concentration of 1-200 mg/l and optimum pH, contact time and doses. The residual concentrations of metals in the water samples were analysed after filtration by AAS.

### 3.3.3 Desorption experiments

Desorption of adsorbed metals (Cu(II), Pb(II), Zn(II) and Cd(II)) from exhausted biosorbents (GG, CW, BP, ML and POFS) were studied with 8 types of solvent including tap water, milli-Q water, distilled water, 0.1N $H_2SO_4$, 0.1N HCl, 0.1N $HNO_3$, 0.1N NaOH and 0.1 N $CH_3COOH$. Pre-adsorbed biosorbents (0.5g) were taken in 100 ml of above mentioned medium and shaken at 120 rpm for 6 hr. After filtering the eluent, the residual metals concentration were analysed by AAS. The eluted biosorbent was washed repeatedly with Milli-Q water to remove any residual desorbing solution and placed into metal containing water for the next adsorption cycle.

### 3.3.4 Adsorption and desorption equilibriums

The experiments for equilibrium isotherm for adsorption of metals (Cu(II), Pb(II), Zn(II) and Cd(II)) onto biosorbents (GG, CW, BP, ML and POFS) were carried out at different initial concentrations of metals (1-500 mg/l) at optimum experiments' conditions. Powdered biosorbents of 0.05, 0.5 and 1 g was thoroughly mixed with 100 ml water contain pre-determined metals concentration. Sixteen Erlenmeyers were put in a rotary shaker (120 rpm) for 2-8 hours at room temperature. Reaction mixtures were then filtered and analysed with AAS for metals. Adsorption capacities ($q_e$) at specified time (t) were calculated as:

$$q_{e\text{-}A} = \frac{V(C_o - C_e)}{m} \qquad (3.8)$$

where, $q_{e\text{-}A}$, is the equilibrium adsorption capacity (mg/g); $C_o$ and $C_e$, the initial and equilibrium metals concentrations in the water (mg/l), respectively; V, volume of used water (l); and m, the mass of used bioadsorbent (g).


**Figure 3.4** A typical platform shaker where all the batch experiments are conducted

The filtrate powder of biosorbents were washed with Milli-Q water to remove any residual desorbing metals and used for desorption equilibrium in 100 ml of the most suitable eluent found from section 3.3.4 with similar process of adsorption equilibrium. Desorption capacities ($q_e$) at specified time (t) were calculated as:

$$q_{e\text{-}D} = \frac{V(C_o - C_e)}{m} \qquad (3.9)$$

where, $q_{e\text{-}D}$, is the desorption capacity (mg/g); $C_o$ and $C_e$, the initial metals on biosorbent and equilibrium metals concentrations in the eluent (mg/l), respectively; V, volume of used eluent (l); and m, the mass of used bioadsorbent (g).

### 3.3.5 Adsorption and desorption kinetics

Time dependent experiments for adsorption (kinetics) of metals (Cu(II), Pb(II), Zn(II) and Cd(II)) onto biosorbents (GG, CW, BP, ML and POFS) were performed in 1l water at 120 rpm at room temperature. Three metals concentrations (10, 50 and 100 mg/l) were selected for kinetics adsorptions. Powdered biosorbents (5g) were thoroughly

mixed with water and 5 ml of mixed water sample were collected for a predetermined period (Figure 3.5). These processes were continued for 2-4 hours depending upon biosorbent type and optimum contact time. Collected water was filtered by Whatman™ GF/C-47mm ϕ circle (GE Healthcare, Buckinghamshire, UK) filter and analysed with AAS (Contra®AA 300, Analytikjena, Germany) in terms of metals. The metals concentration retained in the bioadsorbent phase ($q_{t\text{-}A,}$ mg/g) was calculated by the following expression:

$$q_{t\text{-}A} = \frac{(C_o - C_t)V}{m} \qquad (3.10)$$

where: $C_o$ and $C_t$ are the initial and concentrations of the copper at 't' time in the water (mg/l), 'V' is the water volume (l) and m is the mass of the biosorbent (g).


**Figure 3.5** A typical flocculator where all kinetics adsorption and desorption experiments conducted

The filtrate powder of biosorbents were washed with Milli-Q water to remove any residual desorbed metals and used for desorption kinetics in 1L of the most suitable eluent found from section 3.3.4 with similar process of adsorption kinetics. The metals desorbed from bioadsorbent phase ($q_{t\text{-}D,}$ mg/g) were calculated by the following expression:

$$q_{t\text{-}D} = \frac{(C_o - C_t)V}{m} \qquad (3.11)$$

where: $C_o$ and $C_t$ are the initial metals on biosorbents and concentrations of the metals at 't' time in the eluent (mg/l), 'V' is the eluent volume (l) and m is the mass of the biosorbent (g).

### 3.3.6 Binary, ternary and quaternary adsorption

For binary studies, the desired combinations of Cu-Pb, Pb-Cd, Cd-Zn, Cd-Cu, Cu-Zn and Pb-Zn ions were obtained by diluting 1000 mg/l of stock solutions of metal ions and mixing them in the test medium. Before mixing the biosorbents, the pH of each test solution was adjusted to the required value with 0.1N $H_2SO_4$/NaOH. Similarly, the ternary solution of Pb-Cd-Zn, Cu-Pb-Cd, Cu-Pb-Zn and Cu-Cd-Zn were prepared and the quaternary solution of Cu-Pb-Cd-Zn was prepared with the required dilution from stock solutions. The binary, ternary and quaternary adsorptions were conducted at optimum experimental conditions. The concentrations of heavy metal ions remained in solution were determined by Atomic Adsorption Spectroscopy (AAS) after samples were filtered by Whatman filter. The measurements methods for multiple metals were devised for binary, ternary and quaternary systems and used for the specific tests in AAS.

### 3.3.7 Lab-scale column experiments toward the application

Fixed bed column experiments were conducted using borosilicate glass columns of 2 cm internal diameter and 54 cm length. The column was packed with biosorbents (GG, CW, BP, ML and POFS) between two supporting layers of mesh and cotton wool to prevent floating of the biosorbent from the outlet. The schematic diagram of the column is shown in Fig.3.6. The column studies were conducted to evaluate the effects of various parameters viz., initial metals concentration, the flow rate, and the bed depth.

The metals bearing water was passed through the bed in the up-flow mode at a different loading (volumetric flow rate) rate of 2.07, 3.89 and 4.04 l/h with bed height and metals concentration of 2.25 cm and 10 mg/l, respectively. The bed depths were selected at 2.25 cm, 4.5 cm and 9 cm. For the studies with different bed depths, the initial metals concentration and loading rate used was 10 mg/l and 2.07 l/h. The

column was also run with higher metals concentrations of 5 mg/l and 20 mg/l keeping the bed depth of 2.25 cm and the flow rate 2.07 l/h.

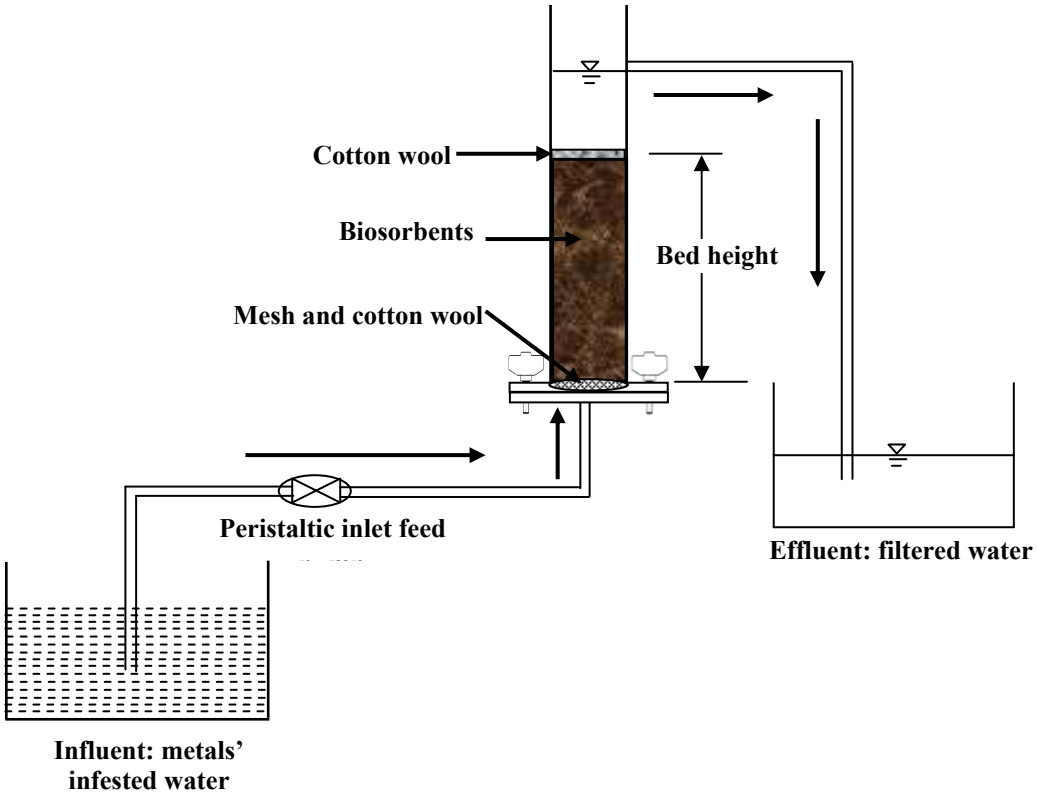


**Figure 3.6** The schematic diagram of the constructed column with all components

### 3.3.8 Flame atomic absorption spectroscopy

The quantitative analysis of heavy metals during adsorption studies were measured by Atomic Adsorption Spectroscopy (AAS) (Contra®AA 300, Analytikjena, Germany). The techniques used for the quantitative analysis of heavy metals are discussed in this section. Flame atomic absorption spectroscopy (FAAS) works based on the theory of the Beer-Lambert law. In quantitative determinations using FAAS, combustion flames provide a means of converting analytes (metals) in solution to atoms in the vapour phase freed of their chemical surroundings. These free atoms are then transformed into excited electronic states by absorption of radiant energy from an external source. The flame that contains the free atoms serves as a sample cell. The free atoms absorb radiation focussed on the cell from an external source to the flame. The incident radiation absorbed by the free atoms in moving from the ground state to an excited

state provides the analytical data (Beaty and Kerber; Wright et al., 1996). The sample is sprayed into the flame as a form of aerosol where the analytes (metals) ions are converted into free atoms. Once formed, the free atoms absorb radiation of a specific wavelength from an external source (hollow cathode lamp) and the amount of radiation absorbed is detected and determined by FAAS.

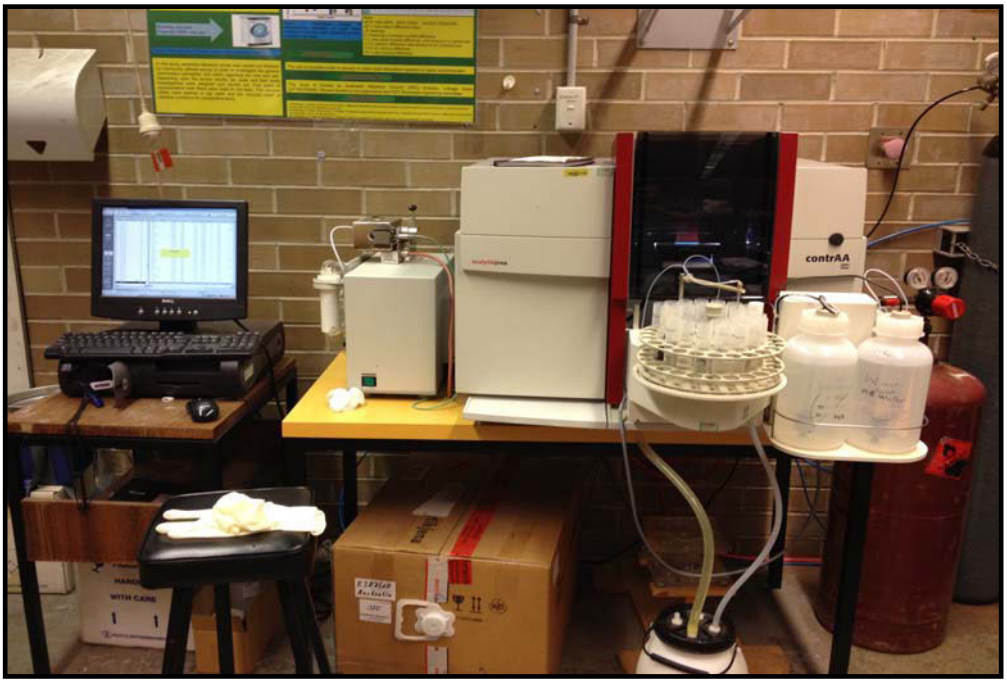


**Figure 3.7** An Atomic Adsorption Spectroscopy (AAS) (Contra®AA 300, Analytikjena, Germany)

As the number of atoms in the light path increases, the amount of light absorbed increases in a predictable way. Measuring the amount of light absorbed allows a quantitative determination of the amount of analyte element present in solution. The ease and speed at which precise and accurate measurements can be made with this technique have made FAAS one of the most popular methods for the determination of metals. The work on the adsorption of heavy metals carried out in this study during the evaluation of the various adsorbents prepared has employed atomic absorption spectroscopy. The concentrations of heavy metals' ions remained in solution were determined by Atomic Adsorption Spectroscopy (AAS) (Contra®AA 300, Analytikjena, Germany) (Figure 3.7) after samples were filtered with Whatman™ GF/C-47mm ϕ circle (GE Healthcare, Buckinghamshire, UK). The measurements

methods for multiple metals were devised for single, binary, ternary and quaternary systems in AAS and used for the specific tests.

## 3.4 Data analysis

The equilibrium data for adsorption and desorption are fitted with different non-linear forms of isotherm models by modelling with MS Excel and MATLAB® (R2010b) programming (Appendices I and II). All equilibrium model parameters were computed, evaluated and optimised by non-linear analyses. The evaluation of fitness of the model equations with experimental data were signified by the coefficient of determination ($R^2$), non-linear error functions: the residual root mean square error (RMSE) and the chi-square test ($\chi^2$) (Hossain et al., 2012). The standard equations are as follows:

$$R^2 = \frac{1 - \sum_{n=1}^{n} (q_{e.n} - q_{m.n})^2}{\sum_{n=1}^{n} (q_{e.n} - \overline{q_{e.n}})^2} \quad (3.12)$$

$$RMSE = \sqrt{\frac{1}{n-1} \sum_{n=1}^{n} (q_{e.n} - q_{m.n})^2} \quad (3.13)$$

$$\chi^2 = \sum_{n=1}^{n} \frac{(q_{e.n} - q_{m.n})^2}{q_{e.n}} \quad (3.14)$$

where, '$q_e$' is the equilibrium sorption capacity found from the batch experiment, '$q_m$' is the prediction from the isotherm model for corresponding to '$C_e$' and 'n' is the number of observations. The small values of RMSE and $\chi^2$ indicate the better model fitting and the similarity of model with the experimental data respectively (Ho et al., 2002).

The kinetics data for adsorption and desorption were fitted to the different kinetics models. The parameters of the models are optimised by non-linear analyses with MS Excel and MATLAB® (R2010b) programming (Appendix I and Appendix II). Along with the coefficient of determination ($R^2$), the degree of fitness of kinetics models were judged by two non-linear errors: the normalized standard deviation (NSD) and average relative error (ARE)(Hossain et al., 2012). The equations are defined as:

$$NSD = 100 \times \sqrt{\frac{1}{N-1}\sum_{i=1}^{N}\left[\frac{q_{t.e} - q_{t.m}}{q_{t.e}}\right]_i}^2 \quad (3.15)$$

$$ARE = \frac{100}{N}\sum_{i=1}^{N}\left[\frac{q_{t.e} - q_{t.m}}{q_{t.e}}\right]_i \quad (3.16)$$

where, $q_{t.e}$ and $q_{t.m}$ (mg/g) are experimental ('e') and model ('m') predicted amount of metals adsorbed onto biosorbents at time 't' and 'N' is the number of observations made. The smaller values of NSD and ARE will indicate the better fitted model.

Faculty of Engineering and Information Technology
University of Technology, Sydney (UTS)

# Chapter 4

# Biosorption of Cu(II), Pb(II), Cd(II) and Zn(II) from aqueous solution onto garden grass

## 4.1 Introduction

Biosorption is the uptake process that naturally takes place in metal substances or metallic species by biological means. Biosorbents come under the following categories: bacteria, fungi, algae, industrial waste, agricultural waste and other polysaccharide materials. Among them, agricultural wastes have the most potent source of producing biosorbents as they have no-known prominent utilization except composting. Biosorbents production may add value to the agro-waste and eventually reduced the agro-wastes management problems all over the world. Agro-materials are usually composed of lignin and cellulose as major constituents. In addition, this may also include other polar functional groups of lignin which includes alcohols, aldehydes, ketones, carboxylic, phenolic and ether groups (Lu et al., 2010). These groups have the ability to some extent bind heavy metals by giving of an electron pair from these groups, thus forming complexes with metal ions in the solution. As a result , different biosorbents were developed for metals removal from aqueous solution such as Rubber wood dust (Kalavathy et al., 2005), Peanut shells (Wilson et al., 2006), *Ceiba pentandra* hulls (Madhava Rao et al., 2006), Hazelnut husk (Madhava Rao et al., 2006), Tree fern (Ho et al., 2002b), Irish peat moss (Sen Gupta et al., 2009), Cellulose pulp waste (Ulmanu et al., 2003), Compost (Ulmanu et al., 2003), Wheat bran (Ozer et al., 2004) and Macro algae (Cochrane et al., 2006). Overall, all types of biomaterials have shown good biosorption capacities towards cations.

Typically, grass is abandoned after mowing garden lawns and parks. Several of tons of garden grass all over Australia are mowed and dumped by the City Corporation. A certain procedure was taken to prepare biosorbents from this readily and considerably available GG. First and foremost, this research was used for Cu(II), Pb(II), Cd(II) and Zn(II) removals from aqueous solutions and also used for desorption studies towards the possible regeneration of GG.

The main objectives of this work are: (i) to characterize the physicochemical parameters of GG such as specific surface area, surface morphology and structure, functional groups; (ii) to evaluate the effects of experimental conditions on Cu(II), Pb(II), Zn(II) and Cd(II) removals such as pH, biosorbents dose, rpm, contact time, initial metals concentration, particle sizes and temperature; (iii) to regenerate biosorbents using various solvents; (iv) to determine the maximum biosorption and desorption capacities

of GG based on several isotherm models; (v) to discuss the biosorption and desorption kinetics of metals onto GG, and (vi) to evaluate the antagonism of metals in multi-metals system.

## 4.2 Results and discussion

### 4.2.1 Characterisation of garden grass

To determine the characteristics of a biosorbent before using is essential in context selection for a particular heavy- metal removal from water and wastewater. The characterisation of garden grass (GG) was evaluated by SEM, XRD, FTIR and BET surface area techniques. The following sections are the findings of the GG characterisation.

#### 4.2.1.1 Surface structure

The surface structure of GG was examined by SEM as the procedure described in Chapter 3, section 3.3.1.1. The micrograph prepared by SEM showed in Figure 4.1 and it revealed some significant feature of the structure.

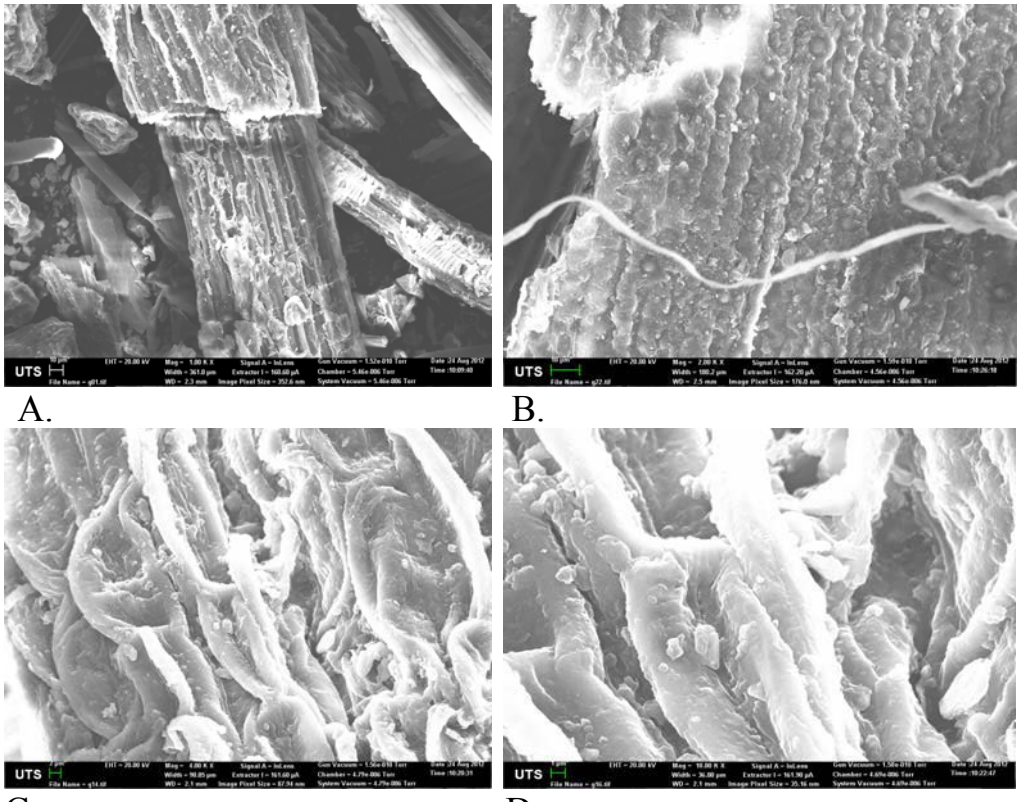


**Figure 4.1** SEM micrograph of garden grass with different magnifications (A. 1KX, B. 2 KX, C. 4 KX and D. 10 KX)

GG has a rough surface with heterogeneous, irregular, tubular and porous cavities (Figure 4.1A) (Lü et al., 2010). In higher magnification (Figure 4.1B), the surface of GG's particles is formed with multiple porous layers. In 4KX and 10 KX magnifications, the porous surfaces consisted of nodule -like thread and have formed hollow cavities (Chen et al., 2011). It indicates the high surface area and pore volume of the GG (Chen et al., 2011). It also disclosed the high binding sites. Therefore, it is presumed that, there is a good possibility for a metal to be trapped and adsorbed into the binding sites of the surface.

#### 4.2.1.2 X-ray mapping

The exhausted GG (with copper) were examined by SEM and a X-ray mapping was prepared and showed in Figure 4.2. A significant visual change was noticed on the surface of GG exhausted with copper compare to the normal GG SEM-image. The surface of biosorbents (Figure 4.2 (a)) is irregular, tubular and porous, and indicates the presence of high surface area and pore volume (Chen et al., 2011).

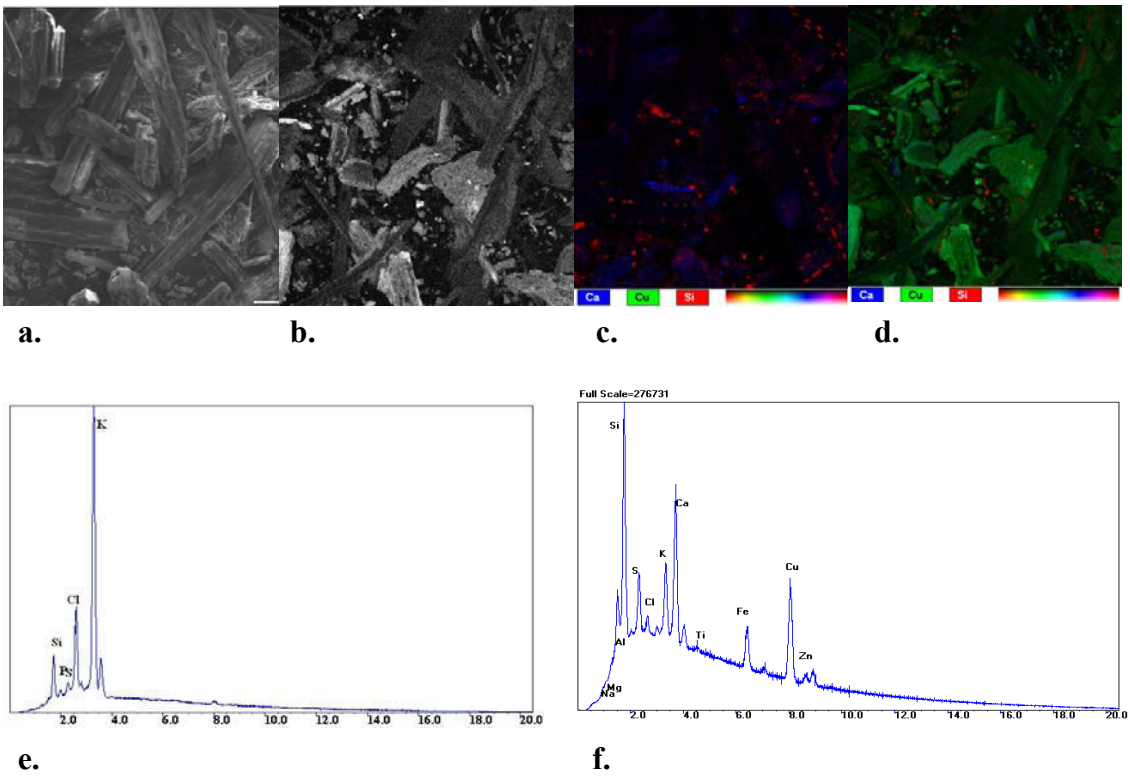


**Figure 4.2** X-ray mapping of (a) Garden grass (b) Garden grass exhausted with copper (c) Colour mapping of garden grass (d) Colour mapping of garden grass exhausted with copper (e) Spectra of garden grass (f) Spectra of garden grass exhausted with copper

These large pores and surface areas are important factors that could lead to high uptakes of Cu(II) in this study. As compared to the images of Figures 4.2 (a) and (b), significant visual changes were noticed on the surface of biosorbents exhausted with Cu(II) (Figure 4.2 (b)). The white dots are the adsorbed copper on to the surface of biosorbents (Figure 4.2 (b)) and showed the affinity of copper onto the garden grass. The presence of adsorbed copper becomes clear from elemental X-ray mapping of exhausted GG (Figure 4.2.e) compare to the normal GG spectra GG (Figure 3.f). The spectra also showed major constituents of GG, which are K, Ca, Mg, Fe and S.

The X-ray mapping of GG exhausted with Pb(II), Cd(II) and Zn(II) ions are presented in the micrograph in Figure 4.3 (a, b and c). Similar to the Cu(II) biosorption, Pb(II), Cd(II) and Zn(II) ions are visible in the micrograph as white dots. It is noticeable that Pb(II) and Cd(II) ions are adsorbed more than Zn(II) ions as it appeared more dots in Figure 4.3(a) and Figure 4.3(b) than Figure 4.3(c). From this, it is predicted that garden grass can adsorb more Pb(II) and Cd(II) ions than Zn(II) ions.

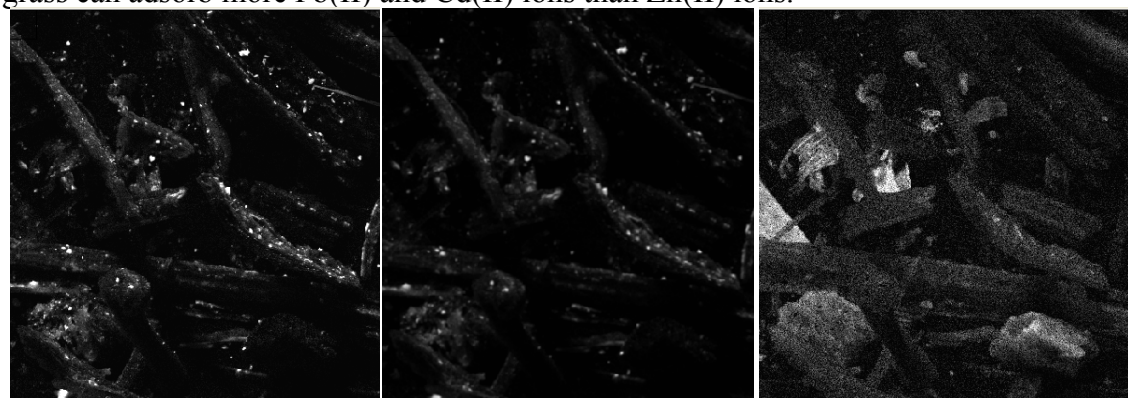

**a.** **b.** **c.**

**Figure 4.3** X-ray mapping micrograph of GG exhausted with metals
(a. Exhausted with Pb(II), b. Exhausted with Cd(II) and c. Exhausted with Zn(II))

#### 4.2.1.3 Functional groups

Biosorbents consist of complex organic and inorganic materials such as proteins, lipids, carbohydrate polymers and sometimes metals. Chemisorptions and ions exchange mostly depend on the available functional groups in a particular biosorbent and eventually metals biosorption depend on it. Carbon-oxygen and carbon bonds are the attracting and stimulating bond of metals biosorption (Ricordel et al., 2001). Functional groups of GG were discovered by FTIR spectra and showed in Figure 4.4. The FTIR of GG was prepared according to the procedure mentioned in Chapter 3, Section 3.3.1.3. This FTIR spectrum showed that there were several functional groups detected on the

surface of GG. The broad peaks detected in spectra were lied between 3640 to 3610 $cm^{-1}$ and 3500-3200 $cm^{-1}$ band which is O-H stretch for free hydroxyl and H-bonded groups (Lü et al., 2010). Other broad peak of the stretch were obtained between 3000 to 2850 $cm^{-1}$ and 1000-650 $cm^{-1}$ band which are C-H stretch and =C-H bend for alkanes (Lu et al., 2010; Pons et al., 2004). Carboxylic acids groups (C=O stretch and C-O stretch) were found for 1760-1665 $cm^{-1}$ and 1320-1000 $cm^{-1}$ band (Pons et al., 2004). Amines group was found between 1650-1580 $cm^{-1}$ band. Thus, hydroxyl and Carboxyl groups of GG could be very effective for capturing cations like Pb(II), Cu(II), Cd(II) and Zn(II) ions (Sheng et al., 2004).

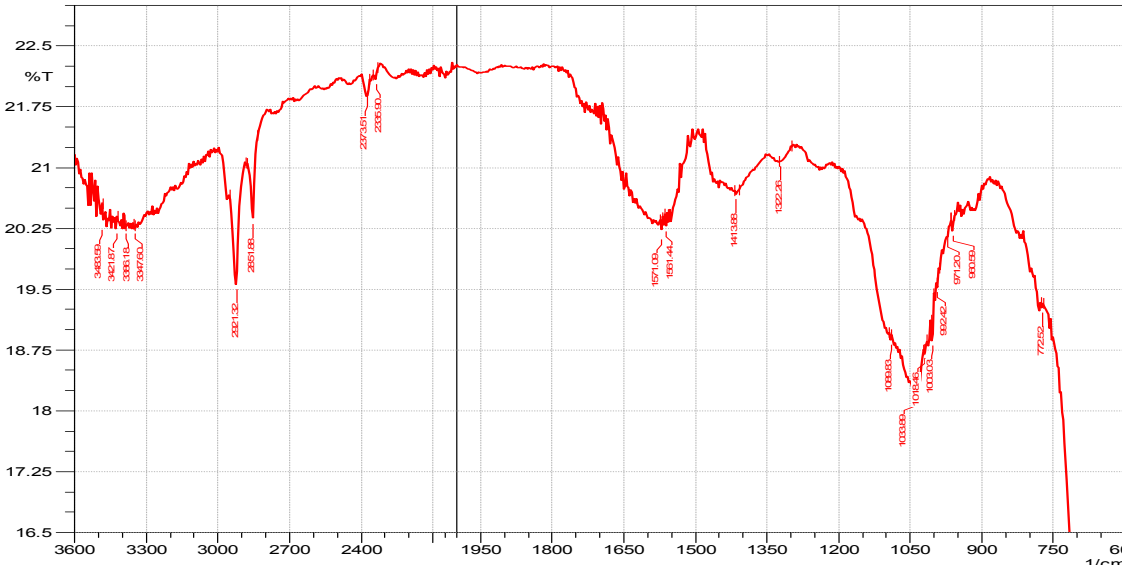


**Figure 4.4** The FTIR spectra with predicted peaks for functional groups of garden grass

#### 4.2.1.4 Specific surface area

The metal -biosorption capacity, surface properties and active functional groups of any biosorbents could be explored from characterisation. Surface properties of GG were examined through BET. The surface properties of GG was measured and tabulated in Table 4.1. Green grass (GG) has the BET surface area of 21.28 $m^2/g$ which was comparable with the biosorbents produced from agro wastes and the use of metal removal from aqueous solution (Hossain et al., 2012). These biosorbents have noticeable micropore and mesopore area with a magnitude of 6.07$m^2/g$ and 21.17$m^2/g$. All pores of GG are mesopore (100%) and total pore volume was 0.03$cm^3/g$. In addition, the mean micropore and mesopore sizes of the GG's powder were found to be 8.71 and 40.18 Å, respectively, suggesting that this biosorbent has fallen within the region of mesopore based on IUPAC-classification (Arias et al., 2005). The high pore area, pore volume and pore sizes indicated the numerous binding sites on the GG surfaces (Lu et al., 2010).

**Table 4.1** Surface parameters of garden grass from BET test

| Parameter of garden grass | Methods | Values |
|---|---|---|
| 1. Surface area | BET surface area | 21.28 $m^2/g$ |
| | Langmuir surface area | -37.42 $m^2/g$ |
| 2. Pore Area | | |
| i. Micropore area | DR method | 6.07 $m^2/g$ |
| | t-plot (statistical thickness = 3.50≈7.00) | 0.12 $m^2/g$ |
| | Horvath-Kawazoe method | 1.11 $m^2/g$ |
| ii. Mesopore area | BJH biosorption | 21.17 $m^2/g$ |
| | BJH desorption | 24.34 $m^2/g$ |
| 3. Pore volume | | |
| i. Micropore volume | DR method | 0.00 $cm^3/g$ |
| | t-plot (statistical thickness = 3.50≈7.00) | -0.01 $cm^3/g$ |
| | Horvath-Kawazoe method | 0.00 $cm^3/g$ |
| ii. Mesopore volume | BJH biosorption | 0.03 $cm^3/g$ |
| | BJH desorption | 0.03 $cm^3/g$ |
| 4. Pore size | | |
| i. Micropore size | DR method | 8.71 Å |
| | t-plot (statistical thickness = 3.50≈7.00) | -1069.53 Å |
| | Horvath-Kawazoe method | 14.98 Å |
| ii. Mesopore size | BJH biosorption | 40.18 Å |
| | BJH desorption | 37.23 Å |

## 4.2.2 Affecting factors on biosorptions

### 4.2.2.1 Effect of pH

It is commonly understandable that the pH of water affects the metal-biosorbent interaction, solubility of the metal ions, and the charge of the functional groups of biosorbent so as pH is one of the most important parameters for any biosorption process (Memon et al., 2008). It is theoretically and experimentally proved that the Cu(II), Cd(II), Zn(II) and Pb(II) metals precipitates as a form of $Cu(OH)_2$, $Cd(OH)_2$, $Zn(OH)_2$ and $Pb(OH)_2$ in aqueous at the pH of 7.36, 9.08, 10.1 and 7.18 respectively (Kusvuran et al., 2012; Sampaio et al., 2009). In this study, biosorption experiments were carried out between the pH of 2 and 8 (Figure 4.5). A negative charge of any biosorbent (in aqueous solution) can be correlated with metal biosorption and it varies with water pH depending on isoelectric pH of the biosorbent. In general, the biosorption capacity of garden grass increases with the increase of pH under some limited conditions such as constant temperature and out of range metal precipitate pH with hydroxide anion (Conrad and Bruun Hansen, 2007). In this study, the biosorption capacity of garden grass was enhanced with an increase of pH from 1.5 to 6.5 (Figure 4.5) for all four metals. The amount of Cu(II) adsorbed has increased from 12.2 to 76.15%, resulted with an increase of 6.5-fold by increasing pH solution from 2.0 to 6.5. The percentage

biosorption of Cd(II) at pH 2.0 and 6.0 corresponded to 13.25% and 83.56%, respectively, and 7.56-fold increase was observed. The amount of Pb(II) adsorbed was 15.85% and 94.87% between pH 2.0 and 6.5, respectively, and 6.5-fold increment was observed. Similarly, 5.8-fold increase was found for Zn(II) removals and it was 9.74 to 58.29% for the pH of 2.0 and 6.5. The similar results were also reported in the literature (Chen et al., 2011; Hameed, 2009). To avoid metal precipitation, the whole experiments were conducted between 6.0 and 6.5 pH. As the pH of prepared medium with distilled water was very close to 6.0, there were no practical pH adjustments for all the experiments. Therefore, the experimental processes became environment friendly.

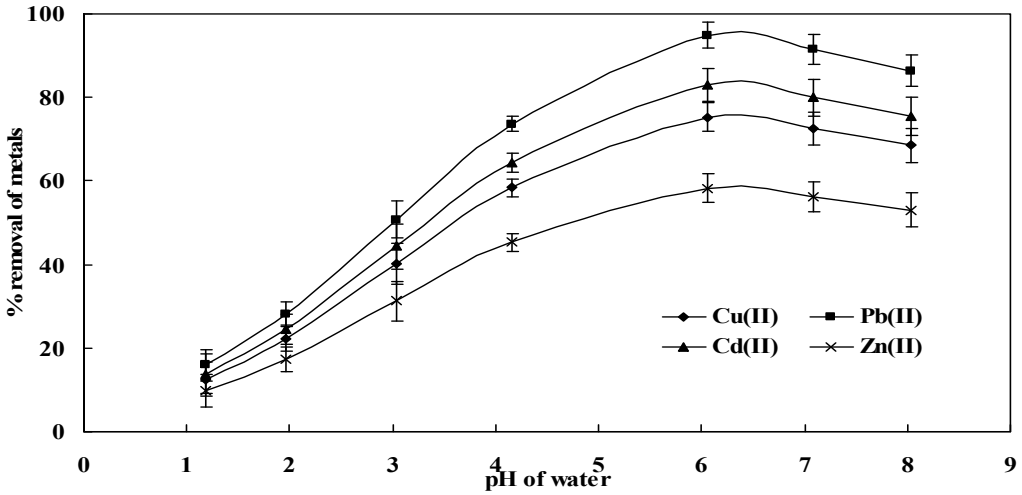


**Figure 4.5** Effect of pH on Cd(II), Cu(II), Zn(II) and Pb(II) biosorptions ($C_o$ = 10 mg/l; dose = 0.5g/100ml)

#### 4.2.2.2 Effect of initial concentration and contact time

The effect of contact times and initial Cu(II), Pb(II), Cd(II) and Zn(II) ions concentrations were studied according to the procedure described in Chapter 3, Sections 3.3.2.4 and 3.3.2.5 and showed in Figure 4.6. Three initial metals concentrations (10, 50 and 100 mg/l) and 0.5g dose of GG were used for 7 hours experiments with optimum conditions. It is generally noticeable that the biosorption capacity for four metals has increased with the increase in metal concentration from 10 mg/l to 100 mg/l in the water and the elapsed time (Figure 4.6). As the metal concentration (Cu(II), Pb(II), Cd(II) and Zn(II)) in the test water was increased, the unit biosorption of Cu(II), Pb(II), Cd(II) and Zn(II) on GG increased from 14.06 to 137.12 mg/g, 16.96 to156.08 mg/g, 14.82 to 141.66 mg/g and 10.42 to 99.51 mg/g; respectively. The equilibrium times for biosorption of metals onto GG were different for different metals and different concentrations. The ranges of equilibrium times were between 45 to 200 minutes. The

equilibrium times were short (45-60 minutes) for low concentration (10 mg/l) and longer (120-360 minutes) for higher concentration (50 mg/l and 100 mg/l). The results are consistent with other studies (Namasivayam et al., 2007). To make it proportion, 3 hours equilibrium time was adapted for the rest of the experiments.

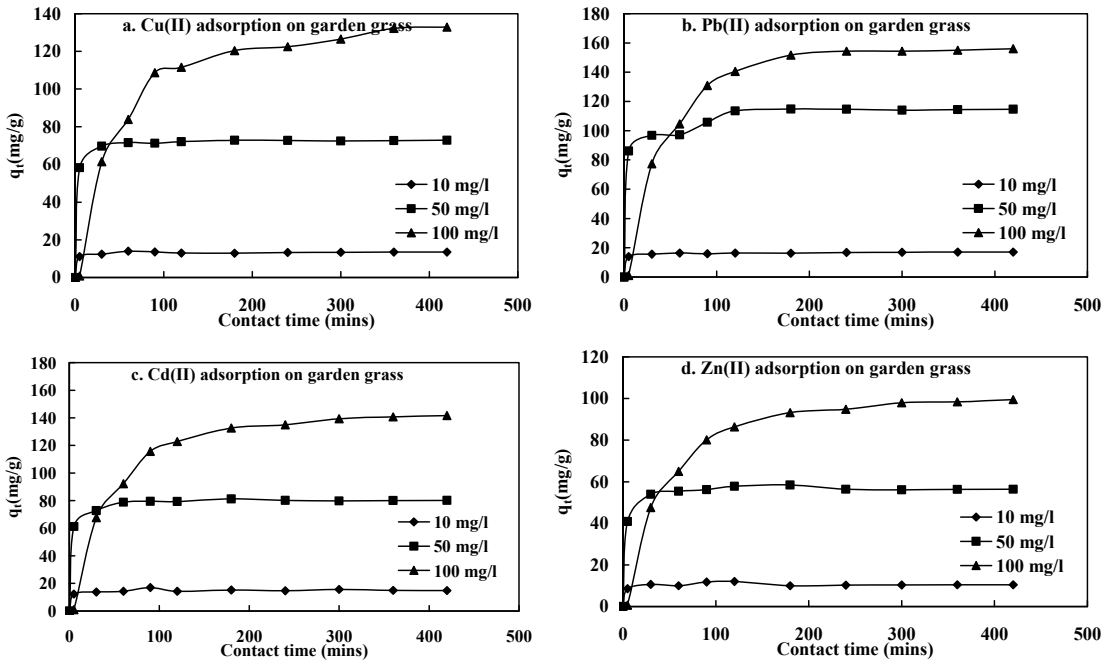


**Figure 4.6** Effects of contact time and initial metals concentration on removals of Cu(II), Pb(II), Cd(II) and Zn(II) from water by garden grass

### 4.2.2.3 Effect of doses

Effect of GG doses (g) on Cu(II), Pb(II), Cd(II) and Zn(II) biosorption were conducted (according to Chapter 3, Section 3.3.3.2) at initial concentrations of 1, 5, 10 and 15 mg/l, while the GG doses were varied from 0.5, 1, 2, 5, 10 and 20 g/l. The effect of biosorbent doses on the percentage removal of Cu(II), Pb(II), Cd(II) and Zn(II) is shown in Figure 4.7. Surprisingly, similar trends of biosorption are found for all four metals in the different experiments (Figure 4.4 (a, b, c and d)). The results indicated that the percentage removal of Cu(II), Pb(II), Cd(II) and Zn(II) has rapidly increased while increasing the doses to 5 g/l and thereafter remained unchanged. At equilibrium, the percentage removal increased from 50 to 84% and an increase in dose from 0.5 to 5 g/l for all four metals. The increase in percentage removal was due to the increase of the available biosorption surfaces and sites (Anwar et al., 2010). Maximum Cu(II), Pb(II), Cd(II) and Zn(II) removal was found from 5 g/l GG dose and 10 mg/l initial concentration and therefore adopted this dose and metals concentration for the rest of the studies.

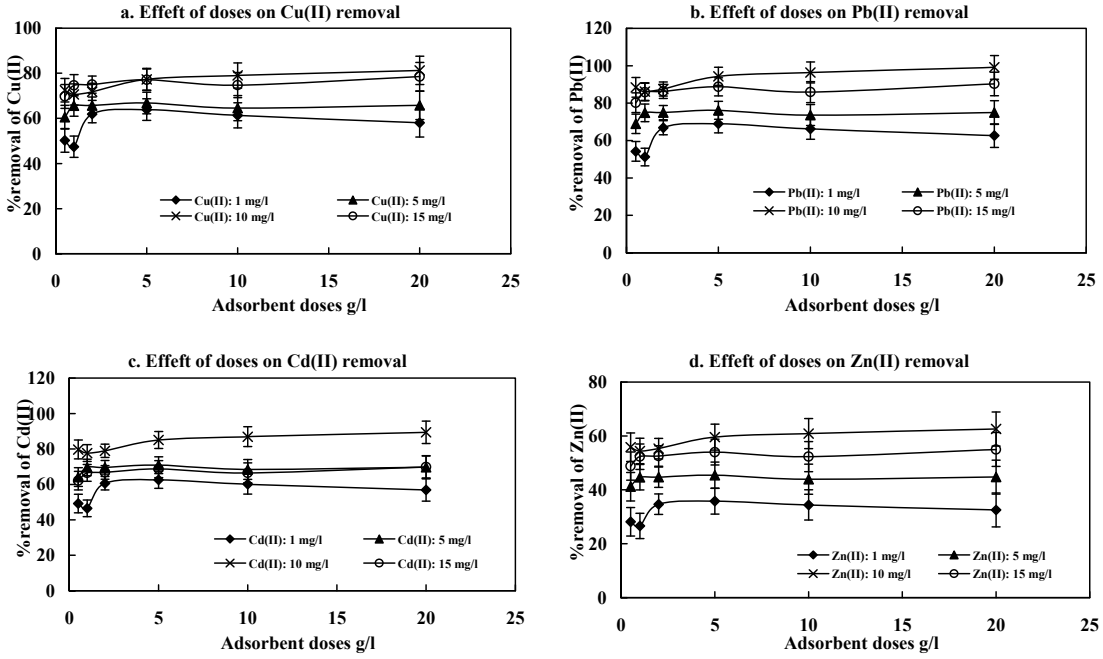


**Figure 4.7** Effects of doses of biosorbents on removals of Cu(II), Pb(II), Cd(II) and Zn(II) from water**.**

### 4.2.2.4 Effect of particle size

Cu(II), Pb(II), Cd(II) and Zn(II) biosorption capacities at three particle sizes of GG are shown in Figure 4.8 (a, b, c and d). It is apparently observed that the monolayer biosorption capacity ($q_m$) of Cu(II), Pb(II), Cd(II) and Zn(II) increased with decreasing in particle size. Langmuir parameters $q_m$ and k for each of the three particle sizes were calculated and are listed in Table 4.2. It is evident that the $q_m$ for each particle size, increased from 6.064 to 11.173 mg/g, 7.641 to 14.078 mg/g, 6.670 to 2.29 mg/g and 4.669 to 8.603 mg/g while the particle size decreased from 150 to <75 μm for Cu(II), Pb(II), Cd(II) and Zn(II) respectively. This may be featured to the larger specific surface area available for biosorption with smaller particles at a constant mass of GG during the process (Wong et al., 2003).

The specific surface area, S, can be measured from the monolayer coverage ($q_m$) for each particle sizes by the following equation (Wong et al., 2003):

$$S = \frac{q_m . A . N_A}{M_A} \qquad (4.1)$$

where, S is the specific surface area of GG ($m^2/g$), $q_m$ the monolayer biosorption capacity, gram metal per gram of GG, $N_A$, the Avogadro number ($6.02\times10^{23}$), A, the

cross-sectional area of metal ion ($m^2$) and $M_A$, is the molecular weight of a metal. For Cu(II) ion, the molecular weight was 63.5 and the cross-sectional areas of Cu(II) were determined to be $1.58\times10^{-18}$ $m^2$ ($Cu^{2+}$ radius is 1.57 Å and 1 angstrom = $1.0 \times 10^{-10}$ metres) in a close packed monolayer (Wong et al., 2003).

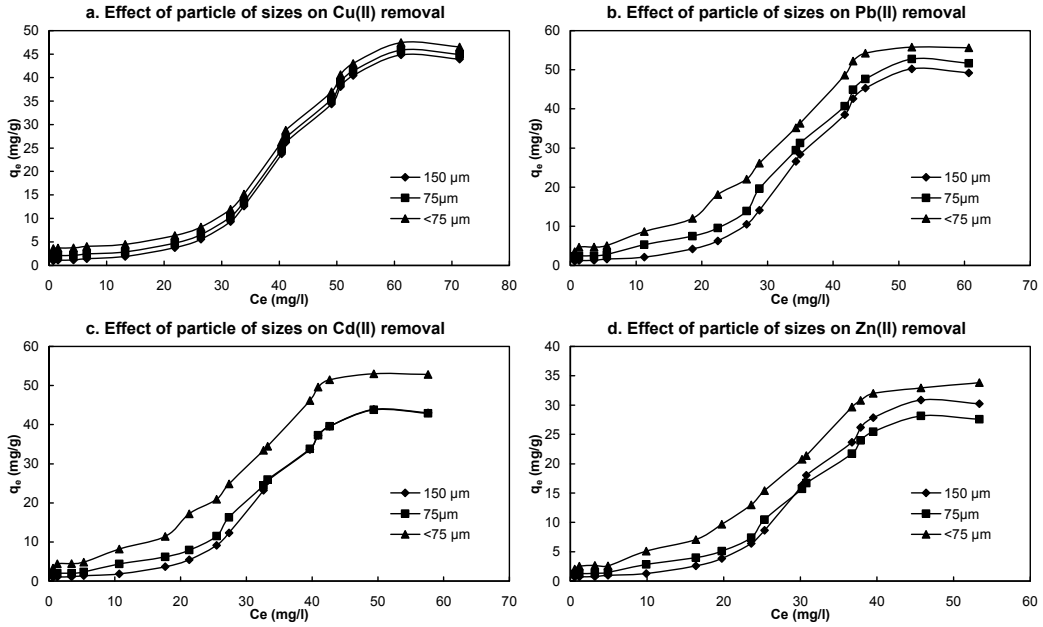


**Figure 4.8** Effects of particle sizes of biosorbents on removals of Cu(II), Pb(II), Cd(II) and Zn(II) from water**.**

The specific surface areas of GG was calculated (Table 4.2) and the maximum specific surface area of GG was 167.36 $m^2/g$ for <75 µm particle size which is higher than BET surface area (Table 4.1). Similarly, the occupied surface area by Pb(II) [atomic radius: 1.81 Å], Cd(II) [atomic radius: 1.71 Å] and Zn(II) [atomic radius: 1.53 Å] onto GG are also calculated and tabulated in Table 4.2.

**Table 4.2** Calculated parameters depends on the particle sizes of garden grass

| Metals | Particle size (µm) | Langmuir Isotherm | | | Surface area of particle ($m^2/g$) |
|---|---|---|---|---|---|
| | | $q_m$ (mg/g) | $K_L$ (l/mg) | $R^2$ | |
| Cu(II) | 150 | 6.064 | 0.204 | 0.986 | 90.836 |
| | 75 | 8.439 | 0.310 | 0.989 | 126.404 |
| | <75 | 11.173 | 0.459 | 0.995 | 167.362 |
| Pb(II) | 150 | 7.641 | 0.257 | 0.996 | 101.736 |
| | 75 | 10.633 | 0.200 | 0.999 | 141.572 |
| | <75 | 14.078 | 0.178 | 0.999 | 187.445 |
| Cd(II) | 150 | 6.670 | 0.224 | 0.996 | 95.196 |
| | 75 | 9.283 | 0.241 | 0.999 | 132.471 |
| | <75 | 12.290 | 0.105 | 0.999 | 175.395 |
| Zn(II) | 150 | 4.669 | 0.157 | 0.976 | 69.944 |
| | 75 | 6.498 | 0.239 | 0.979 | 97.331 |
| | <75 | 8.603 | 0.153 | 0.995 | 128.869 |

The maximum specific surface areas are 187.445, 175.395 and 128.869 $m^2/g$ for <75 μm particle size which areas are higher than the BET surface area. Among the four metals, the surface area calculated from Pb(II) biosorption is greater than Cu(II), Cd(II) and Zn(II). This is due to the more absorption taking place ($q_m$) in the garden grass.

#### 4.2.2.5 Effect of temperature

To measure the thermodynamic parameters, the experiments were conducted (according to Chapter 3, Section 3.3.2.7) at different temperatures in the range of 293-343°K for Cu(II), Pb(II), Cd(II) and Zn(II) biosorption. The thermodynamic parameters such as ΔG° (standard Gibb's free energy change), ΔH° (enthalpy change) and ΔS° (entropy change) were estimated and evaluated according to its feasibility and nature of biosorption process by using standard equations available in literature (Sarin et al., 2006). The Gibb's free energy change of the process is related to equilibrium constant $K_c$. The thermodynamic equilibrium constant ($K_c$) of the biosorption is defined as the ratio of $C_a$ (mg of adsorbate adsorbed per litre) and $C_e$ (the equilibrium concentration of solution, mg/l) (Sarin et al., 2006). According to thermodynamics, the Gibb's free energy change is also related to the enthalpy change (ΔH°) and entropy change (ΔS°) at constant temperature by the van't Hoff equation

$$\ln K_c = \frac{\Delta S^o}{R} - \frac{\Delta H^o}{R}.\frac{1}{T} \qquad (4.2)$$

where, R is the gas constant (8.314 J/ mol °K) and T is the temperature (K).

The values of enthalpy have changed (ΔH°) and the entropy changes (ΔS°) were calculated from the slope and intercept of the plot ***lnKc*** vs. ***1/T***. The calculated values of thermodynamic parameters for Cu(II), Pb(II), Cd(II) and Zn(II) biosorption are reported in Table 4.3. A negative value of ΔH° is indicated that the biosorption process is exothermic in nature. A positive value of the free energy (ΔG°) is indicated that the biosorption process is non-spontaneous in nature (Sarin et al., 2006). It was also noted that the changes in free energy decreases with the rise of temperature but it exhibits a non-normal nature in biosorption (Sengil and Özacar, 2008). Possibly, this could be due to the temperature increase hence decelerates the biosorption processes. The ΔG° for copper biosorption was within the range of 4.452 to 13.660 kJ/mol and thus the biosorption was principally physical biosorption for Cu(II) (Sengil and Özacar, 2008). Possibly, this could be because of the increase of temperature.

**Table 4.3** Thermodynamic parameters for the biosorption of metals by garden grass

| Metals | Temperature (°K) | $q_m$ (mg/g) | Kc | ΔG (kJ/mol) | ΔH° (kJ/mol) | ΔS° (J/mol°K) |
|---|---|---|---|---|---|---|
| Cu(II) | 293 | 7.83 | 0.004 | 13.660 | -0.0021 | 0.0034 |
| | 303 | 49.26 | 0.008 | 12.079 | | |
| | 313 | 4.25 | 0.070 | 6.909 | | |
| | 323 | 6.33 | 0.146 | 5.175 | | |
| | 343 | 4.98 | 0.210 | 4.452 | | |
| Pb(II) | 293 | 9.866 | 0.005 | -15.709 | -0.0031 | 0.0012 |
| | 303 | 62.067 | 0.011 | -13.891 | | |
| | 313 | 5.355 | 0.089 | -7.945 | | |
| | 323 | 7.976 | 0.184 | -5.951 | | |
| | 343 | 6.275 | 0.265 | -5.120 | | |
| Cd(II) | 293 | 8.613 | 0.004 | -14.616 | -0.0051 | 0.0023 |
| | 303 | 54.186 | 0.009 | -12.924 | | |
| | 313 | 4.675 | 0.077 | -7.395 | | |
| | 323 | 6.963 | 0.160 | -5.537 | | |
| | 343 | 5.478 | 0.231 | -4.764 | | |
| Zn(II) | 293 | 6.029 | 0.003 | -10.518 | -0.0029 | 0.0056 |
| | 303 | 37.930 | 0.006 | -9.301 | | |
| | 313 | 3.273 | 0.054 | -5.319 | | |
| | 323 | 4.874 | 0.112 | -3.985 | | |
| | 343 | 3.835 | 0.162 | -3.428 | | |

The negative values of enthalpy change ΔH° indicate the exothermic nature of the biosorption process. With the increase of temperature from 293° K to 343° K, the ΔG° values decrease from -5.120 to -15.709 kJ/mol for Pb(II), -4.7638 to -14.616 kJ/mol for Cd(II) and decrease from-3.4282 to-10.518 kJ/mol for Zn(II), respectively. Generally, the absolute magnitude of the change in free energy for physisorption is between -20 and 0 kJ/mol and chemisorption has a range of -80 to -400 kJ/mol (Yu et al., 2001). The change in free energy for biosorption of Pb(II), Cd(II) and Zn(II) onto GG are in the range of -20 and 0 kJ/mol. Therefore, this process can be considered as physisorption (Yu et al., 2001). The negative ΔG° values at various temperatures indicate that the biosorption process is spontaneous. A positive value of ΔS° revealed an increased randomness between solid-solution interfaces during the biosorption of Cu(II) on GG (Sengil and Özacar, 2008).

#### 4.2.2.6 Effect of shaking speed

The effect of shaking speed on biosorption of Cu(II), Pb(II), Cd(II) and Zn(II) were studied (Chapter 3, section 3.3.2.3) over the range of 30-200 rpm for 3h with 100 ml water containing 10 mg/l metals ions and 0.5 g of GG. Figure 4.9 indicates that the

percentage biosorption increases as the shaking speed increased to all four metals, reaching to its peak and again drops to lower values at higher rpm. It resulted a maximum 96.23% Pb(II) biosorption at 130 rpm, 88% Cu(II) biosorption at 120 rpm, 78.64% Cd(II) biosorption at 120 rpm and 56.83% Zn(II) biosorption at 125 rpm. These biosorption poses higher removal at different shaking speed for four metals, so a nearly value of 120 rpm was employed as standard for other experiment. At low and high speeds, the metal removals were lower than the optimum. Low speed could not spread the particles properly in the water by providing active binding sites for biosorption of metal ions (Memon et al., 2008). It resulted in an accumulation of GG in the bottom of water and it buried the active binding sites. On the other hand, the high speed vigorously spreading the particles of GG in the water and did not allow sufficient time to bind with metal ions (Anwar et al., 2010).

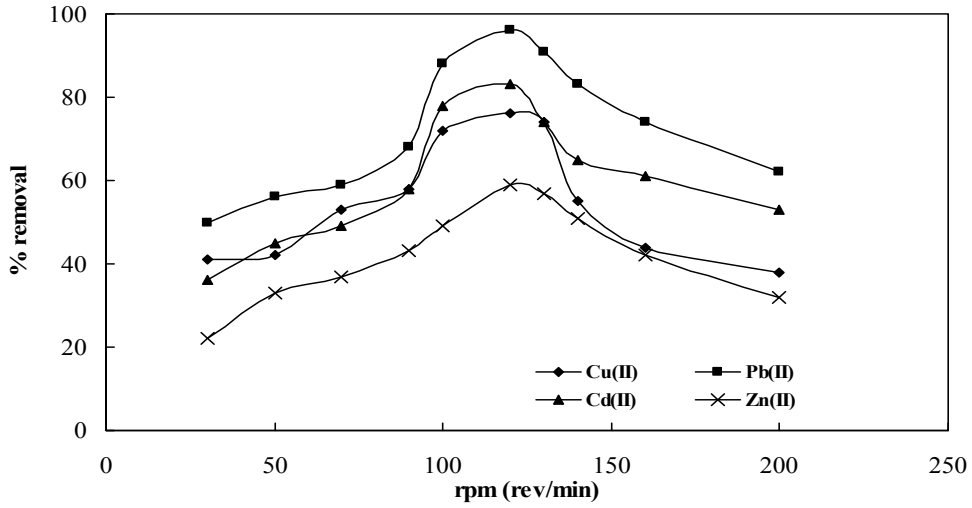


**Figure 4.9** Effect of shaking speed on removal of Cu(II), Pb(II), Cd(II) and Zn(II) ($C_o$: 10 mg/l; d: 0.5 g; t: 3 h: pH: 6-6.5; rpm: 120; T: 20°C)

### 4.2.3 Regeneration of garden grass

In water and wastewater, treatment systems and regeneration of used biosorbents are crucial to repeated use of biosorbents and it reduces the material cost for treatment operation. The adsorbed metals on biosorbents are not completely reversible as reported by several observations on literature (Davis and Upadhyaya, 1996). In this experiments, eight eluent such as tap water, milli-Q water, distilled water, 0.1N $H_2SO_4$, 0.1N HCl, 0.1N $HNO_3$, 0.1N NaOH and 0.1 N $CH_3COOH$ were used for Cu(II), Pb(II), Cd(II) and Zn(II) desorption from pre-loaded GG. As shown in Figure 4.10 (a, b, c and d), biosorption of metals onto GG is easily regenerated by a small amount of 0.1N $H_2SO_4$. The results showed that the 95% of Cu(II), 97% of Pb(II), 79% of Cd(II) and 56% of

Zn(II) were recovered with 0.1 N $H_2SO_4$ from metal-loaded GG (0.5g). The other two acids 0.1 N HCl and 0.1 N $HNO_3$ showed similar efficiencies for recovering the metals. In the desorption system $H^+$ released from the acids which replaced metal cations ($Cu^{2+}$, $Pb^{2+}$, $Cd^{2+}$ and $Zn^{2+}$) on the surface of the GG.

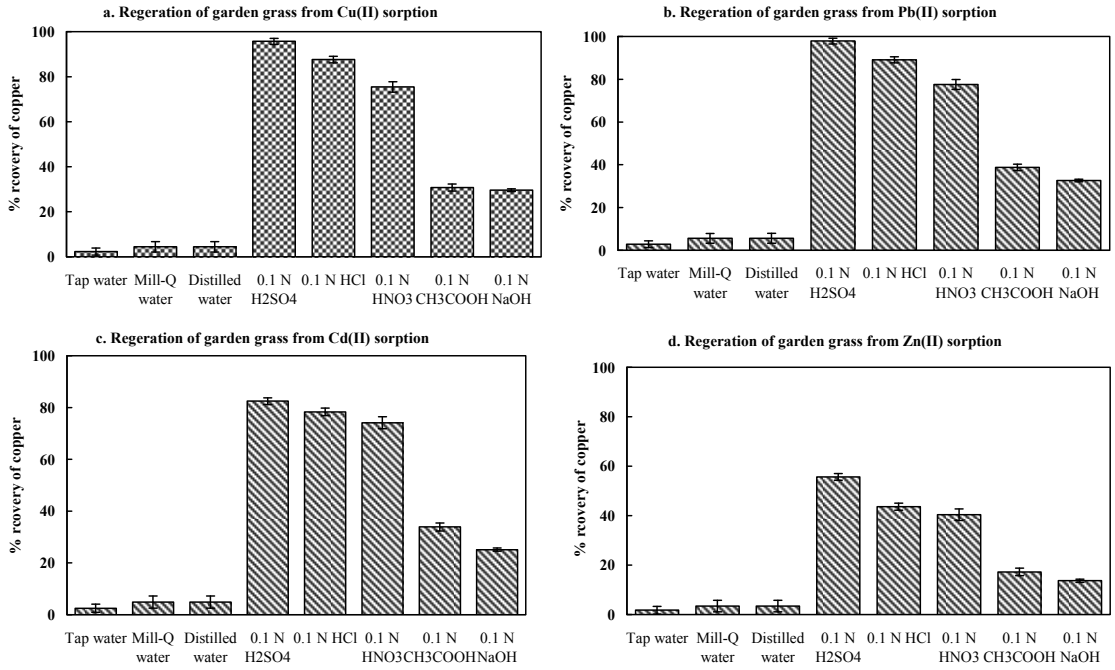


**Figure 4.10** Regeneration of garden grass after biosorption of Cu(II), Pb(II), Cd(II) and Zn(II) ions ($V_o$: 100; d: 0.5 g; t: 3 h; rpm: 120; T: 20°C).

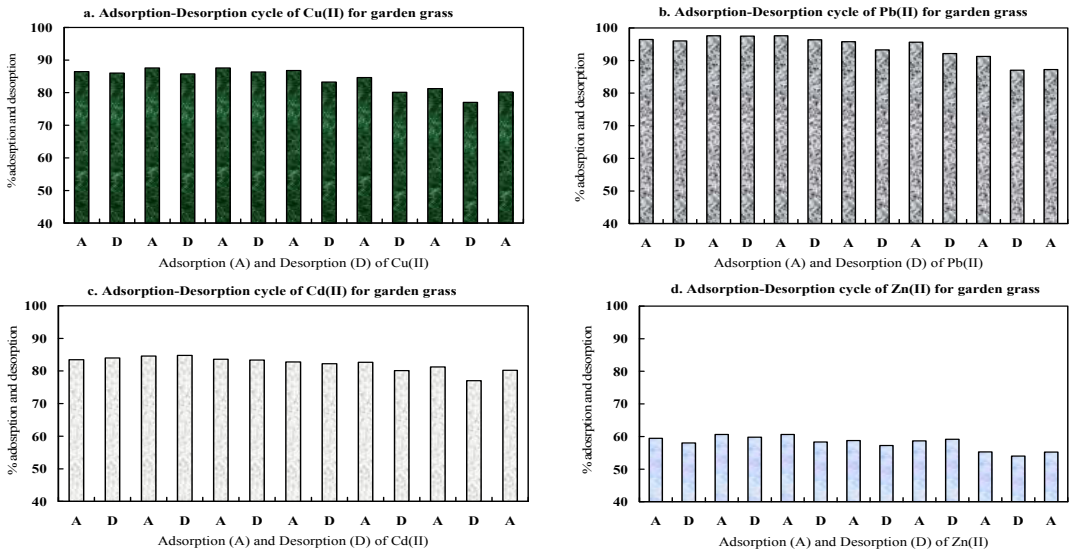


**Figure 4.11** Biosorption and desorption cycle for Cu(II), Pb(II), Cd(II) and Zn(II) onto garden grass ($V_o$: 100 l; d: 0.5 g; t: 3 h; rpm: 120; T: 20°C)

To obtain the reusability of GG, the biosorption and desorption cycles are repeated five times with the best eluent 0.1N $H_2SO_4$ for Cu(II), Pb(II), Cd(II) and Zn(II) and the

results were plotted in Figure 4.11 (a, b, c and d). It is observed that in the first two cycles, biosorption efficiency have slightly increased after the desorption for all four metals. It is presumed that the acid works as a pre-treatment for enhancing efficiency of GG. Latter the regeneration efficiency for GG decreased gradually as the biosorption and desorption continued (Figure 4.11). It is predicted that consecutive acid dissolution poses on the GG surfaces and destroyed the biding sites. The regenerated GG could be used till five times with minor deviation of efficiency.

### 4.2.4 Biosorption and desorption isotherm

It is essential to develop an appropriate model for better perception of the mechanism and to assess the biosorption and desorption characteristics and magnitude based on the suitable model obeyed by the GG. Biosorption and desorption were conducted with 0.05, 0.5 and 1 g doses in between 1-500 mg/l metals concentration (Chapter 3, section 3.3.4). In this study, biosorption and desorption of Cu(II), Pb(II), Cd(II) and Zn(II) onto GG were assessed and compared by popular two two-parameter and two three-parameter isotherm models. The two-parameter models (Langmuir and Freundlich isotherms) and three-parameter models (Redlich-Peterson and Sip isotherms) were fitted with experimental data by non-linear modelling. The models' parameters were measured and optimised by non-linear regression modelling by MATLAB® (R2010b) (Appendix I). The models' fitness was signified by the coefficient of determination ($R^2$), non-linear error functions, the residual root mean square error (RMSE) and the chi-square test ($\chi^2$) (Chapter 3, Section 3.4). The predictions of models' parameters are presented in Figure 4.11 for Cu(II), Figure 4.12 for Pb(II), Figure 4.13 for Cd(II) and Figure 4.14 for Zn(II). The experimented, calculated and predicted parameter four models are tabulated in Table 4.4 for Cu(II), Table 4.5 for Pb(II), Table 4.6 for Cd(II) and Table 4.7 for Zn(II).

#### 4.2.4.1 Copper (II) biosorption and desorption equilibriums

For the Cu(II) biosorption, all the used models have shown good fitness with the experimental data depending on doses as the $R^2$ lies between 0.971 and 0.999. Compare to the three used doses (0.05, 0.5 and 1g), the data obtained from 1g dose have posed better fitness to all models. Langmuir isotherm model was found reasonably fitted to the data, with a coefficient determination ($R^2$) of 0.999, the residual root mean square error (RMSE) of 2.023 and the chi-square test ($\chi^2$) of 0.90 for 1g dose of GG (Table 4.4).

Likewise, the data obtained from desorption of 1g dose was better fitted with Langmuir model as it is produced high $R^2$ (0.983), low RMSE (0.0002) and small $\chi^2$ (1.485) values (Table 4.4). Freundlich isotherm model was in moderate agreement between the experimental data and model prediction, with $R^2$ of 0.997 for 1g doses of biosorption (Table 4.4). The slight high residual root means square error (27.621) and chi-square test (5.165) values indicate a slight disagreement with the experimental data. On the other hand, desorption data showed moderate fitness with low $R^2$ (0.970), low RMSE (0.9697) and big $\chi^2$ (3.564) values.

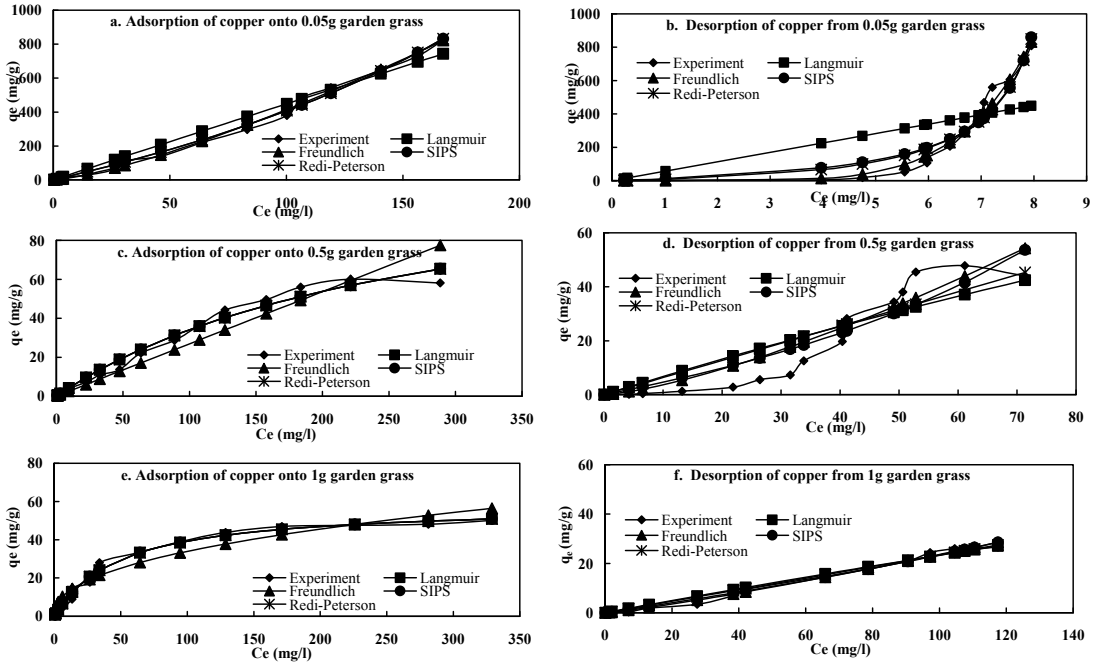


**Figure 4.12** Isotherm modelling of biosorption and desorption of Cu(II) onto garden grass with different doses ($C_o$: 1-500 mg/l; d: 0.05-1 g; t: 3 h: pH: 6-6.5; rpm: 120; T: 20°C)

On the contrary, both the three-parameter models (SIP and Redlich-Peterson isotherms) were found to be better fitted with the experimental data than two-parameter models for both biosorption and desorption processes. The models seemed to confirm remarkably higher degree of fitness with regard to the plots as well as parameters for all used doses (Table 4.4 and Figure 4.12). The predicted $R^2$ values from SIPS model were 0.992, 0.979 and 0.990 for biosorption and 0.939, 0.872 and 0.991 for desorption of 0.05, 0.5 and 1g doses, respectively. While the $R^2$ values from Redlich-Peterson model were 0.992, 0.979 and 0.990 for biosorption and 0.947, 0.832 and 0.987 for desorption of the used three doses. Significantly low RMSE and small $\chi^2$ values were observed for both

biosorption and desorption from the both three-parameter model (Table 4.4) which reveals the good agreement between the experimental data and models' prediction.

**Table 4.4** Isotherm parameters for biosorption and desorption of Cu(II) onto GG

| Isotherm models | Parameters | Biosorption | | | Desorption | | |
|---|---|---|---|---|---|---|---|
| | | Doses | | | Doses | | |
| | | 0.05g | 0.5g | 1g | 0.05g | 0.5g | 1g |
| **Experimental** | $q_m$(mg/g) | 26.2 ±5.9 | 46.23±4.2 | 58.569±1.9 | 18.765±8.9 | 36.258±5.6 | 48.366±4.8 |
| **1. Langmuir** $q_e = \frac{q_m K_L C_e}{1 + K_L C_e}$ | $q_m$(mg/g) | 96.07 | 127.664 | 58.338 | 115.51 | 319.017 | 319.033 |
| | $K_L$ (l/g) | 0.0001 | 0.004 | 0.021 | 0.0005 | 0.002 | 0.001 |
| | $R_L$ | 0.98-1.0 | 0.48-0.99 | 0.19-0.98 | 0.99-0.99 | 0.87-0.99 | 0.92-0.99 |
| | $R^2$ | 0.971 | 0.979 | 0.999 | 0.510 | 0.881 | 0.983 |
| | Δ°G | -22.02 | -13.68 | -9.461 | -18.56 | -14.96 | -17.41 |
| | $\chi^2$ | 0.0366 | 0.431 | 0.90 | 11.042 | 0.033 | 1.485 |
| | RMSE | 50.262 | 3.394 | 2.023 | 203.18 | 8.368 | 0.0002 |
| **2. Freundlich** $q_e = K_F C_e^{1/n}$ | $K_F$(mg/g.l) | 0.886 | 0.268 | 4.743 | 0.003 | 0.157 | 0.102 |
| | n | 0.749 | 1.000 | 2.341 | 0.167 | 0.730 | 0.848 |
| | $R^2$ | 0.994 | 0.917 | 0.997 | 0.983 | 0.889 | 0.970 |
| | $\chi^2$ | 42.301 | 20.346 | 5.165 | $5X10^6$ | 6.411 | 3.564 |
| | RMSE | 22.405 | 7.013 | 27.621 | 37.472 | 31.584 | 0.9697 |
| **3. SIPS** $q_e = \frac{K_s C_e^{\beta_s}}{1 + \alpha_s C_e^{\beta_s}}$ | $K_s$(l/g) | 3.201 | 0.464 | 1.200 | 10.645 | 0.434 | 0.195 |
| | $\alpha_S$ (l/mg) | -0.002 | 0.0036 | 0.021 | -0.113 | -0.006 | -0.002 |
| | $\beta_S$ | 1.000 | 1.000 | 1.000 | 1.000 | 1.000 | 1.000 |
| | $R^2$ | 0.992 | 0.979 | 0.990 | 0.939 | 0.872 | 0.991 |
| | $\chi^2$ | 3.519 | 0.431 | 0.899 | 0.842 | 0.016 | 0.001 |
| | RSME | 0.886 | 0.422 | 0.403 | 18.233 | 1.470 | 0.215 |
| **4. Redlich-Peterson** $q_e = \frac{K_{RP} C_e}{1 + \alpha_{RP} C_e^{\beta}}$ | $K_{RP}$ (l/g) | 3.201 | 0.464 | 1.200 | 2.406 | 3.229 | 3.622 |
| | $\alpha_{RP}$(l/mg) | -0.002 | 0.004 | 0.021 | -0.656 | 4.080 | 14.495 |
| | β | 1.000 | 1.000 | 1.000 | 0.192 | 00 | 000 |
| | $R^2$ | 0.992 | 0.979 | 0.990 | 0.947 | 0.832 | 0.987 |
| | $\chi^2$ | 0.056 | 0.431 | 0.900 | 0.001 | 0.029 | $4X10^{-7}$ |
| | RSME | 4.636 | 0.416 | 0.403 | 15.542 | 2.406 | 0.452 |

The validations of biosorption isotherm models were measured by percentage deviation between experimental values of $q_e$ and models' prediction of $q_e$. All isotherm models studied for both biosorption and desorption of Cu(II) onto 1g GG showed high $R^2$ values (more than 0.9). It specifies the opportunity of simultaneous validity of multiple models and corresponding maxims. It was also observed that the distribution of the average percent deviation was reduced from more than 5% to less than 3% from two parameter models to three parameter models. In comparison of all the three fitness parameters (namely, coefficient of determination ($R^2$), the residual root mean square error (RMSE) and the chi-square test ($\chi^2$)), both three-parameter models are most suitable for understanding the biosorption and desorption mechanisms of Cu(II) onto GG. Therefore, the best fitting order of the models is concluded to be SIPS=Redlich-Peterson> Langmuir> Freundlich.

### 4.2.4.2 Lead (II) biosorption and desorption equilibriums

The parameters from Langmuir, Freundlich, SIPS and Redlich-Peterson presented in Table 4.5 were obtained by fitting the experimental data to the non-linear form of equations (MATLAB modelling: Appendix I). By comparing the coefficient of determination ($R^2$ : 0.999, 0.991 and 1.00) obtained from four sorption models, it can be observed that the Langmuir model for single-metal provides the best fitness for the sorption of the Pb(II) ions onto 0.05, 0.5 and 1g GG (Table 4.5).

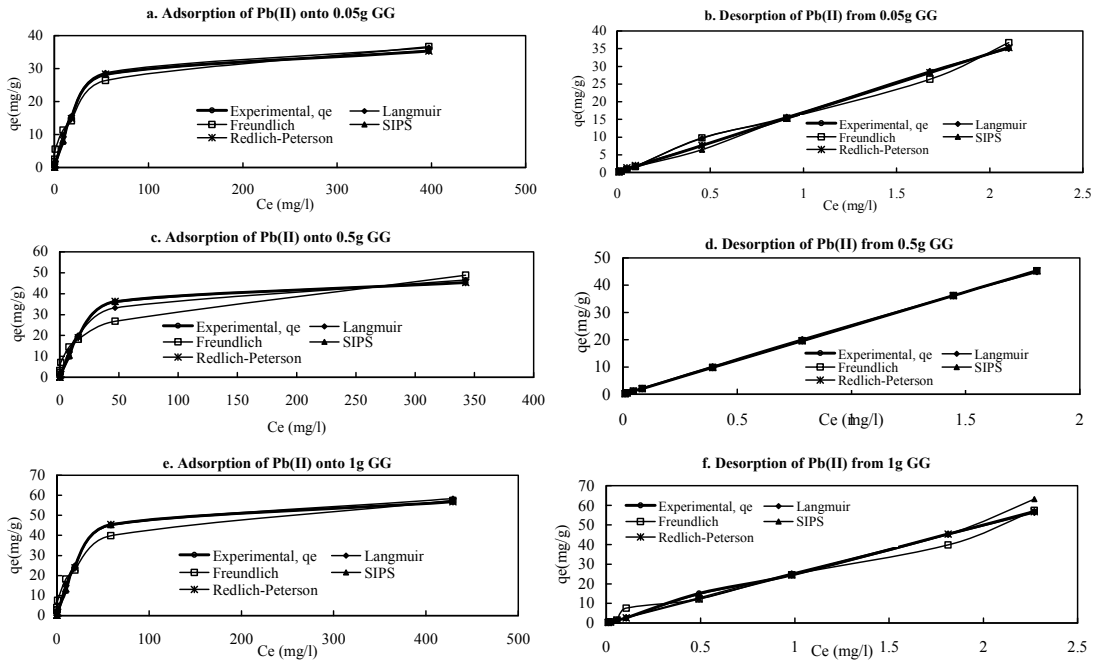


**Figure 4.13** Isotherm modelling of biosorption and desorption of Pb(II) onto garden grass with different doses ($C_o$: 1-500 mg/l; d: 0.05-1 g; t: 3 h: pH: 6-6.5; rpm: 120; T: 20°C).

The appropriateness of the Langmuir model to the experimental data signifies monolayer capacities on the GG surface by Pb(II). On the other hand, the Langmuir model also poses good agreement with desorption of Pb(II) from preloaded GG ($R^2$ : 0.995, 1.00 and 0.998). Among the three-parameter models, Redlich-Peterson model showed a good compatibility with experimental data as the $R^2$ lies 0.989, 0.999 and 0.999 for the three used dose of GG (Table 4.5). The other two models Freundlich and SIPS demonstrated moderate fitness with experimental data. Among the three doses, 1g dose has illustrated higher degree of fitness for all fours models as the $R^2$ values were 1.00, 1.00, 1.00 and 0.999 for Langmuir, Freundlich, SIPS and Redlich-Peterson, respectively. Low RMSE and small $\chi^2$ values were found from the 1 g dose (Table 4.5).

**Table 4.5** Isotherm parameters for biosorption and desorption of Pb(II) onto GG

| Isotherm models | Parameters | Biosorption | | | Desorption | | |
|---|---|---|---|---|---|---|---|
| | | Doses | | | Doses | | |
| | | 0.05g | 0.5g | 1g | 0.05g | 0.5g | 1g |
| **Experimental** | **$q_m$(mg/g)** | 37.81± 1.5 | 45.55± 2.5 | 54.21± 2.7 | 34.31± 3.5 | 36.12± 3.8 | 44.43± 3.5 |
| 1. Langmuir $q_e = \frac{q_m K_L C_e}{1 + K_L C_e}$ | $q_m$(mg/g) | 41.273 | 49.727 | 59.175 | 607.8461 | 639.838 | 787.00 |
| | $K_L$ (l/g) | 0.035 | 0.043 | 0.051 | 0.039 | 0.042 | 0.052 |
| | $R_L$ | 0.03-0.99 | 0.06-0.99 | 0.05-0.9 | 0.84-0.99 | 0.94-0.99 | 0.87-0.99 |
| | $R^2$ | 0.999 | 0.991 | 1.00 | 0.995 | 1.000 | 0.998 |
| | Δ°G | -6.368 | -7.673 | -9.131 | -7.3625 | -7.75 | -9.533 |
| | $\chi^2$ | 9.234 | 11.126 | 13.239 | 0.05282 | 0.056 | 0.068 |
| | RMSE | 1.491 | 1.7966 | 2.138 | 0.35454 | 0.373 | 0.459 |
| 2. Freundlich $q_e = K_F C_e^{1/n}$ | $K_F$(mg/g.l) | 6.217 | 7.491 | 8.914 | 23.75 | 25.00 | 30.75 |
| | n | 2.582 | 3.112 | 3.703 | 0.95 | 1.000 | 1.23 |
| | $R^2$ | 0.961 | 0.917 | 1.00 | 0.995 | 1.000 | 0.986 |
| | $\chi^2$ | 11.906 | 14.345 | 17.07 | 4.75E-10 | 5E-10 | 6.15E-10 |
| | RMSE | 4.5801 | 5.5187 | 6.567 | 2.85E-05 | 3E-05 | 3.69E-05 |
| 3. SIPS $q_e = \frac{K_s C_e^{\beta_s}}{1 + \alpha_s C_e^{\beta_s}}$ | $K_s$(l/g) | 0.556 | 0.670 | 0.797 | 23.749 | 24.999 | 30.749 |
| | $\alpha_S$ (l/mg) | 0.012 | 0.0145 | 0.017 | 0.949 | 0.000 | 1.229 |
| | $\beta_S$ | 1.186 | 1.429 | 1.700 | 0.95 | 0.975 | 1.23 |
| | $R^2$ | 0.988 | 0.998 | 1.00 | 0.998 | 1.000 | 0.969 |
| | $\chi^2$ | 139.88 | 168.542 | 200.56 | 9.5E-09 | 1E-08 | 1.23E-08 |
| | RSME | 0.439 | 0.529 | 0.629 | 4.75E-05 | 5E-05 | 6.15E-05 |
| 4. Redlich-Peterson $q_e = \frac{K_{RP} C_e}{1 + \alpha_{RP} C_e^{\beta}}$ | $K_{RP}$ (l/g) | 1.259 | 1.518 | 1.806 | 6.15885 | 6.483 | 7.974 |
| | $\alpha_{RP}$(l/mg) | 0.007 | 0.009 | 0.0107 | -0.70395 | -0.741 | -0.911 |
| | β | 0.997 | 1.202 | 1.431 | 7.97E-08 | 8.39E-08 | 1.03E-07 |
| | $R^2$ | 0.989 | 0.999 | 0.999 | 0.995 | 1.000 | 1.00 |
| | $\chi^2$ | 0.627 | 0.756 | 0.899 | 6.54E-13 | 6.88E-13 | 8.46E-13 |
| | RSME | 0.283 | 0.341 | 0.406 | 1.08E-05 | 1.14E-05 | 1.4E-05 |

In case of desorption, best fitted data were found from 0.5g dose (Table 4.5). The degrees of fitness ($R^2$) were 1.00 for Langmuir, Freundlich, SIPS and Redlich-Peterson models. While the model's prediction parameters from desorption (Table 4.5) were seem to be reasonable with biosorption parameters, the graphs shows a perfect linear fitted curves for all four models and for three used doses (Figure 4.13).

### 4.2.4.3 Cadmium(II) biosorption and desorption equilibriums

In this part, the experimental data from Cd(II) biosorption and desorption onto three doses (0.05, 0.5 and 1 g) of GG are fitted with Langmuir, Freundlich, SIPS and Redlich-Peterson models and presented in Figure 4.14. It can be detected from these curves that the biosorption capacity of Cd(II) increases when there is an increase of equilibrium concentration of Cd(II), then reached a plateau (Figure 4.14(a, c and e)). This is attributed to the surface active sites of biosorbents having become saturated with the concentration of Cd(II). However, desorption data follow the linear form of line (Figure 4.14(b, d and f)).

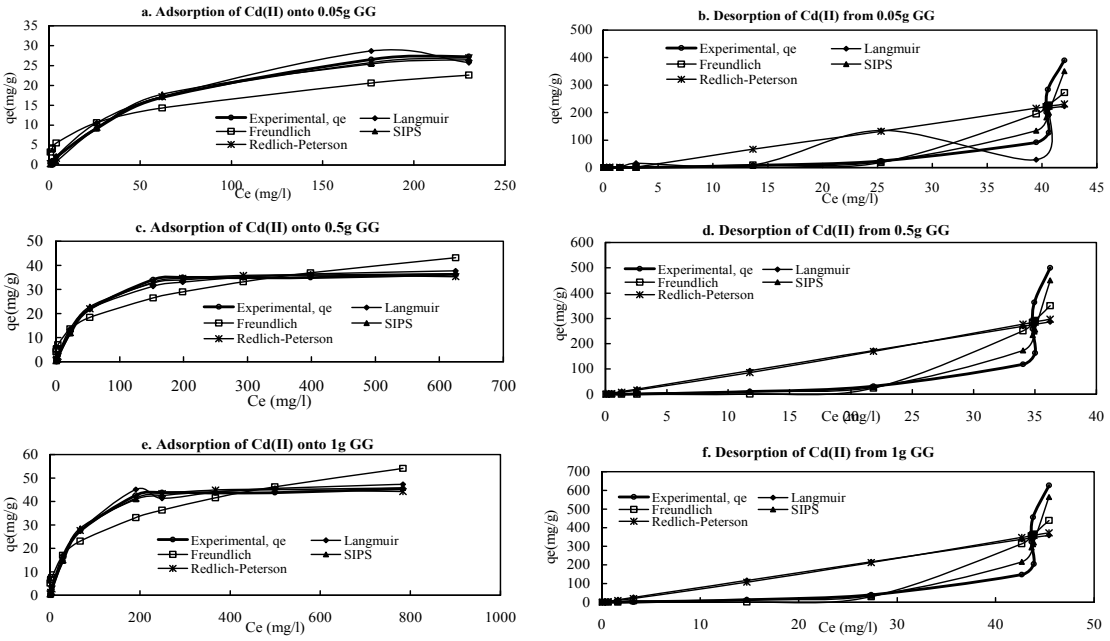


**Figure 4.14** Isotherm modelling of biosorption and desorption of Cd(II) onto garden grass with different doses ($C_o$: 1-500 mg/l; d: 0.05-1 g; t: 3 h: pH: 6-6.5; rpm: 120; T: 20°C)

**Table 4.6** Isotherm parameters for biosorption and desorption of Cd(II) onto GG

| Isotherm models | Parameters | Biosorption | | | Desorption | | |
|---|---|---|---|---|---|---|---|
| | | Doses | | | Doses | | |
| | | 0.05g | 0.5g | 1g | 0.05g | 0.5g | 1g |
| **Experimental** | **$q_m$(mg/g)** | 29.06±2.3 | 35.012±1.7 | 41.66±2.7 | 10.22±3.3 | 10.766±4.7 | 13.242±5.3 |
| 1. Langmuir | $q_m$(mg/g) | 33.56 | 40.438 | 48.12 | 65.683 | 69.140 | 85.04 |
| $q_e = \frac{q_m K_L C_e}{1 + K_L C_e}$ | $K_L$ (l/g) | 0.018 | 0.022 | 0.026 | 8.55E-05 | 0.00009 | 0.0001 |
| | $R_L$ | 0.03-0.9 | 0.06-0.9 | 0.05-0.9 | 0.9-1.0 | 0.9-1.0 | 0.8-1.0 |
| | $R^2$ | 0.923 | 0.992 | 0.998 | 0.737 | 0.565 | 0.695 |
| | Δ°G | -7.676 | -9.248 | -11.005 | -21.40 | -22.53 | -27.71 |
| | $\chi^2$ | 1.563 | 1.8817 | 2.239 | 666.30 | 701.37 | 862.68 |
| | RMSE | 1.255 | 1.5123 | 4.799 | 127.55 | 134.26 | 165.14 |
| 2. Freundlich | $K_F$(mg/g.l) | 3.843 | 4.631 | 5.511 | 1.78E-06 | 1.87E-06 | 2.3E-06 |
| $q_e = K_F C_e^{1/n}$ | n | 2.393 | 2.884 | 3.432 | 0.179 | 0.189 | 0.234 |
| | $R^2$ | 0.954 | 0.989 | 0.992 | 0.602 | 0.739 | 0.909 |
| | $\chi^2$ | 16.439 | 19.807 | 23.57 | 4.7E+12 | 5E+12 | 6.2E+12 |
| | RMSE | 4.280 | 5.1578 | 6.138 | 98.781 | 103.98 | 127.89 |
| 3. SIPS | $K_s$(l/g) | 0.162 | 0.195 | 0.232 | 1.4953 | 1.574 | 1.936 |
| $q_e = \frac{K_s C_e^{\beta_s}}{1 + \alpha_s C_e^{\beta_s}}$ | $\alpha_S$ (l/mg) | 0.004 | 0.005 | 0.005 | -0.2888 | -0.304 | -0.373 |
| | $\beta_S$ | 1.191 | 1.435 | 1.708 | 0.31255 | 0.329 | 0.405 |
| | $R^2$ | 0.998 | 0.999 | 0.999 | 0.8854 | 0.932 | 0.946 |
| | $\chi^2$ | 4.994 | 6.017 | 7.160 | 107.8345 | 113.51 | 139.61 |
| | RSME | 0.218 | 0.263 | 0.31297 | 1.1172 | 1.176 | 1.447 |
| 4. Redlich-Peterson | $K_{RP}$ (l/g) | 0.542 | 0.653 | 0.777 | 3254.178 | 3425.450 | 4213.30 |
| | $\alpha_{RP}$(l/mg) | 0.004 | 0.005 | 0.006 | 582.513 | 613.172 | 754.20 |
| $q_e = \frac{K_{RP} C_e}{1 + \alpha_{RP} C_e^{\beta}}$ | β | 0.975 | 1.175 | 1.398 | -0.101 | -0.107 | -0.131 |
| | $R^2$ | 0.928 | 0.998 | 0.995 | 0.550 | 0.579 | 0.912 |
| | $\chi^2$ | 0.900 | 1.085 | 1.291 | 627.511 | 660.538 | 812.46 |
| | RSME | 0.028 | 0.034 | 0.040 | 18.286 | 19.249 | 23.67 |

Among the four models, SIPS model is proved to be suitable for describing the Cd(II) biosorption onto GG as the $R^2$ values are 0.998, 0.999 and 0.999 for 0.05, 0.5 and 1 g doses (Table 4.6), respectively. Comparatively low RMSE and $\chi^2$ values are obtained from this model. Similarly, desorption data are also explained by the SIPS model. The other three models posed moderate agreement with the experimental data. Along with the doses, the experimental data from Cd(II) onto 0.5 g GG has demonstrated higher degree of fitness (R2: 0.992, 0.989, 0.999 and 0.998) with the models of Langmuir, Freundlich, SIPS and Redlich-Peterson. Nevertheless, data from 1 g dose for desorption showed higher suitability (R2: 0.695, 0.909, 0.946 and 912) with all used models.

#### 4.2.4.4 Zinc(II) biosorption and desorption equilibriums

The biosorption/desorption equilibrium data are easily represented by biosorption/ desorption isotherms, which correspond to the relationship between the mass of the Zn(II) adsorbed per unit mass of GG, $q_e$ and the Zn(II) concentration in water at equilibrium $C_e$. The equilibrium data for Zn(II) biosorption onto GG were compatible to Langmuir, Freundlich, SIPS and Redlich-Peterson models through MATLAB modelling (Appendix I) to identify mechanism involved for biosorption. The models' predictions with experimental data are plotted in Figure 4.15 and the calculated parameters are tabulated in Table 4.7.

Amongst the four models, Langmuir and SIPS models illustrated good agreement with the experimental data as the $R^2$ values were between 0.989 and 0.999 for both models of the three doses (0.05, 0.5 and 1 g). It is found that biosorption data of 1g dose explained properly the Zn(II) biosorption onto GG for all used models because of the higher $R^2$ (between 0.992 to 0.999) values. The data for Zn(II) desorption were not properly fitted with the used four models. Among the model, SIPS model was better to postulate the experimental data as the $R^2$ values were 0.909, 0.951 and 0.987 for 0.05, 0.5 and 1g doses, respectively.

**Table 4.7** Isotherm parameters for biosorption and desorption of Zn(II) onto GG

| Isotherm models | Parameters | Biosorption | | | Desorption | | |
|---|---|---|---|---|---|---|---|
| | | Doses | | | Doses | | |
| | | 0.05g | 0.5g | 1g | 0.05g | 0.5g | 1g |
| **Experimental** | **$q_m$(mg/g)** | 40.13±1.8 | 48.35±2.8 | 57.54±2.4 | 26.189±3.8 | 27.568±4.5 | 33.908±6.3 |
| 1. Langmuir | $q_m$(mg/g) | 50.397 | 60.719 | 72.256 | 27.683 | 29.140 | 35.842 |
| $q_e = \frac{q_m K_L C_e}{1 + K_L C_e}$ | $K_L$ (l/g) | 0.010 | 0.013 | 0.0157 | 6.65E-05 | 0.00007 | 8.61E-05 |
| | $R_L$ | 0.34-0.9 | 0.12-0.9 | 0.23-0.9 | 0.9-1 | 0.99-1 | 0.56-0.9 |
| | $R^2$ | 0.996 | 0.984 | 0.999 | 0.837 | 0.671 | 0.925 |
| | Δ°G | -8.74 | -10.53 | -12.531 | -22.1065 | -23.27 | -28.622 |
| | $\chi^2$ | 6.13 | 7.387 | 8.790 | 455.363 | 479.33 | 589.57 |
| | RMSE | 2.557 | 3.081 | 8.667 | 104.243 | 109.73 | 134.96 |
| 2. Freundlich | $K_F$(mg/g.l) | 3.474 | 4.186 | 4.981 | 7.612 | 8.013 | 9.856 |
| $q_e = K_F C_e^{1/n}$ | n | 1.989 | 2.397 | 2.852 | 1.0317 | 1.086 | 1.336 |
| | $R^2$ | 0.962 | 0.919 | 0.987 | 0.7232 | 0.656 | 0.906 |
| | $\chi^2$ | 22.898 | 27.589 | 32.830 | 477.76 | 502.91 | 618.57 |
| | RMSE | 5.690 | 6.8558 | 8.158 | 106.61 | 112.23 | 138.04 |
| 3. SIPS | $K_s$(l/g) | 0.735 | 0.45 | 0.936 | 3.7734 | 3.972 | 4.885 |
| $q_e = \frac{K_s C_e^{\beta_s}}{1 + \alpha_s C_e^{\beta_s}}$ | $\alpha_S$ (l/mg) | 0.0007 | 0.0009 | 0.001 | -0.43985 | -0.463 | -0.569 |
| | $\beta_S$ | 1.46 | 1.759 | 2.093 | 0.17955 | 0.189 | 0.232 |
| | $R^2$ | 0.998 | 0.997 | 0.999 | 0.903 | 0.951 | 0.987 |
| | $\chi^2$ | 62.163 | 74.896 | 89.126 | 94.1279 | 99.082 | 121.87 |
| | RSME | 0.163 | 0.197 | 0.234 | 7.960 | 8.379 | 10.301 |
| 4. Redlich-Peterson | $K_{RP}$ (l/g) | 0.874 | 0.572 | 0.680 | 46.00 | 48.431 | 59.570 |
| | $\alpha_{RP}$(l/mg) | 0.0008 | 0.001 | 0.001 | 6.59 | 6.941 | 8.537 |
| $q_e = \frac{K_{RP} C_e}{1 + \alpha_{RP} C_e^{\beta}}$ | β | 1.083 | 1.305 | 1.552 | -1.95 | -2.057 | -2.530 |
| | $R^2$ | 0.985 | 0.992 | 0.998 | 0.81 | 0.853 | 0.949 |
| | $\chi^2$ | 3.545 | 4.271 | 5.082 | 571.67 | 601.759 | 740.16 |
| | RSME | 0.413 | 0.498 | 0.593 | 8.98 | 9.453 | 11.62 |

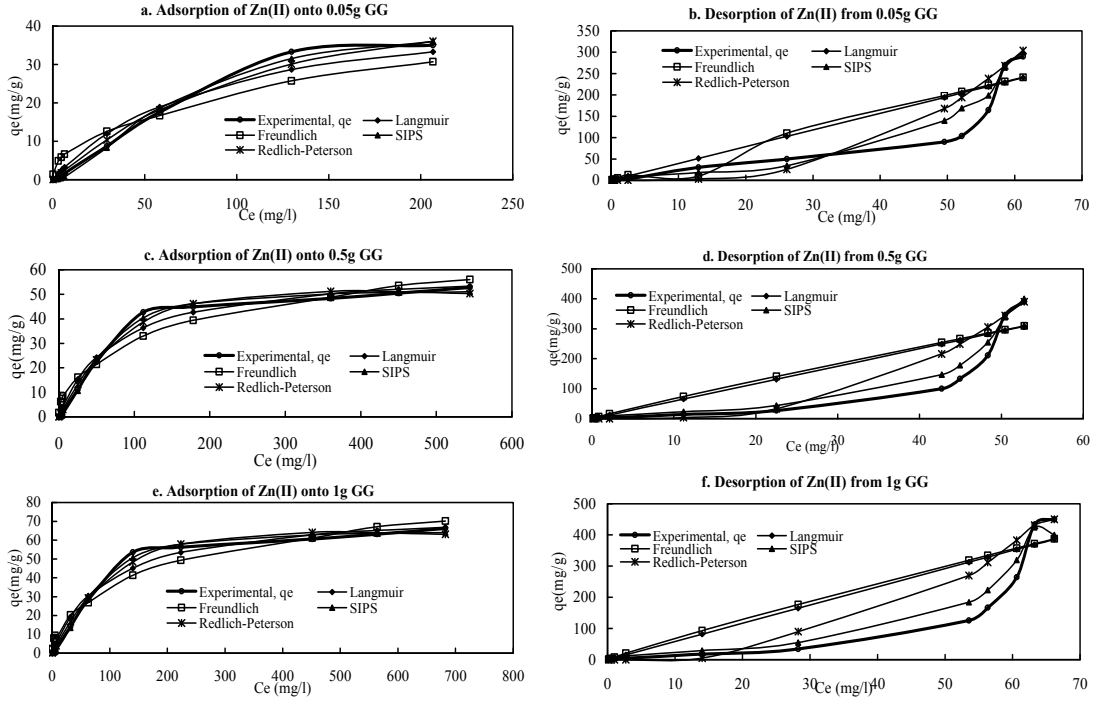


**Figure 4.15** Isotherm modelling of biosorption and desorption of Zn(II) onto garden grass with different doses ($C_o$: 1-500 mg/l; d: 0.05-1 g; t: 3 h: pH: 6-6.5; rpm: 120; T: 20°C)

#### 4.2.4.5 Comparison of Cu(II), Pb(II), Cd(II) and Zn(II) biosorption and desorption with the four used models.

Among the models, SIPS model was better to postulate the experimental data as the $R^2$ values were 0.909, 0.951 and 0.987 for 0.05, 0.5 and 1g doses, respectively.The experimental data were compared with the models' predictions in terms of the nature of fitted models, maximum biosorption capacity ($q_m$, $K_F$, $K_S$, $K_{RP}$), separation factor ($R_L$), energy of biosorption ($K_L$), biosorption intensity(n), and percent deviation (%).

**a) Nature fitted of models**

It is stated from the previous discussion that Zn(II), Pb(II) and Cu(II) biosorption and desorption data are well presented by the Langmuir model that has conventionally been used to compute and contrast the performance of different bio-sorbents (Langmuir, 1918). The formulation of the model is below:

$$q_e = \frac{q_m K_L C_e}{1 + K_L C_e} \qquad (4.3)$$

As the data from Zn(II), Pb(II) and Cu(II) are fitted properly to this model, it can be determined that the metals' ions were the biosorption on the monolayer of GG. It is also be concluded that the metals (Zn(II), Pb(II) and Cu(II)) uptake sites in GG were homogeneous, finite localized sites, identical and equivalent, and there were no lateral interaction and internal obstruction between the adsorbed molecules, even on adjacent sites (Perez-Marin et al., 2007; Vijayaraghavan et al., 2006). Moreover, there was a rapid decrease of the intermolecular attractive forces with the time of biosorption due to the rise of distance between the GG and metals ions (Kundu and Gupta, 2006).

In addition, the data from Cd(II), Zn(II), Pb(II) and Cu(II) biosorption and desorption are expressed well fitness with SIPS model. This model is the combination of Langmuir and Freundlich expressions (Sips, 1948); and can be expressed as:

$$q_e = \frac{K_s C_e^{\beta_s}}{1 + \alpha_s C_e^{\beta_s}} \qquad (4.4)$$

From the fitness of Sips isotherm with all four metals biosorption it can be presumed that the biosorption of metal ions did not only occur in homogeneous sites but also uptakes in heterogeneous surfaces (Foo and Hameed, 2010; Günay et al., 2007).

**b) Maximum biosorption capacity**

The maximum biosorption capacity is the amount of metal ions adsorbed onto biosorbent per unit mass of biosorbent. The parameter of $q_m$, $K_F$, $K_S$, and $K_{RP}$ are the maximum biosorption capacity of biosorbent is computed by Langmuir, SIPS, Freundlich and Redlich-Peterson models. The parameters are tabulated in Table 4.4, Table 4.5, Table 4.6 and Table 4.7.

For Cu(II) biosorption, the Langmuir model properly calculated the maximum biosorption capacity ($q_m$) than other models because it was close to the experimental values (Table 4.4). The $q_m$ values were 96.07, 127.664 and 58.338 mg/g for 0.05, 0.5 and 1g doses, respectively. The calculated parameters from SIPS ($K_S$), Freundlich ($K_F$) and Redlich-Peterson ($K_{RF}$) models are 3.201, 0.464 and 1.20 mg/l; 0.886, 0.268 and 4.743 mg/g; and 3.201, 0.464 and 1.22 mg/g for 0.05, 0.5 and 1g doses; respectively. On the other hand, desorption capacities were not properly found from any models (Table 4.4), though the models were moderately fitted with the experimental data. The maximum biosorption and desorption capacities are selected as 58.57 and 48.34 for Cu(II) that were found from 1 g dose of GG; because this data( from 1 g dose) were consistently fitted (high $R^2$) well to the model.

Among the four metals (Cd(II), Zn(II), Pb(II) and Cu(II)), the data from Pb(II) ions biosorption onto GG have posed best fitness with the four used models (Langmuir, SIPS, Freundlich and Redlich-Peterson). However, the calculated maximum biosorption capacity ($q_m$: 37.81, 45.55 and 54.21 mg/g) was close to the model prediction ($q_m$: 41.27, 49.73 and 59.18 mg/g) from Langmuir model for the three used GG doses. In case of desorption, the Langmuir model over estimated and Redlich-Peterson model under estimated the maximum biosorption capacity (Table 4.5). Freundlich ($K_F$: 23.75, 25.00 and 30.75 mg/g) and SIPS ($K_S$: 23.75, 24.99 and 30.75 mg/g) model predicted moderately similar to the experimental values (37.81, 45.55 and 54.205 mg/g). The maximum biosorption and desorption capacities are suggested to be 54.21 mg/g and 30.75 mg/g from 1g dose, because the experimental data were consistent to the models.

Similar to Pb(II) biosorption, the computed maximum biosorption capacity for the biosorption of Cd(II) ions ($q_m$: 29.06, 35.012 and 41.66 mg/g) were close to the Langmuir model predictions ($q_m$: 33.56, 40.438 and 48.12 mg/g) (Table 4.6). The other three models, SIPS ($K_S$), Freundlich ($K_F$) and Redlich-Peterson ($K_{RF}$) under estimated

the prediction of maximum biosorption capacity for the three used doses (0.05, 0.5 and 1 g). Conversely, Langmuir ($q_m$) and Redlich-Peterson ($K_{RF}$) model over estimated and SIPS ($K_S$) and Freundlich ($K_F$) model under estimated the maximum desorption capacities (Table 4.6). The maximum biosorption and desorption capacities are suggested to be 41.66 mg/g and 13.242 mg/g from 1g dose, because the experimental data coincide with the models.

Similar to Cd(II) and Pb(II) biosorption, the calculated maximum biosorption capacity for the biosorption of Zn(II) ions ($q_m$: 40.131, 48.35 and 57.536 mg/g) were close to the Langmuir model predictions ($q_m$: 50.397, 60.719 and 72.256 mg/g) (Table 4.7). It has under estimated the prediction of maximum biosorption capacity by the SIPS ($K_S$), Freundlich ($K_F$) and Redlich-Peterson ($K_{RF}$) models for the three used doses (0.05, 0.5 and 1 g). On the contrary, Langmuir ($q_m$) model closely estimated the maximum desorption capacities ($q_m$: 27.683, 29.140 and 35.8422 mg/g) with the experimental values ($q_m$: 26.189, 27.568 and 33.908 mg/g) (Table 4.6). The Redlich-Peterson ($K_{RF}$) model over estimated and SIPS ($K_S$) and Freundlich ($K_F$) model under estimated the maximum desorption capacities. The maximum biosorption and desorption capacities are suggested to be 57.536 mg/g and 33.908 mg/g from 1g dose, because the experimental data have shown fair fitness to the models.

**c) Separation factor ($R_L$)**

Separation factor ($R_L$) is known as dimensionless constant, can be used to predict whether an biosorption system is favourable or unfavourable in batch biosorption process (Torab-Mostaedi et al., 2013). $R_L$ was calculated from Langmuir isotherm based equation by the flowing equation (Hanif et al., 2007):

$$R_L = \frac{1}{1 + K_L C_o} \qquad (4.5)$$

where $K_L$ (L/mg) refers to the Langmuir constant and $C_o$ is denoted to the adsorbate initial concentration (mg/L). In this context, lower $R_L$ value reflects that biosorption is more favourable. In a deeper explanation, $R_L$ value indicates the biosorption nature to be either unfavourable.

$R_L > 1$ = unfavourable isotherm (when KL is negative).

$R_L = 1$ = linear isotherm.

$R_L = 0$ =irreversible isotherm.

$0<R_L<1$ = favourable isotherm.

For Cu(II) biosorption, the separation factor ($R_L$) is calculated and the values are between 0.98 to 1, 0.48 to 0.99, and 0.19 to 0.98 for 0.05, 0.5 and 1 g doses respectively, when the Co were 1 to 500 mg/l. In case of desorption, the $R_L$ values are between 0.99 to 0.99, 0.87 to 0.99, and 0.92 to 0.99 for 0.05, 0.5 and 1 g doses respectively (Table 4.4). When it is compared to the values of $R_L$ with condition, it is found that the Cu(II) ions biosorption and desorption are favourable.

The values of $R_L$ are between 0.03 to 0.99, 0.06 to 0.99 and 0.05 to 0.9 for biosorption and, between 0.84 to 0.99, 0.94 to 0.99 and 0.87 to 0.99 for desorption for 0.05, 0.5 and 1 g doses, respectively when the Co were between 1 to 500 mg/l (Table 4.5). It is also revealed that the Pb(II) ions biosorption and desorption are favourable.

Similar to the Pb(II) biosorption and desorption, the values of $R_L$ for Cd(II) biosorption are between 0.03 to 0.9, 0.06 to 0.9 and 0.05 to 0.9 and, for Cd(II) desorption are between 0.9to 1.0, 0.9 to 1.0 and 0.8 to 1.0 for 0.05, 0.5 and 1 g doses, respectively when the Co were between 1 to 500 mg/l (Table 4.6). It is also disclosed that the Cd(II) ions biosorption and desorption are favourable.

The biosorption and desorption isotherm were also favourable for Zn(II) ions on GG, the RL factors were lies between 0.12 to 0.9 for biosorption and 0.56to 0.9 for desorption for all three used doses (Table 4.7).

**d) Energy of biosorption ($K_L$)**

It is constant of Langmuir isotherm that postulates the energy of biosorption ($K_L$). It is found from the Cu(II) (Table 4.4), Pb(II) (Table 4.5), Cd(II) (Table 4.6) and Zn(II) (Table 4.7) biosorption and desorption that all the values of $K_L$ were below the unity(1). So, it can be concluded that the used energy for biosorption and desorption were low, because higher value of $K_L$ indicates the higher energy (Sing and Yu, 1998).

**e) Biosorption intensity (n)**

This constant is calculated from Freundlich isotherm:

$$q_e = K_F C_e^{1/n} \qquad (4.6)$$

where, $q_e$ is the amount of metal ions adsorbed per unit mass of the biosorbents, $C_e$ the equilibrium solution concentration, $K_F$ and n are Freundlich equilibrium coefficients. For favourable biosorption, $0 < n < 1$, while $n > 1$ represents unfavourable biosorption, and $n = 1$ indicates linear biosorption. If $n = 0$, the biosorption process is irreversible (Saha et al., 2010).

Among the four metals, the Pb(II) biosorption and desorption data showed better fitness to the Freundlich isotherm (Table 4.5). The calculated values are 2.582, 3.112 and 3.703 for biosorption and 0.95, 1.00 and 1.23 for desorption of Pb(II) onto 0.05, 0.5 and 1 g doses respectively. Compare to the calculated 'n' values with condition, it is found that the biosorption process of Pb(II) on to GG is unfavourable to heterogeneous surfaces (Foo and Hameed, 2010; Saha et al., 2010).

**f) Percent deviation (%)**

The validation of biosorption isotherm models was measured by percent deviation between experimental values of $q_{e.exp}$ and models' prediction of $q_{e.model}$ and by following equation:

$$\text{Percent deviation} = \frac{\left(q_{e.exp} - q_{e.model}\right)}{q_{e.exp}} \times 100 \qquad (4.7)$$

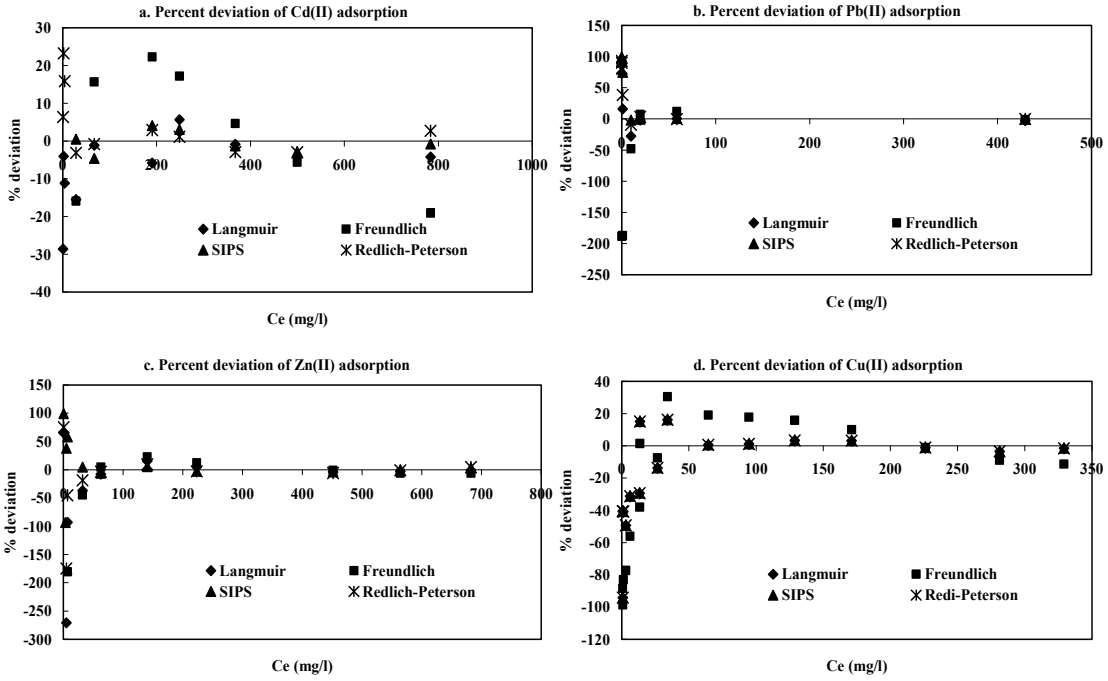


**Figure 4.16** Plots of percent deviation of biosorption capacity of Cu(II), Pb(II), Cd(II) and Zn(II) onto 10 g garden grass.

All four isotherm models (Langmuir, SIPS, Freundlich and Redlich-Peterson) studied for both biosorption of Cu(II), Pb(II), Cd(II) and Zn(II) onto 1g GG showed high $R^2$ values (more than 0.9). It specifies the opportunity of simultaneous validity of multiple models and corresponding maxims. Generally, the percent deviations were higher in the low concentration of metals for all four metals (Cu(II), Pb(II), Cd(II) and Zn(II)) biosorption (Figure 4.16(a, b, c, d)). With the increase of equilibrium concentration, the percentage deviation reduces (Figure 4.16(a, b, c, d)). It is observed that the distribution of the average percent deviation was reduced for more than 5% to 3 % from two parameter models to three parameter models for Cu(II), Pb(II), Cd(II) and Zn(II) (Figure 4.16).

### 4.2.5 Biosorption and desorption kinetics

Initial metal concentration in the water is vital for kinetics and the initial Cu(II), Zn(II), Pb(II) and Cd(II). Concentrations employed during the kinetic studies were 10, 50 and 100 mg/l, which are low compared to the other studies reported (Vargas et al., 2011). The kinetic data for both biosorption and desorption were analysed by a non-linear analyses (MS Excel 2007) using five different kinetic models: Pseudo-first order, Pseudo-second order, Fraction power, Intraparticle diffusion and Avrami equations. The estimated kinetics' parameters are shown in Table 4.8 for Cu(II), Table 4.9 for Zn(II), Table 4.10 for Pb(II), and Table 4.11 for Cd(II) biosorption onto 5g/l doses of GG. The experimental kinetics data with model's prediction are plotted in Figure 4.17 for Cu(II), Figure 4.18 for Zn(II), Figure 4.19 for Pb(II), and Figure 4.20 for Cd(II) biosorption.

The kinetic curve for Cu(II), Zn(II), Pb(II), and Cd(II) ions showed that the amount of biosorption sharply increases with an increasing contact time in the initial stage (0-50 min), and then slowly increases to reach an equilibrium values in approximately 120 min (actual equilibrium time slightly different for different metals but lies in the rage: section: 4.2.2.2). The amount of biosorption increases with the further increase in contact time and it is considered as insignificant effect. A good $R^2$ values of the kinetic data explains the biosorption mechanism of the metal ion on the solid phase (Yang and Al-Duri, 2005). The degree of fitness of kinetics' models were judged by two non-linear errors: the normalized standard deviation (NSD) and average relative error (ARE)(Hossain et al., 2012) (Chapter 3: Section 3.4). In order to evaluate the kinetic mechanism that controls the biosorption process, the Pseudo-first order, Pseudo-second

order, Fraction power, Intraparticle diffusion and Avrami models were employed for the biosorption of Cu(II), Zn(II), Pb(II), and Cd(II) ions on the GG.

#### 4.2.5.1 Pseudo-first-order equation

This equation is also known as Lagergren-first-order equation (Lagergren, 1898) and is widely used model for explaining kinetics biosorption (Rajaei et al., 2013). The mathematical form is:

$$\frac{dq_t}{dt} = k_1(q_e - q_t) \tag{4.8}$$

**Table 4.8** Kinetics parameters of Cu(II) biosorption and desorption onto garden grass

| Kinetic models | Parameters | Biosorption | | | Desorption | | |
|---|---|---|---|---|---|---|---|
| | | Copper concentration | | | Copper concentration | | |
| | | 10mg | 50mg | 100mg | 10mg | 50mg | 100mg |
| **Experimental** | **$q_e$ (mg/g)** | 13.5±0.1 | 72.5±0.2 | 132.26 ±0.5 | 12.49 ±0.32 | 47.98 ±0.62 | 69.51 ±0.73 |
| 1. Pseudo-1st-order $q_t = q_e - q_e e^{(-k_1 t)}$ | $q_e$ (mg/g) | 13.228 | 72.529 | 132.00 | 12.154 | 44.657 | 63.949 |
| | $k_1$ (l/h) | 1.802 | 11.538 | 0.018 | 1.408 | 1.803 | 0.982 |
| | $R^2$ | 0.981 | 0.981 | 0.990 | 0.959 | 0.957 | 0.852 |
| | NSD | 3.843 | 3.543 | 54.92 | 6.318 | 6.224 | 15.005 |
| | ARE | -0.147 | -0.125 | -15.19 | -0.366 | -0.366 | -1.786 |
| 2. Psedo-2nd order $q_t = \frac{k_2 q_e^2 t}{(1 + q_e k_2 t)}$ | $q_e$ (g/mg.min) | 13.313 | 72.938 | 142.55 | 12.195 | 44.757 | 64.434 |
| | $k_2$ (1/h) | 0.364 | 0.192 | 0.000 | 0.232 | 0.105 | 0.022 |
| | $R^2$ | 0.983 | 0.988 | 0.995 | 0.963 | 0.959 | 0.865 |
| | $h=k_2 q_e^2$ | 64.517 | 1023.7 | 3.947 | 35.238 | 211.13 | 91.647 |
| | NSD | 3.513 | 2.892 | 114.66 | 6.172 | 6.115 | 14.811 |
| | ARE | -0.627 | -0.462 | -34.79 | -0.714 | -0.848 | -2.344 |
| 3. Fractional power $q_t = kt^v$ | K(mg/g.min$^v$) | 1.004 | 1.004 | 1.001 | 1.000 | 1.1004 | 1.009 |
| | v | 0.999 | 0.999 | 1.000 | 1.000 | 0.999 | 0.998 |
| | $R^2$ | 1.000 | 1.000 | 1.000 | 1.000 | 1.000 | 1.000 |
| | NSD | 0.009 | 0.003 | 0.041 | 2.1E-12 | 0.007 | 0.055 |
| | ARE | -0.001 | 0.0002 | -0.011 | 2.2E-12 | -0.001 | -0.041 |
| 4. Avrami $q_t = q_e(1 - e^{(-K_{AV} t)^{n_{AV}}})$ | $q_e$ (mg/g) | 13.288 | 72.529 | 132.00 | 12.154 | 44.091 | 63.949 |
| | $K_{AV}$ (/min) | 2.502 | 1.000 | 0.133 | 2.418 | 9.515 | 2.020 |
| | $n_{AV}$ | 0.720 | 25.076 | 0.133 | 0.582 | 25.076 | 0.486 |
| | $R^2$ | 0.981 | 0.984 | 0.990 | 0.959 | 0.931 | 0.852 |
| | NSD | 3.843 | 3.543 | 54.62 | 6.319 | 8.131 | 15.005 |
| | ARE | -0.147 | -0.125 | -15.19 | -0.366 | -0.612 | -1.786 |
| 5. Intraparticle diffusion $q_t = k_p t^{0.5+C}$ | $k_p$(gm/g√min) | 3.340 | 8.159 | 6.587 | 3.079 | 6.029 | 6.365 |
| | C | -0.469 | -0.483 | -0.329 | -0.456 | -0.463 | -0.419 |
| | $R^2$ | 0.999 | 0.997 | 0.866 | 0.985 | 0.990 | 0.955 |
| | NSD | 1.062 | 1.588 | 1536.7 | 3.581 | 2.906 | 7.481 |
| | ARE | -0.013 | -0.022 | -442.5 | -0.167 | -0.079 | -0.675 |

After definite integration within the conditions $q_t = 0$ at $t = 0$ and $q_t = q_t$ at $t = t$, Eq. (4.8) becomes the following:

$$\ln(q_e - q_t) = \ln q_e - k_1 t \tag{4.9}$$

where $q_t$ is the amount of metals' ions biosorption in time 't' (min) (mg/g); $k_1$ the rate constant of the equation (l/min); $q_e$ is the amount of biosorption equilibrium (mg/g). The nonlinear form of the equation/

$$q_t = q_e - q_e e^{(-k_1 t)} \qquad (4.10)$$

Biosorption kinetic data of Cu(II), Zn(II), Pb(II), and Cd(II) ions biosorption and desorption are analysed using the pseudo-first-order rate equation. In reality, it is required that predicted equilibrium biosorption capacity values from model, $q_e$ (model), should resemble to the experimental $q_e$ (exp.) values (Febrianto et al., 2009). Although the coefficient of determination values ($R^2$) are very high (within the rages of 0.981 and 0.998) and NSD and ARE values are low for all four metals biosorption, the experimental $q_e$ values do not agree with the models values (Table 4.8, Table 4.9, Table 4.10, and Table 4.11 for Cd(II)). In desorption process the model fitness is low as the coefficient of determination values ($R^2$) are low and NSD and ARE values are small. This suggests that the biosorption of Cu(II), Zn(II), Pb(II), and Cd(II) ions does not follow pseudo-first-order kinetics properly.

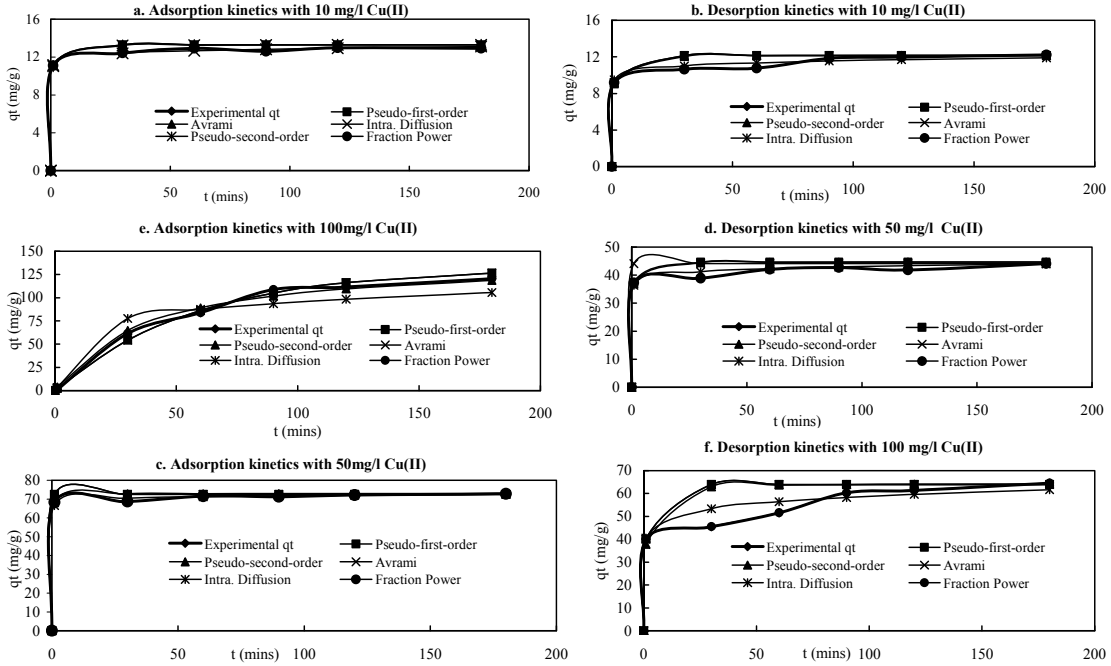


**Figure 4.17** Kinetics modelling of Cu(II) biosorption and desorption onto GG

### 4.2.5.2 Pseudo-second-order equation

The biosorption kinetic data can also be illustrated by pseudo-second-order equation (Ho and McKay, 2000). This model is based on the assumption that the rate-limiting

step may be chemical sorption that involves valance forces through sharing or an exchange of electrons between heavy metal ions and the biosorbents, hence offers the best consistent data for the heavy metal ions (Namasivayam et al., 2007). The mathematical expression is in the following form:

$$\frac{dq_t}{dt} = k_2(q_e - q_t)^2 \qquad (4.11)$$

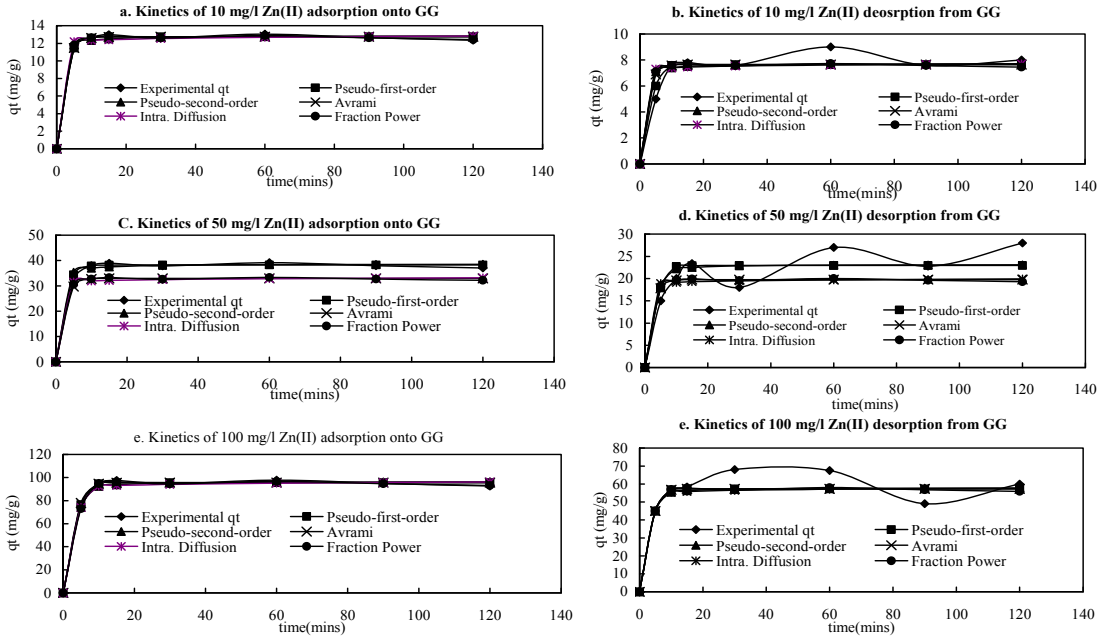


**Figure 4.18** Kinetics modelling of Zn(II) biosorption and desorption onto GG

After the integration within the conditions $q_t$ =0 at t = 0 and $q_t = q_t$ at t = t, Eq. (4.11), it becomes the following:

$$q_t = \frac{k_2 q_e^2 t}{(1 + q_e k_2 t)} \qquad (4.12)$$

where, $k_2$ is the constant rate of the second-order equation (g/mg/min); $q_t$ the amount of biosorption time t (min) (mg/g); $q_e$ is the amount of biosorption equilibrium (mg/g). It was found that the model predicted $q_e$ values agree well with experimental $q_e$ values for biosorption of Cu(II), Zn(II), Pb(II), and Cd(II) ions onto GG (Table 4.8, Table 4.9, Table 4.10, and Table 4.11). In addition, the $R^2$ values are very high (0.983-0.999) and the NSD and ARE values are low and even negative for the three initial concentration for Cu(II), Zn(II), Pb(II), and Cd(II) ions biosorption. This suggests that the pseudo-second-order kinetic model portray that the Cu(II), Zn(II), Pb(II), and Cd(II) ions biosorption onto GG is a rate-limiting step and the chemical sorption may involve by valance forces through sharing or exchange of electrons between heavy metal ions and the biosorbent (Namasivayam and Sangeetha, 2006; Namasivayam et al., 2007).

#### 4.2.5.3 Fractional power equation

The power function equation is an empirical model that describes the relation between the mass of the metals per unit mass of the biosorbent and time 't' to be as follows (Limousin et al., 2007):

$$q_t = kt^v \qquad (2.13)$$

where $q_t$ biosorption capacity at given time (mg/g), k (mg/g.min) and v are adjustment parameters.

**Table 4.9** Kinetics parameters of Zn(II) biosorption and desorption onto garden grass

| Kinetic models | Parameters | Biosorption | | | Desorption | | |
|---|---|---|---|---|---|---|---|
| | | Zinc concentration | | | Zinc concentration | | |
| | | 10mg | 50mg | 100mg | 10mg | 50mg | 100mg |
| **Experimental** | **$q_e$ (mg/g)** | 12.87±0.2 | 39.12±0.4 | 80.123±0.7 | 12.45±1.4 | 16.783±2.5 | 37.123±3.2 |
| 1. Pseudo-1st-order $q_t = q_e - q_e e^{(-k_1 t)}$ | $q_e$ (mg/g) | 12.736 | 38.208 | 82.147 | 7.221 | 21.663 | 46.577 |
| | $k_1$ (l/h) | 0.461 | 1.383 | 0.973 | 0.261 | 0.784 | 1.685 |
| | $R^2$ | 0.998 | 0.994 | 0.993 | 0.975 | 0.897 | 0.949 |
| | NSD | 1.8502 | 5.5506 | 1.934 | 1.049 | 3.147 | 6.766 |
| | ARE | -0.037 | -0.111 | -0.238 | -0.020 | -0.062 | -0.135 |
| 2. Psedo-2nd order $q_t = \frac{k_2 q_e^2 t}{(1 + q_e k_2 t)}$ | $q_e$ (g/mg.min) | 12.756 | 38.664 | 81.176 | 7.307 | 21.92 | 47.133 |
| | $k_2$ (1/h) | 0.166 | 0.498 | 1.070 | 0.094 | 0.282 | 0.607 |
| | $R^2$ | 0.994 | 0.996 | 0.999 | 0.893 | 0.869 | 0.935 |
| | $h=k_2 q_e^2$ | 27.65 | 82.95 | 178.34 | 15.67 | 47.03 | 90.120 |
| | NSD | 2.9158 | 8.747 | 18.807 | 1.653 | 4.759 | 8.663 |
| | ARE | -0.09 | -0.27 | -0.581 | -0.051 | -0.153 | -0.329 |
| 3. Fractional power $q_t = kt^v$ | K(mg/g.min$^v$) | 2.329 | 6.987 | 14.02 | 1.320 | 3.961 | 8.517 |
| | v | 0.666 | 1.998 | 4.397 | 0.377 | 1.132 | 2.436 |
| | $R^2$ | 0.999 | 0.997 | 0.999 | 0.966 | 0.899 | 0.963 |
| | NSD | 1.475 | 4.425 | 3.514 | 0.836 | 2.508 | 5.394 |
| | ARE | -0.12 | -0.36 | -0.774 | -0.068 | -0.204 | -0.436 |
| 4. Avrami $q_t = q_e(1 - e^{(-K_{AV} t)^{n_{AV}}})$ | $q_e$ (mg/g) | 12.736 | 38.208 | 82.147 | 7.221 | 21.663 | 46.577 |
| | $K_{AV}$ (/min) | 2.369 | 7.107 | 15.28 | 1.343 | 4.029 | 8.663 |
| | $n_{AV}$ | 0.195 | 0.585 | 1.258 | 0.110 | 0.331 | 0.713 |
| | $R^2$ | 0.998 | 0.994 | 0.999 | 0.915 | 0.927 | 0.964 |
| | NSD | 1.850 | 5.55 | 7.933 | 1.048 | 3.146 | 4.765 |
| | ARE | -0.037 | -0.111 | -0.239 | -0.020 | -0.062 | -0.135 |
| 5. Intraparticle diffusion $q_t = k_p t^{0.5+C}$ | $k_p$(gm/g√min) | 11.884 | 35.652 | 74.652 | 6.738 | 20.214 | 43.461 |
| | C | -0.484 | -0.452 | -0.422 | -0.274 | -0.823 | -1.770 |
| | $R^2$ | 0.990 | 0.997 | 0.998 | 0.859 | 1.684 | 3.720 |
| | NSD | 3.903 | 11.709 | 25.174 | 2.213 | 6.639 | 8.273 |
| | ARE | -0.151 | -0.453 | -0.973 | -0.085 | -0.256 | -0.452 |

This simple kinetic and fractional power model was tested for biosorption and desorption of Cu(II), Zn(II), Pb(II), and Cd(II) onto GG . Table 4.8, Table 4.9, Table 4.10, and Table 4.11 show the estimated parameters of the model. The results indicated that this model was able to describe properly the time-dependent Cu(II), Zn(II), Pb(II), and Cd(II) biosorption and desorption by GG as the value of $R^2$ were unity for all initial

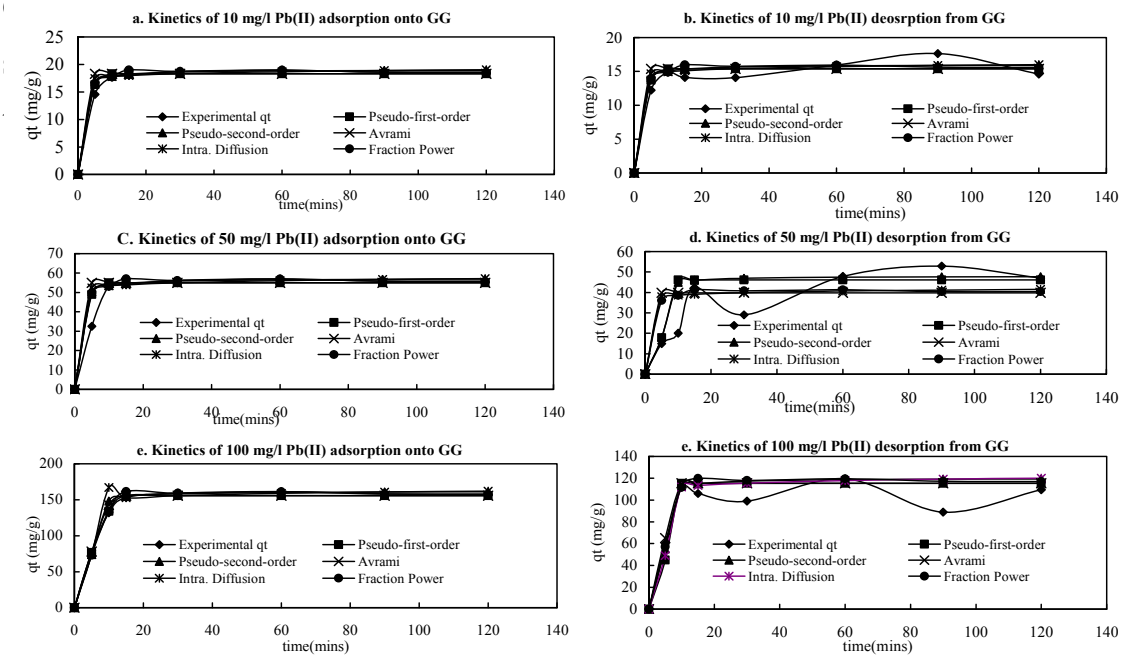


**Figure 4.19** Kinetics modelling of Pb(II) biosorption and desorption onto GG

**Table 4.10** Kinetics parameters of Pb(II) biosorption and desorption onto garden grass

| Kinetic models | Parameters | Biosorption | | | Desorption | | |
|---|---|---|---|---|---|---|---|
| | | Lead concentration | | | Lead concentration | | |
| | | 10mg | 50mg | 100mg | 10mg | 50mg | 100mg |
| **Experimental** | **$q_e$ (mg/g)** | 18.99±0.3 | 56.99±0.5 | 122.54±0.8 | 16.47±2.2 | 49.41±2.5 | 66.24±3.5 |
| 1. Pseudo-1st-order | $q_e$ (mg/g) | 18.311 | 54.933 | 118.106 | 15.875 | 47.626 | 82.399 |
| | $k_1$ (l/h) | 7.188 | 21.564 | 46.362 | 6.231 | 4.912 | 40.196 |
| $q_t = q_e - q_e e^{(-k_1 t)}$ | $R^2$ | 0.984 | 0.992 | 0.989 | 0.853 | 0.854 | 0.867 |
| | NSD | 5.116 | 15.348 | 22.998 | 4.435 | 11.306 | 28.609 |
| | ARE | -0.245 | -0.735 | -0.580 | -0.212 | -0.337 | -1.37 |
| 2. Psedo-2nd order | $q_e$ (g/mg.min) | 19.043 | 57.129 | 122.827 | 16.510 | 39.530 | 46.491 |
| | $k_2$ (1/h) | 0.079 | 0.237 | 0.509 | 0.068 | 0.205 | 0.441 |
| $q_t = \frac{k_2 q_e^2 t}{(1 + q_e k_2 t)}$ | $R^2$ | 0.998 | 0.994 | 0.999 | 0.865 | 0.895 | 0.890 |
| | $h=k_2 q_e^2$ | 28.47 | 85.41 | 178.631 | 24.683 | 74.05 | 159.208 |
| | NSD | 2.108 | 6.324 | 11.597 | 1.827 | 5.482 | 11.788 |
| | ARE | -0.052 | -0.156 | -0.335 | -0.045 | -0.135 | -0.290 |
| 3. Fractional power | $K$(mg/g.min$^v$) | 0.999 | 1.997 | 5.443 | 0.866 | 2.598 | 5.586 |
| | v | 1.000 | 1.00 | 1.45 | 0.867 | 1.601 | 0.592 |
| $q_t = kt^v$ | $R^2$ | 1.000 | 1.00 | 1.00 | 0.987 | 0.901 | 0.892 |
| | NSD | 0.002 | 0.003 | 0.012 | 0.001 | 0.005 | 0.011 |
| | ARE | -0.002 | -0.006 | -0.02 | -0.003 | -0.005 | -0.011 |
| 4. Avrami | $q_e$ (mg/g) | 18.311 | 54.933 | 118.106 | 15.876 | 47.626 | 102.39 |
| $q_t=q_e(1-e^{(-K_{AV}t)^{n_{AV}}})$ | $K_{AV}$ (/min) | 3.459 | 10.377 | 22.311 | 2.998 | 8.996 | 19.343 |
| | $n_{AV}$ | 13.46 | 20.38 | 36.817 | 11.669 | 35.00 | 75.270 |
| | $R^2$ | 0.984 | 0.998 | 0.999 | 0.895 | 0.986 | 0.976 |
| | NSD | 5.116 | 15.348 | 32.998 | 4.435 | 13.306 | 28.609 |
| | ARE | -0.245 | -0.735 | -1.580 | -0.212 | -0.637 | -1.370 |
| 5. Intraparticle diffusion | $k_p$(gm/g√min) | 16.671 | 51.013 | 98.528 | 14.453 | 43.361 | 93.226 |
| | C | -0.472 | -0.316 | -0.444 | -0.409 | -0.227 | -1.639 |
| $q_t = k_p t^{0.5+C}$ | $R^2$ | 0.992 | 0.996 | 0.994 | 0.860 | 0.880 | 0.947 |
| | NSD | 3.498 | 10.494 | 22.562 | 3.032 | 9.098 | 19.561 |
| | ARE | -0.128 | -0.384 | -0.826 | -0.110 | -0.332 | -0.715 |

### 4.2.5.4 Avrami kinetic equation

The Avrami kinetic equation was used to describe the biosorption and desorption kinetics of Cu(II), Zn(II), Pb(II), and Cd(II) onto GG. This equation determines some kinetic parameters, such as possible changes of the biosorption and desorption rates in the function of the initial metals concentration and the biosorption/desorption time, as well as the determination of fractionery kinetic orders (Lopes et al., 2003). The equation of Avrami kinetic model presents Avrami exponential that is a fractionery number related with the possible changes of the biosorption mechanism that takes place during the biosorption process. So the mechanism biosorption could follow multiple kinetic orders that are changed during the contact of the metals with the biosorbents (Lopes et al., 2003).

$$q_t = q_e\left[1 - e^{(-t.k_{AV})^{nAV}}\right] \qquad (4.14)$$

Where, $K_{AV}$ is the Avrami kinetic constant and $n_{AV}$ is another constant, which is related to the biosorption mechanisms changes.

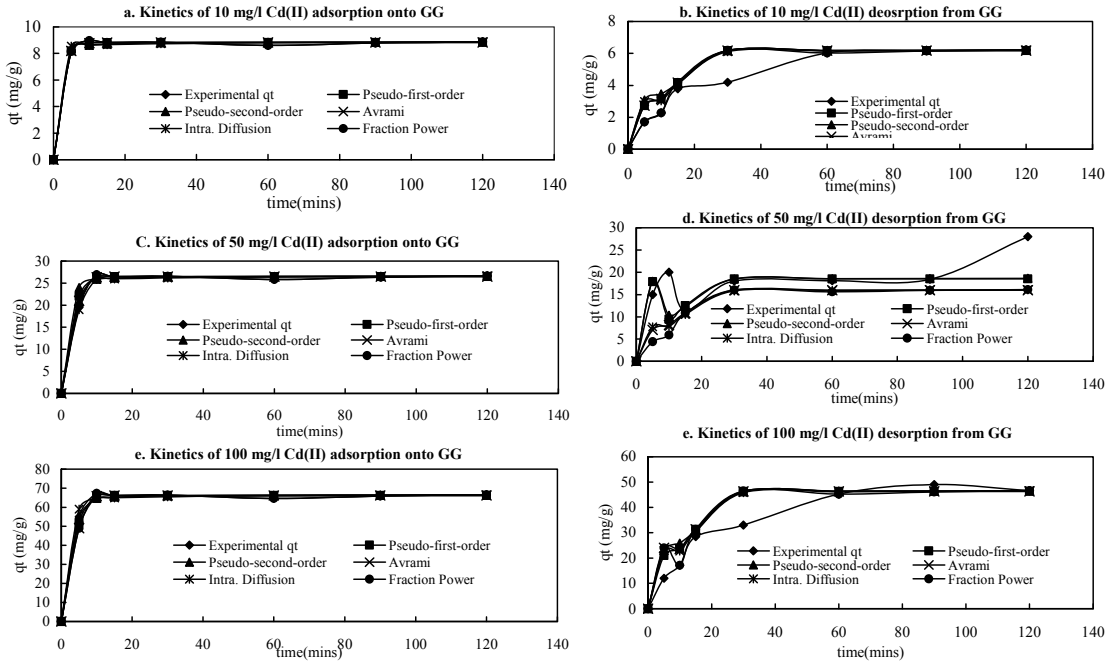


**Figure 4.20** Kinetics modelling of Cd(II) biosorption and desorption onto GG

The conformity between the experimental data and the model-predicted values were found from $R^2$, NSD and ARE values (Table 4.8, Table 4.9, Table 4.10, and Table 4.11). The fractionery number ($n_{AV}$) predicted from biosorption and desorption processes were less than unity except 50 mg/l for Cu(II), 100 mg/l for Zn(II), 100 mg/l

for Cd(II) and; 10, 50, and 100 mg/l for Pb(II) concentration. This suggested that the biosorption process in 50 mg/l for Cu(II), 100 mg/l for Zn(II), 100 mg/l for Cd(II) and; 10, 50, and 100 mg/l for Pb(II) concentration were more than one stages of biosorption.

**Table 4.11** Kinetics parameters of Cd(II) biosorption and desorption onto garden grass

| Kinetic models | Parameters | Biosorption | | | Desorption | | |
|---|---|---|---|---|---|---|---|
| | | Cadmium concentration | | | Cadmium concentration | | |
| | | 10mg | 50mg | 100mg | 10mg | 50mg | 100mg |
| **Experimental** | **$q_e$ (mg/g)** | 8.81±0.3 | 19.54±0.6 | 42.21±0.9 | 5.88±1.3 | 13.16±2.8 | 29.49±5.3 |
| 1. Pseudo-1st-order $q_t = q_e - q_e e^{(-k_1 t)}$ | $q_e$ (mg/g) | 8.824 | 19.765 | 44.27 | 5.885 | 13.183 | 29.531 |
| | $k_1$ (l/h) | 0.524 | 1.173 | 2.629 | 0.349 | 0.782 | 1.753 |
| | $R^2$ | 0.999 | 0.999 | 0.999 | 0.966 | 0.892 | 0.943 |
| | NSD | 1.386 | 3.104 | 3.954 | 0.924 | 2.070 | 4.638 |
| | ARE | -0.023 | -0.51 | -0.115 | -0.015 | -0.034 | -0.076 |
| 2. Psedo-2nd order $q_t = \frac{k_2 q_e^2 t}{(1 + q_e k_2 t)}$ | $q_e$ (g/mg.min) | 8.893 | 19.920 | 44.621 | 5.931 | 13.286 | 29.762 |
| | $k_2$ (1/h) | 0.357 | 0.799 | 1.791 | 0.238 | 0.533 | 1.194 |
| | $R^2$ | 0.996 | 0.998 | 0.994 | 0.964 | 0.888 | 0.933 |
| | $h=k_2 q_e^2$ | 28.203 | 63.172 | 141.51 | 18.811 | 42.137 | 94.388 |
| | NSD | 2.319 | 5.194 | 11.635 | 1.546 | 3.464 | 7.761 |
| | ARE | -0.056 | -0.125 | -0.281 | -0.037 | -0.083 | -0.187 |
| 3. Fractional power $q_t = kt^v$ | K(mg/g.min$^v$) | 1.019 | 2.282 | 4.112 | 0.679 | 1.522 | 2.410 |
| | v | 0.992 | 2.222 | 4.977 | 0.661 | 1.482 | 3.319 |
| | $R^2$ | 1.000 | 1.000 | 1.000 | 0.967 | 0.894 | 0.946 |
| | NSD | 0.027 | 0.060 | 0.135 | 0.018 | 0.040 | 0.090 |
| | ARE | 0.001 | 0.002 | 0.005 | 0.0006 | 0.0014 | 0.003 |
| 4. Avrami $q_t=q_e(1-e^{(-K_{AV}t)^{n_{AV}}})$ | $q_e$ (mg/g) | 8.824 | 18.7654. | 42.275 | 5.885 | 13.183 | 29.531 |
| | $K_{AV}$ (/min) | 1.818 | 072 | 9.121 | 1.212 | 2.716 | 6.084 |
| | $n_{AV}$ | 0.288 | 0.645 | 1.445 | 0.192 | 0.430 | 0.963 |
| | $R^2$ | 0.999 | 0.999 | 0.999 | 0.966 | 0.892 | 0.943 |
| | NSD | 1.386 | 3.104 | 5.954 | 0.924 | 2.070 | 4.638 |
| | ARE | -0.023 | -0.041 | -0.115 | -0.015 | -0.034 | -0.076 |
| 5. Intraparticle diffusion $q_t = k_p t^{0.5+C}$ | $k_p$(gm/g√min) | 8.389 | 18.191 | 41.092 | 5.595 | 12.533 | 28.075 |
| | C | -0.488 | -0.493 | -0.448 | -0.325 | -0.729 | -0.633 |
| | $R^2$ | 0.995 | 0.995 | 0.992 | 0.863 | 0.886 | 0.930 |
| | NSD | 2.876 | 6.442 | 7.430 | 1.918 | 4.296 | 9.625 |
| | ARE | -0.082 | -0.183 | -0.411 | -0.054 | -0.122 | -0.274 |

### 4.2.5.5 Intra-particle diffusion model

Biosorption and desorption kinetic data from Cu(II), Zn(II), Pb(II), and Cd(II) biosorption onto GG were further used to define whether the intra-particle diffusion is rate limiting and also to find the diffusion constant rate, $k_p$ (mg/g min^0.5). Intra-particle diffusion model (Srihari and Das, 2008) is presented by the relationship between specific biosorption and the square root of time, according to the following equation:

$$q_t = k_p t^{0.5+C} \qquad (4.15)$$

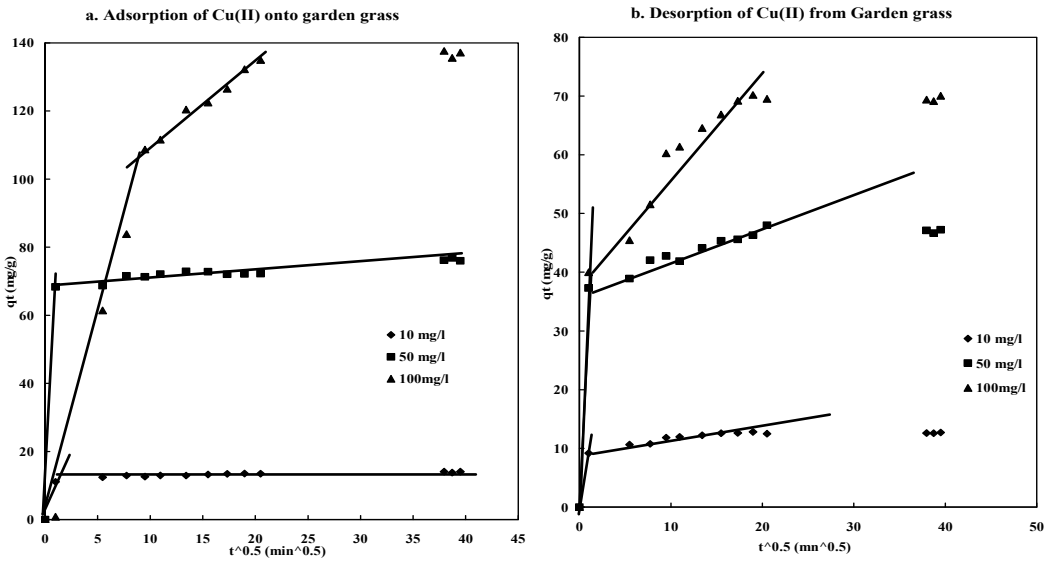


**Figure 4.21** Plots for intra-particle diffusion kinetic model of garden grass for biosorption and desorption of Cu(II) ($C_o$: 10, 50, 100 mg/l; d: 0.5 g; t: 24h: pH: 6-6.5; rpm: 120; T: 20°C)

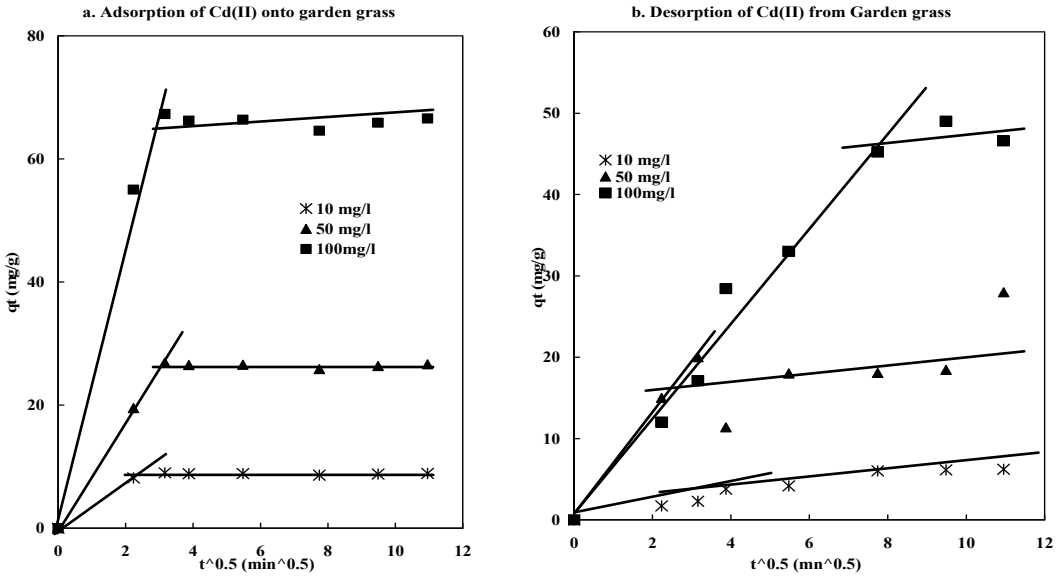


**Figure 4.22** Plots for intra-particle diffusion kinetic model of garden grass for biosorption and desorption of Cd(II) ($C_o$: 10, 50, 100 mg/l; d: 0.5 g; t: 24h: pH: 6-6.5 ; rpm: 120; T: 20°C).

A plot between qt versus t^0.5 for Cu(II), Cd(II), Pb(II) and Zn(II) biosorption and desorption onto GG is shown in Figure 4.21, Figure 4.22, Figure 4.23 and Figure 4.24; respectively. From the Figure, it is revealed that all plots are multi-linear i.e. multi-staged plot for both biosorption and desorption. There are two clear steps visible in the plots which are indeed general type of graphs, i.e. at the first stage and at the second stage.

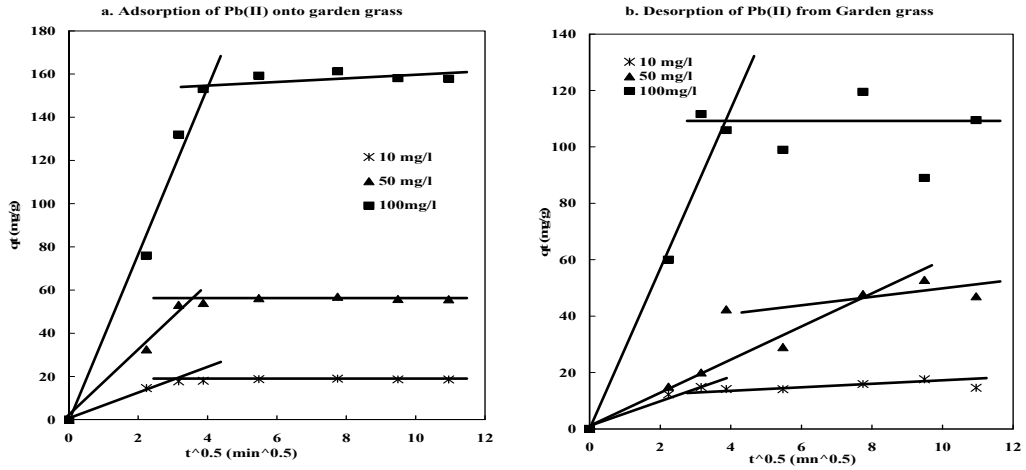


**Figure 4.23** Plots for intra-particle diffusion kinetic model of garden grass for biosorption and desorption of Pb(II) ($C_o$: 10, 50, 100 mg/l; d: 0.5 g; t: 24h: pH: 6-6.5; rpm: 120; T: 20°C).

The initial or first stage may also be attributed to the boundary layer diffusion effect, while the second stage may be due to intra-particle diffusion effects (Srihari and Das, 2008). In the present study, the constant rate ($k_p$) for biosorption and desorption are higher and it follows an increasing trend with the increase of initial copper concentration (Table 4.8, Table 4.9, Table 4.10, and Table 4.11). Therefore, the slope of the top portion which has a linear portion may be defined as a rate parameter ($k_p$) and a characteristic of the biosorption and desorption rate in the region, where intra-particle diffusion was reported to be the rate-limiting factor (Cochrane et al., 2006) for Cu(II), Cd(II), Pb(II) and Zn(II) biosorption and desorption onto GG.

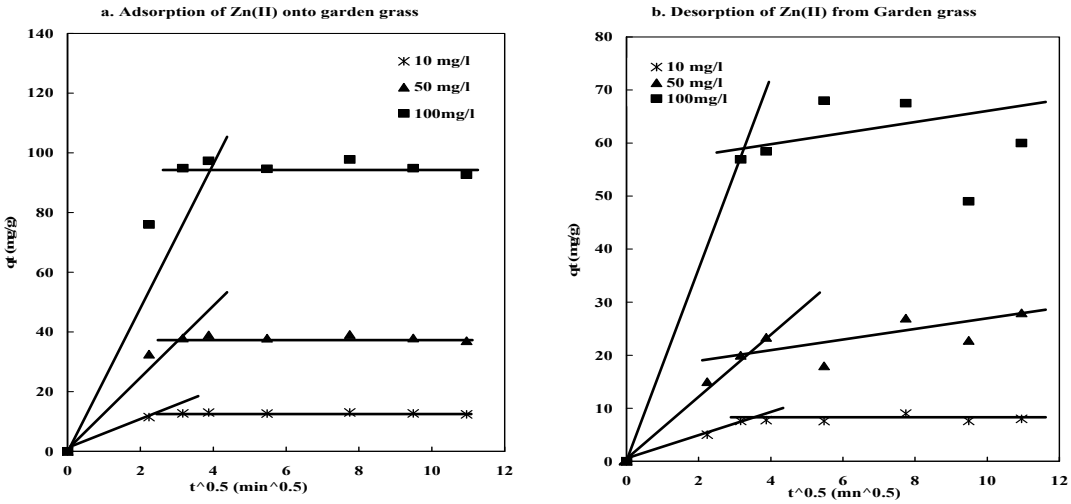


**Figure 4.24** Plots for intra-particle diffusion kinetic model of garden grass for biosorption and desorption of Zn(II) ($C_o$: 10, 50, 100 mg/l; d: 0.5 g; t: 24h: pH: 6-6.5; rpm: 120; T: 20°C)

### 4.2.6 Multimetals biosorption

Wastewaters may contain more than one metal ion and therefore, the examination of multiple simultaneous metal interactions is very important for accurate representation of biosorption data (Hammaini et al., 2003). In these circumstances, Langmuir isotherm can be modified to multi-metals isotherm with some interaction factor (Padilla-Ortega et al., 2013; Srivastava et al., 2008):

$$q_{e.i} = \frac{q_{m.i} K_{L.i}(C_i)}{1 + \sum_{j=1}^{N} K_{L.j}(C_j)} \tag{4.16}$$

In case of four metals concentration in water, the biosorption system can be formulated by reforming the equation (4.16) for quaternary solution of Cu(II)-Pb(II)-Cd(II)-Zn(II) system:

For Cu(II): $$q_{e.Cu} = \frac{q_{m.Cu} K_{L.Cu}(C_{Cu})}{1 + K_{L.Cu}C_{e.Cu} + K_{L.Pb}C_{e.Pb} + K_{L.Cd}C_{e.Cd} + K_{L.Zn}C_{e.Zn}} \tag{4.17}$$

For Pb(II): $$q_{e.Pb} = \frac{q_{m.Pb} K_{L.Pb}(C_{Pb})}{1 + K_{L.Cu}C_{e.Cu} + K_{L.Pb}C_{e.Pb} + K_{L.Cd}C_{e.Cd} + K_{L.Zn}C_{e.Zn}} \tag{4.18}$$

For Cd(II): $$q_{e.Cd} = \frac{q_{m.Cd} K_{L.Cd}(C_{Cd})}{1 + K_{L.Cu}C_{e.Cu} + K_{L.Pb}C_{e.Pb} + K_{L.Cd}C_{e.Cd} + K_{L.Zn}C_{e.Zn}} \tag{4.19}$$

And for Zn(II): $$q_{e.Zn} = \frac{q_{m.Zn} K_{L.Zn}(C_{Zn})}{1 + K_{L.Cu}C_{e.Cu} + K_{L.Pb}C_{e.Pb} + K_{L.Cd}C_{e.Cd} + K_{L.Zn}C_{e.Zn}} \tag{4.20}$$

Biosorption equilibrium is established when the concentration of metal ion in water ($C_e$) is in dynamic with that in the solid matrix ($q_e$). The competitive biosorption among the Cu(II), Pb(II), Cd(II) and Zn(II) in the quaternary systems [Cu(II)-Pb(II)-Cd(II)-Zn(II)] were conducted in batch system between 1 to 200mg/l initial concentration for 3 hours at 120 rpm and room temperature with 0.5g of biosorbent. The calculated parameters from the quaternary Langmuir isotherms are reported in Table 4.12 and plotted in Figure 4.24. This isotherm model was successfully fitted to the competitive biosorption of Cu(II)-Pb(II)-Cd(II)-Zn(II) onto GG.

**Table 4.12** Isotherm parameters from quaternary metals [Cd(II)-Cu(II)-Zn(II)-Pb(II)] biosorption

| For Pb(II) | For Cu(II) | For Cd(II) | For Zn(II) |
|---|---|---|---|
| $q_{m\text{-}Pb}$ = 41.101mg/g | $q_{m\text{-}Cu}$ = 19.951mg/g | $q_{m\text{-}Cd}$ = 19.878 mg/g | $q_{m\text{-}Zn}$ = 16.334mg/g |
| $K_{L\text{-}Cu}$ = 0.047 l/g | $K_{L\text{-}Cu}$ = 0.408 l/g | $K_{L\text{-}Cu}$ = -0.055 l/g | $K_{L\text{-}Cu}$ = 4.917 l/g |
| $K_{L\text{-}Cd}$ = 0.040 l/g | $K_{L\text{-}Cd}$ = 0.011 l/g | $K_{L\text{-}Cd}$ = 0.043 l/g | $K_{L\text{-}Cd}$ = 0.245 l/g |
| $K_{L\text{-}Zn}$ = -0.151 l/g | $K_{L\text{-}Zn}$ = -0.484 l/g | $K_{L\text{-}Zn}$ = 0.181 l/g | $K_{L\text{-}Zn}$ = -3.251 l/g |
| $K_{L\text{-}Pb}$ = 0.157 l/g | $K_{L\text{-}Pb}$ = 0.090 l/g | $K_{L\text{-}Pb}$ = -0.279 l/g | $K_{L\text{-}Pb}$ = -5.013 l/g |
| $R^2$ = 0.998 | $R^2$ = 0.992 | $R^2$ = 0.997 | $R^2$ = 0.988 |

The biosorption capacities of Cu(II), Pb(II), Cd(II) and Zn(II) from four metals [Cu(II)-Pb(II)-Cd(II)-Zn(II)] system were compared to the molar uptake values of metals predicted with the quaternary Langmuir isotherm (eqs. 4.17-4.20). As shown in Figure 4.25, the model perfectly estimated the parameters of all four metals' uptake as the predicted lines and experimental plots are close enough. It is also visible from $R^2$ values that are 0.998, 0.992, 0.997 and 0.988 for Pb(II), Cu(II), Cd(II) and Zn(II) ions biosorption from quaternary system. Apparently, the Cu(II), Pb(II), Zn(II) and Cd(II) uptakes are underestimated as the magnitude of the biosorption capacities (Table 4.12: 19.951, 41.101, 16.334 and 19.878 mg/g) are lower than the single metal system(Table 4.4, Table 4.5, Table 4.6 and Table 4.7) (Papageorgiou et al., 2009; Şengil and Özacar, 2009; Xue et al., 2009).

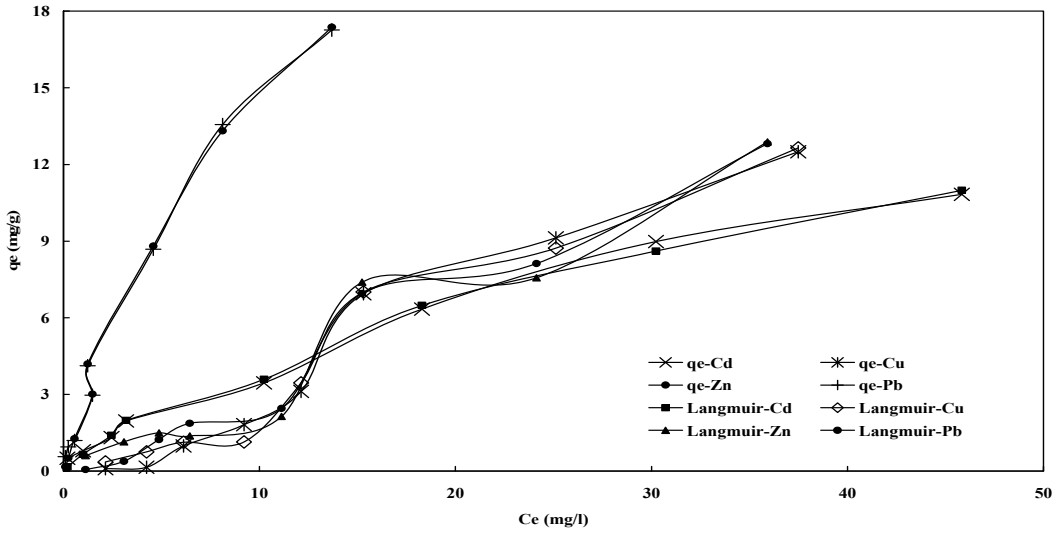


**Figure 4.25** Quaternary biosorption among the Cu(II), Pb(II), Cd(II) and Zn(II) in the four metals system of Cd(II)-Pb(II)-Cu(II)-Zn(II).

The parameter of $K_L$ values of the Langmuir isotherm indicates the affinity of a biosorbent for the two, three or four metal ions. The greater the value of these parameters, the lesser is the affinity for a metal ion (Kusvuran et al., 2012; Şengil and Özacar, 2009). The values of $K_{L\text{-}Cu}$, $K_{L\text{-}Pb}$, $K_{L\text{-}Zn}$, and $K_{L\text{-}Cd}$ are slightly higher in the case of multimetals system than the value of $K_L$ derived for the single metal system (Table 4.4, Table 4.5, Table 4.6 and Table 4.7). This means that the affinity of GG biosorbent for metal ions was reduced in multi-metals metal system. It is found from monolayer biosorption capacity ($q_m$) that the Pb(II) uptake was higher than the other

metals uptake (Table 4.12). It is speculated that garden grass has greater affinity towards Pb(II) ions than Cd(II), Zn(II) and Cu(II) ions.

### 4.2.6.1 Antagonism of multi-metals system

It is has been discussed in the literature (Leyva-Ramos et al., 2001) that the multi-metal Langmuir model provides a reasonable fit to the multi-metals biosorption data , as long as the $q_m$ values for each metal calculated from single-metal are similar to multi-metal systems. On the other hand, the prediction for $q_m$ values from quaternary system are lower than the single metals system (Kumar et al., 2008; Şengil and Özacar, 2009). The antagonism between the metals' ions is the internal competition. The real wastewater is the mixture of several metals' matrices and antagonism is the common activity among the metals (Raize et al., 2004). To understand the antagonism of real wastewater a quaternary system isotherm was conducted. To visualise the antagonism among the four metals surface diagram was constructed and plotted in Figure 4.26(a, b, c and d).

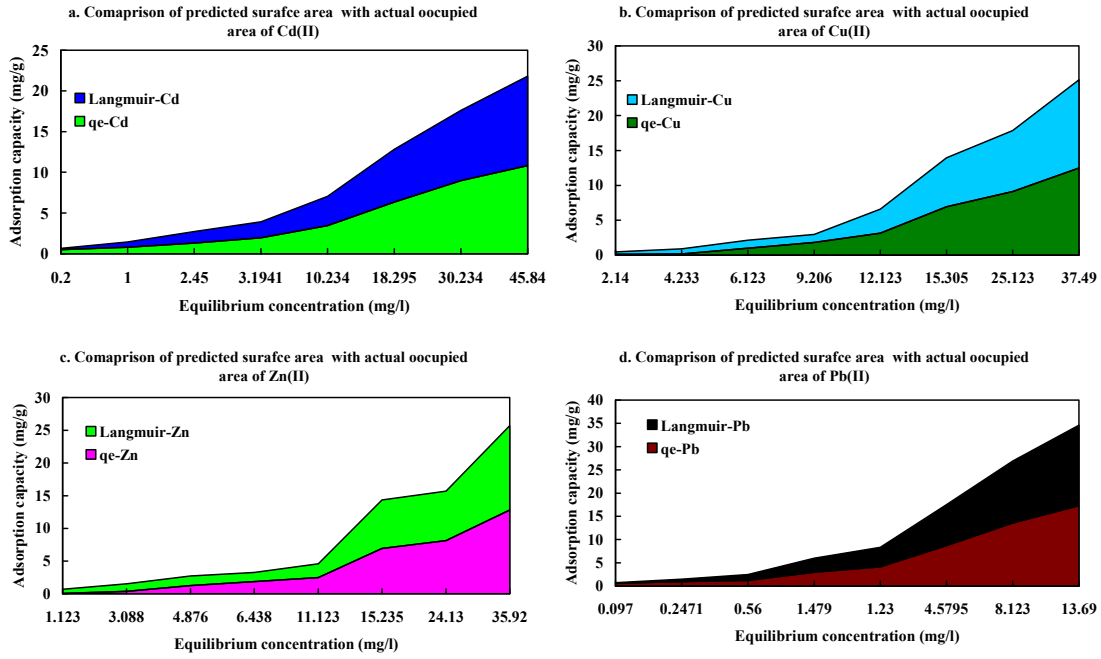


**Figure 4.26** Experimental and model predicted surface areas in terms of biosorption capacity of metals in surface diagram for quaternary metals biosorption onto GG.

It is revealed that the Pb(II) ions presented a higher affinity for the binding sites of the GG than the Cu(II), Cd(II) and Zn(II) ions. In other words, the GG was much more selective towards Pb(II) than to other three metals in the competitive biosorption. The Pb(II) ions presented strong antagonism against the biosorption of Cu(II), Zn(II) and Cd(II) ions in the quaternary system. This behaviour could not be predicted from the

single metal biosorption system. It is also found from Figure 4.26 (a, b, c and d) that Pb(II) ions took higher surface area than other metals. On the other hand, the most binding sites of GG are occupied by Pb(II) ions in competitive system (Raize et al., 2004; Şengil and Özacar, 2009). It is also found from Figure 4.26 that the occupied surface area increases with the increase of initial concentration of metals (0 to 18 mg/l) in the quaternary system. Also, the values of model prediction are similar to the experimental values as both surfaces are nearly equal in magnitude.

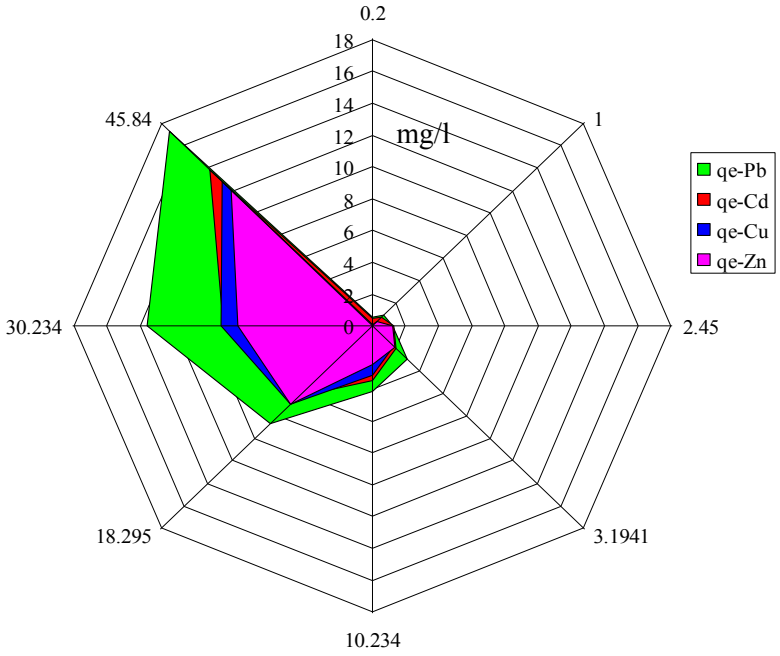


**Figure 4.27** Engaged area in terms of capacity of metals in radar diagram for quaternary metals biosorption onto GG.

As the Pb(II) ions occupied the higher spiral surface of radar plot, the superior attraction toward GG is depicted (Apiratikul and Pavasant, 2006; Raize et al., 2004). Similarly, Cd(II) and Cu(II) ions possess similar antagonism as the uptake capacities were almost same (19.878 and 19.951mg/g) among the four- metal (Table 4.12). Zn(II) ions appeared as the lowest magnitude of affection towards GG though its prediction from single was different(Padilla-Ortega et al., 2013; Şengil and Özacar, 2009).

It is also found that dominant Pb(II) ions uptakes were reduced only to 24.17%, whereas Cd(II), Cu(II) and Zn(II) ions uptake is decreased to 52.29%, 65.94% and 71.60% for quaternary systems. The highest suppression was on Zn(II) in four metals system though Zn(II) has the second highest capacity in the single metal biosorption. It is found

that in a single metal system the Pb(II) uptake was in the third level (54.205 mg/g) in comparison to Cu(II) (58.569 mg/g : first), Zn(II) (57.530 mg/g: second) and Cd(II) (41.66 mg/g: fourth). However, it is dominated in quaternary systems. Therefore, it can be presumed that GG had high affinity to Pb(II) ions than other metals or other metals (Cd(II), Cu(II) and Zn(II) could not pose enough antagonism to decrease the biosorption of Pb(II) ions. In other words, antagonism is a co-metalled dependent for particular metals (Niu et al., 2013; Xue et al., 2009).

## 4.3 Conclusion

- Greatly abandoned garden grass was transformed into biosorbents for removal of toxic Pb(II), Cd(II), Cu(II) and Zn(II) ions from aqueous solutions. The biosorbent preparation method is very simple. First, collect the garden grass (GG). Second, remove the dirt. Next, wash the collected grass. Finally, let it dry in an oven for 24 hours with 105°C and grind it into powder. The experimental results and model prediction revealed that garden grass has effectively removed the Pb(II), Cd(II), Cu(II) and Zn(II) ions from single and multi-metal water systems.
- From characterization (BET and SEM tests), the results showed that GG has a significant specific surface area and potential binding sites in the internal surface of the biosorbents' particles. From FTIR, it was found that cation (Pb(II), Cu(II), Cd(II) and Zn(II)) binding groups such as hydroxyl and carboxyl groups were present in the biosorbents.
- The equilibrium biosorption and desorption data were better described by the Langmuir, and SIPS models though Pb(II) biosorption were also explained by Freundlich model in heterogeneous surfaces.
- Kinetic biosorption and desorption data were adequately explained ($R^2$: 0.992-0.999) by the pseudo-second-order kinetic model for Pb(II), Cu(II), Cd(II) and Zn(II) though pseudo-first-order kinetic model have higher fitness. As the biosorption processes showed higher agreement with pseudo-second-order kinetic model, the biosorption reaction goes to more than one time on the surface of GG. It is happed for all used initial concentration (Co: 10, 50 and 100 mg/l) for Pb(II) as the $n_{AV}$ values (13.46, 20.38 and 36.817 for biosorption and 11.669, 35.00 and 75.270 for desorption) are more than unity. However, it did

not occurred for lower concentration (10 and 50 mg/l) for Cu(II), Cd(II) and Zn(II) biosorption except higher concentration (100 mg/l). The results from the intraparticle diffusion model suggested that intraparticle diffusion was the rate controlling step for Pb(II), Cu(II), Cd(II) and Zn(II) biosorption and desorption onto GG.

- From the results and discussion, it can be recommended that garden grass (GG) biosorbents has the potential capabilities for removal of Pb(II), Cu(II), Cd(II) and Zn(II) ions from single as well as multi-metals water systems.

Faculty of Engineering and Information Technology
University of Technology, Sydney (UTS)

# Chapter 5

# Removal of Cu(II), Pb(II), Cd(II) and Zn(II) from aqueous solution using cabbage bio-wastes

## 5.1 Background

Recently, agricultural waste materials and biomass for the removal of metal ions has been explored (Gupta and Ali, 2004; Sud et al., 2008). By-products or wastes from large-scale agro-production are attracting attention from researchers for use in removing heavy metals from water and wastewater (Garg et al., 2007; Zhang et al., 2010). A wide variety of agricultural waste materials such as modified EFB (Ibrahim et al., 2010), meranti sawdust (Rafatullah et al., 2009), bagasse fly ash (Gupta and Ali, 2004), rubber tree leaf powder(Hanafiah et al., 2006), *Saraca indica* leaf powder (Goyal et al., 2008), tree fern (Ho et al., 2004), ligin from woods (Demirbas, 2004), corncobs (Reddad et al., 2002), moss peat (Summers et al., 1995) and activated carbon prepared from apricot stone (Kobya et al., 2005), coconut shell (Sekar et al., 2004) and other materials are being used for metals removal from water as low-cost alternatives to expensive biosorbents.

Cabbage (*brassica oleracea*) is a commonly used vegetable all over the world. From farmland to dining table, while travelling this path, enormous amounts of agro, market and kitchen wastes are produced by this vegetable. On average, 30-50% of the raw product is wasted in the form of stems and leaves when processing for selling from the farm, selling in markets and while processing for cooking in the kitchen (Choi et al., 2002; Das and Ghosh, 2009).

Twenty million tonnes of food wastes are produced each year in Australia and only 10% of food waste is recycled. The other 90% is sent to landfills (SCECA (Senate Standing Committee on Environment Communications and the Arts, 2008). Cabbage waste (CW) contains more water and therefore readily decompose and create unpleasant environmental consequences (Ngu and Ledin, 2005). The research reported here tried to produce biosorbent materials from CW to be used with Pb(II), Cd(II), Cu(II) and Zn(II) in their removal from water. The purposes of this study were to characterize the biosorbents and to evaluate the Pb(II), Cd(II), Cu(II) and Zn(II) uptake capacities and compare them to other options. The uptake data were evaluated by isotherm models. The effects of the experimental parameters such as contact time, pH, doses and initial Pb(II), Cd(II), Cu(II) and Zn(II) concentrations on adsorption were also investigated. Discovery of the equilibriums and order of reaction at the surface of the biosorbent were also attempted. Multi-metals adsorption of Pb(II), Cd(II), Cu(II) and Zn(II) from binary,

ternary and quaternary systems were examined to characterise the effects of antagonisms among the metals ions.

## 5.2 Results and discussion

### 5.2.1 Characterisation of biosorbent

The metals adsorption capacities, surface properties and active functional groups of potential biosorbents were explored and characterised. The characterisation of a biosorbent is important in the context of uses for selectivity of metals' ions and exploring binding sites and functional groups for ion exchange or chemisorption. In this context, the biosorbent was characterised by SEM, FTIR and BET tests.

#### 5.2.1.1 Surface morphology

The surface structures of biosorbent was analysed by SEM (Chapter 3, Section 3.3.1.1) and is shown in Figure 5.1.

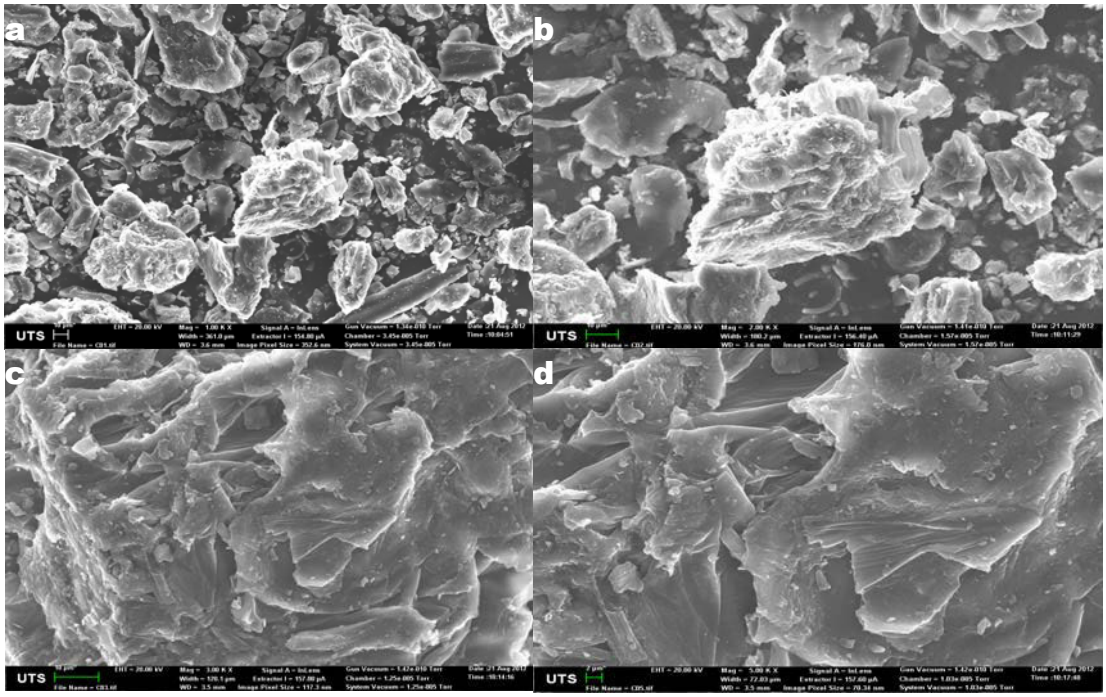


**Figure 5.1** Micro-graphs of cabbage taken by SEM

The micro-graphs revealed that it contained asymmetrical particles (Figure 5.1(a)). In lower magnification, the heterogeneous structures are noticed [Figure 5.1(a) and Figure 5.1(b)]. From higher magnification [Figures 5.1(c) and (d)], the surface of the particles seem to be built with uneven, asymmetric steps and pores. It is presumed that

irregularly shaped particles have more internal biding or uptakes places and adsorb more metals (Hossain et al., 2013).

### 5.2.1.2 Functional groups

Functional groups were the influencing parameters of biosorbents regarding the metals adsorption. The functional groups of CW were evaluated by FTIR (Chapter 3, Section 3.3.1.3) and FTIR spectra of cabbage-biosorbent are shown in Figure 5.2. Chemisorptions and ions exchange mostly depends on the available functional groups in a particular biosorbent (Xue et al., 2009). Carbon-oxygen and carbon bonds are the attracting and stimulating bond for metals adsorption (Kusvuran et al., 2012; Ricordel et al., 2001). The major functional groups found were O-H stretch-free hydroxyl for alcohols/phenols (3624.54 $cm^{-1}$), O-H stretch for carboxylic acids (between 3300-2500 $cm^{-1}$), C-N stretch for aliphatic amines (1024.25 $cm^{-1}$), C-O stretch for alcohols/ carboxylic acids/esters/ethers (between 1320-1000 $cm^{-1}$), =C-H bend for alkanes (between 1000-650 $cm^{-1}$) and C-H "OOH" for aromatics (817.85 $cm^{-1}$). Among the functional groups, hydroxyl, amines and carboxyl groups could bind heavy metal ions with adsorbents (Kongsuwan et al., 2009; Sheng et al., 2004a).

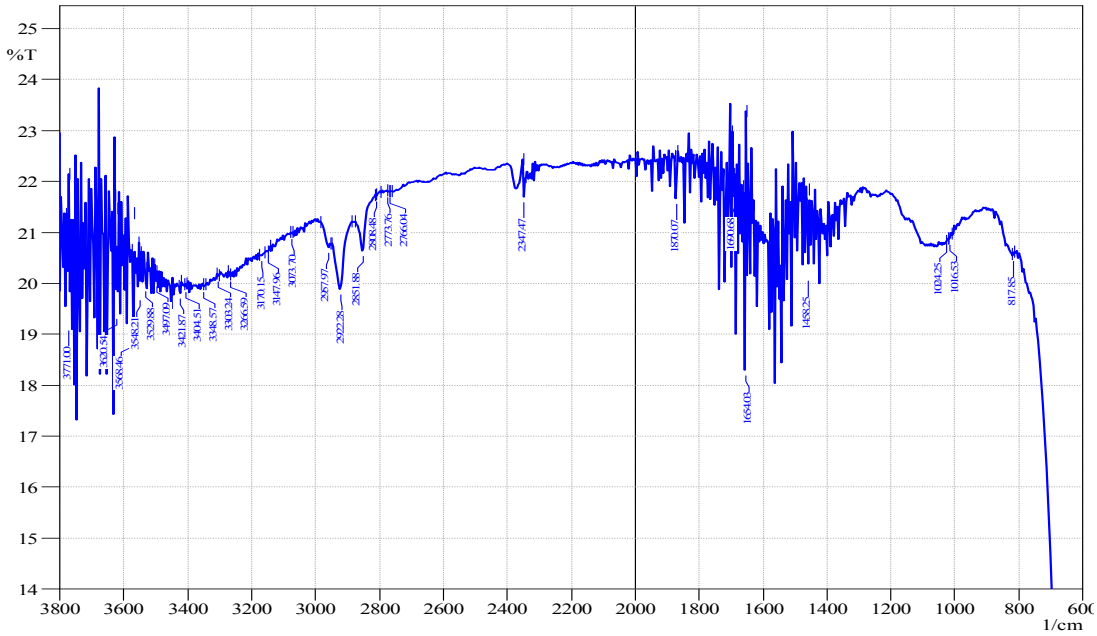


**Figure 5.2** FTIR spectra of the biosorbent from cabbage wastes

### 5.2.1.3 Specific surface area

Surface properties of cabbage were examined by BET testing. The surface properties of cabbage were measured according to methods explained in Chapter 3, Section 3.3.1.4

and tabulated in Table 5.1. The biosorbents have a BET surface area of 1.0265 $m^2/g$ which is lower than conventional biosorbents available in literature. However, it is comparable with the biosorbents produced from agro wastes and used for metals removal from aqueous solution (Hossain et al., 2012).

This biosorbents have noticeable micropore and mesopore areas with magnitudes of 1.01$m^2/g$ and 0.0165$m^2/g$. Most of the pores of cabbage are micropores (95%) and total pore volume was 0.05$cm^3/g$. In addition, the mean mesopore and mesopore sizes of the cabbage were found to be 5.61 and 1.16 Å, respectively, suggesting that this biosorbent falls within the region of micropore based on IUPAC-classification (Arias et al., 2005). The high pore area, pore volume and pore sizes are indicated by the numerous binding sites on the cabbage surfaces (Lu et al., 2010).

**Table 5.1** Surface parameters of cabbage wastes from BET test

| Parameter of garden grass | Methods | Values |
|---|---|---|
| 1. Surface area | BET surface area | 1.0265 $m^2/g$ |
| | Langmuir surface area | -7.32 $m^2/g$ |
| 2. Pore Area | | |
| i. Micropore area | DR method | 1.01$m^2/g$ |
| | t-plot (statistical thickness = 3.50~7.00) | 0.17 $m^2/g$ |
| | Horvath-Kawazoe method | 1.01 $m^2/g$ |
| ii. Mesopore area | BJH adsorption | 0.0165 $m^2/g$ |
| | BJH desorption | 0.304 $m^2/g$ |
| 3. Pore volume | | |
| i. Micropore volume | DR method | 0.05 $cm^3/g$ |
| | t-plot (statistical thickness = 3.50~7.00) | -0.01 $cm^3/g$ |
| | Horvath-Kawazoe method | 0.00 $cm^3/g$ |
| ii. Mesopore volume | BJH adsorption | |
| | BJH desorption | 0.01 $cm^3/g$ |
| 4. Pore size | | 0.01 $cm^3/g$ |
| i. Micropore size | DR method | |
| | t-plot (statistical thickness = 3.50~7.00) | 5.61 Å |
| | Horvath-Kawazoe method | -1006.33 Å |
| | | 12.67 Å |
| ii. Mesopore size | BJH adsorption | |
| | BJH desorption | 1.16 Å |
| | | 2.14 Å |

## 5.2.2 Affecting factors on the performance of biosorption

### 5.2.2.1 pH

The adsorption capacity of cabbage increased with the increase of pH from 2.2 to 7.0 at constant temperature (Conrad and Bruun Hansen, 2007; Kusvuran et al., 2012) (Figure 5.3).

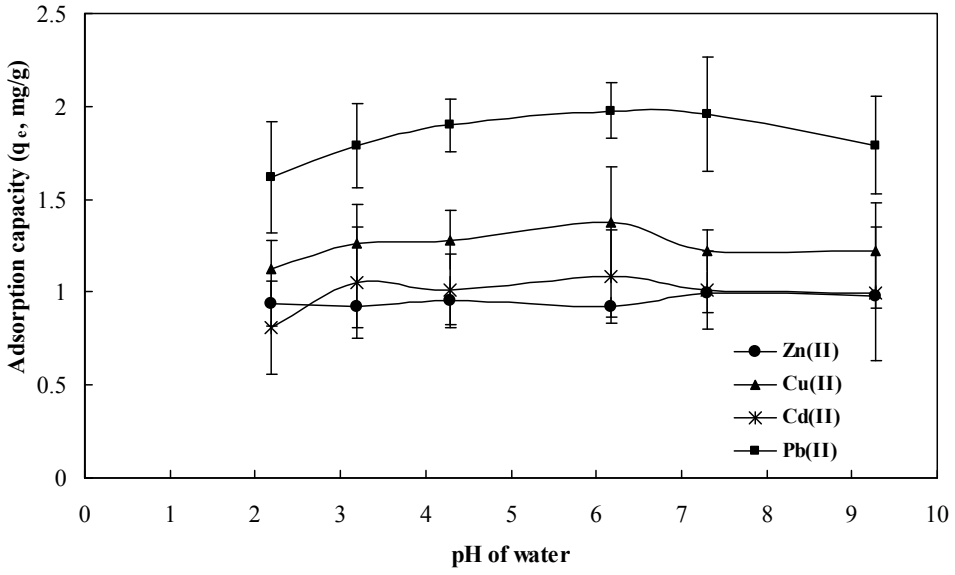


**Figure 5.3** Effect of pH on Cd(II), Cu(II), Zn(II) and Pb(II) adsorptions (Co = 10 mg/l; dose= 0.5g/100ml)

The amount of Cu(II) adsorbed increased from 1.126 to 1.375mg/g with an increase of 1.22-fold when the pH was increased from 2.0 to 6.0. The adsorption capacity of Cd(II) at pH 2.0 and 6.0 corresponded to 0.811mg/g and 1.101mg/g, respectively, amounting to an observed 1.35-fold increase. The amount of Pb(II) adsorbed was found to be 1.616 and 1.977mg/g between pH 2.0 and 6.0, respectively, and a 1.22-fold increment was observed. Similarly, a 1.10-fold increase was found for Zn(II) removals and it was 0.936 to 0.999mg/g for the pH of 2.0 and 7.0. Similar results are also reported in the literature (Conrad and Bruun Hansen, 2007; Demirbas, 2008; Hossain et al., 2012). To avoid metal precipitation, all experiments adopted pH between 6.0 and 6.5.

#### 5.2.2.2 Contact time

The effect of contact time on removal of Cd(II), Cu(II), Zn(II) and Pb(II) by the powder of cabbage was investigated to obtain the equilibrium time (Chapter 3, Section 3.3.2.4) and the results plotted in Figure 5.4. In the first stage (until 10 min), the biosorption process was rapid and during this period a large amount of Cd(II), Cu(II), Zn(II) and Pb(II) were removed from the water (Figure 5.4). This may have occurred as the vast amount of available binding sites on the biosorbent in the first stage (Memon et al., 2008). The second stage was much slower and it reached equilibriums after different times for different initial metals concentrations.

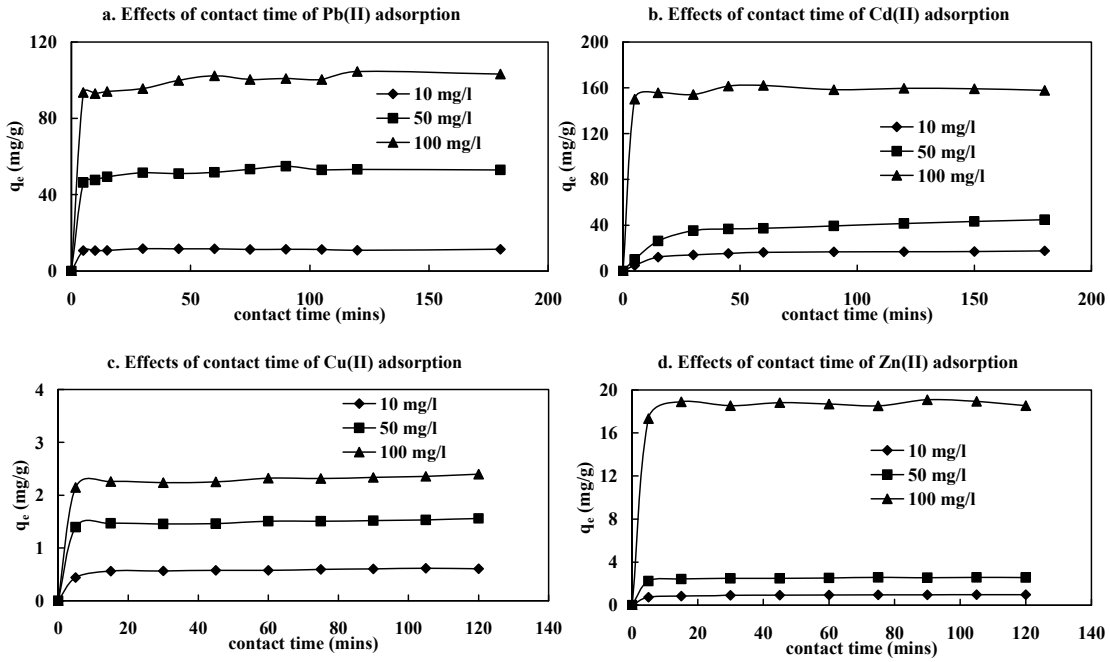


**Figure 5.4** Effects of contact times on the removals of Pb (II), Cd(II), Cu(II) and Zn(II) from water by CW.

The Pb(II) adsorption processes reached equilibriums at 20, 45 and 50 mins for initial concentrations of 10, 50 and 100 mg/l, respectively. Similarly, Cd(II), Cu(II) and Zn(II) adsorption reached equilibrium at 50, 50 and 60 mins; 30, 25 and 25 mins; and, 30, 30 and 30 mins for initial concentrations of 10, 50 and 100 mg/l, respectively. These equilibriums times for Pb(II), Cd(II), Cu(II) and Zn(II) adsorption onto cabbage are rapid and comparable to equilibrium time in the literature (Montazer-Rahmati et al., 2011). The rapid kinetics has an important practical potential for developing metal biosorption systems with cabbage.

### 5.2.2.3 Doses

Effects of doses (g) of cabbage on adsorption of Pb(II), Cd(II), Cu(II) and Zn(II) ions were conducted at 10 mg/l initial metals concentration, while the cabbage doses were varied from 0.1, 0.25, 0.5, 1, 2, 5, 7.5 and 10 g/l (Chapter 3, section 3.3.2.2). The effect of biosorbent doses on the percents removal of Pb(II), Cd(II), Cu(II) and Zn(II) are shown in Figure 5.5. The results indicated that the percent removals of Pb(II), Cd(II), Cu(II) and Zn(II) rapidly increased with increased doses of cabbage and declined after reached its highest values. The maximum Pb(II) removals (99.78%) were found at a 5 g/l dose of cabbage. Similarly the maximum Cd(II), Cu(II) and Zn(II) removals (95.41, 73.56 and 78.65%) were obtained at 5, 6 and 6 g/l doses of cabbage, respectively. To make them comparable, 5 g/l was adopted for all the experiments in this study.

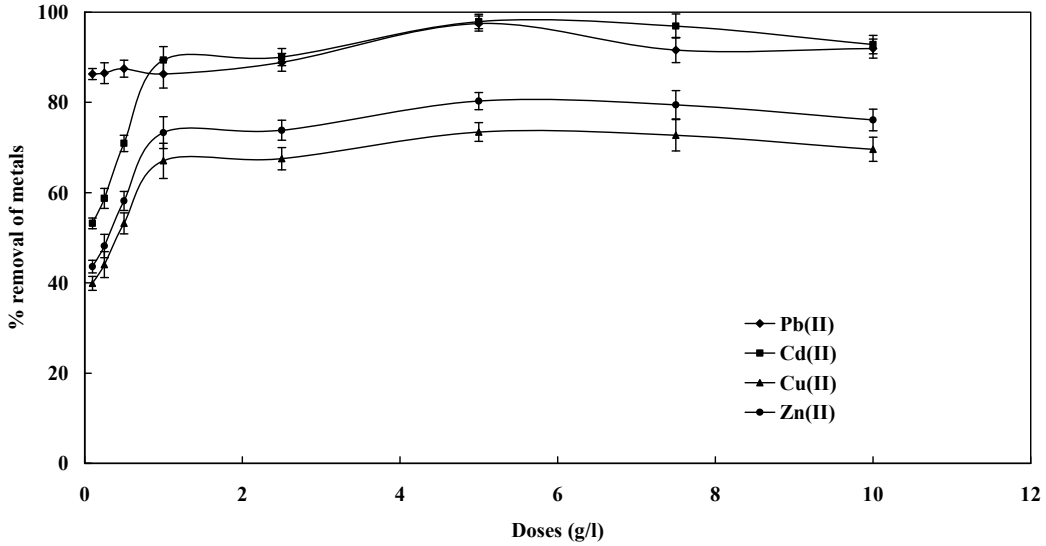


**Figure 5.5** Effects of different doses on the removals of Pb(II), Cd(II), Cu(II) and Zn(II) from water by cabbage biosorbents.

### 5.2.2.4 Initial metals concentration

The effects of varying Pb(II), Cd(II), Cu(II) and Zn(II) concentrations (1 to 100 mg/l) on percentage of removals were conducted while the other four parameters were kept constant (pH:6-6.5; dose: 5 g/l, rpm: 120 and t:180 mins) (according to Chapter 3, Section 3.3.2.5) and is shown in Figure 5.6.

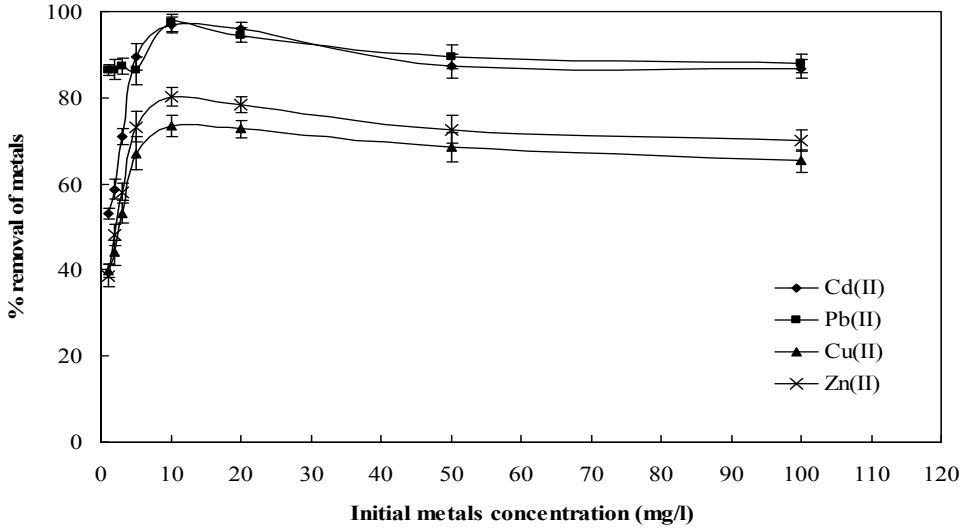


**Figure 5.6** Effect of initial concentrations of Pb(II), Cd(II), Cu(II) and Zn(II) on the percent removal by CW.

The adsorption of metals ions by the adsorbent initially increased rapidly with the increase in Pb(II), Cd(II), Cu(II) and Zn(II) concentrations and slowed down when metals concentrations reached 10 mg/l (Figure 5.6). The initial rapid increase in the

uptake of metals can be attributed to the interactions between the metal ions and the available active sites of the adsorbent (Han et al., 2007; Mustafiz et al., 2002). At higher concentrations more Pb(II), Cd(II), Cu(II) and Zn(II) ions are left un-adsorbed in solution due to the saturation of binding sites. The removal decreases after reaching peaks at 98, 96, 73 and 80% for Pb(II), Cd(II), Cu(II) and Zn(II) respectively and was due to total saturation of the binding sites of the cabbage at same dose (5g/l) with available metals ions at higher concentration (20-100 mg/l). These results are similar to the observations made in this study with removal of metals by other biosorbents available in the literature (Han and Bai, 2010; Kakitani et al., 2006; Pan et al., 2006).

### 5.2.3 Regeneration of biosorbent

The regeneration of biosorbents is a decisive step in the reprocessing and recapturing of valuable metals. It is also involved in reducing the operating cost for any type of water treatment. Several researchers report that adsorbed metals on adsorbents can not be completely recovered (Davis and Upadhyaya, 1996). In this experiment, eight eluents such as tap water, milli-Q water, distilled water, 0.1N $H_2SO_4$, 0.1N HCl, 0.1N $HNO_3$, 0.1N NaOH and 0.1 N $CH_3COOH$ were used for Cu(II), Pb(II), Cd(II) and Zn(II) desorption from cabbage (according to Chapter 3, Section 3.3.3). The batch results of adsorption and desorption with eight eluents plotted in Figure 5.7. As shown in Figure 5.7 (a, b, c and d), adsorption of metals onto cabbage is easily regenerated by a small amount of 0.1N $H_2SO_4$. Among the eluents, the highest 86.67, 70.67, 82.34 and 69.74% recovery of Pb(II), Cu(II), Cd(II) and Zn(II) were obtained by 0.1N $H_2SO_4$ eluents from cabbage (Figures 5.7(a), (b), (c) and (d)). Adsorbed cations ($Cu^{2+}$, $Pb^{2+}$, $Cd^{2+}$ and $Zn^{2+}$) could be replaced by $H^+$ released from acids in the desorption systems (Wankasi et al., 2005).

For obtaining multiple uses of cabbage, the adsorption and desorption cycles were repeated four times with best eluent 0.1N $H_2SO_4$ for Pb(II), Cu(II), Cd(II) and Zn(II) and the results are shown in Figure 5.8 (a, b, c and d). The regeneration efficiency for cabbage decreased gradually after one cycle as the adsorption and desorption continued (Figure 5.8). It is presumed that biosorbent can not be completely recovered from metals adsorption. In the present case, it is observed that the soft cabbage tissues could not withstand acid dissolution stresses and biding sites were destroyed. The regenerated cabbage could be used twice with minor deviation of efficiency

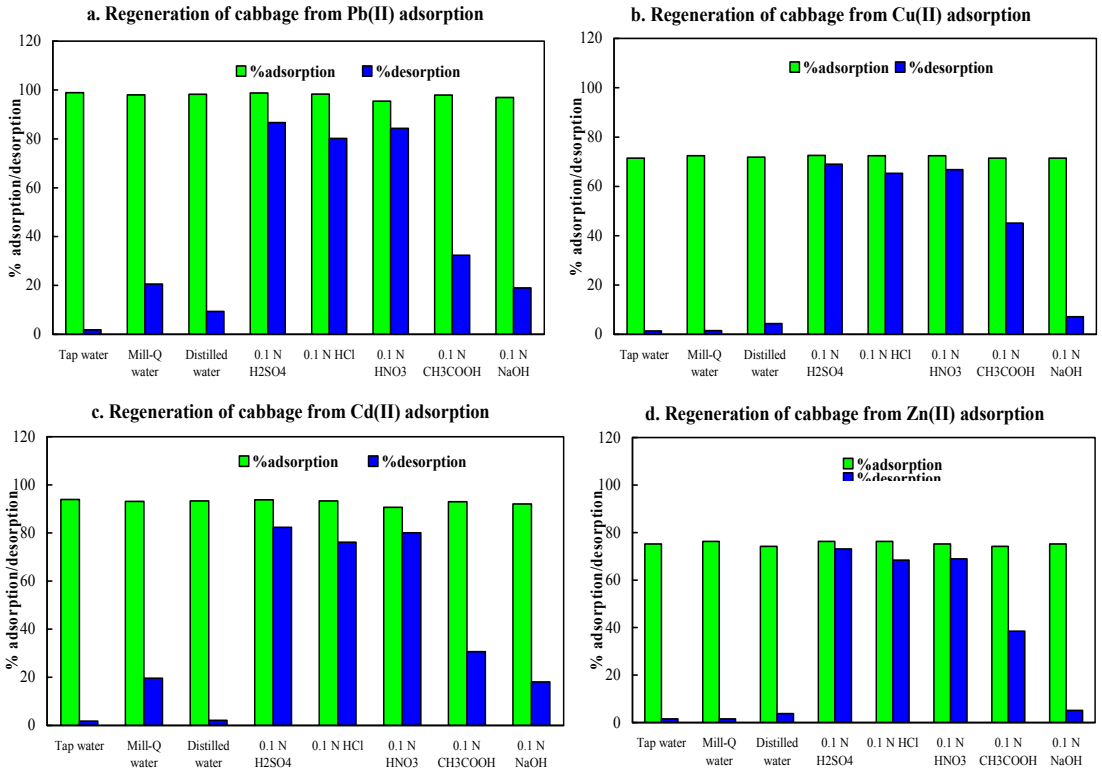


**Figure 5.7** Regeneration of cabbage by different eluent from Pb(II), Cu(II), Cd(II) and Zn(II) adsorption($V_o$: 100; d: 0.5 g; t: 3 h; rpm: 120; T: 20°C).

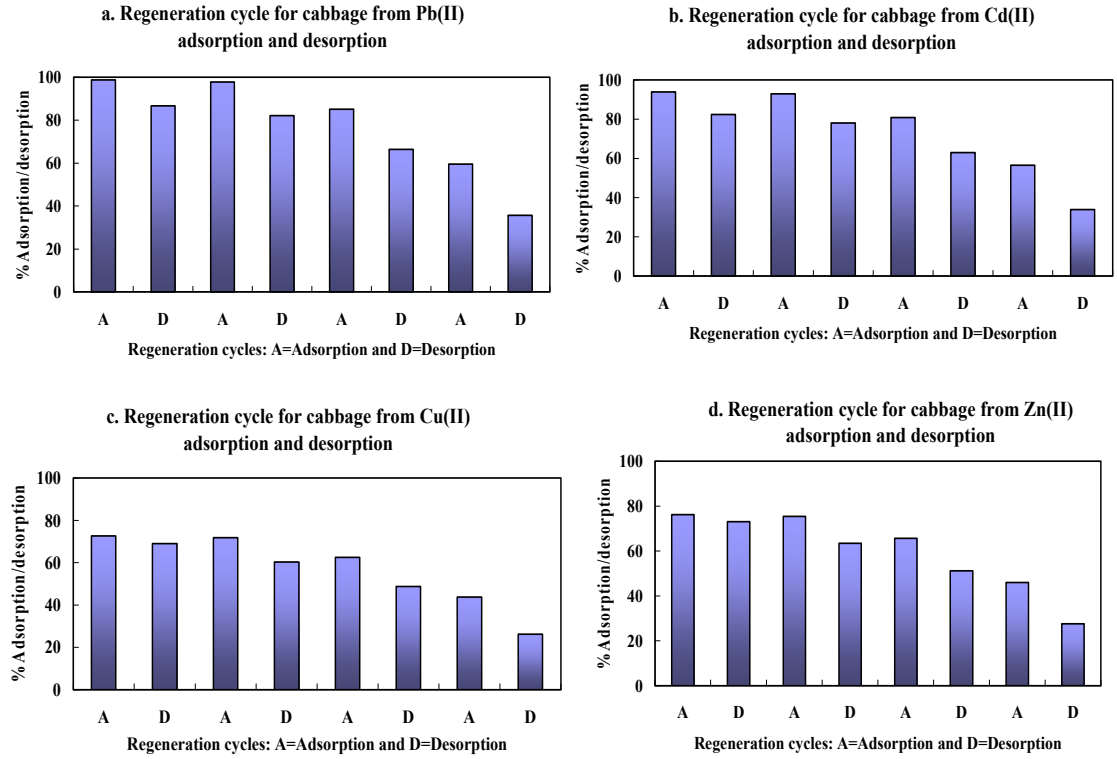


**Figure 5.8** Regeneration cycles of cabbage from Pb(II), Cu(II), Cd(II) and Zn(II) adsorption and desorption by 0.1N $H_2SO_4$. ($V_o$: 100; d: 0.5 g; t: 3 h; rpm: 120; T: 20°C)

## 5.2.4 Kinetics of adsorption and desorption

Kinetics is the process of time dependent adsorption. These parameters are useful for process design of water and wastewater treatment systems when using adsorbents or biosorbents. Inversely, the desorption processes is the reverse of adsorption kinetics. The kinetics of adsorption experiments were conducted in 10 mg/l, 50 mg/l and 100 mg/l metal concentrations for three hours (Chapter 3, section 3.3.5). The desorption experiments were conducted with CW exhausted with 10 mg/l, 50 mg/l and 100 mg/l metals ions in 1litre 0.1N $H_2SO_4$ solution for three hours.

The results of kinetics parameters are calculated from the adsorption and desorption data of Pb(II), Cu(II), Cd(II) and Zn(II) ions onto the surfaces of CW with elapsed time. These parameters represent the characters of biomaterials and forecast the metals adsorption processes as either chemical adsorption or physical adsorption or cation exchange processes (Ho and McKay, 1998). Four kinetics models namely Pseudo-first-order, Pseudo-second-order, Elovich and Avrami were used to describe the kinetics data obtained from both adsorption and desorption. The fitness was evaluated by a coefficient of determination, $R^2$ (Chapter 3, section 3.4). The models' parameters were optimised through non-linear analyses by 'solver' add-in, in MS Excel (Appendix II). The normalized standard deviation (NSD) and average relative error (ARE) (Hossain et al., 2012) were also calculated to judge the fitness of models (Chapter 3, section 3.4). The experimental as well as predicted models for used four models are shown in Figure 5.9 for Pb(II), Figure 5.10 for Cd(II), Figure 5.11 for Cu(II), and Figure 5.12 for Zn(II). The predicted and experimental parameters are tabulated in Table 5.2 for pseudo-first-order kinetics, in Table 5.3 for pseudo-second-order kinetics, in Table 5.4 for Elovich kinetics and in Table 5.4 for Avrami kinetics. On the whole, the kinetics data were well fitted with the models used ($R^2$: 0.967-0.999) for Pb(II), Cu(II), Cd(II) and Zn(II) adsorption and desorption onto the biosorbents.

### 5.2.4.1 Pseudo-first-order kinetics

The pseudo-first order model is the earliest known equation relating the adsorption rate based on the adsorption capacity (Gürses et al., 2006). This equation is also named as the Lagergren-first-order equation (Ho, 2004). This is the broadly employed model for explaining kinetics relation of adsorption reactions (Rajaei et al., 2013). The mathematical form is:

$$\frac{dq_t}{dt} = k_1(q_e - q_t) \quad (5.1)$$

After definite integration within the conditions $q_t$ =0 at t = 0 and $q_t = q_t$ at t = t, Eq. (5.1) becomes the following:

$$\ln(q_e - q_t) = \ln q_e - k_1.t \quad (5.2)$$

where $q_t$ is the amount of metals' ions adsorption in time 't' (min) (mg/g); $k_1$ the rate constant of the equation (l/min); $q_e$ is the amount of adsorption equilibrium (mg/g). The nonlinear form of the equation:

$$q_t = q_e - q_e e^{(-k_1 t)} \quad (5.3)$$

The analysed data (Table 5.2) showed that the experimental data for adsorption are well fitted with this (Eq.5.3) model as the $R^2$ values lies between 0.983 and 0.999. In case of desorption, this model showed good agreement with experimental data from Pb(II), Cu(II) and Zn(II) desorption ($R^2$: 0.930-0.999), but was not well fitted with Cd(II) desorption (Table 5.2).

**Table 5.2** Parameters of pseudo-first-order kinetics for Pb(II), Cd(II), Cu(II) and Zn(II) adsorption onto and desorption from cabbage

| Metals | Parameters | Adsorption | | | Desorption | | |
|---|---|---|---|---|---|---|---|
| | | **10 mg/l** | **50 mg/l** | **100 mg/l** | **10 mg/l** | **50 mg/l** | **100 mg/l** |
| **Experimental** | **$q_e$ (mg/g)** | 11.741 | 53.654 | 95.64 | 2.594 | 39.726 | 87.696 |
| | **Equili. time, t (mins)** | 20 | 45 | 50 | 30 | 20 | 60 |
| **Pb(II)** | $q_e$ (mg/g) | 11.275 | 52.061 | 99.567 | 2.568 | 40.119 | 90.809 |
| | $k_1$ (l/h) | 0.564 | 0.407 | 0.533 | 0.194 | 3.688 | 2.965 |
| | $R^2$ | 0.989 | 0.986 | 0.986 | 0.930 | 0.998 | 0.998 |
| | NSD | 3.153 | 3.664 | 3.719 | 9.687 | 1.526 | 1.516 |
| | ARE | -0.094 | -0.101 | -0.128 | -0.299 | -0.023 | -0.026 |
| **Experimental** | **$q_e$ (mg/g)** | 16.316 | 45.38 | 161.46 | 5.544 | 16.316 | 52.288 |
| | **Equili. time, t (mins)** | 50 | 50 | 60 | 60 | 60 | 60 |
| **Cd(II)** | $q_e$ (mg/g) | 16.753 | 41.446 | 158.52 | 5.308 | 17.138 | 51.782 |
| | $k_1$ (l/h) | 0.073 | 0.060 | 0.587 | 0.211 | 0.247 | 3.000 |
| | $R^2$ | 0.991 | 0.983 | 0.998 | 0.967 | 0.898 | 0.797 |
| | NSD | 4.490 | 5.824 | 1.577 | 7.049 | 12.359 | 22.421 |
| | ARE | -0.248 | -0.521 | -0.025 | 7.049 | -1.094 | -3.669 |
| **Experimental** | **$q_e$ (mg/g)** | 0.616 | 2.336 | 18.321 | 0.362 | 1.519 | 13.121 |
| | **Equili. time, t (mins)** | 30 | 25 | 25 | 60 | 120 | 120 |
| **Cu(II)** | $q_e$ (mg/g) | 0.589 | 2.309 | 18.086 | 0.342 | 1.489 | 13.066 |
| | $k_1$ (l/h) | 0.267 | 0.530 | 0.476 | 2.999 | 2.999 | 2.999 |
| | $R^2$ | 0.992 | 0.995 | 0.999 | 0.928 | 0.990 | 0.991 |
| | NSD | 3.029 | 2.272 | 0.995 | 11.484 | 3.359 | 3.499 |
| | ARE | -0.059 | -0.051 | -0.009 | -1.065 | -0.111 | -0.115 |
| **Experimental** | **$q_e$ (mg/g)** | 0.965 | 2.528 | 18.813 | 0.651 | 1.556 | 9.899 |
| | **Equili. time, t (mins)** | 30 | 30 | 30 | 90 | 60 | 120 |
| **Zn(II)** | $q_e$ (mg/g) | 0.942 | 2.530 | 18.750 | 0.622 | 1.551 | 9.806 |
| | $k_1$ (l/h) | 0.289 | 0.433 | 0.517 | 2.999 | 0.433 | 0.517 |
| | $R^2$ | 0.983 | 0.996 | 0.999 | 0.935 | 0.996 | 0.999 |
| | NSD | 4.719 | 2.045 | 1.068 | 10.209 | 2.0454 | 1.068 |
| | ARE | -0.130 | -0.038 | -0.012 | -0.895 | -0.038 | -0.012 |

For Pb(II) adsorption, the data are sufficiently fitted with the pseudo-first order model as the $R^2$ values are 0.989, 0.986 and 0.986 for the initial Pb(II) concentration of 10, 50 and 100 mg/l respectively (Table 5.2). The small values of NSD (3.153, 3.664 and 3.719) and negative values of ARE (-0.094, -0.101 and -0.128) for the used three initial concentration revealed the suitability of the model to postulate the Pb(II) adsorption onto cabbage. Similarly, desorption data also showed good consistency ($R^2$: 0.930, 0.998 and 0.998) with experimental data (Table 5.2). The predicted equilibrium capacity ($q_e$: 11.275 mg/g) was similar to the experimental $q_e$ (11.741 mg/g) for 10 mg/l initial concentration, but other values were different. Likewise adsorption, the predicted equilibrium capacity (2.568 mg/g) was similar to the experimental $q_e$ (2.594 mg/g).

Cd(II) adsorption data are well fitted with the pseudo-first order model but desorption data are not fitted properly, except at 10 mg/l concentration. The degree of fitness ($R^2$) found was 0.991, 0.983 and 0.998 for 10, 50 and 100 mg/l respectively (Table 5.2) for adsorption of Cd(II). These values are 0.967, 0.898 and 0.797 for desorption of Cd(II) for the used three initial Cd(II) concentration. Small values of NSD and ARE for both adsorption and desorption indicated that the model is suitable to describe the adsorption and desorption processes. The experimental equilibrium capacities for adsorption and desorption ($q_e$: 16.316 and 5.544 mg/g) are close to the model's prediction ($q_e$: 16.753 and 5.308 mg/g) for 10 mg/l initial Cd(II) concentration.

The adsorption and desorption of Cu(II) and Zn(II) onto cabbage posed similar trends of agreement with the pseudo-first order model. The coefficient of determination ($R^2$) are 0.992, 0.995 and 0.999 for adsorption; and 0.928, 0.990 and 0.991 for desorption of Cu(II) while the initial Cu(II) concentration were 10, 50 and 100 mg/l respectively (Table 5.2). These $R^2$ values were 0.983, 0.996 and 0.999 for Zn(II) adsorption and 0.935, 0.996 and 0.999 for Zn(II) desorption while initial Zn(II) concentrations were of 10, 50 and 100 mg/l respectively (Table 5.2). The experimental and model predicted equilibrium capacities are 2.336 mg/l and 2.309 mg/l for Cu(II) adsorption and; 2.528 mg/l and 2.530 mg/l for Zn(II) adsorption while initial Cu(II) and Zn(II) concentration were 50 mg/l. In case of desorption, the experimental and model predicted equilibrium capacities are 0.362 and 0.342 mg/l for Cu(II) desorption from 50 mg/l; and 0.651 and 0.622 mg/g for 10 mg/l; 1.556 and 1.551 mg/g for 50 mg/l; and 9.899 and 9.806 mg/g for 100 mg/l. It seems that Zn(II) adsorption and desorption are better fitted with the

pseudo-first-order model than Cu(II) adsorption and desorption. But it is different from Pb(II) and Cd(II) adsorption and desorption.

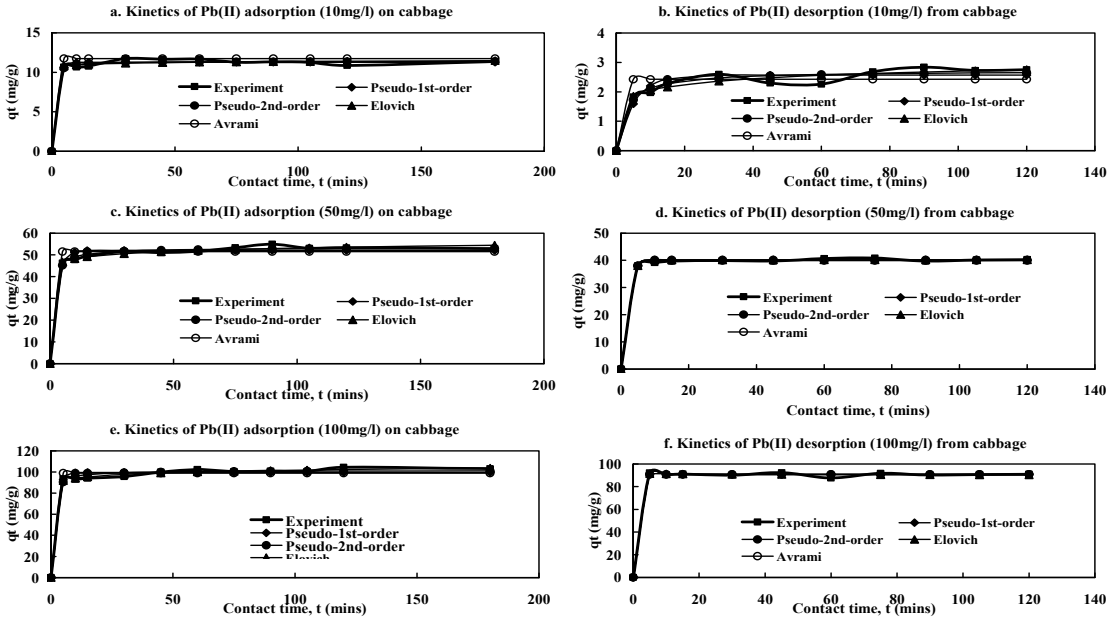


**Figure 5.9** Kinetics modelling of adsorption and desorption of Pb(II) onto cabbage ($C_o$: 50 mg/l; d: 0.5 g; t: 3 h: pH: 6-6.5; rpm: 120; T: room temp.)

Generally the pseudo-first-order kinetics constant, $k_1$ indicates the rate of adsorption reaction. This value provides valuable information about the mechanism of adsorption and subsequently investigation of the controlling mechanism of the biosorption process as either mass transfer or chemical reaction (Khan et al., 2012; Montazer-Rahmati et al., 2011; Omorogie et al., 2012; Patil et al., 2011). This parameter is useful to obtain the optimum operating conditions for industrial-scale batch processes. If $k_1>1$, the adsorption reaction is more than one times and the adsorption mechanism is not physisorption. Likewise, if $k_1<1$, the adsorption reaction is less than one times and the mechanism involved is generally physical sorption or complexation of metals ions with biosorbent (Ho et al., 2004; Ho and Ofomaja, 2006a; Horsfall and Spiff, 2005). Considering the above condition, it is obvious that Pb(II), Cu(II), Cd(II) and Zn(II) ions adsorption processes are fall under the second condition, because $k_1$ values were less than unity for the three initial metal concentrations used (10, 50 and 100 mg/l) and for four metals (Table 5.2). In other words the Pb(II), Cu(II), Cd(II) and Zn(II) ions adsorption mechanism was physical sorption or complexation with cabbage. Conversely, desorption processes showed mixed adsorption mechanisms as the $k_1$

values are less than and greater than unity for different initial exhausted metals concentrations and metals.

### 5.2.4.2 Pseudo-second-order kinetics

The kinetic data from the biosorption of Pb(II), Cu(II), Cd(II) and Zn(II) ions onto cabbage are illustrated by pseudo-second-order equation. This model is based on the assumption that the rate-limiting step may be chemical sorption involving valance forces through sharing or exchange of electrons between heavy metal ions and the adsorbent and offers the best consistent data for the heavy metal ions (Namasivayam et al., 2007). The mathematical expression (Ho and McKay, 2000) is in the following form:

$$\frac{dq_t}{dt} = k_2\left(q_e - q_t\right)^2 \qquad (5.4)$$

After integration within the conditions $q_t$ =0 at t = 0 and $q_t$ = $q_t$ at t = t, Eq. (5.4) becomes the following (Demirbas et al., 2004):

$$q_t = \frac{k_2 q_e^2 t}{(1 + q_e k_2 t)} \qquad (5.5)$$

where the $k_2$, rate constant of pseudo-second-order adsorption (g/(mg min)) and $q_e$, adsorption capacity is at equilibrium (mg/g). The initial adsorption rate of metal was calculated by the following equation (Ho, 2004):

$$h = k_2 q_e^2 \qquad (5.6)$$

The experimental and model predicted parameters are tabulated in Table 5.3. Surprisingly, the adsorption and desorption data showed better fitness ($R^2$: 0.992-0.999 for adsorption and $R^2$: 0.955-0.999 for desorption) with the pseudo-second-order model than the pseudo-first-order model.

This implies that chemisorption controlled the reaction rate of Pb(II), Cu(II), Cd(II) and Zn(II) ions adsorption onto and desorption from CW (Ho and McKay, 2000). The $k_2$ values from pseudo-second-order kinetics which determine the adsorption process occur in two reactions. The first one is fast and reaches equilibrium quickly and the second is a slower reaction that can continue for long time periods (Ho and McKay, 2000; Ho and Ofomaja, 2006b). But the values of $k_2$ are less than unity for adsorption of Pb(II), Cu(II), Cd(II) and Zn(II) ions adsorption onto cabbage which implies the mechanism of Pb(II), Cu(II), Cd(II) and Zn(II) ions adsorption is not chemisorption. In the case of

desorption, the $k_2$ values are more than unity for Pb(II) and Cu(II) desorption from cabbage but are less than one for Cd(II) and Zn(II) desorption. It is noticeable that model fitness and $k_2$ values revealed the opposite proposition for adsorption and desorption mechanisms of Pb(II), Cu(II), Cd(II) and Zn(II) ions onto cabbage.

**Table 5.3** Parameters of pseudo-second-order kinetics for Pb(II), Cd(II), Cu(II) and Zn(II) adsorption onto and desorption from cabbage

| Metals | Parameters | Adsorption | | | Desorption | | |
|---|---|---|---|---|---|---|---|
| | | 10 mg/l | 50 mg/l | 100 mg/l | 10 mg/l | 50 mg/l | 100 mg/l |
| **Experimental** | **$q_e$ (mg/g)** | 11.741 | 53.654 | 95.64 | 2.594 | 39.726 | 87.696 |
| **Pb(II)** | $q_e$ (g/mg.min) | 11.410 | 53.282 | 101.454 | 2.714 | 40.134 | 90.797 |
| | $k_2$ (1/h) | 0.212 | 0.021 | 0.016 | 0.126 | 9.604 | 6.657 |
| | $R^2$ | 0.992 | 0.995 | 0.993 | 0.955 | 0.998 | 0.998 |
| | $h=k_2q_e^2$(mg/g.min) | 27.604 | 0.996 | 166.27 | 0.929 | 15469 | 54880 |
| | NSD | 2.700 | 2.049 | 2.591 | 7.570 | 1.530 | 1.5194 |
| | ARE | -0.072 | -0.033 | -0.059 | -0.399 | -0.048 | -0.003 |
| **Experimental** | **$q_e$ (mg/g)** | 16.316 | 45.38 | 161.46 | 5.544 | 16.316 | 52.288 |
| **Cd(II)** | $q_e$ (g/mg.min) | 18.575 | 46.873 | 159.66 | 5.052 | 18.232 | 59.104 |
| | $k_2$ (1/h) | 0.005 | 0.002 | 0.019 | 0.135 | 0.018 | 0.004 |
| | $R^2$ | 0.990 | 0.989 | 0.998 | 0.966 | 0.970 | 0.988 |
| | $h=k_2q_e^2$(mg/g.min) | 1.856 | 3.592 | 485.21 | 3.439 | 6.055 | 13.334 |
| | NSD | 9.703 | 10.712 | 1.3533 | 8.294 | 9.124 | 5.342 |
| | ARE | -2.257 | -2.730 | -0.018 | 5.688 | -0.399 | -9.5E-05 |
| **Experimental** | **$q_e$ (mg/g)** | 0.616 | 2.336 | 18.321 | 0.362 | 1.519 | 13.121 |
| **Cu(II)** | $q_e$ (g/mg.min) | 0.611 | 2.336 | 18.280 | 0.366 | 1.518 | 13.330 |
| | $k_2$ (1/h) | 0.851 | 0.891 | 0.105 | 1.445 | 1.372 | 0.147 |
| | $R^2$ | 0.996 | 0.997 | 0.998 | 0.998 | 0.999 | 0.999 |
| | $h=k_2q_e^2$(mg/g.min) | 0.3183 | 4.860 | 34.978 | 0.193 | 3.160 | 26.102 |
| | NSD | 2.046 | 1.823 | 1.305 | 1.935 | 1.780 | 1.361 |
| | ARE | -0.050 | -0.031 | -0.019 | -0.047 | -0.029 | -0.021 |
| **Experimental** | **$q_e$ (mg/g)** | 0.965 | 2.528 | 18.813 | 0.651 | 1.556 | 9.899 |
| **Zn(II)** | $q_e$ (g/mg.min) | 0.979 | 2.575 | 18.750 | 0.663 | 1.576 | 9.878 |
| | $k_2$ (1/h) | 0.557 | 0.503 | 0.517 | 0.835 | 0.829 | 0.254 |
| | $R^2$ | 0.997 | 0.999 | 0.999 | 0.999 | 1.000 | 0.999 |
| | $h=k_2q_e^2$(mg/g.min) | 0.534 | 3.332 | 181.90 | 0.3664 | 2.059 | 24.766 |
| | NSD | 2.056 | 0.958 | 1.068 | 1.923 | 0.881 | 1.407 |
| | ARE | 0.0001 | -0.006 | -0.012 | 0.004 | -0.005 | -0.021 |

In addition to $R^2$, significantly low NSD and ARE values were also obtained from pseudo-second-order for all metals adsorption and desorption which further advocates the fitness of the pseudo-second-order model and chemisorption process (Ho and McKay, 2000). Experimental and predicted values of equilibrium adsorption capacities ($q_e$) showed better consistencies with the pseudo-second-order model than the pseudo-first-order model. Thus, it can be concluded that the pseudo-second-order model is the better model to describe the Pb(II), Cu(II), Cd(II) and Zn(II) ions adsorption onto and desorption from cabbage.

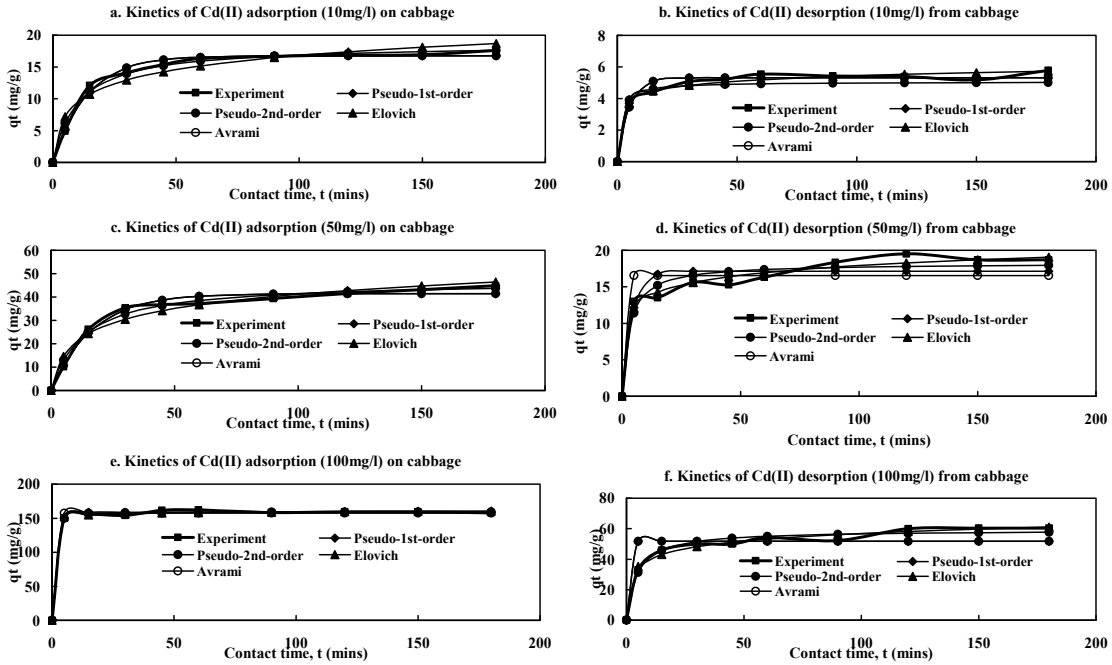


**Figure 5.10** Kinetics modelling of adsorption and desorption of Cd(II) onto cabbage ($C_o$: 50 mg/l; d: 0.5 g; t: 3 h: pH: 6-6.5; rpm: 120; T: room temp.)

### 5.2.4.3 Elovich equation

The Elovich equation assumes that the active sites of the biosorbent are heterogeneous (Cheung et al., 2003) and therefore exhibit different activation energies for chemisorption (Gupta and Babu, 2006). Teng and Hsieh (Teng and Hsieh, 1998) proposed that constant $\alpha$ is related to the rate of chemisorption and $\beta$ is related to the surface coverage. The Elovich model is presented by the following equation (Clayton and Chien, 1980):

$$q_t = \beta.\ln(\alpha\beta t) \qquad (5.7)$$

where, α is the initial adsorption rate (mg/g/min) and β is desorption constant (g/mg).

This model provides the best fit to the experimental data, as can be seen for the different error and $R^2$ values are shown in Table 5.4. For Pb(II), the degree of fitness ($R^2$) for model prediction and experimental data are 0.989, 0.968 and 0.974 for adsorption and 0.968, 0.998 and 0.998 for desorption for the used 10, 50 and 100 mg/l metals concentration, respectively. The $R^2$ values are 0.972, 0.979 and 0.999 for adsorption and 0.989, 0.990 and 0.993 for desorption of Cd(II) from cabbage for used three Cd(II) concentrations. Similarly, the ($R^2$) values are found to be 0.995, 0.999 and 0.998 from adsorption and 0.994, 0.999 and 0.997 from desorption of Cu(II). The most fitted data

were found from Zn(II) adsorption and desorption as the $R^2$ values are 0.999, 0.999 and 0.996 for adsorption and 0.998, 0.999 and 0.998 for desorption. Significantly low and small values of 'NSD' and 'ARE' are found for all metals (Pb(II), Cd(II), Cu(II) and Zn(II)) adsorption and desorption which also dignify the model's association of metals adsorption onto and desorption from cabbage.

**Table 5.4** Parameters of Elovich model for Pb(II), Cd(II), Cu(II) and Zn(II) adsorption onto and desorption from cabbage

| Metals | Parameters | Adsorption | | | Desorption | | |
|---|---|---|---|---|---|---|---|
| | | 10 mg/l | 50 mg/l | 100mg/l | 10 mg/l | 50 mg/l | 100mg/l |
| **Pb(II)** | α [mg/(g.min)] | 10.506 | 43.264 | 86.353 | 1.391 | 40.000 | 92.033 |
| | β (g/mg) | 0.187 | 2.152 | 3.334 | 0.285 | 0.033 | -0.339 |
| | $R^2$ | 0.998 | 0.968 | 0.974 | 0.968 | 0.998 | 0.998 |
| | NSD | 2.972 | 1.749 | 1.571 | 6.639 | 1.522 | 1.459 |
| | ARE | -0.089 | -0.033 | -0.024 | -0.430 | -0.023 | -0.021 |
| **Cd(II)** | α [mg/(g.min)] | 2.007 | 8.871 | 148.50 | 3.125 | 9.017 | 23.546 |
| | β (g/mg) | 3.212 | 0.342 | 2.328 | 0.502 | 1.932 | 7.238 |
| | $R^2$ | 0.972 | 0.979 | 0.999 | 0.989 | 0.990 | 0.993 |
| | NSD | 17.746 | 16.996 | 1.613 | 5.038 | 4.995 | 4.548 |
| | ARE | -3.349 | -3.464 | -0.026 | -0.298 | -0.193 | -0.259 |
| **Cu(II)** | α [mg/(g.min)] | 0.391 | 2.037 | 16.343 | 0.245 | 1.335 | 12.110 |
| | β (g/mg) | 0.048 | 0.067 | 0.413 | 0.025 | 0.040 | 0.245 |
| | $R^2$ | 0.995 | 0.999 | 0.998 | 0.994 | 0.999 | 0.997 |
| | NSD | 3.691 | 1.206 | 2.259 | 4.170 | 1.078 | 2.479 |
| | ARE | -0.158 | -0.014 | -0.052 | -0.195 | -0.011 | -0.062 |
| **Zn(II)** | α [mg/(g.min)] | 0.627 | 2.118 | 18.592 | 0.445 | 1.321 | 9.127 |
| | β (g/mg) | 0.077 | 0.101 | 0.829 | 0.045 | 0.054 | 0.153 |
| | $R^2$ | 0.999 | 0.999 | 0.996 | 0.998 | 0.999 | 0.998 |
| | NSD | 1.405 | 1.081 | 2.890 | 2.270 | 1.360 | 2.073 |
| | ARE | -0.029 | -0.013 | -0.079 | -0.067 | -0.020 | -0.043 |

A higher value of α [10.506 43.264 and 86.353 mg/(g.min) for Pb(II); 2.007, 8.871 and 148.50 mg/(g.min) for Cd(II); 0.391, 2.037 and 16.343 mg/(g.min) for Cu(II) and; 0.627, 2.118 and 18.592 mg/(g.min) for Zn(II) adsorption] and low values of β (between 0.048 and 3.334 for all metals adsorption) also showed that the adsorption mechanism is chemisorptions (Gupta and Torres, 1998). It can presumed from the above discussion the Pb(II), Cd(II), Cu(II) and Zn(II) ions adsorption happened on the heterogeneous catalyst surfaces of biosorbent (Cheung et al., 2003). In fact, it was found from SEM and FTIR analysis of the cabbage that this material contains a heterogeneous surface with different functional groups which could uptake or adsorb metals cations (Cheung et al., 2003). Very similar results are found from the desorption processes of Pb(II), Cd(II), Cu(II) and Zn(II) ions from cabbage.

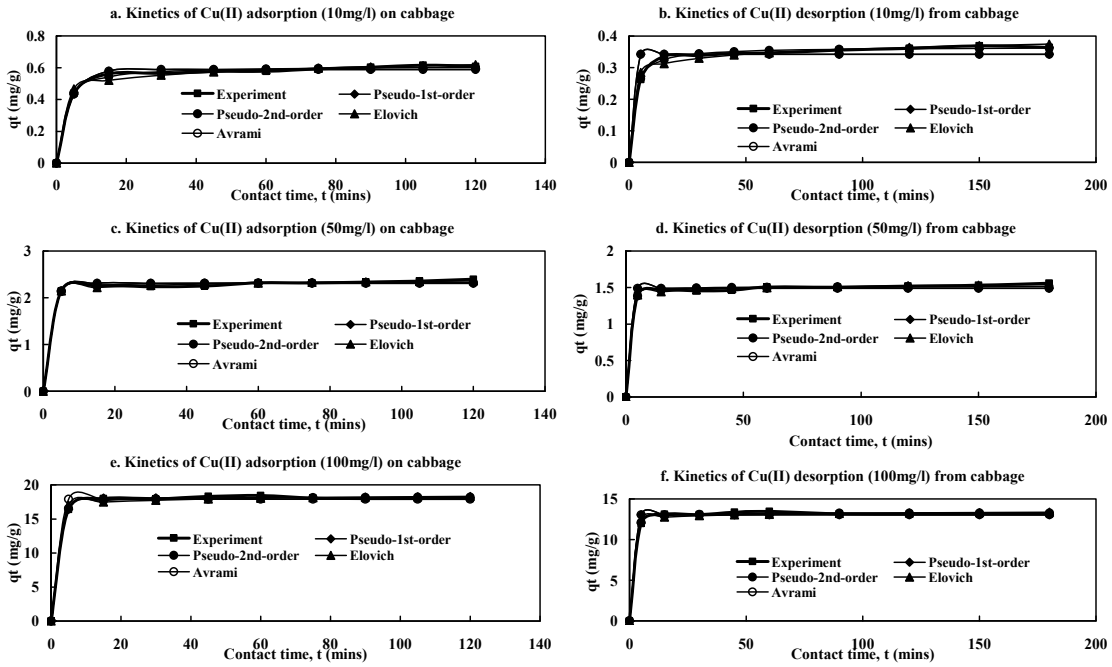


**Figure 5.11** Kinetics modelling of adsorption and desorption of Cu(II) onto cabbage ($C_o$: 50 mg/l; d: 0.5 g; t: 3 h: pH: 6-6.5; rpm: 120; T: room temp.)

### 5.2.4.4 Avrami kinetic equation

The Avrami kinetic equation determines some kinetic parameters, as possible changes of the adsorption and desorption rates in function of the initial metals concentration and the adsorption/desorption time, as well as the determination of fractionery kinetic orders (Lopes et al., 2003). The equation of Avrami kinetic model presents Avrami exponential that is a fractionery number related with the possible changes of the adsorption mechanism that takes place during the adsorption process. So the mechanism of adsorption could follow multiple kinetic orders that are changed during the contact of the metals with the biosorbents (Lopes et al., 2003).

$$q_t = q_e\left[1 - e^{(-t.k_{AV})^{nAV}}\right] \qquad (5.8)$$

where, $K_{AV}$ is the Avrami kinetic constant and $n_{AV}$ is fractionery kinetic orders, which is related to the adsorption mechanisms changes.

**Table 5.5** Parameters of Avrami model for Pb(II), Cd(II), Cu(II) and Zn(II) adsorption onto and desorption from cabbage

| Metals | Parameters | Adsorption | | | Desorption | | |
|---|---|---|---|---|---|---|---|
| | | 10 mg/l | 50 mg/l | 100 mg/l | 10 mg/l | 50 mg/l | 100mg/l |
| **Experimental** | **$q_e$ (mg/g)** | 11.741 | 53.654 | 95.64 | 2.594 | 39.726 | 87.696 |
| **Pb(II)** | $q_e$ (mg/g) | 11.741 | 51.474 | 98.894 | 2.424 | 39.906 | 90.806 |
| | $K_{AV}$ (/min) | 2.000 | 1.005 | 3.299 | 2.006 | 1.000 | 2.000 |
| | $n_{AV}$ | 10.00 | 25.076 | 5.695 | 10.00 | 25.076 | 10.00 |
| | $R^2$ | 0.960 | 1.000 | 0.982 | 0.902 | 1.000 | 0.999 |
| | NSD | 6.320 | 5.328 | 4.196 | 16.075 | 1.611 | 1.516 |
| | ARE | -5.337 | -0.515 | -0.173 | -2.269 | 0.568 | -0.023 |
| **Experimental** | **$q_e$ (mg/g)** | 16.316 | 45.38 | 161.46 | 5.544 | 16.316 | 52.288 |
| **Cd(II)** | $q_e$ (mg/g) | 16.753 | 41.446 | 157.58 | 5.308 | 16.554 | 51.782 |
| | $K_{AV}$ (/min) | 0.038 | 0.035 | 2.000 | 0.131 | 21.968 | 21.968 |
| | $n_{AV}$ | 1.941 | 1.723 | 2.001 | 1.613 | 3.380 | 3.380 |
| | $R^2$ | 0.996 | 0.991 | 0.998 | 0.987 | 0.937 | 0.917 |
| | NSD | 4.490 | 5.825 | 2.424 | 7.049 | 15.710 | 22.420 |
| | ARE | -0.248 | -0.522 | -0.057 | -0.084 | -2.245 | -3.669 |
| **Experimental** | **$q_e$ (mg/g)** | 0.616 | 2.336 | 18.321 | 0.362 | 1.519 | 13.121 |
| **Cu(II)** | $q_e$ (mg/g) | 0.589 | 2.309 | 17.899 | 0.342 | 1.489 | 13.066 |
| | $K_{AV}$ (/min) | 0.091 | 0.184 | 3.996 | 2.000 | 2.000 | 2.000 |
| | $n_{AV}$ | 2.941 | 2.879 | 3.123 | 2.00 | 2.00 | 2.00 |
| | $R^2$ | 0.997 | 0.998 | 0.997 | 0.973 | 0.997 | 0.997 |
| | NSD | 3.028 | 2.272 | 3.499 | 11.483 | 3.359 | 3.499 |
| | ARE | -0.055 | -0.051 | -0.115 | -1.065 | -0.111 | -0.115 |
| **Experimental** | **$q_e$ (mg/g)** | 0.965 | 2.528 | 18.813 | 0.651 | 1.556 | 9.899 |
| **Zn(II)** | $q_e$ (mg/g) | 0.942 | 2.497 | 18.750 | 0.639 | 1.551 | 9.724 |
| | $K_{AV}$ (/min) | 0.181 | 1.000 | 0.517 | 0.173 | 0.256 | 1.609 |
| | $n_{AV}$ | 1.598 | 2.999 | 2.999 | 1.668 | 1.691 | 1.896 |
| | $R^2$ | 0.994 | 0.994 | 1.000 | 0.994 | 0.999 | 0.998 |
| | NSD | 4.719 | 4.649 | 1.068 | 4.719 | 2.045 | 2.890 |
| | ARE | -0.130 | -0.201 | -0.011 | -0.130 | -0.037 | -0.079 |

The Avrami kinetic equation was used to describe the kinetics of Cu(II), Zn(II), Pb(II), and Cd(II) adsorption onto and desorption from cabbage. This equation determines some kinetic parameters namely possible changes of the adsorption rates in function of the initial lead and cadmium concentration and the adsorption time, as well as the determination of fractionery kinetic orders (Lopes et al., 2003). The conformity between the experimental data and the model-predicted values were found from $R^2$, NSD and ARE values (Table 5.5). The overall fitness of this model with experimental data from adsorption and desorption of Cu(II), Zn(II), Pb(II), and Cd(II) are excellent as the $R^2$ values lies between 0.960 and 1.00 for used 10, 50 and 100 mg/l metals concentration. In addition, the model predicted equilibrium ($q_e$) capacities (11.741, 51.475 and 98.894 mg/g for Pb(II) adsorption and; 2.424, 39.906 and 90.806 mg/g for Pb(II) desorption) are close to the experimental equilibrium ($q_e$) capacities (11.741, 53.654 and 95.640 for Pb(II) adsorption and; 2.594, 29.726 and 87.696 mg/g for Pb(II) desorption). Similarly

the experimental equilibrium ($q_e$) capacities are close enough to the model prediction for Cd(II), Cu(II) and Zn(II) adsorption and desorption (Table 5.5). The values of $q_e$ for both adsorption and desorption processes were similar to pseudo-second-order and close to experimental values. From above discussion it can be decided that this model is suitably describe the kinetics processes of adsorption and desorption.

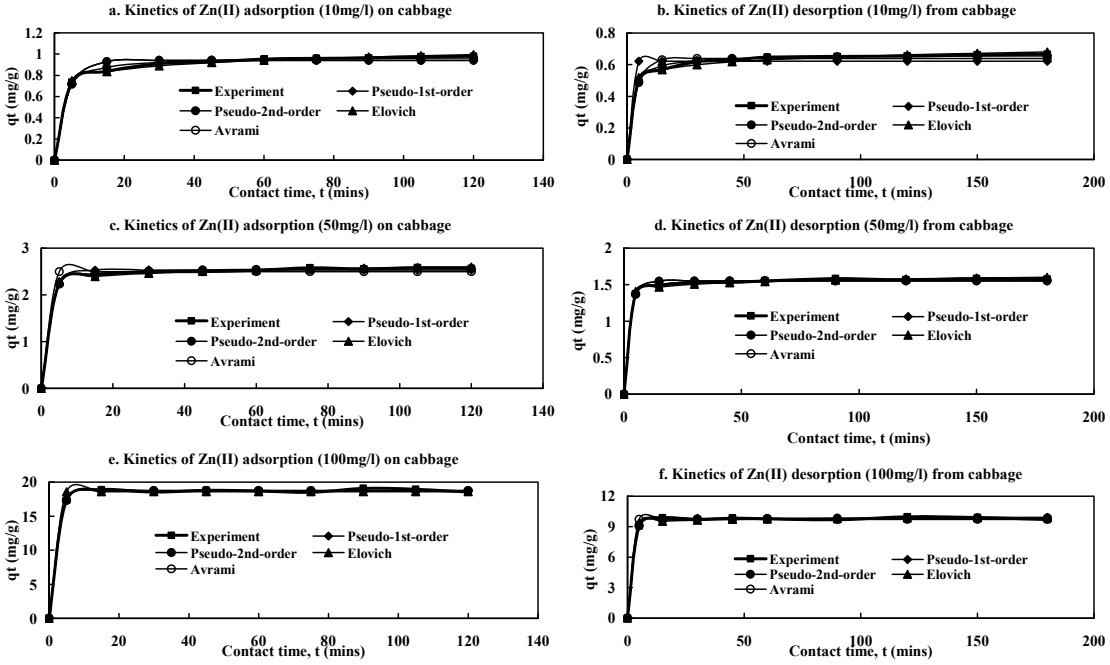


**Figure 5.12** Kinetics modelling of adsorption and desorption of Zn(II) onto cabbage ($C_o$: 50 mg/l; d: 0.5 g; t: 3 h: pH: 6-6.5; rpm: 120; T: room temp.)

The fractionary numbers ($n_{AV}$) predicted from adsorption processes were greater than unity ($n_{AV}$>1) for Cu(II), Zn(II), Pb(II), and Cd(II) adsorption onto and desorption from cabbage which indicated the reaction order (greater than first order) of adsorption and desorption processes are more than one. It could be assumed that Cu(II), Zn(II), Pb(II), and Cd(II) adsorption followed several orders during the processes. These findings postulated that the possible changes occurred on adsorption and desorption mechanisms during the processes. Therefore, the adsorption mechanisms of Cu(II), Zn(II), Pb(II), and Cd(II) onto cabbage followed multiple kinetic orders (Lopes et al., 2003).

## 5.2.5 Adsorption and desorption equilibrium

An equilibrium isotherm denotes the relationship between the amounts of adsorbate (metals) removed from water per unit of mass of biosorbent and equivalent metals concentration in water, at constant temperature and at equilibrium state (Abd El-Latif

and Elkady, 2010; Blazquez et al., 2010; Kicsi et al., 2010). In this study, experimental data from Pb(II), Cd(II), Cu(II), and Zn(II) adsorption and desorption at equilibrium were judged with prediction of parameters of six isotherm models namely two two-parameter models: Langmuir and Freundlich models and four three-parameter models: SIPS, Redlich-Peterson, Koble-Corrigan and Khan Models. Non-linear regression analyses the data on the base of original form of isotherm equation and eventually avoids errors. Therefore non-linear regression (MATLAB bases program) was used to estimate and optimise the parameters (Appendix I).

The predicted and experimental data from adsorption and desorption are plotted in Figure 5.13 for Pb(II), Figure 5.14 for Cd(II), Figure 5.13 for Cu(II) and Figure 5.13 for Zn(II). The calculated and experimental parameters are presented in Table 5.6 for Langmuir isotherm model, Table 5.7 for Freundlich isotherm model, Table 5.8 for SIPS isotherm model, Table 5.9 for Redlich-Peterson isotherm model, Table 5.10 for Koble-Corrigan isotherm model, and Table 5.11 for Khan Isotherm model. The agreement between experimental and model prediction data are judged by $R^2$ (coefficient of determination), RMSE (residual root mean square error) and $\lambda^2$ (chi-square test) (Chapter 3, section 3.4) for both adsorption and desorption of Pb(II), Cd(II), Cu(II), and Zn(II) onto and from biosorbent of cabbage.

#### 5.2.5.1 The Langmuir isotherm

Langmuir assumption was for monolayer adsorption onto a surface containing a finite number of identical sites (Aksu, 2005; Kumar et al., 2008). The assumptions of Langmuir isotherm are chemisorptions of metals at a fixed number of well-defined sites, one ion in each site, energetically equivalent sites, and no interaction between the ions (Buasri et al., 2012; Bulgariu and Bulgariu, 2012; Fourest and Roux, 1992; Semerjian, 2010). The Langmuir equation is formulated as (Langmuir, 1918):

$$q_e = \frac{q_m K_L C_e}{1 + K_L C_e} \tag{5.9}$$

where, $C_e$ (mg/l) and $q_e$ (mg/g) are the equilibrium concentrations of metals in the water and equilibrium adsorption on biosorbent phase, respectively. $q_m$ is a Langmuir constant that expresses the maximum metal uptake (mg/g) and $K_L$ is also a Langmuir constant related to the energy of adsorption and affinity of the biosorbent. This widely applied model is used to describe experimental data of Pb(II), Cd(II), Cu(II) and Zn(II) ions adsorption and desorption. The sorption data were fitted to the non-linear form of

Langmuir isotherm model (Eq. 5.9) and parameters are evaluated by $R^2$, RMSE and $\chi^2$ values. The plots of adsorption capacity ($q_e$,mg/g) against equilibrium concentration ($C_e$) from experiment and model prediction data are shown in Figure 5.13, Figure 5.14, Figure 5.15 and Figure 5.16 and a very good coincide curves were obtained. The data of parameters are tabulated in Table 5.6.

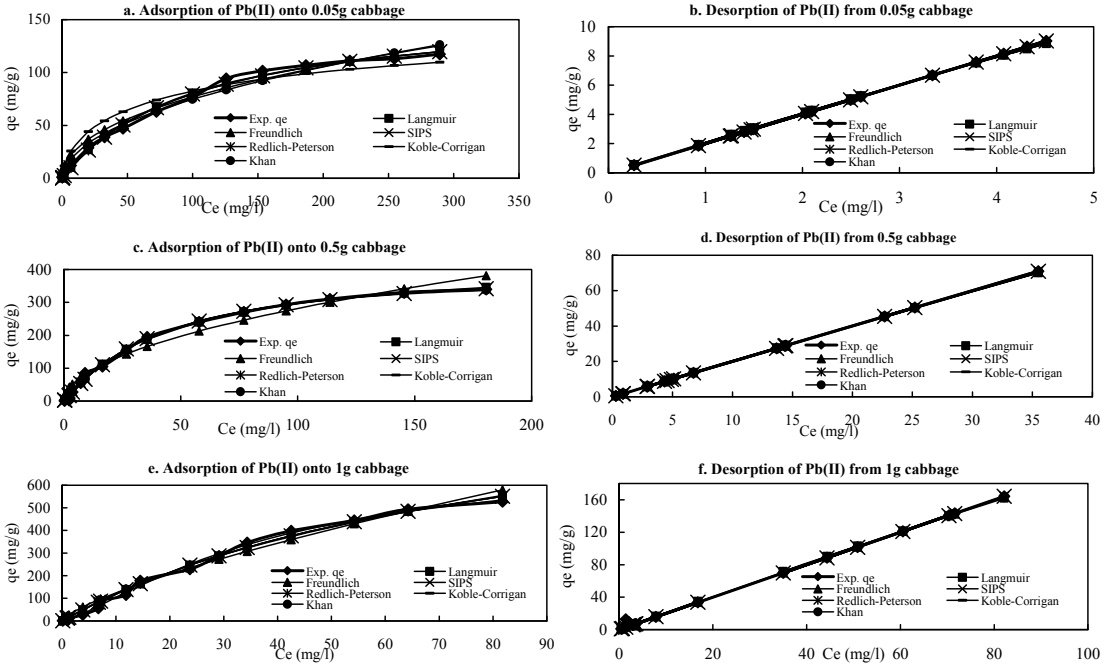


**Figure 5.13** Isotherm modelling of adsorption and desorption of Pb(II) onto cabbage with different doses ($C_o$: 1-500 mg/l; d: 0.05-1 g; t: 3 h: pH: 6-6.5; rpm: 120; T: 20°C)

This isotherm was found to be well fitted with experimental data for Pb(II), Cd(II), Cu(II) and Zn(II) ions adsorption onto and desorption from CW. It resulted a good coefficient of determination values ($R^2$:0.990 to 0.999 for adsorption, and; 0.963-1.00 for desorption) and small RMSE and $\chi^2$ values, which show the fitness of the Langmuir isotherm with the experimental data from both adsorption and desorption processes. The value of $R^2$ is higher than the values of Freundlich isotherm and similar to three-parameter models.

It is noticeable that the Langmuir equation maintained a better fitness with the experimental data for both adsorption and desorption for all metals (Table 5.6). The monolayer saturation capacities ($q_m$) were found to be 60.213, 60.568 and 113.525 mg/g for adsorption of Pb(II) onto 0.05, 0.5 and 1g doses, respectively, which are close to experimental data (16.97, 61.267 and 89.373 mg/g); but the nearest was for 0.5g doses.

In case of desorption of Pb(II), the model showed good consistency with experimental data but over predicted the monolayer saturation capacities ($q_m$) (Table 5.6).

**Table 5.6** The predicted and experimental parameters of Langmuir isotherm model for adsorption and desorption of Pb(II), Cd(II), Cu(II) and Zn(II) onto CW

| Name of metals | Parameters | Adsorption | | | Desorption | | |
|---|---|---|---|---|---|---|---|
| | | Doses | | | Doses | | |
| | | 0.05g | 0.5g | 1g | 0.05g | 0.5g | 1g |
| Experimental | **$q_m$(mg/g)** | 16.97 | 61.267 | 89.373 | 15.154 | 30.173 | 53.67 |
| Pb(II) | $q_m$(mg/g) | 60.213 | 60.568 | 113.525 | 61.962 | 171.635 | 409.210 |
| | $K_L$ (l/g) | 0.010 | 0.021 | 0.012 | 0.026 | 0.001 | 0.001 |
| | $R_L$ | 0.25-0.99 | 0.21-0.99 | 0.99-0.53 | 0.99-0.93 | 0.99-0.98 | 0.99-0.93 |
| | $R^2$ | 0.996 | 0.996 | 0.992 | 0.997 | 1.000 | 1.000 |
| | Δ°G | -11.19 | -9.426 | -10.78 | -8.921 | -16.41 | -17.14 |
| | $\chi^2$ | 3.819 | 2.555 | 0.0024 | 0.0029 | 0.0004 | 0.0028 |
| | RMSE | 3.121 | 8.219 | 17.207 | 0.1425 | 0.3318 | 1.0904 |
| Experimental | **$q_m$(mg/g)** | 40.9 | 22.123 | 65.876 | 30.11 | 41.598 | 460.675 |
| Cd(II) | $q_m$(mg/g) | 35.587 | 20.568 | 66.628 | 67.201 | 53.819 | 402.812 |
| | $K_L$ (l/g) | 0.019 | 0.021 | 0.002 | 0.010 | 0.009 | 0.007 |
| | $R_L$ | 0.28-0.98 | 0.21-0.99 | 0.69-0.99 | 0.38-0.99 | 0.21-0.98 | 0.42-0.99 |
| | $R^2$ | 0.994 | 0.996 | 0.990 | 0.986 | 0.988 | 0.994 |
| | Δ°G | -9.637 | -9.426 | -14.72 | -11.18 | -9.950 | -12.13 |
| | $\chi^2$ | 9.030 | 2.554 | 0.743 | 0.0868 | 0.057 | 0.0037 |
| | RMSE | 18.495 | 8.219 | 24.191 | 13.405 | 11.930 | 7.0725 |
| Experimental | **$q_m$(mg/g)** | 17.772 | 14.231 | 13.879 | 6.634 | 5.592 | 4.996 |
| Cu(II) | $q_m$(mg/g) | 20.796 | 17.247 | 15.667 | 7.288 | 6.899 | 6.711 |
| | $K_L$ (l/g) | 0.216 | 0.018 | 0.016 | 0.041 | 0.037 | 0.326 |
| | $R_L$ | 0.64-0.99 | 0.14-0.98 | 0.25-0.99 | 0.22-0.99 | 0.15-0.99 | 0.56-0.99 |
| | $R^2$ | 0.998 | 0.991 | 0.994 | 0.992 | 0.991 | 0.998 |
| | Δ°G | -10.672 | -9.727 | -8.7543 | -9.256 | -8.038 | -7.744 |
| | $\chi^2$ | 0.158 | 0.140 | 0.261 | 0.062 | 0.056 | 0.049 |
| | RMSE | 0.708 | 0.559 | 0.531 | 0.258 | 0.224 | 0.972 |
| Experimental | **$q_m$(mg/g)** | 12.236 | 9.864 | 7.560 | 4.288 | 5.425 | 4.309 |
| Zn(II) | $q_m$(mg/g) | 13.919 | 11.225 | 8.956 | 5.059 | 6.731 | 5.105 |
| | $K_L$ (l/g) | 0.546 | 0.044 | 0.020 | 0.534 | 0.060 | 0.025 |
| | $R_L$ | 0.25-0.99 | 0.05-0.97 | 0.11-0.99 | 0.08-0.99 | 0.05-0.98 | 0.11-0.99 |
| | $R^2$ | 0.999 | 0.991 | 0.997 | 0.995 | 0.963 | 0.997 |
| | Δ°G | -9.455 | -7.625 | -9.59 | -6.786 | -6.874 | -8.953 |
| | $\chi^2$ | 0.256 | 0.190 | 0.025 | 0.926 | 0.1041 | 0.014 |
| | RMSE | 0.507 | 0.425 | 0.170 | 0.746 | 0.514 | 0.097 |

The maximum adsorption capacities, $q_m$, were calculated as 35.587, 20.568 and 66.629 for Cd(II) adsorption, 20.796, 17.247 and 15.667 for Cu(II) adsorption, and 13.919 11.225, 8.956 and 10.515 for Zn(II) adsorption from 0.05, 0.5 and 1g dose respectively (Table 5.6). The predictions were similar to the experimental values as they are 40.90, 22.123 and 65.876 mg/g for Cd(II); 17.772, 14.231 and 13.879 mg/g for Cu(II), and 12.236, 9.864 and 7.560 mg/g for Zn(II) ions adsorption for from 0.05, 0.5 and 1g dose respectively.

These results revealed that Langmuir isotherm model properly explained the equilibrium adsorption of Pb(II), Cd(II), Cu(II) and Zn(II) onto CW. Similar results are found for metals adsorption onto different biosorbent in literature and comparable to the adsorption capacities of other biosorbent materials (Cai et al., 2012; Hossain et al., 2013; Niu et al., 2013). Similar results are found for desorption of Cd(II), Cu(II) and Zn(II) from cabbage. The negative values of Gibbs free energy, ΔG° from both adsorption and desorption of Pb(II), Cd(II), Cu(II) and Zn(II) confirmed that the processes are feasible and spontaneous in nature (Akbar et al., 2007; Barros et al., 2004). The values of '$K_L$' are less than unity ($K_L$<1) for all metals adsorption and desorption and that indicates the higher affinity (Anwar et al., 2010).

The essential characteristics of Langmuir isotherm can be articulated in terms of a dimensionless constant named separation factor, $R_L$, which is defined as:

$$R_L = \frac{1}{\left(1 + K_L C_o\right)} \qquad (5.10)$$

The value of $R_L$ indicates the shape of the isotherms to be either unfavourable ($R_L$ > 1, when $K_L$ is negative), linear ($R_L$ = 1), favourable (0 < $R_L$ <1) or irreversible ($R_L$ = 0) (Kadirvelu et al., 2002; Lasheen et al., 2012; Rajaei et al., 2013; Repo et al., 2010; Wan et al., 2010). The $R_L$ values were found to vary within a range, 0.21-0.99 and 0.93-0.99 for Pb(II) adsorption and desorption; 0.21-0.99 and 0.21-0.99 for Cd(II) adsorption and desorption; 0.14-0.99 and 0.15-0.99 for Cu(II) adsorption and desorption and; 0.05-0.99 and 0.05-0.99 for Zn(II) adsorption and desorption onto and from CW, respectively. The used initial Pb(II), Cd(II), Cu(II) and Zn(II) concentration values of 1-500 mg/l. They fallen into the range of 0 to 1 which indicates favourable adsorption and desorption processes. Similar findings also observed by the other biosorption processes in literature (Mckay et al., 1982).

Apart from Cd(II), it was observed a mixed proportional relationship between the adsorption capacity and ionic radius (Cu = 73, Zn = 74, Cd = 95 and Pb = 77.5 nm) (Kusvuran et al., 2012). When ionic radius of heavy metals were increased (Pb(II)>Cu(II)), the maximum adsorption capacities were observed in order of $q_m$ (Pb) > $q_m$ (Cu) (Table 1). Similarly when Cd(II)>Zn(II) in ionic radius the adsorption capacity were $q_m$(Cd) > $q_m$(Zn) (Table 5.6), but it was different between Cu(II) and Zn(II). When the results were evaluated together, ionic radius order and maximum adsorption capacity order formed in the order of Cd(II)>Pb(II)>Zn(II)>Cu(II) and

$q_m(Pb)>q_m(Cd)>q_m(Cu)>q_m(Zn)$, respectively. Similar findings are available in literature (Cai et al., 2012; Papageorgiou et al., 2009).

### 5.2.5.2 Freundlich isotherm

The Freundlich isotherm is an exponential equation which assumes that the concentration of adsorbates (metals) on the biosorbent surface increases with the adsorbates concentration. Hypothetically, using this expression, an infinite amount of adsorption can occur on the heterogeneous surface of biosorbent (Freundlich, 1906; Hannachi et al., 2010; Hannachi et al., 2009). The equation is widely used in heterogeneous systems:

$$q_e = K_F C_e^{1/n} \tag{5.11}$$

where $K_F$ (l/g) and n are Freundlich constants characteristic of the system, indicating the adsorption capacity and adsorption intensity, respectively.

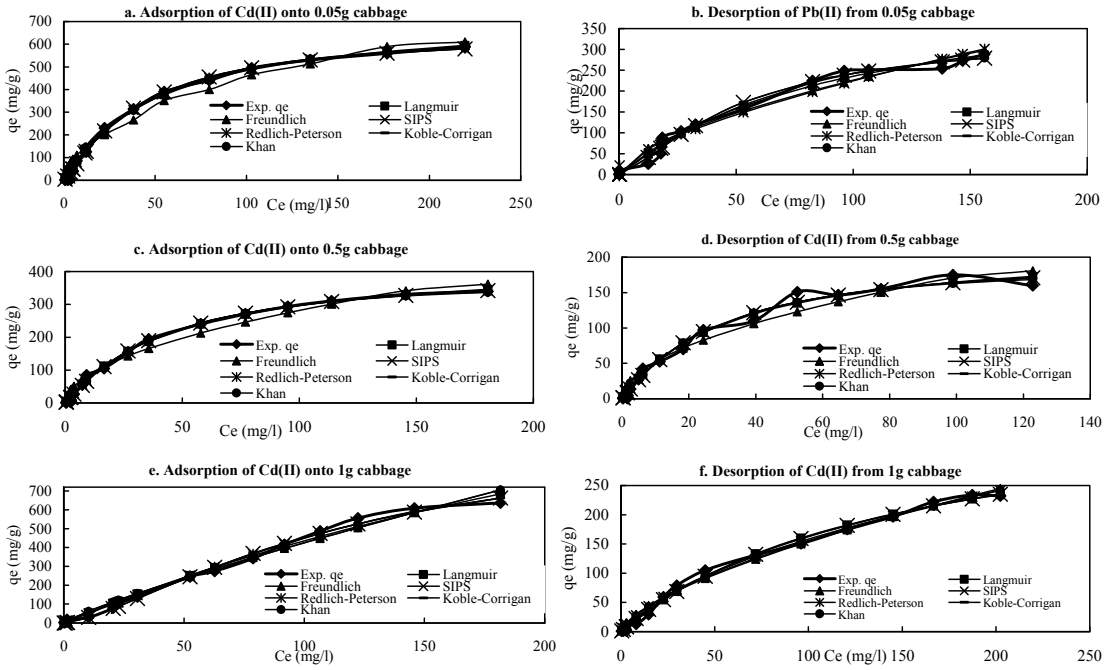


**Figure 5.14** Isotherm modelling of adsorption and desorption of Cd(II) onto cabbage with different doses ($C_o$: 1-500 mg/l; d: 0.05-1 g; t: 3 h: pH: 6-6.5; rpm: 120; T: 20°C)

The Freundlich parameters provide valuable physical information about metal biosorption onto biosorbents. The adsorption and desorption data for Pb(II), Cd(II), Cu(II) and Zn(II) ions onto and from cabbage are fitted to the Freundlich model and the calculated parameters are tabulated in Table 5.7. The fitness of data with the Freundlich model are low compared to using five models as the $R^2$ values lies between 0.903 to 0.997 (Table 5.7) for Pb(II), Cd(II), Cu(II) and Zn(II) adsorption. In case of desorption,

the Zn(II) desorption process did not follow the Freundlich model properly because the $R^2$ are 0.899, 0.881 and 0.931 for the exhausted metal concentration of 10, 50 and 100 mg/l respectively. But the other three metals (Pb(II), Cd(II) and Cu(II)) desorption processed obeyed the Freundlich model. The equivalent maximum adsorption capacity for Freundlich constant, $K_F$ values are lower than the magnitudes of experimental and predicted capacity of the Langmuir isotherm (Table 5.6). But, a high value of Freundlich constant $K_F$ suggests easiness in biosorption of metal ion onto the cabbage. The present study shows that $K_F$ for Cd(II) biosorption was the higher than Pb(II), Cu(II) and Zn(II) biosorption. Several authors report that biosorbent with high $K_F$ often have high $q_m$ as well (Al-Degs et al., 2006; Singh et al., 2007), however, this pattern was not observed in this study. The Freundlich parameter n is a measure of intensity of metal biosorption by the biosorbents. The value of n<1 suggests that biosorption of metal ion on the biosorbent is practically favourable (Gupta and Babu, 2009; Unnithan and Anirudhan, 2001). In this study, the values of n were >1 for all the used metals, thus suggesting that Pb(II), Cd(II), Cu(II) and Zn(II) biosorption are not favourable onto cabbage.

**Table 5.7** The predicted and experimental parameters of Freundlich isotherm model for adsorption and desorption of Pb(II), Cd(II), Cu(II) and Zn(II) onto CW

| Metals | Parameters | Adsorption | | | Desorption | | |
|---|---|---|---|---|---|---|---|
| | | Doses | | | Doses | | |
| | | 0.05g | 0.5g | 1g | 0.05g | 0.5g | 1g |
| Experimental | $q_m$(mg/g) | 16.97 | 61.267 | 89.373 | 5.154 | 30.173 | 53.67 |
| Pb(II) | $K_F$ ($mg^{(1-n)}$ $g^{-1}$ $l^n$) | 7.175 | 26.277 | 23.067 | 2.000 | 2.001 | 2.005 |
| | n | 1.972 | 1.942 | 1.366 | 1.000 | 1.000 | 1.001 |
| | $R^2$ | 0.985 | 0.966 | 0.980 | 1.000 | 1.000 | 1.000 |
| | $\chi^2$ | 10.916 | 126.96 | 101.164 | 3E-06 | 7E-06 | 0.0002 |
| | RMSE | 5.8316 | 24.904 | 27.8986 | 0.0012 | 0.0024 | 0.016 |
| Experimental | $q_m$(mg/g) | 40.9 | 22.123 | 65.876 | 30.11 | 41.598 | 460.67 |
| Cd(II) | $K_F$ ($mg^{(1-n)}$ $g^{-1}$ $l^n$) | 40.089 | 26.277 | 8.535 | 13.084 | 10.254 | 7.409 |
| | n | 1.925 | 1.942 | 1.178 | 1.616 | 1.289 | 1.518 |
| | $R^2$ | 0.951 | 0.966 | 0.984 | 0.974 | 0.983 | 0.989 |
| | $\chi^2$ | 281.7 | 126.96 | 54.542 | 163.15 | 110.309 | 40.828 |
| | RMSE | 50.761 | 24.904 | 30.034 | 18.488 | 12.899 | 9.6133 |
| Experimental | $q_m$(mg/g) | 17.772 | 14.231 | 13.879 | 6.634 | 5.592 | 4.996 |
| Cu(II) | $K_F$ ($mg^{(1-n)}$ $g^{-1}$ $l^n$) | 1.88 | 1.490 | 1.341 | 0.878 | 0.792 | 1.696 |
| | n | 2.268 | 2.439 | 2.1951 | 2.768 | 2.439 | 2.4632 |
| | $R^2$ | 0.997 | 0.982 | 0.988 | 0.998 | 0.982 | 0.986 |
| | $\chi^2$ | 3.31 | 3.695 | 3.323 | 1.544 | 1.477 | 1.997 |
| | RMSE | 0.904 | 0.775 | 0.697 | 0.473 | 0.310 | 0.788 |
| Experimental | $q_m$(mg/g) | 12.236 | 9.864 | 7.560 | 4.288 | 5.425 | 4.309 |
| Zn(II) | $K_F$ ($mg^{(1-n)}$ $g^{-1}$ $l^n$) | 2.744 | 1.831 | 2.895 | 1.457 | 1.175 | 0.564 |
| | n | 4.016 | 3.240 | 2.623 | 2.835 | 3.150 | 2.623 |
| | $R^2$ | 0.972 | 0.903 | 0.931 | 0.899 | 0.881 | 0.931 |
| | $\chi^2$ | 8.678 | 7.716 | 4.618 | 4.830 | 4.998 | 2.632 |
| | RMSE | 1.995 | 1.3706 | 0.8562 | 0.187 | 0.919 | 0.488 |

### 5.2.5.3 Sips isotherm

For describing the adsorption onto heterogeneous surfaces, Sips (1948) has proposed a model that combines the Langmuir and Freundlich isotherm. At low sorbates (metals) concentrations it effectively reduces to a Freundlich isotherm, while at high sorbate concentrations it predicts a monolayer adsorption capacity characteristic of the Langmuir isotherm. The Sips model takes the following form (Sips, 1948):

$$q_e = \frac{K_s C_e^{\beta_s}}{1 + \alpha_s C_e^{\beta_s}} \tag{5.12}$$

Where, $K_S$ is maximum adsorption capacity (mg/g) and $\alpha_s$ is Sips constant related to energy of adsorption.

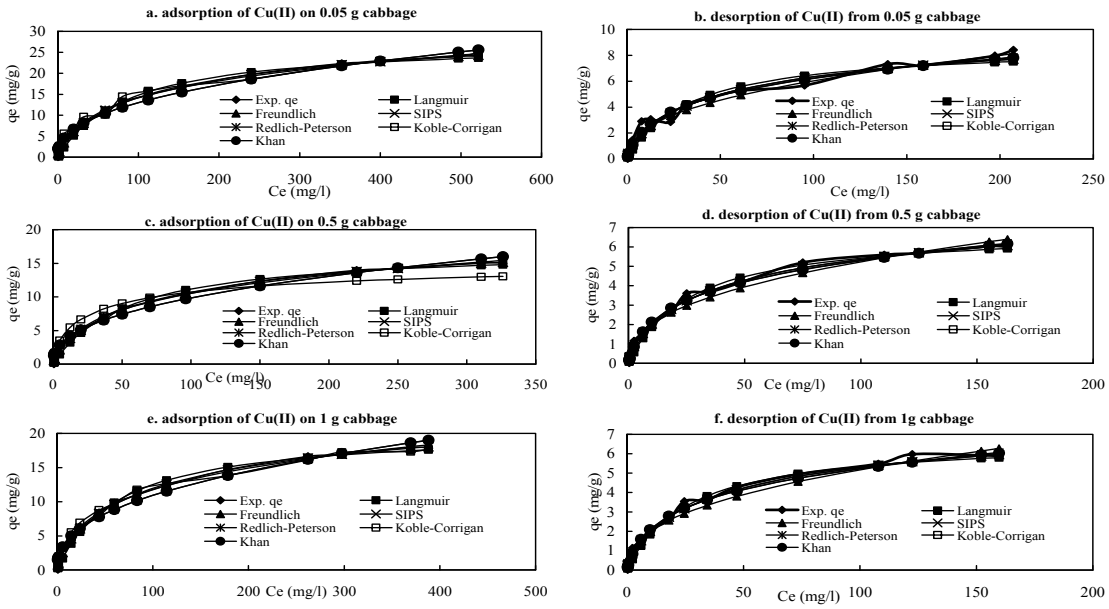


**Figure 5.15** Isotherm modelling of adsorption and desorption of Cu(II) onto cabbage with different doses ($C_o$: 1-500 mg/l; d: 0.05-1 g; t: 3 h: pH: 6-6.5; rpm: 120; T: 20°C).

The equilibrium data from Pb(II), Cd(II), Cu(II) and Zn(II) ions adsorption and desorption are fitted with Sips model and the calculated parameters are shown in Table 5.8. The degrees of fitness ($R^2$) of the model with adsorption data are comparable to Langmuir model as the values lie between 0.968 and 0.997 for the doses of 0.05, 0.5 and 1g for all four metals. However, the desorption data showed higher agreement with this model with the $R^2$ values of 1.00, 1.00 and 1.00 for Pb(II), 0.990, 0.948 and 0.994 for Cd(II), 0.991, 0.997 and 0.988 for Cu(II), and 0.985, 0.966 and 0.998 for Zn(II) for dose of 0.05, 0.5 and 1g, respectively. The maximum adsorption capacity, $K_S$ values are lower than Langmuir, Freundlich, Redlich-Peterson, Koble-Corrigan and Khan models.

**Table 5.8** The predicted and experimental parameters of SIPS isotherm model for adsorption and desorption of Pb(II), Cd(II), Cu(II) and Zn(II) onto CW

| Metals | Parameters | Adsorption | | | Desorption | | |
|---|---|---|---|---|---|---|---|
| | | Doses | | | Doses | | |
| | | 0.05g | 0.5g | 1g | 0.05g | 0.5g | 1g |
| Experimental | $q_m$(mg/g) | 16.97 | 61.267 | 89.373 | 5.154 | 30.173 | 53.67 |
| Pb(II) | Ks(l/g) | 1.633 | 36.932 | 13.344 | 2.000 | 2.006 | 2.109 |
| | $\alpha_S$ (l/mg) | 0.010 | 0.017 | 0.0120 | -2.1E-06 | -6.8E-06 | 0.0004 |
| | $\beta_S$ | 0.989 | 1.101 | 1.003 | 1.006 | 1.008 | 0.981 |
| | $R^2$ | 0.996 | 0.997 | 0.992 | 1.000 | 1.000 | 1.000 |
| | $\chi^2$ | 3.666 | 1.485 | 0.0024 | 2E-11 | 2.3E-08 | 0.004 |
| | RSME | 0.695 | 0.996 | 4.70276 | 1.1E-05 | 0.00156 | 0.021 |
| Experimental | $q_m$(mg/g) | 40.9 | 22.123 | 65.876 | 30.11 | 41.598 | 460.675 |
| Cd(II) | Ks(l/g) | 7.735 | 6.931 | 1.043 | 1.364 | 2.346 | 3.136 |
| | $\alpha_S$ (l/mg) | 0.0118 | 0.017 | 0.001 | 0.004 | 0.009 | 0.007 |
| | $\beta_S$ | 1.204 | 1.100 | 1.449 | 1.399 | 2.991 | 0.961 |
| | $R^2$ | 0.996 | 0.997 | 0.995 | 0.990 | 0.948 | 0.994 |
| | $\chi^2$ | 4.192 | 1.485 | 34.436 | 1.013 | 1.520 | 0.049 |
| | RSME | 2.856 | 0.996 | 2.555 | 0.690 | 1.357 | 0.780 |
| Experimental | $q_m$(mg/g) | 17.772 | 14.231 | 13.879 | 6.634 | 5.592 | 4.996 |
| Cu(II) | Ks(l/g) | 0.932 | 0.761 | 0.849 | 0.562 | 0.501 | 0.882 |
| | $\alpha_S$ (l/mg) | 0.042 | 0.035 | 0.315 | 0.068 | 0.057 | 0.516 |
| | $\beta_S$ | 0.828 | 0.719 | 0.471 | 0.858 | 0.719 | 0.372 |
| | $R^2$ | 0.968 | 0.997 | 0.997 | 0.991 | 0.997 | 0.988 |
| | $\chi^2$ | 0.724 | 0.477 | 0.293 | 0.239 | 0.191 | 0.188 |
| | RSME | 0.504 | 0.042 | 0.378 | 0.194 | 0.017 | 0.146 |
| Experimental | $q_m$(mg/g) | 12.236 | 9.864 | 7.560 | 4.288 | 5.425 | 4.309 |
| Zn(II) | Ks(l/g) | 0.526 | 0.284 | 0.107 | 0.282 | 0.238 | 0.082 |
| | $\alpha_S$ (l/mg) | 0.338 | 0.027 | 0.0126 | 0.329 | 0.037 | 0.017 |
| | $\beta_S$ | 1.996 | 1.209 | 1.136 | 1.893 | 1.224 | 1.136 |
| | $R^2$ | 0.992 | 0.993 | 0.998 | 0.985 | 0.966 | 0.998 |
| | $\chi^2$ | 0.792 | 0.058 | 0.003 | 0.024 | 0.027 | 0.002 |
| | RSME | 0.483 | 0.039 | 0.007 | 0.016 | 0.019 | 0.004 |

### 5.2.5.4 Redlich-Peterson isotherm

Redlich and Peterson (Redlich and Peterson, 1959) proposed an empirical equation to represent equilibrium data:

$$q_e = \frac{K_{RP} C_e}{1 + \alpha_{RP} C_e^{\beta}} \qquad \text{where } \beta \leq 1 \qquad (5.13)$$

where $K_{PR}$ (l/g), $\alpha_{PR}$ (l/mg) and $\beta$ are Redlich-Peterson isotherm constants which lie between 0 and 1. This equation reduces to a linear isotherm in the case of low surface coverage and to a Langmuir isotherm when $\beta$ =1.

Redlich-Peterson isotherm was used to evaluate the adsorption and desorption of Pb(II), Cd(II), Cu(II) and Zn(II) ions onto and from cabbage. The calculated and experimental parameters are tabulated in Table 5.9. It is found from Table 5.9 that this model shows a

good association ($R^2$: 0.987-0.997) with experimental data for all four metals using three doses. Desorption data also fit well with this model. The isotherm constant, $K_{PR}$ which is equivalent to maximum adsorption capacity were lower than the Langmuir model and experimental data. Amazingly, β values are greater than unity for Pb(II), Cd(II) and Zn(II) ions adsorption and desorption which indicate that the isotherm is a monolayer of Langmuir (Table 5.9). But, Cu(II) adsorption and desorption were adsorpted and desorpted onto the heterogeneous surface of cabbage because β<1.0 (Adie et al., 2010; Artola et al., 2000).

**Table 5.9** The predicted and experimental parameters of Redlich-Peterson isotherm model for adsorption and desorption of Pb(II), Cd(II), Cu(II) and Zn(II) onto CW

| Metals | Parameters | Adsorption | | | Desorption | | |
|---|---|---|---|---|---|---|---|
| | | Doses | | | Doses | | |
| | | **0.05g** | **0.5g** | **1g** | **0.05g** | **0.5g** | **1g** |
| **Experimental** | **$q_m$(mg/g)** | 16.97 | 61.267 | 89.373 | 5.154 | 30.173 | 53.67 |
| **Pb(II)** | $K_{RP}$ (l/g) | 1.575 | 8.363 | 13.344 | 5.980 | 0.985 | 7.411 |
| | $\alpha_{RP}$ (l/mg) | 0.010 | 0.012 | 0.012 | 1.990 | 1.507 | 2.705 |
| | β | 1.00 | 1.085 | 1.00 | 1.000 | 1.00 | 1.00 |
| | $R^2$ | 0.996 | 0.997 | 0.992 | 1.00 | 1.000 | 1.000 |
| | $\chi^2$ | 3.9886 | 2.268 | 0.0024 | 3E-13 | 5E-20 | 2E-18 |
| | RSME | 0.6606 | 1.593 | 4.7028 | 4E-06 | 7E-09 | 1E-07 |
| Experimental | $q_m$(mg/g) | 40.9 | 22.123 | 65.876 | 30.11 | 41.598 | 460.675 |
| **Cd(II)** | $K_{RP}$ (l/g) | 12.057 | 8.363 | 4.866 | 4.040 | 7.572 | 5.938 |
| | $\alpha_{RP}$ (l/mg) | 0.008 | 0.012 | 1.96E-06 | 0.001 | 0.08 | 0.247 |
| | β | 1.139 | 1.085 | 2.321 | 1.39589 | 2.512 | 0.523 |
| | $R^2$ | 0.995 | 0.997 | 0.995 | 0.989 | 0.978 | 0.993 |
| | $\chi^2$ | 7.661 | 2.268 | 1.006 | 0.0408 | 0.083 | 0.472 |
| | RSME | 5.199 | 1.593 | 4.432 | 0.5786 | 1.064 | 2.488 |
| Experimental | $q_m$(mg/g) | 17.772 | 14.231 | 13.879 | 6.634 | 5.592 | 4.996 |
| **Cu(II)** | $K_{RP}$ (l/g) | 0.874 | 0.725 | 0.655 | 0.698 | 0.619 | 0.572 |
| | $\alpha_{RP}$ (l/mg) | 0.184 | 0.182 | 0.168 | 0.358 | 0.344 | 0.372 |
| | β | 0.906 | 0.755 | 0.695 | 0.844 | 0.745 | 0.556 |
| | $R^2$ | 0.994 | 0.997 | 0.993 | 0.994 | 0.997 | 0.986 |
| | $\chi^2$ | 0.188 | 0.349 | 0.141 | 0.656 | 0.148 | 0.302 |
| | RSME | 0.543 | 0.045 | 0.435 | 0.336 | 0.028 | 0.244 |
| Experimental | $q_m$(mg/g) | 12.236 | 9.864 | 7.560 | 4.288 | 5.425 | 4.309 |
| **Zn(II)** | $K_{RP}$ (l/g) | 0.908 | 0.467 | 0.143 | 0.752 | 0.375 | 0.105 |
| | $\alpha_{RP}$ (l/mg) | 0.458 | 0.037 | 0.009 | 0.042 | 0.048 | 0.011 |
| | β | 1.636 | 1.019 | 1.097 | 1.913 | 1.026 | 1.101 |
| | $R^2$ | 0.998 | 0.991 | 0.998 | 0.987 | 0.963 | 0.998 |
| | $\chi^2$ | 0.198 | 0.177 | 0.016 | 0.086 | 0.097 | 0.008 |
| | RSME | 0.284 | 0.091 | 0.023 | 0.043 | 0.049 | 0.017 |

### 5.2.5.5 Koble-Corrigan isotherm

The Koble-Corrigan model is another three-parameter empirical model for the representing equilibrium adsorption data. It is a combination of the Langmuir and Freundlich isotherm type models (Koble and Corrigan, 1952) and is given by:

$$q_e = \frac{A_{KC} C_e^p}{1 + B_{KC} C_e^p} \qquad (5.14)$$

where $A_{KC}$, $B_{KC}$ and p are the Koble-Corrigan parameters (Cheung et al., 2000; Do Duong, 1998).

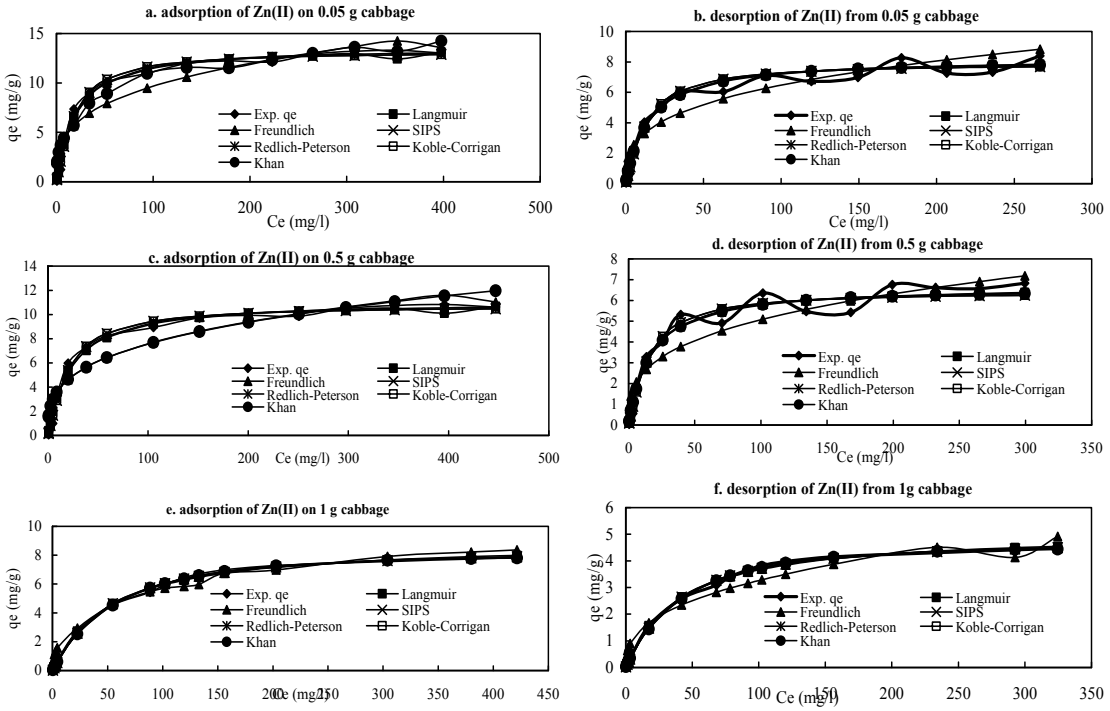


**Figure 5.16** Isotherm modelling of adsorption and desorption of Zn(II) onto cabbage with different doses ($C_o$: 1-500 mg/l; d: 0.05-1 g; t: 3 h: pH: 6-6.5; rpm: 120; T: 20°C)

Koble-Corrigan isotherm model was used to describe the equilibrium adsorption and desorption data for Pb(II), Cd(II), Cu(II) and Zn(II) ions and the parameters are showed in Table 5.10. Like other models, the Koble-Corrigan isotherm model showed higher fitness with experimental data as the $R^2$ values lie between 0.944 and 0.998 for adsorption of Pb(II), Cd(II), Cu(II) and Zn(II) ions onto cabbage (Table 5.10). Similarly, desorption data also showed good agreement ($R^2$: 0.989-1.00) with this model. The values of constant p are grater than unity (p>1) for Pb(II), Cd(II) and Zn(II) ions adsorption onto cabbage and it indicates the isotherm is approaching the Langmuir form. But p values are less than unity (p<1) for Cu(II) adsorption which revealed the adsorption onto heterogenous surface (Aksu and Isoglu, 2005; Asci et al., 2007).

**Table 5.10** The predicted and experimental parameters of Koble-Corrigan isotherm model for adsorption and desorption of Pb(II), Cd(II), Cu(II) and Zn(II) onto CW

| Metals | Parameters | Adsorption | | | Desorption | | |
|---|---|---|---|---|---|---|---|
| | | Doses | | | Doses | | |
| | | 0.05g | 0.5g | 1g | 0.05g | 0.5g | 1g |
| Experimental | $q_m$(mg/g) | 16.97 | 61.267 | 89.373 | 5.154 | 30.173 | 53.67 |
| Pb(II) | $A_{KC}$ | 1.702 | 6.908 | 5.735 | 2.024 | 2.001 | 2.00099 |
| | $B_{KC}$ | 0.010 | 0.017 | 0.008 | 0.049 | 0.00001 | 0.0001 |
| | p | 1.078 | 1.101 | 1.324 | 1.140 | 0.999 | 0.999 |
| | $R^2$ | 0.996 | 0.997 | 0.996 | 0.999 | 1.000 | 1.000 |
| | $\chi^2$ | 3.326 | 1.474 | 4.299 | 0.018 | 4E-07 | 4E-07 |
| | RSME | 0.594 | 1.012 | 0.083 | 0.040 | 0.0004 | 0.0013 |
| Experimental | $q_m$(mg/g) | 40.9 | 22.123 | 65.876 | 30.11 | 41.598 | 460.675 |
| Cd(II) | $A_{KC}$ | 7.731 | 6.908 | 1.162 | 1.367 | 2.506 | 3.271 |
| | $B_{KC}$ | 0.012 | 0.017 | 0.001 | 0.004 | 0.008 | 0.007 |
| | p | 1.204 | 1.101 | 1.419 | 1.399 | 2.622 | 0.947 |
| | $R^2$ | 0.996 | 0.997 | 0.995 | 0.990 | 0.974 | 0.994 |
| | $\chi^2$ | 4.189 | 1.474 | 28.84 | 1.008 | 1.841 | 0.076 |
| | RSME | 2.858 | 1.012 | 2.811 | 0.676 | 1.897 | 0.844 |
| Experimental | $q_m$(mg/g) | 17.772 | 14.231 | 13.879 | 6.634 | 5.592 | 4.996 |
| Cu(II) | $A_{KC}$ | 1.984 | 1.607 | 1.611 | 1.637 | 0.501 | 0.488 |
| | $B_{KC}$ | 0.182 | 0.100 | 0.638 | 0.09 | 0.057 | 0.516 |
| | p | 0.712 | 0.651 | 0.416 | 0.859 | 0.718 | 0.318 |
| | $R^2$ | 0.998 | 0.944 | 0.996 | 0.996 | 0.997 | 0.987 |
| | $\chi^2$ | 1.723 | 1.060 | 0.292 | 0.554 | 0.191 | 0.188 |
| | RSME | 0.534 | 0.212 | 0.194 | 0.908 | 0.017 | 0.049 |
| Experimental | $q_m$(mg/g) | 12.236 | 9.864 | 7.560 | 4.288 | 5.425 | 4.309 |
| Zn(II) | $A_{KC}$ | 0.526 | 0.284 | 0.107 | 0.282 | 0.238 | 0.82 |
| | $B_{KC}$ | 0.322 | 0.026 | 0.013 | 0.039 | 0.037 | 0.017 |
| | p | 1.996 | 1.209 | 1.1368 | 1.088 | 1.223 | 1.136 |
| | $R^2$ | 0.992 | 0.993 | 0.998 | 0.989 | 0.966 | 0.998 |
| | $\chi^2$ | 0.719 | 0.058 | 0.0031 | 0.231 | 0.026 | 0.002 |
| | RSME | 0.486 | 0.039 | 0.0069 | 0.169 | 0.019 | 0.004 |

### 5.2.5.6 Khan isotherm

Khan (Khan et al., 1996) have suggested a generalized isotherm for pure solutions. Khan isotherm is given as:

$$q_e = \frac{q_m b_k C_e}{(1 + b_k C_e)^{a_k}} \qquad (5.15)$$

where $q_m$ and $b_K$ is the Khan model constant and $a_K$ is the Khan model exponent.

The adsorption and desorption data for Pb(II), Cd(II), Cu(II) and Zn(II) ions onto and from cabbage are evaluated with Khan model and the calculated data are tabulated in Table 5.11. This model poses moderate fitness with experimental data because $R^2$ values were between 0.905 and 0.998 for adsorption from the three doses (0.05, 0.5 and 1g) of the four metals. Similar results also found from desorption data. The predicted values of $q_m$ for all the four metals by this model (Table 5.11) are higher than the

experimental values and other models' predictions. But, the values of $b_K$ and $a_K$ were near unity which implies the fitness of the model for both metals adsorption and onto and from biosorbents. From this it is presumed that the model over-estimated the $q_m$ though fitness was quiet good.

**Table 5.11** The predicted and experimental parameters of Khan isotherm model for adsorption and desorption of Pb(II), Cd(II), Cu(II) and Zn(II) onto CW

| Metals | Parameters | Adsorption | | | Desorption | | |
|---|---|---|---|---|---|---|---|
| | | Doses | | | Doses | | |
| | | 0.05g | 0.5g | 1g | 0.05g | 0.5g | 1g |
| Experimental | $q_m$(mg/g) | 16.97 | 61.267 | 89.373 | 5.154 | 30.173 | 53.67 |
| Pb(II) | $q_m$ (mg/g) | 7.768 | 69.897 | 93.387 | 32.344 | 16.344 | 16.954 |
| | $b_k$ (l/mg) | 1.000 | 0.014 | 0.024 | 0.143 | 0.122 | 0.132 |
| | $a_k$ (l/mg) | 0.507 | 1.207 | 0.674 | -1.7E-05 | -4.1E-06 | -4E-06 |
| | $R^2$ | 0.986 | 0.996 | 0.991 | 1.000 | 1.000 | 1.000 |
| | $\chi^2$ | 0.025 | 2.366 | 2E-05 | 2E-11 | 3E-11 | 7E-11 |
| | RSME | 0.537 | 1.374 | 5.0484 | 1E-05 | 6E-05 | 4E-05 |
| Experimental | $q_m$(mg/g) | 40.9 | 22.123 | 65.876 | 30.11 | 41.598 | 460.675 |
| Cd(II) | $q_m$ (mg/g) | 99.036 | 29.897 | 14.706 | 62.192 | 47.659 | 31.133 |
| | $b_k$ (l/mg) | 0.012 | 0.014 | 0.542 | 0.001 | 0.0008 | 0.145 |
| | $a_k$ (l/mg) | 1.239 | 1.207 | 0.156 | 9.766 | 7.226 | 0.389 |
| | $R^2$ | 0.994 | 0.996 | 0.985 | 0.989 | 0.975 | 0.992 |
| | $\chi^2$ | 8.073 | 2.366 | 0.129 | 0.052 | 0.039 | 0.276 |
| | RSME | 5.787 | 1.378 | 3.579 | 0.137 | 0.104 | 1.138 |
| Experimental | $q_m$(mg/g) | 17.772 | 14.231 | 13.879 | 6.634 | 5.592 | 4.996 |
| Cu(II) | $q_m$ (mg/g) | 24.876 | 20.673 | 18.057 | 2.896 | 2.383 | 2.974 |
| | $b_k$ (l/mg) | 0.348 | 0.279 | 0.211 | 0.616 | 0.193 | 0.198 |
| | $a_k$ (l/mg) | 0.708 | 0.590 | 0.531 | 0.846 | 0.718 | 0.638 |
| | $R^2$ | 0.996 | 0.983 | 0.988 | 0.996 | 0.997 | 0.987 |
| | $\chi^2$ | 1.464 | 1.167 | 1.503 | 0.292 | 0.116 | 0.128 |
| | RSME | 0.256 | 0.188 | 0.692 | 0.036 | 0.003 | 0.006 |
| Experimental | $q_m$(mg/g) | 12.236 | 9.864 | 7.560 | 4.288 | 5.425 | 4.309 |
| Zn(II) | $q_m$ (mg/g) | 23.343 | 18.825 | 12.750 | 6.546 | 7.140 | 7.80 |
| | $b_k$ (l/mg) | 0.949 | 0.754 | 0.012 | 0.480 | 0.054 | 0.015 |
| | $a_k$ (l/mg) | 0.656 | 0.694 | 1.173 | 0.989 | 1.021 | 1.173 |
| | $R^2$ | 0.991 | 0.905 | 0.998 | 0.998 | 0.963 | 0.998 |
| | $\chi^2$ | 1.434 | 1.406 | 0.017 | 0.881 | 0.099 | 0.009 |
| | RSME | 0.996 | 0.154 | 0.022 | 0.477 | 0.053 | 0.012 |

### 5.2.5.7 Comparison of models fitness

Cabbage proved to be an effective biosorbent for removing Pb(II), Cd(II), Cu(II) and Zn(II) from water. For equilibrium studies, the isotherms were evaluated using parameters $q_m$, $R^2$, and RMSE and $\chi^2$. With respect to the best prediction of the $q_m$ value, when compared to the experimental value, the isotherms followed the order: Langmuir > Khan > Freundlich > Koble-Corrigan > Redlich-Peterson > Sips. With respect to the best fit ($R^2$), the order was Langmuir > Koble-Corrigan > Redlich-Peterson > Khan > Freundlich > Sips. In the case of RMSE and $\chi^2$ values, the fitness order is Koble-Corrigan > Redlich-Peterson > Sips > Khan > Langmuir > Freundlich.

## 5.2.6 Multimetals adsorption

The equilibrium data for a single metal adsorption can be normally interpreted by the Langmuir isotherm (Langmuir, 1918), which is represented mathematically as:

$$q_{e.i} = \frac{q_{m.i} K_{L.i} C_{e.i}}{1 + K_{L.i} C_{e.i}} \tag{5.16}$$

This isotherm can be modified to multi-metals isotherm with some interaction factor (Padilla-Ortega et al., 2013; Srivastava et al., 2008):

$$q_{e.i} = \frac{q_{m.i} K_{L.i}(C_i)}{1 + \sum_{j=1}^{N} K_{L.j}(C_j)} \tag{5.17}$$

### 5.2.6.1 Adsorption behaviour in binary solutions

The adsorption behaviour of metals ions in binary solution can be evaluated by the Langmuir multi-metals isotherm. When the metals solution is double (i =2) in water, i.e. in binary solution, the equation (5.17) becomes as follows for the Pb(II)-Cd(II) solution:

For Pb(II): $$q_{e.Pb} = \frac{q_{m.Pb} K_{L.Pb}(C_{Pb})}{1 + K_{L.Pb} C_{e.Pb} + K_{L.Cd} C_{e.Cd}} \tag{5.18}$$

For Cd(II): $$q_{e.Cd} = \frac{q_{m.Cd} K_{L.Cd}(C_{Cd})}{1 + K_{L.Pb} C_{e.Pb} + K_{L.Cd} C_{e.Cd}} \tag{5.19}$$

Similarly the equation (5.17) can be transformed for the binary solution of Cu(II)-Pb(II), Cd(II)-Zn(II), Cd(II)-Cu(II), Cu(II)-Zn(II) and Pb(II)-Zn(II) adsorption system.

Adsorption equilibrium is established when the concentration of metal ions in water ($C_e$) is in balance with that in the solid matrix ($q_e$). This level of equilibrium concentration depends substantially on the initial concentration of the metals and the binary isotherm results (Figure 5.17). The sorption parameters of binary adsorptions of Pb(II)-Cd(II), Cu(II)-Pb(II), Cd(II)-Zn(II), Cd(II)-Cu(II), Cu(II)-Zn(II) and Pb(II)-Zn(II) ions are shown in Table 5.12. The adsorption experiments of the binary systems were carried out using pairs of metal ions with equal initial concentration. In this case, the mass ratios of initial concentrations of Pb(II)-Cd(II), Cu(II)-Zn(II), Cu(II)-Pb(II), Pb(II)-Zn(II), Cd(II)-Zn(II) and Cd(II)-Cu(II) were 1:1 over a metal concentration range of 1 to 500 mg/L and an adsorbent dose of 5 g/l.

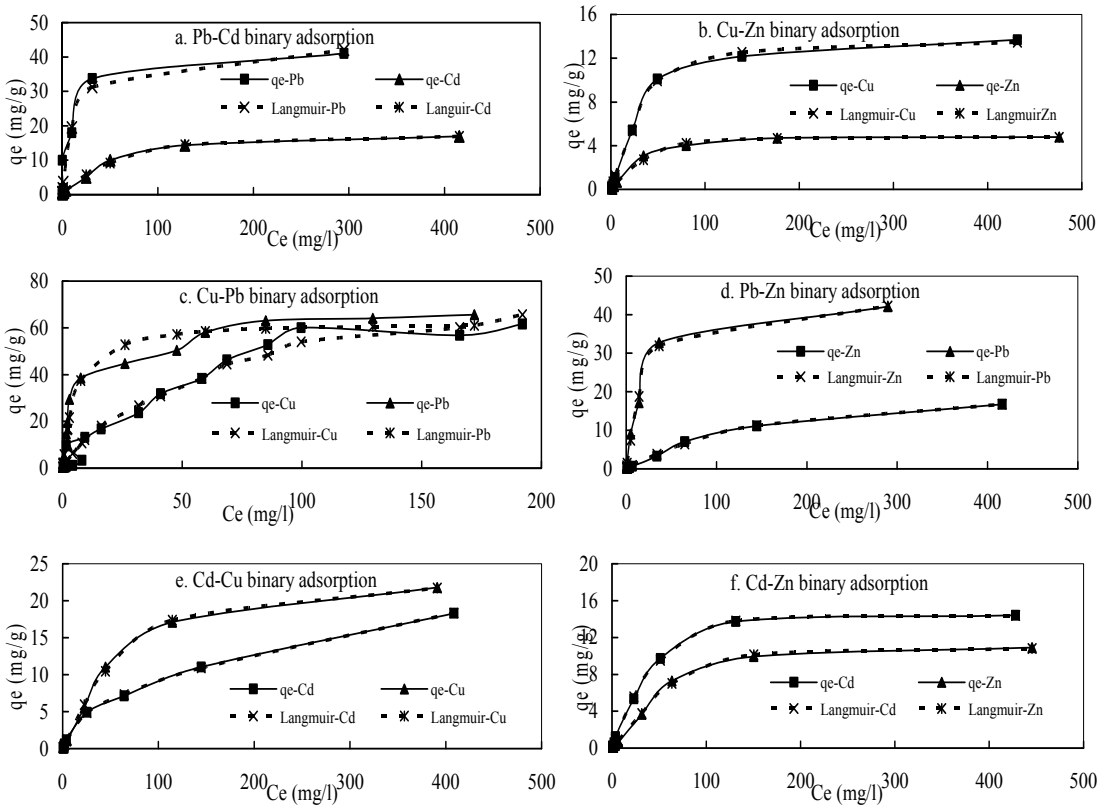


**Figure 5.17** Equilibrium of binary adsorption of Pb(II)-Cd(II), Cu(II)-Pb(II), Cd(II)-Zn(II), Cd(II)-Cu(II), Cu(II)-Zn(II) and Pb(II)-Zn(II) ions on CW.

It is noted that $q_e$ for the adsorption of Pb(II) and Cd(II) are dominant in the binary adsorption system (Kongsuwan et al., 2009). Langmuir isotherms (Eqs.5.17 and 5.18) were selected to discuss experimental data and the maximum adsorption capacities are 43.907, 7.140, 60.311, 42.942, 18.030 and 16.66 mg/g for Pb(II), Cu(II), Pb(II), Pb(II), Cd(II) and Cu(II) ions in binary sorption of Pb(II)-Cd(II), Cu(II)-Zn(II), Cu(II)-Pb(II), Pb(II)-Zn(II), Cd(II)-Zn(II) and Cd(II)-Cu(II) systems, respectively. It is noted that the adsorption capacity for Pb(II) was higher than that of Cd(II),Cu(II) and Zn(II) because Pb(II) could bind with a greater variety of functional groups (Kongsuwan et al., 2009). The maximum adsorption capacities of Cd(II), Zn(II), Cu(II) and Pb(II) obtained from binary metals sorption that were less than those obtained from the single metal system (Table 5.12; Kumar et al., 2008; Zhu et al., 2012).

**Table 5.12** Calculated parameters from Langmuir model for binary adsorption of Pb(II)-Cd(II), Cu(II)-Pb(II), Cd(II)-Zn(II), Cd(II)-Cu(II), Cu(II)-Zn(II) and Pb(II)-Zn(II) ions on CW

| Pb(II)-Cd(II) | Cu(II)-Zn(II) | Cu(II)-Pb(II) |
|---|---|---|
| **For Pb(II):** | **For Cu(II):** | **For Cu(II):** |
| $q_{m\text{-}Pb}$ =43.907 mg/g | $q_{m\text{-}Cu}$ = 7.140 mg/g | $q_{m\text{-}Cu}$ = 9.447 mg/g |
| $K_{L\text{-}Pb}$ = 0.079 l/g | $K_{L\text{-}Cu}$ = 0.041 l/g | $K_{L\text{-}Cu}$ = 0.031 l/g |
| $K_{L\text{-}Cd}$ = 0.0001 l/g | $K_{L\text{-}Zn}$ = -0.0197 l/g | $K_{L\text{-}Pb}$ = -0.013 l/g |
| $R^2$ = 0.944 | $R^2$ = 0.999 | $R^2$ = 0.971 |
| **For Cd(II):** | **For Zn(II):** | **For Pb(II):** |
| $q_{m\text{-}Cd}$ =18.582 mg/g | $q_{m\text{-}Zn}$ = 4.760 mg/g | $q_{m\text{-}Pb}$ = 60.311 mg/g |
| $K_{L\text{-}Pb}$ = 0.079 l/g | $K_{L\text{-}Cu}$ = 0.041 l/g | $K_{L\text{-}Cu}$ = 0.031 l/g |
| $K_{L\text{-}Cd}$ = 0.0001 l/g | $K_{L\text{-}Zn}$ = -0.0197 l/g | $K_{L\text{-}Pb}$ = -0.013 l/g |
| $R^2$ = 0.996 | $R^2$ = 0.988 | $R^2$ = 0.971 |

| Pb(II)-Zn(II) | Cd(II)-Zn(II) | Cd(II)-Cu(II) |
|---|---|---|
| **For Pb(II):** | **For Cd(II):** | **For Cd(II):** |
| $q_{m\text{-}Pb}$ = 42.942 mg/g | $q_{m\text{-}Cd}$ =18.030mg/g | $q_{m\text{-}Cd}$ = 16.280 mg/g |
| $K_{L\text{-}Pb}$ = 0.036 l/g | $K_{L\text{-}Cd}$ = 0.060 | $K_{L\text{-}Cd}$ = 0.041 l/g |
| $K_{L\text{-}Zn}$ = -0.050 l/g | $K_{L\text{-}Zn}$ = -0.044 | $K_{L\text{-}Cu}$ = -0.0306 l/g |
| $R^2$ = 0.997 | $R^2$ = 0.999 | $R^2$ = 0.999 |
| **For Zn(II):** | **For Zn(II):** | **For Cu(II):** |
| $q_{m\text{-}Zn}$ = 9.460 mg/g | $q_{m\text{-}Zn}$ =11.053mg/g | $q_{m\text{-}Cu}$ = 16.660 mg/g |
| $K_{L\text{-}Pb}$ = 0.036 l/g | $K_{L\text{-}Cd}$ = 0.060 l/g | $K_{L\text{-}Cd}$ = 0.041 l/g |
| $K_{L\text{-}Zn}$ = -0.050 l/g | $K_{L\text{-}Zn}$ = -0.044 l/g | $K_{L\text{-}Cu}$ = -0.0306 l/g |
| $R^2$ = 0.997 | $R^2$ = 0.998 | $R^2$ = 0.999 |

### 5.2.6.2 Adsorption behaviour in ternary solutions

In the case of the three metals in the test solution, the equation (5.17) can be rewritten as (for Cu(II)-Pb(II)-Cd(II) ternary adsorption system as an example):

for Cu(II): $$q_{e.Cu} = \frac{q_{m.Cu} K_{L.Cu} (C_{Cu})}{1 + K_{L.Cu} C_{e.Cu} + K_{L.Pb} C_{e.Pb} + K_{L.Cd} C_{e.Cd}} \quad (5.20)$$

for Pb(II): $$q_{e.Pb} = \frac{q_{m.Pb} K_{L.Pb} (C_{Pb})}{1 + K_{L.Cu} C_{e.Cu} + K_{L.Pb} C_{e.Pb} + K_{L.Cd} C_{e.Cd}} \quad (5.21)$$

and for Cd(II): $$q_{e.Cd} = \frac{q_{m.Cd} K_{L.Cd} (C_{Cd})}{1 + K_{L.Cu} C_{e.Cu} + K_{L.Pb} C_{e.Pb} + K_{L.Cd} C_{e.Cd}} \quad (5.22)$$

Similarly, the equation (5.17) can be rewritten for Pb(II)-Cd(II)-Zn(II), Cu(II)-Pb(II)-Zn(II) and Cu(II)-Cd(II)-Zn(II) adsorption systems.

Wastewaters may contain more than one type of metal ion and therefore, the examination of multiple metal interactions simultaneously is very important for accurate representation of adsorption data (Hammaini et al., 2003). The competitive adsorption among the Cu(II), Pb(II), Cd(II) and Zn(II) in the ternary systems were conducted in

batch system between 1 to 200 mg/l initial concentration for 3 hours at 120 rpm and room temperature. The adsorption parameters are tabulated in Table 5.13 and plotted in Figure 5.18.

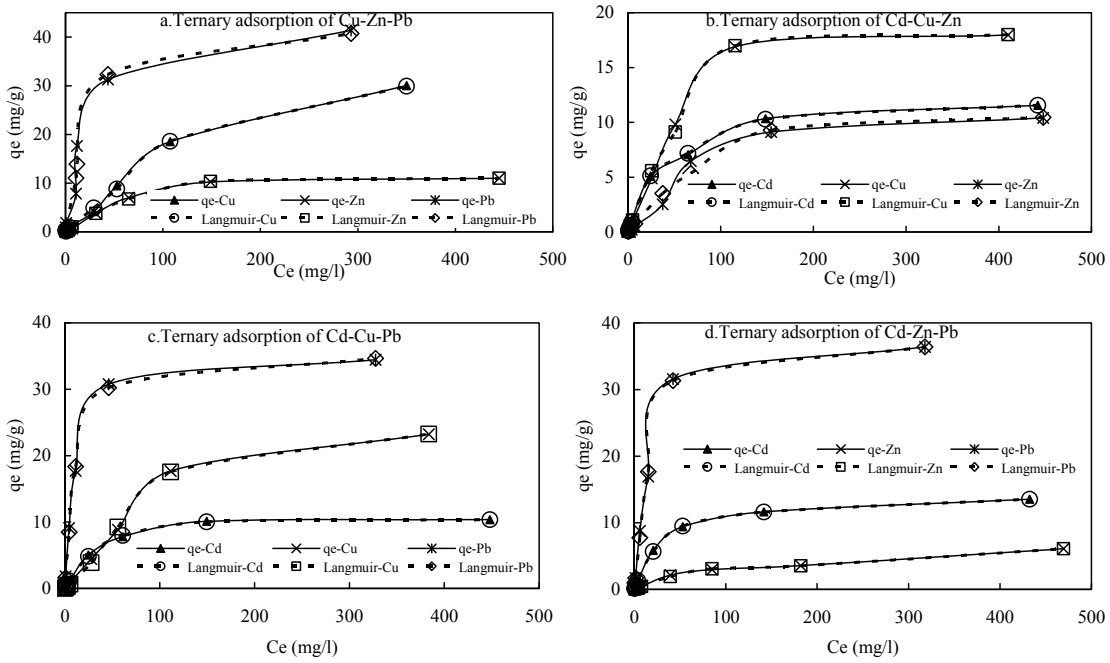


**Figure 5.18** Ternary adsorption of among the Cu(II), Pb(II), Cd(II) and Zn(II) in the ternary systems of Cd(II)-Pb(II)-Cu(II), Cd(II)-Pb(II)-Zn(II), Cu(II)-Cd(II)-Zn(II) and Cu(II)-Pb(II)-Zn(II)

The experimental data were well fitted with the ternary adsorption model (eq.5.20-5.22) as the $R^2$ were 0.998, 0.999 and 0.999 for Cd(II), Cu(II), and Pb(II) of the Cd-Cu-Pb system; 0.999, 0.994 and 0.999 for Cd(II), Zn(II) and Pb(II) of the Cd(II)-Zn(II)-Pb(II) system; 0.999, 0.997 and 0.982 for Cd(II), Cu(II) and Zn(II) of the Cd-Cu-Zn system; and 0.999, 0.997 and 0.985 for Cu(II), Zn(II) and Pb(II) of the Cu-Zn-Pb system; respectively. The lowest adsorption capacity for Cu(II), Cd(II), Zn(II) and Pb(II) ions were observed in this system rather than the single and binary systems (Table 5.6, and Table 5.12). These types of results are found for different biosorbents (Kusvuran et al., 2012; Verma et al., 2008). The ionic charge, ionic radius, and electrode potential affect adsorption capacity and it decreases in the multi-metal adsorption system with respect to single metal adsorption capacity (Padilla-Ortega et al., 2013; Zhu et al., 2012). The adsorption capacities of cabbage were found to be 12.264, 8.785 and 40.963mg/g for the Cd(II)-Cu(II)-Pb(II) system, 7.587, 1.828 and 50.216mg/g for the Cd(II)-Zn(II)-Pb(II) system, 4.965, 7.584 and 5.844mg/g for the Cd(II)-Cu(II)-Zn(II) system, and 8.194, 6.380 and 22.803mg/g for the Cu(II)-Zn(II)-Pb(II) system, respectively (Table 5.13).

**Table 5.13** Ternary adsorption parameters calculated from Langmuir model for Pb(II), Cd(II), Cu(II) and Zn(II) adsorption.

| Cd(II)-Pb(II)-Cu(II) | Cd(II)-Pb(II)-Zn(II) | Cu(II)-Cd(II)-Zn(II) | Cu(II)-Pb(II)-Zn(II) |
|---|---|---|---|
| **For Cd(II)** | **For Cd(II)** | **For Cd(II)** | **For Cu(II)** |
| $q_{m\text{-}Cd}$ =12.264 mg/g | $q_{m\text{-}Cd}$ = 7.587 mg/g | $q_{m\text{-}Cd}$ = 4.965 mg/g | $q_{m\text{-}Cu}$ = 8.194 mg/g |
| $K_{L\text{-}Cu}$ = -0.007 l/g | $K_{L\text{-}Zn}$ = -0.016 l/g | $K_{L\text{-}Cu}$ = 0.009 l/g | $K_{L\text{-}Zn}$ = -0.017 l/g |
| $K_{L\text{-}Cd}$ = 0.023 l/g | $K_{L\text{-}Cd}$ = 0.046 l/g | $K_{L\text{-}Cd}$ = 0.041 l/g | $K_{L\text{-}Cu}$ = 0.025 l/g |
| $K_{L\text{-}Pb}$ = 0.010 l/g | $K_{L\text{-}Pb}$ = -0.006 l/g | $K_{L\text{-}Zn}$ = -0.034 l/g | $K_{L\text{-}Pb}$ = 0.001 l/g |
| $R^2$ = 0.998 | $R^2$ = 0.999 | $R^2$ = 0.999 | $R^2$ = 0.999 |
| **For Cu(II)** | **For Zn(II)** | **For Cu(II)** | **For Zn(II)** |
| $q_{m\text{-}Cu}$ = 8.785 mg/g | $q_{m\text{-}Zn}$ = 1.828 mg/g | $q_{m\text{-}Cu}$ = 7.584 mg/g | $q_{m\text{-}Zn}$ = 6.380 mg/g |
| $K_{L\text{-}Cd}$ = 0.002 l/g | $K_{L\text{-}Zn}$ = -0.009 l/g | $K_{L\text{-}Cu}$ = 0.034 l/g | $K_{L\text{-}Zn}$ = 0.002 l/g |
| $K_{L\text{-}Cu}$ = -0.011 l/g | $K_{L\text{-}Cd}$ = 0.031 l/g | $K_{L\text{-}Cd}$ = 0.003 l/g | $K_{L\text{-}Cu}$ = 0.006 l/g |
| $K_{L\text{-}Pb}$ = 0.012 l/g | $K_{L\text{-}Pb}$ = -0.018 l/g | $K_{L\text{-}Zn}$ = -0.025 l/g | $K_{L\text{-}Pb}$ = 0.009 l/g |
| $R^2$ = 0.999 | $R^2$ = 0.994 | $R^2$ = 0.997 | $R^2$ = 0.997 |
| **For Pb(II)** | **For Pb(II)** | **For Zn(II)** | **For Pb(II)** |
| $q_{m\text{-}Pb}$ = 40.963 mg/g | $q_{m\text{-}Pb}$ = 50.216 mg/g | $q_{m\text{-}Zn}$ = 5.844 mg/g | $q_{m\text{-}Pb}$ = 22.803 mg/g |
| $K_{L\text{-}Cu}$ = -0.012 l/g | $K_{L\text{-}Zn}$ = -0.009 l/g | $K_{L\text{-}Cu}$ = 0.018 l/g | $K_{L\text{-}Zn}$ = -0.009 l/g |
| $K_{L\text{-}Pb}$ = 0.063 l/g | $K_{L\text{-}Cd}$ = 0.006 l/g | $K_{L\text{-}Cd}$ = 0.002 l/g | $K_{L\text{-}Cu}$ = 0.006 l/g |
| $K_{L\text{-}Cd}$ = 0.003 l/g | $K_{L\text{-}Pb}$ = 0.036 l/g | $K_{L\text{-}Zn}$ = -0.010 l/g | $K_{L\text{-}Pb}$ = 0.036 l/g |
| $R^2$ = 0.999 | $R^2$ = 0.999 | $R^2$ = 0.982 | $R^2$ = 0.985 |

### 5.2.6.3 Adsorption behaviour in quaternary solutions

In the case of four metals in water, the adsorption system can be formulated by reforming the equation (5.17) for the quaternary solution of the Cu(II)-Pb(II)-Cd(II)-Zn(II) system:

For Cu(II): $$q_{e.Cu} = \frac{q_{m.Cu} K_{L.Cu} (C_{Cu})}{1 + K_{L.Cu} C_{e.Cu} + K_{L.Pb} C_{e.Pb} + K_{L.Cd} C_{e.Cd} + K_{L.Zn} C_{e.Zn}} \quad (5.23)$$

For Pb(II): $$q_{e.Pb} = \frac{q_{m.Pb} K_{L.Pb} (C_{Pb})}{1 + K_{L.Cu} C_{e.Cu} + K_{L.Pb} C_{e.Pb} + K_{L.Cd} C_{e.Cd} + K_{L.Zn} C_{e.Zn}} \quad (5.24)$$

For Cd(II): $$q_{e.Cd} = \frac{q_{m.Cd} K_{L.Cd} (C_{Cd})}{1 + K_{L.Cu} C_{e.Cu} + K_{L.Pb} C_{e.Pb} + K_{L.Cd} C_{e.Cd} + K_{L.Zn} C_{e.Zn}} \quad (5.25)$$

And for Zn(II): $$q_{e.Zn} = \frac{q_{m.Zn} K_{L.Zn} (C_{Zn})}{1 + K_{L.Cu} C_{e.Cu} + K_{L.Pb} C_{e.Pb} + K_{L.Cd} C_{e.Cd} + K_{L.Zn} C_{e.Zn}} \quad (5.26)$$

The calculated parameters from the quaternion Langmuir isotherms are summarised in Table 5.14. This isotherm model successfully fitted the competitive adsorption of Cu(II)-Pb(II)-Cd(II)-Zn(II) onto the biosorbent prepared from cabbage.

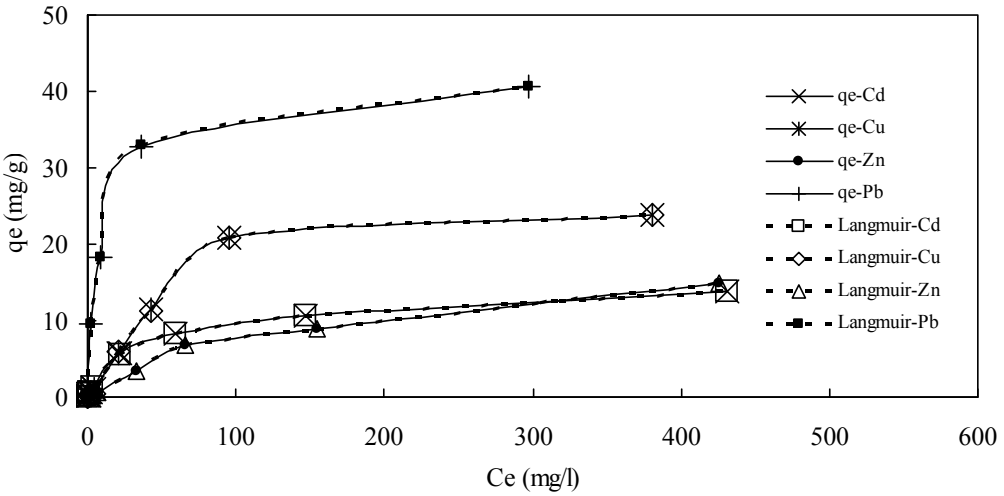


**Figure 5.19** Quaternary adsorption of among the Cu(II), Pb(II), Cd(II) and Zn(II) in the four metals system of Cd(II)-Pb(II)-Cu(II)-Zn(II).

The adsorption capacities of Cu(II), Pb(II), Cd(II) and Zn(II) from four metals in the (Cu-Pb-Cd-Zn) system were compared to the molar uptake values of metals predicted with the quaternary Langmuir isotherm (eqs. 5.23-5.26). As showed in this Figure 5.19, the model perfectly estimated the parameters for all fours metals uptake as the predicted lines and experimental plots are close enough. However, it overestimated the molar uptake of Zn(II) and showed the similar adsorption capacity (10.170mg/g) with single metal systems (Table 5.6). But Cu(II), Pb(II) and Cd(II) uptakes are underestimated as the magnitude of the adsorption capacities (2.415mg/g, 15.085mg/g and 8.697mg/g) are lower than the single metals system (Papageorgiou et al., 2009; Şengil and Özacar, 2009; Xue et al., 2009).

**Table 5.14** Isotherm parameters of Langmuir model of quaternary metals [Cd(II)-Cu(II)-Zn(II)-Pb(II)] adsorption

| **For Cd(II)** | **For Cu(II)** | **For Zn(II)** | **For Pb(II)** |
|---|---|---|---|
| $q_{m\text{-}Cd}$ = 8.697 mg/g | $q_{m\text{-}Cu}$ = 2.415 mg/g | $q_{m\text{-}Zn}$ = 10.170 mg/g | $q_{m\text{-}Pb}$ = 15.085 mg/g |
| $K_{L\text{-}Cu}$ = 0.0034 l/g | $K_{L\text{-}Cu}$ = -0.039 l/g | $K_{L\text{-}Cu}$ = -0.063 l/g | $K_{L\text{-}Cu}$ = -0.052 l/g |
| $K_{L\text{-}Cd}$ = 0.050 l/g | $K_{L\text{-}Cd}$ = 0.038 l/g | $K_{L\text{-}Cd}$ = 0.004 l/g | $K_{L\text{-}Cd}$ = 0.055 l/g |
| $K_{L\text{-}Zn}$ = -0.014 l/g | $K_{L\text{-}Zn}$ = -0.022 l/g | $K_{L\text{-}Zn}$ = 0.029 l/g | $K_{L\text{-}Zn}$ = -0.034 l/g |
| $K_{L\text{-}Pb}$ = -0.015 l/g | $K_{L\text{-}Pb}$ = 0.029 l/g | $K_{L\text{-}Pb}$ = 0.038 l/g | $K_{L\text{-}Pb}$ = 0.038 l/g |
| $R^2$ = 0.999 | $R^2$ = 0.998 | $R^2$ = 0.999 | $R^2$ = 0.998 |

The parameter of $K_L$ values of the Langmuir isotherm indicates the affinity of a biosorbent for the two or three or four metal ions; the greater the value of these parameters, the lesser is the affinity for a metal ion (Kusvuran et al., 2012; Şengil and Özacar, 2009). The values of $K_{L\text{-}Cu}$, $K_{L\text{-}Pb}$, $K_{L\text{-}Zn}$, and $K_{L\text{-}Cd}$ are higher in the case of the binary, ternary and quaternary system than the value of $K_L$ derived for the single metal

system (Table 5.6, Tables 5.12, Tables 5.13 and Tables 5.14). This means that the affinity of cabbage biosorbent for metal ions was reduced in multi-metals metal systems.

### 5.2.6.4 Antagonism of multi-metals system

It is found from available literature (Leyva-Ramos et al., 2001) that the multi-metal Langmuir model provides a reasonable fit to the multi-metals adsorption data as long as the $q_m$ values for each metal calculated from single-metal are similar to each other. But the prediction for $q_m$ values from all binary, ternary and quaternary system are lower than for single metals system (Kumar et al., 2008; Şengil and Özacar, 2009). The antagonism between the metals' ions is the internal competition. In this regard, the 3D surface plots of Cu(II)-Zn(II), Pb(II)-Cd(II), Cd(II)-Zn(II), Cu(II)-Cd(II) and Pb(II)-Cu(II) are prepared for binary systems and shown in Figure 5.20 and Figure 5.21. The area plot for the ternary systems (Cd(II)-Pb(II)-Cu(II), Cd(II)-Pb(II)-Zn(II), Cu(II)-Cd(II)-Zn(II) and Cu(II)-Pb(II)-Zn(II)) is shown in Figure 5.22; and the spider diagram for the quaternary system (Cd(II)-Pb(II)-Cu(II)-Zn(II)) is given in Figure 5.23.

The effect of the presence of Zn(II) for adsorbing Cu(II) is graphed in Figure 5.20(A). The competitive adsorption surface of Cu(II) showed that the presence of Zn(II) drastically reduced the uptake of Cu(II). A moderate reduction of the uptake of Cu(II) can be noted when compare to a single metal system (from 10.315 to 7.140mg/g). On the other hand the effect of the presence Cu(II) on the capacity of Zn(II) adsorption is shown in Figure 5.20(B). The effect is stronger and reduced to half of the uptake of Zn(II) (from 8.970 to 4.760mg/g) though the surface is perfectly slanting evenly (El-Bayaa et al., 2009; Padilla-Ortega et al., 2013). In the Pb(II)-Cd(II) system the effects of Pb(II) and Cd(II) ions on the uptake of Cd(II) and Pb(II) ions are plotted in Figure 5.20(C) and Figure 5.20(D) respectively. Reduced Pb(II) and Cd(II) uptake was found. Both metals posed high aggression on the competitive adsorption as the 3D graph surface is shown to be uneven (Leyva-Ramos et al., 2001).

Similarly, the partial aggression on the adsorption of Cd(II) and Zn(II) in Cd(II)-Zn(II), Cu(II) and Cd(II) in Cu(II)-Cd(II), and; Pb(II) and Cu(II) in the Pb(II)-Cu(II) binary system are plotted in Figure 5.21(A) and Figure 5.21(B); Figure 5.21(C) and Figure 5.21(D); and Figure 5.21(E) and Figure 5.21(F), respectively. From Figure 5.21 it is found that strong antagonisms were found between the metals but the dominancy of

Pb(II) and Cd(II) uptake did not change with their counter pairs of metals (Apiratikul and Pavasant, 2006; El-Bayaa et al., 2009). High affinity of cabbage toward the Pb(II) and Cd(II) ions are internal causes (functional groups) for the significant adsorption of those metals.

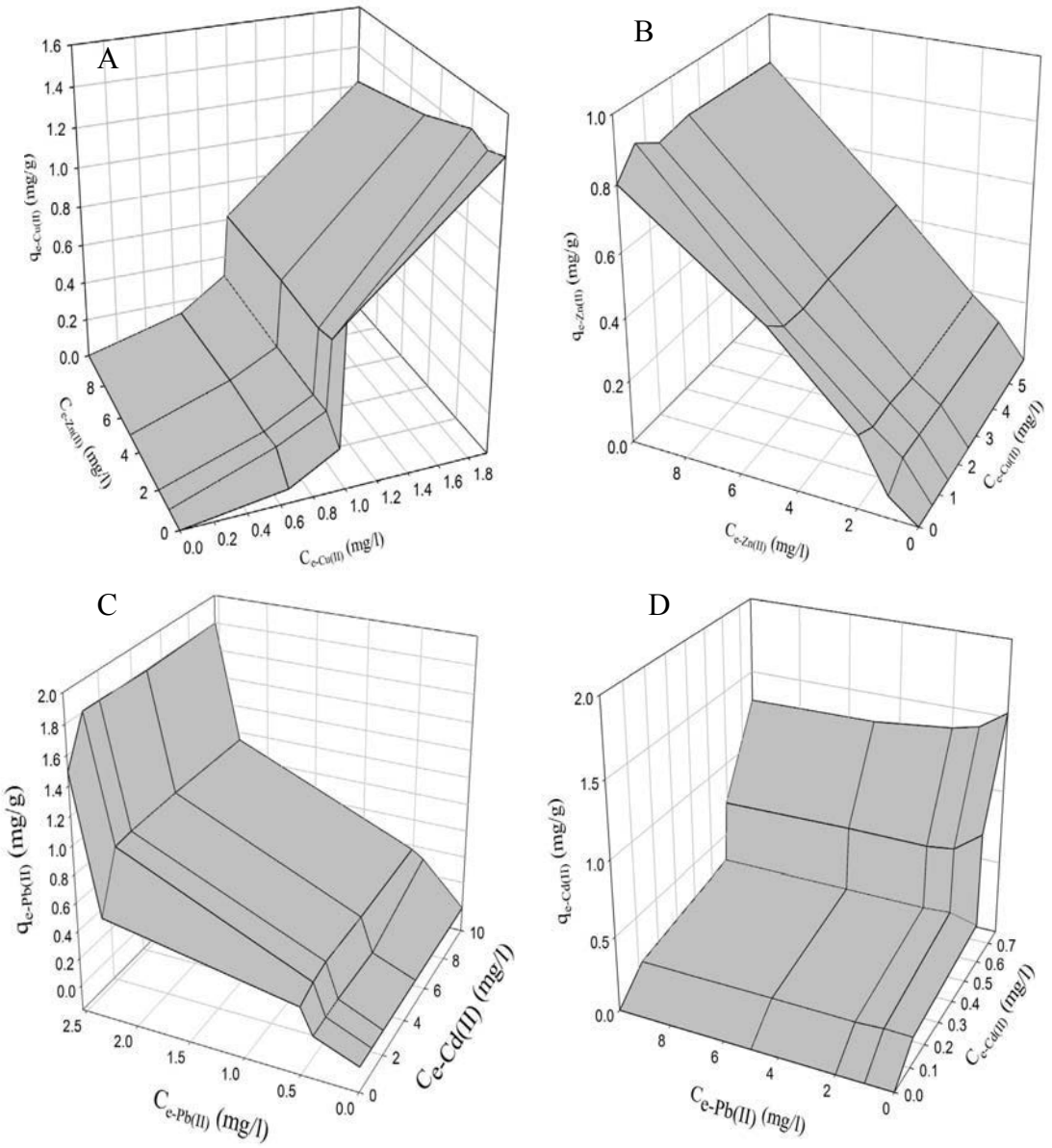


**Figure 5.20** Antagonism among the metals for Cu(II)-Zn(II) (A&B) and Pb(II)-Cd(II) (C&D) binary system.

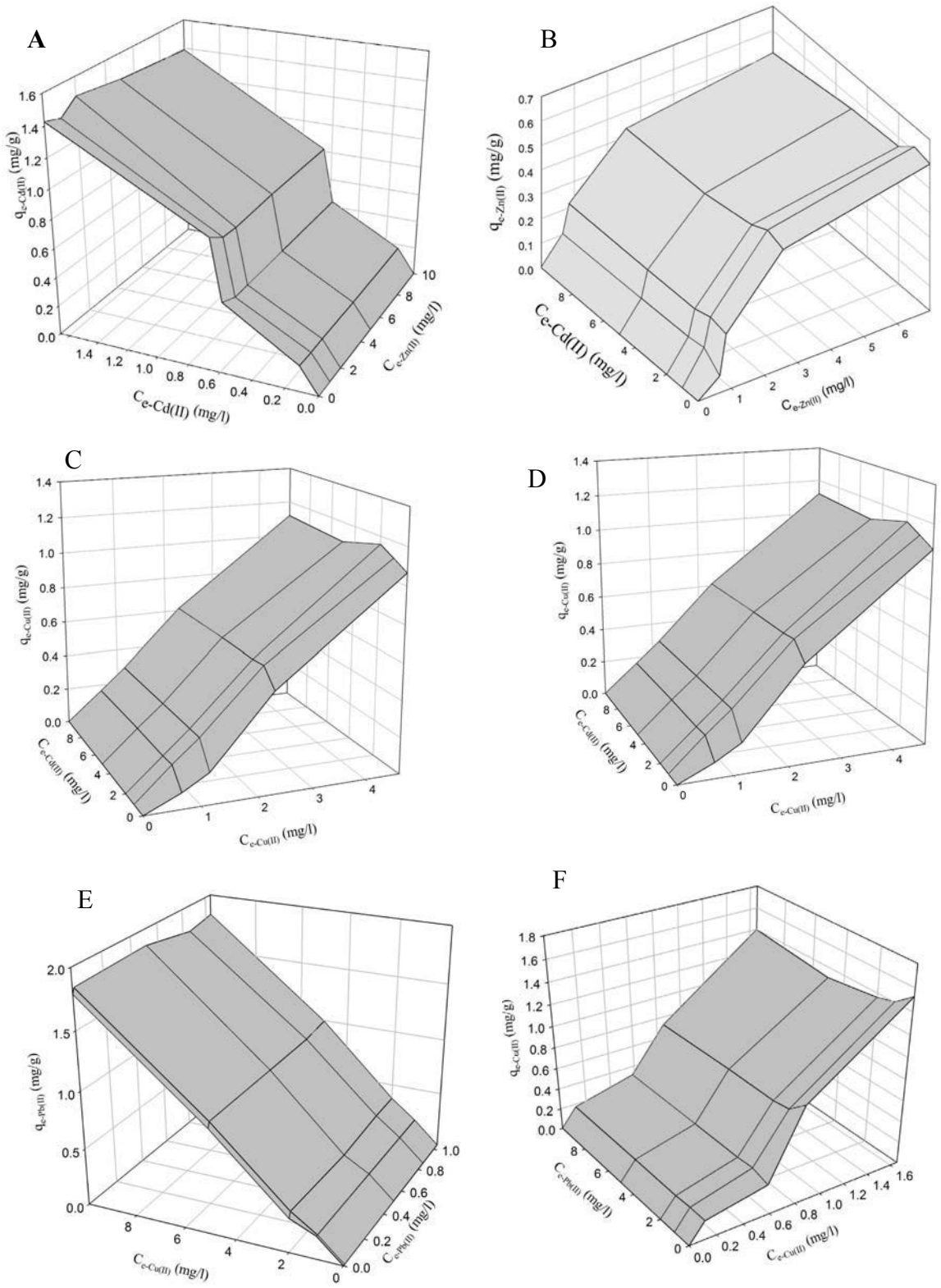


**Figure 5.21** Antagonism among the metals for Cd(II)-Zn(II) (A&B), Cu(II)-Cd(II) (C&D) and Pb(II)-Cu(II) (E&F) binary system.

For instance, in Cd(II)-Zn(II) system Cd(II) uptake(18.030 mg/g), and in Pb(II)-Cu(II) system Pb(II) (60.311mg/g) uptake were more than their pairs of Zn(II) and Cu(II) (Table 5.6 and Tables 5.12,). Figure 5.21(A), Figure 5.21(C) and Figure 5.21(E) also depicted the arguments as the surface is more even than the surface of counter metals. But, a significant change was found in Cu-Cd system where Cu(II) uptake increased (from 10.315mg/g in the single metal system to 20.660mg/g in the binary system) in the presence of Cd(II) ions. It is also notable that Zn(II) adsorption slightly increased in the binary system (11.053mg/g) with the presence of Cd(II) ions. It might be predicted that the presence of Cd(II) ions enhances the uptake of Cu(II) and Zn(II) when considering of minor change of its own uptake (Papageorgiou et al., 2009).

The results of the ternary system are demonstrated in the surface plot of Figure 5.22 (a, b, c and d). There it is revealed that the Pb(II) ions presented a higher affinity for the binding sites of the cabbage than the Cu(II), Cd(II) and Zn(II) ions. In other words, the cabbage was much more selective towards Pb(II) than to the other three metals in the competitive adsorption.

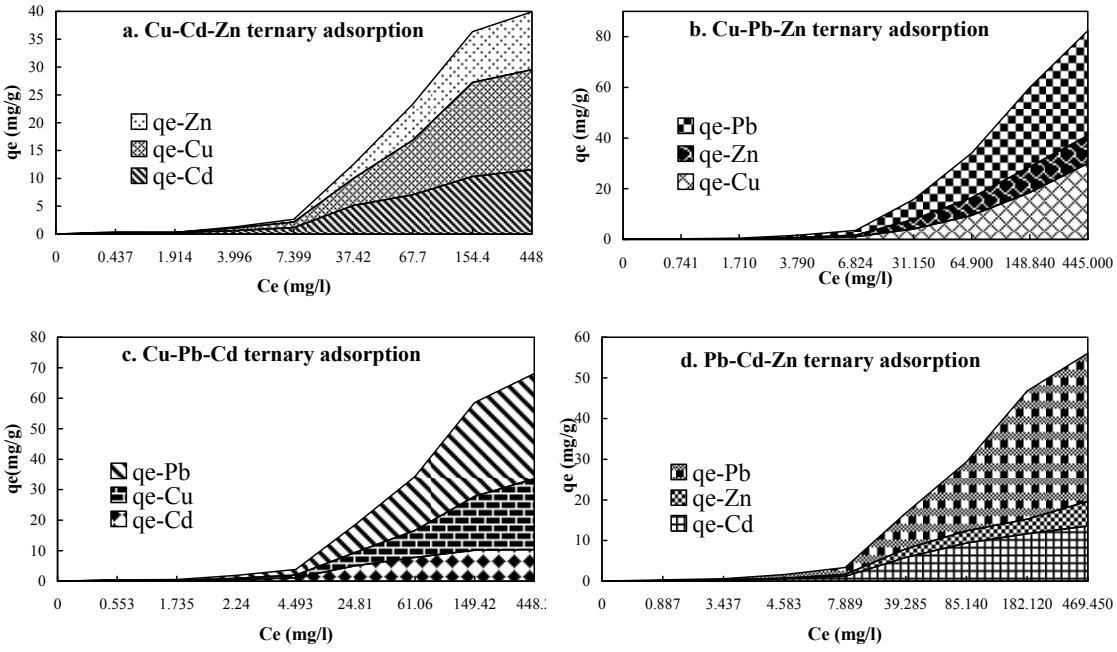


**Figure 5.22** Occupied physical surface area of metals in terms of capacity for ternary metals adsorption system onto cabbage.

The Pb(II) ions presented strong antagonism against the adsorption of Cu(II) and Cd(II) ions in Cu(II)-Pb(II)-Cd(II), against of Cd(II) and Zn(II) ions in theCd(II)-Pb(II)-Zn(II) system; and against the Cu(II) and Zn(II) in the Cu-Pb-Zn system whereas the Cu(II)

and Cd(II) ions, Cd(II) and Zn(II) ions, and Cu(II) and Zn(II) ions exhibited only light antagonism against the adsorption of Pb(II) (Apiratikul and Pavasant, 2006; El-Bayaa et al., 2009; Padilla-Ortega et al., 2013; Şengil and Özacar, 2009). This behaviour could not be predicted from the single metal adsorption system. It is also found from Figure 5.22 (b, c and d) that Pb(II) ions took higher surface area than other metals. In other words, the most binding sites of cabbage are occupied by Pb(II) ions in a competitive system (Raize et al., 2004; Şengil and Özacar, 2009).

Real wastewater is a mixture of several metals matrices and antagonism is the common activity among the metals (Raize et al., 2004). To understand the antagonism of real wastewater a quaternary system isotherm was conducted. To visualise the antagonism among the four metals spider diagram was constructed and plotted in Figure 5.23. As the Pb(II) ions occupied the higher spiral surface of spider plot, the superior attraction toward cabbage is depicted (Apiratikul and Pavasant, 2006; Raize et al., 2004). Similarly, Cu(II) ions possess the second higher antagonism though the maximum uptake capacity for Cu(II) was lowest (2.415mg/g) among the four-metals (Table 5.14). Cd(II) and Zn(II) ions appeared with a same magnitude of affection towards cabbage though their prediction from single and binary system was different (Padilla-Ortega et al., 2013; Şengil and Özacar, 2009).

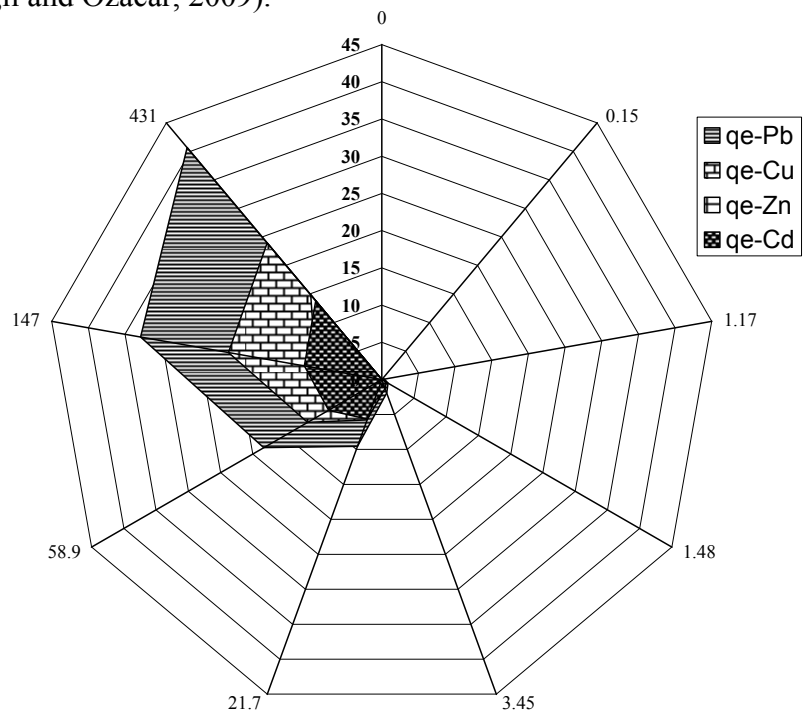


**Figure 5.23** Engaged area in terms of capacity of metals in spider diagram for quaternary metals adsorption onto cabbage.

The percent reduction in adsorption capacities in the competitive systems (binary, ternary and quaternary) were calculated by the following expression:

$$\%\ \text{reduced} = \frac{\left(q_m \text{ from single metal system} - q_m \text{ from multi - metal system}\right)}{q_m \text{ from single metal system}} \times 100$$

It was also found that dominant Pb(II) ions uptakes were reduced to 28.33%, 1.6% and 29.91% for the binary system, 33%, 18% and 62.781% for the ternary system, and 75.37% for quaternary system. The Cd(II) ions uptake is decreased to 16%, 18.50% and 26.4% for binary, 44.56%, 65.71% and 77.56% for ternary and 60.7% for quaternary systems. It is apparent that the highest decline is observed for Pb(II) and Cd(II) ions in all adsorption systems. Conversely, the Cu(II) and Zn(II) posed mixed trends (decrease and increase) for adsorption capacities. The Cu(II) and Zn(II) ions increased to 29% and 1.5% for Cd-Cu and Cd-Zn binary system. But it dropped for binary, ternary and quaternary system with other co-metals. So, it may presumed that Cd(II) ions acted as a stimulate for Cu(II) and Zn(II). In the other words, antagonism is co-metal dependent for particular metals (Niu et al., 2013; Xue et al., 2009).

## 5.3 Conclusions

The cabbage based biosorbent was an effective agro-waste biosorbent for Pb(II), Cd(II), Cu(II) and Zn(II) ions removal from aqueous solutions. It has significant higher specific surface and metals binding functional groups. Three-parameter models (Redlich-Peterson, Koble-Corrigan and SIPS) and two-parameter models (Langmuir and Freundlich) showed good fitness with equilibrium adsorption data. Kinetic adsorption data were satisfactorily fitted by the pseudo-second order, Elovich and Avrami kinetic models. Desorption data also showed good agreement with equilibrium and kinetics models.

As adsorption systems with multi-metal containing effluents is more relevant to practical cases, comparative adsorption of the individual metal ions from single, binary, ternary and quaternion systems of Cu(II), Pb(II), Zn(II) and Cd(II) metals were used and the data were fitted to the mono- and multi-metal Langmuir models. Although cabbage had a higher adsorption capacity for Pb(II) and Cd(II) in a single-metal situation, the equilibrium uptakes of Pb(II) and Cd(II) in the binary, ternary and quaternary mixture decreased because of the levels of interference between these metals.

Faculty of Engineering and Information Technology
University of Technology, Sydney (UTS)

# Chapter 6

# Banana peels – a novel bio-waste for removal of Cu(II), Pb(II), Cd(II) and Zn(II) from aqueous solution

## 6.1 Background

Biosorbents derived from a suitable agro-biomass, can be used for the effective removal and recovery of heavy metals from wastewater (Raize et al., 2004). Agro-wastes are abundant in nature or can be found as by-products or waste from agro-industry, and are cheap and effective without need of pre-processing. Recent studies on the removal of heavy metals using numerous types of biosorbent are reported in the literature. In this context, agricultural wastes such as banana peels have been used as biosorbents for copper adsorption. Banana peels are readily available, low cost and environmentally friendly bio-materials. A step here taken for preparing biosorbents from banana peels (BP) for removal of Cu(II), Pb(II), Cd(II) and Zn(II) from water.

The main aims of this study were to prepare biosorbents and characterize them including evaluation of the effectiveness of banana peels (BP) for Cu(II), Pb(II), Cd(II) and Zn(II) removal by determining the maximum adsorption capacities. The effects of experimental conditions on the removal are also examined. The regeneration of exhausted banana peels and recovery of Cu(II), Pb(II), Cd(II) and Zn(II) were examined. Adsorption and desorption equilibrium were evaluated with isotherm models. The adsorption and desorption kinetic characteristics were determined using kinetics models. The thermodynamics of adsorption were also evaluated. To evaluate antagonism among the metals ions (Cu(II), Pb(II), Cd(II) and Zn(II)), multimetal adsorption was conducted and evaluated.

## 6.2 Results and discussion

### 6.2.1 Environment friendly preparation

Formations of particle size and shape, surface morphology, as well as specific surface area of biosorbent, fully depend on the preparation method. In addition, easy to prepare, easy to use, hazard free and environment friendly treatments are the requirement for the sustainable preparation of biosorbents. In these circumstances, this research adopted a simple and non-treated preparation method rather than the expensive and high-tech and non-environment friendly acid/base treated methods (Al-Asheh et al., 2000; Al-Rub, 2006; Özcan et al., 2005). The novelty of this research is that banana peels were simply cut, washed, dried, ground to powder, and then used for experiments.

### 6.2.2 Characterisation of BP

The characterisations are processes to explore the surface properties, active functional groups and adsorption mechanism. It is an important step for biosorbent in the context of uses for selectivity of metals' ions, explore binding sites and functional groups for ion exchange or chemisorption. In this context, the banana peels were characterised by SEM, FTIR and BET tests.

#### 6.2.2.1 Surface morphology of BP

Zeiss (JEOL-JSM-35CF, UK) Scanning Electronic Microscope (SEM), operating in variable pressure (VP) mode at 0.3 Tor and 20kV accelerating voltage was used for studying the surface morphology of the banana peels (Chapter 3, Section 3.3.1.1). The SEM images were taken with four magnifications and are shown in Figure 6.1 (A, B, C and D). Figure 6.1(A) shows the banana peels, revealing the combination of small and large particles, heterogeneous rough and porous surfaces with crater-like pores. Similar characteristics are found for other biosorbents (Memon et al., 2008b). These micro-rough textured and porous surfaces are found on the particles of banana peels (Figure 6.1(B)), which was expected to promote the uptake of metals ions (Annadurai et al., 2002). In higher magnifications of 5KX and 10KX, Figures 6.1(C) and (D), the porous particle has huge internal spaces where metals ions can be entrapped and adsorbed. Similar propositions are mentioned in literature (Albarelli et al., 2011).

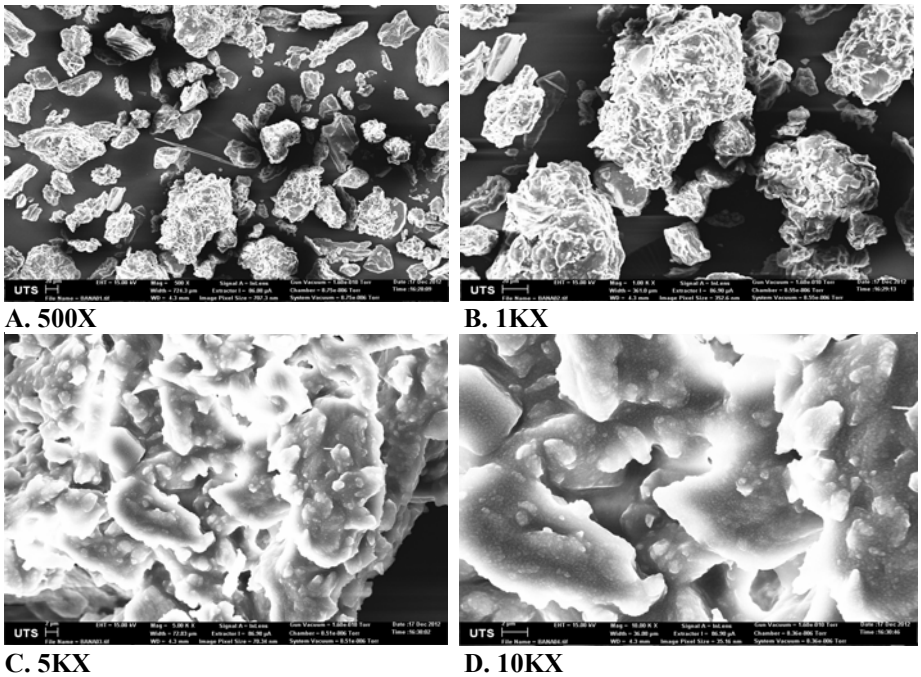


**Figure 6.1** BSE (backscattered electron) images of banana peels taken by SEM

### 6.2.2.2 Functional groups on the surfaces of BP

To understand the nature of the functional groups present in banana peels, the Fourier Transform Infrared Spectroscopy (FTIR) spectra were obtained by SHIMADZU FTIR 8400S (Kyoto, Japan) (Chapter 3, Section 3.3.1.3). FT-IR spectra (Figure 6.2) displayed a number of peaks and indicated a complex nature of the biosorbent. Bands appearing at 3620.54, between 3537.60-3348.57, 3147.96-3102.63, 2957.97-2850.91, 2360.97-2347.47, 1654.03, 1560.48, 1459.21-1411.95 and 996.28-936.48 $cm^{-1}$ were assigned to OH stretch, free hydroxyl (Alcohols, phenols), OH stretch, H-bonded (Alcohols, phenols), OH stretch (carboxylic acids), ≡C-H stretch (alkanes), C≡N stretch (Nitriles), -C=C- stretch (alkanes), N-H bend (primary amines), C-H bend (alkanes) and O-H bend (carboxylic acid or ester); respectively. Among the functional groups carboxylic acid and hydroxyl groups could play major role for metals ions adsorption (Annadurai et al., 2003; Memon et al., 2008b).

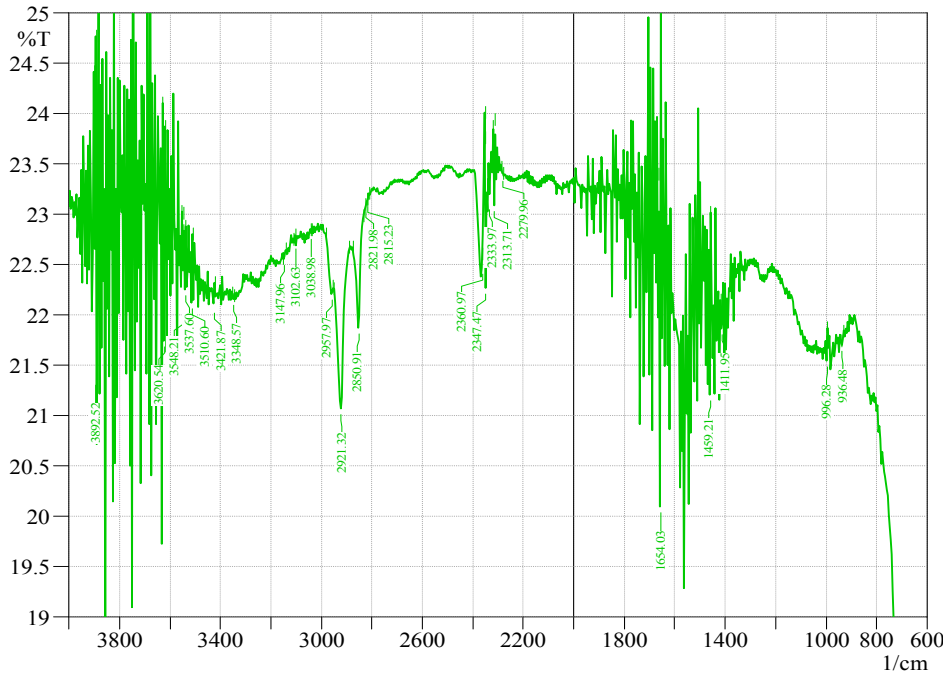


**Figure 6.2** Fourier Transform Infrared Spectroscopy (FTIR) spectra of BP

### 6.2.2.3 Specific surface area of BP

The BET surface areas of banana peels were determined from $N_2$ adsorption isotherm by Nano Porosity System (Micrometrics ASAP 2020, Mirae SI, Korea) and are tabulated in Table 6.1. The BET surface area, Langmuir surface area and average pore diameter of banana peels were 22.59 $m^2/g$, 4.82 $m^2/g$ and 8.71 Å, respectively. This BET area (specific surface area) was higher than chitosan flakes and pine bark (Ngah

and Fatinathan, 2006; Vázquez et al., 2007) but lower than palm oil fruit shell (Hossain et al., 2012a). In contrast, the surface area was low compared to pyrolysed produced activated carbon. However, it could be acceptable as it was produced from the non-treated, low cost and simple processes. The micropore area is 2.70 $m^2/g$ (DR Method) while the mesopore areas are 22.14 $m^2/g$ (BJH Adsorption) and 26.10 $m^2/g$ (BJH Desorption). According to International Union of Pure and Applied Chemistry (IUPAC) classification, the majority of pores are mesopore (83%). The mean micropore and mesopore diameter of banana peels particle are 8.71 Å and 43.01 Å respectively.

**Table 6.1** Surface parameters of banana peels from BET test

| Parameter of garden grass | Methods | Values |
|---|---|---|
| 1. Surface area | BET surface area | 22.59 $m^2/g$ |
| | Langmuir surface area | - 4.82 $m^2/g$ |
| 2. Pore area | | |
| i. Micropore area | DR method | 2.70 $m^2/g$ |
| | t-plot (statistical thickness = 3.50~7.00) | -35.91$m^2/g$ |
| | Horvath-Kawazoe method | 0.36 $m^2/g$ |
| ii. Mesopore area | BJH adsorption | 22.14 $m^2/g$ |
| | BJH desorption | 26.10$m^2/g$ |
| 3. Pore volume | | |
| i. Micropore volume | DR method | 0.00 $cm^3/g$ |
| | t-plot (statistical thickness = 3.50~7.00) | 0.00 $cm^3/g$ |
| | Horvath-Kawazoe method | 0.00 $cm^3/g$ |
| ii. Mesopore volume | BJH adsorption | 0.03 $cm^3/g$ |
| | BJH desorption | 0.02 $cm^3/g$ |
| 4. Pore size | | |
| i. Micropore size | DR method | 8.71 Å |
| | t-plot (statistical thickness = 3.50~7.00) | 2.54 Å |
| | Horvath-Kawazoe method | 14.69 Å |
| ii. Mesopore size | BJH adsorption | 43.01 Å |
| | BJH desorption | 30.81 Å |

### 6.2.3 Affecting factors on the performance of biosorption

The experimental conditions such as pH, particle size, dose, contact time, shaking speed, thermal effect on the adsorption of Cu(II), Pb(II), Cd(II) and Zn(II) were investigated for banana peels (BP) according to procedures in Chapter 3, Section 3.3.2.

#### 6.2.3.1 pH of water

The effects of pH on the removal of Cu(II), Pb(II), Cd(II) and Zn(II) ions by BP were conducted between pH 2 and 8 and are shown in Figure 6.3 (Chapter 3, Section 3.3.2.1). Generally, the adsorption capacities of banana peels for removing Cu(II), Pb(II), Cd(II) and Zn(II) ions were strongly affected by the pH (Figure 6.3). The

adsorption capacities of Cu(II) were increased from 0.7 mg/g to 1.76 mg/g with the increase in pH from pH 2 to pH 6. Similarly, the adsorption capacities were increased 0.43 to 1.36 mg/g for Pb(II); 0.74 to 2.00 mg/g for Cd(II); and 0.32 to 1.28 mg/g for Zn(II) with the creases of pH from 2 to 6; respectively. The metals adsorption was significantly increased between pH 4 and 6 for all metals. Among the metals, Cd(II) adsorption was almost level between pH 3 and 6. The highest removals were found within pH 5.5 and 6.5 for all four metals. To make it similar, pH 6.0-6.5 was adopted for the whole range of experiments. The adsorption capacities decreased after pH 6. Low adsorption capacities were observed at both low and high pH. At low pH, $H_3O^+$ ion competes with $Cu^{2+}$, $Pb^{+2}$, $Cd^{+2}$ and $Zn^{+2}$ for binding and surrounded hydronium ions ($H^+$), preventing the metals ions from approaching the binding sites, and this could be responsible for low adsorption capacities (Karthikeyan et al., 2007). At higher pH, the binding site may not be activated in basic condition (Demirbas et al., 2009). Above the pH of 6, the Cu(II), Cd(II), Zn(II) and Pb(II) started precipitating as $Cu(OH)_2$, $Cd(OH)_2$, $Zn(OH)_2$ and $Pb(OH)_2$ respectively in aqueous solution (Kusvuran et al., 2012; Sampaio et al., 2009); removal after 6.5 was not completed by adsorption (Memon et al., 2008a).

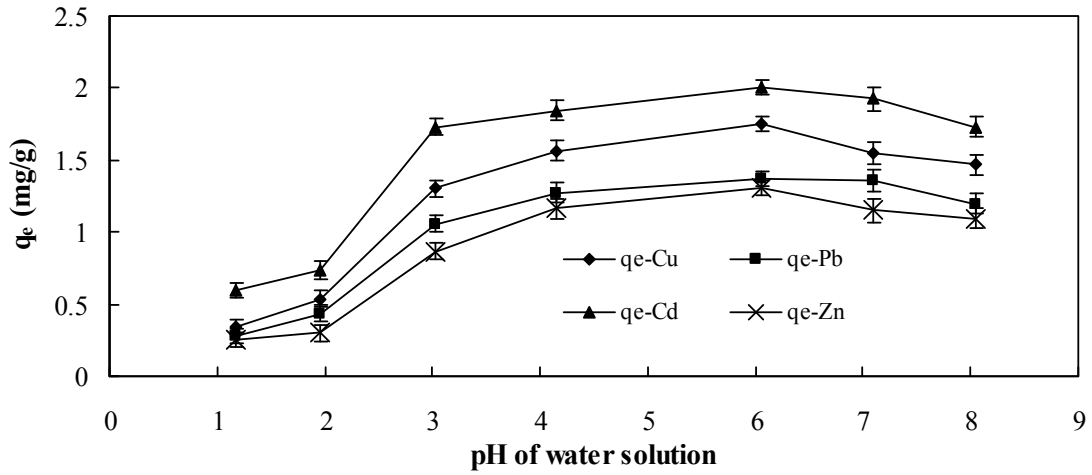


**Figure 6.3** Effect of of pH on the removal of Cu(II), Pb(II), Cd(II) and Zn(II) by BP

### 6.2.3.2 Particle sizes

The ground banana peels were graded with standard sieves to six particles sizes of 600, 420, 300, 150, 75 and < 75 μm. Banana peels (0.5g) from each graded sizes were added to six Erlenmeyer with 100 ml water containing 10 mg/l Cu(II), Pb(II), Cd(II) and Zn(II) concentration and shaken for 6 hrs at 120 rpm at pH of 6-6.5 (Chapter 3, section 3.3.2.6). Figure 6.4 indicates that the removal of Cu(II), Pb(II), Cd(II) and Zn(II) were

increased by decreasing the particle sizes. The percent removal of Cu(II), Pb(II), Cd(II) and Zn(II) increased from 1.49 to 1.92 mg/g, 1.19 to 1.53 mg/g, 1.81 to 2.33 mg/g, and 0.74 to 1.09 mg/g when decreasing particle sizes from 600µm to <75µm; respectively. This behaviour can be attributed to the effective surface area increasing as the particle size decreased and as a consequence of more adsorption (Ozacar et al., 2008; Şengil and Özacar, 2009; Yurtsever and Sengil, 2009).

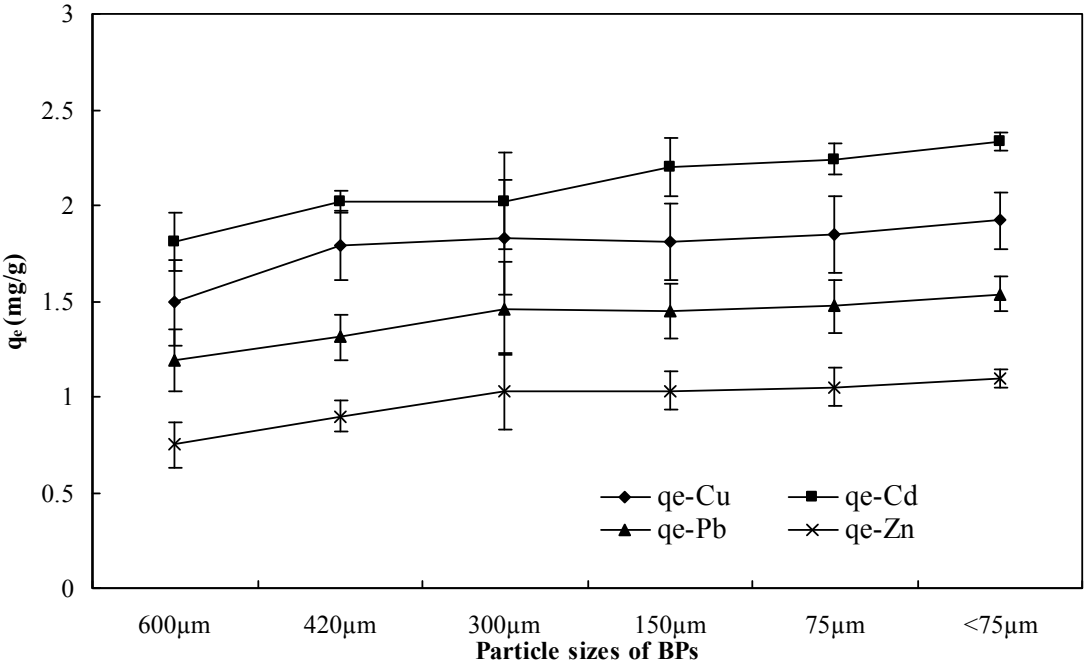


**Figure 6.4** Effect of particle sizes of BP on the removal of Cu(II), Pb(II), Cd(II) and Zn(II).

### 6.2.3.3 Doses

The effect of different doses on the removals of Cu(II), Pb(II), Cd(II) and Zn(II) were tested with 0.5, 1, 2, 5, 10, 20, 50 and 100 g/l doses in 10 mg/l metals concentrations at pH 6-6.5, rpm 120 and for 3 hours (Chapter 3, section3.3.2.2). The experimental results are shown in Figure 6.5. Dose dependent experiments showed that metals removal was low at lower doses and gradually increased with increasing in doses (Figure 6.5). Latter at higher doses, metals removals decreased. The highest Cu(II), Pb(II), Cd(II) and Zn(II) removal were 80, 82, 60 and 46% respectively with a dose of 5g/l**.** At higher doses, the partial aggregation among the available active binding sites retards the metals' adsorption onto banana peels (Anwar et al., 2010). The lack of active binding sites at lower doses retards the metals adsorption onto banana peel (Karthikeyan et al., 2007). Thus, 5g/l (0.5 g/100ml) of banana peels was chosen to use for other experiments.

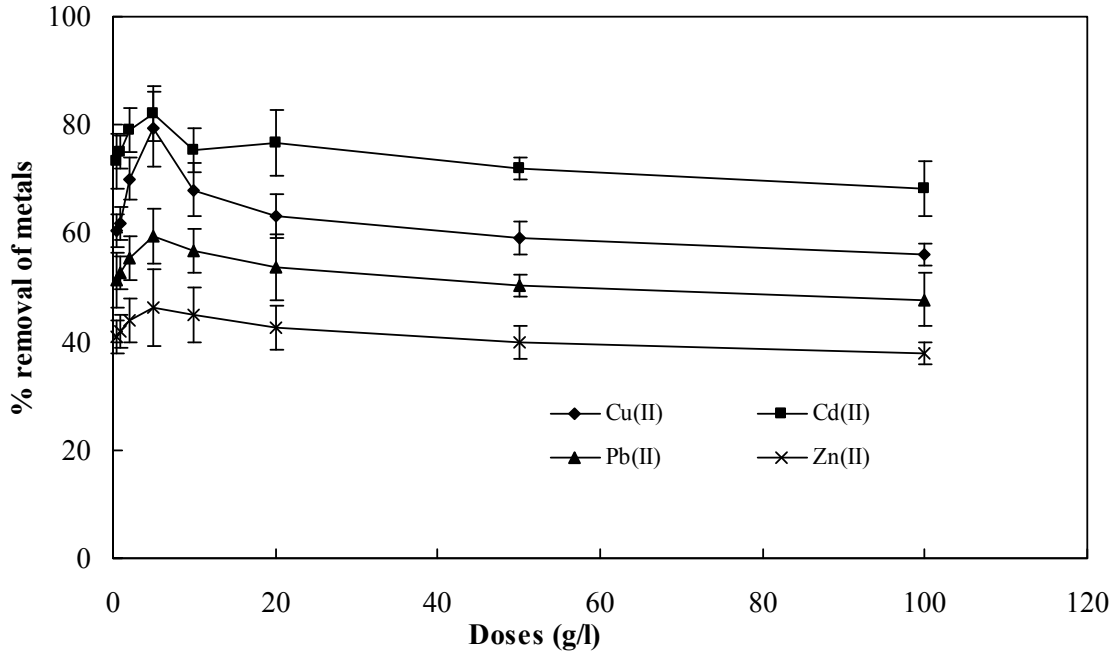


**Figure 6.5** Effect on the removal of Cu(II), Pb(II), Cd(II) and Zn(II) for the doses of banana peels

### 6.2.3.4 Contact Time

The effect of contact time on removal of Cu(II), Pb(II), Cd(II) and Zn(II) were tested with initial concentrations (Co) of 10, 20, 50, 100 and 200 mg/l with a dose of 5 g/l banana peels at 120 rpm and room temperature for 2 hours (Chapter 3, Section 3.3.2.4). The experimental results are plotted in Figure 6.6(a, b, c and d). The adsorption rate of copper, cadmium, lead and zinc were found to be relative faster than those reported for other biosorbents (Karthikeyan et al., 2007). The rate of Cu(II), Pb(II), Cd(II) and Zn(II) removal was very rapid during first 30 min, and thereafter, the rate of removal remained stable. There were no significant increases in adsorption after 50 mins. The Cu(II), Pb(II), Cd(II) and Zn(II) adsorption onto banana peels reached equilibrium after 1h. Higher removal capacity was found at higher initial concentrations of Cu(II), Pb(II), Cd(II) and Zn(II) (Figure 6.6). Initially, there were large numbers of vacant active binding sites available at the first phase of the experiment and large amount of metals ions were bound rapidly on banana peels at the first stage of adsorption. The binding sites shortly become limited, and the remaining vacant surface sites are difficult to be occupied by Cu(II), Pb(II), Cd(II) and Zn(II) ions due to the formation of repulsive forces between the metals ions on the solid surface and the liquid phase (Achak et al., 2009; Srivastava et al., 2006). Besides, the mesopores become saturated at the initial

stage of adsorption where the metal ions are adsorbed (Anwar et al., 2010). As a result, the driving force of mass transfer between liquid and solid phase in an aqueous adsorption system decreases with time elapse. Further, the metal ions have to pass through the deeper surface of the pores for binding and encounter much larger resistance which the slowing down of the adsorption during the later phase of adsorption (Srivastava et al., 2006).

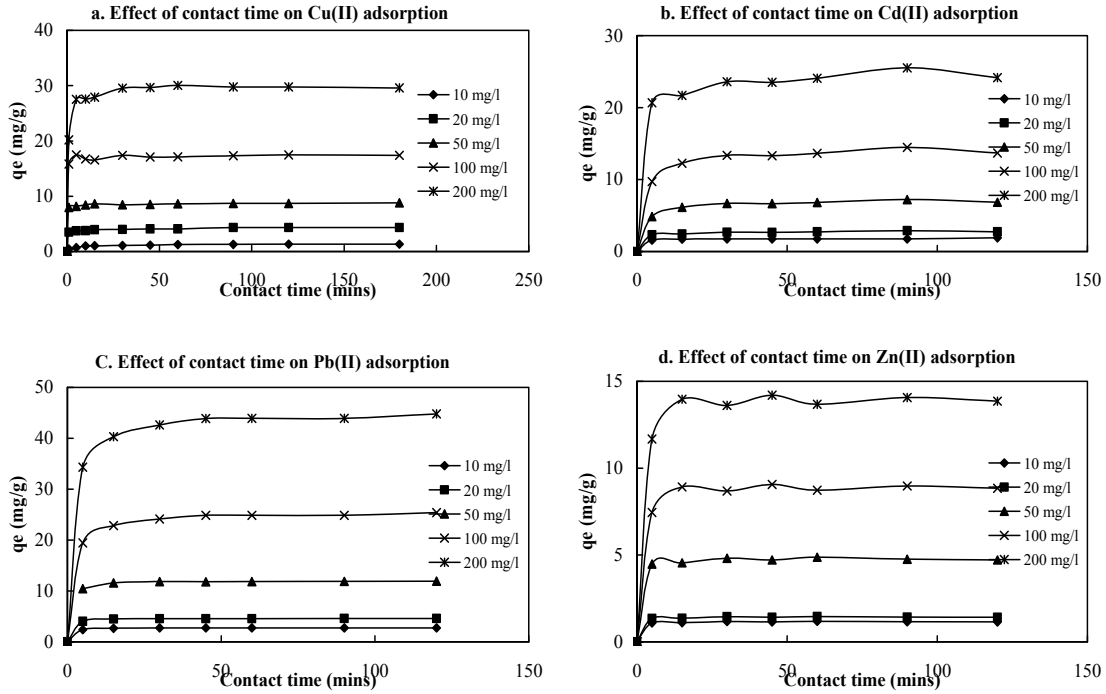


**Figure 6.6** Effect on the removal of Cu(II), Pb(II), Cd(II) and Zn(II) for the doses of banana peels

### 6.2.3.5 Shaking speed

The effect of shaking speed on adsorption of Cu(II), Pb(II), Cd(II) and Zn(II) was studied over the range of 30-200 rpm for 2h with 100 ml water containing 10 mg/l initial concentration and 0.5 g of banana peels (Chapter 3, Section 3.3.2.3). The results are plotted in Figure 6.7. Figure 6.7 indicates that the % removal of metals increased with increased shaking speed and reached the maximum at near 120 rpm. The maximum % removals were found to be 88% for Cd(II) at 110 rpm, 85% for Cu(II) at 120 rpm, 74% for Pb(II) at 120 rpm and 57% for Zn(II) at 120 rpm. At higher speeds, the % removal of metals again decreased. This shaking speed was employed for other experiments. At low and high speeds, the Cu(II), Pb(II), Cd(II) and Zn(II) removal were lower than optimum values (Anwar et al., 2010; Munaf et al., 2009; Qaiser et al., 2009). Low speed could not spread the particles properly in the water for providing active

binding sites for adsorption of metals ions. It resulted in accumulation of banana peels in the bottom of water and buried the active binding sites (Anwar et al., 2010). On the other hand, the high speed tests vigorously spread the particles of banana peels in the water and did not allow sufficient time to bind with copper ions (Reddy et al., 1999).

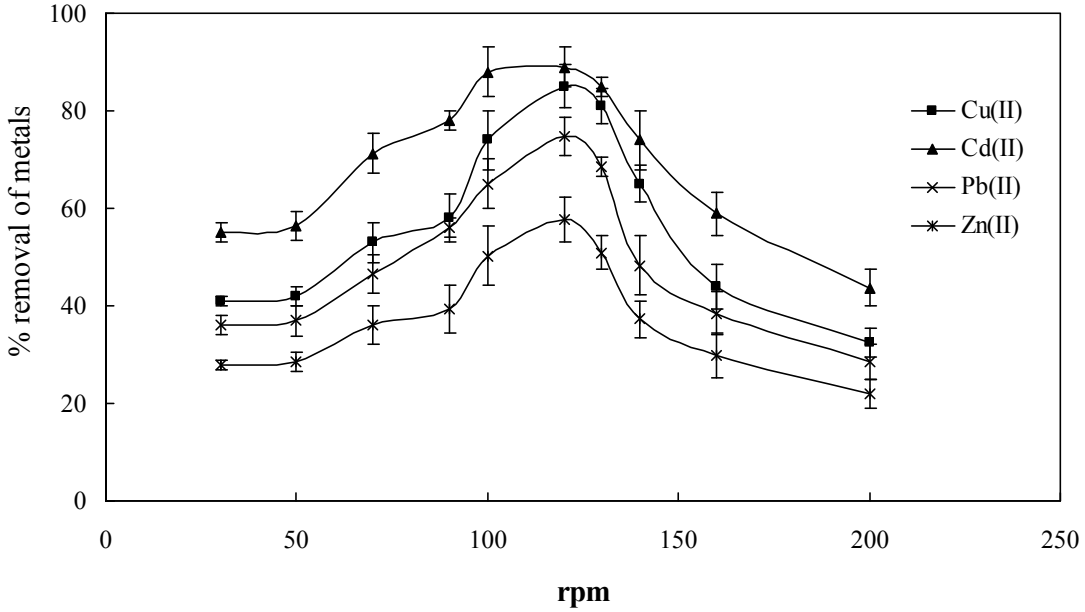


**Figure 6.7** Effect of shaking speed on removal of Cu(II), Pb(II), Cd(II) and Zn(II) (t: 24h; $C_o$: 10 mg/l; d: 5 g/l; T: 20°C; pH: 6-6.5)

### 6.2.3.6 Thermodynamic Parameters

Normally temperature stimulates the molecules, functional groups and surface morphology of the biosorbent and metals during adsorptions processes. To determine the thermal effects of Cu(II), Pb(II), Cd(II) and Zn(II) adsorption onto banana peels, temperature variation experiments were conducted at 30, 40, 50 and 70°C, with an initial Cu(II), Pb(II), Cd(II) and Zn(II) concentrations between 1-200 mg/l and with 0.5g per 100 ml water. The results show that the equilibrium adsorptions ($q_m$) were decreased with an increase in temperature (Table 6.2), suggesting that higher temperature helped to desorb the metals or retard the metals' ions adsorption onto banana peels. From the data the thermodynamic parameters such as Gibbs free energy (ΔG°), enthalpy change (ΔH°), and entropy change (ΔS°) were calculated. The magnitude of ΔG° (kJ/mol) was calculated using the following equation:

$$\Delta G^o = -RT\ln K_a \qquad (6.1)$$

where, R is universal gas constant, 0.008314 kJ/mol °K; T is absolute temperature (°K) and $K_a$ the sorption equilibrium constant from Langmuir and Temkin Isotherm and ΔH° (kJ/mol) and was calculated by the following equation:

$$\Delta H^o = \Delta G^o + T\Delta S^o \qquad (6.2)$$

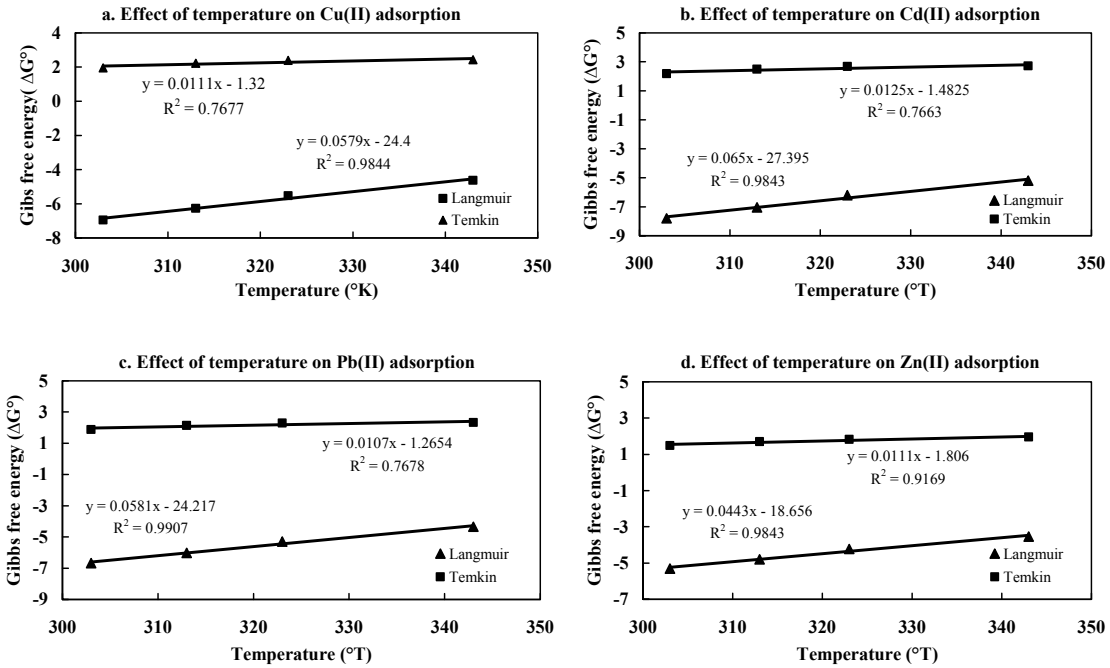


**Figure 6.8** Plots of Gibbs free energy (ΔG°) versus Temperature (°T) for Cu(II), Cd(II), Pb(II) and Zn(II) adsorption onto BP.

A plot of ΔG° versus T was found to be linear (Figure 6.8) and both values of ΔH° and ΔS° were calculated from the slope and intercept. The thermodynamic parameters calculated for both Langmuir isotherm and Temkin isotherm are shown in Table 6.2. The ΔG° values were opposite in nature (-ve and +ve) calculated from Langmuir and Temkin isotherm for the used four metals. The negative nature of ΔG° has confirmed that the adsorption process was spontaneous in nature (Dogar et al., 2010; Hristodor et al., 2010; Memon et al., 2008b). The values of ΔG° were decreased from -6.95 to -4.63 kJ/mol for Langmuir isotherm and increased from 1.95 to 2.43 kJ/mol for Temkin isotherm for Cu(II) adsorption at temperature increases from 30 to 70°C. Similarly, ΔG° was decreased from -7.799 to -5.195 kJ/mol for Cd(II), -6.667 to -4.441 for Pb(II) and -5.312 to -3.539 for Zn(II) adsorption from Langmuir isotherm. In addition, ΔG° was increased from 2.189 to 2.723 for Cd(II), 1.872 to 2.328 for Pb(II) and 1.492 to 1.855 for Zn(II) adsorption for Temkin isotherm. The positive value of ΔH° (for all metals

respectively : Table 6.2) indicated that the adsorption reaction was endothermic and had strong affinity of banana peels towards Cu(II), Pb(II), Cd(II) and Zn(II) ions. It also suggested that some structural changes occurred in metals' ions and banana peels (Gupta and Rastogi, 2008). In addition, the negative value of ΔS° (for all metals : Table 6.2) also suggested that the adsorption was enthalpy driven and spontaneous in nature (Baker et al., 2010; Fukuoka et al., 2010; Memon et al., 2008b; Murphy and Erkey, 1997).

**Table 6.2** Calculated value of thermodynamic parameters for the equilibrium adsorption of Cu(II), Pb(II), Cd(II) and Zn(II) onto banana peels

| Metals | Temp. °C | $q_m$ (mg/g) | ΔG°(kJ/mol) | | ΔH°(kJ/mol) | | ΔS° (kJ/mol.°K) | |
|---|---|---|---|---|---|---|---|---|
| | | | Langmuir | Temkin | Langmuir | Temkin | Langmuir | Temkin |
| Cu(II) | 30 | 4.082 | -6.945 | 1.950 | 0.057 | 0.011 | -24.40 | -1.32 |
| | 40 | 2.203 | -6.268 | 2.224 | | | | |
| | 50 | 0.710 | -5.521 | 2.391 | | | | |
| | 70 | 0.884 | -4.626 | 2.425 | | | | |
| Cd(II) | 30 | 4.584 | -7.799 | 2.189 | 0.065 | 0.125 | -27.4 | -1.483 |
| | 40 | 2.474 | -7.039 | 2.498 | | | | |
| | 50 | 0.797 | -6.200 | 2.685 | | | | |
| | 70 | 0.993 | -5.195 | 2.723 | | | | |
| Pb(II) | 30 | 3.918 | -6.667 | 1.872 | 0.058 | 0.0107 | -24.217 | -1.265 |
| | 40 | 2.115 | -6.017 | 2.135 | | | | |
| | 50 | 0.682 | -5.300 | 2.295 | | | | |
| | 70 | 0.848 | -4.441 | 2.328 | | | | |
| Zn(II) | 30 | 3.122 | -5.312 | 1.492 | 0.0443 | 0.0111 | -18.656 | -1.806 |
| | 40 | 1.685 | -4.795 | 1.701 | | | | |
| | 50 | 0.543 | -4.223 | 1.829 | | | | |
| | 70 | 0.676 | -3.539 | 1.855 | | | | |

## 6.2.4 Regeneration of banana peels

The regeneration of used biosorbent is decisive for repetitive use of biosorbent and decrease expenditure for the operation in water and wastewater treatment systems. Several observations literature reported that the adsorbed metals on biosorbent cannot be entirely reversible (Davis and Upadhyaya, 1996). Eight eluents such as tap water, milli-Q water, distilled water, 0.1N $H_2SO_4$, 0.1N HCl, 0.1N $HNO_3$, 0.1N NaOH and 0.1 N $CH_3COOH$ were used for Cu(II), Cd(II), Pb(II) and Zn(II) desorption from BP and showed in Figure 6.9. It is found from Figure 6.9 (a, b, c and d) that adsorbed metals are easily renewed by a small amount of 0.1N $H_2SO_4$. The maximum desorption were found to be 95% of Cu(II), 98% of Pb(II), 96% of Cd(II) and 82% of Zn(II) with 0.1 N $H_2SO_4$ from metal-loaded BP (0.5g). The other two acids such as 0.1 N HCl and 0.1 N $HNO_3$ demonstrated similar efficiencies for recovering the metals. In the desorption system $H^+$

released from the acids which replaced metal cation ($Cu^{2+}$, $Pb^{2+}$, $Cd^{2+}$ and $Zn^{2+}$) on the surface of the BP (Wang et al., 2008; Wei et al., 2009).

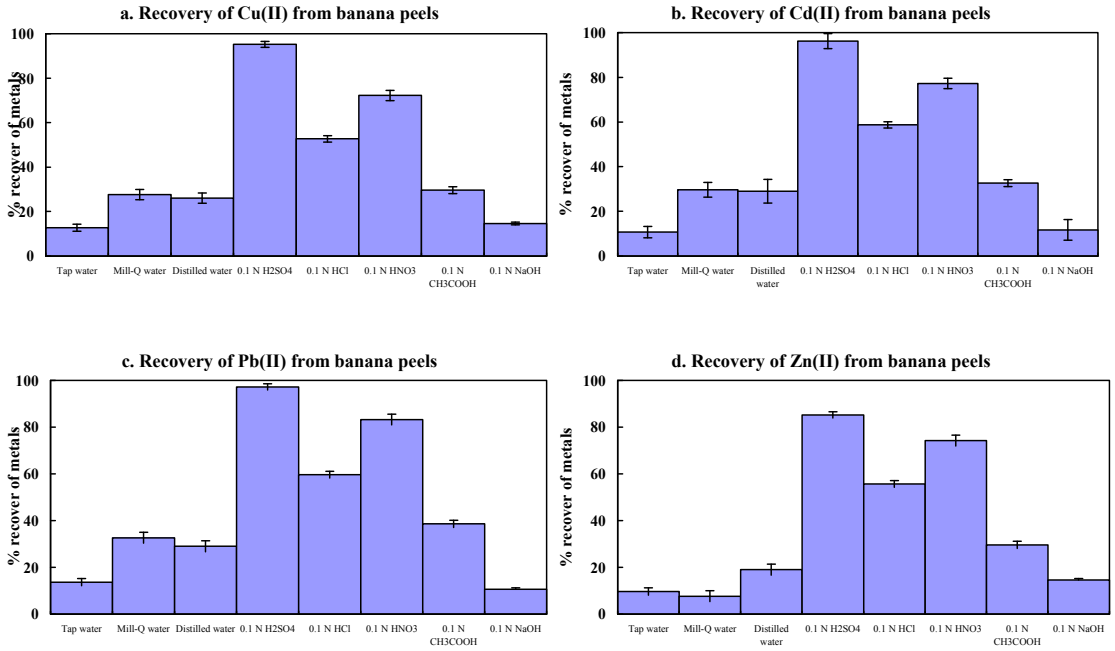


**Figure 6.9** Regeneration of banana peels from Cu(II), Pb(II), Cd(II) and Zn(II) from adsorption

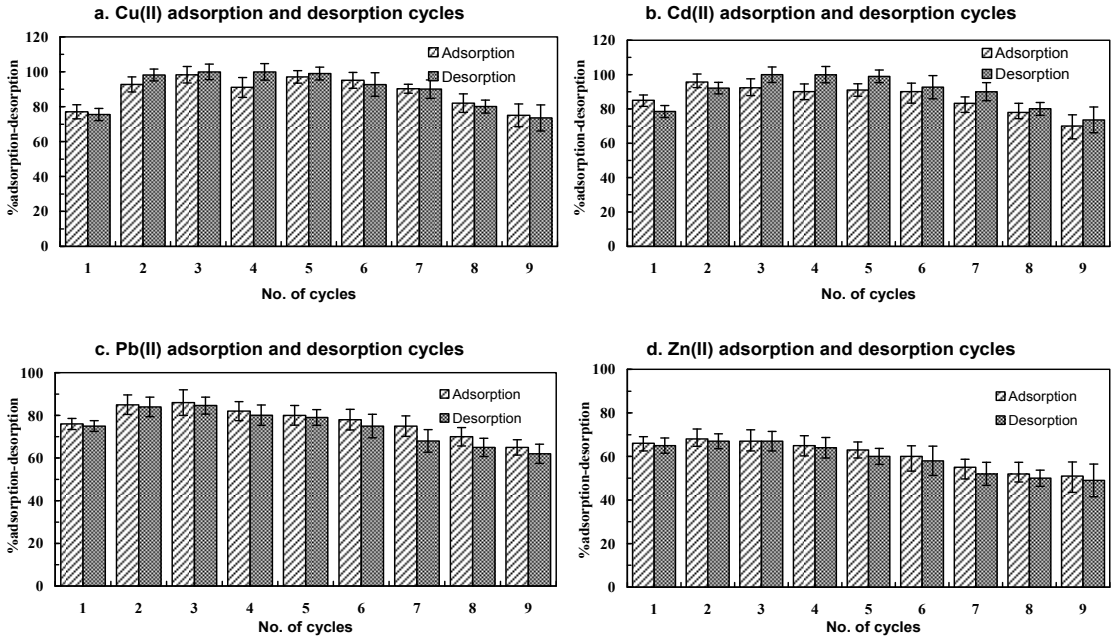


**Figure 6.10** Regeneration cycles of banana peels from Cu(II), Pb(II), Cd(II) and Zn(II) from adsorption

For exploring the repetitive uses of BP, the adsorption and desorption cycles were repeated nine times with best eluent 0.1N $H_2SO_4$ and the results are plotted in Figure 6.10 (a, b, c and d). After the first phase of the desorption process, both the adsorption and desorption efficiency were significantly increased. The acid solution might dissolve

the organic portion of banana peels and activate the binding site, and consequently help to increase the efficiency. It is presumed that acid works as a pre-treatment for BP which enhances efficiency. The regeneration efficiency for BP decreased gradually as the adsorption and desorption continue (Figure 6.10). It is predicted that consecutive acid dissolution imposes stresses on the BP surfaces and destroyed the binding sites. The regenerated BP could be used seven times with only minor loss of efficiency.

### 6.2.5 Modelling of adsorption and desorption isotherms

Adsorption, as well as desorption process, can be quantified by isotherm equations. These processes help to understand the adsorption and desorption behaviour of biosorbents. The equilibrium adsorption/desorption isotherms articulate the specific relation between the adsorbates and degree of adsorption/desorption onto the surfaces of biosorbent at equilibrium condition. At equilibrium isotherms provide fundamental physicochemical data for assessing the pertinence of biosorbents to use for adsorption/desorption processes for treatment systems. Adsorption/desorption equilibrium is normally considered through an isotherm equation. The parameters used to derive a mathematical equation are related to the surface properties and affinity of the biosorbent.

In the recent past, the fitness of an isotherm model with experimental data was typically measured based on $r^2$ value (correlation coefficient) obtained from linear regression. It is assumed that the isotherm giving a $r^2$ value nearer to unity was considered to be best fitted (Myers, 1990). To obtain a linear form from non-linear isotherm equations, a transformation is made which unconditionally modified their error structure and violated the error variance and normality of assumption (Myers, 1990; Ratkowski, 1990). Conversely, non-linear regression optimisation offers a more complex and mathematically precise method for determining isotherm parameters (Malek and Farooq, 1996). But an error judgment is still required to evaluate the fitness of the isotherm prediction to the experimental results (Foo and Hameed, 2010; McKay et al., 1999; Ofomaja, 2010).

In this study, five isotherm models were employed, namely Langmuir, SIPS, Redlich-Peterson, Radke-Prausnitz, and Brouers-Sotolongo and describe elements of the

adsorption/desorption of Cu(II), Cd(II), Pb(II) and Zn(II) onto banana peels (According to Chapter 3, section 3.3.4). Non-linear regression modelling was formulated for the five isotherms for the both adsorption and desorption processes. The fitness of the model with experimental data is judged by coefficient of determination ($R^2$) (Hossain et al., 2012b). Two non-linear error functions such as the residual root mean square error (RMSE) and the chi-square test ($\chi^2$) were examined (Hossain et al., 2012b; Montazer-Rahmati et al., 2011). The isotherm parameters were determined by minimising the respective error function across the concentration range studied using MATLAB programming (Appendices I). The smaller RMSE value indicates the better model fitting. The size of the value of $\chi^2$ indicates the similarity of model with the experimental data (Ho et al., 2000; Montazer-Rahmati et al., 2011). The model predictions and experimental data are plotted in Figure 6.11 for Cu(II), Figure 6.12 for Cd(II), Figure 6.13 for Pb(II) and Figure 6.14 for Zn(II). The predicted, and experimental values of parameters are tabulated in Table 6.3 for Cu(II), Table 6.4 for Cd(II), Table 6.5 for Pb(II) and Table 6.6 for Zn(II).

#### 6.2.5.1 Langmuir isotherm

Langmuir theory explains the monolayer coverage of adsorbate (i.e. metals) over a homogenous biosorbent surface. The isotherm is based on the assumption that adsorption takes place at specific homogenous sites within the biosorbent (Langmuir, 1918). Once an adsorbate molecule occupies a site, no further adsorption can take place at that site. Thus, the equilibrium value can be achieved, and the saturated monolayer curve can be obtained from the model equation. This isotherm was applied to quantify and contrast the performance of adsorption and desorption of Cu(II), Cd(II), Pb(II) and Zn(II) onto banana peels. The condition assumed similarly for the desorption process. The mathematical equation of the model is shown inside each table (Table 6.3 for Cu(II), Table 6.4 for Cd(II), Table 6.5 for Pb(II) and Table 6.6 for Zn(II)).

The maximum metal adsorption and desorption were estimated from the Langmuir model where they could not be reached in the experiments. That is to say, the model predictions for maximum adsorption capacities are more than just the experimental ones. The adsorption process was followed closely for the Langmuir isotherm as $R^2$ values are 0.995, 0.989, 0.998 for Cu(II) biosorption, 0.997, 0.997 and 0.997 for Cd(II) biosorption, 0.997, 0.997 and 0.997 for Pb(II) biosorption, and 0.993, 0.993 and 0.993

for Zn(II) biosorption onto 0.05, 0.5 and 1g doses; respectively. In desorption processes 0.993, 0.975 and 1.00 for Cu(II) desorption; 0.997, 0.989 and 0.996 for Cd(II) desorption; 0.999, 0.992 and 0.998 for Pb(II) desorption; and, 0.999, 0.999 and 0.999 for Zn(II) desorption from 0.05, 0.5 and 1g doses; respectively. It was found from $R^2$ values the Cd(II) and Pb(II) biosorption has posed higher fitness with model than Cu(II) and Zn(II) biosorption. So, the metals preference order for banana peels is Cd(II) = Pb(II) > Zn(II) > Cu(II). On the other hand, desorption data showed higher agreement with the Langmuir model. It is also noted that the desorption did not follow the curve-linear, but it followed the almost straight line-linear (Figure 6.11 for Cu(II), Figure 6.12 for Cd(II), Figure 6.13 for Pb(II) and Figure 6.14 for Zn(II).

**Table 6.3** Parameters of isotherm models for adsorption and desorption of Cu(II) onto and from banana peels

| Isotherm models | Para-meters | Adsorption | | | Desorption | | |
|---|---|---|---|---|---|---|---|
| | | Doses | | | Doses | | |
| | | **0.05g** | **0.5g** | **1g** | **0.05g** | **0.5g** | **1g** |
| Experimental | $q_m$(mg/g) | 240.6 | 44.14 | 19.27 | 78.105 | 13.472 | 6.72 |
| 1. Langmuir $q_e = \frac{q_m K_L C_e}{1 + K_L C_e}$ | $q_m$(mg/g) | 98.30 | 58.90 | 20.37 | 337.05 | 657.81 | 49.511 |
| | $K_L$ (l/g) | 0.020 | 0.013 | 0.016 | 0.001 | 0.000 | 0.001 |
| | $R_L$ | 0.22-0.99 | 0.19-0.99 | 0.16-0.99 | 0.94-0.99 | 0.97-1 | 0.87-0.99 |
| | $R^2$ | 0.995 | 0.989 | 0.998 | 0.993 | 0.975 | 1.000 |
| | Δ°G | -9.535 | -10.54 | -10.05 | -18.09 | -21.88 | -14.85 |
| | $\chi^2$ | 7.827 | 0.240 | 0.036 | 0.024 | 0.0245 | 4E-06 |
| | RMSE | 0.0003 | 1.914 | 0.323 | 0.937 | 0.9226 | 0.038 |
| 2. SIPS $q_e = \frac{K_s C_e^{\beta_s}}{1 + \alpha_s C_e^{\beta_s}}$ | $K_s$(l/g) | 01.794 | 0.317 | 0.440 | 0.816 | 0.190 | 0.100 |
| | $\alpha_S$ (l/mg) | 0.007 | 0.006 | 0.020 | -0.001 | -0.028 | -0.003 |
| | $\beta_S$ | 1.370 | 1.251 | 0.912 | 1.00 | 0.610 | 0.916 |
| | $R^2$ | 0.992 | 0.991 | 0.998 | 0.961 | 0.991 | 1.000 |
| | $\chi^2$ | 63.695 | 11.447 | 0.659 | 9.833 | 1.747 | 0.0167 |
| | RSME | 09.926 | 01.974 | 0.369 | 5.786 | 0.648 | 0.0297 |
| 3.Redlich-Peterson $q_e = \frac{K_{RP} C_e}{1 + \alpha_{RP} C_e^{\beta}}$ | $K_{RP}$ (l/g) | 2.860 | 0.778 | 0.344 | 0.054 | 0.891 | 0.194 |
| | $\alpha_{RP}$(l/mg) | 2.150 | 0.013 | 0.020 | -0.904 | 11.478 | 0.939 |
| | β | 0.001 | 1.00 | 0.974 | 0.009 | 0.001 | 0.001 |
| | $R^2$ | 0.989 | 0.989 | 0.998 | 0.963 | 0.976 | 1.000 |
| | $\chi^2$ | 12.635 | 4.977 | 1.362 | 8.188 | 5.199 | 6E-17 |
| | RSME | 6.723 | 1.892 | 0.406 | 5.225 | 0.671 | 5E-09 |
| 4.Radke-Prausnitz $q_e = \frac{\alpha_R r_R C_e^{\beta_R}}{\alpha_R + r_R C_e^{\beta_R - 1}}$ | $\alpha_R$ (l/g) | 4.582 | 0.525 | 0.344 | 0.881 | 0.071 | 0.100 |
| | $r_R$ (l/mg) | 1050. 8 | 1050.9 | 17.394 | 1050.78 | 1050.8 | 1050.78 |
| | $\beta_R$ | -0.219 | -0.496 | 0.027 | 0000 | 1.000 | 0.864 |
| | $R^2$ | 0.993 | 0.995 | 0.998 | 0.996 | 0.976 | 1.000 |
| | $\chi^2$ | 13.795 | 7.553 | 1.361 | 26.865 | 5.1990. | 5E-09 |
| | RSME | 10.007 | 1.640 | 0.406 | 9.570 | 671 | 3E-05 |
| 5.Brouers-Sotolongo $q_e = q_m[1 - \exp(-K_{BS}(C_e)^{\alpha}]$ | $q_m$(mg/g) | 247.50 | 46.310 | 17.88 | 247.034 | 247.02 | 247.026 |
| | $K_{BS}$(l/mg) | 0.020 | 0.014 | 0.031 | 0.003 | 0.000 | 0.000 |
| | α | 0.978 | 1.00 | 0.790 | 1.067 | 1.273 | 1.0094 |
| | $R^2$ | 0.993 | 0.994 | 0.998 | 0.759 | 0.986 | 1.000 |
| | $\chi^2$ | 11.967 | 5.71 | 0.301 | 27.249 | 21.363 | 0.0003 |
| | RSME | 10.118 | 1.6688 | 0.3162 | 9.611 | 0.5355 | 0.0042 |

The maximum adsorption capacity ($q_m$) onto banana peels were 298.30, 58.90, 20.37 mg/g for Cu(II) biosorption; 76.113, 35.667 and 47.972 mg/g for Cd(II) biosorption; 320.729, 117.311 and 158.370 mg/g for Pb(II) biosorption; and 70.502, 38.441 and 51.896 mg/g for Zn(II) biosorption onto 0.05, 0.5 and 1g doses; respectively. It is noticeable that the model predicted $q_m$ values are higher than the experimental values for all four metals (Table 6.3 for Cu(II), Table 6.4 for Cd(II), Table 6.5 for Pb(II) and Table 6.6 for Zn(II)). Desorption processes showed much higher values of $q_m$ than experiments. It might be said that the higher predictions are because the desorption process follows linear and hysteresis processes. So, the non-linear analysis could not predict the real values.

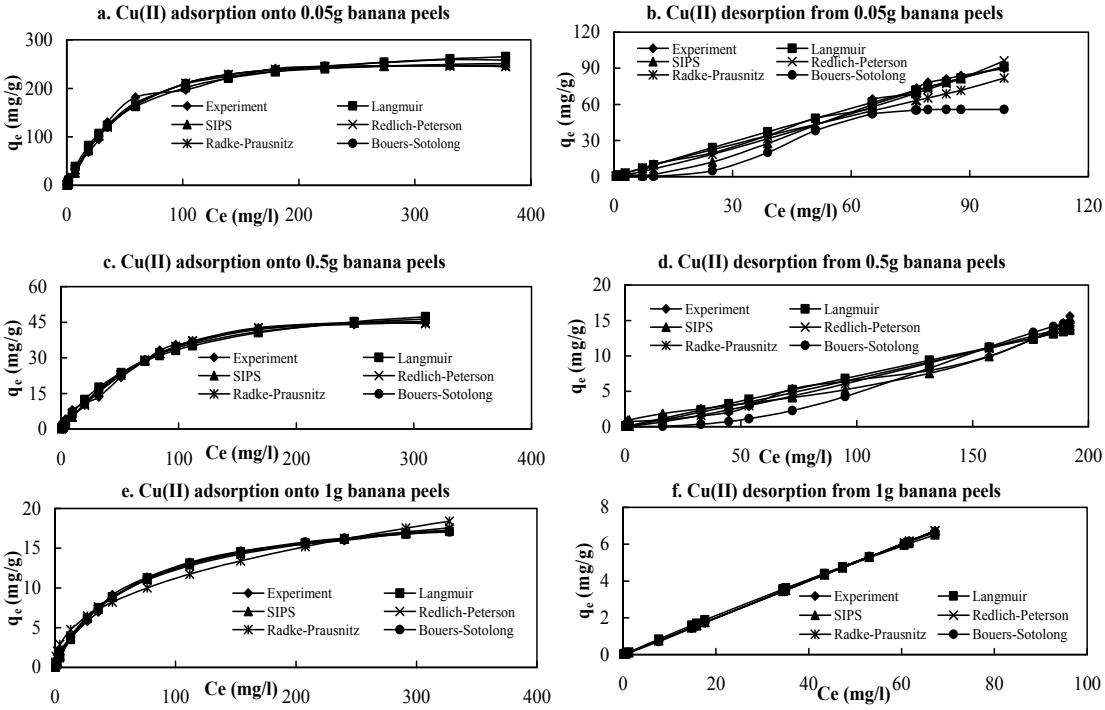


**Figure 6.11** Isotherm modelling of adsorption and desorption of Cu(II) onto and from banana peels ($C_o$: 1-500 mg/l; d: 0.05-1 g; t: 3h: pH: 6-6.5; rpm: 120; T: 20°C)

The constant $K_L$ represents the affinity between the banana peels and metals ions (Cu(II), Cd(II), Pb(II) and Zn(II)). Lower values of $K_L$ (<1) for both adsorption and desorption process (Table 6.3 for Cu(II), Table 6.4 for Cd(II), Table 6.5 for Pb(II) and Table 6.6 for Zn(II)), revealed that affinity among the BP and metals ions are weak (Davis et al., 2003). Significantly low RMSE and chi-square values were observed in the case of Langmuir model for both adsorption and desorption equilibrium. It was observed that the Langmuir model adequately describes the adsorption and desorption processes.

Separation factor ($R_L$) could predict the favourability of adsorption and desorption processes (Torab-Mostaedi et al., 2013). $R_L$ was calculated from Langmuir isotherm based equation by the flowing equation (Hanif et al., 2007):

$$R_L = \frac{1}{1 + K_L C_o} \tag{4.5}$$

where $K_L$ (l/mg) refers to the Langmuir constant and $C_o$ denotes the adsorbate initial concentration (mg/l). In this context, lower $R_L$ values reflect adsorption that is more favourable. At a level, $R_L$ value indicates the adsorption nature to be either favourable or unfavourable.

$R_L > 1$ = unfavourable isotherm.

$R_L = 1$ = linear isotherm.

$R_L = 0$ =irreversible isotherm.

$0<R_L<1$ = favourable isotherm.

The calculated separation factor ($R_L$) are between 0.22 to 0.99, 0.19 to 0.99, and 0.16 to 0.98 for 0.05, 0.5 and 1 g doses respectively for Cu(II) adsorption, when Co were 1 to 500 mg/l. In case of desorption, the $R_L$ values are between 0.94 to 0.99, 0.97 to 1, and 0.87 to 0.99 for 0.05, 0.5 and 1 g doses respectively (Table 6.3). When it is compared the values of $R_L$ with condition, is found that the Cu(II) ions adsorption onto and desorption from BP are favourable. The values of $R_L$ are between 0.03 to 0.99, 0.04 to 0.99 and 0.03 to 0.9 for Cd(II) adsorption and, between 0.83 to 0.99, 0.88 to 0.99 and 0.89 to 0.99 for desorption for 0.05, 0.5 and 1 g doses, respectively when the Co were between 1 to 500 mg/l (Table 6.4). Cd(II) ions adsorption and desorption are also favourable. Similar to the Cd(II) adsorption and desorption, the values of $R_L$ are between 0.21 to 0.99, 0.21 to 0.96 and 0.21 to 0.99 for Pb(II) adsorption and, are between 0.92 to 0.99, 0.92 to 0.99 and 0.85 to 0.99 for Pb(II) desorption for 0.05, 0.5 and 1 g doses, respectively when the Co were between 1 and 500 mg/l (Table 6.5). It is also disclosed that the pB(II) ions adsorption and desorption on BP are favourable. The adsorption and desorption isotherms were also favourable for Zn(II) ions on BP, and the RL factors were also found between 0.04 to 0.96 for adsorption and 0.83 to 0.99 for desorption for all three doses (Table 6.6).

#### 6.2.5.2 SIPS isotherm

SIPS isotherm is an empirical and hybrid equation which was derived from the combination of Langmuir and Freundlich isotherms (Volesky, 2003). The key

suitability of the isotherm is that it has the ability to fit with a wide variety of equilibrium data when both Langmuir and Freundlich models do not fit well (Ismadji and Bhatia, 2001). At low metals concentrations, it changes to the Freundlich isotherm and at high metals concentrations, it calculates a monolayer sorption capacity characteristic like Langmuir isotherm. This model was fitted with experimental data for both adsorption and desorption processes of Cu(II), Cd(II), Pb(II) and Zn(II) onto banana peels. The predictions are plotted in Figure 6.11 for Cu(II), Figure 6.12 for Cd(II), Figure 6.13 for Pb(II) and Figure 6.14 for Zn(II). The models parameters are tabulated in Table 6.3 for Cu(II), Table 6.4 for Cd(II), Table 6.5 for Pb(II) and Table 6.6 for Zn(II).

**Table 6.4** Parameters of isotherm models for adsorption and desorption of Cd(II) onto and from banana peels

| Isotherm models | Para-meters | Adsorption | | | Desorption | | |
|---|---|---|---|---|---|---|---|
| | | Doses | | | Doses | | |
| | | **0.05g** | **0.5g** | **1g** | **0.05g** | **0.5g** | **1g** |
| Experimental | $q_m$(mg/g) | 74.470 | 35.15 | 50.459 | 14.891 | 3.866 | 5.513 |
| 1. Langmuir | $q_m$(mg/g) | 76.113 | 35.667 | 47.972 | 84.905 | 35.365 | 56.289 |
| $q_e = \frac{q_m K_L C_e}{1 + K_L C_e}$ | $K_L$ (l/g) | 0.120 | 0.084 | 0.110 | 0.004 | 0.004 | 0.003 |
| | $R_L$ | 0.03-0.99 | 0.04-0.99 | 0.03-0.99 | 0.83-0.99 | 0.88-0.99 | 0.89-0.99 |
| | $R^2$ | 0.997 | 0.997 | 0.997 | 0.997 | 0.989 | 0.996 |
| | Δ°G | -5.162 | -6.031 | -5.378 | -13.75 | -13.5 | -14.39 |
| | $\chi^2$ | 0.095 | 0.045 | 0.060 | 0.003 | 1.396 | 0.123 |
| | RMSE | 1.739 | 0.815 | 1.096 | 0.351 | 0.166 | 0.163 |
| 2. SIPS | $K_s$(l/g) | 11.892 | 4.151 | 6.965 | 0.387 | 0.265 | 0.063 |
| $q_e = \frac{K_s C_e^{\beta_s}}{1 + \alpha_s C_e^{\beta_s}}$ | $\alpha_S$ (l/mg) | 0.148 | 0.111 | 0.138 | 0.000 | -0.098 | 0.007 |
| | $\beta_S$ | 0.826 | 0.825 | 0.826 | 0.892 | 0.522 | 1.453 |
| | $R^2$ | 0.999 | 0.999 | 0.999 | 0.997 | 0.992 | 0.994 |
| | $\chi^2$ | 2.060 | 0.965 | 1.299 | 0.774 | 0.839 | 0.432 |
| | RSME | 1.466 | 0.687 | 0.924 | 0.442 | 0.167 | 0.235 |
| 3.Redlich-Peterson | $K_{RP}$ (l/g) | 10.966 | 3.599 | 6.321 | 12.388 | 1.308 | 6.536 |
| $q_e = \frac{K_{RP} C_e}{1 + \alpha_{RP} C_e^{\beta}}$ | $\alpha_{RP}$(l/mg) | 0.191 | 0.137 | 0.175 | 31.131 | 8.252 | 33.404 |
| | β | 0.946 | 0.945 | 0.946 | 0.109 | 0.042 | 0.089 |
| | $R^2$ | 0.998 | 0.998 | 0.998 | 0.997 | 0.990 | 0.996 |
| | $\chi^2$ | 4.935 | 2.312 | 3.114 | 0.776 | 5.125 | 0.166 |
| | RSME | 1.746 | 0.819 | 1.101 | 0.442 | 0.201 | 0.212 |
| 4.Radke-Prausnitz | $\alpha_R$ (l/g) | 19.046 | 3.596 | 6.322 | 4.758 | 4.740 | 4.728 |
| $q_e = \frac{\alpha_R r_R C_e^{\beta_R}}{\alpha_R + r_R C_e^{\beta_R - 1}}$ | $r_R$ (l/mg) | 11.264 | 26.398 | 36.027 | 0.418 | 0.146 | 0.198 |
| | $\beta_R$ | 0.357 | 0.054 | 0.054 | 0.886 | 0.960 | 0.909 |
| | $R^2$ | 0.908 | 0.998 | 0.998 | 0.997 | 0.990 | 0.996 |
| | $\chi^2$ | 47.653 | 2.314 | 3.113 | 0.776 | 5.108 | 0.165 |
| | RSME | 12.329 | 0.818 | 1.101 | 0.442 | 0.209 | 0.212 |
| 5.Brouers-Sotolongo | $q_m$(mg/g) | 73.717 | 34.544 | 46.462 | 41.951 | 39.554 | 41.977 |
| $q_e = q_m[1 - \exp(-K_{BS}(C_e)^{\alpha}]$ | $K_{BS}$(l/mg) | 0.170 | 0.135 | 0.161 | 0.007 | 0.035 | 0.004 |
| | α | 0.637 | 0.637 | 0.638 | 1.009 | 0.989 | 0.952 |
| | $R^2$ | 0.998 | 0.998 | 0.998 | 0.997 | 0.990 | 0.996 |
| | $\chi^2$ | 2.978 | 1.395 | 1.877 | 0.957 | 5.679 | 0.140 |
| | RSME | 1.663 | 0.779 | 1.048 | 0.462 | 0.203 | 0.208 |

This model was the best fitted model for the both adsorption and the desorption data of Cu(II), Cd(II), Pb(II) and Zn(II). The $R^2$ values were 0.992, 0.991 and 0.998 for Cu(II) biosorption; 0.999, 0.999 and 0.999 for Cd(II) biosorption; 0.999, 0.999 and 0.999 for Pb(II) biosorption and, 0.998, 0.998 and 0.998 Zn(II) biosorption onto 0.05, 0.5 and 1 g doses of BP, respectively. Likewise, the biosorption, desorption processes also showed higher fitness with model because the $R^2$ values lie between 0.991 and 1.00 for all fours metals and all three doses. The small RMSE and $\chi^2$ values also prove that this model perfectly describes the equilibrium adsorption. The values of Sips model isotherm constant ($K_s$; l/g) which are similar to maximum adsorption/desorption capacity ($q_m$), are found to be much lower than the experimental and Langmuir model prediction for adsorption and desorption for the doses of 0.05, 0.5 and 1g. The calculated values of exponent, $\beta_S$ lies near unity for both adsorption and desorption of Cu(II), Cd(II), Pb(II) and Zn(II) onto the three doses. It signifies that metals adsorption and desorption are more in the heterogeneous surfaces than monolayer surfaces of BP (Blázquez et al., 2011; Cayllahua and Torem, 2010; Kosasih et al., 2010).

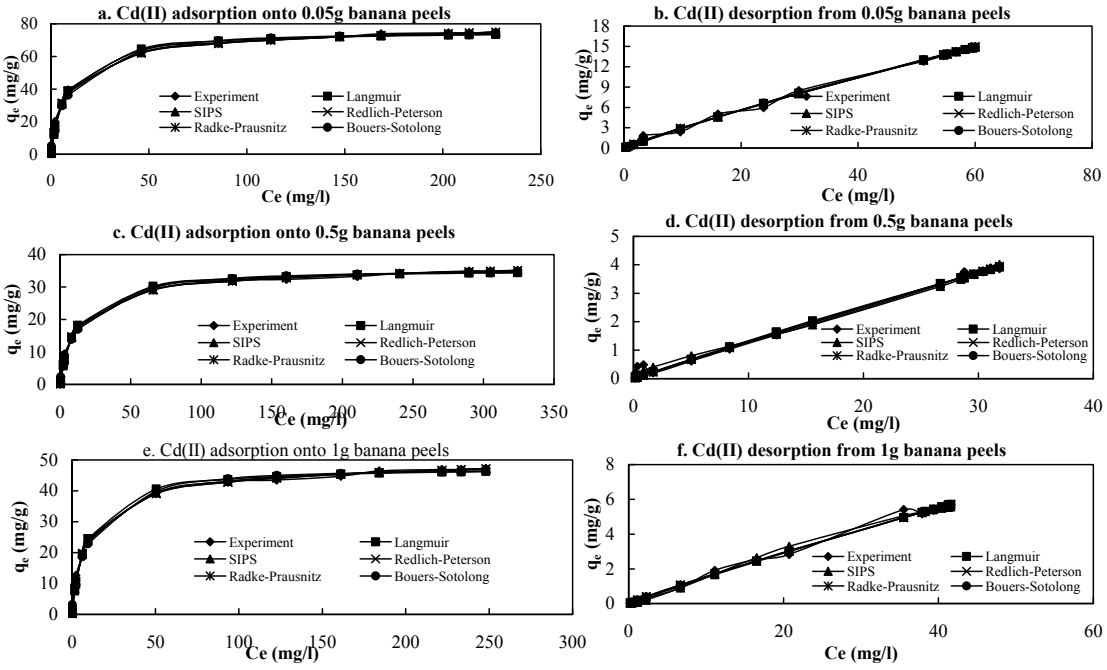


**Figure 6.12** Isotherm modelling of adsorption and desorption of Cd(II) onto and from banana peels ($C_o$: 1-500 mg/l; d: 0.05-1 g; t: 3h: pH: 6-6.5; rpm: 120; T: 20°C)

### 6.2.5.3 Redlich-Peterson isotherm

The Redlich-Peterson isotherm model is also a hybrid equation which incorporates the features of the Langmuir and Freundlich isotherms (Aksu, 2002; Li et al., 2010; Yao et

al., 2010). This model was used for prediction of isotherm constants for both adsorption and desorption of Cu(II), Cd(II), Pb(II) and Zn(II) onto and from banana peels. The model prediction and isotherm constant are plotted in Figure 6.11 for Cu(II), Figure 6.12 for Cd(II), Figure 6.13 for Pb(II) and Figure 6.14 for Zn(II). The models' parameters are tabulated in Table 6.3 for Cu(II), Table 6.4 for Cd(II), Table 6.5 for Pb(II) and Table 6.6 for Zn(II).

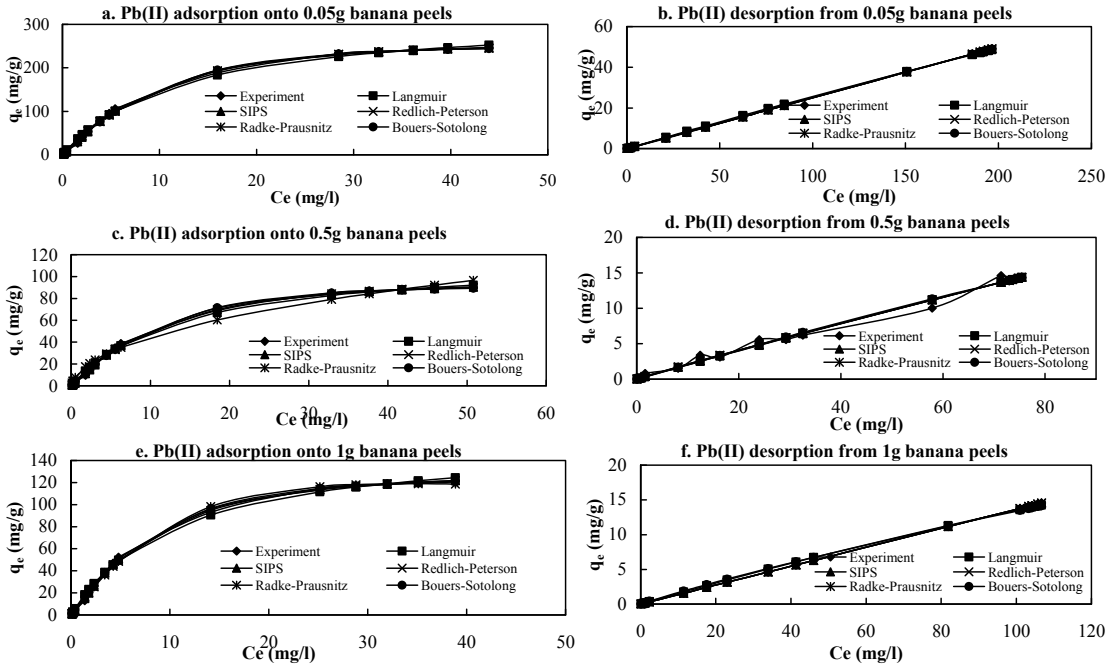


**Figure 6.13** Isotherm modelling of adsorption and desorption of Pb(II) onto and from banana peels ($C_o$: 1-500 mg/l; d: 0.05-1 g; t: 3h: pH: 6-6.5; rpm: 120; T: 20°C)

Similar to SIPS model, this model showed better fitness with the experimental data for the both adsorption and desorption processes. The $R^2$ values are 0.989, 0.989 and 0.998 for Cu(II) biosorption; 0.998, 0.998 and 0.998 for Cd(II) biosorption; 0.998, 0.998 and 0.998 for Pb(II) biosorption; and, 0.996, 0.996 and 0.996 for Zn(II) biosorption for the doses of 0.05, 0.5 and 1 g BP; respectively. Among the fitness, the Cd(II) biosorption showed the best fitted data while Cu(II) was the lowest among the four metals. In the other words, the BP preferences order were Cd(II)>Pb(II)>Zn(II)>Cu(II). The considerably lower values of RMSE and $\chi^2$ also support the above decision. The calculated values of the Redlich-Peterson model isotherm constant, $K_{RP}$ (l/g), which shows as maximum adsorption or desorption capacity, are lower in magnitude (Table 2) than the maximum adsorption or desorption capacity ($q_m$) found from experiment and Langmuir model predictions for all four metals (Table 6.3 for Cu(II), Table 6.4 for

Cd(II), Table 6.5 for Pb(II) and Table 6.6 for Zn(II)). This was not the case with adsorption as desorption posed higher fitness with the experimental data for Cu(II), Cd(II), Pb(II) and Zn(II). The exponent ($\beta_{RP}$) values lies between 0 and 2 (Table 6.5) for all three doses and both adsorption and desorption processes. If β= 1, the adsorption/desorption process follows the Langmuir isotherm and if β = 0, the process follows the Henry's law. In this study, the calculated values of $\beta_{RP}$ were not 0 and 2. It is shown that mixed values revealed that the adsorption/desorption processes follows neither Langmuir nor Henry's law. This is also proved by Sips model predictions. It can thence be presumed that banana peels have heterogeneous surfaces to biosorption.

**Table 6.5** Parameters of isotherm models for adsorption and desorption of Pb(II) onto and from banana peels

| Isotherm models | Para-meters | Adsorption | | | Desorption | | |
|---|---|---|---|---|---|---|---|
| | | Doses | | | Doses | | |
| | | **0.05g** | **0.5g** | **1g** | **0.05g** | **0.5g** | **1g** |
| Experimental | $q_m$(mg/g) | 239.703 | 89.84 | 120.096 | 21.185 | 14.028 | 14.203 |
| 1. Langmuir $q_e = \frac{q_m K_L C_e}{1 + K_L C_e}$ | $q_m$(mg/g) | 320.729 | 117.311 | 158.370 | 630.963 | 203.059 | 95.644 |
| | $K_L$ (l/g) | 0.084 | 0.072 | 0.095 | 0.0004 | 0.001 | 0.002 |
| | $R_L$ | 0.21-0.99 | 0.21-0.96 | 0.21-0.96 | 0.92-0.99 | 0.92-0.99 | 0.85-0.99 |
| | $R^2$ | 0.997 | 0.997 | 0.997 | 0.999 | 0.992 | 0.998 |
| | Δ°G | -6.043 | -6.396 | -5.744 | -18.91 | -16.8 | -15.62 |
| | $\chi^2$ | 10.912 | 3.991 | 5.388 | 0.184 | 1.315 | 0.217 |
| | RMSE | 5.911 | 2.162 | 2.919 | 0.479 | 0.536 | 0.286 |
| 2. SIPS $q_e = \frac{K_s C_e^{\beta_s}}{1 + \alpha_s C_e^{\beta_s}}$ | $K_s$(l/g) | 18.819 | 5.711 | 10.887 | 0.230 | 0.220 | 0.136 |
| | $\alpha_S$ (l/mg) | 0.069 | 0.057 | 0.080 | 0.0002 | 0.000 | 0.000 |
| | $\beta_S$ | 1.288 | 1.288 | 1.288 | 1.023 | 0.969 | 1.006 |
| | $R^2$ | 0.999 | 0.999 | 0.999 | 1.000 | 0.992 | 1.000 |
| | $\chi^2$ | 13.914 | 5.089 | 6.869 | 0.010 | 1.038 | 6E-12 |
| | RSME | 3.028 | 1.108 | 1.495 | 0.056 | 0.459 | 2E-06 |
| 3.Redlich-Peterson $q_e = \frac{K_{RP} C_e}{1 + \alpha_{RP} C_e^{\beta}}$ | $K_{RP}$ (l/g) | 22.786 | 7.399 | 13.017 | 8.503 | 8.190 | 4.766 |
| | $\alpha_{RP}$(l/mg) | 0.029 | 0.031 | 0.040 | 33.013 | 33.088 | 33.952 |
| | β | 1.236 | 1.181 | 1.194 | -1.4E-05 | 0.055 | -9.5E-07 |
| | $R^2$ | 0.998 | 0.998 | 0.998 | 1.000 | 0.993 | 1.000 |
| | $\chi^2$ | 14.259 | 5.431 | 7.286 | 4E-08 | 0.890 | 2E-10 |
| | RSME | 5.274 | 2.012 | 2.679 | 0.0002 | 0.439 | 1E-05 |
| 4.Radke-Prausnitz $q_e = \frac{\alpha_R r_R C_e^{\beta_R}}{\alpha_R + r_R C_e^{\beta_R - 1}}$ | $\alpha_R$ (l/g) | 22.890 | 33.140 | 11.533 | 4.728 | 4.728 | 4.715 |
| | $r_R$ (l/mg) | 758.004 | 19.456 | 757.796 | 0.264 | 0.253 | 0.140 |
| | $\beta_R$ | -0.224 | 0.423 | -0.423 | 0.999 | 0.944 | 0.999 |
| | $R^2$ | 0.998 | 0.981 | 0.997 | 1.000 | 0.993 | 1.000 |
| | $\chi^2$ | 14.367 | 19.911 | 6.519 | 4E-07 | 0.895 | 3E-08 |
| | RSME | 5.324 | 5.199 | 2.699 | 0.0007 | 0.439 | 0.0001 |
| 5.Brouers-Sotolongo $q_e = q_m[1 - \exp(-K_{BS}(C_e)^{\alpha}]$ | $q_m$(mg/g) | 246.925 | 90.316 | 121.927 | 205.755 | 41.974 | 115.685 |
| | $K_{BS}$(l/mg) | 0.092 | 0.079 | 0.104 | 0.001 | 0.004 | 0.002 |
| | α | 1.024 | 1.0244 | 1.024 | 1.078 | 1.059 | 0.924 |
| | $R^2$ | 0.998 | 0.998 | 0.998 | 1.000 | 0.991 | 0.997 |
| | $\chi^2$ | 13.677 | 5.003 | 6.754 | 0.122 | 1.316 | 0.381 |
| | RSME | 5.179 | 1.895 | 2.558 | 0.187 | 0.475 | 0.391 |

### 6.2.5.4 Radke-Prausnitz model

The Radke-Prausnitz isotherm is a simple empirical expression having three degrees of freedom (Vijayaraghavan et al., 2006; Volesky, 2003). It is a slightly different isotherm equation with three adjustable parameters and was developed by Radke and Prausnitz (Radke and Prausnitz, 1972) based on the thermodynamically ideal solution concept for dilute solutions. This isotherm can be valid for a wide range of concentrations (Vargas et al., 2011). This model was used for both adsorption and desorption of Cu(II), Cd(II), Pb(II) and Zn(II) onto and from banana peels. The model prediction and isotherm constant are plotted in Figure 6.11 for Cu(II), Figure 6.12 for Cd(II), Figure 6.13 for Pb(II) and Figure 6.14 for Zn(II). The model's parameters are tabulated in Table 6.3 for Cu(II), Table 6.4 for Cd(II), Table 6.5 for Pb(II) and Table 6.6 for Zn(II).

**Table 6.6** Parameters of isotherm models for adsorption and desorption of Zn(II) onto and from banana peels

| Isotherm models | Para-meters | Adsorption | | | Desorption | | |
|---|---|---|---|---|---|---|---|
| | | Doses | | | Doses | | |
| | | **0.05g** | **0.5g** | **1g** | **0.05g** | **0.5g** | **1g** |
| Experimental | $q_m$(mg/g) | 64.649 | 35.654 | 48.1329 | 12.456 | 5.705 | |
| 1. Langmuir | $q_m$(mg/g) | 70.502 | 38.441 | 51.896 | 111.121 | 48.584 | 32.683 |
| $q_e = \frac{q_m K_L C_e}{1 + K_L C_e}$ | $K_L$ (l/g) | 0.065 | 0.050 | 0.065 | 0.003 | 0.004 | 0.005 |
| | $R_L$ | 0.04-0.96 | 0.06-0.96 | 0.06-0.96 | 0.88-0.99 | 0.88-0.99 | 0.83-0.99 |
| | $R^2$ | 0.993 | 0.993 | 0.993 | 0.999 | 0.999 | 0.999 |
| | Δ°G | -6.645 | -7.298 | -6.645 | -14.57 | -13.22 | -12.92 |
| | $\chi^2$ | 2.551 | 1.391 | 8.728 | 0.057 | 0.025 | 0.0591 |
| | RMSE | 2.492 | 1.359 | 1.834 | 0.143 | 0.061 | 0.0974 |
| 2. SIPS | $K_s$(l/g) | 2.066 | 0.779 | 1.522 | 0.258 | 0.207 | 0.222 |
| $q_e = \frac{K_s C_e^{\beta_s}}{1 + \alpha_s C_e^{\beta_s}}$ | $\alpha_S$ (l/mg) | 0.031 | 0.022 | 0.031 | 0.000 | 0.000 | 0.000 |
| | $\beta_S$ | 1.374 | 1.374 | 1.374 | 0.992 | 0.974 | 0.865 |
| | $R^2$ | 0.998 | 0.998 | 0.998 | 1.000 | 1.000 | 0.998 |
| | $\chi^2$ | 3.282 | 1.788 | 2.419 | 0.0012 | 0.006 | 0.154 |
| | RSME | 1.446 | 0.788 | 1.065 | 0.0172 | 0.025 | 0.138 |
| 3.Redlich-Peterson | $K_{RP}$ (l/g) | 3.747 | 1.566 | 2.762 | 9.880 | 6.800 | 2.765 |
| | $\alpha_{RP}$(l/mg) | 0.033 | 0.025 | 0.033 | 38.520 | 34.773 | 19.277 |
| $q_e = \frac{K_{RP} C_e}{1 + \alpha_{RP} C_e^{\beta}}$ | β | 1.092 | 1.090 | 1.091 | -6.6E-06 | -0.001 | -5.6E-05 |
| | $R^2$ | 0.996 | 0.996 | 0.996 | 1.000 | 1.000 | 1.000 |
| | $\chi^2$ | 8.893 | 4.861 | 6.557 | 2E-09 | 7E-06 | 3E-08 |
| | RSME | 2.505 | 1.367 | 1.845 | 3E-05 | 0.0016 | 5E-05 |
| 4.Radke-Prausnitz | $\alpha_R$ (l/g) | 4.148 | 39.669 | 2.752 | 18.433 | 18.433 | 8.878 |
| | $r_R$ (l/mg) | 91.241 | 6.806 | 84.866 | 0.253 | 0.248 | 0.193 |
| $q_e = \frac{\alpha_R r_R C_e^{\beta_R}}{\alpha_R + r_R C_e^{\beta_R - 1}}$ | $\beta_R$ | -0.051 | 0.305 | -0.092 | 0.999 | 0.922 | 0.907 |
| | $R^2$ | 0.995 | 0.906 | 0.996 | 1.000 | 0.999 | 0.999 |
| | $\chi^2$ | 10.179 | 27.741 | 6.529 | 1E-08 | 0.049 | 0.067 |
| | RSME | 2.747 | 5.942 | 1.843 | 9E-05 | 0.0752 | 0.099 |
| 5.Brouers-Sotolongo | $q_m$(mg/g) | 63.980 | 34.885 | 43.891 | 49.781 | 49.342 | 5.915 |
| $q_e = q_m[1 - \exp(-K_{BS}(C_e)^{\alpha}$ | $K_{BS}$(l/mg) | 0.058 | 0.045 | 4.28E-08 | 0.004 | 0.0002 | 0.001 |
| | α | 0.942 | 0.942 | 6.824 | 1.095 | 1.956 | 2.189 |
| | $R^2$ | 0.994 | 0.994 | 0.951 | 1.000 | 0.963 | 0.992 |
| | $\chi^2$ | 9.177 | 5.004 | 15.06 | 0.043 | 19.437 | 18.873 |
| | RSME | 2.849 | 1.554 | 5.339 | 0.058 | 0.616 | 0.295 |

Similar to other models, Radke-Prausnitz isotherm revealed the good fitness to the experimental data for both adsorption and desorption of Cu(II), Cd(II), Pb(II) and Zn(II) from banana peels. Significantly higher $R^2$ values are found from both adsorption and desorption of Cu(II), Cd(II), Pb(II) and Zn(II) ions onto BP. The constant $r_R$ which is equivalent to adsorption capacities are much higher than the experimental and Langmuir isotherm (Table 6.3, Table 6.4, Table 6.5 and Table 6.6). The low RMSE and $\chi^2$ values also resolve the fitness of the model.

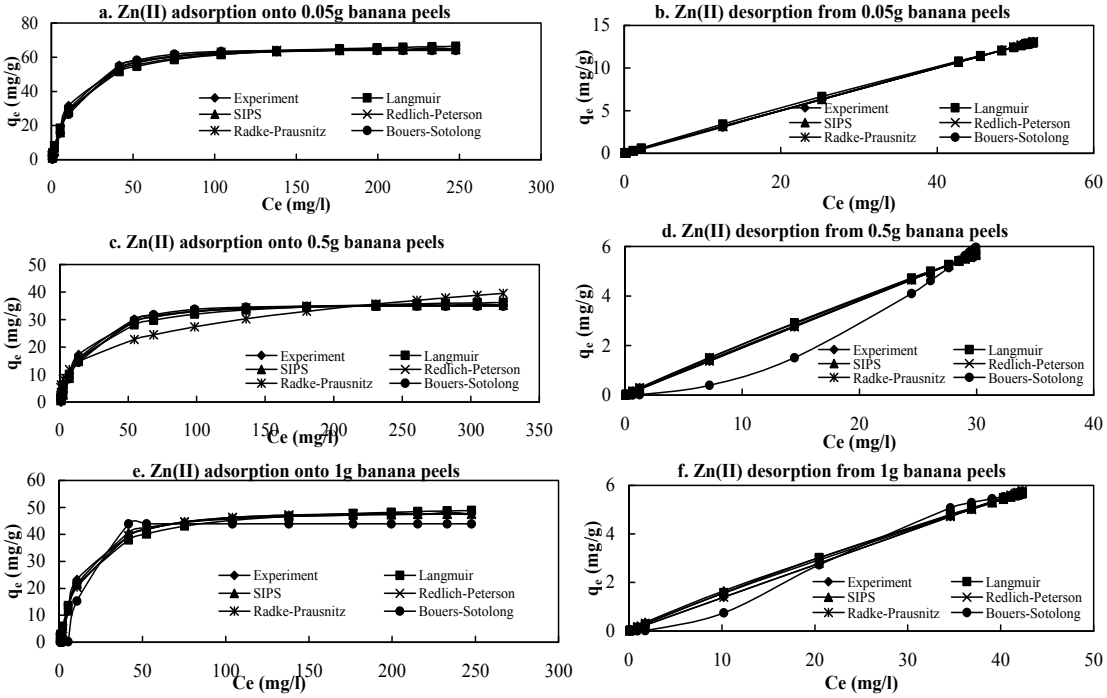


**Figure 6.14** Isotherm modelling of adsorption and desorption of Zn(II) onto and from banana peels ($C_o$: 1-500 mg/l; d: 0.05-1 g; t: 3h: pH: 6-6.5; rpm: 120; T: 20°C)

### 6.2.5.5 The Brouers-Sotolongo isotherm

Besides the theory of adsorption on a non-uniform surface by Langmuir, the Brouers-Sotolongo model assumes that the surface comprises a finite number of patches of sites with equal energy (Ncibi et al., 2008a; Vargas et al., 2011). It is given by a deformed exponential (Weibull) function (Altenor et al., 2009). This model was used to fit with experimental data of Cu(II), Cd(II), Pb(II) and Zn(II) adsorption and desorption. The predicted data were plotted in Figure 6.11 for Cu(II), Figure 6.12 for Cd(II), Figure 6.13 for Pb(II) and Figure 6.14 for Zn(II). The model's parameters are tabulated in Table 6.3 for Cu(II), Table 6.4 for Cd(II), Table 6.5 for Pb(II) and Table 6.6 for Zn(II). Similar to other models this model showed higher agreement with experimental data as the R2 values lies between 0.991 and 1.00. The predicted $q_m$ values for adsorption and

desorption equilibrium were similar and quiet higher than the other models. The values of $K_{BS}$ lie between 0 and 1 which implies the heterogeneity of the banana peels surface. It is also depicted from SEM data and other models.

#### 6.2.5.6 Model results comparison

It is indispensable to uncover an appropriate model for better understanding the adsorption/desorption mechanism. It is also needed to measure the adsorption/ desorption characteristics and magnitude based on the suitable model obeyed by banana peels. In this regard, Langmuir, SIPS, Redlich-Peterson, Radke-Prausnitz and Brouers-Sotolongo isotherm models were considered and compared against experimental data for the goodness of fit. The model predictions are plotted in Figure 6.11 for Cu(II), Figure 6.12 for Cd(II), Figure 6.13 for Pb(II) and Figure 6.14 for Zn(II). The models parameters are tabulated in Table 6.3 for Cu(II), Table 6.4 for Cd(II), Table 6.5 for Pb(II) and Table 6.6 for Zn(II). The fitness/suitability of the models was evaluated based on the study of $R^2$, RMSE and $\chi^2$ values. Among the three doses of banana peels (i.e. 0.05, 0.5 and 1g per 100 ml water) only experimental data for 1g doses from both adsorption and desorption equilibrium for Cu(II) were properly fitted with all five models because the $R^2$ values remained 0.998 to 1 and also RMSE and $\chi^2$ values were low. But the data for Cd(II), Pb(II) and Zn(II) adsorption and desorption from all doses (i.e. 0.05, 0.5 and 1g per 100 ml water) showed higher fitness.

In this study, it was found that only the two-parameter model (Langmuir) was less fitted with experimental data when compared to other three-parameter (Sips, Redlich-Peterson, Radke-Prausnitz and Brouers-Sotolongo model) models used. This may have occurred due to the heterogeneity of the banana peels surfaces as the Langmuir model assumes a homogeneous surface. All three-parametric models (SIPS, Redlich-Peterson, Radke-Prausnitz, and Brouers-Sotolongo) were found to fit the experimental data and seemed to show remarkably similar degrees of fitness with regard to the plots (Figure 6.11, Figure 6.12, Figure 6.13 and Figure 6.14) as well as parameters (Table 6.3, Table 6.4, Table 6.5 and Table 6.6). According to fitness and models parameters, the order of preference of model is SIPS>Redlich-Peterson>Radke-Prausnitz>Brouers-Sotolongo> Langmuir. The preference of metals by BP is Cd(II)>Pb(II)>Zn(II)>Cu(II).

### 6.2.6 Biosorption and desorption kinetics

The kinetic adsorption/desorption data can be used to understand the dynamics of the adsorption reactions in terms of rate constant. In the adsorption process prediction of the rate-limiting step is an important factor. Kinetic studies help to identify the adsorption process and to predict the required economical design of wastewater treatment mechanism. For a solid-liquid adsorption, the solute transfer in the adsorption process can be either external mass transfer (boundary layer diffusion) for nonporous medium or intra-particle diffusion for porous medium or both mechanisms (Ncibi et al., 2008b). Since the kinetics parameters provide important information for designing and modelling the adsorption/desorption processes, it is important to point out the initial copper concentrations employed during the kinetic studies (Ho and McKay, 1999). In this study, three initial Cu(II), Cd(II), Pb(II) and Zn(II) concentrations (10, 50 and 100 mg/l) were used for adsorption and desorption kinetics (According to Chapter 3, Section 3.3.5). The nonlinear regression analysis method was used to fit the kinetic models with the help of the MS Excel Spreadsheet and optimised with '**Solver tool'** (Appendices II).

Recent studies have shown that the nonlinear method is more valid than the linear method for fitting either the kinetics model or isotherm models (Ho and McKay, 1999). The kinetic data for adsorption and desorption were analysed using four different kinetic models: pseudo-first-order, pseudo-second-order, Avrami and Intra particle diffusion equations. The conformity between the experimental data and the model-predicted values is expressed by $R^2$ (Hossain et al., 2012b). Besides the $R^2$ values the applicability of kinetics models were demonstrated through the normalized standard deviation (NSD) and average relative error (ARE) values (Behnamfard and Salarirad, 2009). The nonlinear fitting curves of the pseudo-first-order, pseudo-second-order, Avrami and Intra particle diffusion equations for adsorption and desorption of Cu(II), Cd(II), Pb(II) and Zn(II) on banana peels are presented in Figure 6.16 for Cu(II), Figure 6.17 for Cd(II), Figure 6.18 for Pb(II) and Figure 6.19 for Zn(II). The kinetic model parameters are shown in Table 6.7 for Cu(II) Table 6.8 for Cd(II), Table 6.9 for Pb(II) and Table 6.10 for Zn(II).

#### 6.2.6.1 Pseudo-first order model

The pseudo-first-order model is the earliest known equation describing the adsorption rate based on the adsorption capacity. The pseudo-second order model describes the

adsorption process as being controlled by chemisorption which involves valency forces through sharing or exchange of electron between the solvent and the sorbate (Aharoni and Tompkins, 1970; Ho et al., 2000). Adsorption kinetics involves the relationship between the adsorption capacities and adsorption time. The pseudo-first order model is the earliest known equation relating the adsorption rate based on the adsorption capacity (Gürses et al., 2006). This equation is also named as Lagergren-first-order equation (Ho, 2004). This is the broadly employed model for explaining the kinetics relation of the adsorption reaction (Rajaei et al., 2013). The mathematical form is shown in the tables for all metals (Table 6.7 for Cu(II) Table 6.8 for Cd(II), Table 6.9 for Pb(II) and Table 6.10 for Zn(II)).

**Table 6.7** Kinetics parameters of Cu(II) adsorption and desorption onto banana peels

| Kinetic models | Parameters | Adsorption | | | Desorption | | |
|---|---|---|---|---|---|---|---|
| | | Cu(II) concentration | | | Cu(II) concentration | | |
| | | **10mg** | **50mg** | **100mg** | **10mg** | **50mg** | **100mg** |
| **Experimental** | $q_e$ (mg/g) | 1.336 | 8.628 | 17.229 | 1.099 | 7.101 | 14.264 |
| 1. Pseudo-1st-order | $q_e$ (mg/g) | 1.268 | 8.556 | 17.169 | 1.039 | 7.042 | 14.130 |
| | $k_1$ (l/h) | 0.178 | 2.691 | 2.547 | 0.168 | 2.691 | 2.547 |
| $q_t = q_e - q_e e^{(-k_1 t)}$ | $R^2$ | 0.984 | 0.996 | 0.997 | 0.943 | 0.996 | 0.997 |
| | NSD | 18.975 | 2.095 | 1.851 | 20.002 | 2.095 | 1.851 |
| | ARE | 5.046 | -0.043 | -0.034 | 5.417 | -0.043 | -0.034 |
| 2. Pseudo-2nd-order | $q_e$ (g/mg.min) | 1.338 | 8.603 | 17.169 | 1.099 | 7.080 | 14.190 |
| | $k_2$ (1/h) | 0.237 | 1.314 | 1.596 | 0.271 | 1.597 | 0.809 |
| | $R^2$ | 0.981 | 0.997 | 0.998 | 0.979 | 0.997 | 0.997 |
| $q_t = \frac{k_2 q_e^2 t}{(1 + q_e k_2 t)}$ | $h=k_2 q_e^2$(mg/g.min) | 0.425 | 97.290 | 197.967 | 0.327 | 80.069 | 162.92 |
| | NSD | 11.550 | 1.671 | 1.8513 | 13.03 | 1.601 | 1.946 |
| | ARE | 1.906 | -0.026 | -0.034 | 2.366 | -0.298 | -0.159 |
| 3.Avrami | $q_e$ (mg/g) | 1.262 | 8.556 | 17.169 | 1.039 | 6.994 | 14.019 |
| | $K_{AV}$ (/min) | 0.410 | 1.640 | 1.596 | 0.084 | 9.360 | 9.360 |
| $q_t = q_e\left[1 - e^{(-t k_{AV})^{n_{AV}}}\right]$ | $n_{AV}$ | 0.410 | 1.640 | 1.596 | 1.997 | 2.389 | 2.389 |
| | $R^2$ | 0.963 | 0.998 | 0.998 | 0.963 | 0.995 | 0.995 |
| | NSD | 20.001 | 2.096 | 1.851 | 21.126 | 3.055 | 3.345 |
| | ARE | 5.417 | -0.043 | -0.034 | 5.405 | -0.516 | -0.375 |
| 4. Intra particle diffusion | $k_p$(gm/g√min) | 0.620 | 7.934 | 16.255 | 0.530 | 6.358 | 13.378 |
| | C | -0.335 | -0.480 | -0.486 | -0.335 | 9.000 | -0.486 |
| $q_t = k_p t^{0.5+C}$ | $R^2$ | 0.982 | 1.000 | 0.999 | 0.978 | 1.000 | 0.999 |
| | NSD | 13.748 | 1.192 | 2.077 | 15.534 | 1.082 | 2.077 |
| | ARE | -2.793 | 0.349 | -0.045 | -6.997 | -0.013 | -0.045 |

The analysed data (Table 6.7) revealed that the experimental data for adsorption are well fitted with pseudo-first-order as the $R^2$ values are 0.984, 0.996 and 0.997 for 10, 50 and 100 mg/l initial Cu(II) concentrations respectively. In case of desorption, this model showed good agreement with experimental data from Cu(II) desorption ($R^2$: 0.943, 0.996 and 0.997). The equilibrium adsorption capacities ($q_e$) are 1.268, 8.556 and 17.169 mg/g desorption for 10, 50 and 100 mg/l initial Cu(II) concentrations

respectively. It is seems to be close to the values found from the experiment (Table 6.7). Similar results are also found for desorption equilibrium capacities. The significant small values of NSD and ARE are also found for Cu(II) adsorption kinetics.

For Cd(II) adsorption, the data are moderately fitted with the pseudo-first order model as the $R^2$ values are 0.970, 0.982 and 0.960 for the initial Cd(II) concentration of 10, 50 and 100 mg/l respectively (Table 6.8). The high values of NSD (14.271, 25.099 and 221.458) and some negative values of ARE (3.213, -7.509 and -72.792) for the three initial concentrations used revealed the suitability of the model to postulate the Cd(II) adsorption onto banana peels. Similarly, desorption data also showed good consistency ($R^2$: 0.970, 0.982 and 0.960) with experimental data (Table 6.8). The predicted equilibrium capacity ($q_e$: 1.761, 6.759 and 23.877 mg/g) were similar to experimental $q_e$ (1.811, 7.023 and 23.514 mg/g) for 10, 50 and 100 mg/l initial concentration.

**Table 6.8** Kinetics parameters of Cd(II) adsorption and desorption onto banana peels

| Kinetic models | Parameters | Adsorption | | | Desorption | | |
|---|---|---|---|---|---|---|---|
| | | Cd(II) concentration | | | Cd(II) concentration | | |
| | | **10mg** | **50mg** | **100mg** | **10mg** | **50mg** | **100mg** |
| **Experimental** | $q_e$ (mg/g) | 1.811 | 7.023 | 23.514 | 1.492 | 5.629 | 18.395 |
| 1. Pseudo-1st-order | $q_e$ (mg/g) | 1.761 | 6.759 | 23.877 | 1.450 | 5.563 | 18.679 |
| | $k_1$ (l/h) | 0.261 | 0.190 | 0.243 | 0.261 | 0.190 | 0.243 |
| $q_t = q_e - q_e e^{(-k_1 t)}$ | $R^2$ | 0.970 | 0.982 | 0.960 | 0.970 | 0.982 | 0.960 |
| | NSD | 14.271 | 25.099 | 221.458 | 14.271 | 25.098 | 221.458 |
| | ARE | 3.213 | -7.509 | -72.797 | 3.213 | -7.509 | -72.797 |
| 2. Pseudo-2nd-order | $q_e$ (g/mg.min) | 1.838 | 7.223 | 25.534 | 1.513 | 5.944 | 19.975 |
| | $k_2$ (1/h) | 0.272 | 0.040 | 0.013 | 0.330 | 0.049 | 0.017 |
| | $R^2$ | 0.982 | 0.977 | 0.939 | 0.982 | 0.977 | 0.939 |
| $q_t = \frac{k_2 q_e^2 t}{(1 + q_e k_2 t)}$ | $h=k_2 q_e^2$(mg/g.min) | 0.918 | 2.088 | 8.772 | 0.755 | 1.718 | 6.861 |
| | NSD | 7.155 | 46.886 | 289.161 | 7.588 | 49.710 | 306.699 |
| | ARE | 0.134 | -14.401 | -94.412 | 0.187 | -15.697 | -105.82 |
| 3.Avrami | $q_e$ (mg/g) | 1.761 | 6.759 | 23.877 | 1.299 | 5.563 | 18.679 |
| | $K_{AV}$ (/min) | 0.510 | 0.070 | 0.092 | 9.360 | 0.070 | 0.153 |
| $q_t = q_e\left[1 - e^{(-t k_{AV})^{n_{AV}}}\right]$ | $n_{AV}$ | 0.510 | 2.706 | 2.659 | 2.389 | 2.704 | 1.594 |
| | $R^2$ | 0.981 | 0.987 | 0.971 | 0.773 | 0.987 | 0.971 |
| | NSD | 14.271 | 25.099 | 221.457 | 50.198 | 26.620 | 234.89 |
| | ARE | 3.213 | -7.509 | -72.797 | -13.76 | -8.544 | -82.137 |
| 4. Intra particle diffusion | $k_p$(gm/g√min) | 1.043 | 3.235 | 7.278 | 0.848 | 2.653 | 10.037 |
| | C | -0.378 | -0.329 | -0.220 | -0.373 | -0.329 | -0.359 |
| $q_t = k_p t^{0.5+C}$ | $R^2$ | 0.963 | 0.928 | 0.846 | 0.963 | 0.928 | 0.896 |
| | NSD | 20.665 | 126.877 | 327.006 | 20.156 | 126.341 | 600.335 |
| | ARE | -3.975 | -37.815 | -98.533 | -4.089 | -37.385 | -193.29 |

Pb(II) adsorption and desorption data are well fitted with the pseudo-first order model as the $R^2$ values are same (0.995, 0.981 and 0.975) for both processes (Table 6.9). The equilibrium adsorption/desorption capacities ($q_e$: 2.728, 11.849 and 24.713 mg/g for

adsorption; 2.062, 8.958 and 21.251 mg/g for desorption) are closed to experimental values for both adsorption (2.736, 11.907 and 25.713 mg/g) and desorption (2.068, 9.001 and 20.672 mg/g) of 10, 50 and 100 mg/l initial Pb(II) concentrations. Small values of NSD and ARE for both adsorption and desorption indicating that the model is suitable to describes the adsorption and desorption processes.

The adsorption and desorption of Zn(II) onto BP posed similar trends of agreement with pseudo-first order model. The coefficient of determination ($R^2$) are 0.996, 0.995 and 0.995 for adsorption; and 0.996, 0.963 and 0.995 for desorption of Zn(II) while the initial Zn(II) concentrations were 10, 50 and 100 mg/l respectively (Table 6.10). The experimental and model predicted equilibrium capacities are 1.146, 4.758 and 8.77 mg/g for Zn(II) adsorption and; 0.943, 3.942 and 6.346 mg/g for Zn(II) desorption while initial Zn(II) concentrations were 10, 50 and 100 mg/l. It seems that Zn(II) adsorption and desorption are better fitted with pseudo-first-order model.

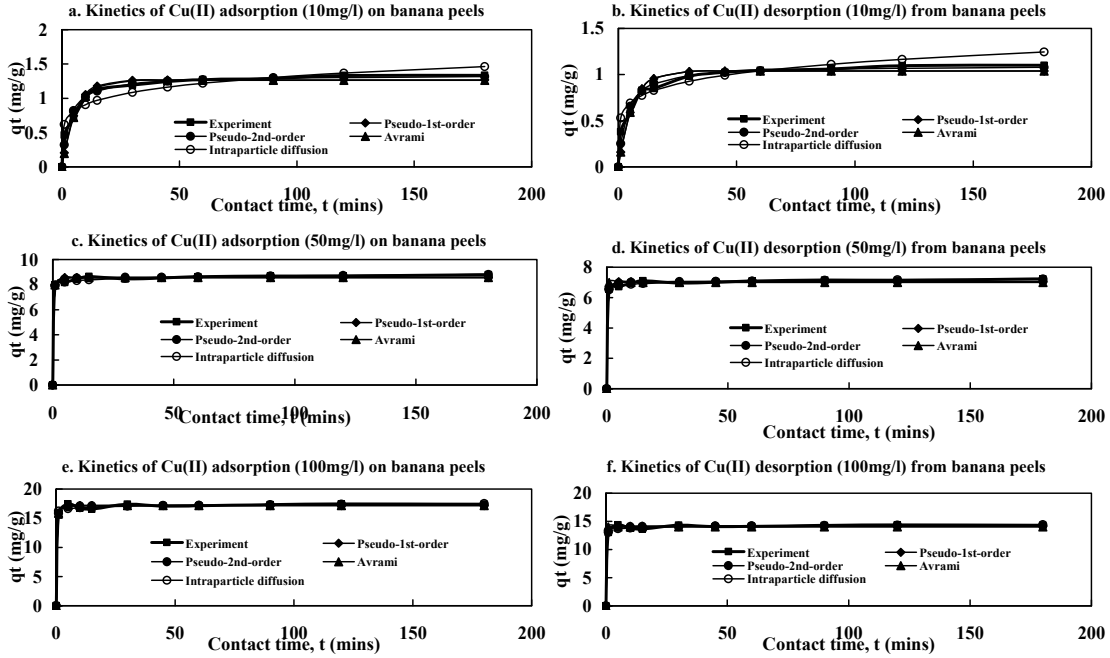


**Figure 6.15** Kinetics modelling of adsorption and desorption of Cu(II) onto banana peels ($C_o$: 50 mg/l; d: 0.5 g; t: 3 h: pH: 6-6.5; rpm: 120; T: room temp.)

Normally $k_1$ (pseudo-first-order kinetics constant) designates the rate of adsorption reaction. This value provides valuable information about the mechanism of adsorption and subsequently investigation of the controlling mechanism of the biosorption process as either mass transfer or chemical reaction (Khan et al., 2012; Montazer-Rahmati et al., 2011; Omorogie et al., 2012; Patil et al., 2011). This parameter is useful to obtain the

optimum operating conditions for industrial-scale batch processes. If $k_1>1$, the adsorption reaction is more than one times and adsorption mechanism is not physisorption. Likewise, if $k_1<1$, the adsorption reaction is one times and involves a mechanism that is generally physical sorption or complexation of metals ions with biosorbent (Ho et al., 2004; Ho and Ofomaja, 2006a; Horsfall and Spiff, 2005).

Considering the above condition, it is obvious that Pb(II), Cu(II), Cd(II) and Zn(II) ions adsorption processes fall under the second condition, because $k_1$ values were less than unity when using the three initial metal concentrations (10, 50 and 100 mg/l) (Table 6.7, Table 6.8, Table 6.9 and Table 6.10). In other words the Pb(II), Cu(II), Cd(II) and Zn(II) ions adsorption mechanism was physical sorption or complexation with BP. Conversely, desorption processes showed similar trend of mechanism as the $k_1$ values are less than unity for different initial exhausted metals concentration and metals.

**Table 6.9** Kinetics parameters of Pb(II) adsorption and desorption onto banana peels

| Kinetic models | Parameters | Adsorption | | | Desorption | | |
|---|---|---|---|---|---|---|---|
| | | Pb(II) concentration | | | Pb(II) concentration | | |
| | | 10mg | 50mg | 100mg | 10mg | 50mg | 100mg |
| **Experimental** | $q_e$ (mg/g) | 2.736 | 11.907 | 25.7123 | 2.068 | 9.001 | 20.6722 |
| 1. Pseudo-1st-order | $q_e$ (mg/g) | 2.728 | 11.849 | 24.826 | 2.062 | 8.958 | 21.251 |
| | $k_1$ (l/h) | 0.359 | 0.308 | 0.223 | 0.359 | 0.308 | 0.223 |
| $q_t = q_e - q_e e^{(-k_1 t)}$ | $R^2$ | 0.995 | 0.981 | 0.975 | 0.995 | 0.981 | 0.975 |
| | NSD | 7.574 | 29.368 | 65.799 | 7.574 | 29.368 | 65.799 |
| | ARE | -2.106 | -9.008 | -21.057 | -2.106 | -9.008 | -21.058 |
| 2. Pseudo-2nd-order | $q_e$ (g/mg.min) | 2.863 | 12.518 | 26.539 | 2.165 | 9.464 | 22.717 |
| | $k_2$ (1/h) | 0.200 | 0.037 | 0.012 | 0.264 | 0.049 | 0.014 |
| | $R^2$ | 0.967 | 0.948 | 0.961 | 0.967 | 0.948 | 0.961 |
| $q_t = \frac{k_2 q_e^2 t}{(1 + q_e k_2 t)}$ | $h=k_2 q_e^2$(mg/g.min) | 1.638 | 5.837 | 8.636 | 1.238 | 4.413 | 7.3926 |
| | NSD | 18.909 | 46.356 | 96.498 | 19.992 | 49.128 | 102.350 |
| | ARE | -4.862 | -13.695 | -30.482 | -4.901 | -14.705 | -34.107 |
| 3. Avrami | $q_e$ (mg/g) | 2.728 | 11.849 | 24.826 | 2.062 | 8.958 | 21.251 |
| | $K_{AV}$ (/min) | 0.230 | 0.229 | 0.084 | 0.214 | 1.670 | 0.147 |
| $q_t = q_e\left[1 - e^{(-t k_{AV})^{n_{AV}}}\right]$ | $n_{AV}$ | 1.563 | 1.343 | 2.672 | 1.683 | 0.184 | 1.520 |
| | $R^2$ | 0.997 | 0.987 | 0.982 | 0.997 | 0.987 | 0.978 |
| | NSD | 7.574 | 29.368 | 65.799 | 8.031 | 31.146 | 69.780 |
| | ARE | -2.106 | -9.008 | -21.057 | -2.297 | -9.988 | -24.130 |
| 4. Intra particle diffusion | $k_p$(gm/g√min) | 1.685 | 6.895 | 12.802 | 1.274 | 5.151 | 11.481 |
| | C | -0.385 | -0.374 | -0.348 | -0.385 | -0.369 | -0.350 |
| $q_t = k_p t^{0.5+C}$ | $R^2$ | 0.929 | 0.908 | 0.915 | 0.929 | 0.908 | 0.912 |
| | NSD | 51.031 | 104.547 | 221.683 | 51.031 | 102.962 | 233.752 |
| | ARE | -12.46 | -29.153 | -67.928 | -12.46 | -29.209 | -75.975 |

### 6.2.6.2 Pseudo-second order model

The data from the kinetic biosorption and desorption of Cu(II), Cd(II), Pb(II) and Zn(II) ions onto and from banana peels are explained by the pseudo-second-order equation. This model is based on the assumption that the rate-limiting step may be chemical

sorption involving valance forces through sharing or exchange of electrons between heavy metal ions and the adsorbent and offers the best consistent data for the heavy metal ions (Namasivayam et al., 2007). The mathematical expression (Ho and McKay, 2000) of the equation is shown in tables (Table 6.7 for Cu(II) Table 6.8 for Cd(II), Table 6.9 for Pb(II) and Table 6.10 for Zn(II)).

The model predicted and experimental parameters are summarised in Table 6.7 for Cu(II) Table 6.8 for Cd(II), Table 6.9 for Pb(II) and Table 6.10 for Zn(II). Surprisingly, the adsorption and desorption data for Cu(II) showed similar fitness ($R^2$: 0.981, 0.997 and 0.999 for adsorption and $R^2$: 0.979, 0.997 and 0.997 for desorption) with the pseudo-second-order model and the pseudo-first-order model. The model predicted $q_e$ values (1.338 8.603 and 17.169 mg/g for adsorption; and, 1.099, 7.080 and 14.190 mg/g for desorption) are near to the experimental values (1.336, 8.628 and 17.229 mg/g for adsorption; and 1.099, 7.101 and 14.264 mg/g for desorption). This implies that along with physio-adsorption, the chemisorption also controlled the reaction rate of Cu(II) ions adsorption onto and desorption from BP wastes (Ho and McKay, 2000).

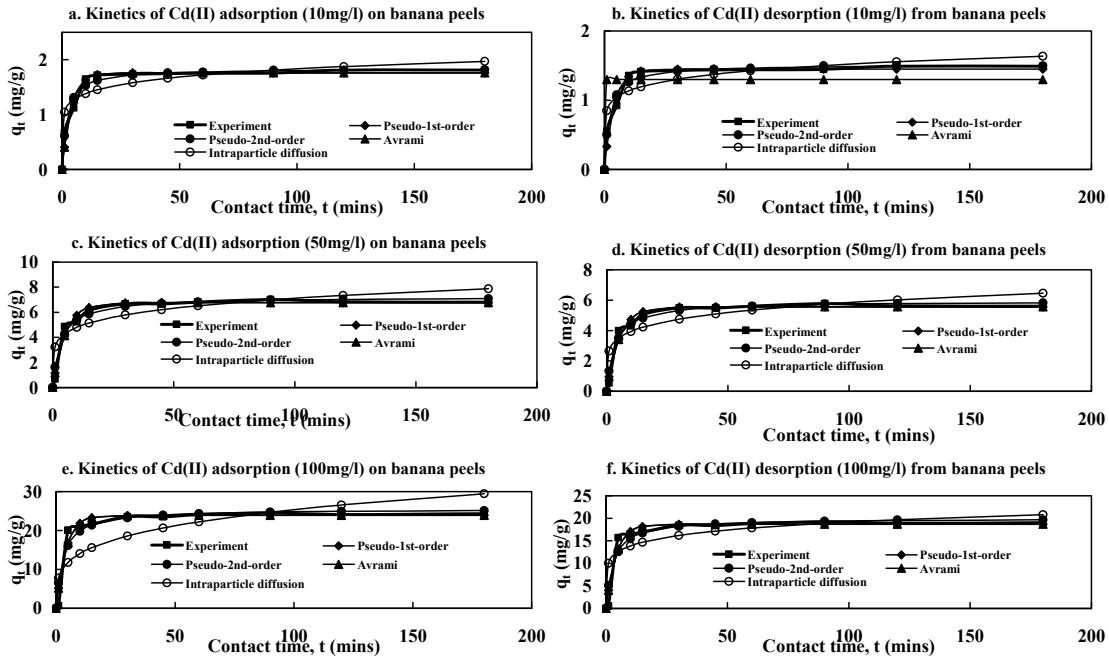


**Figure 6.16** Kinetics modelling of adsorption and desorption of Cd(II) onto banana peels ($C_o$: 50 mg/l; d: 0.5 g; t: 3 h: pH: 6-6.5; rpm: 120; T: room temp.)

For Cd(II) adsorption and desorption kinetics are also fitted by the pseudo-second-order model and the predictions are plotted in Figure 6.17. The kinetic model parameters are shown in Table 6.8 for Cd(II). The values of $R^2$ indicate that this data also fitted with

this model like other metals. The equilibrium adsorption/desorption capacities ($q_e$) of Cd(II) are 1.838, 7.223 and 25.536 mg/g for 10, 50 and 100 mg/l respectively and are close to the experimental values (1.811, 7.023 and 23.514 mg/g). The magnitude of $q_e$ values for desorption are also almost the same for the model predictions and the experimental values. This prediction is also same as Cu(II) adsorption, i.e. chemisorption controls the Cd(II) adsorption along with physio-sorption (Ho and McKay, 2000).

Similar to other metals, the Pb(II) adsorption and desorption data posed a good fitness with the pseudo-second-order kinetics model as the $R^2$ values are 0.967, 0.948 and 0.961 for adsorption and 0.967, 0.948 and 0.961 for desorption. The $q_e$ values are similar to the experimental values (Table 6.9). In addition, the Zn(II) adsorption and desorption data also showed higher fitness with this model (Table 6.10). The predicted $q_e$ values (1.194, 4.963 and 9.232 mg/g for adsorption; and 0.982, 4.154 and 6.674 mg/g for desorption) are similar to the experimental values (1.182, 4.813 and 8.726 mg/g for adsorption; and 0.973, 4.719 and 6.491 mg/g for desorption). From these predictions, it is also concluded that Pb(II) and Zn(II) also follow the chemisorption along with physio-adsorption (Ho and McKay, 2000).

The pseudo-second-order constant, $k_2$ which explains that the adsorption process is occurring in more than one stage of reactions. The first one is fast and reaches equilibrium quickly and the second is a slower reaction that can continue for long time periods (Ho and McKay, 2000; Ho and Ofomaja, 2006b). The values of $k_2$ are less than unity for adsorption of Cd(II), Pb(II) and Zn(II) ions adsorption onto BP. But the $k_2$ values for Cu(II) adsorption are more than unity for 50 and 100 mg/l initial Cu(II) concentration but not 10 mg/l. This implies that the mechanism of Pb(II), Cd(II) and Zn(II) ions adsorption is not chemisorption along with physio-adsorption. But the Cu(II) adsorption may be chemisorption along with physio-adsorption. In case of desorption, similar values of $k_2$ are found. It is notable that model fitness and $k_2$ values depict the opposite proposition for adsorption and desorption mechanisms of Pb(II), Cu(II), Cd(II) and Zn(II) ions onto BP.

In addition to $R^2$, significantly low NSD and ARE values were also obtained from pseudo-second-order for all metals adsorption and desorption which further advocate the fitness of the pseudo-second-order model and chemisorption process (Ho and

McKay, 2000). Experimental and predicted values of equilibrium adsorption capacities ($q_e$) showed good consistencies between the pseudo-second-order model with the pseudo-first-order model. So, it can be concluded that both pseudo-first-order and pseudo-second-order models are able to illustrate the Pb(II), Cu(II), Cd(II) and Zn(II) ions adsorption onto and desorption from banana peels.

### 6.2.6.3 Avrami kinetic equation

This model describes the possible changes of the adsorption and desorption rates is a function of the initial metals concentration and the adsorption/desorption time, as well as the determination of fractional kinetic orders (Lopes et al., 2003). The equation of Avrami kinetic model presents Avrami exponential that is a fractionery number related to the possible changes of the adsorption mechanism that takes place during the adsorption process. So the adsorption mechanism could follow multiple kinetic orders that change during the contact of the metals with the biosorbents (Lopes et al., 2003). The mathematical equation of the model is shown in the tables with other parameters (Table 6.7 for Cu(II) Table 6.8 for Cd(II), Table 6.9 for Pb(II) and Table 6.10 for Zn(II)). The predictions as well as experimental data are plotted in Figure 6.16 for Cu(II), Figure 6.17 for Cd(II), Figure 6.18 for Pb(II) and Figure 6.19 for Zn(II).

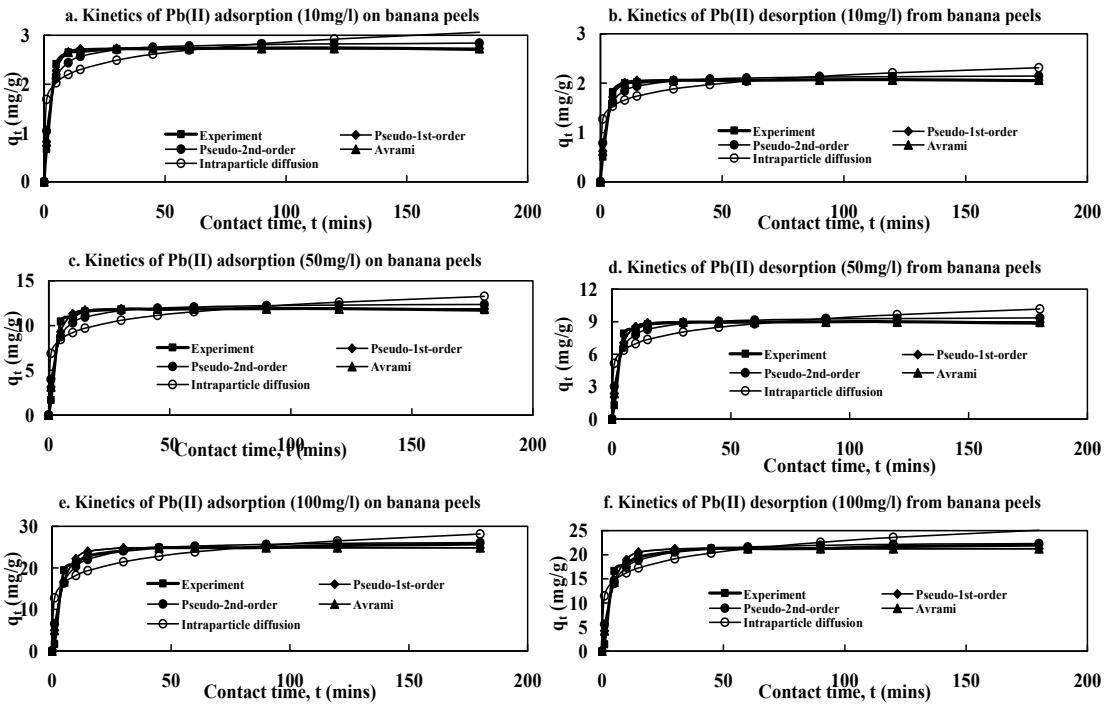


**Figure 6.17** Kinetics modelling of adsorption and desorption of Pb(II) onto banana peels ($C_o$: 50 mg/l; d: 0.5 g; t: 3 h: pH: 6-6.5; rpm: 120; T: room temp.)

The Avrami kinetic equation was used to describe the kinetics of Cu(II), Cd(II), Pb(II) and Zn(II) adsorption onto and desorption from banana peels. The overall fitness of this model with experimental data from adsorption and desorption of Cu(II), Cd(II), Pb(II), and Zn(II) are excellent as the $R^2$ values lies between 0.963 and 0.999 for used 10, 50 and 100 mg/l metals concentration (Table 6.7).

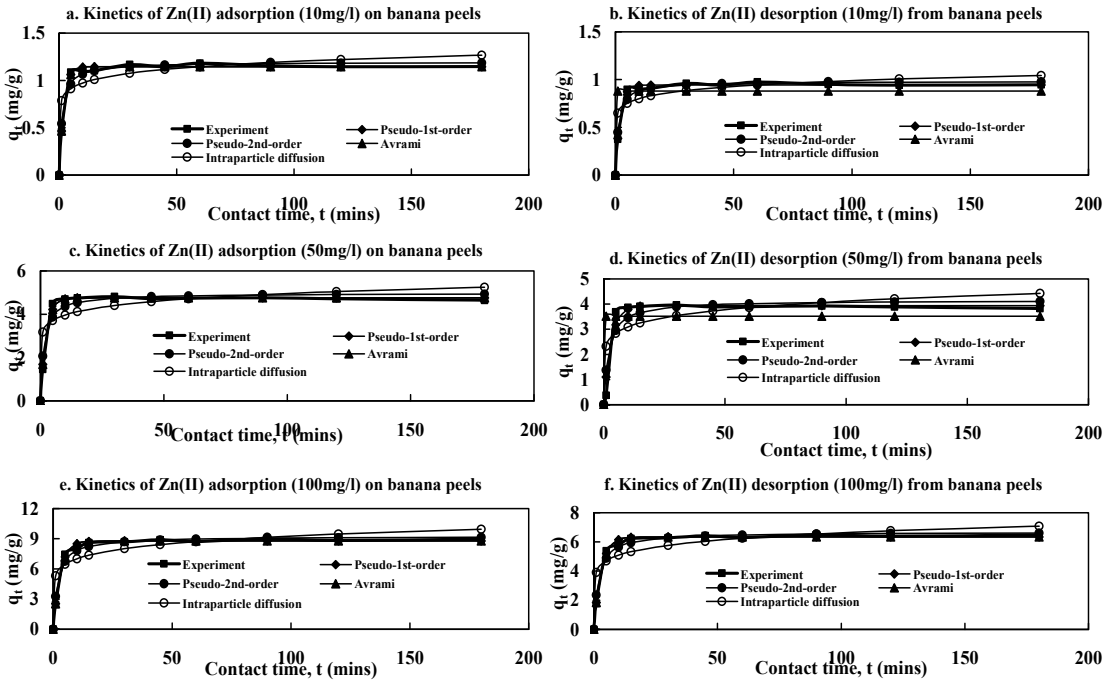


**Figure 6.18** Kinetics modelling of adsorption and desorption of Zn(II) onto banana peels ($C_o$: 50 mg/l; d: 0.5 g; t: 3 h: pH: 6-6.5; rpm: 120; T: room temp.)

In addition, the model predicted equilibrium ($q_e$) capacities (1.262, 8.556 and 17.169 mg/g for Cu(II) adsorption and; 1.039, 6.994 and 14.09 mg/g for Cu(II) desorption) are close to the experimental equilibrium ($q_e$) capacities (1.336, 8.628 and 17.229 for Cu(II) adsorption and; 1.099, 7.101 and 14.264 mg/g for Pb(II) desorption). Similarly, the experimental equilibrium ($q_e$) capacities are close enough to the model prediction for Cd(II), Cu(II) and Zn(II) adsorption and desorption (Tables 6.8, 6.9 and 6.10). The values of $q_e$ for both adsorption and desorption processes were similar to pseudo-second-order and close to experimental values. From the above discussion, it noted that this model suitably describes the kinetics processes of adsorption and desorption. The errors functions NSD and ARE are significantly smaller for all three initial concentrations and four metals.

**Table 6.10** Kinetics parameters of Zn(II) adsorption and desorption onto banana peels

| Kinetic models | Parameters | Adsorption | | | Desorption | | |
|---|---|---|---|---|---|---|---|
| | | Zn(II) concentration | | | Zn(II) concentration | | |
| | | 10mg | 50mg | 100mg | 10mg | 50mg | 100mg |
| **Experimental** | $q_e$ (mg/g) | 1.182 | 4.813 | 8.726 | 0.973 | 4.719 | 6.491 |
| 1. Pseudo-1st-order $q_t = q_e - q_e e^{(-k_1 t)}$ | $q_e$ (mg/g) | 1.146 | 4.758 | 8.777 | 0.943 | 3.942 | 6.346 |
| | $k_1$ (l/h) | 0.524 | 0.436 | 0.342 | 0.524 | 0.328 | 0.342 |
| | $R^2$ | 0.996 | 0.995 | 0.995 | 0.996 | 0.963 | 0.995 |
| | NSD | 2.486 | 5.626 | 2.909 | 2.486 | 64.716 | 2.909 |
| | ARE | -0.247 | -1.447 | -0.344 | -0.247 | -20.565 | -0.344 |
| 2. Pseudo-2nd-order $q_t = \frac{k_2 q_e^2 t}{(1 + q_e k_2 t)}$ | $q_e$ (g/mg.min) | 1.194 | 4.963 | 9.232 | 0.982 | 4.154 | 6.674 |
| | $k_2$ (1/h) | 0.699 | 0.144 | 0.059 | 0.849 | 0.119 | 0.082 |
| | $R^2$ | 0.981 | 0.961 | 0.984 | 0.981 | 0.914 | 0.984 |
| | $h=k_2 q_e^2$(mg/g.min) | 0.996 | 3.543 | 5.046 | 0.819 | 2.0517 | 3.648 |
| | NSD | 7.697 | 15.225 | 11.597 | 8.081 | 94.429 | 12.277 |
| | ARE | -1.406 | -3.564 | -2.785 | -1.171 | -30.191 | -2.867 |
| 3. Avrami $q_t = q_e\left[1 - e^{(-t k_{AV})^{n_{AV}}}\right]$ | $q_e$ (mg/g) | 1.146 | 4.758 | 8.777 | 0.879 | 3.521 | 6.346 |
| | $K_{AV}$ (/min) | 0.724 | 0.160 | 0.218 | 9.360 | 9.360 | 2.024 |
| | $n_{AV}$ | 0.724 | 2.733 | 1.567 | 2.388 | 2.389 | 0.169 |
| | $R^2$ | 0.997 | 0.997 | 0.997 | 0.823 | 0.661 | 0.997 |
| | NSD | 2.486 | 5.626 | 2.909 | 47.908 | 296.522 | 3.011 |
| | ARE | -0.247 | -1.447 | -0.345 | -11.00 | -95.657 | -0.625 |
| 4. Intra particle diffusion $q_t = k_p t^{0.5+C}$ | $k_p$(gm/g√min) | 0.787 | 3.169 | 5.303 | 0.648 | 2.324 | 3.907 |
| | C | -0.408 | -0.403 | -0.379 | -0.408 | -0.376 | -0.385 |
| | $R^2$ | 0.954 | 0.931 | 0.945 | 0.954 | 0.882 | 0.945 |
| | NSD | 25.756 | 40.631 | 39.796 | 25.756 | 173.618 | 41.030 |
| | ARE | -4.823 | -9.152 | -9.100 | -4.823 | -52.405 | -9.081 |

The $n_{AV}$ (fractionary number) predicted from adsorption processes were greater than unity ($n_{AV}$>1) for Cu(II), Cd(II), Pb(II) and Zn(II) adsorption onto and desorption from banana peels which signified that the reaction order is greater than first order for both adsorption and desorption processes. From $n_{AV}$ values, it could be concluded that Cu(II), Zn(II), Pb(II) and Cd(II) adsorption followed several orders during the processes. These finding suggested that possible changes occurred on adsorption and desorption mechanism during the processes; therefore, the adsorption mechanism of Cu(II), Cd(II), Pb(II) and Zn(II) onto banana peels followed multiple kinetic orders (Lopes et al., 2003).

### 6.2.6.4 Intra-particle diffusion model

The kinetic data from adsorption and desorption processes of Cu(II), Cd(II), Pb(II) and Zn(II) from banana peels were further applied to decide whether the intra-particle diffusion is rate limiting. The diffusion rate constant, $k_p$ (mg/g-min$^{0.5}$) was also found for four metals in three initial metals concentrations (10, 50 and 100 mg/l). The intra-particle diffusion model (Weber and Morris, 1963) is characterized by the relationship

between specific adsorption and the square root of time (Clayton and Chien, 1980). This relation also keeps same for desorption kinetics.

The model predictions are shown in Figure 6.16 for Cu(II), Figure 6.17 for Cd(II), Figure 6.18 for Pb(II) and Figure 6.19 for Zn(II). The kinetic model parameters are shown in Table 6.7 for Cu(II) Table 6.8 for Cd(II), Table 6.9 for Pb(II) and Table 6.10 for Zn(II). If data exhibits multi-linear plots, then two or more steps influence the sorption process. The external resistance to mass transfer surrounding the particle is considered to be significant only in the early stage of adsorption, whereas the second linear portion dominated the gradual adsorption stage with intra-particle diffusion (Srihari and Das, 2008). Indeed, the plots were found to be general in type, i.e. at the first stage and at the second stage they are distinct. It is also noticeable from figures (Figure 6.16 for Cu(II), Figure 6.17 for Cd(II), Figure 6.18 for Pb(II) and Figure 6.19 for Zn(II)) the lines belong to this model are different from other models' predictions. The rapid first stage and slower second stage are distinctly visible in the figures.

The experimental data moderately fitted with model prediction as the $R^2$ values were little bit low compared to other models. In the present study, the adsorption rate constant ($k_p$) were found to be increasing (0.620 to 16.255 for Cu(II); 1.043 to 7.278 for Cd(II); 1.685 to 12.802 for Pb(II) and 0.787 to 5.303 for Zn(II)) with increasing of initial metal concentrations (10 to 100 mg/l). However, the desorption rate constant ($k_p$) followed increasing trends for all four metals. Therefore, the rate parameter ($k_p$) characterises that the adsorption and desorption rate where intra-particle diffusion has been reported to be the rate-limiting factor (Venkata Mohan et al., 2002).

### 6.2.7 Multimetals adsorption

It is well known that wastewaters have complex matrices and contain several metal ions with other pollutants. So, the inspection of multiple metal interactions concurrently is very significant for exact demonstration of adsorption data (Hammaini et al., 2003). For this reason, Langmuir single-metal isotherm can be adapted to multi-metals isotherm with some interaction factor (Padilla-Ortega et al., 2013; Srivastava et al., 2008):

$$q_{e.i} = \frac{q_{m.i} K_{L.i}(C_i)}{1 + \sum_{j=1}^{N} K_{L.j}(C_j)} \qquad (6.1)$$

The adsorption system for multi-metals can be formulated by modification of the equation (6.1) for quaternary solution of Cu(II)-Pb(II)-Cd(II)-Zn(II) system:

For Cu(II): $$q_{e.Cu} = \frac{q_{m.Cu} K_{L.Cu} (C_{Cu})}{1 + K_{L.Cu} C_{e.Cu} + K_{L.Pb} C_{e.Pb} + K_{L.Cd} C_{e.Cd} + K_{L.Zn} C_{e.Zn}}$$ (6.2)

For Pb(II): $$q_{e.Pb} = \frac{q_{m.Pb} K_{L.Pb} (C_{Pb})}{1 + K_{L.Cu} C_{e.Cu} + K_{L.Pb} C_{e.Pb} + K_{L.Cd} C_{e.Cd} + K_{L.Zn} C_{e.Zn}}$$ (6.3)

For Cd(II): $$q_{e.Cd} = \frac{q_{m.Cd} K_{L.Cd} (C_{Cd})}{1 + K_{L.Cu} C_{e.Cu} + K_{L.Pb} C_{e.Pb} + K_{L.Cd} C_{e.Cd} + K_{L.Zn} C_{e.Zn}}$$ (6.4)

And for Zn(II): $$q_{e.Zn} = \frac{q_{m.Zn} K_{L.Zn} (C_{Zn})}{1 + K_{L.Cu} C_{e.Cu} + K_{L.Pb} C_{e.Pb} + K_{L.Cd} C_{e.Cd} + K_{L.Zn} C_{e.Zn}}$$ (6.5)

Equilibrium is reached in an adsorption when the concentration of metal ions in water ($C_e$) was in dynamic with that in the solid matrix ($q_e$). The competitive adsorption of the Cu(II), Pb(II), Cd(II) and Zn(II) in the quaternary systems [Cu(II)-Pb(II)-Cd(II)-Zn(II)] were conducted in batch system. The initial concentrations were 1 to 200 mg/l and the experiments were conducted for 3 hours at 120 rpm and room temperature with 0.5g of banana peels. The model parameters are calculated and tabulated in Table 6.11. The experimental and predicted data is plotted in Figure 6.19. Generally it appeared that the isotherm model was successfully fitted to the competitive adsorption of Cu(II)-Pb(II)-Cd(II)-Zn(II) onto banana peels.

The maximum adsorption capacities ($q_m$) of Cu(II), Pb(II), Cd(II) and Zn(II) from quaternary system [Cu(II)-Pb(II)-Cd(II)-Zn(II)] were estimated and compared to the molar uptake values of metals predicted with single metal Langmuir isotherm. As shown in this Figure 6.19, the model perfectly estimated the parameters for all fours metals adsorption because the predicted lines and experimental plots coincided.

**Table 6.11** Isotherm parameters from quaternary metals [Cd(II)-Cu(II)-Zn(II)-Pb(II)] adsorption

| **For Pb(II)** | **For Cu(II)** | **For Cd(II)** | **For Zn(II)** |
|---|---|---|---|
| $q_{m\text{-}Pb}$ = 83.279mg/g | $q_{m\text{-}Cu}$ = 20.058 mg/g | $q_{m\text{-}Cd}$ = 19.233mg/g | $q_{m\text{-}Zn}$ = 4.343mg/g |
| $K_{L\text{-}Cu}$ = -0.004l/g | $K_{L\text{-}Cu}$ = 0.019 l/g | $K_{L\text{-}Cu}$ = 0.009 l/g | $K_{L\text{-}Cu}$ = -0.036 l/g |
| $K_{L\text{-}Cd}$ = 0.014 l/g | $K_{L\text{-}Cd}$ = 0.026 l/g | $K_{L\text{-}Cd}$ = 0.059 l/g | $K_{L\text{-}Cd}$ = 0.089 l/g |
| $K_{L\text{-}Zn}$ = -0.006 l/g | $K_{L\text{-}Zn}$ = -0.012 l/g | $K_{L\text{-}Zn}$ = 0.0004 l/g | $K_{L\text{-}Zn}$ = 0.017 l/g |
| $K_{L\text{-}Pb}$ = 0.024 l/g | $K_{L\text{-}Pb}$ = -0.019 l/g | $K_{L\text{-}Pb}$ = -0.047 l/g | $K_{L\text{-}Pb}$ = -0.065 l/g |
| $R^2$ = 0.982 | $R^2$ = 0.995 | $R^2$ = 0.997 | $R^2$ = 1.00 |

It is also noticeable that the $R^2$ values are near to unity (0.982, 0.995, 0.997 and 1.00 for Pb(II), Cu(II), Cd(II) and Zn(II) ions). Apparently the Cu(II), Cd(II), Pb(II) and Zn(II) uptakes are underestimated as the magnitude of the adsorption capacities (Table 6.11: 20.058, 19.233, 83.279 and 4.343 mg/g) are lower than the single metals system (Table 6.3 for Cu(II): 58.90 mg/g, Table 6.4 for Cd(II): 35.667 mg/g, Table 6.5 for Pb(II): 117.311 mg/g and Table 6.6 for Zn(II): 38.441 mg/g). Similar findings are found in literature (Papageorgiou et al., 2009; Şengil and Özacar, 2009; Xue et al., 2009).

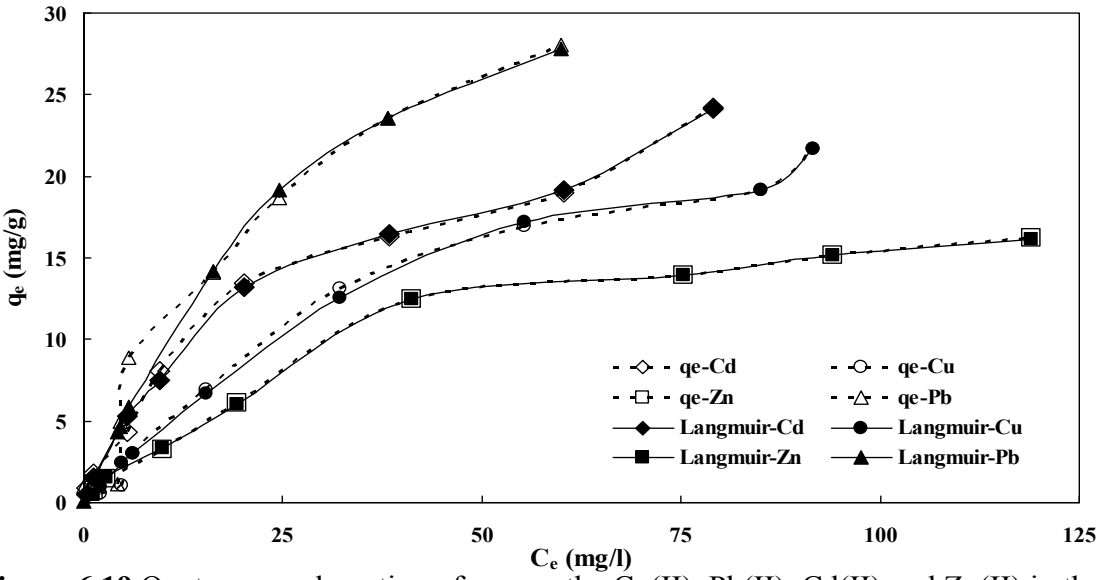


**Figure 6.19** Quaternary adsorption of among the Cu(II), Pb(II), Cd(II) and Zn(II) in the four metals system of Cd(II)-Pb(II)-Cu(II)-Zn(II).

The parameter of Langmuir isotherm, $K_L$ indicates the affinity between a biosorbent and metals ions. The greater the value of these parameters, the lesser is the affinity for a metal ion (Kusvuran et al., 2012; Şengil and Özacar, 2009). It is noticeable that the value of $K_{L\text{-}Cu}$, $K_{L\text{-}Pb}$, $K_{L\text{-}Zn}$, and $K_{L\text{-}Cd}$ predicted from multimetals system are lower than the value of single metal systems (Tables 6.3, 6.4, 6.5 and 6.6). This means that the affinity of BP for metal ions was still strong in a multi-metals metal system. The monolayer adsorption capacities ($q_m$) are higher than the values from multi-metals uptake (Table 6.11). Banana peels have greater affinity towards all metals ions (Cu(II), Cd(II), Pb(II) and Zn(II)) in the multimetals system.

### 6.2.7.1 Antagonism among metals ions

The multi-metals isotherm shows a logical agreement to the multi-metals adsorption data as long as the $q_m$ values for each metal calculated from single-metal are similar to multi-metals systems (Leyva-Ramos et al., 2001). However, the prediction for $q_m$ values

from a quaternary system are lower than single metals system and similar results found in literature (Kumar et al., 2008; Şengil and Özacar, 2009). The internal competition to be uptaken by biosorbent among the metals' ions is known as antagonism. Real wastewater is a mixture of several metals matrices and antagonism frequently happens (Raize et al., 2004). To understand the antagonism in real wastewater an equilibrium isotherm was conducted for the quaternary system. To visualise the antagonism among the four metals surface diagram was constructed and plotted in Figure 6.20 (a, b, c and d).

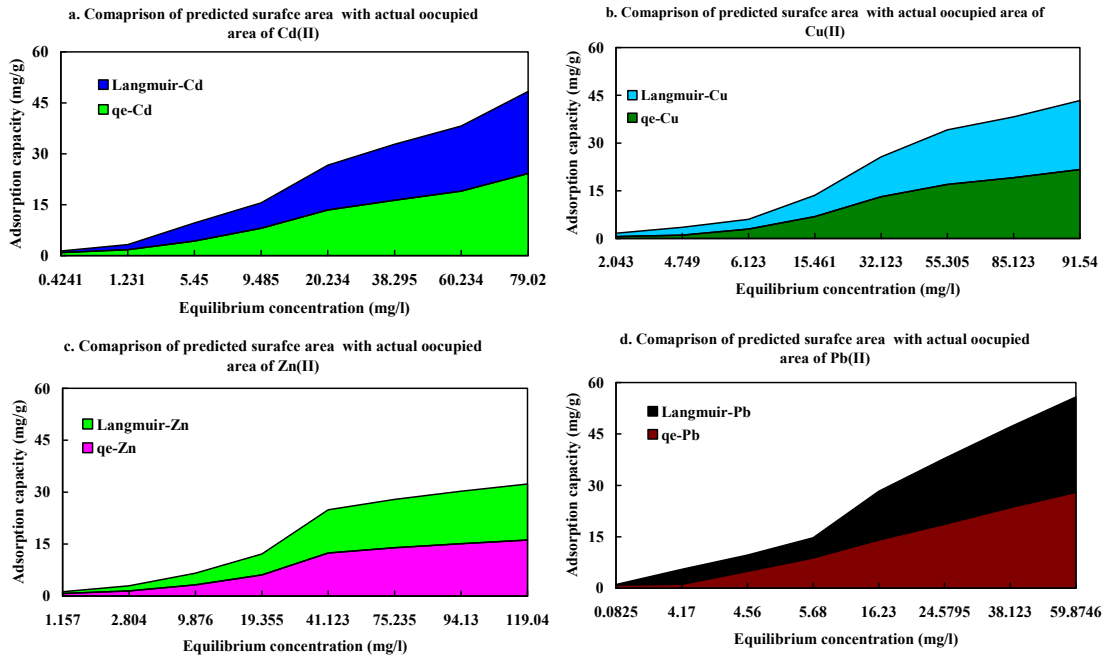


**Figure 6.20** Experimental and model predicted surface areas in terms of adsorption capacity of metals in surface diagram for quaternary metals adsorption onto BP.

The Pb(II) ions posed a stronger affinity towards BP than the Cu(II), Cd(II) and Zn(II) ions and the affinity increased with the increasing of equilibrium concentration of Pb(II) (Figure 6.20(d)). The Pb(II) ions presented strong antagonism against the adsorption of Cu(II), Zn(II) and Cd(II) ions in the quaternary system. A single metal system cannot pose this behaviour. When comparing the data in Figure 6.20 (a, b, c and d) it is found that Pb(II) ions took higher surface areas than other metals. In other word the most binding sites of BP are occupied by Pb(II) ions in a competitive system (Raize et al., 2004; Şengil and Özacar, 2009). The occupied surface area increases with the increases of metals concentration in the quaternary system (Figure 6.20). The model predictions

are similar to the experimental values as the both surface are nearly equal in magnitude for all four metals.

BP has posed superior attraction toward the Pb(II) ions because it occupies the higher spiral surface of the radar plot (Figure 6.21) and similar to other observations predicted in the literature (Apiratikul and Pavasant, 2006; Raize et al., 2004). Figure 6.21 reveals that Cd(II) and Cu(II) ions have similar antagonism as they engage in equal areas of BP. It is noticeable that Zn(II) ions showed the lowest amount of affection towards BP (Padilla-Ortega et al., 2013; Şengil and Özacar, 2009).

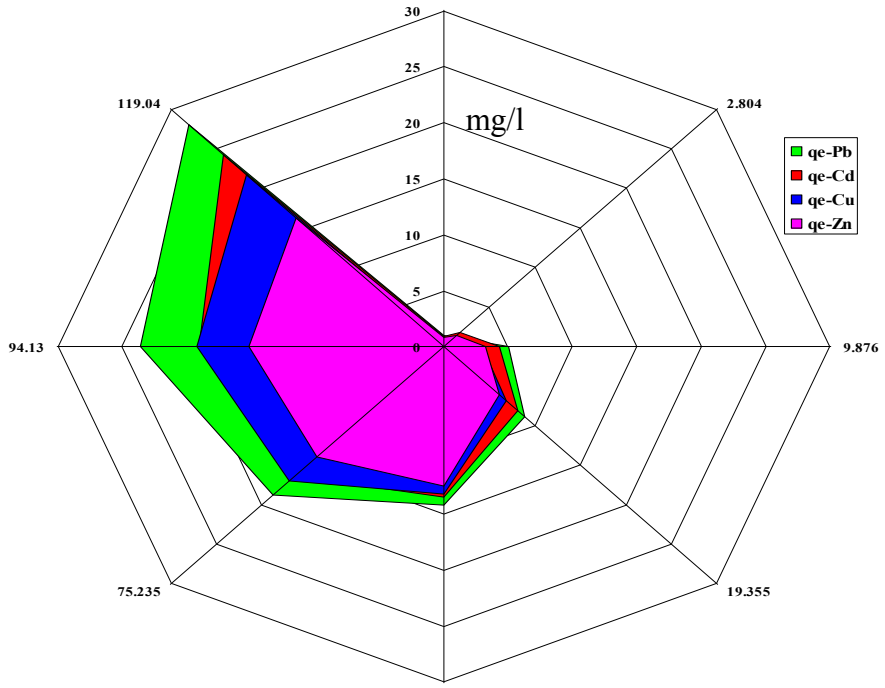


**Figure 6.21** Engaged area in terms of capacity of metals in radar diagram for quaternary metals adsorption onto BP.

It was also found that Pb(II) ions was dominated to be uptaken by BP in preference to Cu(II), Cd(II) and Zn(II) ions. The Pb(II) uptakes were reduced to only 29.01%, whereas Cd(II), Cu(II) and Zn(II) ions uptake is decreased to 46.08%, 64.52% and 88.70% in quaternary systems. Zn(II) ions faced the highest suppression compared to other metals. It was found that in a single metal system the Pb(II) uptake was in the first level (117.311 mg/g) in comparison to Cu(II) (58.90 mg/g : second), Zn(II) (38.441 mg/g: third) and Cd(II) (35.667 mg/g: fourth). It also dominated in quaternary systems. Thus, it can be deduced that BP had higher affinity to Pb(II) ions than Cd(II), Cu(II) and

Zn(II) which could not pose enough antagonism to decrease the adsorption of Pb(II) ions. Besides this they were suppressed (Niu et al., 2013; Xue et al., 2009).

### 6.3 Conclusion

Banana peels are a low cost and readily available material for preparing biosorbents. This study has explored that economically viable biosorbent for Cu(II), Cd(II), Pb(II) and Zn(II) removal from water. The banana peels could be regenerated and reused seven times without reducing efficiency. The data from adsorption and desorption equilibrium were well fitted with five isotherm models with showing a significant degrees of fitness ($R^2 \approx 0.999$). The Langmuir model predicted the maximum equilibrium adsorption and desorption capacities from a 1g dose and the values found are higher than some biosorbents. The kinetics of adsorption of Cu(II), Cd(II), Pb(II) and Zn(II) onto banana peels could follow pseudo-first-order, pseudo-second-order and Avrami equations. The adsorption mechanisms are physio-sorption and chemisorption and the adsorption processes are rate controlling.

Desorption processes were also well fitted with kinetics models. The reuse of banana peels was viable as the desorption study revealed. Hence, the banana peels based biosorbent can be a favourable alternative for metals removal from water and wastewater.

Faculty of Engineering and Information Technology
University of Technology, Sydney (UTS)

# Chapter 7

# Maple leaves: a bio-waste for removal of Cu(II), Pb(II), Cd(II) and Zn(II) from aqueous solution

## 7.1 Background

The lignocellulosic solid wastes generated from agricultural, plantation and forestry sectors have been emphasized as an alternative potential biosorbent for the removal and recovery of heavy metal ions from the waters and wastewaters (Demirbas, 2008). A wide variety of agricultural waste materials such as modified EFB of palm oil (Ibrahim et al., 2010), meranti sawdust (Rafatullah et al., 2009a), Olive tree pruning waste (Blázquez et al., 2011), Nordmann fir (Kay et al., 2009), Groundnut hull (Qaiser et al., 2009), Green alga (*Ulva lactuca*) biomass (Sarı and Tuzen, 2008), Cotton waste biomass (Riaz et al., 2009), Modified peanut sawdust (Li et al., 2007), Grape stalks (Martínez et al., 2006) and activated carbon prepared from apricot stone (Kobya et al., 2005) and coconut shell (Sekar et al., 2004) are used for heavy metals removal from water as they are low-cost biosorbents.

Maple trees have played a key role in commercial, environmental and aesthetic issues to temperate and polar regions of world (Rahman and Islam, 2009; Witek-Krowiak et al., 2010). Maple wood has a great demand for flooring, furniture, interior woodwork, veneer and small woodenware due to its hardness, toughness and other properties. Maple is therefore cultivated timber and roadside decoration (Witek-Krowiak et al., 2010). Consequently, huge quantities of maple leaves (ML) are produced and dumped every year. To date, no commercial uses of maple leaves are found in the world and they create waste management problems. Hence, this study endeavoured to make biosorbent from maple leaves by grinding it into powder.

In this chapter, maple leaves powder (ML) was evaluated for its ability to adsorb Pb(II), Cd(II), Cu(II) and Zn(II) ions from aqueous solutions. It was characterised by FTIR, BET, SEM and X-ray mapping. The effect of contact time, pH of the solution, initial concentration of metals ions and dosage of the adsorbents, particle sizes and temperature on the removal of Pb(II), Cd(II), Cu(II) and Zn(II) ions were studied. Adsorption and desorption isotherm and probable mechanism of biosorption were investigated. It is also determined the kinetics characteristics of Pb(II), Cd(II), Cu(II) and Zn(II) adsorption and desorption on the surface of maple leaves.

## 7.2 Results and Discussion

### 7.2.1 Characterisation of biosorbent

The characterisations of biosorbents and biosorbent processes involve exploring the surface properties, active functional groups and adsorption mechanism. It is an important step for biosorbents in the context of uses for selectivity of metals' ions, exploring binding sites and discovering functional groups for ion exchange or chemisorption. In this context, the ML was characterised by SEM, FTIR and BET tests.

#### 7.2.1.1 Surface area of ML

The metals adsorption capacity, surface properties and active functional groups of biosorbents can be explored through certain characterisations. Surface area of ML was examined by BET test (Chapter 3, Section 3.3.1.4). BET surface properties are tabulated in Table 7.1.

**Table 7.1** BET characteristics of biosorbent produced from maple leaves.

| Parameter | Methods | Values |
|---|---|---|
| 1. Surface area | BET surface area | 10.94 $m^2/g$ |
| | Langmuir surface area | -38.12 $m^2/g$ |
| 2. Pore Area | | |
| i. Micropore area | DR method | 3.53 $m^2/g$ |
| | t-plot (statistical thickness = 3.50~7.00) | -2.36 $m^2/g$ |
| | Horvath-Kawazoe method | 0.58 $m^2/g$ |
| ii. Mesopore area | BJH adsorption | 14.88 $m^2/g$ |
| | BJH desorption | 26.31 $m^2/g$ |
| 3. Pore Volume | | |
| i. Micropore volume | DR method | 0.00 $cm^3/g$ |
| | t-plot (statistical thickness = 3.50~7.00) | -0.00 $cm^3/g$ |
| | Horvath-Kawazoe method | 0.00 $cm^3/g$ |
| ii. Mesopore volume | BJH adsorption | 0.02 $cm^3/g$ |
| | BJH desorption | 0.04 $cm^3/g$ |
| 4. Pore Size | | |
| i. Micropore size | DR method | 8.71 Å |
| | t-plot (statistical thickness = 3.50~7.00) | 36.14 Å |
| | Horvath-Kawazoe method | 14.38 Å |
| ii. Mesopore Size | BJH adsorption | 41.46 Å |
| | BJH desorption | 32.44 Å |

The BET surface area of ML is 10.94$m^2/g$ which was comparable with the biosorbents produced from agro wastes and used for metals removal from aqueous solution (Hossain et al., 2012b). The total pore volume of the ML's powder was 0.02 $cm^3/g$ and most of the pore volume was mesopore (100%). In addition, the mean micropore and mesopore sizes of the ML were found to be 8.71 and 41.46 Å, respectively, suggesting

that this biosorbent was fallen within the definition of *mesopore* based on International Union of Pure and Applied Chemistry (IUPAC) classification (Arias et al., 2005). The high pore area, pore volume and pore sizes are indicated in the numerous binding sites on the ML surfaces (Lu et al., 2010).

#### 7.2.1.2 Surface morphology

The surface structure of ML was analysed using a scanning electron microscope (SEM) with different magnifications (according to Chapter 3, section 3.3.1.1). The micrograph prepared by SEM showed in Figure 7.1 (A, B, C and D) and it revealed some significant feature of structures. It is noticed from lower magnification that asymmetrical and irregular sized particles are present in the ML (Figure 7.1 A). It is also become more visible at higher magnification (Figure 7.1 B). The micro-graphs at further magnification reveal the presence of rough surfaces of ML particles (Figure 7.1 C).

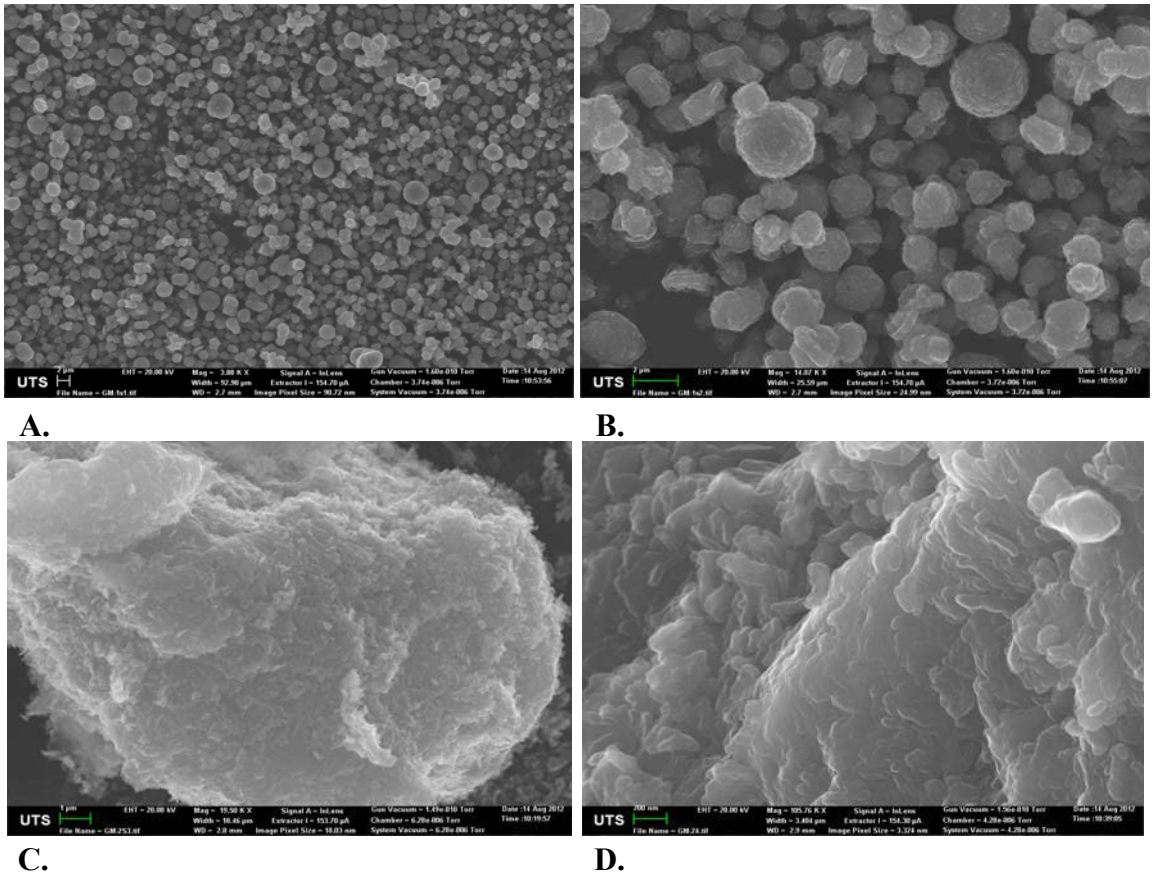


**Figure 7.1** SEM micrograph of ML with different magnifications (A. 3KX, B. 14 KX, C. 19.5 KX and D. 105 KX).

A ML particle's surface made from nodule like structures and presence spaces between two nodules which is clearly visible from higher magnification (Figure 7.1 D). Similar findings are found for other biosorbents in the literatures (Lü et al., 2010). This signifies

the high internal surface area or binding sites of the ML which are responsible for high metals adsorption (Chen et al., 2011).

### 7.2.1.3 X-ray mapping

The metals loaded ML were examined by SEM and an X-ray mapping were prepared. It is shown in Figure 7.2 (according to Chapter 3, section 3.3.1.2). A significant visual change was noticed on the surface of ML exhausted with lead when compared to normal MLs' SEM-image. The particles of biosorbents (Figure 7.2 (a)) are irregular, tubular and rough, indicating the presence of high surface area and pore volume (Chen et al., 2011). These large pores and surface areas are important factors that could lead to high uptakes of metals ions in this study. A significant visual transformation (filled dark spaces between the particles) is noticed on the surface of biosorbents exhausted with lead when compared to the images of (Figure 7.2 (a)) and (Figure 7.2 (b)).

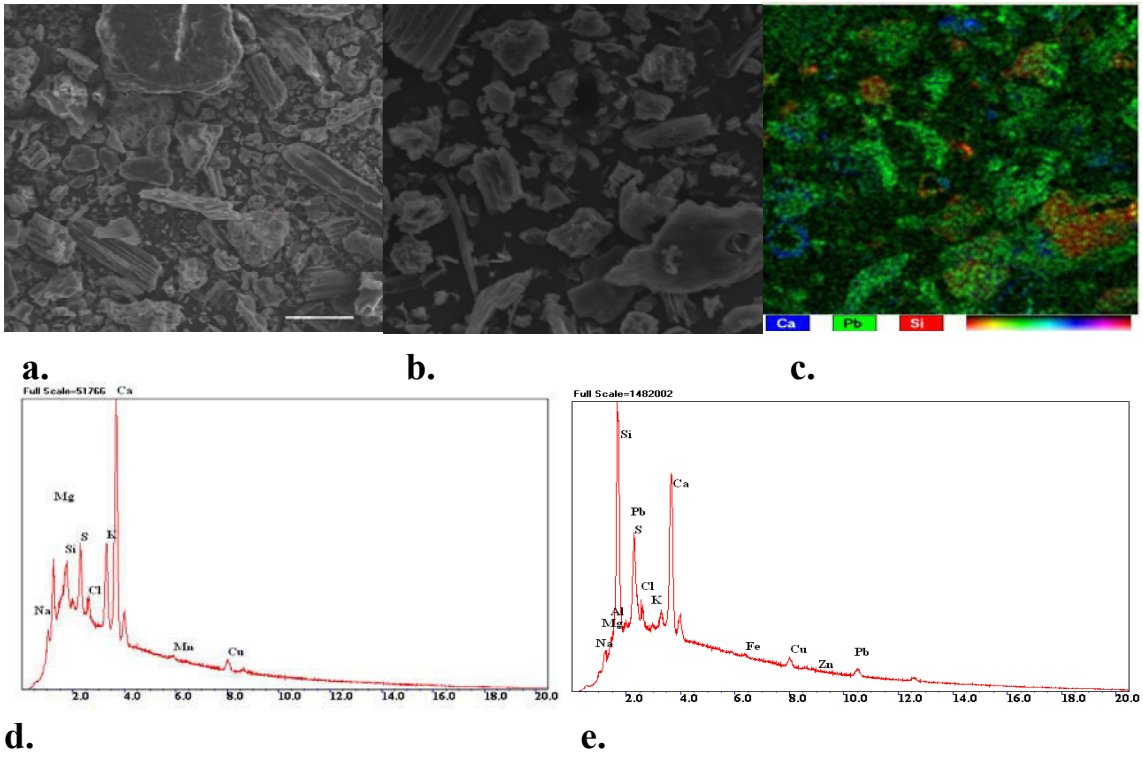


**Figure 7.2** SEM micrograph 150× (HWOF=600µm) (a) Maple leaves (b) Maple leaves exhausted with lead (c) X-ray mapping of maple leaves exhausted with lead (d) Spectra of maple leaves (e) Spectra of maple leaves exhausted with metals.

The green dots are the adsorbed Pb(II) onto the surface of biosorbents (Figure 7.2 (c)) and show the affinity of Pb(II) onto ML. The presence of adsorbed Pb(II), Cu(II) and Zn(II) becomes clear from elemental XRD spectra of exhausted ML (Figure 7.2.e) while

comparing the spectra from normal ML (Figure 7.2 d). Similar results are reported in the literature (Mohapatra et al., 2009; Zhang et al., 2010; Zuo et al., 2012). The XRD spectrum of maple leaves shows the constituents' elements of maple leaves like Na, Mg, Ca, K, S, Cl etc.

### 7.2.1.3 Functional groups

Functional groups were the influencing parameters of metals adsorption onto biosorbents. The functional groups that are present in ML are studied by Fourier transform infrared spectroscopy (FTIR). FTIR spectra for maple leaves powder (ML) is shown in Figure 7.3.

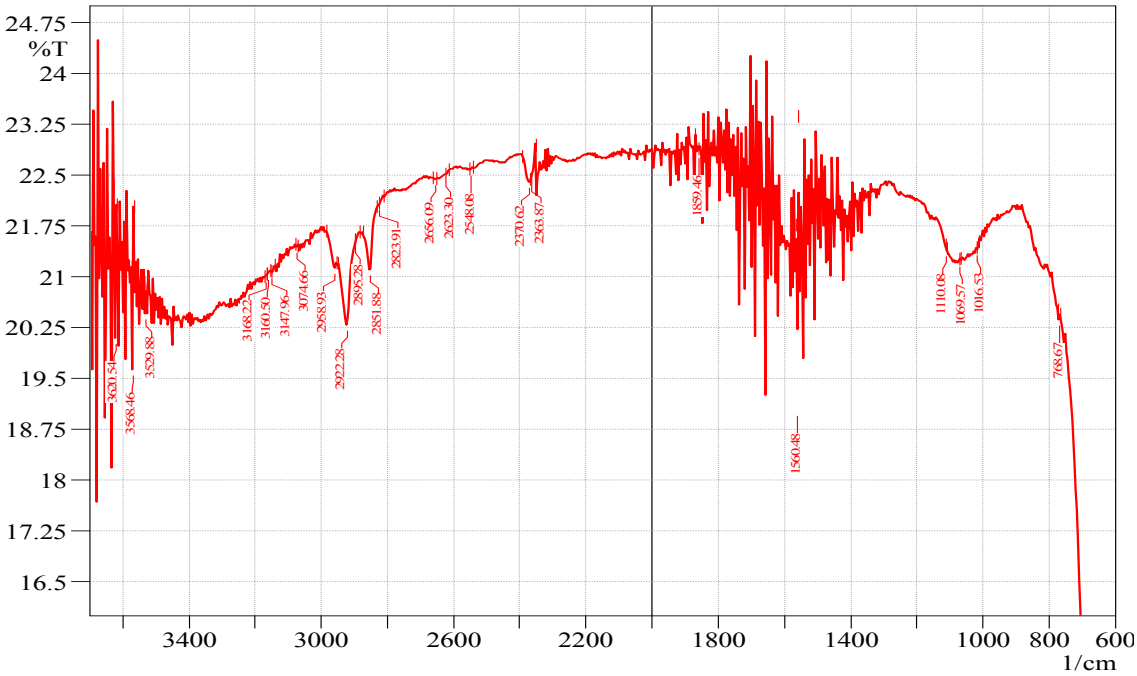


**Figure 7.3** The Fourier transforms infrared spectroscopy (FTIR) spectra of maple leaves powder (ML).

The major functional groups found from spectra were O-H stretch-free hydroxyl for alcohols/phenols (3624.54 $cm^{-1}$), O-H stretch for carboxylic acids (between 3300-2500 $cm^{-1}$), C-N stretch for aliphatic amines (1024.25$cm^{-1}$), C-O stretch for alcohols/carboxylic acids/esters/ethers (between 1320-1000 $cm^{-1}$), =C-H bend for alkanes (between 1000-650 $cm^{-1}$) and C-H "OOH" for aromatics (817.85$cm^{-1}$) (Pons et al., 2004). The behaviour of carbon-oxygen bonds and carbon bonds on the surface of the biosorbents attract and stimulate the metal's adsorption (Ricordel et al., 2001). Functional groups like hydroxyl and carboxyl groups could able to bind with cations of

metal's ions (Hanafiah et al., 2006; Lopes et al., 2005; Rahman and Islam, 2009; Witek-Krowiak et al., 2010; Yu et al., 2003).

### 7.2.2 Affecting factors on the performance of biosorption

The experimental conditions such as pH, particle sizes, doses, contact time, thermal effect on the adsorption of Pb(II), Cd(II), Cu(II) and Zn(II) were investigated for maple leaves (ML) according to Chapter 3, Section 3.3.2.

#### 7.2.1.1 Influence of pH

The pH value is one of the most influential parameters which affects the adsorption behaviour of metal ions from aqueous solutions. The influence of pH on the adsorption of Pb(II), Cd(II), Cu(II) and Zn(II) ions were studied within the range of pH 2.0-9.5 (Chapter 3, section 3.3.2.1) and the results are presented in Figure 7.4. At the beginning of adsorption processes, the uptake of Pb(II), Cd(II), Cu(II) and Zn(II) ions increases with an increase of pH. Similar results are also reported in the literature for various biomass (Anwar et al., 2010). A sharp increase in the biosorption occurred for all four metals in the pH range 2.5 to 4.5.

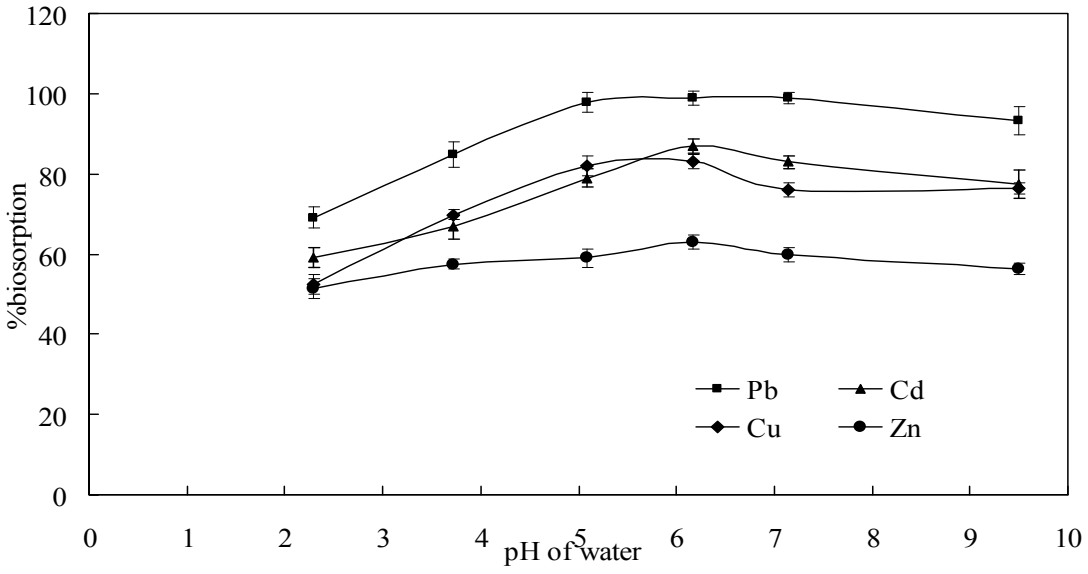


**Figure 7.4** Effect of pH on the removal of Pb(II), Cd(II), Cu(II) and Zn(II).

The maximum biosorption was found to be 98.99% for Pb(II), 86.99% for Cd(II), 82.67% for Cu(II) and 63.12% for Zn(II) ions between pH 6 to 6.5. Therefore, all the biosorption experiments were carried out between pH 6.0-6.5. At pH values higher than pH 6.5, metal ions precipitated and biosorption studies at these pH values could not be performed (Romera et al., 2008). At low values of pH the decrease in the removal

efficiency could be due to the fact that the mobility of the hydrogen ($H^+$) ions is higher than that of the metal ions and it reacts with active sites before adsorbing the metal ions (Akbar et al., 2010).

### 7.2.1.2 Influence of biosorbent and initial metals concentrations

The optimisation to determine the best doses of biosorbent for adsorptions of Pb(II), Cd(II), Cu(II) and Zn(II) ions was accomplished with five initial metals concentrations (1-15 mg/l) and between 0.01 to 3 g doses (Chapter 3, section 3.3.2.2). The adsorption results are plotted in Figure 7.5 (a, b, c and d). It is generally found that the removals are low at lower concentration (1, 2.5 and 5 mg/l) and lower doses (0.01, 0.02 and 0.5 g/l). In low metals concentrations there are not enough available of ions to be uptaken by biosorbent (Sanchez-Viveros et al., 2010). For low doses the binding sites are occupied by metals ions quickly and as a result there is no further uptake (Singh et al., 2008).

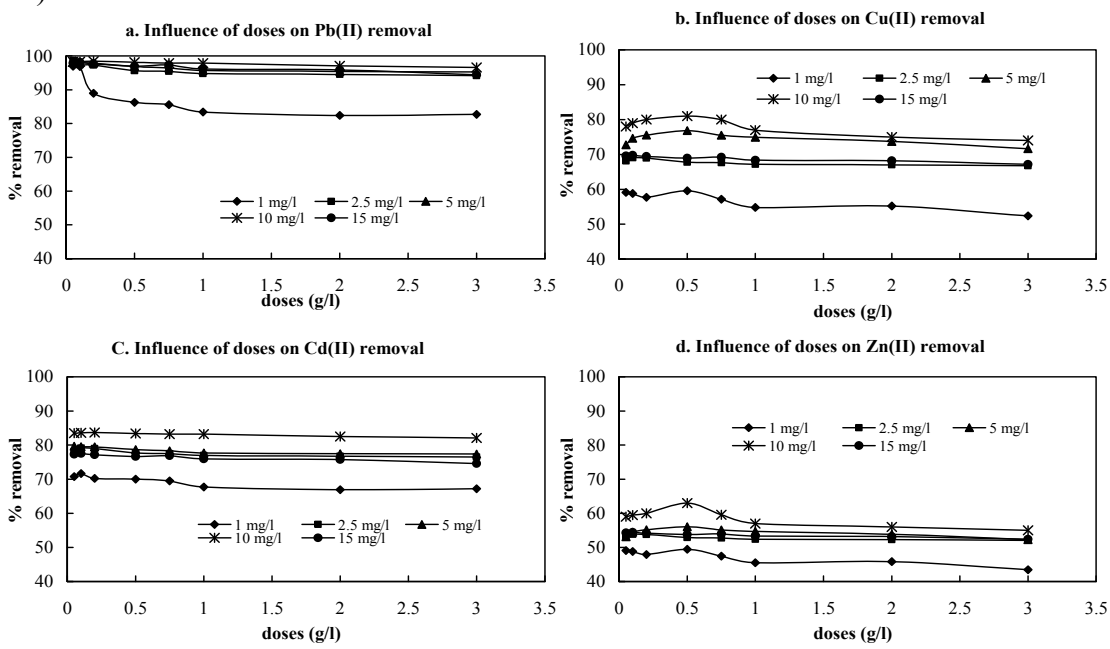


**Figure 7.5** Effect of ML doses on the removal of Pb(II), Cd(II), Cu(II) and Zn(II).

On the other hand, higher metals concentration and doses also showed low removal. This may happen due to lack of binding sites for higher metals concentration and shortage of ions for higher doses (Apiratikul and Pavasant, 2008; Aydin et al., 2008; Grimm et al., 2008). Among the five initial lead concentration 10 mg/l showed higher removals, 98.2% for Pb(II), 81% for Cu(II), 84% for Cd(II) and 64% for Zn(II) ions than other concentrations used. Among the doses, 5g/l resulted in higher removal for

Pb(II), Cd(II), Cu(II) and Zn(II) ions. Therefore, the selection was that of 0.5g ML for 100 ml (5g/l) of water and 10 mg/l of metals for the other studies.

### 7.2.1.3 Influence of contact time and initial concentration

The contact time affected the extent of adsorption of metals ions. The experiment for the effect of contact times are conducted in 5 initial metals concentrations (10, 25, 50, 100 and 200 mg/l) according to Chapter 3, section 3.3.2.4. Figure 7.6 (a, b, c and d) shows the variation in the extent of adsorption capacity (mg/g) of Pb(II), Cd(II), Cu(II) and Zn(II) ions onto ML at room temperature. As it can be seen from Figure 7.6 (a, b, c and d), the amount of the adsorbed Pb(II), Cd(II), Cu(II) and Zn(II) onto ML increases with time and initial metals concentrations. After some point of time, it reaches a constant value beyond which no more metals ions are removed from solution.

The time required to attain these states of equilibrium is termed as equilibrium time and the amount of metals adsorbed at the equilibrium time reflects the maximum adsorption capacity under those operating conditions. The rapid adsorptions were found in the initial stages of adsorption processes. This may be explained by a rapid adsorption on the outer surface, followed by slower adsorption inside the pores (Bulgariu and Bulgariu, 2012; Chen et al., 2011). The second stage was much slower than the first and reached equilibrium after 5, 5, 6, 15 and 20 min for 10, 25, 50, 100 and 200 mg/l Pb(II) concentration, respectively.

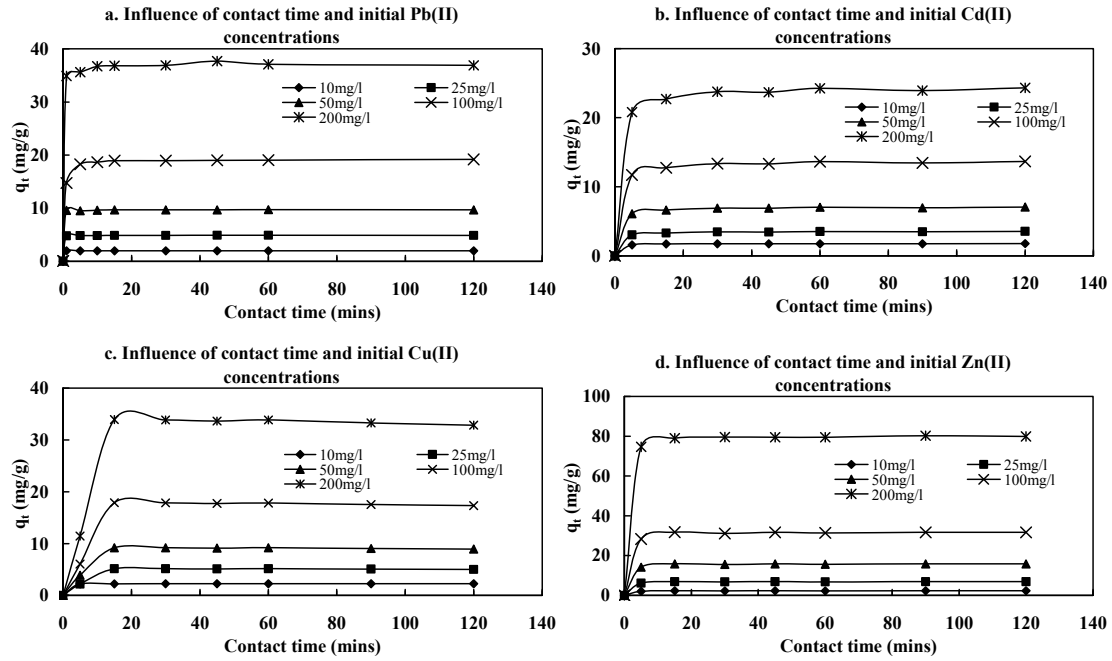


**Figure 7.6** Effect of contact time and initial Pb(II), Cd(II), Cu(II) and Zn(II) concentrations.

Similarly the Cd(II) adsorption reached equilibrium at 5, 10, 15, 30 and 40 minutes for 10, 25, 50, 100 and 200 mg/l concentration, respectively. The equilibrium was a little bit slower for Cu(II) and it is reached equilibrium at 10, 30, 40, 45 and 50 minutes for the same initial concentrations. But Zn(II) adsorption followed the same trend as Pb(II) and Cd(II) and showed equilibrium values after 5, 5, 10, 15 and 25 minutes for 10, 25, 50, 100 and 200 mg/l concentration, respectively. Similar results are reported for other biosorbents (Areco et al., 2013; Gorgievski et al., 2013; Kizilkaya et al., 2013; Ronda et al., 2013; Witek-Krowiak, 2012). This rapid kinetics has an important practical potentiality in developing of metal biosorption system with maple leaves (Montazer-Rahmati et al., 2011).

#### 7.2.1.4 Influence of particle sizes

Adsorption isotherms of Pb(II), Cd(II), Cu(II) and Zn(II) ions onto four particle sizes of ML are shown in Figure 7.7 (a, b, c and d). It is noticed from figure that the amount of metals ions adsorbed was higher for small particle sizes than large particles. The isotherm parameters of $q_m$ and K were calculated by Langmuir model and tabulated in Table 7.2 for all four metals. It was apparent that $q_m$, the monolayer coverage for each particle size, increased from 26.5957 to 60.9756 mg/g for Pb(II); 24.216 to 51.768 mg/g for Cd(II), 18.518 to 44.836 mg/g for Cu(II) and 18.837 to 38.519 mg/g for Zn(II) with decreasing particle size from 300 to <75 μm. This trend might indicate that small particle sizes have the larger specific surface area which might bind more metals (Schiewer and Volesky, 2000). For larger particles, the diffusion resistance to mass transport is high and most of the internal surface of the particle may not be utilized for adsorption. Consequently, the amount of Pb(II) adsorbed is small (Patil et al., 2011). Similar trends have been seen in adsorption of metals onto other biosorbents (Anwar et al., 2010).

The specific surface areas (S) of ML are calculated for all used metals using the following equation (Ho et al., 2002) and the results are shown in Table 7.2:

$$S = \frac{q_m . A . N_A}{M_A} \qquad (7.1)$$

where S is the specific surface area of ML ($m^2/g$), $q_m$ the monolayer adsorption capacity (mg/g), $N_A$ the Avogadro number ($6.02\times10^{23}$/mol), 'A' the cross-sectional area of metals ion ($m^2$) and 'M' is the molecular weight of metals. For $Pb^{2+}$ ion, the molecular

weight was 207.2 g/mol and the cross-sectional areas of $Pb^{2+}$ were determined to be 24062.5 $pm^2$ ($Pb^{2+}$ radius was 175 pm (pico meter and 1 pm = $1\times10^{-12}$ m)) in a close packed monolayer. Hence, the specific surface area was calculated for $Pb^{2+}$ (Table 7. 2) and it was found that the maximum specific surface area of ML (4.263 $m^2/g$ for <75µm particle size) was lower than the BET surface area (Table 7.1).

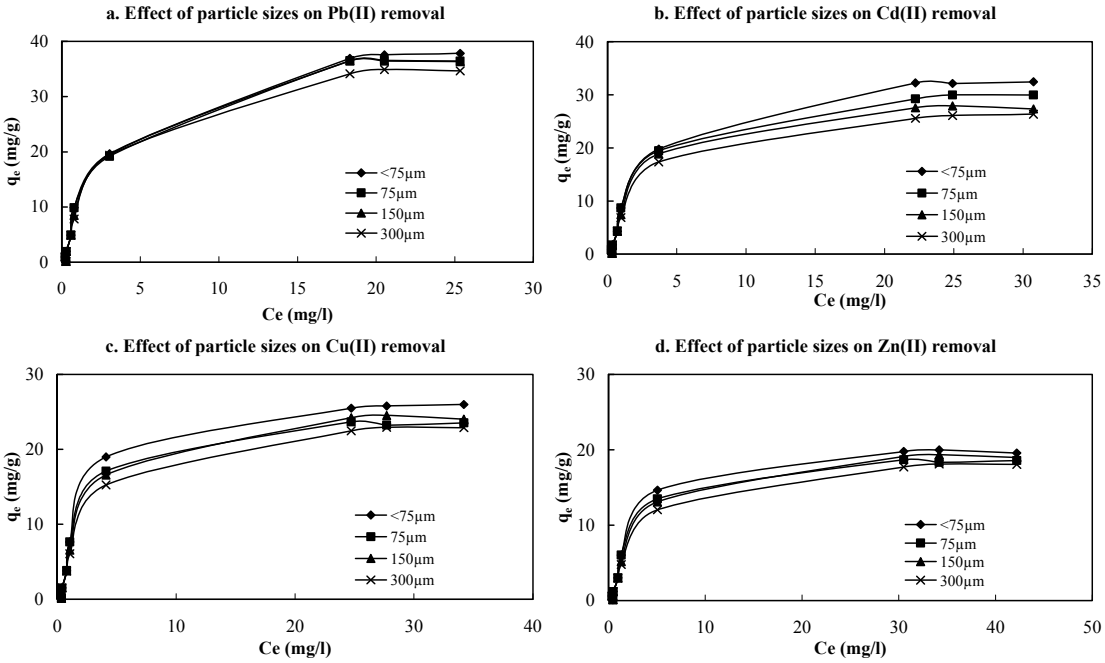


**Figure 7.7** Effect of particle sizes of ML on removal of Pb(II), Cd(II), Cu(II) and Zn(II) ions.

**Table 7.2** Effects of particle sizes of ML for Pb(II), Cd(II), Cu(II) and Zn(II) adsorption

| Metals | Particle size (µm) | Langmuir Isotherm | | | Surface area of particle ($m^2/g$) |
|---|---|---|---|---|---|
| | | $q_m$ (mg/g) | K (l/mg) | $R^2$ | |
| **Pb(II)** | 300 | 26.595 | 0.182 | 0.949 | 1.859 |
| | 150 | 41.428 | 0.106 | 0.993 | 3.194 |
| | 75 | 39.525 | 0.209 | 0.983 | 2.763 |
| | <75 | 60.976 | 0.308 | 0.983 | 4.263 |
| **Cd(II)** | 300 | 24.216 | 0.188 | 0.998 | 1.509 |
| | 150 | 33.252 | 0.191 | 0.989 | 2.953 |
| | 75 | 36.206 | 0.681 | 0.993 | 2.999 |
| | <75 | 51.768 | 0.964 | 0.996 | 3.789 |
| **Cu(II)** | 300 | 18.518 | 0.437 | 0.998 | 1.592 |
| | 150 | 32.027 | 0.799 | 0.994 | 2.792 |
| | 75 | 31.601 | 0.577 | 0.976 | 2.699 |
| | <75 | 44.836 | 0.928 | 0.997 | 3.938 |
| **Zn(II)** | 300 | 18.837 | 0.188 | 0.998 | 1.565 |
| | 150 | 27.860 | 0.696 | 0.987 | 2.787 |
| | 75 | 29.717 | 0.367 | 0.998 | 1.797 |
| | <75 | 38.519 | 0.987 | 0.999 | 2.993 |

For Cu(II) ion, the molecular weight was 63.5 and the cross-sectional areas of Cu(II) were determined to be $1.58\times10^{-18}$ $m^2$ ($Cu^{2+}$ radius is 1.57 Å and 1 angstrom = $1.0 \times 10^{-10}$ metres) in a close packed monolayer (Wong et al., 2003). The specific surface areas of ML was calculated (Table 7.2) and the maximum specific surface area of ML was 44.836 $m^2/g$ for <75 μm particle size which is lower than BET surface area (Table 7.1). Similarly the occupied surface area by Cd(II)[ atomic radius: 1.71 Å] and Zn(II)[ atomic radius: 1.53 Å] are calculated and tabulated in Table 7.2. For both metals, the calculated surface areas are lower than the BET surface areas (Table 7.1).

### 7.2.1.5 Biosorption thermodynamics

Temperature is considered as a stimulating agent for any biosorbent because it affects the molecules, functional groups and surface morphology of the biosorbent and metals during biosorption processes. Temperature variation experiments were conducted at 30, 40, 50 and 70°C, with initial Pb(II), Cd(II), Cu(II), and Zn(II) concentrations between 1-200 mg/l and with 0.5g per 100 ml water for exploring the effects on metals adsorption onto ML. From the data the thermodynamic parameters such as Gibbs free energy (ΔG°), enthalpy change (ΔH°), and entropy change (ΔS°) were calculated. The magnitude of ΔG° (kJ/mol) was calculated using the following equation:

$$\Delta G^{o} = -RT\ln K \qquad (7.2)$$

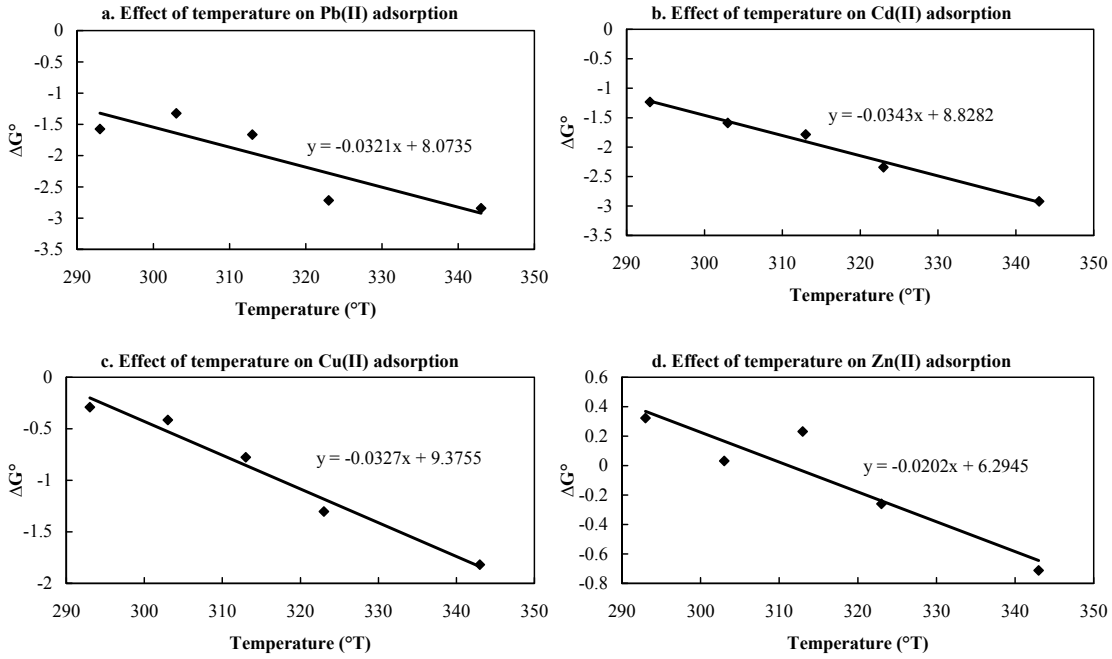


**Figure 7.8** Plots of Gibbs free energy (ΔG°) versus Temperature (°T) for Cu(II), Cd(II), Pb(II) and Zn(II) adsorption onto ML

where, R is universal gas constant, 0.008314 kJ/mol °K; T is absolute temperature (°K) and $K_a$ the sorption equilibrium constant from Langmuir isotherm and ΔH° (kJ/mol) was calculated by the following equation:

$$\Delta H^o = \Delta G^o + T\Delta S^o \qquad (7.3)$$

A linear plot found from ΔG° versus T plotting (Figure 7.8). The values of ΔH° and ΔS° are calculated from the slope and intercept of linear equation showed in Figure 7.8.

The thermodynamic parameters calculated by Langmuir isotherm are shown in Table 7.3. The ΔG° values were negative in nature (-ve) for the used four metals and reveals the adsorption process was spontaneous in nature (Dogar et al., 2010; Hristodor et al., 2010; Memon et al., 2008). The values of ΔG° decreased with increases of temperature from 30 to 70°C. The positive value of ΔH° (for all metals : Table 7.3) indicated that the adsorption reaction was endothermic and has strong affinity of ML towards Cu(II), Pb(II), Cd(II) and Zn(II) ions. This result also suggested some structural changes occurred in metals' ions and maple leaves (Gupta and Rastogi, 2008).

**Table 7.3** Thermodynamic parameters for the adsorption of Pb(II), Cd(II), Cu(II) and Zn(II) ions by ML.

| Metals | Temp. (°K) | ΔG° (kJ/mol) | ΔH° (kJ/mol) | ΔS° (J/mol°K) |
|---|---|---|---|---|
| **Pb(II)** | 293 | -1.574 | -0.321 | 8.0735 |
| | 303 | -1.324 | | |
| | 313 | -1.665 | | |
| | 323 | -2.716 | | |
| | 343 | -2.841 | | |
| **Cd(II)** | 293 | -1.234 | -0.0343 | 8.8282 |
| | 303 | -1.589 | | |
| | 313 | -1.785 | | |
| | 323 | -2.342 | | |
| | 343 | -2.922 | | |
| **Cu(II)** | 293 | -0.291 | -0.0327 | 9.3755 |
| | 303 | -0.415 | | |
| | 313 | -0.778 | | |
| | 323 | -1.302 | | |
| | 343 | -1.817 | | |
| **Zn(II)** | 293 | 0.323 | -0.0202 | 6.2945 |
| | 303 | 0.031 | | |
| | 313 | 0.232 | | |
| | 323 | -0.260 | | |
| | 343 | -0.711 | | |

But this was different for Zn(II) adsorption and it produced both positive and negative ΔG° values. It can be presumed that both endothermic and exothermic reaction occurred in Zn(II) adsorption. In addition, the negative value of ΔS° (for all metals : Table 6.2)

also suggested that the adsorption was enthalpy driven and spontaneous in nature (Baker et al., 2010; Fukuoka et al., 2010; Memon et al., 2008; Murphy and Erkey, 1997).

### 7.2.2 Regeneration of maple leaves

The multiple uses of biosorbent depend on regeneration capability. It can decrease the operation cost for water and wastewater treatment systems. The exhausted biosorbent cannot be entirely reversible though it can be reused depending on conditions (Davis and Upadhyaya, 1996). To explore the reusability of ML, eight eluents such as tap water, milli-Q water, distilled water, 0.1N $H_2SO_4$, 0.1N HCl, 0.1N $HNO_3$, 0.1N NaOH and 0.1 N $CH_3COOH$ were used for desorbing the Pb(II), Cd(II), Cu(II) and Zn(II) ions and showed in Figure 7.9.

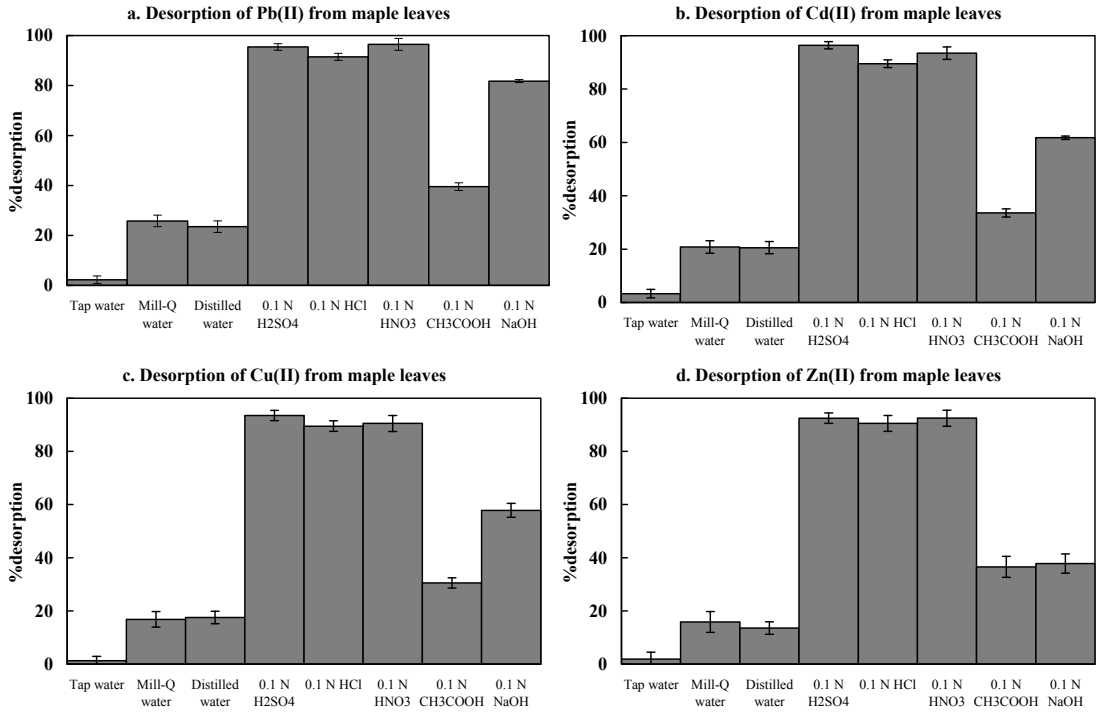


**Figure 7.9** Regeneration of ML from Pb(II), Cd(II), Cu(II) and Zn(II) from adsorption

It was found from Figure 7.9 (a, b, c and d) that small amounts of 0.1N $H_2SO_4$ straightforwardly renovated exhausted ML. The maximum desorption were found at 98.8% of Pb(II), 97% of Cd(II), 92% of Cu(II), and 88% of Zn(II) with 0.1 N $H_2SO_4$ from metal-loaded ML (0.5g). Similar efficiencies for recovering the metals are found from 0.1 N HCl and 0.1 N $HNO_3$. $H^+$ is released in the acidic system and can be

replaced by adsorbed metal cations ($Cu^{2+}$, $Pb^{2+}$, $Cd^{2+}$ and $Zn^{2+}$) on the surface of the ML (Wang et al., 2008; Wei et al., 2009).

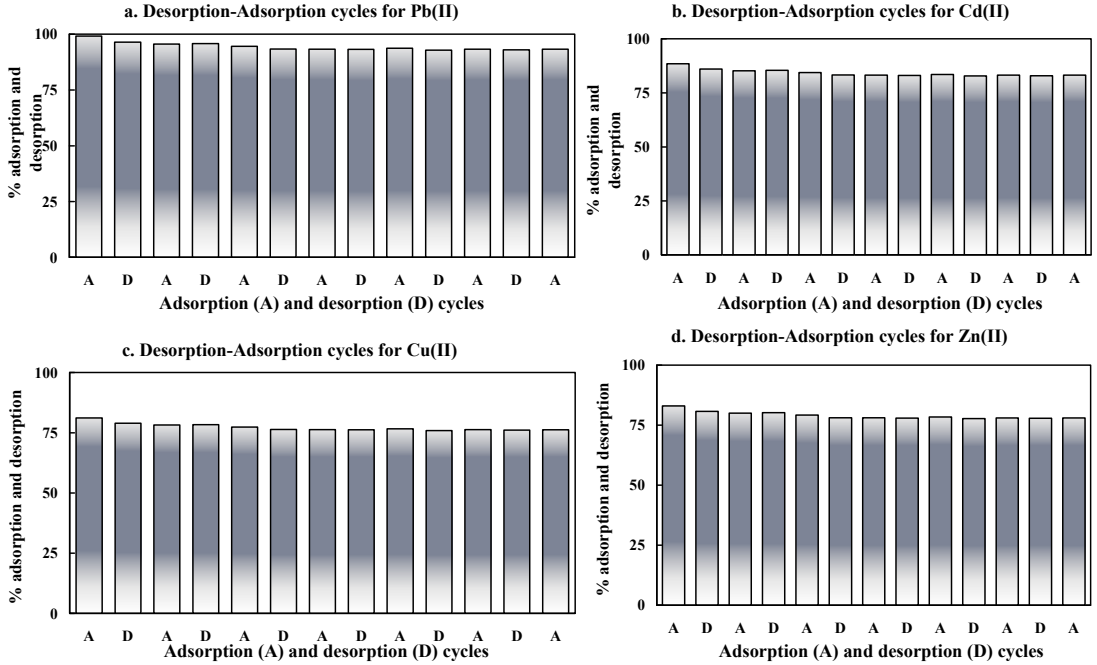


**Figure 7.10** Regeneration cycles of ML from Pb(II), Cd(II), Cu(II), and Zn(II) from adsorption

To investigate the repetitive uses of ML, the adsorption and desorption cycles were repeated seven times with best eluent 0.1N $H_2SO_4$. The results are plotted in Figure 7.10 (a, b, c and d) for Pb(II), Cd(II), Cu(II) and Zn(II) ions desorption and adsorption. Like other biosorbents, the adsorption and desorption efficiency were not increased for ML after the first phase of desorption (Hossain et al., 2012a). It is presumed that acid did not work as a pre-treatment for ML. With the progress of adsorption and desorption processes the regeneration efficiency for ML decreased (Figure 7.10). It is expected that successive acid suspension causes stresses on the ML surfaces and demolished the biding sites. The regenerated ML could be used seven times with minor loss of efficiency.

### 7.2.3 Biosorption and desorption kinetics

Biosorption kinetics are conducted in three initial concentrations (10, 50 and 100 mg/l) for Pb(II), Cd(II), Cu(II) and Zn(II) ions. The desorption kinetics are done with the exhausted biosorbent by 10, 50 and 100 mg/l metals ions (According to Chapter 3, Section 3.3.5). In the kinetics experiment, initial metals concentration is crucial for adsorption. The initial Cu(II), Zn(II), Pb(II) and Cd(II) concentrations used in the

present studies are lower than the kinetics experiments reported in the literature (Vargas et al., 2011).

The kinetic data for both adsorption and desorption were analysed by non-linear analyses (MS Excel 2007) using five different kinetic models, namely Pseudo-first order, Pseudo-second order, Avrami, Elovich and Intraparticle diffusion models. The model fitness is judged by $R^2$, NSD and ARE (Chapter 3, Section 3.4). The model parameters are optimized by non-linear modelling of kinetics model (Appendices II). The estimated kinetics' parameters are shown in Table 7.4 for Pb(II), Table 7.5 for Cd(II), Table 7.6 for Cu(II), and Table 7.7 for Zn(II) adsorption onto 5g/l ML. The experimental data with model's prediction are plotted in Figure 7.11 for Pb(II), Figure 7.12 for Cd(II), Figure 7.13 for Cu(II), and Figure 7.14 for Zn(II) adsorption.

#### 7.2.3.1 Pb(II) biosorption and desorption kinetics

It is clearly found from Figure 7.11 that initially the sorption of Pb(II) ions occurred very rapidly in all metals concentrations and that maximum Pb(II) uptake occurred within the first few minutes of adsorption and reached equilibrium. After an equilibrium time of 20-30min, no additional Pb(II) was adsorbed, suggesting that available sites on the biosorbent are limited to uptake metals ions. The rapid kinetics observed for lead removal by ML has significant practical importance because the kinetics will facilitate smaller reactor volumes, ensuring efficiency and economy (Günay et al., 2007).

Table 7.4 showed the predicted and experimental parameters of kinetics models from adsorption and desorption processes for five models. Generally, the adsorption and desorption kinetics data were well fitted with all models ($R^2 > 0.923$) and the plotting of experimental data and models' prediction data coincided (Figure 7.11). Specifically, the adsorption and desorption data showed better fitness with Pseudo-second-order model than the Pseudo-first-order model (Table 7.4); implying Pb(II) ions adsorption was the rate-controlling step (Ho, 2004). Higher fitness (high $R^2$ and low NSD and ARE values) for Pseudo-second-order model (Table 7.4), obtained from both adsorption and desorption process for the three Pb(II) concentration (10, 50 and 100 mg/l), also reinforced the proposition and argument derived from FTIR spectra (Figure 7.3). Experimental (1.994, 9.720 and 18.954 mg/g for adsorption and 1.219, 6.313 and 13.573 mg/g for desorption) and calculated values (2.027, 9.750 and 19.190 mg/g for

adsorption and 1.199, 6.614 and 13.172 mg/g for desorption) of equilibrium adsorption/desorption capacities ($q_e$) from Pseudo-second-order model are more similar and poses better consistency than the Pseudo-first-order model. Significantly low NSD and ARE values (Table 7.4) were obtained from Pseudo-second-order for both adsorption and desorption processes. These results denoted that the adsorption/ desorption system followed to the Pseudo-second-order kinetics which further advocated that adsorption was the rate-controlling step (Ho, 2004).

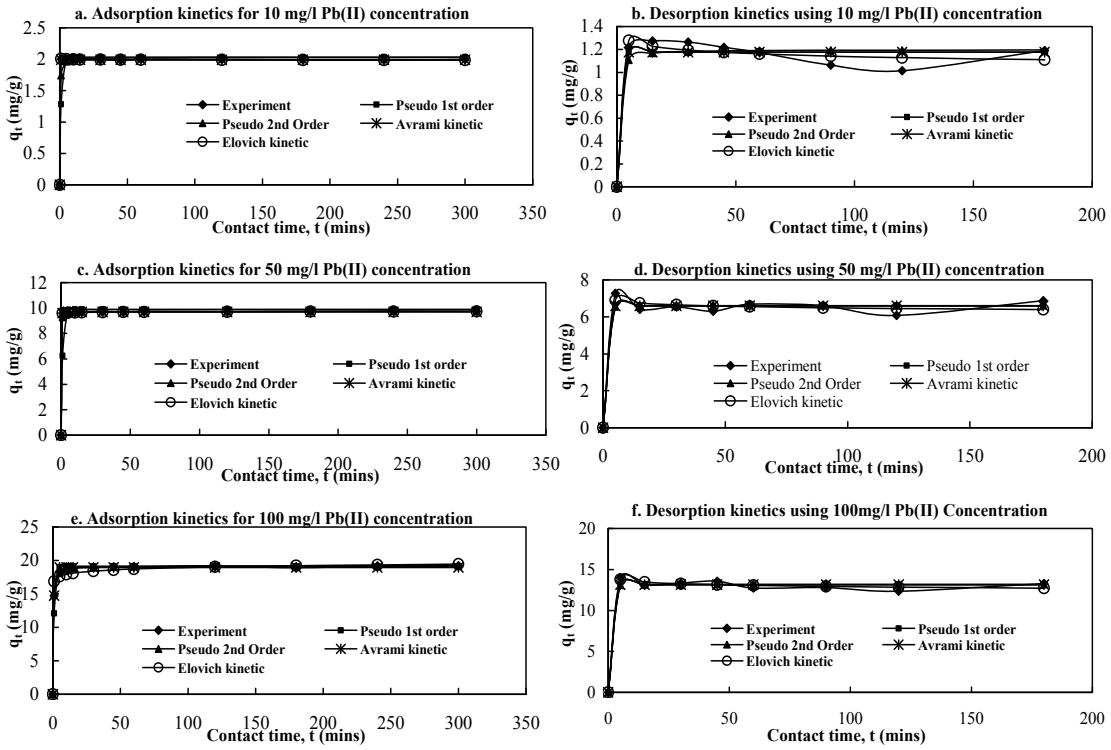


**Figure 7.11** Kinetics modelling of adsorption and desorption of Pb(II) onto maple leaves (Co: 10, 50, 100 mg/l; d: 0.5 g; t: 3 h: pH: 6-6.5; rpm: 120; T: 20°C).

Beside the order equations the data posed a well agreement with Avrami model which determines some kinetic parameters, as possible changes of the adsorption and desorption rates in function of the initial metals concentration and the adsorption/desorption time, as well as the determination of fractionery kinetic orders (Lopes et al., 2003). The overall fitness of this model with experimental data from adsorption and desorption of Pb(II) are excellent as the $R^2$ values lies 1.000, 1.000 and 0.999 for used 10, 50 and 100 mg/l metals concentration, respectively. In addition, the model predicted equilibrium ($q_e$) capacities (1.991, 9.698 and 18.968 mg/g for Pb(II) adsorption and; 1.177, 6.599 and 13.149 mg/g for Pb(II) desorption) are closed to the

experimental equilibrium ($q_e$) capacities (1.994, 9.720 and 18.954 mg/g for adsorption and 1.219, 6.313 and 13.573 mg/g for desorption).

**Table 7.4** Kinetics parameters of Pb(II) adsorption and desorption onto ML

| Kinetic models | Parameters | Adsorption | | | Desorption | | |
|---|---|---|---|---|---|---|---|
| | | Pb(II) concentration | | | Pb(II) concentration | | |
| | | 10mg/l | 50mg/l | 100mg/l | 10mg/l | 50mg/l | 100mg/l |
| Experimental | $q_e$ (mg/g) | 1.994 | 9.720 | 18.954 | 1.219 | 6.313 | 13.573 |
| 1. Pseudo-1st-order $q_t = q_e - q_e e^{(-k_1 t)}$ | $q_e$ (mg/g) | 2.033 | 9.897 | 19.132 | 1.177 | 6.599 | 13.149 |
| | $k_1$ (l/h) | 1.000 | 1.000 | 1.000 | 3.175 | 3.550 | 4.173 |
| | $R^2$ | 0.924 | 0.930 | 0.987 | 0.953 | 0.976 | 0.988 |
| | NSD | 10.996 | 10.716 | 5.646 | 8.430 | 5.421 | 3.945 |
| | ARE | 1.1814 | 1.180 | 0.814 | -0.658 | -0.297 | -0.155 |
| 2. Psedo-2nd order $q_t = \frac{k_2 q_e^2 t}{(1 + q_e k_2 t)}$ | $q_e$ (g/mg.min) | 2.027 | 9.750 | 19.190 | 1.199 | 6.614 | 13.172 |
| | $k_2$ (1/h) | 3.000 | 2.000 | 0.177 | 2.000 | 3.000 | 2.000 |
| | $R^2$ | 0.998 | 0.999 | 1.000 | 0.935 | 0.974 | 0.987 |
| | $h=k_2 q_e^2$ (mg/g.min) | 12.326 | 190.11 | 65.062 | 2.875 | 131.25 | 347.00 |
| | NSD | 4.267 | 0.595 | 0.557 | 9.756 | 5.623 | 4.111 |
| | ARE | 0.013 | -0.004 | -0.007 | -0.731 | -0.309 | -0.162 |
| 3. Avrami $q_t=q_e(1-e^{(-K_{AV}t)^{n_{AV}}})$ | $q_e$ (mg/g) | 1.991 | 9.698 | 18.968 | 1.177 | 6.599 | 13.149 |
| | $K_{AV}$ (/min) | 2.798 | 2.161 | 0.809 | 1.761 | 2.000 | 2.000 |
| | $n_{AV}$ | 2.764 | 2.161 | 1.857 | 1.882 | 2.000 | 2.000 |
| | $R^2$ | 1.000 | 1.000 | 0.999 | 0.953 | 0.976 | 0.988 |
| | NSD | 0.601 | 0.661 | 1.405 | 8.430 | 5.421 | 3.945 |
| | ARE | -0.009 | -0.004 | -0.018 | -0.658 | -0 .297 | -0.155 |
| 4. Elovich $q_t = \beta.\ln(\alpha\beta t)$ | $\alpha$ [mg/(g.min)] | 2.005 | 9.598 | 16.880 | 1.354 | 7.120 | 14.254 |
| | $\beta$ (g/mg) | 0.004 | 0.024 | 0.449 | -0.047 | -0.138 | -0.294 |
| | $R^2$ | 1.000 | 1.000 | 0.978 | 0.354 | 0.200 | 0.442 |
| | NSD | 0.467 | 0.504 | 5.283 | 6.649 | 4.911 | 2.968 |
| | ARE | -0.002 | -0.002 | -0.268 | -0.429 | -0.241 | -0.088 |
| 5. Intraparticle diffusion $q_t = k_p t^{0.5+C}$ | $k_p$(gm/g√min) | 2.089 | 1.837 | 16.983 | 1.377 | 7.244 | 14.299 |
| | C | -0.408 | -0.251 | -0.376 | -0.441 | -0.425 | -0.422 |
| | $R^2$ | 0.997 | 0.985 | 0.987 | 0.969 | 0.981 | 0.993 |
| | NSD | 2.238 | 53.808 | 5.447 | 6.759 | 4.922 | 2.958 |
| | ARE | -1.840 | 48.955 | -0.399 | -1.008 | -0.341 | -0.086 |

The values of $q_e$ for both adsorption and desorption processes were similar to Pseudo-second-order. The fractionery number ($n_{AV}$) predicted from adsorption processes were greater than unity ($n_{AV}>1$) for Pb(II), adsorption onto and desorption from ML which indicated the reaction order of adsorption and desorption processes are more than first order. It can be assumed that Pb(II) adsorption followed several orders during the processes. These findings postulated that possible changes occurred on adsorption and desorption mechanisms during the processes; therefore, the adsorption mechanism of Pb(II) onto ML followed multiple kinetic orders (Lopes et al., 2003). From the above discussion it can be accepted that this model is suitably describe the kinetics processes of adsorption and desorption.

The Elovich equation presumes that the active sites of the biosorbent are heterogeneous (Cheung et al., 2003) and therefore exhibit different activation energies for chemisorption (Gupta and Babu, 2006). Teng and Hsieh (Teng and Hsieh, 1998) proposed that constant $\alpha$ is related to the rate of chemisorption and $\beta$ is related to the surface coverage. The higher fitness of the Elovich equation (Table 7.4) suggested that Pb(II) uptakes happen on the heterogeneous surfaces of ML and the mechanism might be chemisorption.

### 7.2.3.2 Cd(II) biosorption and desorption kinetics

The Cd(II) adsorption onto and desorption from ML follows a trend similar to Pb(II). At the beginning of the sorption process, the Cd(II) biosorption took place very rapidly in all Cd(II) concentrations and maximum Cd(II) uptake occurred within the first few minutes of adsorption, and reached equilibrium. The process came to equilibrium after between 0-30min for both adsorption and desorption for three Cd(II) concentrations. No significant additional Cd(II) ions were adsorbed after equilibrium, showing that available sites on ML become unavailable for Cd(II) ions. The rapid kinetics has significant practical importance, because the kinetics will facilitate smaller reactor volumes, ensuring efficiency and economy (Günay et al., 2007).

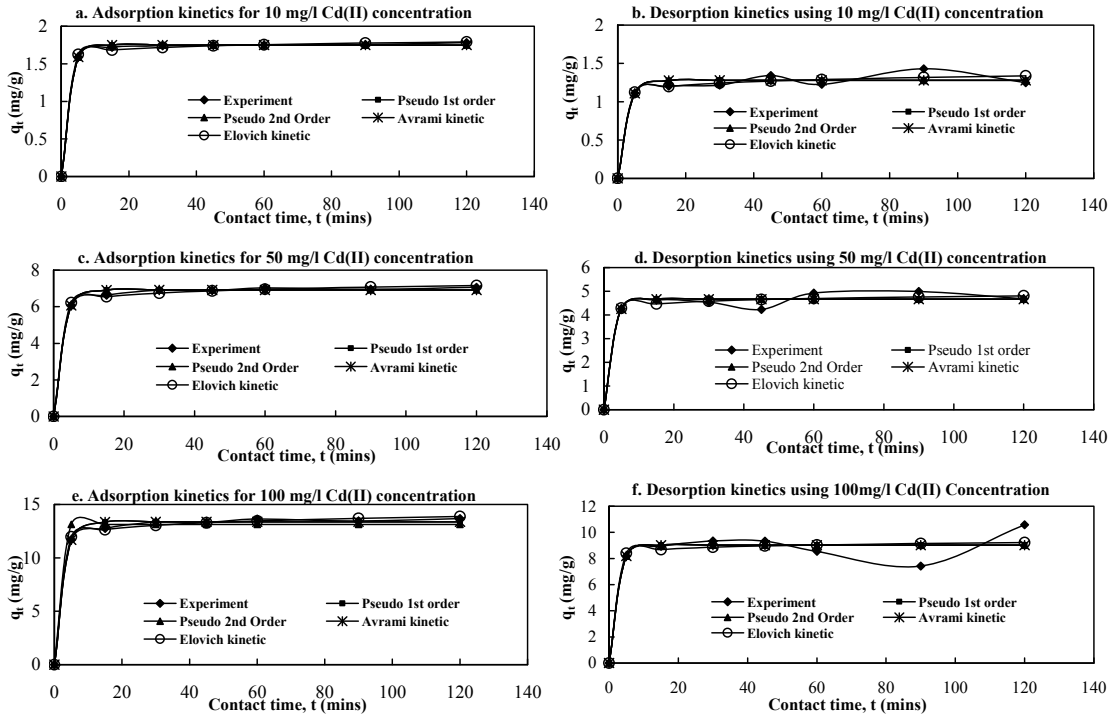


**Figure 7.12** Kinetics modelling of adsorption and desorption of Cd(II) onto maple leaves ($C_o$: 10, 50, 100 mg/l; d: 0.5 g; t: 2h: pH: 6-6.5; rpm: 120; T: 20°C).

The predicted and experimental parameters of kinetics models from adsorption and desorption processes are shown in Table 7.5. Commonly, the adsorption and desorption kinetics data were better fitted with all models ($R^2$: 0.928-1.00) than Pb(II) adsorption and desorption. The plotting of experimental data and models' prediction data are overlapped (Figure 7.12) which signifies the fitness. Surprisingly, the adsorption and desorption data showed good agreement with both the Pseudo-first-order and Pseudo-second-order models (Table 7.5). It is presumed that Cd(II) ions adsorption was not the rate-controlling step (Ho, 2004). The equilibrium adsorption/desorption capacities ($q_e$) from Pseudo-first-order and Pseudo-second-order model are similar to the experimental values. The experimental values are 1.752, 6.957 and 13.459 mg/g for adsorption and 1.342, 4.990 and 9.323 mg/g for desorption which is almost equal to calculated values from Pseudo-first-order: 1.749, 6.917 and 13.376 mg/g for adsorption and 1.278, 4.666 and 9.025 mg/g for desorption and; and from Pseudo-second-order with 1.749, 6.917 and 13.130 mg/g for adsorption and 1.278, 4.666 and 9.025 mg/g for desorption. Considerably lower NSD and ARE values (Table 7.5) were obtained from both model and processes. These results denote that the adsorption/ desorption system followed both single and rate-controlling steps (Ho, 2004).

Along with the order equations, the kinetics also showed good agreement with Avrami model. This model finds out some kinetic parameters, as possible changes of the adsorption and desorption rates in function of the initial metals concentration and the adsorption/desorption time, as well as the determination of fractionary kinetic orders (Lopes et al., 2003). The generally this model showed good fitness with experimental data from adsorption and desorption of Cd(II) are excellent as the $R^2$ values lies 0.999, 0.997 and 0.997 for used 10, 50 and 100 mg/l metals concentration, respectively. The equilibrium ($q_e$) capacities from model prediction are 1.749, 9.917 and 13.373 mg/g for Cd(II) adsorption and; 1.278, 4.666 and 9.025 mg/g for Cd(II) desorption which are closed to the experimental equilibrium ($q_e$) capacities (1.752, 6.957 and 13.459 mg/g for adsorption and 1.342, 4.990 and 9.323 mg/g for desorption).

The values of $q_e$ for both adsorption and desorption processes were similar to Pseudo-first-order and Pseudo-second-order. The fractionary number ($n_{AV}$) are smaller than unity ($n_{AV}<1$) for Cd(II), adsorption onto and desorption from ML. It revealed the reaction order of adsorption and desorption processes are less than first order. It can be

decided that this model suitably describes the kinetics processes of adsorption and desorption.

**Table 7.5** Kinetics parameters of Cd(II) adsorption and desorption onto ML

| Kinetic models | Parameters | Adsorption | | | Desorption | | |
|---|---|---|---|---|---|---|---|
| | | Cd(II) concentration | | | Cd(II)concentration | | |
| | | 10mg/l | 50mg/l | 100mg/l | 10mg/l | 50mg/l | 100mg/l |
| Experimental | $q_e$ (mg/g) | 1.752 | 6.957 | 13.459 | 1.342 | 4.990 | 9.323 |
| 1. Pseudo-1st-order | $q_e$ (mg/g) | 1.749 | 6.917 | 13.376 | 1.278 | 4.666 | 9.025 |
| | $k_1$ (l/h) | 0.479 | 0.421 | 0.413 | 0.404 | 0.488 | 0.476 |
| $q_t = q_e - q_e e^{(-k_1 t)}$ | $R^2$ | 0.999 | 0.997 | 0.997 | 0.972 | 0.980 | 0.928 |
| | NSD | 1.062 | 2.067 | 2.255 | 6.0667 | 5.537 | 11.085 |
| | ARE | -0.01 | -0.036 | -0.043 | -0.375 | -0.297 | -1.149 |
| 2. Psedo-2nd order | $q_e$ (g/mg.min) | 1.749 | 6.917 | 13.130 | 1.278 | 4.666 | 9.025 |
| | $k_2$ (1/h) | 0.479 | 0.421 | 3.958 | 0.404 | 0.488 | 0.476 |
| | $R^2$ | 0.999 | 1.000 | 0.997 | 0.972 | 0.997 | 0.928 |
| $q_t = \frac{k_2 q_e^2 t}{(1 + q_e k_2 t)}$ | $h=k_2 q_e^2$(mg/g.min) | 1.464 | 20.134 | 682.338 | 0.661 | 10.623 | 38.801 |
| | NSD | 1.062 | 2.068 | 5.7324 | 6.067 | 5.537 | 11.085 |
| | ARE | -0.010 | -0.036 | -0.304 | -0.375 | -0.297 | -1.15 |
| 3. Avrami | $q_e$ (mg/g) | 1.749 | 6.917 | 13.376 | 1.278 | 4.666 | 9.025 |
| $q_t=q_e(1-e^{(-K_{AV}t)^{n_{AV}}})$ | $K_{AV}$ (/min) | 0.692 | 0.649 | 0.642 | 0.636 | 0.698 | 0.690 |
| | $n_{AV}$ | 0.692 | 0.648 | 0.642 | 0.636 | 0.698 | 0.690 |
| | $R^2$ | 0.999 | 0.997 | 0.997 | 0.972 | 0.980 | 0.928 |
| | NSD | 1.062 | 2.067 | 2.255 | 6.067 | 5.537 | 11.085 |
| | ARE | -0.010 | -0.036 | -0.043 | -0.375 | -0.297 | -1.15 |
| 4. Elovich | | | | | | | |
| $q_t$ $\beta.\ln(\alpha\beta t)$ | | | | | | | |

and desorption for all Cu(II) concentration. The equilibrium time for Cu(II) ions are more than Pb(II) and Cd(II) adsorption onto ML but lower than other biosorbents reported in literature (Günay et al., 2007). Latter the adsorption processes became slower than first stage and no significant Cu(II) ion adsorption occurred. This means that accessible binding sites on ML become engaged for Cu(II) ions. This rapid kinetics will facilitate smaller reactor volumes, ensuring efficiency and economy (Günay et al., 2007).

The Cu(II) kinetics parameter from experiments and models for both adsorption and desorption processes showed in Table 7.6. The kinetics data of Cu(II) adsorption and desorption were well fitted with all models ($R^2$: 0.976-1.00) except Elovich model. The overlapped plot for experimental and models' prediction data indicates the good fitness (Figure 7.13). Like Cd(II), the experimental data for Cu(II) adsorption and desorption presented excellent harmony with both Pseudo-first-order and Pseudo-second-order models (Table 7.6). It is apparent that Cu(II) ions adsorption was not the rate-controlling step (Ho, 2004).

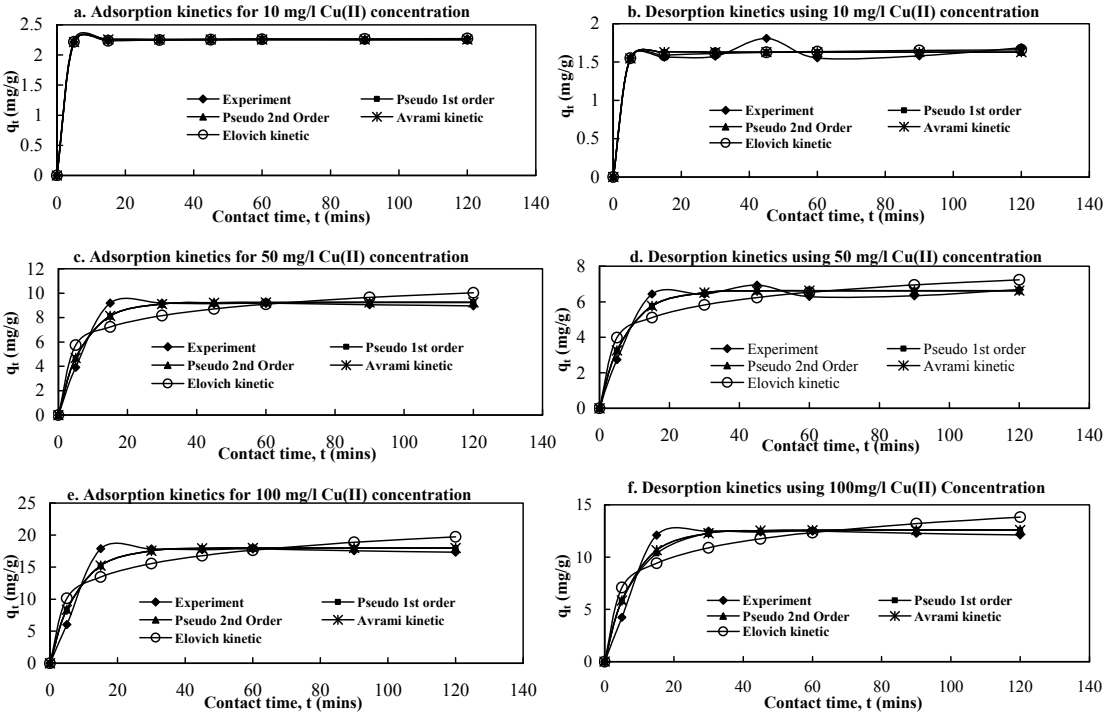


**Figure 7.13** Kinetics modelling of adsorption and desorption of Cu(II) onto maple leaves (Co: 10, 50, 100 mg/l; d: 0.5 g; t: 2h: pH: 6-6.5; rpm: 120; T: 20°C).

Pseudo-second-order models are similar to the experimental values (Table 7.6). Among the three concentrations, the data from 10mg/l posed better fitness with both Pseudo-

first-order and Pseudo-second-order models because $R^2$ values are 1.00 (Table 7.6). The reaction order found from kinetics parameter $k_1$ for Pseudo-first-order and $k_2$ from Pseudo-second-order are less than unity for all three metals' concentrations. Noticeably low NSD and ARE values (Table 7.6) were obtained from both model and processes. These results denoted that the adsorption/ desorption system followed both single and rate-controlling step (Ho, 2005). Similar to Cd(II) and Pb(II) adsorption, the kinetics data for Cu(II) did not follow the Elovich model.

**Table 7.6** Kinetics parameters of Cu(II) adsorption and desorption onto ML.

| Kinetic models | Parameters | Adsorption | | | Desorption | | |
|---|---|---|---|---|---|---|---|
| | | Cu(II) concentration | | | Cu(II)concentration | | |
| | | 10mg/l | 50mg/l | 100mg/l | 10mg/l | 50mg/l | 100mg/l |
| Experimental | $q_e$ (mg/g) | 2.268 | 9.184 | 17.872 | 1.687 | 6.336 | 12.484 |
| 1. Pseudo-1st-order | $q_e$ (mg/g) | 2.256 | 9.238 | 17.983 | 1.629 | 6.629 | 12.588 |
| | $k_1$ (l/h) | 0.787 | 0.142 | 0.125 | 0.602 | 0.135 | 0.125 |
| $q_t = q_e - q_e e^{(-k_1 t)}$ | $R^2$ | 1.000 | 0.978 | 0.961 | 0.978 | 0.976 | 0.961 |
| | NSD | 0.477 | 9.487 | 16.985 | 5.348 | 9.490 | 16.985 |
| | ARE | -0.005 | -2.379 | -5.064 | -0.301 | -2.357 | -5.06 |
| 2. Psedo-2nd order | $q_e$ (g/mg.min) | 2.249 | 9.238 | 17.983 | 1.629 | 6.629 | 12.588 |
| | $k_2$ (1/h) | 0.958 | 0.142 | 0.125 | 0.602 | 0.135 | 0.125 |
| $q_t = \frac{k_2 q_e^2 t}{(1 + q_e k_2 t)}$ | $R^2$ | 1.000 | 0.995 | 0.991 | 0.978 | 0.976 | 0.961 |
| | $h=k_2 q_e^2$(mg/g.min) | 20.028 | 12.085 | 40.472 | 1.596 | 5.936 | 19.831 |
| | NSD | 0.877 | 9.486 | 16.985 | 5.348 | 9.490 | 16.985 |
| | ARE | -0.008 | -2.379 | -5.064 | -0.301 | -2.357 | -5.064 |
| 3. Avrami | $q_e$ (mg/g) | 2.256 | 9.238 | 17.983 | 1.629 | 6.629 | 12.588 |
| $q_t=q_e(1-e^{(-K_{AV}t)^{n_{AV}}})$ | $K_{AV}$ (/min) | 1.729 | 1.619 | 1.407 | 0.358 | 0.084 | 0.354 |
| | $n_{AV}$ | 0.457 | 0.087 | 0.089 | 1.679 | 1.613 | 0.354 |
| | $R^2$ | 1.000 | 0.978 | 0.961 | 0.978 | 0.976 | 0.961 |
| | NSD | 0.476 | 9.486 | 16.985 | 5.348 | 9.490 | 16.985 |
| | ARE | -0.002 | -2.379 | -5.064 | -0.301 | -2.357 | -5.064 |
| 4. Elovich | $\alpha$ [mg/(g.min)] | 2.189 | 3.563 | 5.282 | 1.495 | 2.331 | 3.697 |
| $q_t = \beta.\ln(\alpha\beta t)$ | $\beta$ (g/mg) | 0.017 | 1.351 | 3.020 | 0.034 | 1.025 | 2.114 |
| | $R^2$ | 1.000 | 0.883 | 0.853 | 0.980 | 0.888 | 0.853 |
| | NSD | 0.237 | 22.251 | 30.772 | 5.153 | 21.791 | 30.772 |
| | ARE | -5E-04 | -4.528 | -7.59 | -0.281 | -4.456 | -7.59 |
| 5. Intraparticle diffusion | $k_p$(gm/g$\sqrt{}$min) | 2.189 | 5.391 | 8.606 | 1.499 | 3.349 | 6.024 |
| | C | -0.492 | -0.377 | -0.329 | -0.479 | -0.340 | -0.329 |
| $q_t = k_p t^{0.5+C}$ | $R^2$ | 1.000 | 0.860 | 0.826 | 0.980 | 0.868 | 0.826 |
| | NSD | 0.240 | 29.415 | 38.081 | 5.154 | 26.266 | 38.081 |
| | ARE | -0.001 | -7.108 | -10.010 | -0.282 | -5.871 | -10.01 |

### 7.2.3.4 Zn(II) biosorption and desorption kinetics

Likewise Pb(II), the Zn(II) adsorption and desorption followed a similar trend of adsorption. The Figure 7.14 showed that initially the sorption of Zn(II) ions occurred very rapidly in all metals concentrations and maximum Zn(II) uptake occurred within the first few minutes of adsorption, and then reached equilibrium. After an equilibrium time of 5-30min, no additional Zn(II) was adsorbed, suggesting that available sites on the biosorbent are limited to uptake metals ions. The rapid kinetics will make possible

for smaller reactor volumes, ensuring efficiency and economy in any adsorption process (Günay et al., 2007).

The kinetics data of Zn(II) from experiments and prediction by kinetics models presented in Table 7.7. Generally, the adsorption and desorption kinetics data were well fitted with all used models because $R^2$ values lie between 0.996 and 1.00. The degree of fitness can also be found from the plotting of experimental and models' prediction data because the coincided with each other (Figure 7.14). Surprisingly, the adsorption and desorption data showed good fitness with Pseudo-first-order and Pseudo-second-order models (Table 7.7), implying that Zn(II) ions adsorption was the rate controlling step as well as single steps (Ho, 2004). Significantly low NSD and ARE values are found from both the Pseudo-first-order and Pseudo-second-order models (Table 7.7) for all Zn(II) concentrations (10, 50 and 100 mg/l).

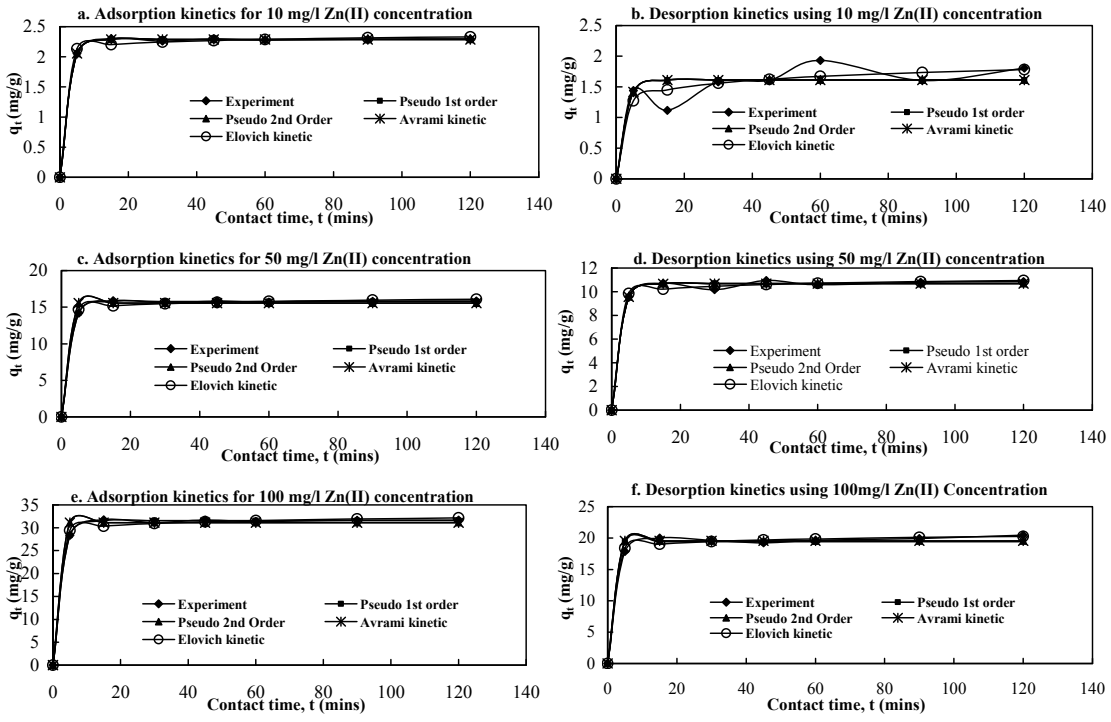


**Figure 7.14** Kinetics modelling of adsorption and desorption of Zn(II) onto maple leaves (Co: 10, 50, 100 mg/l; d: 0.5 g; t: 2h: pH: 6-6.5; rpm: 120; T: 20°C).

The equilibrium adsorption/desorption capacities ($q_e$) from Pseudo-first-order and Pseudo-second-order models are more similar each other and posed better consistency with the experimental data. The experimental $q_e$ values are 2.295, 15.830 and 31.660 mg/g for adsorption and 1.931, 10.942 and 19.934 mg/g for desorption while the calculated values from Pseudo-first-order are 2.288, 15.777 and 31.660 mg/g for

adsorption and 1.612, 10.680 and 19.398 mg/g for desorption; and from Pseudo-second-order are 2.288, 15.547 and 31.094 mg/g for adsorption and 1.612, 10.680 and 19.541 mg/g for desorption (Table 7.7). Significantly low NSD and ARE values (Table 7.7) were obtained from Pseudo-first-order and Pseudo-second-order for both adsorption and desorption processes. These results denoted that the adsorption/ desorption system followed to the Pseudo-first-order and Pseudo-second-order kinetics which further advocated that adsorption was the rate-controlling step (Ho, 2004).

**Table 7.7** Kinetics parameters of Zn(II) adsorption and desorption onto ML.

| Kinetic models | Parameters | Adsorption | | | Desorption | | |
|---|---|---|---|---|---|---|---|
| | | Zn(II) concentration | | | Zn(II)concentration | | |
| | | 10mg/l | 50mg/l | 100mg/l | 10mg/l | 50mg/l | 100mg/l |
| Experimental | $q_e$ (mg/g) | 2.295 | 15.830 | 31.660 | 1.931 | 10.942 | 19.934 |
| 1. Pseudo-1st-order | $q_e$ (mg/g) | 2.288 | 15.777 | 31.554 | 1.612 | 10.680 | 19.398 |
| | $k_1$ (l/h) | 0.458 | 0.458 | 0.458 | 0.423 | 0.453 | 7.228 |
| $q_t = q_e - q_e e^{(-k_1 t)}$ | $R^2$ | 1.000 | 1.000 | 1.000 | 0.853 | 0.996 | 0.987 |
| | NSD | 0.678 | 0.678 | 0.678 | 19.720 | 2.404 | 4.484 |
| | ARE | -0.005 | -0.005 | -0.005 | -2.975 | -0.056 | 0.665 |
| 2. Psedo-2nd order | $q_e$ (g/mg.min) | 2.288 | 15.547 | 31.094 | 1.612 | 10.680 | 19.541 |
| | $k_2$ (1/h) | 1.458 | 2.553 | 2.553 | 0.423 | 0.453 | 7.228 |
| $q_t = \frac{k_2 q_e^2 t}{(1 + q_e k_2 t)}$ | $R^2$ | 1.000 | 0.998 | 0.998 | 0.853 | 0.996 | 0.988 |
| | $h=k_2 q_e^2$(mg/g.min) | 2.399 | 617.02 | 2468.48 | 1.099 | 51.693 | 2759.88 |
| | NSD | 0.678 | 4.245 | 4.248 | 19.72 | 2.404 | 4.4775 |
| | ARE | -0.005 | -0.167 | -0.167 | -2.975 | -0.056 | -0.19 |
| 3. Avrami | $q_e$ (mg/g) | 2.288 | 15.547 | 31.094 | 1.584 | 10.520 | 19.541 |
| $q_t = q_e(1 - e^{(-K_{AV} t)^{n_{AV}}})$ | $K_{AV}$ (/min) | 0.271 | 1.880 | 1.000 | 2.000 | 1.000 | 2.000 |
| | $n_{AV}$ | 1.689 | 2.000 | 2.000 | 2.000 | 2.999 | 1.999 |
| | $R^2$ | 1.000 | 0.998 | 0.989 | 0.843 | 0.986 | 0.988 |
| | NSD | 0.678 | 4.249 | 4.244 | 19.687 | 4.902 | 4.477 |
| | ARE | -0.005 | -0.167 | -0.167 | -3.156 | -0.227 | -0.190 |
| 4. Elovich | $\alpha$ [mg/(g.min)] | 2.032 | 14.016 | 28.032 | 1.015 | 9.280 | 17.426 |
| $q_t = \beta . \ln(\alpha \beta t)$ | $\beta$ (g/mg) | 0.062 | 0.430 | 0.860 | 0.160 | 0.348 | 0.594 |
| | $R^2$ | 0.996 | 0.996 | 0.996 | 0.914 | 0.995 | 0.995 |
| | NSD | 2.533 | 2.537 | 2.534 | 14.511 | 2.857 | 2.618 |
| | ARE | -0.066 | -0.066 | -0.066 | -1.784 | -0.085 | -0.071 |
| 5. Intraparticle diffusion | $k_p$(gm/g√min) | 2.044 | 14.095 | 28.190 | 1.072 | 9.346 | 17.524 |
| | C | -0.473 | -0.473 | -0.473 | -0.392 | -0.467 | -0.470 |
| $q_t = k_p t^{0.5+C}$ | $R^2$ | 0.996 | 0.996 | 0.996 | 0.916 | 2.447 | 0.995 |
| | NSD | 2.573 | 2.573 | 2.573 | 14.187 | 2.887 | 2.635 |
| | ARE | -0.070 | -0.070 | -0.070 | -1.698 | -0.088 | -0.073 |

Along with the order equations, the Zn(II) kinetics data showed a good concurrence with Avrami model which determines the possible changes of the adsorption and desorption rates in function of the initial metals concentration and the adsorption/desorption time, as well as the determination of fractionary kinetic orders (Lopes et al., 2003). The experimental and predicted data from this model showed good agreement because $R^2$ values lies 1.000, 0.998 and 0.989 for used 10, 50 and 100 mg/l

metals concentration, respectively. The desorption data did not quite fit with this model as the $R^2$ values are 0.843, 0.986 and 0.988 for the three exhausted concentrations. In addition, the model predicted equilibrium ($q_e$) capacities (2.288, 15.547 and 31.094 mg/g for Zn(II) adsorption and 1.584, 10.520 and 19.541 mg/g for Zn(II) desorption which are close to the experimental equilibrium ($q_e$) capacities (2.295, 15.830 and 31.660 mg/g for adsorption and 1.931, 10.942 and 19.934 mg/g for desorption). The values of $q_e$ for both adsorption and desorption processes were similar to Pseudo-first-order and Pseudo-second-order. The fractionery number ($n_{AV}$) predicted from adsorption processes were greater than unity ($n_{AV}>1$) for Zn(II), adsorption onto and desorption from ML which indicated the reaction order of adsorption and desorption processes are more than first order. It could be assumed that Zn(II) adsorption followed several orders during the processes. These findings result in postulation of possible changes occurring in adsorption and desorption mechanisms during the processes. Therefore, the adsorption mechanism of Zn(II) onto ML followed multiple kinetic orders (Lopes et al., 2003).

The metal binding active sites of the biosorbent are heterogeneous as presumed by the Elovich model (Cheung et al., 2003) and therefore exhibit different activation energies for chemisorption in the sites (Gupta and Babu, 2006). Teng and Hsieh (1998) proposed that constant $\alpha$ is related to the rate of chemisorption and $\beta$ is related to the surface coverage. The higher fitness of Elovich equation (Table 7.7) recommended that Zn(II) uptakes happen on the heterogeneous surfaces of ML and the mechanism might be chemisorption.

#### 7.2.3.5 Intra-particle diffusion model

Kinetic data from Cu(II), Zn(II), Pb(II), and Cd(II) adsorption onto and desorption from ML were further used to define whether the intra-particle diffusion is rate limiting and also to find the diffusion rate constant, $k_p$ (mg/g min^0.5). The intra-particle diffusion model (Srihari and Das, 2008) is presented as the relationship between specific adsorption and the square root of time:

$$q_t = k_p t^{0.5+C} \tag{7.4}$$

A plot between $q_t$ versus t^0.5 for Pb(II), Cd(II), Cu(II) and Zn(II) adsorption onto ML is shown in Figure 7.15 (a, b, c and d). From the Figure, it is revealed that all plots are multi-linear and multi-staged plots are depicted by two straight lines. Two clear steps

are visible in the plots which are indeed general type of graphs, i.e. at the first stage and at the second stage.

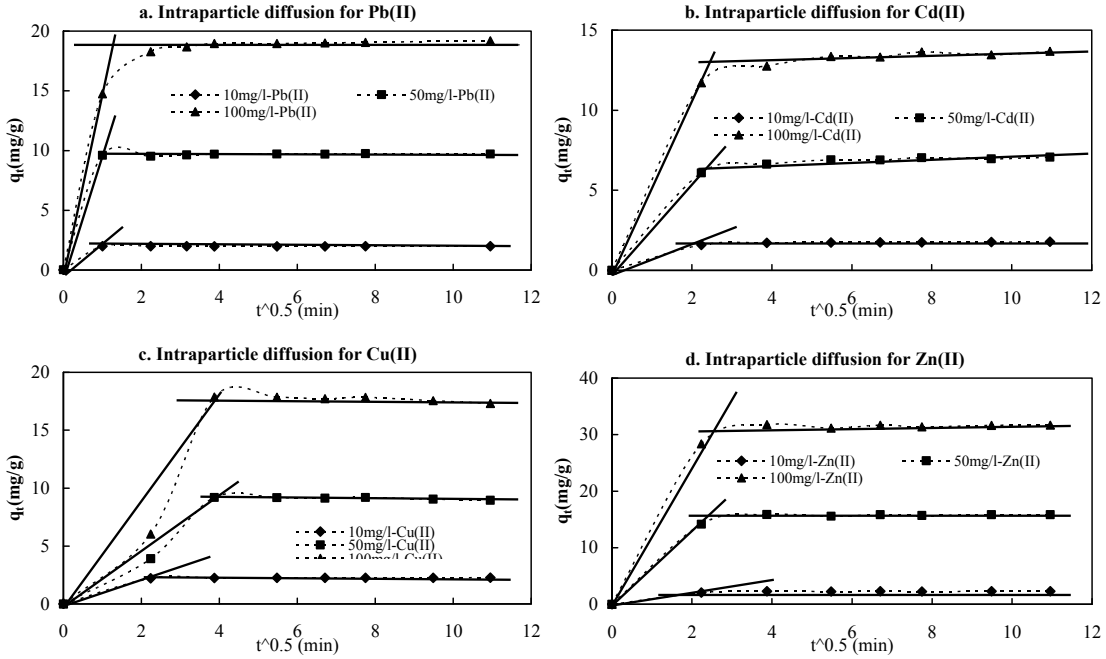


**Figure 7.15** Plots for intra-particle diffusion kinetic model ML for adsorption Pb(II), Cd(II), Cu(II) and Zn(II) ($C_o$: 10, 50, 100 mg/l; d: 0.5 g; t: 2h: pH: 6-6.5; rpm: 120; T: 20°C).

The initial or first stage may also be attributed to the boundary layer diffusion effect, while the second stage may be due to intra-particle diffusion effects (Srihari and Das, 2008). In the present study, the rate constant ($k_p$) for adsorption is higher and follows an increasing trend with the increases of initial Pb(II), Cd(II), Cu(II) and Zn(II) concentrations (Table 7.4, Table 7.5, Table 7.6, and Table 7.7). Therefore, the slope of the top portion which is the linear portion may be defined as a rate parameter ($k_p$) and characteristic of the adsorption rate in the region, where intra-particle diffusion was reported to be the rate-limiting factor (Hanafiah et al., 2006) for Pb(II), Cd(II), Cu(II) and Zn(II) adsorption onto ML.

### 7.2.4 Biosorption and desorption equilibrium

The relationship between the amounts of adsorbate (metals) removed from water per unit of mass of biosorbent and equivalent metals concentration in water, at constant temperature and at equilibrium state is termed as equilibrium (Abd El-Latif and Elkady, 2010; Blazquez et al., 2010; Kicsi et al., 2010). Experimental data from Pb(II), Cd(II), Cu(II), and Zn(II) adsorption and desorption at equilibrium state were judged with five isotherm model: Langmuir, Freundlich, SIPS, Redlich-Peterson and Unilan models. The

isotherm data are analysed by non-linear regression analyses on the base of original form of isotherm equation and eventually avoids errors.

MATLAB software was used to program the non-linear model of the isotherm models. It was used to estimate and optimise the isotherm parameters (Appendix I). The isotherm data from model prediction and experiments are plotted in Figure 7.16, Figure 7.17, Figure 7.18 and Figure 7.19 for Pb(II), Cd(II), Cu(II) and Zn(II), respectively. The models' predicted and experimental parameters are presented in Table 7.8, Table 7.9, Table 7.10 and Table 7.11 for Pb(II), Cd(II), Cu(II) and Zn(II), respectively. The fitness between experimental and model prediction data are evaluated by $R^2$ (coefficient of determination), RMSE (residual root mean square error) and $\lambda^2$ (chi-square test) (Chapter 3, section 3.4) for both adsorption and desorption of Pb(II), Cd(II), Cu(II), and Zn(II) onto and from biosorbent of ML.

#### 7.2.4.1 Isotherm models

The following models are used to describe the adsorption and desorption data of Pb(II), Cd(II), Cu(II), and Zn(II) onto and from biosorbent of ML. The simple theoretical formulations are discussed below.

The most widely used adsorption isotherm is Langmuir model. A basic assumption of the Langmuir theory is that adsorption takes place at specific homogeneous sites within the adsorbent. The saturated monolayer isotherm can be represented as (Langmuir, 1918):

$$q_e = \frac{q_m K_L C_e}{1 + K_L C_e} \tag{7.5}$$

where $C_e$ is the equilibrium concentration (mg/l), $q_e$ is the amount of metal ion adsorbed (mg/g), $q_m$ is the $q_e$ for a complete monolayer (mg/g) and a constant related to adsorption capacity, and b is the constant related to the affinity of the binding sites and the energy of adsorption (l/mg).

Freundlich devised an empirical model, which is based on adsorption on a heterogeneous surface and in a multilayer adsorption manner, and is given by (Thomas et al., 1997) as:

$$q_e = K_F C_e^{1/n} \tag{7.6}$$

where $q_e$ is the amount of metal ions adsorbed per unit mass of the adsorbent, $C_e$ the equilibrium solution concentration, and $K_F$ and n are Freundlich equilibrium coefficients. For favourable adsorption, $0 < n < 1$, while $n > 1$ represents unfavourable adsorption, and $n = 1$ indicates linear adsorption. If $n = 0$, the adsorption process is irreversible (Abia and Asuquo, 2006).

An empirical isotherm equation is proposed by Sips, which is often expressed as (Sips, 1948),

$$q_e = \frac{K_s C_e^{\beta_s}}{1 + \alpha_s C_e^{\beta_s}} \qquad (7.7)$$

where $q_e$ is the amount of metal ions adsorbed per unit mass of the adsorbent, $C_e$ the equilibrium solution concentration and n is the Sips constant.

Redlich and Peterson (1959) proposed an empirical equation to represent equilibrium data:

$$q_e = \frac{K_{RP} C_e}{1 + \alpha_{RP} C_e^{\beta}} \qquad \text{where } \beta \leq 1 \qquad (7.8)$$

where $K_{PR}$ (l/g), $\alpha_{PR}$ (l/mg) and $\beta$ are Redlich-Peterson isotherm constants which lies between 0 and 1. This equation reduces to a linear isotherm in the case of low surface coverage and to a Langmuir isotherm when $\beta = 1$.

Unilan equation is an empirical equation having three degrees of freedom and is often used for gas phase adsorption on heterogeneous surface. This empirical equation assumed applicability of local Langmuir isotherm and uniform distribution of energy (Do Duong, 1998; Ismadji and Bhatia, 2000) and also introduced a parameter "s" to account the heterogeneity of the system. This equation has a Henry's law limit so it can be applicable at very small adsorbate loadings (Ismadji and Bhatia, 2000). The Unilan equation has the following form:

$$q_e = \frac{1}{2} q_m S \ln(1 + be^S) \qquad (7.9)$$

where s and d=temperature dependent model constants.

### 7.2.4.2 Equilibrium of Pb(II) adsorption and desorption

The obtained isotherm parameters at 0.05, 0.5 and 1g/100ml doses for adsorption and desorption are given in Table 7.8 and plotted in Figure 7.16. Among two-parameter models, the Langmuir model better fitted with experimental data than the Freundlich model for both adsorption and desorption processes, which was recognized by high $R^2$ and low RMSE and small $\chi^2$ values. Among the three doses of ML (0.05, 0.5 and 1 g), the best fitted data were found from 1 g dose for adsorption and from 0.05g for desorption process. The maximum adsorption and desorption capacities were 50.267 and 150.680 mg/g for 1 g and 0.05 g doses respectively for well fitted data.

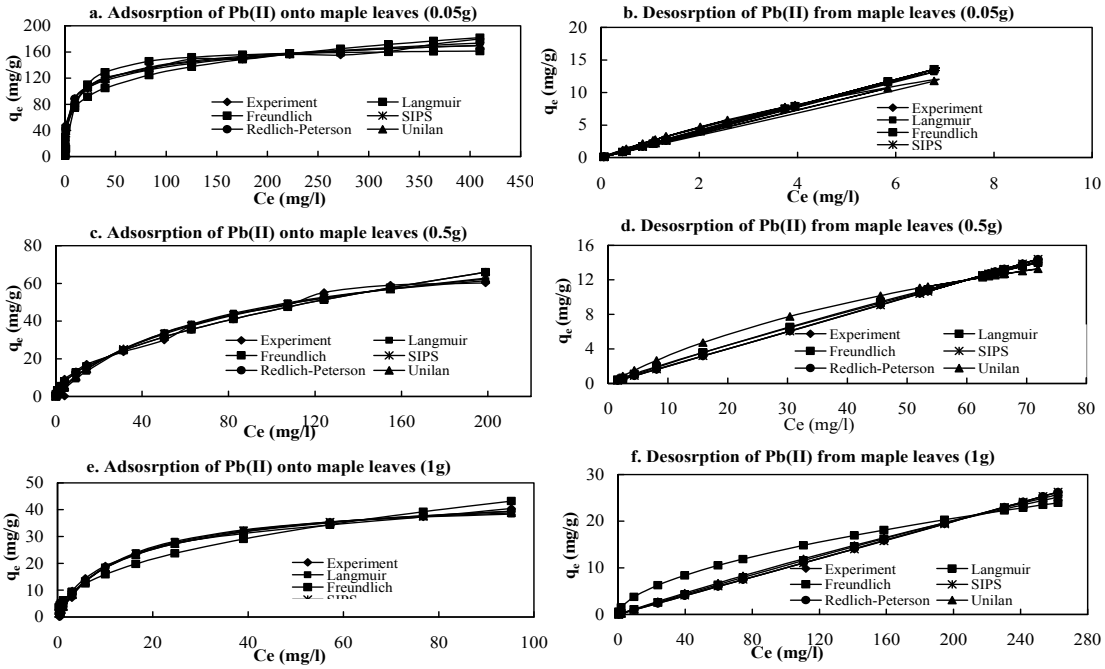


**Figure 7.16** Isotherm modelling of adsorption and desorption of Pb(II) onto ML with different doses (Co: 1-500 mg/l; d: 0.05-1 g; t: 3 h: pH: 6-6.5; rpm: 120; T: 20°C).

To verify the experimental data, three-parameter models were better in description of equilibrium isotherm than the two-parameter ones. Very high values of $R^2$ (above 0.991) and low values of RMSE and $\chi^2$ for both adsorption and desorption processes suggest that these models could be used to describe the equilibrium Pb(II) uptake as well as desorbs (Figure 7.16 and Table 7.8). The predicted $R^2$ values from Sips model were 0.991, 0.988 and 0.994 for adsorption and 1.00, 1.00 and 1.00 for desorption while doses were 0.05, 0.5 and 1g respectively. On the other hand, the $R^2$ values from Redlich-Peterson model were 0.994, 0.982 and 0.995 for adsorption and 1.00, 1.00 and 1.00 for desorption of the used three doses. Similarly, the $R^2$ values for the Unilan

model were 0.994, 0.987 and 0.995 for adsorption and 0.998, 0.974 and 0.996 for desorption. Significantly low RMSE and small $\chi^2$ values were observed for both adsorption and desorption from the three three-parameter models (Table 7.8) which revealed the good agreement between the experimental data and models' predictions. On comparison of the values of coefficient of determination ($R^2$), the residual root mean square error (RMSE) and the chi-square test ($\chi^2$), both the three-parameter models were most appropriate for describing the adsorption and desorption mechanisms of Pb(II) onto ML. Therefore, the best fitting order of the models was concluded to be Redlich-Peterson=Unilan> SIPS > Langmuir> Freundlich.

**Table 7.8** The prediction of isotherm models for adsorption and desorption of Pb(II) on maple leaves.

| Isotherm models | Para-meters | Adsorption | | | Desorption | | |
|---|---|---|---|---|---|---|---|
| | | Doses | | | Doses | | |
| | | **0.05g** | **0.5g** | **1g** | **0.05g** | **0.5g** | **1g** |
| Experimental | $q_m$(mg/g) | 125.95 | 66.722 | 50.267 | 150.68 | 60.26 | 120.056 |
| **1. Langmuir** | $q_m$(mg/g) | 165.79 | 84.890 | 43.857 | 136.840 | 82.127 | 150.05 |
| $q_e = \frac{q_m K_L C_e}{1 + K_L C_e}$ | $K_L$ (l/g) | 0.088 | 0.013 | 0.073 | 0.016 | 0.003 | 0.001 |
| | $R_L$ | 0.02-0.99 | 0.27-0.98 | 0.12-0.97 | 0.98-0.99 | 0.84-0.99 | 0.83-0.99 |
| | $R^2$ | 0.961 | 0.986 | 0.994 | 0.999 | 0.998 | 0.997 |
| | Δ°G | -5.918 | -10.55 | -6.371 | -10.12 | -14.27 | -17.44 |
| | $\chi^2$ | 0.899 | 0.861 | 1.011 | 0.0041 | 0.0075 | 0.0007 |
| | RMSE | 13.356 | 2.797 | 1.212 | 0.1591 | 0.268 | 0.5624 |
| **2. Freundlich** | $K_F$ (mg/g.l) | 43.701 | 3.778 | 5.687 | 2.000 | 0.294 | 1.076 |
| $q_e = K_F C_e^{1/n}$ | n | 4.218 | 1.849 | 2.247 | 1.000 | 1.104 | 1.795 |
| | $R^2$ | 0.968 | 0.981 | 0.962 | 1.000 | 0.998 | 0.917 |
| | $\chi^2$ | 54.622 | 12.910 | 17.671 | $1.5x10^{-9}$ | 0.284 | 14.781 |
| | RMSE | 12.622 | 3.206 | 2.961 | $2.1x10^{-5}$ | 0.239 | 2.971 |
| **3. SIPS** | Ks(l/g) | 45.442 | 2.014 | 3.620 | 2.000 | 0.252 | 0.134 |
| $q_e = \frac{K_s C_e^{\beta_s}}{1 + \alpha_s C_e^{\beta_s}}$ | $\alpha_S$ (l/mg) | 0.212 | 0.018 | 0.079 | 0.006 | 0.003 | 0.001 |
| | $\beta_S$ | 0.479 | 0.805 | 0.923 | 1.000 | 0.913 | 0.926 |
| | $R^2$ | 0.991 | 0.988 | 0.994 | 1.000 | 1.000 | 1.000 |
| | $\chi^2$ | 8.192 | 1.656 | 1.253 | $1.8X10^{-6}$ | 0.012 | 0.005 |
| | RSME | 0.644 | 0.069 | 0.231 | $1X10^{-13}$ | 0.004 | 0.014 |
| **4. Redlich-Peterson** | $K_{RP}$ (l/g) | 148.618 | 18.331 | 3.976 | 169.966 | 5.867 | 6.327 |
| | $\alpha_{RP}$ (l/mg) | 2.284 | 4.359 | 0.150 | 83.980 | 23.587 | 62.274 |
| $q_e = \frac{K_{RP} C_e}{1 + \alpha_{RP} C_e^{\beta}}$ | β | 0.836 | 0.477 | 0.888 | $2x10^{-5}$ | 0.045 | 0.002 |
| | $R^2$ | 0.994 | 0.982 | 0.995 | 1.000 | 1.000 | 1.000 |
| | $\chi^2$ | 4.565 | 3.004 | 1.236 | $3x10^{-9}$ | 0.0078 | $2x10^{-19}$ |
| | RSME | 0.392 | 0.318 | 0.282 | $5x10^{-5}$ | 0.0444 | $3x10^{-8}$ |
| **5. Unilan** | $q_m$ (mg/g) | 7.241 | 47.785 | 17.641 | 23.052 | 23.026 | 25.059 |
| $q_e = \frac{1}{2} q_m S \ln(1 + b e^S)$ | S (l/mg) | 6.058 | 1.426 | 1.677 | 4.704 | 1.195 | 4.713 |
| | b (l/g) | 0.014 | 0.010 | 0.052 | 0.0001 | 0.009 | 0.0001 |
| | $R^2$ | 0.994 | 0.987 | 0.995 | 0.998 | 0.974 | 0.996 |
| | $\chi^2$ | 3.812 | 0.988 | 1.244 | 0.006 | 0.115 | 0.001 |
| | RMSE | 0.069 | 0.447 | 0.274 | 0.063 | 0.273 | 0.157 |

The other mono-component Langmuir constant, $K_L$, indicates the affinity for the binding of Pb(II) ions. The essential characteristics of the Langmuir isotherm have been

described by the term separation factor or equilibrium constant $R_L$, which is defined as $R_L = 1/(1+K_LC_o)$ (where $C_o$ is the initial concentration of Pb(II), and $K_L$ is its Langmuir constant). This indicates the nature of adsorption as

$R_L > 1$ (unfavourable),

$0<R_L < 1$ (favourable),

$R_L = 0$ (irreversible),

$R_L = 1$ (linear).

The values of $R_L$ in the present investigation have been found to be below 1.0 for both adsorption and desorption of Pb(II) from ML, showing that the adsorption/desorption of Pb(II) is very favourable. The values of 1/n from Freundlich models are also found to be less than unity for both adsorption and desorption processes, which suggests favourable adsorption and desorption behaviours of Pb(II) onto ML. In addition the Gibb's free energy ($\Delta°G$) are negative in magnitude which reveals the exothermic nature of adsorption processes.

**7.2.4.3 Equilibrium of Cd(II) adsorption and desorption**

The Cd(II) ions adsorption and desorption data from 0.05, 0.5 and 1g/100ml doses are tabulated in Table 7.9 and plotted in Figure 7.17. It is found from analysed data (Table 7.9) that the Langmuir model better fitted with experimental data than the Freundlich model among two-parameter models for both adsorption and desorption processes. High $R^2$ and low RMSE and small $\chi^2$ values from Langmuir model proved the fitness (Table 7.9). The best fitted data were found from 0.5 g dose for adsorption and from 0.05g for desorption process for Cd(II). The maximum adsorption and desorption capacities were 60.980 and 43.372 mg/g for 0.5g and 0.05g doses respectively for well fitted data.

Three three-parameter models namely, Sips, Redlich-Peterson and Unilan were used to evaluate the Cd(II) adsorption and desorption data and showed better fitness than the two-parameter models. Overall, very high $R^2$ (above 0.962) values and low RMSE and $\chi^2$ values are found for both adsorption and desorption processes. It is thus recommended that three-parameter models could be used properly to illustrate the equilibrium of Cd(II) adsorption and desorption (Figure 7.17 and Table 7.9). The coefficients of determination ($R^2$) for Sips model were 0.998, 0.999 and 0.997 for

adsorption and 0.994, 1.00 and 0.990 for desorption for 0.05, 0.5 and 1g dose, respectively.

**Table 7.9** The prediction of isotherm models for adsorption and desorption of Cd(II) on maple leaves.

| Isotherm models | Para-meters | Adsorption | | | Desorption | | |
|---|---|---|---|---|---|---|---|
| | | Doses | | | Doses | | |
| | | **0.05g** | **0.5g** | **1g** | **0.05g** | **0.5g** | **1g** |
| Experimental | $q_m$(mg/g) | 57.412 | 60.980 | 37.008 | 43.372 | 38.234 | 23.445 |
| **1. Langmuir** | $q_m$(mg/g) | 107.589 | 93.368 | 39.599 | 96.719 | 100.000 | 25.562 |
| $q_e = \frac{q_m K_L C_e}{1 + K_L C_e}$ | $K_L$ (l/g) | 0.021 | 0.012 | 0.044 | 0.031 | 0.151 | 0.068 |
| | $R^2$ | 0.991 | 0.993 | 0.962 | 0.984 | 0.963 | 0.959 |
| | $R_L$ | 0.27-0.99 | 0.30-0.99 | 0.06-0.99 | 0.27-0.99 | 0.52-0.99 | 0.05-0.99 |
| | Δ°G | -9.409 | -10.811 | -7.623 | -8.436 | -4.597 | -6.555 |
| | $\chi^2$ | 5.723 | 3.338 | 9.705 | 0.182 | 0.034 | 0.100 |
| | RMSE | 2.678 | 1.955 | 3.031 | 3.138 | 4.030 | 2.024 |
| **2. Freundlich** | $K_F$ (mg/g.l) | 5.919 | 3.303 | 5.895 | 6.548 | 9.155 | 4.368 |
| $q_e = K_F C_e^{1/n}$ | n | 1.823 | 1.731 | 2.981 | 1.812 | 1.011 | 2.964 |
| | $R^2$ | 0.954 | 0.964 | 0.855 | 0.946 | 1.000 | 0.865 |
| | $\chi^2$ | 25.589 | 16.749 | 37.083 | 24.931 | 0.849 | 23.402 |
| | RMSE | 5.885 | 4.425 | 5.915 | 5.771 | 0.286 | 3.684 |
| **3. SIPS** | Ks(l/g) | 0.747 | 0.338 | 0.037 | 0.948 | 9.218 | 0.057 |
| $q_e = \frac{K_s C_e^{\beta_s}}{1 + \alpha_s C_e^{\beta_s}}$ | $\alpha_S$ (l/mg) | 0.009 | 0.005 | 0.001 | 0.013 | -0.018 | 0.003 |
| | $\beta_S$ | 1.403 | 1.358 | 2.426 | 1.492 | 0.930 | 2.526 |
| | $R^2$ | 0.998 | 0.999 | 0.997 | 0.994 | 1.000 | 0.990 |
| | $\chi^2$ | 0.090 | 0.054 | 20.969 | 0.173 | 0.013 | 20.364 |
| | RSME | 0.067 | 0.110 | 0.187 | 0.139 | 0.038 | 0.131 |
| **4. Redlich-Peterson** | $K_{RP}$ (l/g) | 1.748 | 58.694 | 1.219 | 2.278 | 200.761 | 1.351 |
| | $\alpha_{RP}$ (l/mg) | 0.002 | 17.323 | 0.007 | 0.002 | 20.930 | 0.022 |
| $q_e = \frac{K_{RP} C_e}{1 + \alpha_{RP} C_e^{\beta}}$ | β | 1.459 | 0.425 | 1.275 | 1.570 | 0.011 | 1.170 |
| | $R^2$ | 0.996 | 0.965 | 0.981 | 0.992 | 1.000 | 0.968 |
| | $\chi^2$ | 0.119 | 1.358 | 0.062 | 0.095 | 0.849 | 0.054 |
| | RSME | 0.311 | 0.929 | 0.358 | 0.297 | 0.093 | 0.254 |
| **5. Unilan** | $q_m$ (mg/g) | 21.083 | 20.924 | 5.332 | 934.880 | 26.325 | 927.311 |
| $q_e = \frac{1}{2} q_m S \ln(1 + be^S)$ | S (l/mg) | 0.003 | 0.002 | 0.014 | 0.323 | 0.001 | 0.166 |
| | b (l/g) | 3.218 | 2.993 | 3.217 | 0.031 | 8.233 | 0.068 |
| | $R^2$ | 0.984 | 0.988 | 0.926 | 0.984 | 0.995 | 0.959 |
| | $\chi^2$ | 0.278 | 0.165 | 0.393 | 0.184 | 0.005 | 0.101 |
| | RMSE | 0.676 | 0.461 | 0.506 | 0.649 | 0.292 | 0.306 |

The Redlich-Peterson model posed high fitness ($R^2$: 0.996, 0.965 and 0.981 for adsorption and 0.992, 1.00 and 0.968 for desorption) with experimental data but a little bit lower than fitness of Sips model (Table 7.9). The other three-parameter model, the Unilan model showed good fitness with experimental data but it is lower than the fitness of other two three-parameter models. Considerably low RMSE and small $\chi^2$ values were observed for both adsorption and desorption from the three three-parameter models (Table 7.9) which revealed the good agreement between the experimental data and models' prediction. On comparison of the values of coefficient of determination ($R^2$), the residual root mean square error (RMSE) and the chi-square test ($\chi^2$), both the three-

parameter models were most appropriate for describing the adsorption and desorption mechanisms of Cd(II) onto ML. Therefore, the best fitting order of the models was concluded to be Sips>Redlich-Peterson>Unilan> Langmuir> Freundlich.

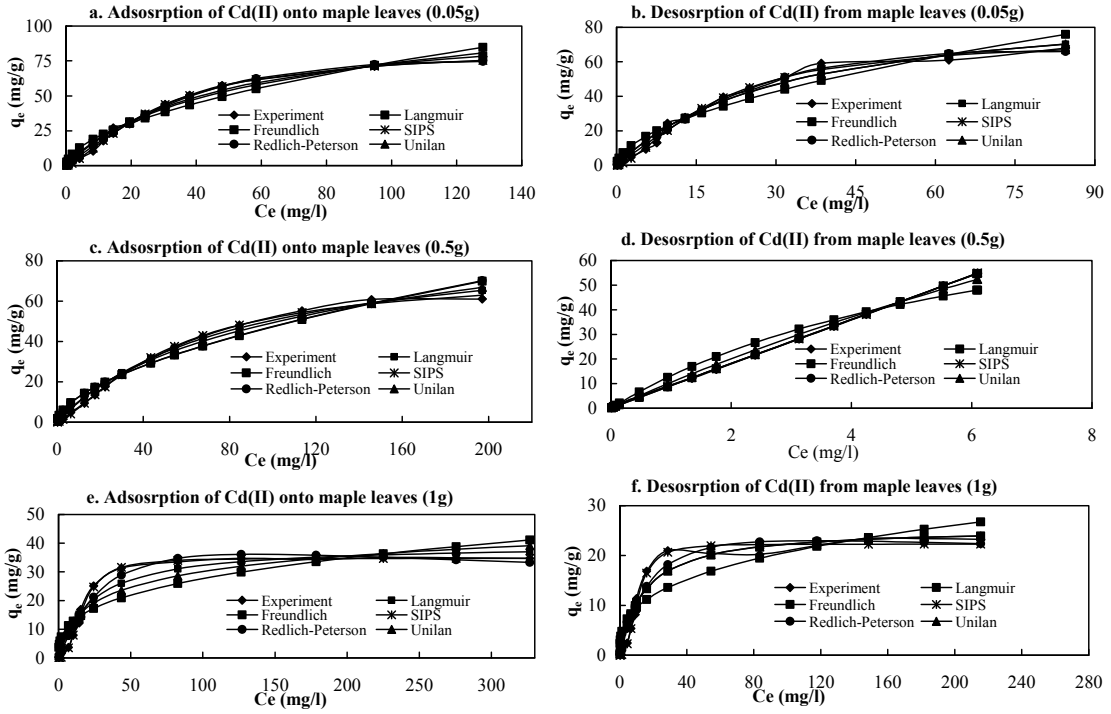


**Figure 7.17** Isotherm modelling of adsorption and desorption of Cd(II) onto ML with different doses (Co: 1-500 mg/l; d: 0.05-1 g; t: 3 h: pH: 6-6.5; rpm: 120; T: 20°C).

The Langmuir constant, $K_L$ for mono-component adsorption that is indicated the biosorption affinity of biosorbent. The magnitudes of $K_L$ are less than unity for both adsorption and desorption of three doses which signifies the strong affinity of Cd(II) adsorption. The separation factor or equilibrium constant $R_L$ explains the essential characteristics of the Langmuir isotherm. The calculated values of $R_L$ for both adsorption and desorption of Cd(II) stayed below the unity which confirmed favourability of Cd(II) adsorption/desorption onto and from ML. The values of 1/n from Freundlich models are found to be greater than unity for both adsorption and desorption processes, which advocates un-favourability. In addition the values of Gibb's free energy (Δ°G) are negative in magnitude which reveals the exothermic nature of adsorption processes.

### 7.2.4.4 Equilibrium of Cu(II) adsorption and desorption

The adsorption and desorption data of Cu(II) onto and from ML were evaluated by five isotherm models. The calculated and experimental data from 0.05, 0.5 and 1g/100ml doses are tabulated in Table 7.10 and plotted in Figure 7.18. The analysed data showed (Table 7.10) that the Langmuir model posed better fitness with experimental data than the Freundlich model for both adsorption and desorption processes. Significantly high $R^2$, low RMSE and small $\chi^2$ values are found from the Langmuir model and it proves the fitness (Table 7.10). Among the used doses the data from 0.5g dose for adsorption and from 0.05g for desorption posed higher fitness with the Langmuir model. The maximum adsorption and desorption capacities were 27.368 and 93.201 mg/g for 0.5g and 0.05g doses respectively for well fitted data.

**Table 7.10** The prediction of isotherm models for adsorption and desorption of Cu(II) on maple leaves.

| Isotherm models | Para-meters | Adsorption | | | Desorption | | |
|---|---|---|---|---|---|---|---|
| | | Doses | | | Doses | | |
| | | **0.05g** | **0.5g** | **1g** | **0.05g** | **0.5g** | **1g** |
| Experimental | $q_m$(mg/g) | 270.600 | 27.368 | 30.239 | 93.201 | 13.863 | 18.212 |
| **1. Langmuir** | $q_m$(mg/g) | 313.947 | 36.602 | 34.534 | 147.559 | 17.438 | 18.097 |
| $q_e = \frac{q_m K_L C_e}{1 + K_L C_e}$ | $K_L$ (l/g) | 0.030 | 0.010 | 0.034 | 0.065 | 0.026 | 0.058 |
| | $R^2$ | 0.991 | 0.994 | 0.991 | 0.991 | 0.961 | 0.983 |
| | $R_L$ | 0.08-0.94 | 0.21-0.99 | 0.08-0.99 | 0.08-0.99 | 0.18-0.99 | 0.11-0.99 |
| | Δ°G | -8.540 | -11.148 | -8.226 | -6.649 | -8.867 | -6.935 |
| | $\chi^2$ | 37.264 | 1.007 | 4.099 | 2.393 | 0.004 | 0.170 |
| | RMSE | 11.130 | 0.876 | 1.224 | 5.241 | 1.137 | 0.869 |
| **2. Freundlich** | $K_F$ (mg/g.l) | 38.591 | 2.077 | 4.446 | 23.944 | 1.524 | 2.527 |
| $q_e = K_F C_e^{1/n}$ | n | 2.789 | 2.179 | 2.789 | 2.788 | 2.211 | 2.536 |
| | $R^2$ | 0.915 | 0.961 | 0.915 | 0.915 | 0.912 | 0.943 |
| | $\chi^2$ | 179.176 | 10.293 | 19.709 | 84.741 | 7.561 | 7.589 |
| | RMSE | 34.749 | 2.261 | 3.822 | 16.351 | 1.712 | 1.597 |
| **3. SIPS** | Ks(l/g) | 2.604 | 0.128 | 0.344 | 3.696 | 0.044 | 0.882 |
| $q_e = \frac{K_s C_e^{\beta_s}}{1 + \alpha_s C_e^{\beta_s}}$ | $\alpha_S$ (l/mg) | 0.009 | 0.004 | 0.011 | 0.028 | 0.003 | 0.050 |
| | $\beta_S$ | 1.424 | 1.280 | 1.424 | 1.425 | 1.743 | 1.083 |
| | $R^2$ | 0.998 | 0.996 | 0.998 | 0.998 | 0.972 | 0.983 |
| | $\chi^2$ | 0.137 | 0.020 | 0.015 | 0.407 | 2.023 | 0.110 |
| | RSME | 1.217 | 0.079 | 0.134 | 0.552 | 0.110 | 0.010 |
| **4. Redlich-Peterson** | $K_{RP}$ (l/g) | 6.937 | 22.750 | 0.867 | 7.013 | 0.276 | 1.071 |
| | $\alpha_{RP}$ (l/mg) | 0.007 | 11.511 | 0.008 | 0.017 | 0.000 | 0.062 |
| $q_e = \frac{K_{RP} C_e}{1 + \alpha_{RP} C_e^{\beta}}$ | β | 1.200 | 0.531 | 1.202 | 1.207 | 1.719 | 0.989 |
| | $R^2$ | 0.998 | 0.962 | 0.998 | 0.998 | 0.978 | 0.983 |
| | $\chi^2$ | 2.617 | 1.144 | 0.287 | 1.722 | 0.005 | 0.175 |
| | RSME | 0.438 | 0.439 | 0.043 | 0.199 | 0.008 | 0.052 |
| **5. Unilan** | $q_m$ (mg/g) | 30.207 | 116.875 | 626.425 | 16.716 | 17.078 | 927.311 |
| $q_e = \frac{1}{2} q_m S \ln(1 + b e^{\delta})$ | S (l/mg) | 0.002 | 0.010 | 0.034 | 0.011 | 0.024 | 0.058 |
| | b (l/g) | 4.543 | 0.563 | 0.235 | 3.850 | 1.033 | 0.140 |
| | $R^2$ | 0.969 | 0.994 | 0.991 | 0.969 | 0.958 | 0.983 |
| | $\chi^2$ | 7.300 | 0.066 | 0.440 | 4.013 | 0.009 | 0.171 |
| | RMSE | 2.516 | 0.110 | 0.187 | 1.014 | 0.113 | 0.048 |

Sips, Redlich-Peterson and Unilan model which known as three-parameters model were used to explain the Cu(II) adsorption and desorption. Surprisingly similar to Pb(II) and Cd(II) three-parameter models showed better fitness than the two-parameter models. On the whole, very high $R^2$ (above 0.969) values, low RMSE and small $\chi^2$ values are found for both adsorption and desorption of Cu(II) onto ML. Therefore it is assumed that three-parameter models are the best model to demonstrate the equilibrium of Cu(II) adsorption and desorption (Figure 7.18 and Table 7.10). Among the three three-parameter models, the Sips model showed better agreement with the experimental data of Cu(II) adsorption and desorption, because the $R^2$ values were 0.998, 0.999 and 0.998 for adsorption and 0.998, 0.972 and 0.983 for desorption for 0.05, 0.5 and 1g doses respectively.

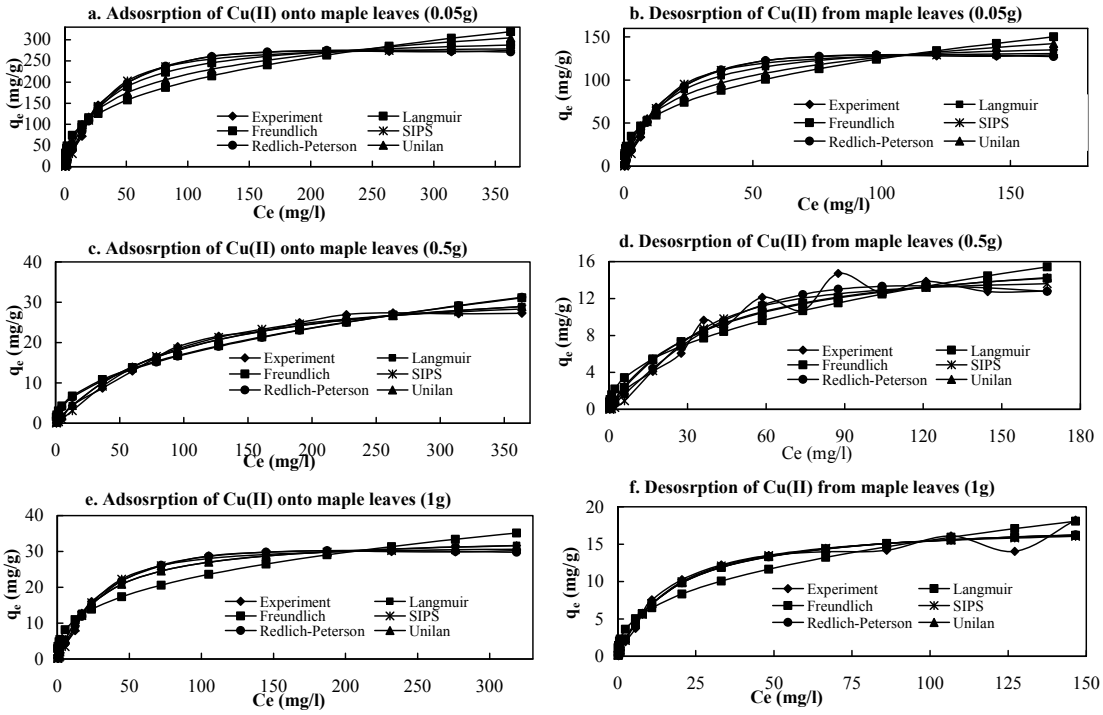


**Figure 7.18** Isotherm modelling of adsorption and desorption of Cu(II) onto ML with different doses (Co: 1-500 mg/l; d: 0.05-1 g; t: 3 h: pH: 6-6.5; rpm: 120; T: 20°C)

The second three-parameter model Redlich-Peterson also showed good agreement with experimental data as the $R^2$ values were 0.998, 0.962 and 0.998 for adsorption and 0.998, 0.978 and 0.983 for desorption (Table 7.10). These $R^2$ values are lower than the fitness of Sips model (Table 7.10). The third, the Unilan model also showed good fitness with experimental data but it is lower than the fitness of other models. Noticeably low RMSE and small $\chi^2$ values were found from all three-parameter models

(Table 7.10) which prove the conformity between the experimental data and models' prediction. On comparison of the values of coefficient of determination ($R^2$), the residual root mean square error (RMSE) and the chi-square test ($\chi^2$), both of the three-parameter models were most appropriate for describing the adsorption and desorption mechanisms of Cu(II) onto ML. Therefore, the best fitting order of the models was concluded to be Sips>Redlich-Peterson>Unilan> Langmuir> Freundlich.

$K_L$ is a constant for the Langmuir model which shows the biosorption affinity between metal ions and biosorbent. For Cu(II), the $K_L$ values are less than unity for both adsorption and desorption of three doses. This is noted as indicating that there is a strong affinity between ML and Cu(II) ions. $R_L$ is known as a separation factor or equilibrium constant which describes the essential fitness quality of the Langmuir isotherm. The $R_L$ values are below the one which validated the favourability of Cu(II) adsorption/desorption onto and from ML. The opposite proposition is found from Freundlich models because 1/n values are greater than unity for both adsorption and desorption processes, which signifies the non-favourability of Cu(II) adsorption/ desorption. In addition the values of Gibb's free energy ($\Delta°G$) are negative in magnitude which reveals the exothermic nature of adsorption processes.

#### 7.2.4.5 Equilibrium of Zn(II) adsorption and desorption

The equilibrium data from Zn(II) ions adsorption and desorption onto and from ML are assessed by five isotherm models. Among the models, Langmuir and Freundlich are two-parameter and Sips, Redlich-Peterson and Unilan are three-parameter models. The model predicted and experimental data from 0.05, 0.5 and 1g/100ml doses are presented in Table 7.11 and plotted in Figure 7.19. It can be presumed from data analysed (Table 7.11) that the Langmuir model posed better fitness with experimental data than the Freundlich model. Notably high $R^2$ (>0.972), low RMSE and small $\chi^2$ values are found from Langmuir model which demonstrated the fitness (Table 7.11) of the model with experimental data. It is notably found that the data from 1g dose for adsorption and from 1g for desorption process illustrated higher fitness with this model. The maximum adsorption and desorption capacities were 29.94 and 11.976 mg/g for 0.5g and 0.05g doses respectively for well fitted data.

Similar to Pb(II), Cd(II) and Cu(II) adsorption data, the Zn(II) adsorption and desorption data showed better fitness with three-parameter models than the two-

parameter models. Generally, very high $R^2$ (above 0.971) values, low RMSE and small $\chi^2$ values are found for both adsorption and desorption of Zn(II) onto ML. Hence it is suggested that three-parameter models are the best models to express the equilibrium of Zn(II) adsorption and desorption (Figure 7.19 and Table 7.11). Noticeably low RMSE and small $\chi^2$ values were found from all three-parameter models (Table 7.11) which prove the conformity between the experimental data and models' predictions. The Sips model showed the better agreement with the experimental data among the three three-parameter models. The fitness of the Sips model are found from high values of $R^2$ which are 0.994, 0.991 and 0.996 for adsorption and 0.998, 0.988 and 0.986 for desorption for 0.05, 0.5 and 1g doses, respectively. In addition, low RMSE and small $\chi^2$ values also revealed the fitness of this model.

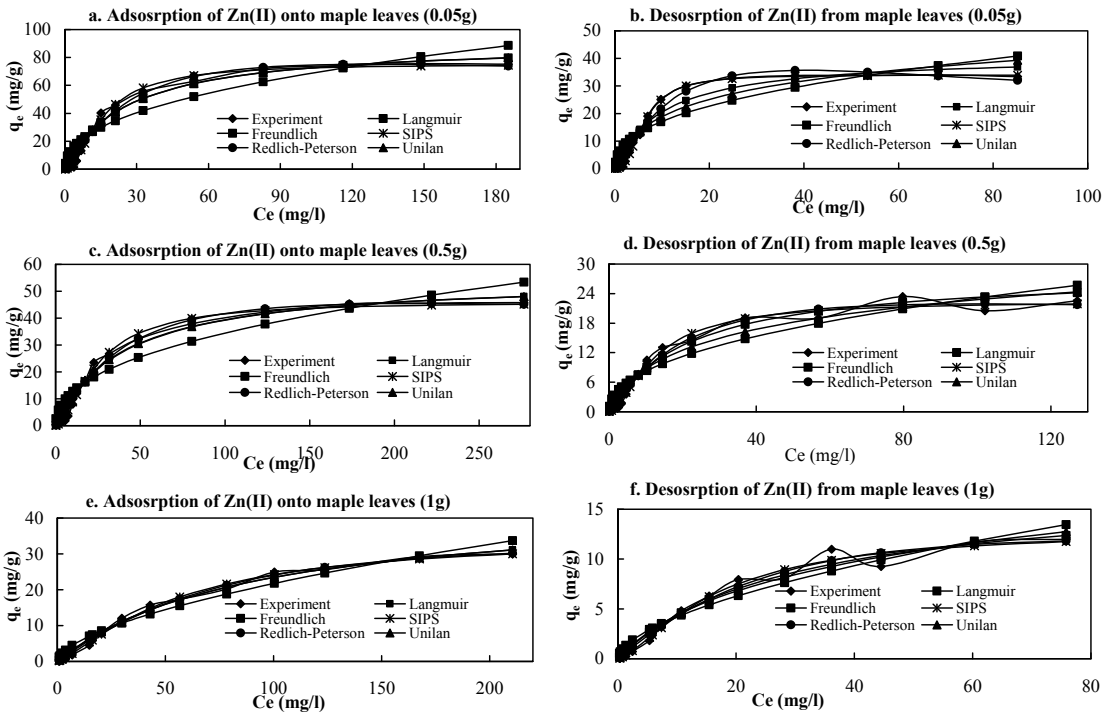


**Figure 7.19** Isotherm modelling of adsorption and desorption of Zn(II) onto ML with different doses (Co: 1-500 mg/l; d: 0.05-1 g; t: 3 h: pH: 6-6.5; rpm: 120; T: 20°C)

The Redlich-Peterson model which is used to verify the Zn(II) adsorption and desorption data, showed excellent harmony with experimental data as the $R^2$ values were 0.982, 0.983 and 0.994 for adsorption and 0.976, 0.980 and 0.982 for desorption(Table 7.11). But these values ($R^2$) are lower than the values of $R^2$ of Sips model (Table 7.11). Unilan model which is also three-parameter model articulated good fitness with experimental data but it is lower than the fitness of other three-parameter

models. On comparison of the values of coefficient of determination ($R^2$), the residual root mean square error (RMSE) and the chi-square test ($\chi^2$), both the three-parameter models were most appropriate for describing the adsorption and desorption mechanisms of Zn(II) onto ML. Therefore, the best fitting order of the models was concluded to be Sips>Redlich-Peterson>Unilan> Langmuir> Freundlich.

**Table 7.11** The prediction of isotherm models for adsorption and desorption of Zn(II) on maple leaves

| Isotherm models | Para-meters | Adsorption | | | Desorption | | |
|---|---|---|---|---|---|---|---|
| | | Doses | | | Doses | | |
| | | **0.05g** | **0.5g** | **1g** | **0.05g** | **0.5g** | **1g** |
| Experimental | $q_m$(mg/g) | 75.579 | 45.72 | 29.94 | 34.011 | 20.525 | 11.976 |
| **1. Langmuir** | $q_m$(mg/g) | 90.843 | 55.024 | 44.292 | 41.287 | 28.365 | 17.116 |
| $q_e = \frac{q_m K_L C_e}{1 + K_L C_e}$ | $K_L$ (l/g) | 0.039 | 0.025 | 0.011 | 0.099 | 0.045 | 0.034 |
| | $R_L$ | 0.972 | 0.979 | 0.992 | 0.944 | 0.971 | 0.978 |
| | $R^2$ | 0.12-0.99 | 0.13-0.99 | 0.30-0.99 | 0.11-0.99 | 0.15-0.99 | 0.28-0.99 |
| | Δ°G | -7.929 | -8.988 | -10.944 | -5.638 | -7.542 | -8.215 |
| | $\chi^2$ | 27.191 | 11.844 | 3.766 | 0.118 | 0.085 | 0.159 |
| | RMSE | 5.253 | 2.696 | 1.047 | 3.540 | 1.549 | 0.688 |
| **2. Freundlich** | $K_F$ (mg/g.l) | 9.274 | 4.730 | 1.439 | 6.733 | 2.940 | 1.115 |
| $q_e = K_F C_e^{1/n}$ | n | 2.314 | 2.320 | 1.697 | 2.465 | 2.234 | 1.738 |
| | $R^2$ | 0.889 | 0.899 | 0.962 | 0.830 | 0.903 | 0.943 |
| | $\chi^2$ | 67.242 | 35.451 | 11.277 | 42.228 | 16.457 | 5.552 |
| | RMSE | 10.460 | 5.936 | 2.229 | 6.164 | 2.825 | 1.108 |
| **3. SIPS** | Ks(l/g) | 0.651 | 0.279 | 0.187 | 0.461 | 0.437 | 0.224 |
| $q_e = \frac{K_s C_e^{\beta_s}}{1 + \alpha_s C_e^{\beta_s}}$ | $\alpha_S$ (l/mg) | 0.009 | 0.006 | 0.005 | 0.014 | 0.019 | 0.017 |
| | $\beta_S$ | 1.708 | 1.586 | 1.307 | 2.332 | 1.549 | 1.450 |
| | $R^2$ | 0.994 | 0.991 | 0.996 | 0.998 | 0.988 | 0.986 |
| | $\chi^2$ | 1.697 | 8.048 | 1.040 | 11.568 | 0.021 | 0.026 |
| | RSME | 0.397 | 0.165 | 0.086 | 0.023 | 0.085 | 0.024 |
| **4. Redlich-Peterson** | $K_{RP}$ (l/g) | 2.706 | 1.124 | 0.421 | 2.869 | 1.067 | 0.478 |
| | $\alpha_{RP}$ (l/mg) | 0.007 | 0.006 | 0.002 | 0.011 | 0.012 | 0.006 |
| $q_e = \frac{K_{RP} C_e}{1 + \alpha_{RP} C_e^{\beta}}$ | β | 1.278 | 1.227 | 1.272 | 1.448 | 1.253 | 1.359 |
| | $R^2$ | 0.982 | 0.983 | 0.994 | 0.976 | 0.980 | 0.982 |
| | $\chi^2$ | 0.080 | 0.220 | 0.312 | 0.048 | 0.063 | 0.128 |
| | RSME | 1.175 | 0.570 | 0.240 | 0.799 | 0.272 | 0.113 |
| **5. Unilan** | $q_m$ (mg/g) | 53.103 | 38.835 | 31.867 | 5.372 | 4.030 | 2.889 |
| $q_e = \frac{1}{2} q_m S \ln(1 + b e^S)$ | S (l/mg) | 0.327 | 0.319 | 1.265 | 3.850 | 3.526 | 3.819 |
| | b (l/g) | 0.038 | 0.025 | 0.008 | 0.011 | 0.007 | 0.003 |
| | $R^2$ | 0.971 | 0.975 | 0.990 | 0.905 | 0.955 | 0.972 |
| | $\chi^2$ | 0.177 | 0.091 | 0.397 | 0.201 | 0.129 | 0.180 |
| | RMSE | 1.468 | 0.723 | 0.333 | 0.718 | 0.304 | 0.164 |

The constant of the Langmuir model, $K_L$ demonstrates the biosorption affinity between metal ions and biosorbent. The $K_L$ values are less than unity for both adsorption and desorption of three doses for Zn(II). This signifies that there is strong affinity between ML and Zn(II) ions. The separation factor, $R_L$ shows the suitability of Langmuir isotherm to demonstrate the metals adsorption. The $R_L$ values for Zn(II) adsorption are below the one which authenticated the favourability of Zn(II) adsorption/desorption.

But 1/n values from Freundlich models differ with the favourability of Zn(II) adsorption and desorption because these values are greater than unity for both adsorption and desorption processes. In addition the values of Gibb's free energy (Δ°G) are negative in magnitude which reveals the exothermic nature of adsorption processes.

#### 7.2.4.6 Comparison of fitness for Pb(II), Cd(II), Cu(II) and Zn(II)

The fitness of Pb(II), Cd(II), Cu(II) and Zn(II) adsorption and desorption data are judged on the basis of $R^2$, RMSE and $\chi^2$ values for different models. It was found that the fitness trends are Pb(II)>Cd(II)>Zn(II)>Cu(II) for adsorption onto ML; but it is Pb(II)>Cd(II)>Cu(II) >Zn(II) for desorption. The Langmuir model describes the monolayer adsorption onto homogeneous surfaces while Freundlich better resembles the adsorption onto heterogeneous surfaces. From the analysed data, it was found that Pb(II), Cd(II), Cu(II) and Zn(II) adsorption did not show proper agreement with the Langmuir and Freundlich models. Conversely, the adsorption data for Pb(II), Cd(II), Cu(II) and Zn(II) showed excellent fitness with Sips, Redlich-Peterson and Unilan which mainly describes the combined characteristics of Langmuir and Freundlich. So, it can be decided that ML has both homogeneous and heterogeneous surfaces.

#### 7.2.4.7 Adsorption mechanism

From the hints of FT-IR analysis (hydroxyl and carboxylic groups) and activation energy evaluation, the high $R^2$, $\chi^2$ and RMSE values for the Langmuir isotherm and; high $R^2$, NSD and ARE values for the Pseudo-second-order kinetic model, and reasonable fixed values for metals biosorption revealed that adsorption could be a chelation bond between the Pb(II), Cd(II), Cu(II) and Zn(II) ion and ML. However, the high $R^2$ values of three-parameter isotherms suggest that more than one mechanism such as physiosorption, chemisorption and complexation may be involved for metals ions adsorption. Therefore, the analyses of the results make it very difficult to assign a definite mechanism for the sorption of Pb(II), Cd(II), Cu(II) and Zn(II) ions onto maple leaves.

### 7.2.5 Multimetals adsorption

The Langmuir isotherm can be used to evaluate the equilibrium data for a single metal adsorption (Langmuir, 1918), which is represented mathematically as follows:

$$q_{e.i} = \frac{q_{m.i} K_{L.i} C_{e.i}}{1 + K_{L.i} C_{e.i}} \qquad (7.10)$$

With a simple modification this model can be used to multi-metals isotherm (Padilla-Ortega et al., 2013; Srivastava et al., 2008):

$$q_{e.i} = \frac{q_{m.i} K_{L.i}(C_i)}{1 + \sum_{j=1}^{N} K_{L.j}(C_j)} \qquad (7.11)$$

### 7.2.5.1 Adsorption behaviour in binary solutions

Langmuir multi-metals isotherm can be employed for binary metals adsorption. When the metals content is double (i =2) in water; i.e. the equation (7.11) becomes as follows (in Pb(II)-Cd(II) solution):

For Pb(II): $$q_{e.Pb} = \frac{q_{m.Pb} K_{L.Pb}(C_{Pb})}{1 + K_{L.Pb} C_{e.Pb} + K_{L.Cd} C_{e.Cd}} \qquad (7.12)$$

For Cd(II): $$q_{e.Cd} = \frac{q_{m.Cd} K_{L.Cd}(C_{Cd})}{1 + K_{L.Pb} C_{e.Pb} + K_{L.Cd} C_{e.Cd}} \qquad (7.13)$$

Similarly the equation(7.11) can be transformed for the binary solution of Cu(II)-Pb(II), Cd(II)-Zn(II), Cd(II)-Cu(II), Cu(II)-Zn(II) and Pb(II)-Zn(II) adsorption system.

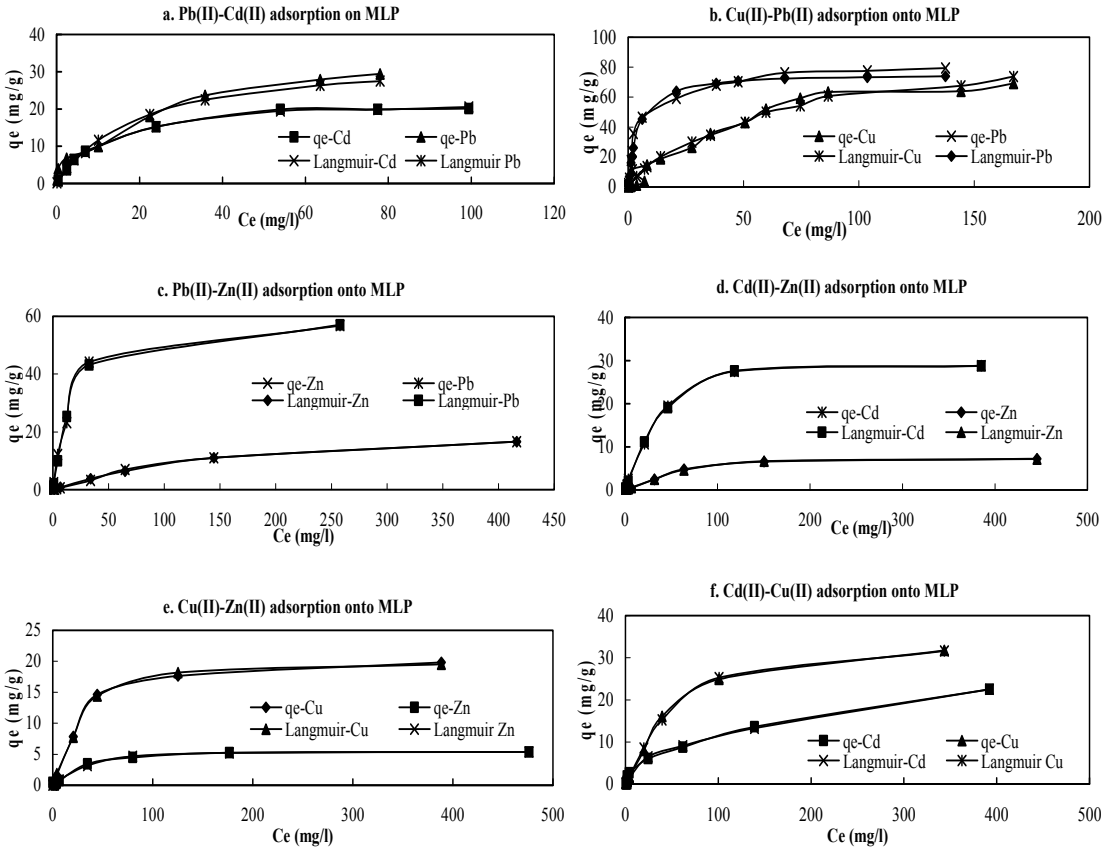


**Figure 7.20** Equilibrium of binary adsorption of Pb(II)-Cd(II), Cu(II)-Pb(II), Cd(II)-Zn(II), Cd(II)-Cu(II), Cu(II)-Zn(II) and Pb(II)-Zn(II) ions on ML.

When the concentration of metal ions in water ($C_e$) is in balance with that in the solid matrix ($q_e$), equilibrium is established. This level of equilibrium concentration depends significantly on the initial concentration of the metals and the binary isotherm results are plotted in Figure 7.20. The isotherm parameters of binary adsorptions of Pb(II)-Cd(II), Cu(II)-Pb(II), Cd(II)-Zn(II), Cd(II)-Cu(II), Cu(II)-Zn(II) and Pb(II)-Zn(II) ions are shown in Table 7.12. The binary isotherm experiments were carried out using pairs of metal ions with equal initial concentration and the concentrations were between 1 to 500 mg/l and an adsorbent dose of 5 g/l. In this case, the mass ratios of initial concentrations of Pb(II)-Cd(II), Cu(II)-Zn(II), Cu(II)-Pb(II), Pb(II)-Zn(II), Cd(II)-Zn(II) and Cd(II)-Cu(II) were 1:1.

The adsorption of Pb(II) and Cu(II) are dominant in the binary adsorption system for ML and almost similar results were found for other biosorbents in the literature (Kongsuwan et al., 2009). The binary form of the Langmuir isotherm (Eqs.7.12 and 7.13) used to examine experimental data with isotherm programming. The adsorption showed a significantly higher degree of fitness ($R^2$: 0.955-0.999) with metal ions adsorption (Table 7.12).

**Table 7.12** Calculated parameters from Langmuir model for binary adsorption of Pb(II)-Cd(II), Cu(II)-Pb(II), Cd(II)-Zn(II), Cd(II)-Cu(II), Cu(II)-Zn(II) and Pb(II)-Zn(II) ions on ML

| **Pb(II)-Cd(II)** | **Cu(II)-Zn(II)** | **Cu(II)-Pb(II)** |
|---|---|---|
| For Pb(II): | For Cu(II): | For Cu(II): |
| $q_{m\text{-}Pb}$ = 34.019 mg/g | $q_{m\text{-}Cu}$ = 10.354 mg/g | $q_{m\text{-}Cu}$ = 25.898 mg/g |
| $K_{L\text{-}Pb}$ = 0.050 l/g | $K_{L\text{-}Cu}$ = 0.046 l/g | $K_{L\text{-}Cu}$ = 0.036 l/g |
| $K_{L\text{-}Cd}$ = -0.004 l/g | $K_{L\text{-}Zn}$ = -0.019 l/g | $K_{L\text{-}Pb}$ = -0.016 l/g |
| $R^2$ = 0.955 | $R^2$ = 0.998 | $R^2$ = 0.971 |
| For Cd(II): | For Zn(II): | For Pb(II): |
| $q_{m\text{-}Cd}$ = 28.360 mg/g | $q_{m\text{-}Zn}$ = 5.420 mg/g | $q_{m\text{-}Pb}$ = 45.396 mg/g |
| $K_{L\text{-}Pb}$ = 0.022 l/g | $K_{L\text{-}Cu}$ = -0.045 l/g | $K_{L\text{-}Cu}$ = -0.0069 l/g |
| $K_{L\text{-}Cd}$ = 0.073 l/g | $K_{L\text{-}Zn}$ = 0.03 l/g | $K_{L\text{-}Pb}$ = 0.185 l/g |
| $R^2$ = 0.998 | $R^2$ = 0.989 | $R^2$ = 0.981 |
| **Pb(II)-Zn(II)** | **Cd(II)-Zn(II)** | **Cd(II)-Cu(II)** |
| For Pb(II): | For Cd(II): | For Cd(II): |
| $q_{m\text{-}Pb}$ = 37.971 mg/g | $q_{m\text{-}Cd}$ =8.057 mg/g | $q_{m\text{-}Cd}$ = 6.899 mg/g |
| $K_{L\text{-}Pb}$ = 0.040 l/g | $K_{L\text{-}Cd}$ = 0.067 l/g | $K_{L\text{-}Cd}$ = 0.054 l/g |
| $K_{L\text{-}Zn}$ = -0.050 l/g | $K_{L\text{-}Zn}$ = -0.044 l/g | $K_{L\text{-}Cu}$ = -0.046 l/g |
| $R^2$ = 0.997 | $R^2$ = 0.999 | $R^2$ = 0.991 |
| For Zn(II): | For Zn(II): | For Cu(II): |
| $q_{m\text{-}Zn}$ = 27.88 mg/g | $q_{m\text{-}Zn}$ =7.295 mg/g | $q_{m\text{-}Cu}$ = 19.985 mg/g |
| $K_{L\text{-}Pb}$ = 0.0013 l/g | $K_{L\text{-}Cd}$ = -0.031 l/g | $K_{L\text{-}Cd}$ = -0.055 l/g |
| $K_{L\text{-}Zn}$ = 0.005 l/g | $K_{L\text{-}Zn}$ = 0.01 l/g | $K_{L\text{-}Cu}$ = 0.014 l/g |
| $R^2$ = 0.997 | $R^2$ = 0.998 | $R^2$ = 0.996 |

The maximum adsorption capacities ($q_m$) are 34.019 and 28.360 mg/g for Pb(II) and Cd(II) in Pb(II)-Cd(II) binary system, 10.354 and 5.420mg/g for Cu(II) and Zn(II) in Cu(II)-Zn(II) binary system, 28.898 and 45.396 mg/g for Cu(II) and Pb(II) in Cu(II)-Pb(II) binary system, 37.971 and 27.88 mg/g for Pb(II) and Zn(II) in Pb(II)-Zn(II) binary system, 8.057 and 7.295 mg/g for Cd(II) and Zn(II) in Cd(II)-Zn(II) binary system, and 6.899 and 19.985 mg/g for Cd(II) and Cu(II) in Cd(II)-Cu(II) binary system (Table 7.12). It is observed that the adsorption capacity for Pb(II) was higher than that of Cd(II), Cu(II) and Zn(II) because the variety of functional groups on the surface of ML could uptake more Pb(II) ions than other metals (Kongsuwan et al., 2009). It is also noticeable that the maximum adsorption capacities for Pb(II), Cd(II), Cu(II) and Zn(II) obtained from binary metals sorption are less than those obtained from the single metal system (Table 7.8, Table 7.9, Table 7.10 and Table 7.11). Similar results also found in the literature (Kumar et al., 2008; Zhu et al., 2012).

#### 7.2.5.2 Adsorption behaviour in ternary solutions

The equation 7.11 can be rephrased for Cu(II)-Pb(II)-Cd(II) ternary adsorption system as:

for Cu(II): $$q_{e.Cu} = \frac{q_{m.Cu} K_{L.Cu} (C_{Cu})}{1 + K_{L.Cu} C_{e.Cu} + K_{L.Pb} C_{e.Pb} + K_{L.Cd} C_{e.Cd}} \quad (7.14)$$

for Pb(II): $$q_{e.Pb} = \frac{q_{m.Pb} K_{L.Pb} (C_{Pb})}{1 + K_{L.Cu} C_{e.Cu} + K_{L.Pb} C_{e.Pb} + K_{L.Cd} C_{e.Cd}} \quad (7.15)$$

and for Cd(II): $$q_{e.Cd} = \frac{q_{m.Cd} K_{L.Cd} (C_{Cd})}{1 + K_{L.Cu} C_{e.Cu} + K_{L.Pb} C_{e.Pb} + K_{L.Cd} C_{e.Cd}} \quad (7.16)$$

Similarly, the equation (7.11) can be rewritten for Pb(II)-Cd(II)-Zn(II), Cu(II)-Pb(II)-Zn(II) and Cu(II)-Cd(II)-Zn(II) adsorption systems.

Normally, wastewaters contain multi-metal ions and therefore, the evaluation of multiple metal interactions concurrently is very significant for accurate representation of adsorption data (Hammaini et al., 2003). Competitive adsorptions were performed in batch system in the ternary systems between 1 to 200 mg/l initial concentration of Pb(II), Cd(II), Cu(II) and Zn(II) ions for 3 hours at 120 rpm and room temperature. The multi-metal isotherm parameters are tabulated in Table 7.13 and plotted in Figure 7.21.

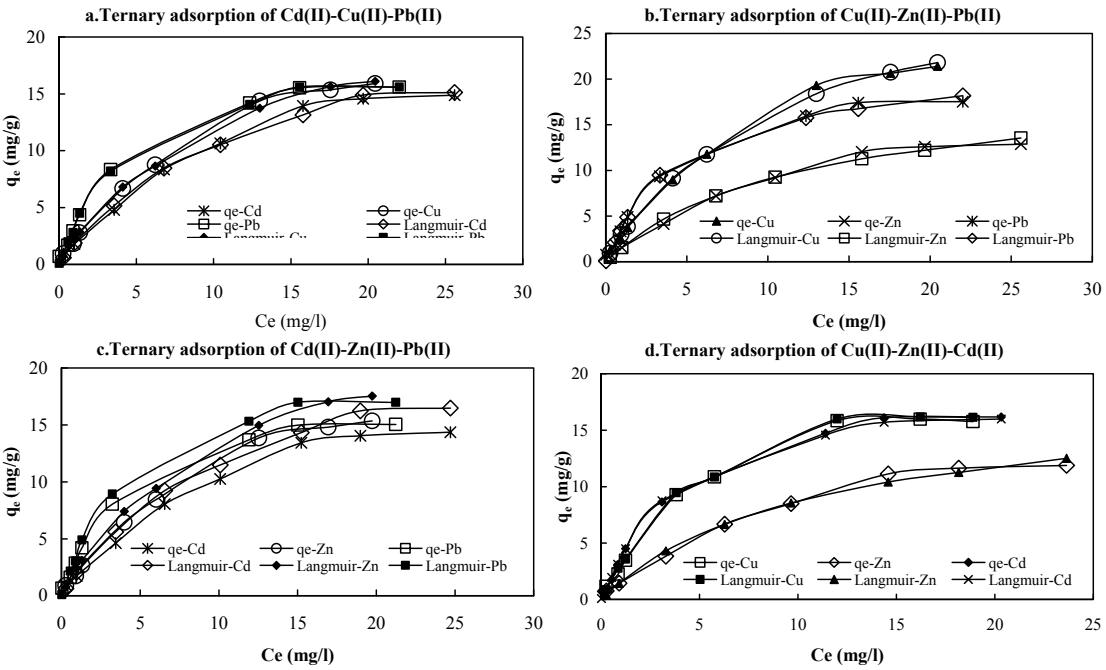


**Figure 7.21** Ternary adsorption of among the Cu(II), Pb(II), Cd(II) and Zn(II) in the ternary systems of Cd(II)-Pb(II)-Cu(II), Cd(II)-Pb(II)-Zn(II), Cu(II)-Cd(II)-Zn(II) and Cu(II)-Pb(II)-Zn(II)

It is found from the analysed data that experimental data showed good agreement with the ternary isotherm model (eq.7.14, 7.15 and 7.16) as the $R^2$ were 0.995, 0.997 and 0.999 for Cd(II), Pb(II), and Cu(II) of Cd(II)-Pb(II)-Cu(II) system; 0.996, 0.996 and 0.996 for Cd(II), Pb(II) and Zn(II) of Cd(II)-Pb(II)-Zn(II) system; 0.993, 0.994 and 0.992 for Cu(II), Cd(II) and Zn(II) of Cu(II)-Cd(II)-Zn(II)system; and 0.994, 0.995 and 0.993 for Cu(II), Pb(II) and Zn(II) of Cu(II)-Pb(II)-Zn(II) system, respectively. In ternary system, the maximum adsorption capacity ($q_m$) were found lower than single metal system for Cu(II), Cd(II), Zn(II) and Pb(II) ions (Table 7.8, Table 7.9, Table 7.10, Table 7.11 and Table 7.13). Similar results are found for other biosorbents in the literature (Kusvuran et al., 2012; Verma et al., 2008).

Different characteristics of metal ions such as ionic charge, ionic radius, and electro-potential affect adsorption capacities (Zhu et al., 2012). Eventually it reduces the capacities in the multi-metal adsorption system with respect to single metal adsorption capacity (Padilla-Ortega et al., 2013; Zhu et al., 2012). The maximum adsorption capacities were found to be 14.664, 44.061 and 22.416 mg/g for Cd(II)-Pb(II)-Cu(II) system, 17.587, 35.743 and 9.254 mg/g for Cd(II)-Pb(II)-Zn(II) system, 12.478, 14.837

and 8.743 mg/g for Cu(II)-Cd(II)-Zn(II) system, and 17.456, 32.768 and 9.230 mg/g for Cu(II)-Pb(II)-Zn(II) system, respectively for ML in ternary (Table 7.13).

**Table 7.13** Ternary adsorption parameters calculated from Langmuir model for Pb(II), Cd(II), Cu(II) and Zn(II) adsorption

| Cd(II)-Pb(II)-Cu(II) | Cd(II)-Pb(II)-Zn(II) | Cu(II)-Cd(II)-Zn(II) | Cu(II)-Pb(II)-Zn(II) |
|---|---|---|---|
| **For Cd(II)** | **For Cd(II)** | **For Cu(II)** | **For Cu(II)** |
| $q_{m\text{-}Cd}$ =14.664 mg/g | $q_{m\text{-}Cd}$ = 17.587 mg/g | $q_{m\text{-}Cu}$ = 12.478 mg/g | $q_{m\text{-}Cu}$ = 17.456 mg/g |
| $K_{L\text{-}Cu}$ = -0.083 l/g | $K_{L\text{-}Zn}$ = -0.048 l/g | $K_{L\text{-}Cu}$ = 0.053 l/g | $K_{L\text{-}Zn}$ = -0.024 l/g |
| $K_{L\text{-}Cd}$ = 0.139 l/g | $K_{L\text{-}Cd}$ = 0.093 l/g | $K_{L\text{-}Cd}$ = 0.098 l/g | $K_{L\text{-}Cu}$ = 0.086 l/g |
| $K_{L\text{-}Pb}$ = 0.027 l/g | $K_{L\text{-}Pb}$ = -0.076 l/g | $K_{L\text{-}Zn}$ = -0.058 l/g | $K_{L\text{-}Pb}$ = 0.075 l/g |
| $R^2$ = 0.995 | $R^2$ = 0.996 | $R^2$ = 0.993 | $R^2$ = 0.994 |
| **For Pb(II)** | **For Pb(II)** | **For Cd(II)** | **For Pb(II)** |
| $q_{m\text{-}Pb}$ = 44.061 mg/g | $q_{m\text{-}Pb}$ = 35.743 mg/g | $q_{m\text{-}Cd}$ = 14.837 mg/g | $q_{m\text{-}Pb}$ = 32.768 mg/g |
| $K_{L\text{-}Cu}$ = -0.111 l/g | $K_{L\text{-}Zn}$ = -0.018 l/g | $K_{L\text{-}Cu}$ = 0.065 l/g | $K_{L\text{-}Zn}$ = -0.023 l/g |
| $K_{L\text{-}Pb}$ = 0.257 l/g | $K_{L\text{-}Cd}$ = -0.023 l/g | $K_{L\text{-}Cd}$ = 0.073 l/g | $K_{L\text{-}Cu}$ = 0.057 l/g |
| $K_{L\text{-}Cd}$ = 0.032 l/g | $K_{L\text{-}Pb}$ = 0.087 l/g | $K_{L\text{-}Zn}$ = -0.056 l/g | $K_{L\text{-}Pb}$ = 0.089 l/g |
| $R^2$ = 0.999 | $R^2$ = 0.996 | $R^2$ = 0.994 | $R^2$ = 0.995 |
| **For Cu(II)** | **For Zn(II)** | **For Zn(II)** | **For Zn(II)** |
| $q_{m\text{-}Cu}$ = 22.416 mg/g | $q_{m\text{-}Zn}$ = 9.254 mg/g | $q_{m\text{-}Zn}$ = 8.743 mg/g | $q_{m\text{-}Zn}$ = 9.230 mg/g |
| $K_{L\text{-}Cd}$ = 0.051 l/g | $K_{L\text{-}Zn}$ = 0.017 l/g | $K_{L\text{-}Cu}$ = 0.036 l/g | $K_{L\text{-}Zn}$ = 0.034 l/g |
| $K_{L\text{-}Cu}$ = 0.075 l/g | $K_{L\text{-}Cd}$ = -0.053 l/g | $K_{L\text{-}Cd}$ = 0.072 l/g | $K_{L\text{-}Cu}$ = 0.079 l/g |
| $K_{L\text{-}Pb}$ = -0.02 l/g | $K_{L\text{-}Pb}$ = -0.027 l/g | $K_{L\text{-}Zn}$ = -0.023 l/g | $K_{L\text{-}Pb}$ = 0.017 l/g |
| $R^2$ = 0.997 | $R^2$ = 0.996 | $R^2$ = 0.992 | $R^2$ = 0.993 |

### 7.2.5.3 Adsorption behaviour in quaternary solutions

The adsorption system for four metals system in water can be devised by modification of the equation 7.11 for quaternary solution [Cu(II)-Pb(II)-Cd(II)-Zn(II)] system:

For Cu(II): $$q_{e.Cu} = \frac{q_{m.Cu} K_{L.Cu} (C_{Cu})}{1 + K_{L.Cu} C_{e.Cu} + K_{L.Pb} C_{e.Pb} + K_{L.Cd} C_{e.Cd} + K_{L.Zn} C_{e.Zn}} \quad (7.17)$$

For Pb(II): $$q_{e.Pb} = \frac{q_{m.Pb} K_{L.Pb} (C_{Pb})}{1 + K_{L.Cu} C_{e.Cu} + K_{L.Pb} C_{e.Pb} + K_{L.Cd} C_{e.Cd} + K_{L.Zn} C_{e.Zn}} \quad (7.18)$$

For Cd(II): $$q_{e.Cd} = \frac{q_{m.Cd} K_{L.Cd} (C_{Cd})}{1 + K_{L.Cu} C_{e.Cu} + K_{L.Pb} C_{e.Pb} + K_{L.Cd} C_{e.Cd} + K_{L.Zn} C_{e.Zn}} \quad (7.19)$$

And for Zn(II): $$q_{e.Zn} = \frac{q_{m.Zn} K_{L.Zn} (C_{Zn})}{1 + K_{L.Cu} C_{e.Cu} + K_{L.Pb} C_{e.Pb} + K_{L.Cd} C_{e.Cd} + K_{L.Zn} C_{e.Zn}} \quad (7.20)$$

The isotherm data are fitted with the quaternary Langmuir model and the parameters are summarised in Table 7.14. It is found that quaternary data showed good agreement with the isotherm model. The experimental and model predictions are plotted in Figure 7.22 and Figure 7.23.

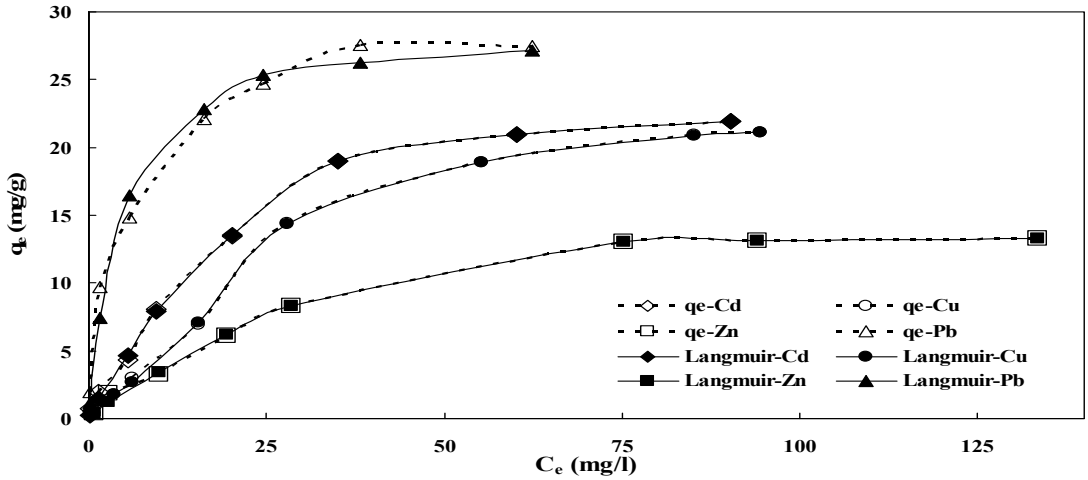


**Figure 7.22** Quaternary adsorption of among the Cu(II), Pb(II), Cd(II) and Zn(II) in the four metals system of Cd(II)-Pb(II)-Cu(II)-Zn(II)

The maximum adsorption capacities ($q_m$) for four metals [Cd(II)-Pb(II)-Cu(II)-Zn(II)] system were compared to the molar uptake values of metals predicted with single metal system. It is found that the model absolutely assessed the parameters for all fours metals uptake because the predicted lines and experimental plots are close enough (Figure 7.22). A clear comparison of metal adsorption and prediction can be viewed in Figure 7.23. The adsorption capacities increases with the increased of initial metals concentration and adsorbed areas are equal to the predicted areas (Figure 7.23). The maximum adsorption capacities ($q_m$) are 45.248, 13.633, 9.652 and 7.984 mg/g for Pb(II), Cd(II), Cu(II) and Zn(II) respectively, but these values are lower than the single metals system. The competitions among the metal ions reduces the adsorption capacities (Papageorgiou et al., 2009; Şengil and Özacar, 2009; Xue et al., 2009).

**Table 7.14** Isotherm parameters of Langmuir model for quaternary metals [Cd(II)-Cu(II)-Zn(II)-Pb(II)] adsorption

| For Pb(II) | For Cd(II) | For Zn(II) | For Cu(II) |
|---|---|---|---|
| $q_{m\text{-}Pb}$ = 45.248 mg/g | $q_{m\text{-}Cd}$ = 13.633 mg/g | $q_{m\text{-}Zn}$ = 9.652 mg/g | $q_{m\text{-}Cu}$ = 7.984 mg/g |
| $K_{L\text{-}Cu}$ = -0.003 l/g | $K_{L\text{-}Cu}$ = -0.013 l/g | $K_{L\text{-}Cu}$ = -0.017 l/g | $K_{L\text{-}Cu}$ = -0.002 l/g |
| $K_{L\text{-}Cd}$ = 0.014 l/g | $K_{L\text{-}Cd}$ = 0.080 l/g | $K_{L\text{-}Cd}$ = 0.048 l/g | $K_{L\text{-}Cd}$ = 0.072 l/g |
| $K_{L\text{-}Zn}$ = -0.006 l/g | $K_{L\text{-}Zn}$ = -0.004 l/g | $K_{L\text{-}Zn}$ = 0.025 l/g | $K_{L\text{-}Zn}$ = 0.007 l/g |
| $K_{L\text{-}Pb}$ = 0.214 l/g | $K_{L\text{-}Pb}$ = -0.031 l/g | $K_{L\text{-}Pb}$ = -0.038 l/g | $K_{L\text{-}Pb}$ = -0.09 l/g |
| $R^2$ = 0.987 | $R^2$ = 0.999 | $R^2$ = 0.998 | $R^2$ = 1.000 |

The Langmuir constant, $K_L$ signifies the affinity of biosorbent towards the metal ions; th greater the value of these parameters, the lesser is the affinity (Kusvuran et al., 2012; Şengil and Özacar, 2009). The values of $K_{L\text{-}Cu}$, $K_{L\text{-}Pb}$, $K_{L\text{-}Zn}$, and $K_{L\text{-}Cd}$ are higher in the case of the binary, ternary and quaternary system than the value of $K_L$ derived for the

single metal system (Table 7.8, Table 7.9, Table 7.10, Table 7.11 and Table 7.13). This means that the affinity of ML biosorbent for metal ions was reduced in a multi-metals metal system.

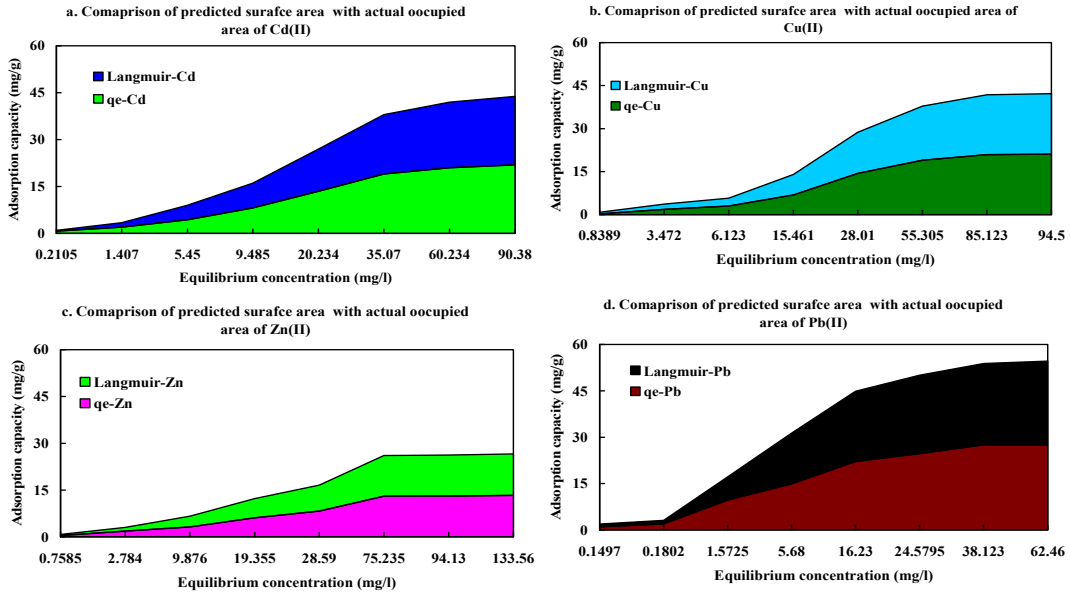


**Figure 7.23** Experimental and model predicted surface areas in terms of adsorption capacity of metals in surface diagram for quaternary metals adsorption onto ML

### 7.2.5.4 Antagonism of multi-metals system

The multi-metal Langmuir model gives a logical fit to the adsorption data from multimetals as long as the $q_m$ values for each metal calculated from single-metal are similar to each (Leyva-Ramos et al., 2001). However, the $q_m$ values from single metals systems are found to be lower than the values from binary, ternary and quaternary. Similar results reported in the literature (Kumar et al., 2008; Şengil and Özacar, 2009). The internal competitions among the metals ions reduce the adsorption capacities (Şengil and Özacar, 2009). This competition is termed as antagonism. To visualise the antagonism, 3D surface plots are constructed for the binary system adsorption of Pb(II)-Cd(II), Cd(II)-Cu(II), Cu(II)-Pb(II), Cu(II)-Zn(II), Cd(II)-Zn(II) and Zn(II)-Pb(II). The 3D for the binary systems are shown in Figure 7.24 and Figure 7.25. The area plot for ternary system (Cd(II)-Pb(II)-Cu(II), Cd(II)-Pb(II)-Zn(II), Cu(II)-Cd(II)-Zn(II) and Cu(II)-Pb(II)-Zn(II)) is shown in Figure 7.26; and the spider diagram for quaternary system (Cd(II)-Pb(II)-Cu(II)-Zn(II)) is given in Figure 7.27.

The presence of Cd(II) during the adsorbing of Pb(II) ions is showed in Figure 7.24(A). It is found the from the adsorption surface of Figure 7.24 that Pb(II) adsorption reduces in the presence of Cd(II). A reasonable reduction of the uptake of Pb(II) is found in

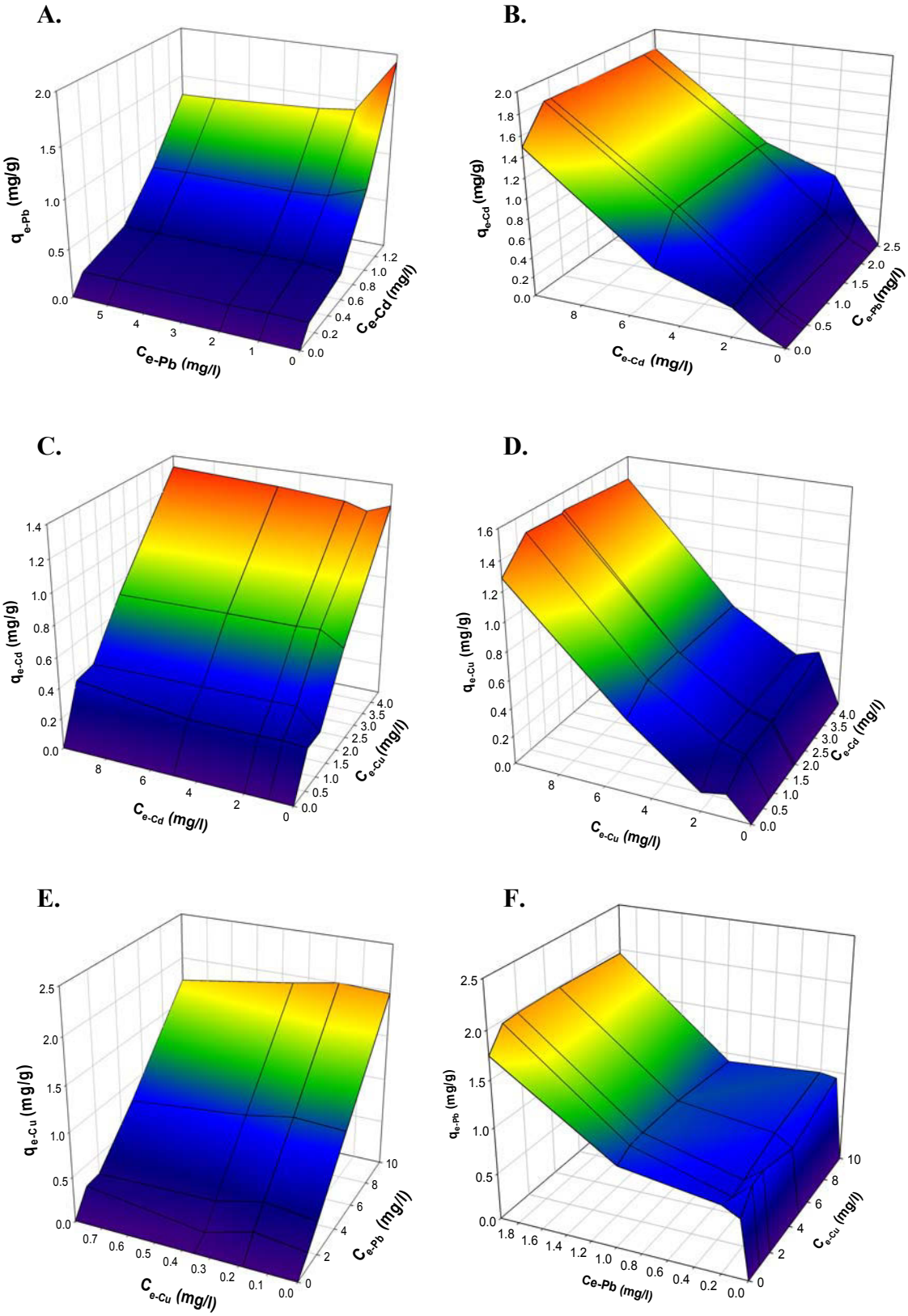


Figure 7.24 Antagonism among the metals for Pb(II)-Cd(II) (A & B), Cd(II)-Cu(II) (C & D) and Cu(II)-Pb(II) (E & F) binary system.

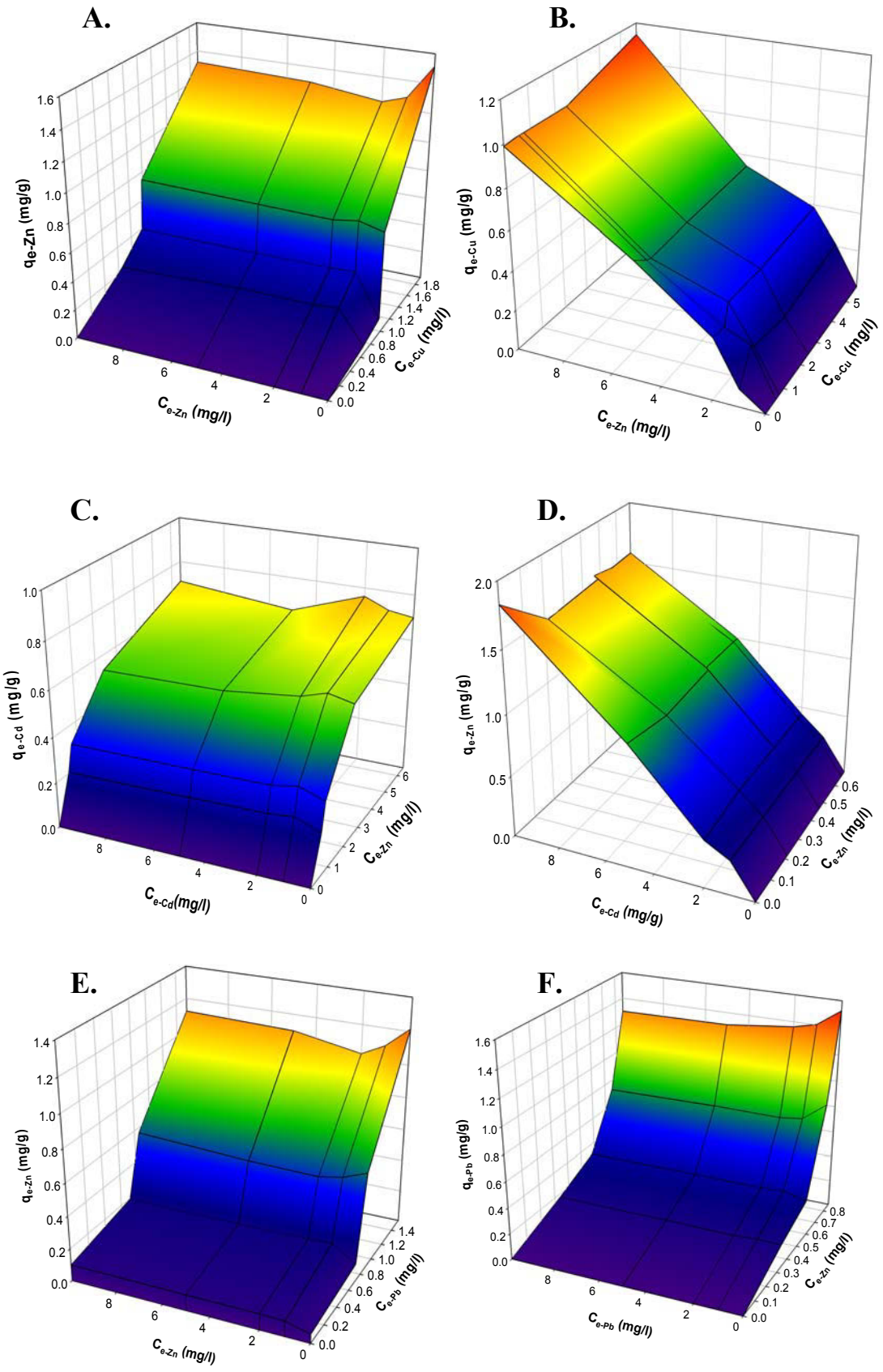


Figure 7.25 Antagonism among the metals for Cu(II)-Zn(II) (A&B), Cd(II)-Zn(II) (C&D) and Zn(II)-Pb(II) (E&F) binary system.

comparison to a single metal system (from 50.267 to 35.019 mg/g). Besides this the effect of the presence Pb(II) on the capacity of Cd(II) adsorption is plotted in Figure 7.24(B). It is found that the effect is strong and uptake of Cd(II) reduced from 60.980 to 28.360 mg/g. The uptake surface is perfectly slanting evenly which suggests even antagonism by Pb(II) ions over the whole adsorption process (El-Bayaa et al., 2009; Padilla-Ortega et al., 2013).

The effects of the existence of Cd(II) and Cu(II) ions on the uptake of Cd(II) and Pb(II) in Cd(II)-Cu(II) system are plotted in Figure7.24(C) and Figure 7.24(D) respectively. The Cd(II) and Cu(II) adsorption reduced to 6.899 and 19.985 mg/g in binary system from 60.980 and 27.360 mg/g in single metal system. The almost uneven 3D surfaces indicate the even aggression by the Cd(II) and Cu(II) ions (Leyva-Ramos et al., 2001). The antagonism of Cu(II) and Pb(II) ions in the Cu(II)-Pb(II) system are plotted in Figure 7.24(E) and Figure 7.24(F). Significantly reduced adsorption capacities are found for Cu(II) and Pb(II) ions in the Cu(II)-Pb(II) system. The Cu(II) and Pb(II) ions adsorption capacities reduced to 25.898 and 45.396 mg/g from 27.368 and 50.267 mg/g respectively. Likewise, the antagonism on the adsorption of Cu(II) and Zn(II) in Cu(II)-Zn(II), Cd(II) and Zn(II) in Cd(II)-Zn(II), and Zn(II) and Pb(II) in Cu(II)-Pb(II) binary system are plotted in Figure 7.25(A) and Figure 7.25(B); Figure 7.25(C) and Figure 7.25(D); and Figure 7.25(E) and Figure 7.25(F), respectively.

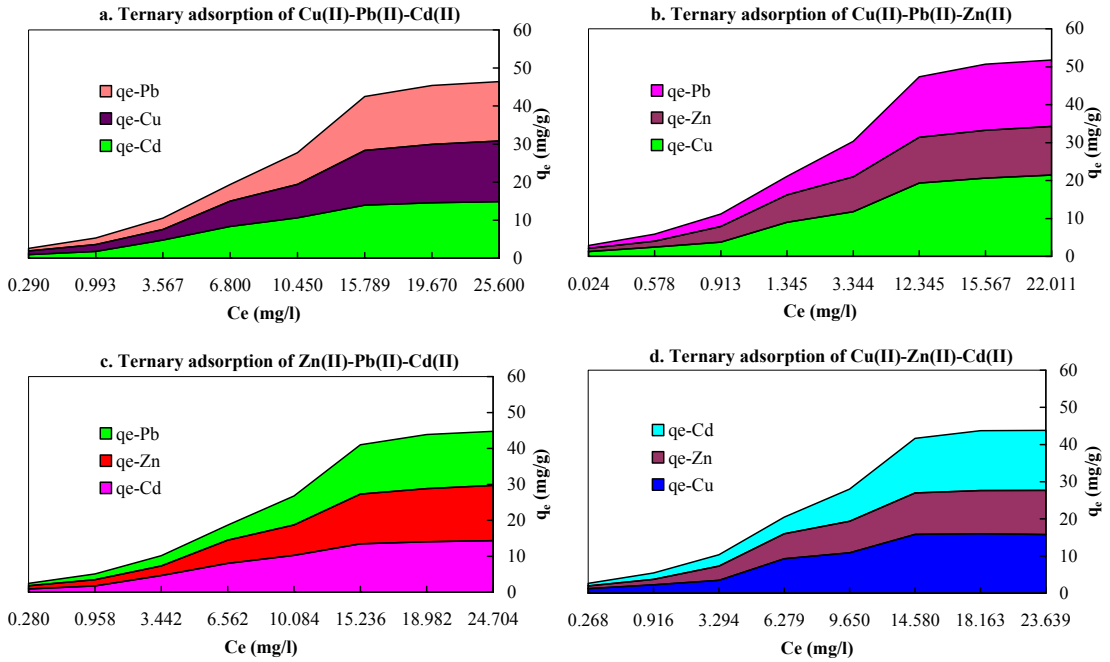


**Figure 7.26** Occupied physical surface area of metals in terms of capacity for ternary metals adsorption system onto ML

In general strong antagonisms were found between the metals. The Pb(II) and Cu(II) showed dominance over their counter pairs of metals. Similar findings are reported in the literature (Apiratikul and Pavasant, 2006; El-Bayaa et al., 2009). The Pb(II) and Cu(II) ions have high affinity to ML. In the Cu(II)-Zn(II) system Cu(II) and Zn(II) ions uptake are 10.354 and 5.420 mg/g which is lower than the single metals system (27.368 and 29.94 mg/g). The uneven adsorption surfaces (Figure 7.25(A) and Figure 7.25(B)) also depict the effects. As found from Figure 7.25(C) and Figure 7.25(D), Cd(II) and Zn(II) ions posed similar type of antagonism to each other. This is perhaps related to their similar looking surfaces found from the 3D plots (Figure 7.25(C) and Figure 7.25(D)). The adsorption capacities are 8.057 and 7.295 mg/g for Cd(II) and Zn(II) in binary system while it are 60.980 and 29.94 mg/l in a single metal system. For the Zn(II)-Pb(II) system, Zn(II) posed a higher antagonism than Pb(II) as the Figure 7.25(F) shows. It is also established from adsorption capacities because the Pb(II) ion adsorption reduced to 37.971 mg/g from 50.267 mg/g while Zn(II) ions adsorption reduced to 27.88 mg/g from 29.94 mg/g.

The ternary systems adsorption are demonstrated in the surface plot of Figure 7.26 (a, b, c and d). It is seen that the Pb(II) ions presented a higher affinity for the binding sites of the ML than the Cu(II), Cd(II) and Zn(II) ions. In other words, the ML was much more selective towards Pb(II) than to other three metals in the competitive adsorption.
The Pb(II) and Cu(II) ions showed strong antagonism against their co-ions. The Pb(II) ion posed high antagonism against the adsorption of Cu(II) and Cd(II) ions in Cu(II)-Pb(II)-Cd(II), against of Cd(II) and Zn(II) ions in Cd(II)-Pb(II)-Zn(II) system; and against of Cu(II) and Zn(II) in Cu-Pb-Zn system whereas the Cu(II) and Cd(II) ions, Cd(II) and Zn(II) ions; and Cu(II) and Zn(II) ions exhibited light antagonism against the adsorption of Pb(II) (Apiratikul and Pavasant, 2006; El-Bayaa et al., 2009; Padilla-Ortega et al., 2013; Şengil and Özacar, 2009). This behaviour could not be predicted from the single metal adsorption system. It is also found from binary systems (b, c and d) that Pb(II) ions took higher surface area than other metals. In other words, most binding sites of ML are occupied by Pb(II) and Cu(II) ions in ternary systems (Raize et al., 2004; Şengil and Özacar, 2009).

Mixtures of several metals matrices are found in real wastewater and antagonism is the common action among the ions (Raize et al., 2004). To more closely emulate the

antagonism of actual wastewater metals, a quaternary system isotherm was conducted. To visualise the antagonism among the four metals, a spider diagram was constructed and plotted in Figure 7.27. Higher spiral surface occupied by Pb(II) in the spider plot shows the superior attraction of Pb(II) ions by ML (Apiratikul and Pavasant, 2006; Raize et al., 2004). Similarly, Cu(II) and Cd(II) ions possess the second highest antagonism. Zn(II) ions showed lower magnitude of spiral surfaces though their prediction from single and binary systems was different. Similar findings are reported in the literature (Padilla-Ortega et al., 2013; Şengil and Özacar, 2009).

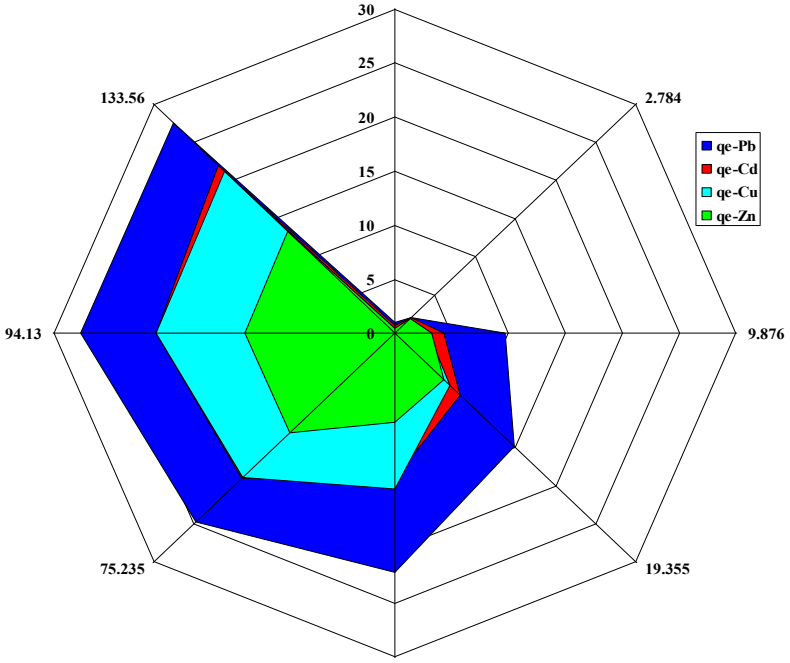


**Figure 7.27** Engaged area in terms of capacity of metals in spider diagram for quaternary metals adsorption onto ML.

The percent reduction in adsorption capacities in the competitive systems (binary, ternary and quaternary) were calculated by the following expression:

$$\%\ \text{reduced} = \frac{\left(q_m\ \text{from single metal system} - q_m\ \text{from multi - metal system}\right)}{q_m\ \text{from single metal system}} \times 100$$

Dominant Pb(II) ion uptakes were reduced to 32.33%, 9.6% and 24.46% for a binary system and; 12.34%, 28.89 % and 34.81% for a ternary system; and 9.98% for a quaternary system. The Cd(II) ions uptake is decreased to 62.167%, 5.59% and 26.97% for binary, 75.95%, 71.16% and 75.67% for ternary and 77.64 % for quaternary systems. The Cu(II) adsorption capacities declined to 62.17%, 5.59% and 26.98 % for

binary; 18.09%, 54.41% and 36.22% for ternary and 64.73% for quaternary systems. Similar to other metals Zn(II) ions adsorption capacities declined to 81.90%, 6.88% and 75.63% for binary; 69.09%, 70.80% and 69.17% for ternary and 73.33% for quaternary systems. It is apparent that adsorption capacities dropped for binary, ternary and quaternary system with the presence of co-metals. In the other words, antagonism is co-metal dependent (Niu et al., 2013; Xue et al., 2009).

## 7.3 Conclusions

Maples leaves were found to be an effective biosorbent for the removal of Pb(II), Cd(II), Cu(II) and Zn(II) from aqueous solutions. Biosorption kinetics follows a Pseudo-second-order model and Sips isotherm model best reproduces the experimental data. Cations binding functional groups such as hydroxyl and carboxylic groups are found in the surface of ML. SEM-Xray mapping confirmed the presence of adsorbed Pb(II) ions on the ML surfaces. Thermodynamic properties indicate that Pb(II), Cd(II), Cu(II) and Zn(II) biosorption processes are spontaneous and exothermic in nature. The results suggest that pH, doses, initial Pb(II), Cd(II), Cu(II) and Zn(II) concentration, contact time and particle sizes affected the biosorption process. Small particle size (<75μm) poses higher Pb(II), Cd(II), Cu(II) and Zn(II) biosorption than other. Quick equilibrium time (5-20 mins) for different initial Pb(II), Cd(II), Cu(II) and Zn(II) concentration poses practical potentiality of maple leaves as an alternative metal adsorbent. The biosorbent was successfully used in five successive adsorption-desorption cycles. The monolayer capacity of Pb(II), Cd(II), Cu(II) and Zn(II) biosorption is comparable to other biosorbent available in literature. In competitive adsorption systems, Pb(II) and Cu(II) showed dominancy over the other metals ions.

Faculty of Engineering and Information Technology
University of Technology, Sydney (UTS)

# Chapter 8

# Palm oil fruit shells as biosorbent for copper removal from aqueous solution

## 8.1 Background

Several million tonnes of palm oil fruit shells and fibre wastes is produced annually in the tropical countries like Malaysia, Indonesia, Thailand, Columbia, Nigeria, PNG and Ecuador (Chu et al., 2000; Hossain et al., 2012a; Issabayeva et al., 2006; Ofomaja, 2010). Complex agricultural waste materials containing lignin and cellulose which contain some functional groups such as alcohols, aldehydes, ketones, acids phenolic hydroxides and ethers, and it acts as chemical bonding agents for sorption of metals (Ho and Ofomaja, 2006a; Saifuddin and Kumaran, 2005; Tan et al., 2007). Natural abundance and their affinity for heavy metals, palm oil fruit shells stay a cheap and readily available source of bioadsorbents that can be useful for copper removal from water and wastewater. The main aim of this study was to investigate the feasibility of using palm oil fruit shells (POFS) as an efficient adsorbent for the removal of copper from water and wastewater. The sorption is often described by sorption isotherms and modelling of sorption isotherm is the best way to predict and compare sorption performance by adsorbent. Twelve isotherm models were used to predict adsorbent performance. The dynamic behaviour of copper sorption onto the palm oil fruit shells was also calculated from experimental data with kinetic models. To characterise the biosorbent SEM, FTIR and BET test were conducted and evaluated. This study also investigated the effect of pH on copper removal.

## 8.2 Results and discussion

### 8.2.1 Characterization of palm oil fruit shells

The biosorption by a biosorbent depends on the surface properties, active functional groups and adsorption mechanism. Characterisations are an important step for biosorbent in context of uses for selectivity of metals' ions; explore binding sites and functional groups for ion exchange or chemisorption. Therefore, the palm oil fruit shells (POFS) was characterised by SEM, FTIR and BET tests.

#### 8.2.1.1 Surface morphology

Scanning electron microscope (SEM) with different magnifications is used for the study of surface morphology of POFS (according to Chapter 3, section 3.3.1.1). The SEM micrograph showed in Figure 8.1 (A, B, C and D). The micrograph revealed some significant feature of structures. It is visualised from lower magnification that uneven and rough sized particles are contained in the POFS biosorbent (Figure 8.1 A). The

rough surface of the POFS is also become more noticeable at higher magnification (Figure 8.1 B). The micro-graphs reveal the presence of rough surfaces of POFS particles at further magnification (Figure 8.1 C). A POFS particle's surface made from swelling like structures and presence spaces between two lumps which is clearly visible from higher magnification (Figure 8.1 D). Similar results are reported for other biosorbents in the literatures (Lü et al., 2010; Walcarius and Mercier, 2010; Yang et al., 2010; Zhang et al., 2010). This is denoted the high internal surface area or binding sites of the POFS which are responsible for high metals adsorption (Chen et al., 2011).

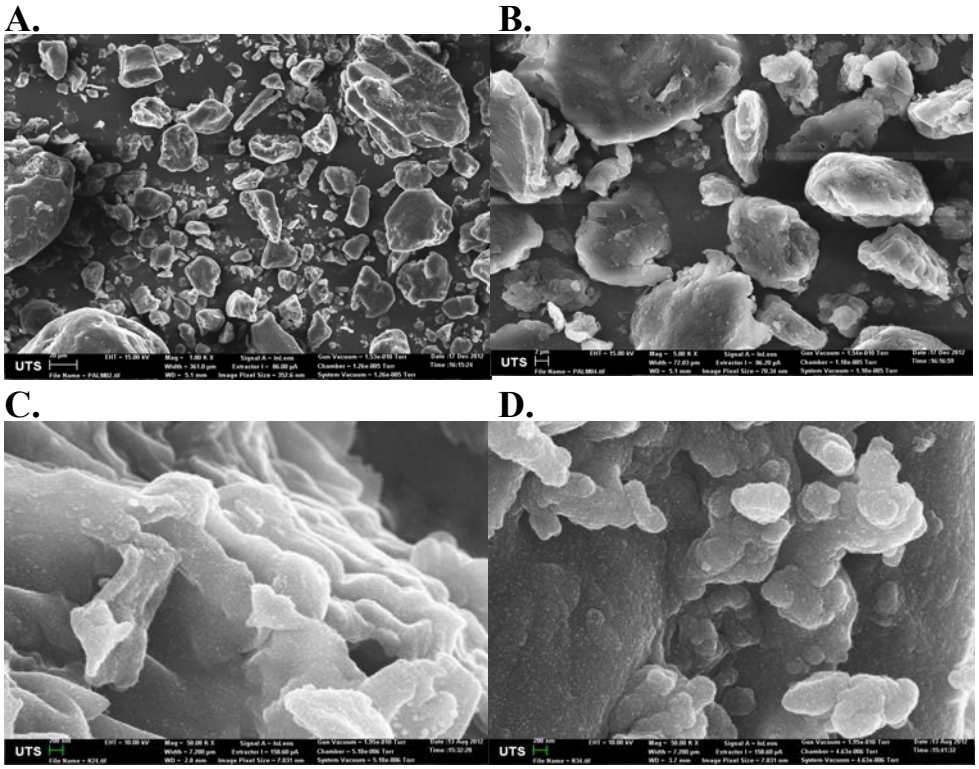


**Figure 8.1** SEM micrograph of POFS with different magnifications (A. 1X, B. 5KX, C. 50X and D. 90KX)

### 8.2.1.2 Surface area of POFS

It is assumed that the metals adsorption capacity depends on the specific surface area of biosorbent. So, exploration of surface area is important for any biosorbent. Surface area of POFS was examined by BET test (Chapter 3, Section 3.3.1.4). The BET surface properties of POFS (<75 μm) are tabulated in Table 8.1. The surface area is 39.76 $m^2/g$ with mesopore surface area of 19.60 $m^2/g$ and micropore surface area 2.14 $m^2/g$. It is comparable with the biosorbents produced from agro wastes (Giaccio et al., 2012; Hossain et al., 2012b; Shinde et al., 2012). The total pore volume of the POFS's powder

was 0.10 $cm^3/g$ and the mesopore and micropore were 70% and 30%. In addition, the mean micropore and mesopore sizes of the POFS were found to be 14.51 and 42.14 Å, respectively, suggesting that this biosorbent was fallen within the region of mesopore based on International Union of Pure and Applied Chemistry (IUPAC) classification (Arias et al., 2005). The high pore area, pore volume and pore sizes are indicated the numerous binding sites on the POFS surfaces (Lu et al., 2010; Thirumavalavan et al., 2010; Velmurugan et al., 2010; Warner et al., 2010).

**Table 8.1** BET characteristics of biosorbent produced from palm oil fruit shells

| Parameter | Methods | Values |
|---|---|---|
| 1. Surface area | BET surface area | 39.76 $m^2/g$ |
| | Langmuir surface area | -11.92 $m^2/g$ |
| 2. Pore Area | | |
| i. Micropore area | DR method | 2.14 $m^2/g$ |
| | t-plot (statistical thickness = 3.50~7.00) | 20.65 $m^2/g$ |
| | Horvath-Kawazoe method | 0.56 $m^2/g$ |
| ii. Mesopore area | BJH adsorption | 19.60 $m^2/g$ |
| | BJH desorption | 25.97 $m^2/g$ |
| 3. Pore volume | | |
| i. Micropore volume | DR method | 0.00 $cm^3/g$ |
| | t-plot (statistical thickness = 3.50~7.00) | -0.01 $cm^3/g$ |
| | Horvath-Kawazoe method | 0.00 $cm^3/g$ |
| ii. Mesopore volume | BJH adsorption | 0.03 $cm^3/g$ |
| | BJH desorption | 0.07 $cm^3/g$ |
| 4. Pore size | | |
| i. Micropore size | DR method | 8.71 Å |
| | t-plot (statistical thickness = 3.50~7.00) | 6.35 Å |
| | Horvath-Kawazoe method | 14.51 Å |
| ii. Mesopore size | BJH adsorption | 40.29 Å |
| | BJH desorption | 42.14 Å |

### 8.2.1.3 Functional groups

Functional groups are important parameters of biosorbents because it plays a vital role in metals adsorption. The functional groups that are present in POFS are studied by Fourier transform infrared spectroscopy (FTIR) (Chapter 3, Section 3.3.1.3). An FTIR spectrum for POFS is shown in Figure 8.2. The major functional groups found from spectra were O-H stretch-free hydroxyl for alcohols/phenols or carboxylic acids (3640–3610 $cm^{-1}$), O–H stretch, H–bonded for alcohols/phenols (3500–3200 $cm^{-1}$), C-N stretch for aliphatic amines (1250–1020 $cm^{-1}$), C-O stretch for alcohols/carboxylic acids/esters/ethers (between 1320-1000 $cm^{-1}$), =C-H bend for alkanes (between 1000-650 $cm^{-1}$) and C-H "OOH" for aromatics (1056.$cm^{-1}$) (Yang et al., 2006b). The

behaviour of carbon-oxygen bonds and carbon bonds on the surface of the biosorbents attract and stimulate the metals adsorption (Ricordel et al., 2001; Yang et al., 2006a). Functional groups like hydroxyl and carboxyl groups could able to bind with cations of metals ions (Rahman and Islam, 2009; Witek-Krowiak et al., 2010; Yu et al., 2003).

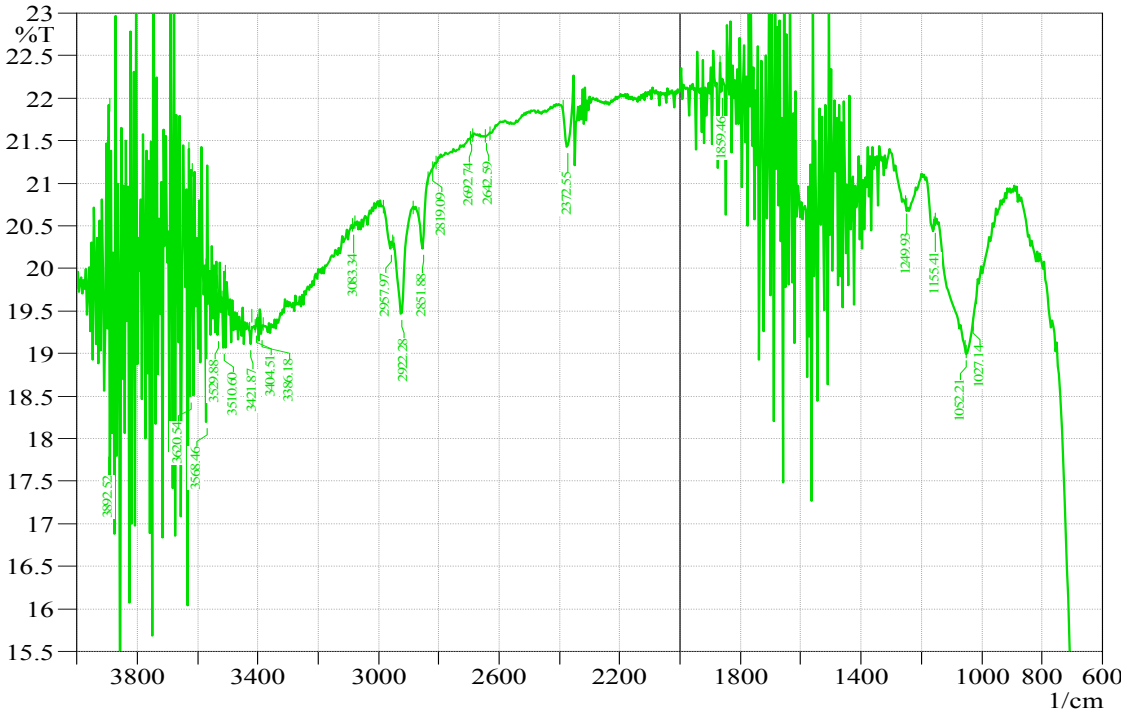


**Figure 8.2** FTIR spectra of palm oil fruit shells (POFS)

### 8.2.2 Effect of pH

pH is a deciding factor for any kind of metal sorption on adsorbents in an aqueous solution. The surface properties of adsorbents, ionic state of functional groups and species of metals are dependent on pH condition (Laus and de Fávere, 2011; Rajaei et al., 2013). To find out the best solution for maximum sorption, the experiments were conducted between the pH of 2 to 8 in 100 ml water with 10 mg/l copper concentration and0.5 g of palm oil fruit shells (POFS) (Chapter 3, section 3.3.2.1). The maximum (98.5%) removal of copper was found at pH 6.5. The pH experiment was kept between 2 to 8, because the speciation diagram has confirmed that $Cu^{2+}$ is the dominant free species below pH 6 which involved in true sorption and above the pH 7 copper starts to precipitate (Komy et al., 2013; Manzoor et al., 2013). The Cu(II) adsorption was greatly increased between pH 4 and 6.5 but decreased after pH 6.5. Low adsorption capacities were observed at both low and high pH of water. At low pH, $H_3O^+$ ion competed with $Cu^{2+}$ for binding and surrounded hydronium ions ($H^+$) preventing the metals ions from

approaching the binding sites, and it could be responsible for low adsorption capacities (Karthikeyan et al., 2007). At higher pH, the binding site may not be activated in basic condition (Demirbas et al., 2009). Above the pH of 6, the Cu(II) started precipitating as $Cu(OH)_2$ in aqueous solution; respectively (Rajaei et al., 2013), so the removal after 6.5 was not completely by adsorption (Zhang et al., 2010).

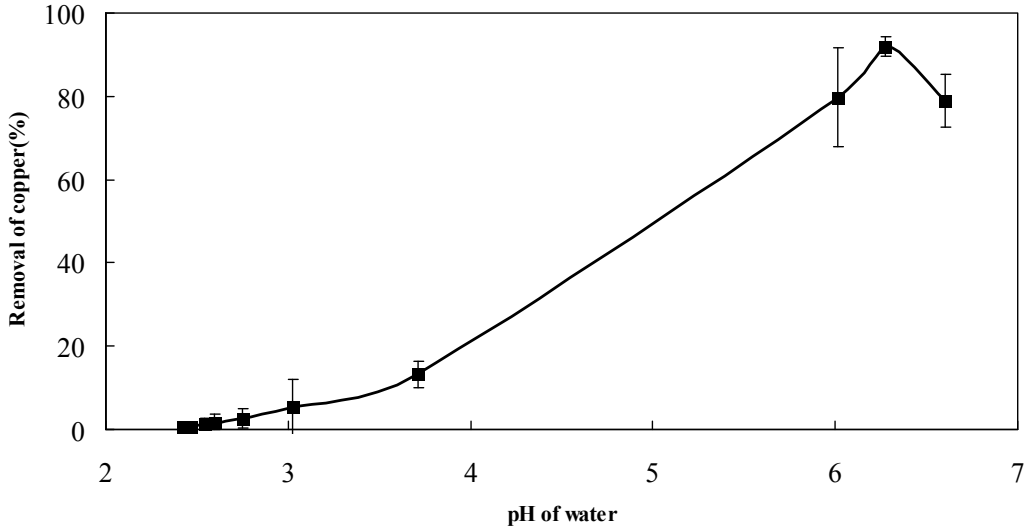


**Figure 8.3** Effect of pH on removal of Cu(II) by POFS

### 8.2.3 Equilibrium sorption modelling

Commonly, a sorption isotherm is an important curve which describes the phenomenon that governing the retention/release or mobility of a metals/substance from the aqueous porous media or aquatic environments to a solid-phase at a constant temperature and pH (Adelaja et al., 2011; Zheng et al., 2010). An equilibrium isotherm describes the relation between the amounts of metals removed from aqueous solution at equilibrium by unit of mass of biosorbents at constant temperature (Hawari and Mulligan, 2006; Matheickal and Yu, 1999; Puyen et al., 2012; Yalcin et al., 2008). Sorption equilibrium is attained when metals containing phase has been contacted with the adsorbent for sufficient time and the metals concentration in the solution become constant. An equilibrium isotherm denotes the relationship between the amounts of adsorbate (metals) removed from the water per unit of mass of biosorbent and equivalent metals concentration in water, at constant temperature and equilibrium state (Abd El-Latif and Elkady, 2010; Blazquez et al., 2010; Kicsi et al., 2010).

Naturally, the statistical correlation, which plays a significant role towards the isotherm modelling, effective design and relevant practice of the sorption systems, is found by graphically expressing the solid-phase against its residual concentration. But linear relation always misleads the nature of isotherm equation because the model equations are devised based of non-linear equation (Gorgievski et al., 2013; Reddy et al., 2012; Torab-Mostaedi et al., 2013). To optimize the design for copper sorption onto palm oil fruit shells, it is important to establish the most appropriate model for equilibrium data. Four 4-parameter model namely Langmuir, Temkin, Jovanovic and Flory-Huggins isotherm; and eight 3-parameter models such as Sips, Redlich-Peterson, Koble-Corrigan, Toth, Radke-Prausnitz, Hill, Brouers-Sotolongo and Vieth-Sladek are used to evaluate the Cu(II) adsorption data. Non-linear regression (MATLAB bases program) was used to estimate and optimise the parameters (Appendix I). The agreement between experimental and model prediction data are judged by $R^2$ (coefficient of determination), RMSE (residual root mean square error) and $\lambda^2$ (chi-square test) (Chapter 3, section 3.4) for both adsorption of Cu(II) onto palm oil fruit shell. An interesting trend in the isotherm modelling is derived for predicting the difference in the physical characteristics of the model parameters. The model predictions with experimental data are plotted in Figure 8.4 and Figure 8.5 for "two-parameter isotherms" and "three-parameter isotherms" respectively. The models parameters with optimised values are tabulated in Table 8.2 and Table 8.3 for "two-parameter isotherms" and "three-parameter isotherms" respectively.

#### 8.2.3.1 Two-parameter models

In order to calculate the different parameters of isotherms models and their capability to correlate with experimental data, the theoretical prediction for 4 'two-parameter isotherm models' were chosen and the parameters are summarized in Table 8.2. Table 8.2 shows that the Langmuir isotherm was best fitted model with the experimental data as it has higher $R^2$ and also the least RMSE and $\chi^2$ values. The Temkin (Temkin and Pyzhev, 1940), Jovanovic (Jovanovic, 1969) and Flory-Huggins isotherm (Horsfall and Spiff, 2005) models also showed fairly good degree of accuracy to the experimental data with relatively high values of $R^2$ and low values of RMSE and $\chi^2$. The plotted line of experimental and predicted data showed that all line (Figure 8.4) are significantly closed together which proved the fitness of the models.

The Langmuir isotherm is the most appropriate among the four 'two-parameter isotherm models' applied to this Cu(II) sorption system. This isotherm assumes monolayer coverage of the adsorbent surface by the copper molecules and that the surface is completely uniform and energetically homogeneous (Rajaei et al., 2013; Yan et al., 2010). Low value of $K_L$ (1.566 l/mg ≈1) indicates the high affinity of Cu(II) ions by palm oil fruit shells (POFS). High $q_m$ (32.455 mg/g) and $R^2$ (0.994) revealed that the palm oil fruit shells are a good biosorbent for copper. Significantly low RMSE and $\chi^2$ values also proved the fitness of the model with experimental data.

**Table 8.2** Isotherm parameter of two-parameter models for copper sorption onto POFS

| Isotherm Models | Parameters | Isotherm Models | Parameters |
|---|---|---|---|
| **1. Langmuir** (Langmuir, 1918) $q_e = \frac{q_m K_L C_e}{1 + K_L C_e}$ | $q_m$ = 32.455 mg/g<br>$K_L$ = 1.566 l/g<br>$R_L$ = 0.060<br>$R^2$ = 0.994<br>Δ°G =-1.092 kJ/mol<br>$\chi^2$ = 5.2041<br>RMSE = 1.479 | **2. Jovanovic** (Jovanovic, 1969) $q_e = q_m\left(1 - e^{K_J C_e}\right)$ | $q_m$ = 28.587 mg/g<br>$K_J$ = -1.237<br>$R^2$ = 0.990<br>$\chi^2$ = 10.291<br>RMSE = 1.861 |
| **3.Tempkin** (Temkin and Pyzhev, 1940) $q_e = \frac{RT}{b_T}\ln(K_T C_e)$ | $b_T$ =1.056373 (kJ/mol)<br>$K_T$ =35.312 l/g<br>$R^2$ = 0.987<br>Δ°G = -8.682<br>$\chi^2$ = 25.694<br>RMSE = 2.149 | **4. Flory-Huggins** (Horsfall and Spiff, 2005) $\frac{\theta}{C_o} = K_{FH}(1-\theta)^n$<br>$\theta = 1 - \frac{C_e}{C_o}$ | $K_{FH}$ = 17.481 mg/g<br>n = 4.359<br>ΔG° = -6.970<br>$R^2$ = 0.986<br>$\chi^2$ = 5972.4<br>RMSE = 2.241 |

The value of Δ°G (1.092 kJ/mol) is fairly lower than other models and the negative value showed the spontaneous exothermic nature of Cu(II) adsorption. Furthermore, the favourability of Cu(II) sorption on palm oil fruit shells was evaluated using a dimensionless constant called separation factor ($R_L$), which is an essential feature of Langmuir isotherm (Langmuir,1918):

$$R_L = \frac{1}{1 + K_L C_o} \qquad (8.1)$$

The values of $R_L$ indicates the type of isotherm to be irreversible ($R_L$ = 0), favourable (0 < $R_L$ < 1), linear ($R_L$ = 1) or unfavourable ($R_L$ > 1). The values of $R_L$ for palm oil fruit shells (0.06) lie between 0 and 1 which confirmed the viability of Cu(II) sorption onto POFS.

The assumption for Jovanovic model is similar to assumptions of Langmuir model (Jovanovic, 1969). It is also represented another approximation for monolayer and localized adsorption without lateral interactions (Allen Jr and Clark, 1977). The

experimental data and model prediction are shown in Table 8.2 and plotted in Figure 8.4. The fairly high $R^2$ (0.990) and low RMSE (1.861) and $\chi^2$ values (10.291) are ascertained the good fitness of the model with experimental data. The equilibrium adsorption capacity (28.587 mg/g) for this model was lower than Langmuir and Temkin's adsorption capacities but higher than Flory-Huggins prediction.

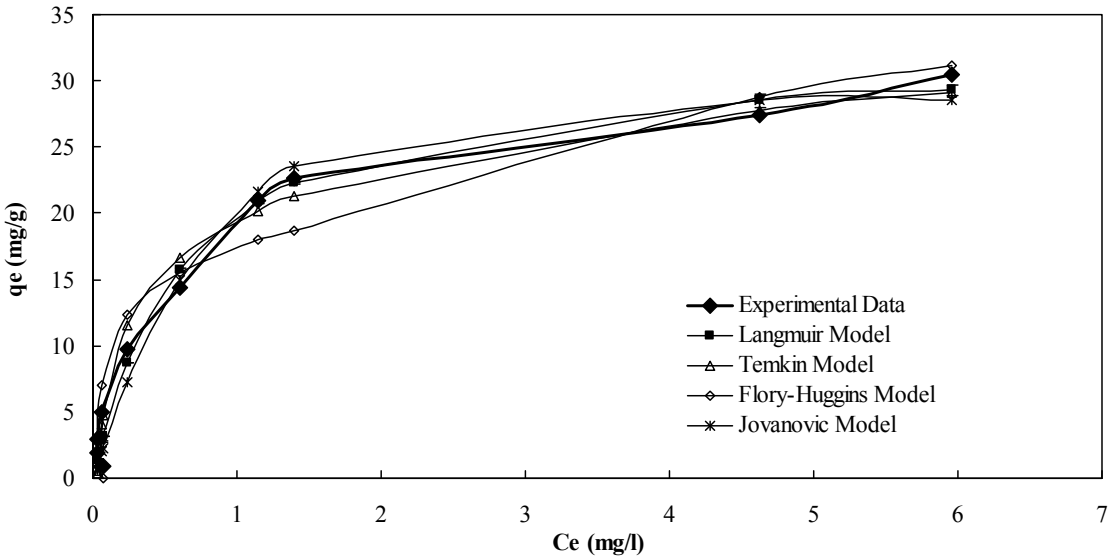


**Figure 8.4** Isotherm modelling of Cu(II) sorption onto palm oil fruit shells for two-parameter models

The assumption of Temkin isotherm is that the heat of sorption is linear rather than logarithmic. The heat of sorption for all ions in layer would reduce linearly with coverage due to sorbate-sorbent interactions (Temkin and Pyzhev, 1940). Temkin constant related to heat of sorption, $b_T$ (kJ/mol); and sorption potential, $K_T$ (l/g) was calculated (Table 8.2). It is found that $K_T$ value is quite higher (35.312 L/g) than the other two-parameter models. The calculated high $R^2$ (0.987) and low RMSE values, and moderate high $\chi^2$ value also implies the applicability of Cu(II) sorption onto POFS. On contrast of equivalent sorption capacity predicted by the Temkin isotherm was significantly higher than other two-parameter models. The sorption heat energy ($\Delta°G$ =8.682 kJ/mol) is higher than Langmuir and Florry-Huggins model which indicates the sorption process is depended on ion-exchange mechanism as the values lies within the ranges of 8-16 kJ/mol (Temkin and Pyzhev, 1940; Wang and Qin, 2005)).

The degree of surface coverage of adsorbent is studied by Flory-Huggins isotherm (Horsfall and Spiff, 2005). Flory-Huggins model equilibrium constant, $K_{FH}$ (17.481mg/g); exponent, n (4.359); $\Delta°G$ (6.970 kJ/mol) with $R^2$ (0.986) and low RMSE

and high $\chi^2$ (Table 8.2) implies the moderate applicability Cu(II) sorption on palm oil fruit shell. As can also be seen in Table 8.2, the Gibbs free energy is negative which indicating spontaneous nature and feasibility of Cu(II) sorption onto palm oil fruit shell and; the sorption is an exothermic reaction (Montazer-Rahmati et al., 2011; Rajaei et al., 2013; Sathasivam and Haris, 2010). On the basis of $R^2$ values, the higher fitted model order is Langmuir> Jovanovic>Temkin >Flory-Huggins.

### 8.2.3.2 Three-parameter models

The predictions of 8 'three-parameter isotherm models' were plotted against the experimental data and showed in Figure 8.5. The calculated parameters are also presented in Table 8.3. The coincided behaviour of models predictions with experimental data (Figure 8.5) revealed that the experimental data showed better fitness with the predictions of 8 three-parameter models rather than the 4 two-parameter models. The values of $R^2$, $\chi^2$ and RMSE are almost similar for all the 8 models and eventually the predicted model graphs overlapped each other (Figure 8.5).

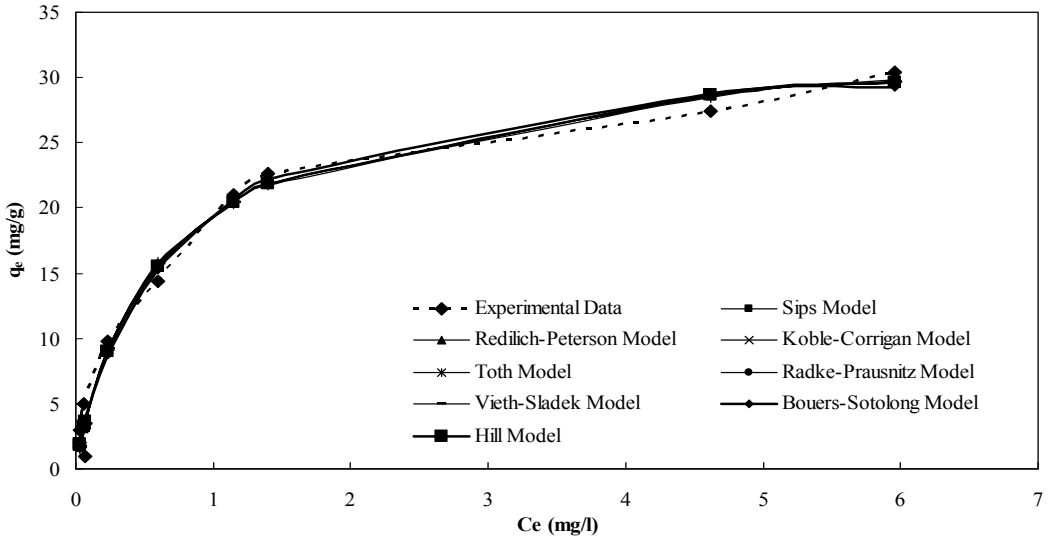


**Figure 8.5** Isotherm modelling of Cu(II) sorption onto POFS for three-parameter models

To describe surface heterogeneity of adsorbent, Sips isotherms is derived with combination of the Langmuir and Freundlich isotherms (Sips, 1948). It provides a rationally accurate prediction of Cu(II) sorption with experimental results showing high $R^2$. High values of constant, $K_S$ (45.275 l/g) and low values of $\chi^2$ and RMSE revealed that this model described properly the Cu(II) sorption onto POFS. The Sips model constant, $\alpha_S$ (1.328 L/mg) and exponent, $\beta_S$ (0.898) were close to unity which also

indicated that the Cu(II) was adsorbed by the functional groups or binding sites on the surface of the palm oil fruit shells (Jacques et al., 2007; Ngah and Fatinathan, 2008; Singh et al., 2008).

**Table 8.3** Isotherm parameter of three-parameter models for Cu(II) sorption onto palm oil fruit shell

| Isotherm Models | Parameters | Isotherm Models | Parameters |
|---|---|---|---|
| **1. Sips** (Sips, 1948) $q_e = \frac{K_s C_e^{\beta_s}}{1 + \alpha_s C_e^{\beta_s}}$ | $K_s$ = 45.275<br>$\alpha_s$ = 1.328<br>$\beta_s$ = 0.898<br>$R^2$ = 0.994<br>$\chi^2$ = 3.797<br>RSME = 1.425 | **2. Redlich-Peterson** (Redlich and Peterson, 1959) $q_e = \frac{K_{RP} C_e}{1 + \alpha_{RP} C_e^{\beta}}$ | $K_{RP}$ = 59.502<br>$\alpha_{RP}$ = 2.054<br>$\beta$ = 0.938<br>$R^2$ = 0.994<br>$\chi^2$ = 4.244<br>RSME = 1.441 |
| **3. Koble-Corrigan** (Koble and Corrigan, 1952) $q_e = \frac{A_{KC} C_e^{p}}{1 + B_{KC} C_e^{p}}$ | $A_{KC}$ = 45.275<br>$B_{KC}$ = 1.328<br>p = 0.898<br>$R^2$ = 0.994<br>$\chi^2$ = 3.797<br>RSME = 1.425 | **4. Toth** (Toth, 1971) $q_e = \frac{q_m C_e}{(b_T + C_e^{n})^{1/n}}$ | $q_m$ = 34.902<br>$b_T$ = 0.608<br>n = 0.813<br>$R^2$ = 0.994<br>$\chi^2$ = 4.043<br>RSME = 1.436 |
| **5. Radke-Prausnitz** (Radke and Prausnitz, 1972) $q_e = \frac{\alpha_R r_R C_e^{\beta_R}}{\alpha_R + r_R C_e^{\beta_R - 1}}$ | $\alpha_R$ = 59.502<br>$r_R$ = 28.974<br>$\beta_R$ = 0.062<br>$R^2$ = 0.994<br>$\chi^2$ = 4.244<br>RSME = 1.441 | **6. Hill** (Hill, 1910) $q_e = \frac{q_m C_e^{n}}{K_D + C_e^{n}}$ | $q_m$ = 34.092<br>$K_D$ = 0.753<br>n = 0.899<br>$R^2$ = 0.994<br>$\chi^2$ = 3.797<br>RSME = 1.425 |
| **7. Brouers-Sotolongo** (Altenor et al., 2009) $q_e = q_m\left[1 - \exp(-K_{BS}(C_e)^{\alpha}\right]$ | $q_m$ = 29.738<br>$K_{BS}$ = 1.063<br>$\alpha$ = 0.770<br>$R^2$ = 0.994<br>$\chi^2$ = 3.492<br>RSME = 1.433 | **8. Vieth-Sladek** (Vieth and Sladek, 1965) $q_e = K_{vs} C_e + \frac{q_m \beta C_e}{1 + \beta C_e}$ | $q_m$ = 28.721<br>$K_{vs}$ = 0.561<br>$\beta$ = 1.946<br>$R^2$ = 0.994<br>$\chi^2$ = 4.444<br>RSME = 1.439 |

Redlich-Peterson isotherm model is a hybrid three-parameter isotherm which also combined the parameters of both Langmuir and Freundlich isotherms (Redlich and Peterson, 1959). This model depends on the concentration in the numerator and an exponential function in the denominator to show equilibrium of sorption system and it can be used for both homogeneous and heterogeneous systems (Wu et al., 2010; Yao et al., 2010). This model has been frequently used in the liquid phase sorption of heavy metals and organic compounds (Ho et al., 2002; Homagai et al., 2010). Although this model have some positive and negative comments about the significant fitness (Lee et al., 2001). This model showed accurate capability for wide range of Cu(II) adsorption data (Table 8.3 and Figure 8.5). High values of sorption capacity, $K_{RP}$ (59.502 mg/g) and $R^2$ (>0.994), low values of model constant, $\alpha_{RP}$, small RMSE and $\chi^2$ (Table 8.3)

ascertained the applicability of Cu(II) sorption onto palm oil fruit shells. As the exponent, β lies between 0 and 1 the model supported the heterogeneous system of sorption (Lee et al., 2001).

Koble-Corrigan model (Koble and Corrigan, 1952) has an exponential dependence on concentration in the numerator and denominator which is usually used with heterogeneous sorption surfaces. The high $R^2$ values (0.994), low $\chi^2$ and RMSE (Table 8.3) revealed the suitability of model for prediction of Cu(II) sorption onto palm oil fruit shells. The low values of exponent 'p' (0.898 <1) suggested that the sorption surface of palm oil fruit shells is heterogeneous (Aksu and Isoglu, 2005; Han et al., 2005; Koble and Corrigan, 1952).

Toth isotherm model (Toth, 1971) is empirically derived to improve fitness of model with experimental data. It is used to describe the heterogeneous sorption systems and can satisfy both low and high concentration of adsorbates (Kosasih et al., 2010; Kumar et al., 2010). This model possessed a high degree of fitness with experimental data (Figure 8.5) as predicted high $R^2$ (0.994) and low $\chi^2$ and RMSE (Table 8.3) values. The low values of model constant, n (0.813<1) revealed the heterogeneity of adsorbent surface (Kosasih et al., 2010; Vargas et al., 2011). The Radke-Prausnitz model (Radke and Prausnitz, 1972) is also shown a good fitness with experimental data as found high $R^2$ (0.994) and low $\chi^2$ and RMSE values (Table 8.3). The exponent $\beta_R$ predicted from this model is close to unity that also proved the applicability and heterogeneity of the model (Montazer-Rahmati et al., 2011; Vijayaraghavan et al., 2006).

The other 3 three-parameter models namely Vieth-Sladek (Vieth and Sladek, 1965), Brouers-Sotolongo (Altenor et al., 2009) and Hill (Hill, 1910) were also used to predict the sorption parameters of Cu(II) onto palm oil fruit shells. The predictions and experimental data are plotted in Figure 8.5 and shown in Table 8.3. It is indicated that the experimental data of Cu(II) sorption are fitted quite well ($R^2$ >0.994) with the above three isotherm models. The applicability is also confirmed by small values of RMSE and $\chi^2$ (Table 8.3). A wide range of sorption capacity (28.721 to 59.502 mg/g) is predicted from the three-parameter models. The maximum equivalent sorption capacity (59.502 mg/g) was found from the prediction of Redlich-Peterson and Radke-Prausnitz models and lowest (28.721 mg/g) for Vieth-Sladek model. According to the degree of

fitness ($R^2$) it can be concluded that all models are suitable to describe the Cu(II) adsorption onto POFS. Thus, based on equivalent sorption capacity and fitness, the order followed by the models are Redilich-Peter>Radke-Prausnitz>SIPS>Koble-Corrigan> Toth>Hill>Brouers-Sotolongo>Vieth-Sladek.

### 8.2.4 Sorption kinetics

Kinetics is a process where metals adsorption depends on time (Iftikhar et al., 2009; Kalavathy et al., 2005; Sari and Tuzen, 2009; Tharanitharan and Srinivasan, 2010). Kinetics parameters are useful for process design of water and wastewater treatment systems (Ho and Ofomaja, 2006a; Li et al., 2006). The kinetics of adsorption experiments were conducted in 10 mg/l Cu(II) concentration for 24 hours (Chapter 3, section 3.3.5). The kinetics parameters are calculated from the adsorption of Cu(II) ions onto POFS with elapsed time. These parameters describe the characters of biomaterials and forecast the metals adsorption processes is either chemical adsorption or physical adsorption or cation exchange processes (Ho and McKay, 1998). Three kinetics models namely Pseudo-second-order, Elovich and Avrami, were used to describe the kinetics data of Cu(II) adsorption. The fitness was evaluated by coefficient of determination, $R^2$ (Chapter 3, section 3.4). The models' parameters were optimised by non-linear analyses by 'solver' add-in, in MS Excel (Appendix II), and the normalized standard deviation (NSD) and average relative error (ARE)(Hossain et al., 2012b) were also calculated to judge the fitness of models (Chapter 3, section 3.4). The predicted models with experimental data are shown in Figure 8.6 and parameter tabulated in Table 8.4. It is found that the Cu(II) adsorption reached equilibrium just after 50 mins. It has a practical significance for process design of biosorbent process (Omorogie et al., 2012).

#### 8.2.4.1 Pseudo-second-order kinetics

The kinetic data from the biosorption of Cu(II) ions onto POFS are illustrated by pseudo-second-order equation. This model based on the assumption that the rate-limiting step may be chemical sorption involving valence forces through sharing or exchange of electrons between heavy metal ions and the adsorbent (Namasivayam et al., 2007). This kinetics's model offers good consistent data for the heavy metal ions. The mathematical equation (Ho and McKay, 2000) is as follows:

$$q_t = \frac{k_2 q_e^2 t}{(1 + q_e k_2 t)} \qquad (5.5)$$

where $k_2$, rate constant of pseudo-second-order adsorption (g/(mg min)) and $q_e$, adsorption capacity at equilibrium (mg/g). The initial adsorption rate of metal was calculated by the following equation (Ho, 2004):

$$h=k_2 q_e^2 \qquad (5.6)$$

The experimental and model predicted parameters are tabulated in Table 8.4. The adsorption data showed good fitness with this model ($R^2$: 0.999). This fitness signify that Cu(II) adsorption happen by chemisorption that controlled by the reaction rate (Ho and McKay, 2000). The kinetics constant, $k_2$ which determine the adsorption process are occurring in two reaction rate, the first one is fast and reaches equilibrium quickly and the second is a slow reaction that can continue for long period (Ho and McKay, 2000; Ho and Ofomaja, 2006b). But the value of $k_2$ (0.205 1/h) is less than unity for adsorption of Cu(II) ions onto POFS which implies the mechanism is not chemisorption (Table 8.4). In addition to $R^2$, significantly low NSD and ARE values are also advocated the fitness of the pseudo-second-order model and chemisorption process (Ho and McKay, 2000). Experimental and predicted values of equilibrium adsorption capacities ($q_e$: 4.704 mg/g) are similar. So, it can be assumed that pseudo-second-order model describes the Cu(II) adsorption onto POFS properly.

**Table 8.4** Kinetics model's parameters of Cu(II) sorption onto POFS

| Kinetics model | Parameters |
|---|---|
| Experimental | $q_e$ = 4.813 mg/g |
| 1. Pseudo-2nd-order<br>$q_t = \frac{K_2 q_e^2 t}{1 + K_2 q_e t}$ | $q_e$ = 4.704 mg/g<br>$K_2$ = 0.205 (1/h)<br>h = 0.963 (mg/g.min)<br>$R^2$ = 0.998<br>NSD = 5.213<br>ARE = 0.241 |
| 2. Elovich<br>$q_t = \beta.\ln(\alpha\beta t)$ | α = 9 x$10^7$ [mg/(g.min)]<br>β = 0.211 (g/mg)<br>$R^2$ = 0.953<br>NSD =2.084<br>ARE =0.109 |
| 3. Avrami<br>$q_t = q_e\left\{1 - \exp\left[-K_{AV}.t\right]^{n_{AV}}\right\}$ | $q_e$= 4.529 mg/g<br>$K_{AV}$ =1.242 (/min)<br>$n_{AV}$ = 1.242<br>$R^2$ = 0.923<br>NSD =8.445<br>ARE =0.652 |

### 8.2.4.2 Elovich equation

The metals adsorbed on the heterogeneous sites of biosorbent and the Elovich equation devised on these assumption (Cheung et al., 2003). It is also demonstrated the different

activation energies used in chemisorption (Gupta and Babu, 2006). Teng and Hsieh (Teng and Hsieh, 1998) proposed that a constant $\alpha$ is related to the rate of chemisorption and $\beta$ is related to the surface coverage. The Elovich model is presented by the following equation (Clayton and Chien, 1980):

$$q_t = \beta.\ln(\alpha\beta t) \qquad (5.7)$$

where, α is the initial adsorption rate (mg/g/min) and β is desorption constant (g/mg).

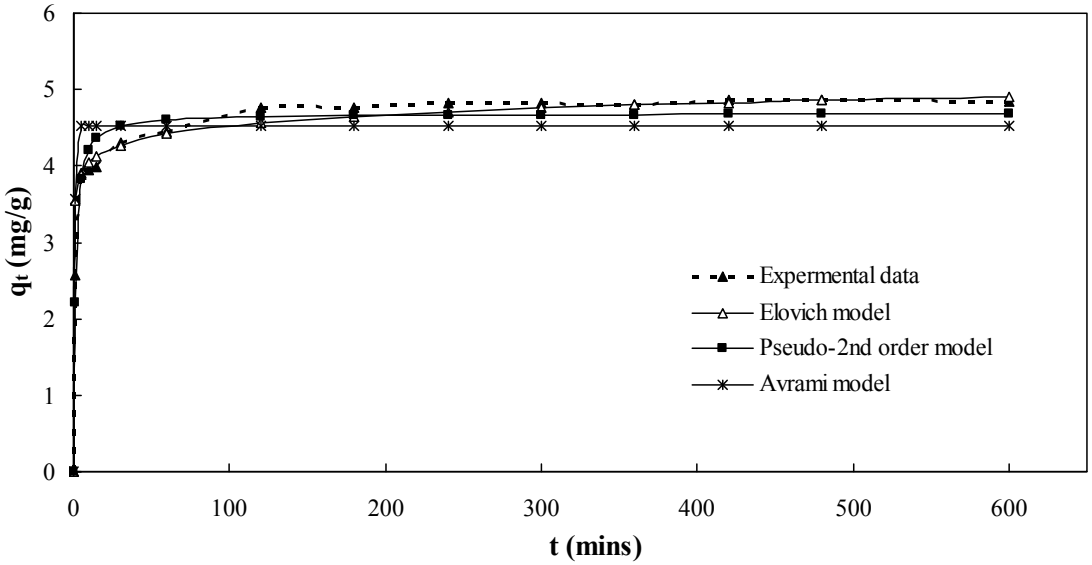


**Figure 8.6** Kinetics modelling of Cu(II) sorption on palm oil fruit shells

This model provides good fitness to the experimental data because $R^2$ is 0.953. Along with significantly low and small values of 'NSD' and 'ARE' are found from Cu(II) adsorption which also dignify the model association of metals adsorption onto POFS. A high value of α [9 x$10^7$ mg/(g.min)] and low values of β (0.211g/mg) also showed that the adsorption mechanism is chemisorptions (Gupta and Torres, 1998). It can presume that Cu(II) ions adsorption happened on the heterogeneous surfaces of POFS (Cheung et al., 2003). In fact, similar findings were found from SEM and FTIR analysis because this material contains heterogeneous surface with different metal lure functional groups (Cheung et al., 2003).

### 8.2.4.3 Avrami kinetic equation

The Avrami kinetic equation determines possible changes of the adsorption rates in function of the initial metals concentrations and the adsorption time, and it is also determined the orders of fractionery kinetic (Lopes et al., 2003). The mechanism of

adsorption could follow multiple kinetic orders that are changed during the contact of the metals with the biosorbents (Avrami, 1939; Lopes et al., 2003).

$$q_t = q_e \left[ 1 - e^{(-t.k_{AV})^{n_{AV}}} \right] \quad (5.8)$$

where, $K_{AV}$ is the Avrami kinetic constant and $n_{AV}$ is fractionery kinetic orders, which is related to the adsorption mechanisms changes.

The Avrami kinetic equation was used to describe the kinetics of Cu(II) adsorption onto POFS. The conformity between the experimental data and the model-predicted values were found from $R^2$, NSD and ARE values (Table 8.4). The overall fitness of this model with experimental data from Cu(II) adsorption is moderate as the $R^2$ values is 0.923. In addition, the model predicted equilibrium capacity ($q_e$) is 4.529 mg/g which is close to the experimental and pseudo-second-order model (4.813 and 4.704 mg/g). From the above discussion it can be decided that this model is suitably described the kinetics processes of Cu(II) adsorption.

The fractionery number ($n_{AV}$) predicted from adsorption process are greater than unity ($n_{AV}$>1.242) which indicate that the reaction order is greater than first order (Borrego and Gonzalez-Doncel, 1998). In this reason, the pseudo-second-order model posed better fitness with data than pseudo-first-order model. So, it could be assumed that Cu(II) adsorption followed more order during the processes. These finding postulated the possible changes occurred on adsorption mechanism during the processes and therefore, the adsorption mechanism of Cu(II) onto POFS followed multiple kinetic orders (Cestari et al., 2004; Lopes et al., 2003).

## 8.3 Conclusion

This research ascertained that palm oil fruit shells (POFS) can be used as a biosorbents for the removal of toxic Cu(II) ions from water and wastewater. Characterisation showed that the surface of POFS is heterogeneous, contains metal hungry functional groups (hydroxyl and carboxyl groups) and hold significantly high specification surface (39.76 $m^2$/g). The equilibrium data were found well fitted the three-parameter isotherm than two-parameter models. The analysis revealed that the sorption system was heterogeneous as the exponents from the prediction of three-parameter models were lies

between 0 and 1. The POFS showed significantly high adsorption capacity (59.502 mg/g), i.e. one gram of POFS can remove 59.502 mg of Cu(II) ions from water. The high $R^2$ (coefficient of determination) values of kinetics model and quick equilibrium (50mins) showed the applicability of Cu(II) removal by palm oil fruit shells.

Faculty of Engineering and Information Technology
University of Technology, Sydney (UTS)

# Chapter 9

# Laboratory-scale fixed bed column experiments for evaluation the applicability of cabbage biosorbent to remove Pb(II), Cd(II), Cu(II) and Zn(II) from aqueous solution

## 9.1 Background

To validate the biosorption data obtained under batch conditions, assessment of sorption performance in a continuously operated column is necessary as the biosorbent uptake capacity is well utilised by metals ions in this completely mixed system (Acheampong et al., 2011). In addition the contact time required to attain equilibrium is different under column operation than batch system (Chandra Sekhar et al., 2003a; Vilar et al., 2008). For column operation, the biosorbent is continuously in contact with freshly metals laded wastewater and subsequently, the concentration in the solution in contact with a given layer of the biosorbent in a column changes very slowly. A fixed-bed column is simple to operate and economically valuable for wastewater treatment (Ahmad and Hameed, 2010; Singh et al., 2009; Sousa et al., 2010). Experiments using a laboratory-scale fixed-bed column of relatively large volume yield performance data that can be used to design a larger pilot and industrial scale plant with a high degree of accuracy(Chandra Sekhar et al., 2003a).

A continuous removal of Pb(II), Cd(II), Cu(II) and Zn(II) from a mixture of artificial wastewater by cabbage waste in a fixed-bed column to determine process design for practical uses are investigated. Further, the breakthrough data obtained for each operating condition were fitted to adsorption models to enable appropriate design and scale up of the biosorption column. The cabbage investigated in this study shown in Chapter 5 was found to be the most effective biosorbent within all of the studied biorbents in this thesis. The conditions got in the Chapter 5, were therefore maintained in the column experiments as well for examining the influence of various operating conditions such as flow rate, bed depth and initial metals concentration on continuous biosorption by cabbage.

## 9.2 Results and discussions

An acrylic column was designed and constructed for conducting the column experiment. Different conditions are used to evaluate the metal biosorption by cabbage waste and the experimental results with discussion are as below.

### 9.2.1 Effect of flow rate

The column was operated at three flow rates of 34.5 ml/min (2.07 l/h), 64.83 ml/min (3.89 l/h) and 67.33 ml/min (4.04 l/h) with bed depth of 2.25 cm, cabbage powder of 5 g

and initial metals concentration of 5 mg/l were kept constant. The breakthrough curves achieved are presented in Figure 9.1(A) for Pb(II), Figure 9.1(B) for Cd(II), Figure 9.1(C) for Cu(II) and Figure 9.1(D) for Zn(II).

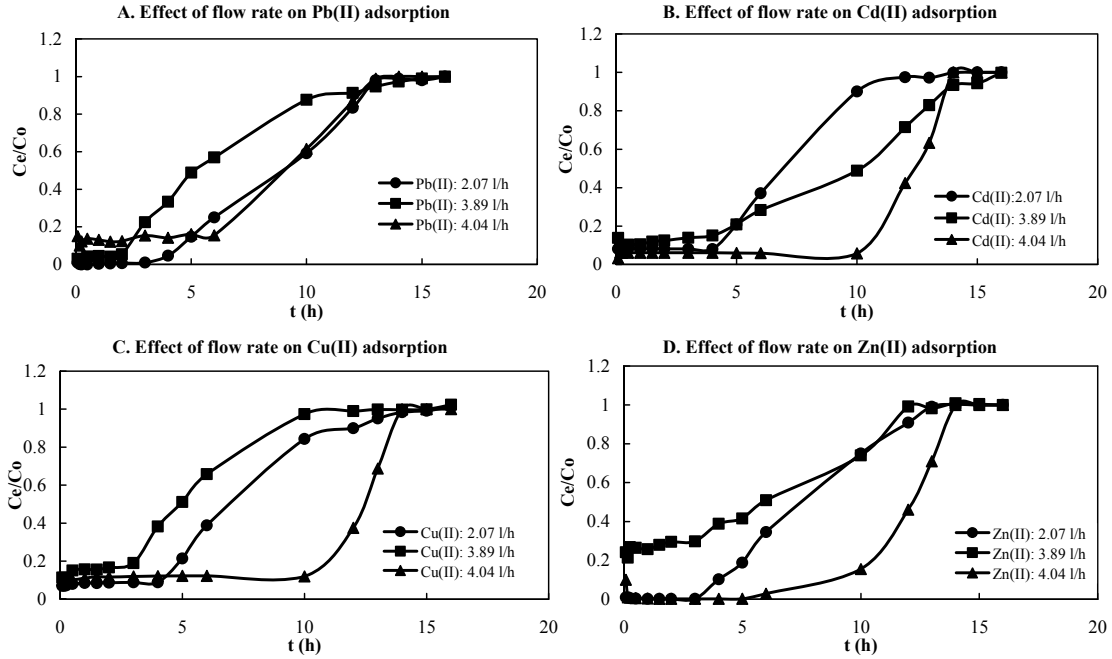


**Figure 9.1** Breakthrough curves for Pb(II), Cd(II), Cu(II) and Zn(II) biosorption onto cabbage at different flow rates (bed depth = 2.25 cm, inlet Pb(II), Cd(II), Cu(II) and Zn(II) concentrations = 5 mg/l, particle size > 0.3 mm, temperature = room temp. and influent pH 6.0-6.5).

Figure 9.1 showed that that the breakthrough time as well as the exhaustion time increased with a decrease in flow rate (from 2.07 to 4.04 l/h) for Pb(II), Cd(II), Cu(II) and Zn(II) adsorption. The slope of the plots from breakthrough time to exhaustion time increased as the flow rate was increased from 2.07 to 4.04 l/h. It means that the breakthrough curve produced steep slopes with the increased flow rate for all metals adsorption. In case of Pb(II) adsorption, the exhaustion time was similar for 2.07 l/h and 4.04 l/h flow rate and earlier for 3.39 l/h flow rates than other two flow rate. A higher flow rate resulted in a lower residence time in the column and vice versa (Acheampong et al., 2013). An increase in the flow rate reduced the contact time between Pb(II), Cd(II), Cu(II) and Zn(II) ions and cabbage waste; and also reduced the volume of effluent efficiently treated before the bed became saturated (Khan et al., 2012; Tunali Akar et al., 2012). Therefore, it decreased the service time of the bed (Figure 9.1 A, B, C and D). Figure 9.1(B, C & D) demonstrates that breakthrough occurs faster at a

higher flow rate for Cd(II), Cu(II) and Zn(II) ions. It might occur due to bypass of flow in a clod formation at low flow rate.

### 9.2.2 Effect of bed depth

The bed depth is an important parameter for design a fixed bed column for continuous wastewater treatment system. In this context, three bed depth (2.25, 4.5 and 9.0 cm) are used for removal of multimetals [Pb(II), Cd(II), Cu(II) and Zn(II)] from an artificial multi-metal solution. The experimental results are showed in Figure 9.2 (A, B, C and D).

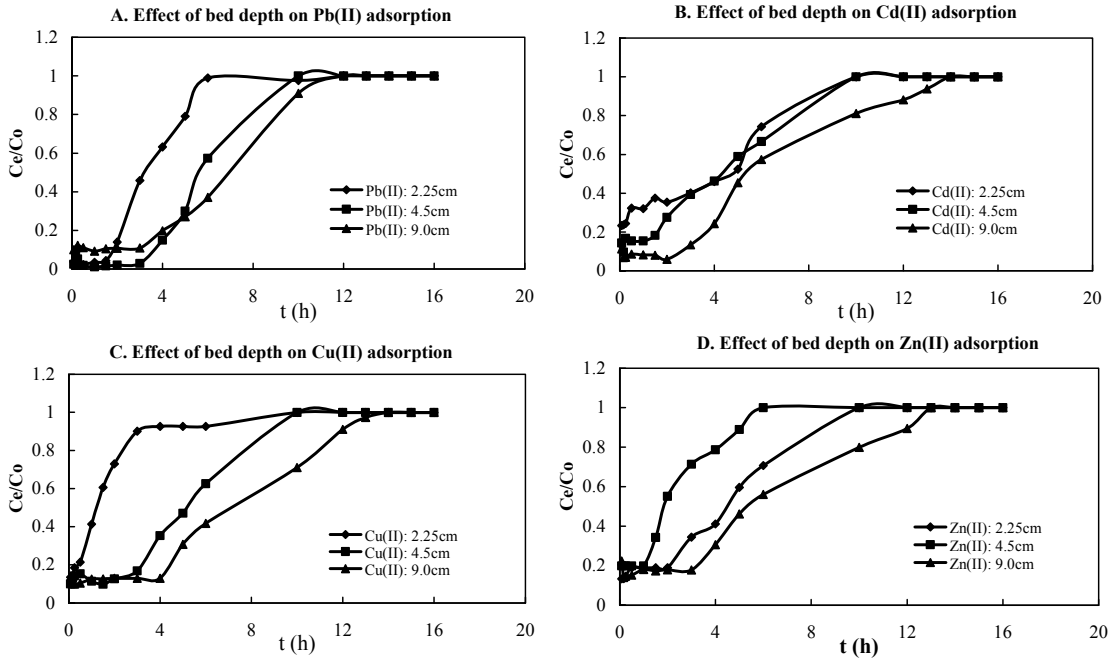


**Figure 9.2** Breakthrough curves for Pb(II), Cd(II), Cu(II) and Zn(II) biosorption onto cabbage at different bed heights ( inlet Pb(II), Cd(II), Cu(II) and Zn(II) concentrations = 9 mg/l, flow rate = 7.07 l/h, particle size > 0.3 mm, temperature = room temp and influent pH 6.0-6.5).

The breakthrough curves obtained for Pb(II), Cd(II), Cu(II) and Zn(II) ions biosorption are illustrated in Figure 9.2 (A, B, C and D) for different bed depth of cabbage (2.25, 4.5 and 9.0 cm), at a constant linear flow rate of 2.07 l/h and metals concentration (9 mg/l). It is visible from the plots (Figure 9.2) that a characteristic 'S' shaped profile generated in ideal biosorption systems. It can be predicted that the breakthrough volume varies with bed depth. Axial dispersion phenomena predominate in the mass transfer and reduce the diffusion of metallic ions when the bed depth is reduced (Malkoc and Nuhoglu, 2006a). The solute (metallic ions) does not have enough time to diffuse into the whole of the adsorbent mass (Taty-Costodes et al., 2005). As observed from Figure

9.2 (A, B, C and D), the treated volume considerably decreased from about 31050 to 20700 ml for Pb(II), 28980 to 12420 ml for Cd(II), 31050 to 12420 for Cu(II) and 31050 to 20700 ml for Zn(II) (Table 9.1) as the bed depth increased from 2.25 to 9.0 cm. At higher bed depth the cabbage biosorbent were not dispersed properly in the used flow rate so as the treated volume is reduced (Sousa et al., 2010; Valderrama et al., 2010).

### 9.2.3 Effect of initial metals concentrations

The effect of varying the inlet metals concentration from 5 to 20 mg/l on the shape of the breakthrough curves was studied at a constant biosorbent bed depth (2.25 cm) and feed flow rate (34.5 ml/min). The resulting breakthrough curves are presented in Figure 9.3(A, B, C and D) for Pb(II), Cd(II), Cu(II) and Zn(II) ions adsorption on to cabbage waste loaded columns.

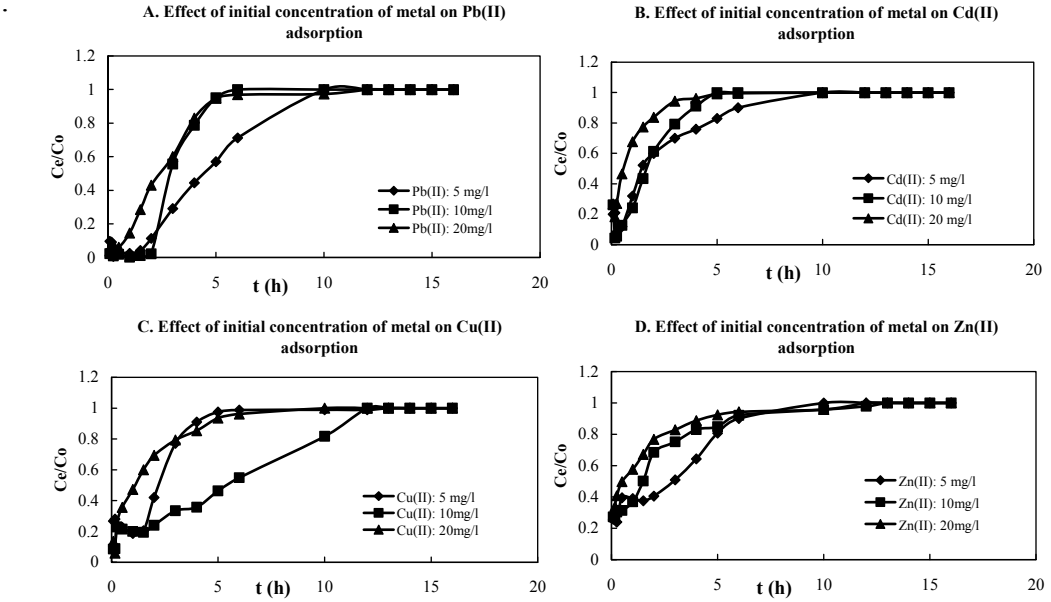


**Figure 9.3** Breakthrough curves for Pb(II), Cd(II), Cu(II) and Zn(II) biosorption onto cabbage at different initial Pb(II), Cd(II), Cu(II) and Zn(II) concentrations ( flow rate = 2.07 l/h, bed depth = 2.25 cm, particle size > 0.3 mm, temperature = room temp, influent pH 6.0-6.5).

The curves show that the breakthrough time decreased with increasing inlet Pb(II), Cd(II), Cu(II) and Zn(II) concentration. The larger the initial concentration ($C_0$) for all metals, the steeper the breakthrough curve and the shorter the breakthrough time (Figure 9.3A, B, C & D). An increase in the inlet concentration reduced the treated volume [31050 ml to 689670 ml for Pb(II); 31050 ml to 588550 ml for Cd(II); 31050 ml to 625670 ml for Cu(II); and 31050 ml to 657980 ml for Zn(II) (Table 9.1)] before the bed

gets saturated. As a high metals concentrations may saturate the biosorbent more quickly, the operation time was decreased. Decreasing the Pb(II), Cd(II), Cu(II) and Zn(II) concentration increases the volume of the feed metals solution that can be treated, shifting the breakthrough curve to the right (Figure 9.3A, B, C & D) (Acheampong et al., 2013). The value of $C_e/C_0$ reached near unity at 10, 7 and 8 h for Pb(II); at 12, 7 and 7 h for Cd(II); at 14, 5 and 7 h for Cu(II); and 8 , 8 and 8 h for Zn(II) for adsorption when the inlet concentrations were 5, 10 and 20 mg/l, respectively.

### 9.2.4 Metals ions uptake at different column operation parameters

The maximum column capacity, $q_{total}$ (mg) for a given set of conditions in the column was calculated from the area under the plot of adsorbed Pb(II), Cd(II), Cu(II) and Zn(II) concentration, $C_{ad}$ (mg/l), versus time as given by the equation (Ahmad and Hameed, 2010):

$$q_{total} = \frac{QA}{1000} = \frac{Q}{1000}\int_{t_0}^{t_{total}} C_{ad}\,dt \qquad (9.1)$$

where $C_{ad} = C_0 - C_e$ (mg/l), $t_{total}$ is the total flow time (min), Q is the flow rate (ml/ min) and A is the area under the breakthrough curve ($cm^2$). The equilibrium uptake ($q_{e(exp)}$), i.e. the amount of Pb(II), Cd(II), Cu(II) and Zn(II) adsorbed (mg) per unit dry weight of biosorbent (mg/g) in the column, was calculated by following equation (Martín-Lara et al., 2012; Mohan and Sreelakshmi, 2008):

$$q_{e(\exp)} = \frac{q_{total}}{m} \qquad (9.2)$$

where *m* is the total dry weight of cabbage waste in the column (g). The total volume treated, $V_{eff}$ (ml), was calculated from the following equation(Futalan et al., 2011):

$$V_{eff} = Q.t_{total} \qquad (9.3)$$

The column data obtained during the experimental run are presented in Table 9.1. Data from laboratory tests is useful for the design of a full-scale biosorption column. It is found that as the flow rate increases, the volume of influent treated increased while the uptake decreased (Table 9.1). The optimum conditions for column operation for Pb(II), Cd(II), Cu(II) and Zn(II) ions biosorption by cabbage wastewater were 5 mg/l for Pb(II), Cd(II), Cu(II) and Zn(II) inlet concentration, 4.5 cm bed depth and 64.83 ml/ min flow rate, which yielded a service time to breakthrough of 8-10 h (Figure 9.2).

**Table 9.1** Uptake of Pb(II), Cd(II), Cu(II) and Zn(II) at different operating conditions (particle size > 0.3 mm, bed depth = 2.25 cm, inlet pH= 6-6.5)

| Metals name | Bed depth, Z (cm) | Flow rate, Q (ml/min) | Initial concen. $C_o$ (mg/l) | Total treated vol., $V_{eff}$ (ml) | Total metals removed, $q_{total}$ (mg) | Equil. adsorption capacity, $q_{e\,(exp)}$ (mg/g) |
|---|---|---|---|---|---|---|
| | 2.25 | 34.5 | 5 | 31050 | 2075.11 | 415.02 |
| | 2.25 | 64.83 | 5 | 58350 | 4814.88 | 962.98 |
| | 2.25 | 67.33 | 5 | 52520 | 2046.77 | 409.35 |
| **Pb(II)** | 4.5 | 34.5 | 10 | 12420 | 871.93 | 87.19 |
| | 9.0 | 34.5 | 10 | 24840 | 2597.07 | 129.85 |
| | 2.25 | 34.5 | 10 | 10350 | 1046.21 | 209.24 |
| | 2.25 | 34.5 | 20 | 20700 | 3130.56 | 626.11 |
| | 2.25 | 34.5 | 5 | 28980 | 1287.89 | 257.58 |
| | 2.25 | 64.83 | 5 | 62240 | 6884.17 | 1376.83 |
| | 2.25 | 67.33 | 5 | 52520 | 3966.57 | 793.31 |
| **Cd(II)** | 4.5 | 34.5 | 10 | 12420 | 1119.25 | 111.93 |
| | 9.0 | 34.5 | 10 | 28980 | 4301.71 | 215.09 |
| | 2.25 | 34.5 | 10 | 10350 | 370.82 | 74.16 |
| | 2.25 | 34.5 | 20 | 12420 | 1105.07 | 221.01 |
| | 2.25 | 34.5 | 5 | 31050 | 1702.19 | 340.44 |
| | 2.25 | 64.83 | 5 | 62240 | 4865.16 | 973.03 |
| | 2.25 | 67.33 | 5 | 52520 | 2381.03 | 476.21 |
| **Cu(II)** | 4.5 | 34.5 | 10 | 12420 | 1175.99 | 117.59 |
| | 9.0 | 34.5 | 10 | 28980 | 3119.46 | 155.97 |
| | 2.25 | 34.5 | 10 | 24840 | 1117.86 | 223.57 |
| | 2.25 | 34.5 | 20 | 12420 | 1237.62 | 247.52 |
| | 2.25 | 34.5 | 5 | 31050 | 2130.14 | 426.03 |
| | 2.25 | 64.83 | 5 | 50570 | 4325.97 | 865.19 |
| | 2.25 | 67.33 | 5 | 52520 | 4309.35 | 861.87 |
| **Zn(II)** | 4.5 | 34.5 | 10 | 10350 | 661.51 | 66.15 |
| | 9.0 | 34.5 | 10 | 28980 | 2879.11 | 143.96 |
| | 2.25 | 34.5 | 10 | 26910 | 622.53 | 124.51 |
| | 2.25 | 34.5 | 20 | 20700 | 1693.43 | 338.69 |

The optimum adsorption capacity was found at 64.83 ml/min flow rate, 2.25 cm bed depth and 5 mg/l initial metal concentrations for Pb(II), Cd(II), Cu(II) and Zn(II) (Table 9.1). This study showed that the biosorption capacities by the column were 962.98, 1376.83, 973.03 and 865.19 mg/g (Table 9.1) for Pb(II), Cd(II), Cu(II) and Zn(II) respectively, which were 15.72, 62.23, 68.23 and 70.71 times better than that obtained in a batch system (Chapter 5, Table 5.6). Similar findings reported in literature (Acheampong et al., 2011). These enhanced capacities by the column method can be featured to the continuously increasing concentration gradient in the interface of the biosorption zone as it passes through the column, whereas the gradient concentration decreases with time in batch systems (Martín-Lara et al., 2012; Sousa et al., 2010). A characterisation study on the cabbage waste prior to biosorption showed that hydroxyl

and carboxylic functional groups were involved in the removal of Pb(II), Cd(II), Cu(II) and Zn(II) from aqueous solutions by this biosorbent, besides micro precipitation and electrostatic attraction forces (Acheampong et al., 2011; Hossain et al., 2013).

### 9.2.5 Influence of functional parameters on breakthrough curves

The column showed well removal capacities at the low flow rate because at the lower flow rate the residence time of the influent was increased, allowing metals ions to diffuse into the pores of the cabbage by means of intra-particle diffusion (Luo et al., 2011). A high flow rate means inadequate time for metals ions [Pb(II), Cd(II), Cu(II) and Zn(II)] to diffuse into the pores of the cabbage, leading to a low uptake capacity and removal efficiency (Ko et al., 2000; Vijayaraghavan et al., 2004). This may be due to the metals ions leaving the column before to be adsorbed and the equilibrium could be attained (Singh and Pant, 2006). As the bed height increased, the metals ions had more time to contact with more cabbage particles, resulting in a higher uptake of Pb(II), Cd(II), Cu(II) and Zn(II) in the column (Table 9.1). Hence, when the bed height increases, the maximum biosorption capacity of the column also increases (Malkoc and Nuhoglu, 2006b). Though, all high bed depth did not show the same trend. At higher bed depth the biosorbent particles stay in compact condition and do not expose to uptake metals ions. The slight increase in the slope of the breakthrough curves (Figure 9.1, Figure 9.2 and Figure 9.3) with increasing bed height resulted in a broadened mass transfer zone. The dynamic force for biosorption is the concentration gradient between the metals ions onto biosorbent and the solution (Oguz and Ersoy, 2010). A high concentration, therefore, provides a large driving force for the biosorption process. However, the saturation of the adsorbent requires much more time. But due to the high driving force, breakthrough is reached before all the active sites of the cabbage waste could be occupied by Pb(II), Cd(II), Cu(II) and Zn(II) ions, leading to a shorter breakthrough time (Figure 9.1, Figure 9.2 and Figure 9.3). The diffusion process is concentration dependent because a change of concentration gradient affects the saturation rate and the breakthrough time (Mondal, 2009).

### 9.2.6 Evaluation of column data by dynamic models

The successful design of a column adsorption process depends on the proper prediction the concentration-time profile or breakthrough curve for effluent parameters. A number of mathematical models have been developed for use in the design of continuous fixed bed biosorption columns. In this work, the Bed Depth Service Time (BDST), Thomas,

Yoon–Nelson and Clark models were used in predicting the behaviour of the breakthrough curve because of their effectiveness.

### 9.2.6.1 Bed Depth Service Time (BDST) model

The Bed Depth Service Time (BDST) is widely used model for designing the column biosorption system (Bohart, 1920; Luo et al., 2011; Mohan and Sreelakshmi, 2008). It assumes that the rate of biosorption is administered by the surface reaction between the metals ions and binding sites of the biosorbent. The BDST model describes the relation between the breakthrough time, often called the service time of the bed and the packed-bed depth of the column. The BDST model rate constant (*Ka*) is not significantly affected by the change in flow rate, and thus the intercept n of the BDST equation remains unchanged when flow rate is changed (Vijayaraghavan and Prabu, 2006). The BDST model equation is as follows:

$$t = \frac{N_0}{C_0 Q} Z - \frac{1}{K_a C_0} \ln\left(\frac{C_0}{C_e} - 1\right) \qquad (9.4)$$

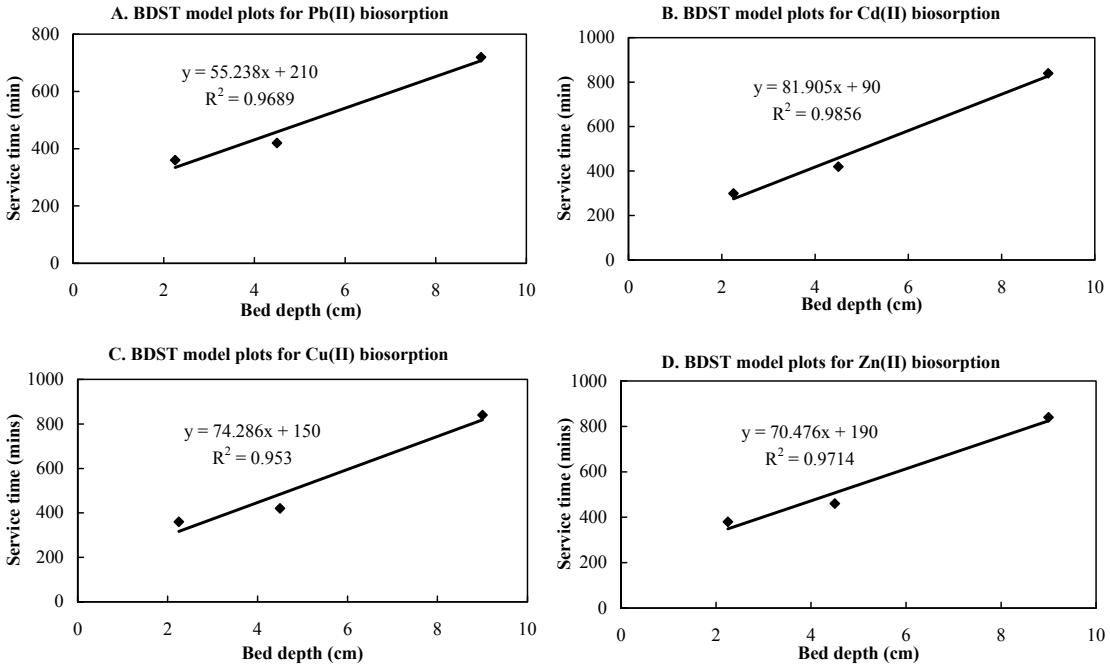


**Figure 9.4** BDST model plots for Pb(II), Cd(II), Cu(II) and Zn(II) biosorption onto cabbage waste at different bed heights (flow rate = 2.07 l/h, initial metals concentration = 10 mg/l, particle size > 0.3, temperature = room temp, inlet pH= 6-6.5).

A plot of t versus bed depth, Z, should yield a straight line where $N_0$ and *Ka* can be evaluated from the slope and intercept (Figure 9.4), respectively. The critical bed depth of column, $Z_0$ is calculated by the following equation:

$$Z_0 = \frac{Q}{K_a N_0} \ln\left(\frac{C_0}{C_e} - 1\right) \quad (9.5)$$

The Figure 9.4 (A, B, C and D) shows the plot of the service time versus bed height for Pb(II), Cd(II), Cu(II) and Zn(II) biosorption onto cabbage waste. The BDST parameters calculated from the slopes and the intercepts of the plots are presented in Table 9.2. The variations of the service time with bed depth are linear for all plots (Figure 9.4), with very high correlation coefficient ($R^2$) values, representing the validity of the BDST model. The most significant principle in the design of fixed-bed biosorption systems is the prediction of the column breakthrough or the shape of the adsorption wave front, which determines the operating life-span of the bed.

**Table 9.2** BDST model parameters for the sorption of Pb(II), Cd(II), Cu(II) and Zn(II) onto cabbage waste at varying bed heights (flow rate = 34.5 ml/min, initial metals concentration = 10 mg/l, particle size > 0.3 mm, temperature = room temp., inlet pH = 6-6.5**)**

| BDST parameters | Pb(II) | Cd(II) | Cu(II) | Zn(II) |
|---|---|---|---|---|
| $N_0$ (mg/l) | 317.607 | 470.959 | 427.145 | 405.237 |
| $K_a$ (l/mg. h) | 0.130 | 0.345 | 0.268 | 0.212 |
| $Z_0$ (cm) | 3.802 | 1.099 | 2.019 | 2.696 |
| $R^2$ | 0.969 | 0.986 | 0.953 | 0.971 |

The BDST model provide an idea of the efficiency of the column under constant operating conditions for achieving a desired Pb(II), Cd(II), Cu(II) and Zn(II) breakthrough level in the column. The values of biosorption rate constant (K*a*) and biosorption capacity ($N_0$) of the column estimated using this model, is shown in (Table 9.2). In addition, these parameter values are also in good agreement with the previous study on batch kinetics of Pb(II), Cd(II), Cu(II) and Zn(II) biosorption using cabbage waste and other biosorbent (Acheampong et al., 2011; Hossain et al., 2013; Malakootian et al., 2008; Malakootian et al., 2009). The BDST model parameters are valuable in scaling up the process for other flow rates without further experimental runs (Vijayaraghavan and Prabu, 2006). Normally, 50% breakthrough curve between t and Z must pass through the origin i.e, the intercept would be zero (Singh et al., 2009); but these studies were not the case (Figure 9.4). It showed that the biosorption of metals ions onto cabbage waste is governed by a more complex mechanism and the biosorption process is limited by the intra-particle diffusion step (Singh et al., 2009). The rate

constant *Ka*, which is a evaluation of the rate of transfer of solute (metals ions) from the fluid phase to the solid phase (biosorbent) (Al-Degs et al., 2009; Chandra Sekhar et al., 2003b), mainly persuaded the breakthrough trend in the column study. For smaller values of *Ka* (Table 9.2), a relatively longer bed is required to avoid breakthrough for cabbage biosorbent (Acheampong et al., 2013). The breakthrough can be eliminated even in smaller bed heights when the value of *Ka* is high (Chandra Sekhar et al., 2003b).

The bed capacity, $N_0$, a process parameter changes with time and is used to predict the performance of the bed if there is a change in the initial metals concentration, $C_0$, to a new value. At a constant flow rate, a greater $N_0$ and a smaller $Z_0$ indicate a higher efficiency for a biosorption material (Acheampong et al., 2013). Generally, *Ka* and $N_0$ are inversely proportional to Z, and the product of *Ka* and $N_0$ is a unique constant for a given adsorbent (Luo et al., 2011). From Table 9.2, $N_0$ is much greater than $Z_0$ for all four metals, indicating that cabbage waste is highly efficient in removing Pb(II), Cd(II), Cu(II) and Zn(II) from aqueous solution. Once the BDST column design parameters are found, fixed bed columns can be designed for deferent flow rates and initial metals concentrations without further experimental runs (Luo et al., 2011; Vijayaraghavan and Prabu, 2006).

**9.2.6.2 The Thomas, Yoon-Nelson and Clark models**

The Thomas model is one of the most extensively applied models in demonstrating the column performance and prediction of breakthrough curves (Thomas, 1944). This model follows the Langmuir model of adsorption-desorption (Vijayaraghavan and Prabu, 2006). It presumes that a negligible axial dispersion happen in the column adsorption since the rate driving force obeys the second-order reversible kinetics (Futalan et al., 2011). The Thomas model equation is as follows:

$$\ln\left(\frac{C_0}{C_t}-1\right)=\frac{k_{TH}q_0m}{Q}-k_{TH}C_0t \qquad (9.6)$$

This model was applied to the experimental data and model parameters were determined from the linear plot. A plot of $\ln\left(\frac{C_0}{C_t}-1\right)$ against 't' gives a straight line from which the values of $k_{TH}$ and $q_0$ are determined from the intercept and the slope, respectively. The calculated parameters are presented in Table 9.3, Table 9.4, Table 9.5 and Table 9.6

for Pb(II), Cd(II), Cu(II) and Zn(II); respectively. The results show that $k_{TH}$ increased with increasing flow rate and initial metals concentration. Generally, $q_0$ increased with flow rate and the initial metals concentration over the entire biosorption period (Tables 9.3, 9.4, 9.5 and 9.6). A good fit ($R^2$ > 0.81-0.99) was obtained for all metals biosorption.

Yoon and Nelson devised a model to examine the breakthrough behaviour of adsorbate gases on activated carbon which is known as Yoon-Nelson model (Yoon and Nelson, 1984). This model was based on the assumption that the rate of decrease in the probability of biosorption of each adsorbate molecule is proportional to the probability of the adsorbate adsorption and the adsorbate breakthrough on the adsorbent (Chen et al., 2012). The formulation of the model is as follows:

$$\ln\left(\frac{C_t}{C_0 - C_t}\right) = k_{YN}t - \tau k_{YN} \qquad (9.7)$$

**Table 9.3** The Thomas, Yoon-Nelson and Clark models parameters for Pb(II) biosorption onto cabbage at different bed heights, flow rate and inlet concentration (particle size >0.3mm, temperature = room temp., inlet pH: 6-6.5)

| Experimental conditions | | | Thomas model Parameters | | | Yoon–Nelson model parameters | | | Clark model parameters | | |
|---|---|---|---|---|---|---|---|---|---|---|---|
| Z (cm) | Q (ml/min) | $C_0$ (mg/l) | $q_0$ (mg/g) | $k_{TH}$ (ml/ mg. min) | $R^2$ | $k_{YN}$ (mg/g) | τ (/min) | $R^2$ | r (/min) | A | $R^2$ |
| 2.25 | 34.5 | 5 | 21.38 | 2.02 | 0.96 | 0.005 | 125.5 | 0.73 | 0.111 | 2.7E +38 | 0.90 |
| 2.25 | 64.83 | 5 | 44.67 | 0.99 | 0.98 | 0.004 | 58.77 | 0.96 | 0.071 | 1.9E +24 | 0.97 |
| 2.25 | 67.33 | 5 | 26.73 | 1.183 | 0.81 | 0.003 | 144.1 | 0.81 | 0.041 | 6.9E +16 | 0.93 |
| 4.5 | 34.5 | 10 | 20.31 | 0.68 | 0.91 | 0.002 | 31.39 | 0.87 | 0.089 | 1.8E +36 | 0.93 |
| 9.0 | 34.5 | 10 | 16.04 | 0.23 | 0.95 | 0.0001 | 1197 | 0.95 | 0.046 | 1.7E +17 | 0.94 |
| 2.25 | 34.5 | 10 | 77.64 | 0.376 | 0.95 | 0.009 | 33.63 | 0.83 | 0.079 | 3.2E +34 | 0.95 |
| 2.25 | 34.5 | 20 | 24.80 | 0.818 | 0.99 | 0.010 | 29.87 | 0.94 | 0.175 | 1.8E +20 | 0.88 |

The magnitudes of the Yoon-Nelson parameters ($k_{YN}$ and $t$) were calculated from the plot of $ln[(C_t/(C_0-C_t)]$ versus $t$ at various operating conditions (Table 9.3, Table 9.4, Table 9.5 and Table 9.6). The $k_{YN}$ values increased with increasing flow rates, while the t values decreased as the flow rate increased. A comparable trends were observed when the initial Pb(II), Cd(II), Cu(II) and Zn(II) concentration were increased (Table 9.3, 9.4,

9.5 and 9.6). The $R^2$ values (Table 9.3, 9.4, 9.5 and 9.6) specify a good fit in all cases, viewing that the Yoon-Nelson model can be used to describe the Pb(II), Cd(II), Cu(II) and Zn(II)-cabbage waste biosorption system.

**Table 9.4** The Thomas, Yoon-Nelson and Clark models parameters for Cd(II) biosorption onto cabbage at different bed heights, flow rate and inlet concentration (particle size >0.3mm, temperature = room temp., inlet pH: 6-6.5)

| Experimental conditions | | | Thomas model Parameters | | | Yoon–Nelson model parameters | | | Clark model parameters | | |
|---|---|---|---|---|---|---|---|---|---|---|---|
| Z (cm) | Q (ml/min) | $C_0$ (mg/l) | $q_0$ (mg/g) | $k_{TH}$ (ml/ mg. min) | $R^2$ | $k_{YN}$ (mg/g) | τ (/min) | $R^2$ | r (/min) | A | $R^2$ |
| 2.25 | 34.5 | 5 | 11.22 | 1.93 | 0.90 | 0.004 | 64.39 | 0.907 | 0.059 | 6.2E +18 | 0.93 |
| 2.25 | 64.83 | 5 | 61.85 | 0.54 | 0.95 | 0.002 | 28 | 0.87 | 0.04 | 1.5E +16 | 0.98 |
| 2.25 | 67.33 | 5 | 69.35 | 0.59 | 0.94 | 0.001 | 6.36 | 0.96 | 0.055 | 5.9E +22 | 0.96 |
| 4.5 | 34.5 | 10 | 32.89 | 0.188 | 0.93 | 0.0002 | 839.5 | 0.94 | 0.038 | 1.8E +14 | 0.93 |
| 9.0 | 34.5 | 10 | 10.78 | 0.437 | 0.96 | 0.003 | 50.78 | 0.94 | 0.055 | 4.3E +18 | 0.97 |
| 2.25 | 34.5 | 10 | 5.21 | 3.206 | 0.90 | 0.009 | 9.802 | 0.95 | 0.208 | 1.1E +19 | 0.81 |
| 2.25 | 34.5 | 20 | 8.21 | 0.752 | 0.97 | 0.015 | 10.82 | 0.99 | 0.037 | 8.5E +4 | 0.81 |

**Table 9.5** The Thomas, Yoon–Nelson and Clark models parameters for Cu(II) biosorption onto cabbage at different bed heights, flow rate and inlet concentration (particle size >0.3mm, temperature = room temp., inlet pH: 6-6.5)

| Experimental conditions | | | Thomas model Parameters | | | Yoon–Nelson model parameters | | | Clark model parameters | | |
|---|---|---|---|---|---|---|---|---|---|---|---|
| Z (cm) | Q (ml/min) | $C_0$ (mg/l) | $q_0$ (mg/g) | $k_{TH}$ (ml/ mg. min) | $R^2$ | $k_{YN}$ (mg/g) | τ (/min) | $R^2$ | r (/min) | A | $R^2$ |
| 2.25 | 34.5 | 5 | 14.97 | 1.43 | 0.95 | 0.004 | 92.20 | 0.88 | 0.058 | 6.1E +18 | 0.95 |
| 2.25 | 64.83 | 5 | 30.38 | 1.08 | 0.98 | 0.008 | 73.4 | 0.94 | 0.047 | 4.4E +14 | 0.98 |
| 2.25 | 67.33 | 5 | 48.49 | 0.639 | 0.98 | 0.00001 | 107.8 | 0.77 | 0.040 | 4.6E +17 | 0.98 |
| 4.5 | 34.5 | 10 | 31.28 | 0.225 | 0.93 | 0.0002 | 687.5 | 0.91 | 0.043 | 1.5E +16 | 0.94 |
| 9.0 | 34.5 | 10 | 7.37 | 0.598 | 0.93 | 0.0017 | 6.471 | 0.88 | 0.044 | 5.6E +16 | 0.94 |
| 2.25 | 34.5 | 10 | 12.30 | 1.042 | 0.92 | 0.0024 | 21.33 | 0.92 | 0.042 | 3.1E +12 | 0.94 |
| 2.25 | 34.5 | 20 | 12.42 | 0.622 | 0.95 | 0.0086 | 11.84 | 0.99 | 0.055 | 1.3E +8 | 0.80 |

Clark model presumes that the biosorption behaviour of pollutants follows the Freundlich adsorption isotherm, and the biosorption rate is determined by the external mass transfer step (Clark, 1987). The model is used for the simulation of breakthrough curves and the equation is as follows:

$$\ln\left[\left(\frac{C_0}{C_e}\right)^{n-1} - 1\right] = \ln A - rt \qquad (9.8)$$

The values of the Clark parameters A and r are determined from the slope and the intercept of plots of $ln((C_0/C_e)^{n-1} - 1)$ versus $t$. The values of the Clark parameters are presented in Table 9.3, Table 9.4, Table 9.5 and Table 9.6 for Pb(II), Cd(II), Cu(II) and Zn(II); respectively. The applicability of the Clark model to this column system is very practicable in the examined range of flow rate, bed depth and initial metals concentration for which their dependence on parameters (Table 9.3, 9.4, 9.5 and 9.6). Generally, the values of r increase with increasing bed height, flow rate and initial metals concentration, while the A values are inversely related to the experimental conditions. However, for this system, it happen opposite for r and A values though the model gave excellent fitting of the experimental data as evident from the high $R^2$ values (Table 9.3, 9.4, 9.5 and 9.6).

**Table 9.6** The Thomas, Yoon–Nelson and Clark models parameters for Zn(II) biosorption onto cabbage at different bed heights, flow rate and inlet concentration (particle size >0.3mm, temperature = room temp., inlet pH: 6-6.5)

| Experimental conditions | | | Thomas model Parameters | | | Yoon–Nelson model parameters | | | Clark model parameters | | |
|---|---|---|---|---|---|---|---|---|---|---|---|
| Z (cm) | Q (ml/min) | $C_0$ (mg/l) | $q_0$ (mg/g) | $k_{TH}$ (ml/ mg. min) | $R^2$ | $k_{YN}$ (mg/g) | τ (/min) | $R^2$ | r (/min) | A | $R^2$ |
| 2.25 | 34.5 | 5 | 18.95 | 1.981 | 0.95 | 0.003 | 82.41 | 0.87 | 0.102 | 1.3E +31 | 0.86 |
| 2.25 | 64.83 | 5 | 52.09 | 0.32 | 0.92 | 0.001 | 245.5 | 0.91 | 0.03 | 1.6E +10 | 0.96 |
| 2.25 | 67.33 | 5 | 75.22 | 0.82 | 0.83 | 0.002 | 169.2 | 0.80 | 0.09 | 1.8E +37 | 0.97 |
| 4.5 | 34.5 | 10 | 29.81 | 0.152 | 0.85 | 0.0003 | 698 | 0.85 | 0.031 | 6.9E +11 | 0.94 |
| 9.0 | 34.5 | 10 | 6.79 | 0.483 | 0.95 | 0.003 | 22.36 | 0.94 | 0.039 | 1.2E +14 | 0.91 |
| 2.25 | 34.5 | 10 | 2.96 | 1.492 | 0.93 | 0.005 | 70.04 | 0.98 | 0.059 | 1.6E +9 | 0.90 |
| 2.25 | 34.5 | 20 | 6.56 | 0.484 | 0.94 | 0.007 | 60.32 | 0.99 | 0.059 | 1.6E +9 | 0.83 |

### 9.2.7 Fixed bed column design

The biosorption capacity predicted by the Thomas model ($q_0$: Table 9.3, 9.4, 9.5 and 9.6) did not show good agreement with those obtained from the experimental results ($q_{e(exp)}$:Table 9.1). This demonstrated that the Thomas model might not adequately portray the biosorption system in this study and is therefore not a suitable model for the

design of the biosorption column, although the $R^2$ (0.81-0.99) value are high to show good fitness.

A layer of liquid film on the adsorbent surface has a direct effect on the mass transfer resistance (Futalan et al., 2011). The higher flow rates enhance the mass transfer of the Pb(II), Cd(II), Cu(II) and Zn(II) ions from the liquid film to the cabbage waste surface, resulting in earlier saturation of the biosorbent bed (Acheampong et al., 2011). The increase in $q_0$ as the flow rate was increased (Table 9.3, 9.4, 9.5 and 9.6) was due to proper dispersion to provide for the Pb(II), Cd(II), Cu(II) and Zn(II) ions to diffuse into the cabbage waste bed (Acheampong et al., 2011; Muhamad et al., 2010; Sen Gupta et al., 2009; Xiang et al., 2010). The dynamic force for biosorption is the concentration difference between the Pb(II), Cd(II), Cu(II) and Zn(II) ions on the cabbage waste and the metals ions remaining in the water (Luo et al., 2006; Luo et al., 2011). Thus, a decrease in initial Pb(II), Cd(II), Cu(II) and Zn(II) ions concentration guide to an increase in the value of $q_0$ and a decrease in $k_{TH}$. To design a biosorption column with the Thomas model should utilise low flow rates as well as low initial Pb(II), Cd(II), Cu(II) and Zn(II) ions concentrations for optimal Pb(II), Cd(II), Cu(II) and Zn(II) uptake. Nevertheless, the deviation between the biosorption capacities measured experimentally and that predicted by the model makes it unsuitable for the cabbage waste columns studied.

The Yoon-Nelson rate constant $k_{YN}$ follows the same trend as the Thomas model rate constant $k_{TH}$ (Table 9.3, 9.4, 9.5 and 9.6) but the magnitudes are lower than $k_{TH}$. The time required for sorbates breakthrough (t) obtained from the Yoon-Nelson model agreed well with the experimental data at all conditions examined. Consequently, the Yoon-Nelson model showed a good illustration of the metals-cabbage waste system. The Yoon-Nelson model has been used successfully to predict the time required for breakthrough of the biosorption of Pb(II), Cd(II), Cu(II) and Zn(II) ions onto different biosorbents (Baral et al., 2009; Chen et al., 2011a; Oliveira et al., 2012; Singh et al., 2009; Vijayaraghavan and Prabu, 2006; Vijayaraghavan and Yun, 2008; Yahaya et al., 2011). These results established that the model set of equations can be used as an appropriate numerical illustration of the biosorption process carried out in continuous flow fixed bed columns for cabbage.

Among the breakthrough models, the Clark model might be assumed a more superior model as it engages both the mass transfer and equilibrium biosorption in predicting the breakthrough phenomena (Acheampong et al., 2013). The earlier work dealing with a batch study on Pb(II), Cd(II), Cu(II) and Zn(II) biosorption using cabbage waste showed that the Freundlich model did not provide a good fit to the experimental equilibrium data (Hossain et al., 2013), and, therefore, the previously obtained Freundlich constant 'n' value was applied to estimate the Clark model parameters in this study. It is evident that the experimental breakthrough curve of Pb(II), Cd(II), Cu(II) and Zn(II) at the different column operating conditions were not well predicted by the Clark model in the low flow rate (Table 9.3, 9.4, 9.5 and 9.6). Thus, the entire breakthrough curve can be designed partially with the Clark model for continuous removal of Pb(II), Cd(II), Cu(II) and Zn(II) by cabbage waste in fixed bed columns.

## 9.3 Conclusions

It was found that fixed-bed systems achieved a better uptake of Pb(II), Cd(II), Cu(II) and Zn(II) by cabbage waste at a lower metals concentration, lower feed flow rate and lower cabbage waste bed-depth. The suitable service time to breakthrough and metals [Pb(II), Cd(II), Cu(II) and Zn(II)] ions concentration were 5-10 h and 10 mg/l, respectively. Among the various models applied to describe the metal breakthrough in the column, the BDST model was able to describe the data properly, whereas prediction of the metals uptake capacity by the Thomas model was poor. The adsorption capacities found by Thomas model were higher than batch system. The Yoon-Nelson model predicted the time required for breakthrough well and can be applied to the entire breakthrough curve. Nevertheless, the entire breakthrough curve was best predicted by the Clark model in the higher flow rate and higher bed depth. The design of a continuous fixed bed column treatment system with cabbage biosorbent for Pb(II), Cd(II), Cu(II) and Zn(II) laden wastewater can thus be reached using the BDST, Yoon-Nelson and Clark breakthrough models.

**Faculty of Engineering and Information Technology**
**University of Technology, Sydney (UTS)**

# Chapter 10

# Conclusions and Recommendations

## 10.1 Conclusions

The present study was mainly focused on the development of a low cost and effective biosorption system for removing Pb(II), Cd(II), Cu(II) and Zn(II) from aqueous solution. For the objectives, agro-waste and bio-waste based biosorbents were prepared from garden grass (GG), cabbage waste (CW), banana peels (BP), maple leaves (ML) and palm oil fruit shells (POFS). The prepared biosorbents were then evaluated for their characteristics; influence of experimental conditions, regeneration and adsorption–desorption properties by using Pb(II), Cd(II), Cu(II) and Zn(II) as model pollutants in aqueous solutions.

### 10.1.1 Characteristics

- All biosorbents are full with microporous to mesoporous particles with uneven structures, asymmetric steps and pores which postulate the high binding sites.
- Metal hungry functional groups such as hydroxyl, amines and carboxyl groups, are present in all biosorbents which responsible for higher adsorption.
- Among the five biosorbent, the POFS and CW pose highest, and lowest BET surface area, respectively.

### 10.1.2 Experimental conditions

- The biosorption of the metals depends on the changes of pH, doses, contact time, temperature, initial concentration of metal and particle sizes.
- The adsorption processes is spontaneous and exothermic in nature

### 10.1.3 Regeneration and reuse

- A small amount 0.1N $H_2SO_4$ could easily regenerate the biosorbent.
- Biosorbents can be reused 5 to 7 times with minor efficiency loss.

### 10.1.4 Equilibrium biosorption

The equilibrium biosorption of metals were examined and the following results are found:

- The initial metals concentration had substantial impacts on the isotherm parameters. Hence, it is necessary to estimate the isotherm parameters of models covering wide range of initial metals concentrations.
- The equilibrium data posed good agreement with three-parameter models ($R^2$: 0.988-1.00) e.g. Sips, Khan, Redlich-Peterson, Unilan models that indicates the

biosorbents contain both monolayer and heterogeneous surfaces to adsorb metals ions.

- Some metals like Cu(II) and Zn(II) ions adsorption data posed good fitness to describe the equilibrium with Freundlich isotherm.
- The Langmuir isotherm predicted efficiently the maximum adsorption capacity ($q_m$) for Pb(II), Cd(II), Cu(II) and Zn(II) ions adsorption which was similar to experimental values.
- The maximum adsorption capacities for Pb(II), Cd(II), Cu(II) and Zn(II) ion adsorption were 120.096, 50.459, 59.502 and 57.53 mg/g from C, BP, POFS and GG, respectively.
- Among the four metals Pb(II) and Cd(II) ions are more uptaken by the biosorbent than other metals ions.
- According to the Pb(II) ions adsorption capacities the order of preference of biosorbent is BP>CW>GG>ML where as it is BP>GG>ML> CW for Cd(II) ions adsorption.
- In the case of Cu(II) adsorption the choice of order is POFS > GG > ML > BP > CW; however, it was GG>BP>ML>CW for Zn(II) biosorption.
- A multi-component system was assumed in the adsorption modelling due to the presence of different components in the wastewater. As Pb(II) and Cd(II) ions was majority uptaken in this multi-component, the maximum reduction was achieved for the both Pb(II) and Cd(II) ions.
- Strong antagonisms were observed in the multimetals adsorption system which is the real condition of normal wastewater. The antagonism increases with increasing the number of metals ions.
- Although there was some good fitness found (e.g. Cu(II) desorption from GG and BP), the desorption data were shown moderate fitness with the isotherm models.

### 10.1.5 Kinetics of biosorption

The kinetics characteristics of metals were examined and the following results are found:

- Kinetics biosorption data from GG, ML, BP, CW and POFS showed good agreement with pseudo-second-order model. Thus the kinetics process best describes by this model.

- The adsorption reactions onto the above biosorbents are more than one as $k_2$ (the reaction constant from order kinetics) and $n_{AV}$ (fractionery kinetic orders from Avrami model) values were greater than unity.
- Along with pseudo-second-order and Avrami, Elovich and Fraction power models also showed good fitness with the kinetics data.
- The biosorption mechanisms were combination of physisorption and chemisorption because the fitness of kinetics data with pseudo-second-order, Avrami and Elovich models implies that. It is also supported by available functional groups on the biosorbents.
- The biosorption process is rate controlling steps that mean the intraparticle diffusion also happen in the second stage of biosorption of metals as the Intraparticle diffusion model posed good fitness with the kinetics data.

### 10.1.6 Laboratory scale test with fixed-bed column

Laboratory scale test with fixed-bed columns were conducted and the following findings are as follows:

- Fixed-bed column system achieved a better uptake of Pb(II), Cd(II), Cu(II) and Zn(II) at a lower metals concentration, lower feed flow rate and lower CW bed-depth than batch system.
- The biosorption capacities from fixed-bed column system were 15.72, 62.23, 68.23 and 70.71 times higher than that obtained in a batch system.
- The appropriate service times to breakthrough and metals ions concentration were 5-10 h and 10 mg/L, respectively.
- The design of a continuous fixed bed column treatment system with CW biosorbent for Pb(II), Cd(II), Cu(II) and Zn(II) laden wastewater can thus be reached using the BDST, Yoon-Nelson and Clark breakthrough models.

Relatively higher fitness ($R^2$), affinity of metals biosorbents and biosorption capacities are found in CW. Thus, CW can be the most effective biosorbent for the removal of Pb(II), Cd(II), Cu(II) and Zn(II) ions from aqueous solution.

## 10.2 Recommendations

Developed five biosorbents (garden grass, cabbage waste, banana peels, maple leaves and palm oil fruit shells) could be regenerated several times and used for the biosorption

of heavy metals without a significant loss in the adsorption capacity. These biosorbents showed improved uptake of heavy metals [Pb(II), Cd(II), Cu(II) and Zn(II) ions can be further investigated under continuous flow conditions for real wastewater. The following recommendation can be made for the future study:

- A pilot-scale column with the developed biosorbent can be conducted for real wastewater.
- As the sole biosorbent showed preference to certain metals, a combined biosorbent with more than one biosorbent could be evaluated for removal of multimetals from wastewater.
- A suitable modification method for preparing the biosorbents can be considered to obtain maximum removal of heavy metals.
- The performance of removal of heavy metals along with organic pollutants can be evaluated by using the developed biosorbents.
- When the biosorbents mixed with water, organic carbon is dissolved and increased organic load in water. Thus, a biosorption system with a bioreactor could be explored for sustainable removals of pollutants (e.g. organic and nutrients) from wastewater.


**Faculty of Engineering and Information Technology**
**University of Technology, Sydney (UTS)**

# References

Abate, G., Masini, J.C. 2005. Influence of pH, ionic strength and humic acid on adsorption of Cd(II) and Pb(II) onto vermiculite. *Colloids and Surfaces a-Physicochemical and Engineering Aspects*, **262**(1-3), 33-39.

Abd El-Latif, M.M., Elkady, M.F. 2010. Equilibrium isotherms for harmful ions sorption using nano zirconium vanadate ion exchanger. *Desalination*, **255**(1-3), 21-43.

Abdel-Aty, A.M., Ammar, N.S., Abdel Ghafar, H.H., Ali, R.K. 2013. Biosorption of cadmium and lead from aqueous solution by fresh water alga Anabaena sphaerica biomass. *Journal of Advanced Research*, **4**(4), 367-374.

Abdel-Ghani, N.T., Elchaghaby, G.A. 2007. Influence of operating conditions on the removal of Cu(II), Zn(II), Cd(II) and Pb(II) ions from wastewater by adsorption. *International Journal of Environmental Science and Technology : (IJEST)*, **4**(4), 451-456.

Abia, A.A., Asuquo, E.D. 2006. Lead (II) and nickel (II) adsorption kinetics from aqueous metal solutions using chemically modified and unmodified agricultural adsorbents. *African Journal of Biotechnology*, **5**(16), 1475-1482.

Abia, A.A., Horsfall Jr, M., Didi, O. 2003. The use of chemically modified and unmodified cassava waste for the removal of Cd, Cu and Zn ions from aqueous solution. *Bioresource Technology*, **90**(3), 345-348.

Abo-El-Enein, S.A., Eissa, M.A., Diafullah, A.A., Rizk, M.A., Mohamed, F.M. 2009. Removal of some heavy metals ions from wastewater by copolymer of iron and aluminum impregnated with active silica derived from rice husk ash. *Journal of Hazardous Materials*, **172**(2-3), 574-579.

Abrego, J. 1997. Comparative evaluation of collectors for metal removal by precipitation/flotation. *Int. J. Environ. Pollut.*, **8**, 208.

Abu-Lail, L., Bergendahl, J.A., Thompson, R.W. 2012. Mathematical modeling of chloroform adsorption onto fixed‐bed columns of highly siliceous granular zeolites. *Environmental Progress and Sustainable Energy*, **31**(4), 591-596.

Achak, M., Hafidi, A., Ouazzani, N., Sayadi, S., Mandi, L. 2009. Low cost biosorbent "banana peel" for the removal of phenolic compounds from olive mill wastewater: Kinetic and equilibrium studies. *Journal of Hazardous Materials*, **166**(1), 117-125.

Acheampong, M.A., Pakshirajan, K., Annachhatre, A.P., Lens, P.N.L. 2013. Removal of Cu(II) by biosorption onto coconut shell in fixed-bed column systems. *Journal of Industrial and Engineering Chemistry*, **19**(3), 841-848.

Acheampong, M.A., Pereira, J.P., Meulepas, R.J., Lens, P.N. 2011. Biosorption of Cu (II) onto agricultural materials from tropical regions. *Journal of Chemical Technology and Biotechnology*, **86**(9), 1184-1194.

Adelaja, O.A., Amoo, I.A., Aderibigbe, A.D. 2011. Biosorption of Lead (II) ions from aqueous solution using Moringa oleifera pods. *Archives of Applied Science Research*, **3**(6), 50-60.

Adie, D.B., Olarinoye, N.O., Oke, I.A., Ismail, A., Lukman, S., Otun, J.A. 2010. Removal of Lead Ions from Aqueous Solutions Using Powdered Corn Cobs. *Canadian Journal of Chemical Engineering*, **88**(2), 241-255.

Agate, A.D. 2003. Bioremediation and biobeneficiation of metals. *New Horizons in Biotechnology*, 215-220.

Agrawal, A., Kumar, V., Pandey, B.D. 2006. Remediation options for the treatment of electroplating and leather tanning effluent containing chromium - A review. *Mineral Processing and Extractive Metallurgy Review*, **27**(2), 99-130.

Ahalya, N., Kanamadi, R.D., Ramachandra, T.V. 2006. Biosorption of iron(III) from aqueous solutions using the husk of Cicer arientinum. *Indian Journal of Chemical Technology*, **13**(2), 122-127.

Ahalya, N., Ramachandra, T., Kanamadi, R. 2003. Biosorption of heavy metals. *Res. J. Chem. Environ*, **7**(4), 71-79.

Aharoni, C., Tompkins, F.C. 1970. Kinetics of Adsorption and Desorption and the Elovich Equation. in: *Advances in Catalysis*, (Eds.) H.P. D.D. Eley, B.W. Paul, Vol. Volume 21, Academic Press, pp. 1-49.

Ahluwalia, S., Goyal, D. 2005. Removal of heavy metals by waste tea leaves from aqueous solution. *Engineering in Life Sciences*, **5**(2), 158-162.

Ahluwalia, S.S., Goyal, D. 2007. Microbial and plant derived biomass for removal of heavy metals from wastewater. *Bioresource Technology*, **98**(12), 2243-2257.

Ahmad, A., Ghufran, R., Faizal, W.M. 2010. Cd(II), Pb(II) and Zn(II) removal from contaminated water by biosorption using activated sludge biomass. *CLEAN–Soil, Air, Water*, **38**(2), 153-158.

Ahmad, A., Hameed, B. 2010. Fixed-bed adsorption of reactive azo dye onto granular activated carbon prepared from waste. *Journal of Hazardous Materials*, **175**(1), 298-303.

Ajmal, M., Rao, R.A.K., Ahmad, R., Ahmad, J. 2000. Adsorption studies on *Citrus reticulata* (fruit peel of orange): removal and recovery of Ni (II) from electroplating wastewater. *Journal of Hazardous Materials*, **79**(1), 117-131.

Ajmal, M., Rao, R.A.K., Ahmad, R., Ahmad, J., Rao, L.A.K. 2001. Removal and recovery of heavy metals from electroplating wastewater by using Kyanite as an adsorbent. *Journal of Hazardous Materials*, **87**(1-3), 127-137.

Akbar, S., Shah, T.H., Anwar, M., Khan, M. 2010. A Study of Cobalt Ions Removal from Aqueous Solutions by Sodium X-Zeolite. *Journal of the Chemical Society of Pakistan*, **32**(3), 331-337.

Akbar, S., Shah, T.H., Shahnaz, R., Sarwar, G. 2007. Thermal studies of synthetic NaX zeolite and its zinc exchanged forms. *Journal of the Chemical Society of Pakistan*, **29**(1), 5-11.

Akhtar, N., Saeed, A., Iqbal, M. 2003. *Chlorella sorokiniana* immobilized on the biomatrix of vegetable sponge of *Luffa cylindrica*: a new system to remove cadmium from contaminated aqueous medium. *Bioresource Technology*, **88**(2), 163-165.

Aksu, Z. 2001. Equilibrium and kinetic modelling of cadmium (II) biosorption by *C. vulgaris* in a batch system: effect of temperature. *Separation and Purification Technology*, **21**(3), 285-294.

Aksu, Z. 2002. Determination of the equilibrium, kinetic and thermodynamic parameters of the batch biosorption of nickel(II) ions onto Chlorella vulgaris. *Process Biochemistry*, **38**(1), 89-99.

Aksu, Z. 2005. Application of biosorption for the removal of organic pollutants: a review. *Process Biochemistry*, **40**(3–4), 997-1026.

Aksu, Z., Balibek, E. 2007. Chromium(VI) biosorption by dried Rhizopus arrhizus: Effect of salt (NaCl) concentration on equilibrium and kinetic parameters. *Journal of Hazardous Materials*, **145**(1-2), 210-220.

Aksu, Z., Dönmez, G. 2003. A comparative study on the biosorption characteristics of some yeasts for Remazol Blue reactive dye. *Chemosphere*, **50**(8), 1075-1083.

Aksu, Z., Gönen, F. 2004. Biosorption of phenol by immobilized activated sludge in a continuous packed bed: prediction of breakthrough curves. *Process Biochemistry*, **39**(5), 599-613.

Aksu, Z., Gonen, F. 2006. Binary biosorption of phenol and chromium(VI) onto immobilized activated sludge in a packed bed: Prediction of kinetic parameters and breakthrough curves. *Separation and Purification Technology*, **49**(3), 205-216.

Aksu, Z., Isoglu, I.A. 2005. Removal of copper(II) ions from aqueous solution by biosorption onto agricultural waste sugar beet pulp. *Process Biochemistry*, **40**(9), 3031-3044.

Aksu, Z., Kutsal, T. 1991. A Bioseparation Process for Removing Lead(Ii) Ions from Waste-Water by Using C-Vulgaris. *Journal of Chemical Technology and Biotechnology*, **52**(1), 109-118.

Albarelli, J.Q., Rabelo, R.B., Santos, D.T., Beppu, M.M., Meireles, M.A.A. 2011. Effects of supercritical carbon dioxide on waste banana peels for heavy metal removal. *The Journal of Supercritical Fluids*, **58**(3), 343-351.

Al-Degs, Y.S., El-Barghouthi, M.I., Issa, A.A., Khraisheh, M.A., Walker, G.M. 2006. Sorption of Zn(II), Pb(II), and Co(II) using natural sorbents: Equilibrium and kinetic studies. *Water Research*, **40**(14), 2645-2658.

Al-Degs, Y.S., Khraisheh, M.A.M., Allen, S.J., Ahmad, M.N. 2009. Adsorption characteristics of reactive dyes in columns of activated carbon. *Journal of Hazardous Materials*, **165**(1-3), 944-949.

Al-Duri, B., Robinson, E., McNerlan, S., Bailie, P. 1995. Hydrolysis of edible oils by lipases immobilized on hydrophobic supports: effects of internal support structure. *Journal of the American Oil Chemists' Society*, **72**(11), 1351-1359.

Algarra, M., Jiménez, M., Rodríguez-Castellón, E., Jiménez-López, A., Jiménez-Jiménez, J. 2005. Heavy metals removal from electroplating wastewater by aminopropyl-Si MCM-41. *Chemosphere*, **59**(6), 779-786.

Allen Jr, R.O., Clark, P.J. 1977. Fluorine in meteorites. *Geochimica Et Cosmochimica Acta*, **41**(5), 581-585.

Allen, S.J., Gan, Q., Matthews, R., Johnson, P.A. 2003. Comparison of optimised isotherm models for basic dye adsorption by kudzu. *Bioresource Technology*, **88**(2), 143-152.

Alluri, H.K., Ronda, S.R., Settalluri, V.S., Jayakumar Singh, B., Suryanarayana, V., Venkateshwar, P. 2007. Biosorption: An eco-friendly alternative for heavy metal removal. *African Journal of Biotechnology*, **6**(25), 2924-2931.

Al-Rub, F.A.A. 2006. Biosorption of zinc on palm tree leaves: Equilibrium, kinetics, and thermodynamics studies. *Separation Science and Technology*, **41**(15), 3499-3515.

Alslaibi, T.M., Abustan, I., Ahmad, M.A., Abu Foul, A. 2013. Preparation of Activated Carbon From Olive Stone Waste: Optimization Study on the Removal of Cu2+, $Cd^{2+}$, $Ni^{2+}$, $Pb^{2+}$, $Fe^{2+}$, and $Zn^{2+}$ From Aqueous Solution Using Response Surface Methodology. *Journal of Dispersion Science and Technology*, null-null.

Altenor, S., Carene, B., Emmanuel, E., Lambert, J., Ehrhardt, J.-J., Gaspard, S. 2009. Adsorption studies of methylene blue and phenol onto vetiver roots activated carbon prepared by chemical activation. *Journal of Hazardous Materials*, **165**(1), 1029-1039.

Al-Tohami, F., Ackacha, M.A., Belaid, R.A., Hamaadi, M. 2013. Adsorption of Zn(II) Ions from Aqueous Solutions by Novel Adsorbent: Ngella Sativa Seeds. *APCBEE Procedia*, **5**(0), 400-404.

Alvarez-Vazquez, H., Jefferson, B., Judd, S.J. 2004. Membrane bioreactors vs conventional biological treatment of landfill leachate: a brief review. *Journal of Chemical Technology and Biotechnology*, **79**(10), 1043-1049.

Amankwah, R.K., Yen, W.T. 2003. Biosorption of heavy metal ions from wastewater by Streptomyces viridosporus. *Hydrometallurgy 2003 Proceedings, Vols 1 and 2*, 1961-1969, 2031.

Amarasinghe, B.M.W.P.K., Williams, R.A. 2007. Tea waste as a low cost adsorbent for the removal of Cu and Pb from wastewater. *Chemical Engineering Journal*, **132**(1–3), 299-309.

Amuda, O., Alade, A. 2006. Coagulation/flocculation process in the treatment of abattoir wastewater. *Desalination*, **196**(1), 22-31.

Amuda, O., Amoo, I. 2007. Coagulation/flocculation process and sludge conditioning in beverage industrial wastewater treatment. *Journal of Hazardous Materials*, **141**(3), 778-783.

An, H.K., Park, B.Y., Kim, D.S. 2001. Crab shell for the removal of heavy metals from aqueous solution. *Water Research*, **35**(15), 3551-3556.

Anand, P., Etzel, J., Friedlaender, F. 1985. Heavy metals removal by high gradient magnetic separation. *Magnetics, IEEE Transactions on*, **21**(5), 2062-2064.

Anderson, C., Brooks, R., Stewart, R., Simcock, R., Robinson, B. 1999. The phytoremediation and phytomining of heavy metals. *Pacrim'99: International*

*Congress on Earth Science, Exploration and Mining around the Pacific Rim, Proceedings*, **99**(4), 127-135.

Angelidis, T., Fytianos, K., Vasilikiotics, G. 1989. Lead recovery from aqueous solution and wastewater by cementation utilising an iron rotating disc. *Resources, Conservation and Recycling*, **2**, 131-138.

Annadurai, G., Juang, R., Lee, D. 2003. Adsorption of heavy metals from water using banana and orange peels. *Water Science & Technology*, **47**(1), 185-190.

Annadurai, G., Juang, R.S., Lee, D.J. 2002. Adsorption of heavy metals from water using banana and orange peels,. *Water Science and Technology*, **47**(1), 185-190.

Annadurai, G., Juang, R.S., Lee, D.J. 2003. Adsorption of heavy metals from water using banana and orange peels. *Water Science and Technology*, **47**(1), 185-190.

Anwar, J., Shafique, U., Waheed uz, Z., Salman, M., Dar, A., Anwar, S. 2010. Removal of Pb(II) and Cd(II) from water by adsorption on peels of banana. *Bioresource Technology*, **101**(6), 1752-1755.

Apiratikul, R., Pavasant, P. 2006. Sorption isotherm model for binary component sorption of copper, cadmium, and lead ions using dried green macroalga, *Caulerpa lentillifera*. *Chemical Engineering Journal*, **119**(2), 135-145.

Apiratikul, R., Pavasant, P. 2008. Sorption of $Cu^{2+}$, $Cd^{2+}$, and $Pb^{2+}$ using modified zeolite from coal fly ash. *Chemical Engineering Journal*, **144**(2), 245-258.

Arain, M.B., Kazi, T.G., Jamali, M.K., Jalbani, N., Afridi, H.I., Baig, J.A. 2008. Speciation of heavy metals in sediment by conventional, ultrasound and microwave assisted single extraction methods: a comparison with modified sequential extraction procedure. *Journal of Hazardous Materials*, **154**(1), 998-1006.

Areco, M.M., Hanela, S., Duran, J., dos Santos Afonso, M. 2012. Biosorption of Cu(II), Zn(II), Cd(II) and Pb(II) by dead biomasses of green alga Ulva lactuca and the development of a sustainable matrix for adsorption implementation. *Journal of Hazardous Materials*, **213–214**(0), 123-132.

Areco, M.M., Saleh-Medina, L., Trinelli, M.A., Marco-Brown, J.L., dos Santos Afonso, M. 2013. Adsorption of Cu(II), Zn(II), Cd(II) and Pb(II) by dead Avena fatua biomass and the effect of these metals on their growth. *Colloids and Surfaces B: Biointerfaces*, **110**(0), 305-312.

Argun, M.E., Dursun, S., Gur, K., Ozdemir, C., Karatas, M., Dogan, S. 2005. Adsorption of copper on modified wood (pine) materials. *Cellulose Chemistry and Technology*, **39**(5-6), 581-591.

Arias, M., Perez-Novo, C., Osorio, F., Lopez, E., Soto, B. 2005. Adsorption and desorption of copper and zinc in the surface layer of acid soils. *Journal of Colloid and Interface Science*, **288**(1), 21-29.

Arpa, C., Basyilmaz, E., Bektas, S., Genc, O., Yurum, Y. 2000. Cation exchange properties of low rank Turkish coals: removal of Hg(II), Cd(II) and Pb(II) from waste water. *Fuel Processing Technology*, **68**(2), 111-120.

Arshad, M., Zafar, M.N., Younis, S., Nadeem, R. 2008. The use of Neem biomass for the biosorption of zinc from aqueous solutions. *Journal of Hazardous Materials*, **157**(2–3), 534-540.

Artola, A., Martin, M., Balaguer, M.D., Rigola, M. 2000. Isotherm model analysis for the adsorption of Cd(II), Cu(II), Ni(II), and Zn(II) on anaerobically digested sludge. *Journal of Colloid and Interface Science*, **232**(1), 64-70.

Asadi, F., Shariatmadari, H., Mirghaffari, N. 2008. Modification of rice hull and sawdust sorptive characteristics for remove heavy metals from synthetic solutions and wastewater. *Journal of Hazardous Materials*, **154**(1–3), 451-458.

Asci, Y., Nurbas, M., Acikel, Y.S. 2007. Sorption of Cd(II) onto kaolin as a soil component and desorption of Cd(II) from kaolin using rhamnolipid biosurfactant. *Journal of Hazardous Materials*, **139**(1), 50-56.

Astier, C., Chaleix, V., Faugeron, C., Ropartz, D., Krausz, P., Gloaguen, V. 2012. Biosorption of lead (ii) on modified barks explained by the hard and soft acids and bases (HSAB) theory. *Bioresources*, **7**(1), 1100-1110.

ATSDR. 1990. Syracuse Research Corporation Agency for Toxic Substances and Disease Registry.

Avrami, M. 1939. Kinetics of phase change. I General theory. *The Journal of Chemical Physics*, **7**, 1103.

Aydin, H., Buluta, Y., Yerlikaya, C. 2008. Removal of copper (II) from aqueous solution by adsorption onto low-cost adsorbents. *Journal of Environmental Management*, **87**(1), 37-45.

Babaei, H., Kheirandish, R., Ebrahimi, L. 2012. The effects of copper toxicity on histopathological and morphometrical changes of the rat testes. *Asian Pacific Journal of Tropical Biomedicine*, **2**(3, Supplement), S1615-S1619.

Babel, S., Kurniawan, T.A. 2003. Low-cost adsorbents for heavy metals uptake from contaminated water: a review. *Journal of Hazardous Materials*, **97**(1-3), 219-243.

Babel, S., Kurniawan, T.A. 2003. Low-cost adsorbents for heavy metals uptake from contaminated water: a review. *Journal of Hazardous Materials*, **97**(1-3), 219-243.

Bae, J.W., Rhee, S.K., Kim, I.S., Hyun, S.H., Lee, S.T. 2002. Increased microbial resistance to toxic wastewater by sludge granulation in upflow anaerobic sludge blanket reactor. *Journal of Microbiology and Biotechnology*, **12**(6), 901-908.

Baek, N., Shin, U., Yoon, J. 2005. A study on the design and analysis of a heat pump heating system using wastewater as a heat source. *Solar Energy*, **78**(3), 427-440.

Bailey, S.E., Olin, T.J., Bricka, R.M., Adrian, D.D. 1999. A review of potentially low-cost sorbents for heavy metals. *Water Research*, **33**(11), 2469-2479.

Baker, E.L., Feldman, R.G., White, R.A., Harley, J.P., Niles, C.A., Dinse, G.E., Berkey, C.S. 1984. Occupational lead neurotoxicity: A behavioral and electrophysiological evaluation. Study design and year one result. *British journal of industrial medicine*, **41**(3), 352-361.

Baker, E.L., Feldman, R.G., White, R.A., Harley, J.P., Niles, C.A., Dinse, G.E., Berkey, C.S. 1984. Occupational lead neurotoxicity: A behavioral and electrophysiological evaluation. Study design and year one result. *British journal of industrial medicine*, **41**(3), 352-361.

Baker, J.R., Satarug, S., Edwards, R.J., Moore, M.R., Williams, D.J., Reilly, P.E.B. 2003. Potential for early involvement of CYP isoforms in aspects of human cadmium toxicity. *Toxicology Letters*, **137**(1–2), 85-93.

Baker, R.J., McCabe, T., O'Brien, J.E., Ogilvie, H.V. 2010. Thermomorphic metal scavengers: A synthetic and multinuclear NMR study of highly fluorinated ketones and their application in heavy metal removal. *Journal of Fluorine Chemistry*, **131**(5), 621-626.

Baker, R.J., McCabe, T., O'Brien, J.E., Ogilvie, H.V. 2010. Thermomorphic metal scavengers: A synthetic and multinuclear NMR study of highly fluorinated ketones and their application in heavy metal removal. *Journal of Fluorine Chemistry*, **131**(5), 621-626.

Bang Mo, K. 1984. Membrane-based solvent extraction for selective removal and recovery of metals. *Journal of Membrane Science*, **21**(1), 5-19.

Baral, S.S., Das, N., Ramulu, T.S., Sahoo, S.K., Das, S.N., Chaudhury, G.R. 2009. Removal of Cr(VI) by thermally activated weed Salvinia cucullata in a fixed-bed column. *Journal of Hazardous Materials*, **161**(2-3), 1427-1435.

Barka, N., Abdennouri, M., El Makhfouk, M., Qourzal, S. 2013. Biosorption characteristics of cadmium and lead onto eco-friendly dried cactus (Opuntia ficus indica) cladodes. *Journal of Environmental Chemical Engineering*, **1**(3), 144-149.

Barriada, J.L., Caridad, S., Lodeiro, P., Herrero, R., de Vicente, M.E.S. 2009. Physicochemical characterisation of the ubiquitous bracken fern as useful biomaterial for preconcentration of heavy metals. *Bioresource Technology*, **100**(4), 1561-1567.

Barros, M.A.S.D., Arroyo, P.A., Sousa-Aguiar, E.F., Tavares, C.R.G. 2004. Thermodynamics of the exchange processes between $K^+$, $Ca^{2+}$ and $Cr^{3+}$ in zeolite NaA. *Adsorption-Journal of the International Adsorption Society*, **10**(3), 227-235.

Basso, M.C., Cerrella, E.G., Cukierman, A.L. 2002. Lignocellulosic Materials as Potential Biosorbents of Trace Toxic Metals from Wastewater. *Industrial & Engineering Chemistry Research*, **41**(15), 3580-3585.

Basso, M.C., Cukierman, A.L. 2008. Biosorption performance of red and green marine macroalgae for removal of trace cadmium and nickel from wastewater. *International Journal of Environment and Pollution*, **34**(1-4), 340-352.

Battistoni, P., Fava, G., Ruello, M.L. 1993. Heavy-Metal Shock Load in Activated-Sludge Uptake and Toxic Effects. *Water Research*, **27**(5), 821-827.

Bayramoglu, G., Arica, M.Y. 2008. Adsorption of Cr(VI) onto PEI immobilized acrylate-based magnetic beads: Isotherms, kinetics and thermodynamics study. *Chemical Engineering Journal*, **139**(1), 20-28.

Bayramoglu, G., Bektas, S., Arica, M.Y. 2003. Biosorption of heavy metal ions on immobilized white-rot fungus Trametes versicolor. *Journal of Hazardous Materials*, **101**(3), 285-300.

Beaty, R.D., Kerber, J.D. 1978. *Concepts, instrumentation and techniques in atomic absorption spectrophotometry,* Perkin-Elmer USA.

Behnamfard, A., Salarirad, M.M. 2009. Equilibrium and kinetic studies on free cyanide adsorption from aqueous solution by activated carbon. *Journal of Hazardous Materials*, **170**(1), 127-133.

Belfort, G. 1984. *Synthetic Membrane Process: Fundamentals and Water Applications*. Access Online via Elsevier.

Ben Hamissa, A.M., Lodi, A., Seffen, M., Finocchio, E., Botter, R., Converti, A. 2010. Sorption of Cd(II) and Pb(II) from aqueous solutions onto Agave americana fibers. *Chemical Engineering Journal*, **159**(1-3), 67-74.

Benhammou, A., Yaacoubi, A., Nibou, L., Tanouti, B. 2005. Adsorption of metal ions onto Moroccan stevensite: kinetic and isotherm studies. *Journal of Colloid and Interface Science*, **282**(2), 320-326.

Beveridge, T.J., Murray, R.G.E. 1980. Sites of metal deposition in the cell wall of Bacillus subtilis. *Journal of Bacteriology*, **141**(2), 876-887.

Bhattacharya, A., et al., Mandal, S., Das, S. 2006. Adsorption of Zn (II) from aqueous solution by using different adsorbents. *Chemical Engineering Journal*, **123**(1), 43-51.

Bhattacharyya, K.G., Gupta, S.S. 2006. Kaolinite, montmorillonite, and their modified derivatives as adsorbents for removal of Cu(II) from aqueous solution. *Separation and Purification Technology*, **50**(3), 388-397.

Bhogal, A., Nicholson, F., Chambers, B., Shepherd, M. 2003. Effects of past sewage sludge additions on heavy metal availability in light textured soils: implications for crop yields and metal uptakes. *Environmental Pollution*, **121**(3), 413-423.

Blanco, A., Sanz, B., Llama, M.J., Serra, J.L. 1999. Biosorption of heavy metals to immobilised Phormidium laminosum biomass. *Journal of Biotechnology*, **69**(2-3), 227-240.

Blazquez, G., Calero, M., Hernainz, F., Tenorio, G., Martin-Lara, M.A. 2010. Equilibrium biosorption of lead(II) from aqueous solutions by solid waste from olive-oil production. *Chemical Engineering Journal*, **160**(2), 615-622.

Blazquez, G., Calero, M., Hernainz, F., Tenorio, G., Martin-Lara, M.A. 2010. Equilibrium biosorption of lead(II) from aqueous solutions by solid waste from olive-oil production. *Chemical Engineering Journal*, **160**(2), 615-622.

Blázquez, G., Martín-Lara, M.A., Tenorio, G., Calero, M. 2011. Batch biosorption of lead(II) from aqueous solutions by olive tree pruning waste: Equilibrium,

kinetics and thermodynamic study. *Chemical Engineering Journal*, **168**(1), 170-177.

Bloom, H., Ayling, G. 1977. Heavy metals in the Derwent Estuary. *Environmental Geology*, **2**(1), 3-22.

Bohart, G., Adams, E. 1920. Some aspects of the behavior of charcoal with respect to chlorine. 1. *Journal of the American Chemical Society*, **42**(3), 523-544.

Bohart, G.S. 1920. Some aspects of the behavior of charcoal with respect to chlorine. *Journal of the American Chemical Society*, **42**(3), 523-543.

Boller, M. 1997. Tracking heavy metals reveals sustainability deficits of urban drainage systems. *Water Science and Technology*, **35**(9), 77-87.

Boota, R., Bhatti, H.N., Hanif, M.A. 2009. Removal of Cu(II) and Zn(II) Using Lignocellulosic Fiber Derived from Citrus reticulata (Kinnow) Waste Biomass. *Separation Science and Technology*, **44**(16), 4000-4022.

Borrego, A., Gonzalez-Doncel, G. 1998. Analysis of the precipitation behavior in aluminum matrix composites from a Johnson-Mehl-Avrami kinetic model. *Mat. Sci. Eng. A*, **252**, 149-152.

Bremner, I. 1974. Heavy metal toxicities. *Quarterly reviews of biophysics*, **7**(01), 75-124.

Brewer, G.J. 2007. Iron and copper toxicity in diseases of aging, particularly atherosclerosis and Alzheimer's disease. *Expermental Biol. Med.*, **232**(2), 323-35.

Brewer, G.J. 2010. Copper toxicity in the general population. *Clin Neurophysiol.*, **121**(4), 459-60.

Bricka, R.M., Hill, D.O. 1989. Metal immobilization by solidification of hydroxide and xanthate sludges. In Environmental Aspects of Stabilization and Solidification of Hazardous and Radioactive Wastes. *American Society for Testing and Materials (ASTM) STP 1033, eds., Philadelphia*, 257-272.

Brower, J.B., Ryan, R.L., Pazirandeh, M. 1997. Comparison of ion-exchange resins and biosorbents for the removal of heavy metals from plating factory wastewater. *Environmental Science and Technology*, **31**(10), 2910-2914.

Brown, P., Atly Jefcoat, I., Parrish, D., Gill, S., Graham, E. 2000. Evaluation of the adsorptive capacity of peanut hull pellets for heavy metals in solution. *Advances in Environmental Research*, **4**(1), 19-29.

Brown, P., Gill, S., Allen, S. 2000. Metal removal from wastewater using peat. *Water Research*, **34**(16), 3907-3916.

Brunauer, S., Emmett, P.H., Teller, E. 1938. Adsorption of Gases in Multimolecular Layers. *Journal of the American Chemical Society*, **60**(2), 309-319.

Buasri, A., Chaiyut, N., Tapang, K., Jaroensin, S., Panphrom, S. 2012. Equilibrium and Kinetic Studies of Biosorption of Zn(II) Ions from Wastewater Using Modified Corn Cob. *APCBEE Procedia*, **3**(0), 60-64.

Bucio, L., Souza, V., Albores, A., Sierra, A., Chávez, E., Cárabez, A., Gutiérrez-Ruiz, M.C. 1995. Cadmium and mercury toxicity in a human fetal hepatic cell line (WRL-68 cells). *Toxicology*, **102**(3), 285-299.

Bulgariu, D., Bulgariu, L. 2012. Equilibrium and kinetics studies of heavy metal ions biosorption on green algae waste biomass. *Bioresource Technology*, **103**(1), 489-493.

Bulut, Y., Tez, Z. 2007. Adsorption studies on ground shells of hazelnut and almond. *Journal of Hazardous Materials*, **149**(1), 35-41.

Burger, J., Gochfeld, M. 2004. Marine Birds as Sentinels of Environmental Pollution. *EcoHealth*, **1**(3), 263-274.

Caeiro, S., Costa, M., Ramos, T., Fernandes, F., Silveira, N., Coimbra, A., Medeiros, G., Painho, M. 2005. Assessing heavy metal contamination in Sado Estuary sediment: an index analysis approach. *Ecological indicators*, **5**(2), 151-169.

Cai, P., Zheng, H., Wang, C., Ma, H., Hu, J., Pu, Y., Liang, P. 2012. Competitive adsorption characteristics of fluoride and phosphate on calcined Mg-Al-$CO_3$ layered double hydroxides. *Journal of Hazardous Materials*, **213–214**(0), 100-108.

Campos, J., Martinez-Pacheco, M., Cervantes, C. 1995. Hexavalent-chromium reduction by a chromate-resistant Bacillus sp. strain. *Antonie van Leeuwenhoek*, **68**(3), 203-208.

Cañizares, P., Pérez, Á., Camarillo, R. 2002. Recovery of heavy metals by means of ultrafiltration with water-soluble polymers: calculation of design parameters. *Desalination*, **144**(1), 279-285.

Caramalau, C., Bulgariu, L., Macoveanu, M. 2009. Adsorption characteristics of Co(II) ions from aqueous solutions on romanian peat moss. *Environmental Engineering and Management Journal*, **8**(5), 1089-1095.

Case, O.P. 1974. Metallic recovery from wastewaters utilising cementation. *EPA-270/2-74-008, U.S. Washington DC*

Caspers, H. 1981. U. Förstner and G. T. W. Wittmann: Metal Pollution in the Aquatic Environment. With Contributions by F. Prosi an J.H. van Lierde. — With 102 figs., 94 ab., 486 pp. Berlin-Heidelberg-New York: Springer-Verlag 1979. ISBN -540 (Berlin) 0-387 (New York) -09307-9 DM 98, US $ 53.90. *Internationale Revue der gesamten Hydrobiologie und Hydrographie*, **66**(2), 277-277.

Caspers, H. 1985. Wim Salomons and Ulrich Förstner: Metals in the Hydrocycle.–With 149 figs, 359 pp. Berlin/New York: Springer Verlag 1984. ISBN 3-540 (Berlin) 0-387 (New York) 12755–0. DM 98, $ 36.60. *Internationale Revue der gesamten Hydrobiologie und Hydrographie*, **70**(6), 876-876.

Castro-González, M.I., Méndez-Armenta, M. 2008. Heavy metals: Implications associated to fish consumption. *Environmental Toxicology and Pharmacology*, **26**(3), 263-271.

Cayllahua, J.E.B., Torem, M.L. 2010. Biosorption of aluminum ions onto Rhodococcus opacus from wastewaters. *Chemical Engineering Journal*, **161**(1-2), 1-8.

Cestari, A.R., Vieira, E.F., Lopes, E.C., da Silva, R.G. 2004. Kinetics and equilibrium parameters of Hg (II) adsorption on silica–dithizone. *Journal of Colloid and Interface Science*, **272**(2), 271-276.

Çetinkaya Dönmez, G., Aksu, Z., Öztürk, A., Kutsal, T. 1999. A comparative study on heavy metal biosorption characteristics of some algae. *Process Biochemistry*, **34**(9), 885-892.

Chakravarty, S., Mohanty, A., Sudha, T.N., Upadhyay, A.K., Konar, J., Sircar, J.K., Madhukar, A., Gupta, K.K. 2010. Removal of Pb(II) ions from aqueous solution by adsorption using bael leaves (Aegle marmelos). *Journal of Hazardous Materials*, **173**(1-3), 502-509.

Chandra Sekhar, K., Kamala, C., Chary, N., Anjaneyulu, Y. 2003. Removal of heavy metals using a plant biomass with reference to environmental control. *International Journal of Mineral Processing*, **68**(1), 37-45.

Chang, A., Page, A., Warneke, J. 1987. Long-term sludge applications on cadmium and zinc accumulation in Swiss chard and radish. *Journal of Environmental Quality*, **16**(3), 217-221.

Chang, M., McBroom, M.W., Scott Beasley, R. 2004. Roofing as a source of nonpoint water pollution. *Journal of Environmental Management*, **73**(4), 307-315.

Chao, Y.-M., Liang, T. 2008. A feasibility study of industrial wastewater recovery using electrodialysis reversal. *Desalination*, **221**(1), 433-439.

Charerntanyarak, L. 1999. Heavy metals removal by chemical coagulation and precipitation. *Water Science and Technology*, **39**(10), 135-138.

Chaufer, B., Deratani, A. 1988. Removal of metal ions by complexation-ultrafiltration using water-soluble macromolecules: Perspective of application to wastewater treatment. *Nuclear and chemical waste management*, **8**(3), 175-187.

Chehregani, A., Noori, M., Yazdi, H.L. 2009. Phytoremediation of heavy-metal-polluted soils: Screening for new accumulator plants in Angouran mine (Iran) and evaluation of removal ability. *Ecotoxicology and Environmental Safety*, **72**(5), 1349-1353.

Chen, B.-Y., Utgikar, V.P., Harmon, S.M., Tabak, H.H., Bishop, D.F., Govind, R. 2000. Studies on biosorption of zinc (II) and copper (II) on *Desulfovibrio desulfuricans*. *International Biodeterioration and Biodegradation*, **46**(1), 11-18.

Chen, C.Y., Yang, C.Y., Chen, A.H. 2011a. Biosorption of Cu(II), Zn(II), Ni(II) and Pb(II) ions by cross-linked metal-imprinted chitosans with epichlorohydrin. *Journal of Environmental Management*, **92**(3), 796-802.

Chen, G. 2004. Electrochemical technologies in wastewater treatment. *Separation and Purification Technology*, **38**(1), 11-41.

Chen, G.Q., Zhang, W. J., Zeng, G. M., Huang, J. H., Wang, L., Shen, G. L. 2011b. Surface-modified *Phanerochaete chrysosporium* as a biosorbent for Cr (VI)-contaminated wastewater. *Journal of Hazardous Materials*, **186**(2), 2138-2143.

Chen, L., Lü, L., Shao, W., Luo, F. 2011. Kinetics and equilibria of Cd(II) adsorption onto a chemically modified lawny grass with H [BTMPP]. *Journal of Chemical and Engineering Data*, **56**(4), 1059-1068.

Chen, S., Ding, C., Han, Y., Fang, Y., Chen, Y. 2012. Study on information fusion algorithm for the miniature AHRS. pp. 114-117.

Cheng, R., Ou, S., Li, M., Li, Y., Xiang, B. 2009. Ethylenediamine modified starch as biosorbent for acid dyes. *Journal of Hazardous Materials*, **172**(2), 1665-1670.

Cheung, C.W., Ko, D.C.K., Porter, J.F., McKay, G. 2003. Binary metal sorption on bone char mass transport model using LAST. *Langmuir*, **19**(10), 4144-4153.

Cheung, C.W., Porter, J.F., McKay, G. 2000. Sorption kinetics for the removal of copper and zinc from effluents using bone char. *Separation and Purification Technology*, **19**(1-2), 55-64.

Chien, S.H., Clayton, W.R. 1980. W. R. Application of Elovich equation to the kinnetcs of phosphate release and sorption on solids. *Soil Sci Am J*, **4**, 265-268.

Choi, M.H., Ji, G.E., Koh, K.H., Ryu, Y.W., Jo, D.H., Park, Y.H. 2002. Use of waste Chinese cabbage as a substrate for yeast biomass production. *Bioresource Technology*, **83**(3), 251-253.

Choi, S.B., Yun, Y.S. 2006. Biosorption of cadmium by various types of dried sludge: An equilibrium study and investigation of mechanisms. *Journal of Hazardous Materials*, **138**(2), 378-383.

Chojnacka, K., Chojnacki, A., Górecka, H. 2005. Biosorption of $Cr^{3+}$, $Cd^{2+}$ and $Cu^{2+}$ ions by blue–green algae *Spirulina sp.*: kinetics, equilibrium and the mechanism of the process. *Chemosphere*, **59**(1), 75-84.

Chong, K.H., Volesky, B. 1995. Description of 2-Metal Biosorption Equilibria by Langmuir-Type Models. *Biotechnology and Bioengineering*, **47**(4), 451-460.

Chu, G.Y., Kim, T.Y., Cho, S.Y., Kang, Y., Kim, S.D., Kim, S.J. 2004. Adsorption characteristics of zinc-cyanide complexes by waste brewery biomass. *Journal of Industrial and Engineering Chemistry*, **10**(4), 551-557.

Chu, K.H., Hashim, M.A., Ng, P.C., Chong, M.T. 2000. Palm oil fuel ash as an adsorbent for heavy metals. *Adsorption Science and Technology*, **2**, 154-158.

Chubar, N., Carvalho, J.R., Correia, M.J.N. 2003. Cork biomass as biosorbent for Cu(II), Zn(II) and Ni(II). *Colloids and Surfaces a-Physicochemical and Engineering Aspects*, **230**(1-3), 57-65.

Clark, R.M. 1987. Evaluating the cost and performance of field-scale granular activated carbon systems. *Environmental Science and Technology*, **21**(6), 573-580.

Clayton, W., Chien, S. 1980. Application of Elovich equation to the kinetics of phosphate release and sorption in soils. *Soil Science Society of America Journal*, **44**(2), 265-268.

Clements, W.H., Vieira, N.K.M., Church, S.E. 2010. Quantifying restoration success and recovery in a metal-polluted stream: a 17-year assessment of physicochemical and biological responses. *Journal of Applied Ecology*, **47**(4), 899-910.

Cochrane, E.L., Lu, S., Gibb, S.W., Villaescusa, I. 2006. A comparison of low-cost biosorbents and commercial sorbents for the removal of copper from aqueous media. *Journal of Hazardous Materials*, **137**(1), 198-206.

Çolak, F., Atar, N., Yazıcıoğlu, D., Olgun, A. 2011. Biosorption of lead from aqueous solutions by Bacillus strains possessing heavy-metal resistance. *Chemical Engineering Journal*, **173**(2), 422-428.

Conrad, K., Bruun Hansen, H.C. 2007. Sorption of zinc and lead on coir. *Bioresource Technology*, **98**(1), 89-97.

Cruver, J., Nusbaum, I. 1974. Application of reverse osmosis to wastewater treatment. *Journal (Water Pollution Control Federation)*, 301-311.

Cushnie, J.G.C. 1985. Electroplating wastewater pollution control technology. *Noyes publications*, 152-219.

Dabrowski, A., Hubicki, Z., Podkościelny, P., Robens, E. 2004. Selective removal of the heavy metal ions from waters and industrial wastewaters by ion-exchange method. *Chemosphere*, **56**(2), 91-106.

Dakiky, M., Khamis, M., Manassra, A., Mer'eb, M. 2002. Selective adsorption of chromium(VI) in industrial wastewater using low-cost abundantly available adsorbents. *Advances in Environmental Research*, **6**(4), 533-540.

Das, A., Ghosh, U. 2009. Solid-state fermentation of waste cabbage by Penicillium Notatum NCIM NO-923 for production and Characterization of cellulases. *Journal of Scientific & Industrial Research*, **68**, 714-718.

Das, N., Vimala, R., Karthika, P. 2008. Biosorption of heavy metals - An overview. *Indian Journal of Biotechnology*, **7**(2), 159-169.

Davis, A.P., Upadhyaya, M. 1996. Desorption of cadmium from goethite (α-FeOOH). *Water Research*, **30**(8), 1894-1904.

Davis, T.A., Volesky, B., Mucci, A. 2003. A review of the biochemistry of heavy metal biosorption by brown algae. *Water Research*, **37**(18), 4311-4330.

de Rome, L., Gadd, G.M. 1987. Copper adsorption by Rhizopus arrhizus, Cladosporium resinae and Penicillium italicum. *Applied Microbiology and Biotechnology*, **26**(1), 84-90.

Dean, J.G., Bosqui, F.L., Lanouette, K.H. 1972. Removing heavy metals from waste water. *Environmental Science and Technology*, **6**(6), 518-522.

Demirbas, A. 2000. Biomass resources for energy and chemical industry. *Energy Edu. Sci. Technol.*, **5** 21-45.

Demirbas, A. 2004. Adsorption of lead and cadmium ions in aqueous solutions onto modified lignin from alkali glycerol delignication. *Journal of Hazardous Materials*, **109**(1-3), 221-226.

Demirbas, A. 2008. Heavy metal adsorption onto agro-based waste materials: A review. *Journal of Hazardous Materials*, **157**(2-3), 220-229.

Demirbas, A. 2009. Agricultural based activated carbons for the removal of dyes from aqueous solutions: A review. *Journal of Hazardous Materials*, **167**(1-3), 1-9.

Demirbas, E., Dizge, N., Sulak, M.T., Kobya, M. 2009. Adsorption kinetics and equilibrium of copper from aqueous solutions using hazelnut shell activated carbon. *Chemical Engineering Journal*, **148**(2-3), 480-487.

Demirbas, E., Kobya, M., Senturk, E., Ozkan, T. 2004. Adsorption kinetics for the removal of chromium(VI) from aqueous solutions on the activated carbons prepared from agricultural wastes. *Water S. A.*, **30**(4), 533-540.

Derome, L., Gadd, G.M. 1991. Use of Pelleted and Immobilized Yeast and Fungal Biomass for Heavy-Metal and Radionuclide Recovery. *Journal of Industrial Microbiology*, **7**(2), 97-104.

Dias, N.L., do Carmo, D.R. 2006. Study of an organically modified clay: Selective adsorption of heavy metal ions and voltammetric determination of mercury(II). *Talanta*, **68**(3), 919-927.

Diaz, E., Ordóñez, S., Vega, A., Coca, J. 2005. Comparison of adsorption properties of a chemically activated and a steam-activated carbon, using inverse gas chromatography. *Microporous and Mesoporous Materials*, **82**(1-2), 173-181.

Díaz, S., Martín-González, A., Carlos Gutiérrez, J. 2006. Evaluation of heavy metal acute toxicity and bioaccumulation in soil ciliated protozoa. *Environment International*, **32**(6), 711-717.

Diniz, V., Volesky, B. 2005. Biosorption of La, Eu and Yb using *Sargassum* biomass. *Water Research*, **39**(1), 239-247.

Do Duong, D. 1998. *Absorption Analysis: Equilibria and Kinetics*. Imperial College Pr.

Dogar, C., Gurses, A., Acikyildiz, M., Ozkan, E. 2010. Thermodynamics and kinetic studies of biosorption of a basic dye from aqueous solution using green algae Ulothrix sp. *Colloids and Surfaces B-Biointerfaces*, **76**(1), 279-285.

Dos Santos, V.C.G., Tarley, C.R.T., Caetano, J., Dragunski, D.C. 2010. Assessment of chemically modified sugarcane bagasse for lead adsorption from aqueous medium. *Water Science and Technology*, **62**(2), 457-465.

Drake, L.R., Rayson, G.D. 1996. Peer Reviewed: Plant-Derived Materials for Metal Ion-Selective Binding and Preconcentration. *Analytical Chemistry*, **68**(1), 22A-27A.

Dubinin, M., Radushkevich, L. 1947. Equation of the characteristic curve of activated charcoal. *Chem. Zentr*, **1**(1), 875.

Dupont, L., Bouanda, J., Dumonceau, J., Aplincourt, M. 2005. Biosorption of Cu(II) and Zn(II) onto a lignocellulosic substrate extracted from wheat bran. *Environmental Chemistry Letters*, **2**(4), 165-168.

Ebau, W., Rawi, C.S.M., Din, Z., Al-Shami, S.A. 2012. Toxicity of cadmium and lead on tropical midge larvae, Chironomus kiiensis Tokunaga and Chironomus javanus Kieffer (Diptera: Chironomidae). *Asian Pacific Journal of Tropical Biomedicine*, **2**(8), 631-634.

Eccles, H. 1995. Removal of heavy metals from effluent streams—Why select a biological process? *International Biodeterioration and Biodegradation*, **35**(1), 5-16.

Ehrlich, H.L. 1997. Microbes and metals. *Applied Microbiology and Biotechnology*, **48**(6), 687-692.

El-Ashtoukhy, E.S.Z., Amin, N.K., Abdelwahab, O. 2008. Removal of lead (II) and copper (II) from aqueous solution using pomegranate peel as a new adsorbent. *Desalination*, **223**(1–3), 162-173.

El-Bayaa, A.A., Badawy, N.A., AlKhalik, E.A. 2009. Effect of ionic strength on the adsorption of copper and chromium ions by vermiculite pure clay mineral. *Journal of Hazardous Materials*, **170**(2-3), 1204-1209.

Erdem, E., Karapinar, N., Donat, R. 2004. The removal of heavy metal cations by natural zeolites. *Journal of Colloid and Interface Science*, **280**(2), 309-314.

Faller, P. 2009. Copper and zinc binding to amyloid-beta: coordination, dynamics, aggregation, reactivity and metal-ion transfer. *Chembiochem.*, **10**(18), 2837-45.

Farajzadeh, M.A., Monji, A.B. 2004. Adsorption characteristics of wheat bran towards heavy metal cations. *Separation and Purification Technology*, **38**(3), 197-207.

Febrianto, J., Kosasih, A.N., Sunarso, J., Ju, Y.-H., Indraswati, N., Ismadji, S. 2009. Equilibrium and kinetic studies in adsorption of heavy metals using biosorbent: A summary of recent studies. *Journal of Hazardous Materials*, **162**(2–3), 616-645.

Feng, N., Guo, X., Liang, S., Zhu, Y., Liu, J. 2011. Biosorption of heavy metals from aqueous solutions by chemically modified orange peel. *Journal of Hazardous Materials*, **185**(1), 49-54.

Feng, N., Zhang, F. 2013. Untreated Chinese Ephedra Residue as Biosorbents for the Removal of $Pb^{2+}$ Ions from Aqueous Solutions. *Procedia Environmental Sciences*, **18**(0), 794-799.

Fiol, N., Villaescusa, I., Martínez, M., Miralles, N., Poch, J., Serarols, J. 2006. Sorption of Pb(II), Ni(II), Cu(II) and Cd(II) from aqueous solution by olive stone waste. *Separation and Purification Technology*, **50**(1), 132-140.

Flemming, C.A., Trevors, J.T. 1989. Copper toxicity and chemistry in the environment: a review. *Water, Air, andamp; Soil Pollution*, **44**(1), 143-158.

Flynn, C.M.J., Carnahan, T.G., Lindstrom, R.E. 1980. Adsorption of heavy metal ions by xanthated sawdust. *Report of Investigations # 8427, United States Bureau of Mines*.

Foo, K.Y., Hameed, B.H. 2010. Insights into the modeling of adsorption isotherm systems. *Chemical Engineering Journal*, **156**(1), 2-10.

Foulkes, E. 2000. Transport of toxic heavy metals across cell membranes. *Proceedings of the Society for Experimental Biology and Medicine*, **223**(3), 234-240.

Fourest, E., Roux, J.C. 1992. Heavy metal biosorption by fungal mycelial by-product: mechanisms and influence of pH. *Applied Microbiology and Biotechnology*, **37**(3), 399-403.

Fourest, E., Roux, J.C. 1992. Heavy metal biosorption by fungal mycelial by-products: Mechanisms and influence of pH. *Applied Microbiology and Biotechnology*, **37**(3), 399-403.

Fowler, B.A. 2009. Monitoring of human populations for early markers of cadmium toxicity: A review. *Toxicology and Applied Pharmacology*, **238**(3), 294-300.

Freundlich, H. 1906. Adsorption in solution. *Phys. Chem.*, **57**, 384-410.

Friis, N., Myers-Keith, P. 1986. Biosorption of uranium and lead by Streptomyces longwoodensis. *Biotechnology and Bioengineering*, **28**(1), 21-28.

Fritzmann, C., Löwenberg, J., Wintgens, T., Melin, T. 2007. State-of-the-art of reverse osmosis desalination. *Desalination*, **216**(1), 1-76.

Fu, F., Wang, Q. 2011. Removal of heavy metal ions from wastewaters: A review. *Journal of Environmental Management*, **92**(3), 407-418.

Fukuoka, S., Kida, T., Nakajima, Y., Tsumagari, T., Watanabe, W., Inaba, Y., Mori, A., Matsumura, T., Nakano, Y., Takeshita, K. 2010. Thermo-responsive extraction of cadmium(II) ion with TPEN-NIPA gel. Effect of the number of polymerizable double bond toward gel formation and the extracting behavior. *Tetrahedron*, **66**(9), 1721-1727.

Futalan, C.M., Kan, C.C., Dalida, M.L., Pascua, C., Wan, M.W. 2011. Fixed-bed column studies on the removal of copper using chitosan immobilized on bentonite. *Carbohydrate Polymers*, **83**(2), 697-704.

Gadd, G. 2000. Microbial interactions with tributyltin compounds: detoxification, accumulation, and environmental fate. *Science of the Total Environment*, **258**(1), 119-127.

Gadd, G.M. 1988. Accumulation of metals by microorganisms and algae. *Biotechnology*, **6**, 401-433.

Gadd, G.M. 2004. Microbial influence on metal mobility and application for bioremediation. *Geoderma*, **122**(2-4), 109-119.

Gadd, G.M. 2009. Biosorption: critical review of scientific rationale, environmental importance and significance for pollution treatment. *Journal of Chemical Technology and Biotechnology*, **84**(1), 13-28.

Gaetke, L.M., Chow, C.K. 2003. Copper toxicity, oxidative stress, and antioxidant nutrients. *Toxicology*, **189**(1–2), 147-163.

Gallego, S.M., Pena, L.B., Barcia, R.A., Azpilicueta, C.E., Iannone, M.F., Rosales, E.P., Zawoznik, M.S., Groppa, M.D., Benavides, M.P. 2012. Unravelling cadmium toxicity and tolerance in plants: Insight into regulatory mechanisms. *Environmental and Experimental Botany*, **83**(0), 33-46.

Gao, C.L., Zhang, W.L., Li, H.B., Lang, L.M., Xu, Z. 2008. Controllable fabrication of mesoporous MgO with various morphologies and their absorption performance for toxic pollutants in water. *Crystal Growth and Design*, **8**(10), 3785-3790.

Gardea-Torresdey, J.L., Becker-Hapak, M.K., Hosea, J.M., Darnall, D.W. 1990. Effect of chemical modification of algal carboxyl groups on metal ion binding. *Environmental Science and Technology*, **24**(9), 1372-1378.

Garg, U., Kaur, M.P., Jawa, G.K., Sud, D., Garg, V.K. 2008. Removal of cadmium (II) from aqueous solutions by adsorption on agricultural waste biomass. *Journal of Hazardous Materials*, **154**(1-3), 1149-1157.

Garg, U.K., Kaur, M.P., Garg, V.K., Sud, D. 2007. Removal of hexavalent chromium from aqueous solution by agricultural waste biomass. *Journal of Hazardous Materials*, **140**(1-2), 60-68.

Garnham, G., Green, M. 1995. Chromate (VI) uptake by and interactions with cyanobacteria. *Journal of Industrial Microbiology*, **14**(3-4), 247-251.

Gavrilescu, M. 2004. Removal of heavy metals from the environment by biosorption. *Engineering in Life Sciences*, **4**(3), 219-232.

Gereli, G., Seki, Y., Murat Kusoglu, I., Yurdakoç, K. 2006. Equilibrium and kinetics for the sorption of promethazine hydrochloride onto K10 montmorillonite. *Journal of Colloid and Interface Science*, **299**(1), 155-162.

Giaccio, L., Cicchella, D., De Vivo, B., Lombardi, G., De Rosa, M. 2012. Does heavy metals pollution affects semen quality in men? A case of study in the metropolitan area of Naples (Italy). *Journal of Geochemical Exploration*, **112**(0), 218-225.

Giguere, V., Ong, E.S., Segui, P., Evans, R.M. 1987. Identification of a receptor for the morphogen retinoic acid. *Nature*, **330**(6149), 624-629.

Giller, K.E., Witter, E., Mcgrath, S.P. 1998. Toxicity of heavy metals to microorganisms and microbial processes in agricultural soils: a review. *Soil Biology and Biochemistry*, **30**(10), 1389-1414.

GLAAS, 2012. Global analysis and assessment of sanitation and drinking-water (GLAAS). *A report by the challenge of extending and sustaining services, WHO*, 1-112.

Goel, J., Kadirvelu, K., Rajagopal, C., Kumar Garg, V. 2005. Removal of lead (II) by adsorption using treated granular activated carbon: batch and column studies. *Journal of Hazardous Materials*, **125**(1), 211-220.

Gold, H., Czupryna, G., Levy, R.D., Calmon, C., Gross, L. 1987. Purifying plating bath by chelate ion exchange, in Metals speciation, separation, and recovery. *edited by Patterson, J.W., and Passino, R., Lewis Publishers, Boca Raton.* , 1-200.

Goldberg, E.D., Gamble, E., Griffin, J.J., Koide, M. 1977. Pollution history of Narragansett Bay as recorded in its sediments. *Estuarine and Coastal Marine Science*, **5**(4), 549-561.

Goldstein, J., Newbury, D., Joy, D., Lyman, C., Echlin, P., Lifshin, E., Sawyer, L., Michael, J. 2003. Scanning electron microscopy and X-ray microanalysis. *Plenum Press, New York*, **3rd edition**, 1-9.

Golob, V., Vinder, A., Simonič, M. 2005. Efficiency of the coagulation/flocculation method for the treatment of dyebath effluents. *Dyes and Pigments*, **67**(2), 93-97.

Gong, R., Ding, Y., Liu, H., Chen, Q., Liu, Z. 2005. Lead biosorption and desorption by intact and pretreated *spirulina maxima* biomass. *Chemosphere*, **58**(1), 125-130.

Gorgievski, M., Božić, D., Stanković, V., Štrbac, N., Šerbula, S. 2013. Kinetics, equilibrium and mechanism of $Cu^{2+,}$ $Ni^{2+}$ and $Zn^{2+}$ ions biosorption using wheat straw. *Ecological Engineering*, **58**(0), 113-122.

Goyal, P., Sharma, P., Srivastava, S., Srivastava, M.M. 2008. Saraca indica leaf powder for decontamination of Pb(II): removal, recovery, adsorbent characterization and equilibrium modeling. *International Journal of Environmental Science and Technology : (IJEST)*, **5**(1), 27-34.

Graeme, K.A., Pollack Jr, C.V. 1998. Heavy metal toxicity, part II: lead and metal fume fever. *The Journal of Emergency Medicine*, **16**(2), 171-177.

Gray, W.G., Schrefler, B.A. 2001. Thermodynamic approach to effective stress in partially saturated porous media. *European Journal of Mechanics-A/Solids*, **20**(4), 521-538.

Gregory, M.W. 1993. Wastewater evaporator system, Google Patents.

Grimm, A., Zanzi, R., Bjornbom, E., Cukierman, A.L. 2008. Comparison of different types of biomasses for copper biosorption. *Bioresource Technology*, **99**(7), 2559-2565.

Günay, A., Arslankaya, E., Tosun, İ. 2007. Lead removal from aqueous solution by natural and pretreated clinoptilolite: Adsorption equilibrium and kinetics. *Journal of Hazardous Materials*, **146**(1-2), 362-371.

Gürses, A., Doğar, Ç., Yalçın, M., Açıkyıldız, M., Bayrak, R., Karaca, S. 2006. The adsorption kinetics of the cationic dye, methylene blue, onto clay. *Journal of Hazardous Materials*, **131**(1), 217-228.

Guibal, E., Lorenzelli, R., Vincent, T., Cloirec, P.L. 1995. Application of silica gel to metal ion sorption: static and dynamic removal of uranyl ions. *Environmental Technology*, **16**(2), 101-114.

Guler, U.A., Sarioglu, M. 2013. Single and binary biosorption of Cu(II), Ni(II) and methylene blue by raw and pretreated Spirogyra sp.: Equilibrium and kinetic modeling. *Journal of Environmental Chemical Engineering*, **1**(3), 369-377.

Gupta, G., Keegan, B. 1998. Bioaccumulation and biosorption of lead by poultry litter microorganisms. *Poultry science*, **77**(3), 400-404.

Gupta, G., Torres, N. 1998. Use of fly ash in reducing toxicity of and heavy metals in wastewater effluent. *Journal of Hazardous Materials*, **57**(1-3), 243-248.

Gupta, S., Babu, B. 2009. Removal of toxic metal Cr (VI) from aqueous solutions using sawdust as adsorbent: equilibrium, kinetics and regeneration studies. *Chemical Engineering Journal*, **150**(2), 352-365.

Gupta, S., Babu, B.V. 2006. Adsorption of Cr(VI) by a low-cost adsorbent prepared from neem leaves. *Proceeding National Conference Environment Conservation*. pp. 175–180.

Gupta, V.K., Ali, I. 2004. Removal of lead and chromium from wastewater using bagasse fly ash-a sugar industry waste. *Journal of Colloid and Interface Science*, **271**(2), 321-328.

Gupta, V.K., Rastogi, A. 2008. Biosorption of lead(II) from aqueous solutions by non-living algal biomass Oedogonium sp and Nostoc sp - A comparative study. *Colloids and Surfaces B-Biointerfaces*, **64**(2), 170-178.

Gupta, V.K., Rastogi, A. 2008. Sorption and desorption studies of chromium(VI) from nonviable cyanobacterium Nostoc muscorum biomass. *Journal of Hazardous Materials*, **154**(1-3), 347-354.

Hameed, B.H. 2009. Grass waste: A novel sorbent for the removal of basic dye from aqueous solution. *Journal of Hazardous Materials*, **166**(1), 233-238.

Hammaini, A., González, F., Ballester, A., Blázquez, M.L., Muñoz, J.A. 2003. Simultaneous uptake of metals by activated sludge. *Minerals Engineering*, **16**(8), 723-729.

Han, R., Li, H., Li, Y., Zhang, J., Xiao, H., Shi, J. 2006. Biosorption of copper and lead ions by waste beer yeast. *Journal of Hazardous Materials*, **137**(3), 1569-1576.

Han, R., Zou, L., Zhao, X., Xu, Y., Xu, F., Li, Y., Wang, Y. 2009. Characterization and properties of iron oxide-coated zeolite as adsorbent for removal of copper (II) from solution in fixed bed column. *Chemical Engineering Journal*, **149**(1), 123-131.

Han, R.P., Zhang, J.H., Zou, W.H., Shi, H., Liu, H.M. 2005. Equilibrium biosorption isotherm for lead ion on chaff. *Journal of Hazardous Materials*, **125**(1-3), 266-271.

Han, W., Bai, R.B. 2010. A Novel Method for Obtaining a High-Concentration Chitosan Solution and Preparing a High-Strength Chitosan Hollow-Fiber Membrane with an Excellent Adsorption Capacity. *Journal of Applied Polymer Science*, **115**(4), 1913-1921.

Han, W., Lu, M., Wang, H., Liu, G. 2007. A novel nano-water-purifying material. *Advanced Materials and Processing Iv*, **29-30**, 367-370

Hanafiah, M.A.K.M., Ngah, W.S.W., Ibrahim, S.C., Zakaria, H., Ilias, W.A.H.W. 2006. Kinetics and thermodynamic study of lead adsorption from aqueous solution onto rubber (Hevea brasiliensis) leaf powder. *Journal of Applied Sciences*, **6**(13), 2762-2767.

Hanif, M.A., Nadeem, R., Bhatti, H.N., Ahmad, N.R., Ansari, T.M. 2007. Ni (II) biosorption by *Cassia fistula* (Golden Shower) biomass. *Journal of Hazardous Materials*, **139**(2), 345-355.

Hansen, H.K., Gutierrez, C., Callejas, J., Cameselle, C. 2013. Biosorption of lead from acidic aqueous solutions using Durvillaea antarctica as adsorbent. *Minerals Engineering*, **46–47**(0), 95-99.

Harland, C.E. 1994. Ion exchange, theory and practice. *The Royal Society of Chethistry, Cambridge.*

Haug, A., Smidsrod, O. 1970. Selectivity of some anionic polymers for divalent metal ions. *Acta Chem Scand*, **24**(3), 843-854.

Hawari, A.H., Mulligan, C.N. 2006. Biosorption of lead(II), cadmium(II), copper(II) and nickel(II) by anaerobic granular biomass. *Bioresource Technology*, **97**(4), 692-700.

Heng, B.C., Zhao, X., Xiong, S., Woei Ng, K., Yin-Chiang Boey, F., Say-Chye Loo, J. 2010. Toxicity of zinc oxide (ZnO) nanoparticles on human bronchial epithelial

cells (BEAS-2B) is accentuated by oxidative stress. *Food and Chemical Toxicology*, **48**(6), 1762-1766.

Hill, A.V. 1910. The possible effects of the aggregation of the molecules of haemoglobin on its dissociation curves. *J physiol*, **40**(4), iv-vii.

Ho, Y. S., Chiu, W.-T., Hsu, C. S., Huang, C.T. 2004. Sorption of lead ions from aqueous solution using tree fern as a sorbent. *Hydrometallurgy*, **73**(1–2), 55-61.

Ho, Y., Huang, C., Huang, H. 2002. Equilibrium sorption isotherm for metal ions on tree fern. *Process Biochemistry*, **37**(12), 1421-1430.

Ho, Y., McKay, G. 1999. The sorption of lead (II) ions on peat. *Water Research*, **33**(2), 578-584.

Ho, Y., Porter, J., McKay, G. 2002. Equilibrium Isotherm Studies for the Sorption of Divalent Metal Ions onto Peat: Copper, Nickel and Lead Single Component Systems. *Water, Air, & Soil Pollution*, **141**(1), 1-33.

Ho, Y.S. 2004. Citation review of Lagergren kinetic rate equation on adsorption reactions. *Scientometrics*, **59**(1), 171-177.

Ho, Y.S. 2004. Comment on "Removal of copper from aqueous solution by aminated and protonated mesoporous aluminas: kinetics and equilibrium," by S. Rengaraj, Y. Kim, C.K. Joo, and J. Yi. *Journal of Colloid and Interface Science*, **276**(1), 255-258.

Ho, Y.S. 2005. Effect of pH on lead removal from water using tree fern as the sorbent. *Bioresource Technology*, **96**(11), 1292-1296.

Ho, Y.S., Huang, C.T., Huang, H.W. 2002. Equilibrium sorption isotherm for metal ions on tree fern. *Process Biochemistry*, **37**(12), 1421-1430.

Ho, Y.S., McKay, G. 1998a. A Comparison of Chemisorption Kinetic Models Applied to Pollutant Removal on Various Sorbents. *Process Safety and Environmental Protection*, **76**(4), 332-340.

Ho, Y.S., McKay, G. 1998b. The kinetics of sorption of basic dyes from aqueous solution by sphagnum moss peat. *The Canadian Journal of Chemical Engineering*, **76**(4), 822-827.

Ho, Y.S., McKay, G. 1999. A multi-stage batch sorption design with experimental data. *Adsorption Science and Technology*, **17**(4), 233-243.

Ho, Y.S., McKay, G. 2000. The kinetics of sorption of divalent metal ions onto sphagnum moss peat. *Water Research*, **34**(3), 735-742.

Ho, Y.S., Ng, J.C.Y., McKay, G. 2000. Kinetics of pollutant sorption by biosorbents: review. *Separation and Purification Reviews*, **29**(2), 189-232.

Ho, Y.S., Ng, J.C.Y., McKay, G. 2000. Kinetics of pollutant sorption by biosorbents: review. *Separation and Purification Reviews*, **29**(2), 189-232.

Ho, Y.S., Ofomaja, A.E. 2006a. Kinetic studies of copper ion adsorption on palm kernel fibre. *Journal of Hazardous Materials*, **137**(3), 1796-1802.

Ho, Y.S., Porter, J.F., McKay, G. 2002. Equilibrium Isotherm Studies for the Sorption of Divalent Metal Ions onto Peat: Copper, Nickel and Lead Single Component Systems. *Water, Air, and Soil Pollution*, **141**(1-4), 1-33.

Ho, Y.S., Wase, D.A.J., Forster, C.F. 1994. Adsorption of divalent copper ions from aqueous solution by sphagnum moss peat. *Process Safety and Environmental Protection: Transactions of the Institution of Chemical Engineers, Part B*, **72**(3), 185-194.

Hogan, M.C., Foreman, K.J., Naghavi, M., Ahn, S.Y., Wang, M., Makela, S.M., Lopez, A.D., Lozano, R., Murray, C.J. 2010. Maternal mortality for 181 countries, 1980–2008: a systematic analysis of progress towards Millennium Development Goal 5. *The Lancet*, **375**(9726), 1609-1623.

Holland, M. 1979. Toxicity of heavy metals. *Australian Veterinary Journal*, **55**(8), 373-373.

Holland, M.K., White, I.G. 1988. Heavy metals and human spermatozoa. III. The toxicity of copper ions for spermatozoa. *Contraception*, **38**(6), 685-695.

Homagai, P.L., Ghimire, K.N., Inoue, K. 2010. Adsorption behavior of heavy metals onto chemically modified sugarcane bagasse. *Bioresource Technology*, **101**(6), 2067-2069.

Hong, K. M., Kim, M.-S., Chung, J.G. 2004. Adsorption characteristics of Ni(II) on γ-type alumina particles and its determination of overall adsorption rate by a differential bed reactor. *Chemosphere*, **54**(7), 927-934.

Hong, S., Nuerdongbai, W., Bing, D., Mao-wu, F. 2006. Removal of Heavy Metals form Wastewater by Using Activated Carbon Adsorption. *Jiangsu Environmental Science and Technology*, S2.

Horsfall, M., Spiff, A.I. 2005. Kinetic studies on the sorption of lead and cadmium ions from aqueous solutions by Caladium bicolor (wild cocoyam) biomass. *Bulletin of the Chemical Society of Ethiopia*, **19**(1), 89-102.

Horsfall, M., Spiff, A.I. 2005a. Effect of metal ion concentration on the biosorption of $Pb^{2+}$ and $Cd^{2+}$ by Caladium bicolor (wild cocoyam). *African Journal of Biotechnology*, **4**(2), 191-196.

Horsfall, M., Spiff, A.I. 2005b. Equilibrium sorption study of $Al^{3+}$, $Co^{2+}$ and $Ag^{+}$ in aqueous solutions by fluted pumpkin (Telfairia Occidentalis HOOK f) waste biomass. *Acta Chimica Slovenica*, **52**(2), 174-181.

Hossain, M.A., Ngo, H.H., Guo, W.S., Nguyen, T.V. 2012a. Biosorption of Cu(II) From Water by Banana Peel Based Biosorbent: Experiments and Models of Adsorption and Desorption. *Journal of Water Sustainability*, **2**(1), 87-104.

Hossain, M.A., Ngo, H.H., Guo, W.S., Nguyen, T.V. 2012a. Palm oil fruit shells as biosorbent for copper removal from water and wastewater: Experiments and sorption models. *Bioresource Technology*, **113**(0), 97-101.

Hossain, M.A., Ngo, H.H., Guo, W.S., Nguyen, T.V., Vigneswaran, S. 2013. Performance of cabbage and cauliflower wastes for heavy metals removal. *Desalination and Water Treatment*, 1-17.

Hossain, M.A., Ngo, H.H., Guo, W.S., Setiadi, T. 2012. Adsorption and desorption of copper(II) ions onto garden grass. *Bioresource Technology*, **121**(0), 386-395.

Hristodor, C., Copcia, V., Lutic, D., Popovici, E. 2010. Thermodynamics and Kinetics of Pb(II) and Hg(II) Ions Removal from Aqueous Solution by Romanian Clays. *Revista De Chimie*, **61**(3), 285-289.

Hsu, M.J., Selvaraj, K., Agoramoorthy, G. 2006. Taiwan's industrial heavy metal pollution threatens terrestrial biota. *Environmental Pollution*, **143**(2), 327-334.

Hu, L., Greer, J.B., Solo-Gabriele, H., Fieber, L.A., Cai, Y. 2013. Arsenic toxicity in the human nerve cell line SK-N-SH in the presence of chromium and copper. *Chemosphere*, **91**(8), 1082-1087.

Hu, Z., Yang, X., Gao, A., WEI, X. 2007. Remediation of mycorrhiza on Cd(II) contaminated soil. *Journal-china university of mining and technology-chinese edition-*, **36**(2), 237.

Hureau, C., Faller, P. 2009. Aβ-mediated ROS production by Cu(II) ions: Structural insights, mechanisms and relevance to Alzheimer's disease. *Biochimie*, **91**(10), 1212-1217.

IARC. 1982. International Agency for Research on Cancer: Chemicals, industrial processes and industries associated with cancer in humans. In IARC monographs. *Eval. Carcinog. Risk. Chem. Hum.*, **1-29**, 149.

Ibrahim, M.N.M., Ngah, W.S.W., Norliyana, M.S., Daud, W.R.W., Rafatullah, M., Sulaiman, O., Hashim, R. 2010. A novel agricultural waste adsorbent for the removal of lead (II) ions from aqueous solutions. *Journal of Hazardous Materials*, **182**(1–3), 377-385.

Iftikhar, A.R., Bhatti, H.N., Hanif, M.A., Nadeem, R. 2009. Kinetic and thermodynamic aspects of Cu(II) and Cr(III) removal from aqueous solutions using rose waste biomass. *Journal of Hazardous Materials*, **161**(2-3), 941-947.

Ige, S.F., Akhigbe, R.E. 2013. Common onion (Allium cepa) extract reverses cadmium-induced organ toxicity and dyslipidaemia via redox alteration in rats. *Pathophysiology*(0).

Igwe, J., Abia, A. 2006. A bioseparation process for removing heavy metals from waste water using biosorbents. *African Journal of Biotechnology*, **5**(11).

Igwe, J.C., Abia, A.A. 2007. Equilibrium sorption isotherm studies of Cd(II), Pb(II) and Zn(II) ions detoxification from waste water using unmodified and EDTA-modified maize husk. *Electronic Journal of Biotechnology*, **10**(4), 536-548.

Igwe, J.C., Abia, A.A., Ibeh, C.A. 2008. Adsorption kinetics and intraparticulate diffusivities of Hg(II), As(III) and Pb(II) ions on unmodified and thiolated coconut fiber. *International Journal of Environmental Science and Technology : (IJEST)*, **5**(1), 83-92.

Iqbal, M., Saeed, A., Zafar, S.I. 2009a. FTIR spectrophotometry, kinetics and adsorption isotherms modeling, ion exchange, and EDX analysis for understanding the mechanism of $Cd^{2+}$ and $Pb^{2+}$ removal by mango peel waste. *Journal of Hazardous Materials*, **164**(1), 161-171.

Iqbal, M., Schiewer, S., Cameron, R. 2009b. Mechanistic elucidation and evaluation of biosorption of metal ions by grapefruit peel using FTIR spectroscopy, kinetics

and isotherms modeling, cations displacement and EDX analysis. *Journal of Chemical Technology and Biotechnology*, **84**(10), 1516-1526.

Ismadji, S., Bhatia, S.K. 2000. Adsorption of flavour esters on granular activated carbon. *The Canadian Journal of Chemical Engineering*, **78**(5), 892-901.

Ismadji, S., Bhatia, S.K. 2001. Characterization of activated carbons using liquid phase adsorption. *Carbon*, **39**(8), 1237-1250.

Issabayeva, G., Aroua, M.K., Sulaiman, N.M. 2006. Electrodeposition of copper and lead on palm shell activated carbon in a flow-through electrolytic cell. *Desalination*, **194**(1-3), 192-201.

Jabeen, R., Ahmad, A., Iqbal, M. 2009. Phytoremediation of Heavy Metals: Physiological and Molecular Mechanisms. *Botanical Review*, **75**(4), 339-364.

Jacques, R.A., Bernardi, R., Caovila, M., Lima, E.C., Pavan, F.A., Vaghetti, J.C.P., Airoldi, C. 2007. Removal of Cu(II), Fe(III), and Cr(III) from aqueous solution by aniline grafted silica gel. *Separation Science and Technology*, **42**(3), 591-609.

Jakobsen, M.R., Fritt-Rasmussen, J., Nielsen, S., Ottosen, L.M. 2004. Electrodialytic removal of cadmium from wastewater sludge. *Journal of Hazardous Materials*, **106**(2), 127-132.

Jamali, M.K., Kazi, T.G., Arain, M.B., Afridi, H.I., Jalbani, N., Kandhro, G.A., Shah, A.Q., Baig, J.A. 2009. Speciation of heavy metals in untreated sewage sludge by using microwave assisted sequential extraction procedure. *Journal of Hazardous Materials*, **163**(2), 1157-1164.

Järup, L. 2003. Hazards of heavy metal contamination. *British medical bulletin*, **68**(1), 167-182.

Javanbakht, V., Zilouei, H., Karimi, K. 2011. Lead biosorption by different morphologies of fungus Mucor indicus. *International Biodeterioration and Biodegradation*, **65**(2), 294-300.

Jeon, C., Park, K.H. 2005. Adsorption and desorption characteristics of mercury(II) ions using aminated chitosan bead. *Water Research*, **39**(16), 3938-3944.

Jianqiu, C., Zhijun, H., Zhiliang, W., Rong, J. 2010. Adsorption characteristic of bioadsorbent for antibiotics. *Technology of Water Treatment*, **12**, 018.

Jiuzhou, D., Feng, C., Jinhu, J., Weiwei, Z., Heng, X. 2012. Biosorption of Lead(ll) in Aqueous Solution by Spent Mushroom Tricholoma lobayense. *Water Environment Research (10614303)*, **84**(4), 291-298.

Johnson, F.O., Gilbreath, E.T., Ogden, L., Graham, T.C., Gorham, S. 2011. Reproductive and developmental toxicities of zinc supplemented rats. *Reproductive Toxicology*, **31**(2), 134-143.

Jortner, B.S. 2008. Effect of stress at dosing on organophosphate and heavy metal toxicity. *Toxicology and Applied Pharmacology*, **233**(1), 162-167.

Jovanovic, D. 1969. physical adsorption of gases I: isotherms for monolayer and multilayer adsorption. *Colloid Polym. Sci*, **235**, 1203-1214.

Kadirvelu, K., Namasivayam, C. 2000. Agricutural by-product as metal adsorbent: sorption of lead (II) from aqueous solution onto Coirpith carbon. *Environmental Technology*, **21**(10), 1091-1097.

Kadirvelu, K., Senthilkumar, P., Thamaraiselvi, K., Subburam, V. 2002. Activated carbon prepared from biomass as adsorbent: elimination of Ni(II) from aqueous solution. *Bioresource Technology*, **81**(1), 87-90.

Kaewsarn, P. 2002. Biosorption of copper(II) from aqueous solutions by pre-treated biomass of marine algae *Padina sp*. *Chemosphere*, **47**(10), 1081-1085.

Kahraman, S., Asma, D., Erdemoglu, S., Yesilada, O. 2005. Biosorption of copper(II) by live and dried biomass of the white rot fungi Phanerochaete chrysosporium and Funalia trogii. *Engineering in Life Sciences*, **5**(1), 72-77.

Kahraman, S., Dogan, N., Erdemoglu, S. 2008. Use of various agricultural wastes for the removal of heavy metal ions. *International Journal of Environment and Pollution*, **34**(1-4), 275-284.

Kakitani, T., Hata, T., Kajimoto, T., Imamura, Y. 2006. A novel extractant for removal of hazardous metals from preservative-treated wood waste. *Journal of Environmental Quality*, **35**(3), 912-917.

Kaksonen, A., Riekkola-Vanhanen, M.-L., Puhakka, J. 2003. Optimization of metal sulphide precipitation in fluidized-bed treatment of acidic wastewater. *Water Research*, **37**(2), 255-266.

Kalavathy, M.H., Karthikeyan, T., Rajgopal, S., Miranda, L.R. 2005. Kinetic and isotherm studies of Cu(II) adsorption onto $H_3PO_4$-activated rubber wood sawdust. *Journal of Colloid and Interface Science*, **292**(2), 354-362.

Kalmykova, Y., Strömvall, A.-M., Steenari, B.-M. 2008. Adsorption of Cd, Cu, Ni, Pb and Zn on *Sphagnum* peat from solutions with low metal concentrations. *Journal of Hazardous Materials*, **152**(2), 885-891.

Kandah, M.I. 2004. Zinc and cadmium adsorption on low-grade phosphate. *Separation and Purification Technology*, **35**(1), 61-70.

Kandah, M.I., Abu Al-Rub, F.A., Al-Dabaybeh, N. 2003. The aqueous adsorption of copper and cadmium ions onto sheep manure. *Adsorption Science & Technology*, **21**(6), 501-509.

Kapoor, A., Viraraghavan, T. 1995. Fungal biosorption-an alternative treatment option for heavy metal bearing wastewaters: a review. *Bioresource Technology*, **53**(3), 195-206.

Kapoor, A., Viraraghavan, T. 1997. Heavy metal biosorption sites in Aspergillus niger. *Bioresource Technology*, **61**(3), 221-227.

Kara, A. 2009. Adsorption of Cr(VI) ions onto Poly(ethylene glycol dimethacrylate-1-vinyl-1,2,4-triazole). *Journal of Applied Polymer Science*, **114**(2), 948-955.

Kara, S., Aydiner, C., Demirbas, E., Kobya, M., Dizge, N. 2007. Modeling the effects of adsorbent dose and particle size on the adsorption of reactive textile dyes by fly ash. *Desalination*, **212**(1-3), 282-293.

Karami, A., Shamsuddin, Z.H. 2010. Phytoremediation of heavy metals with several efficiency enhancer methods. *African Journal of Biotechnology*, **9**(25), 3689-3698.

Karnitz Jr, O., Gurgel, L.V.A., De Melo, J.C.P., Botaro, V.R., Melo, T.M.S., de Freitas Gil, R.P., Gil, L.F. 2007. Adsorption of heavy metal ion from aqueous single metal solution by chemically modified sugarcane bagasse. *Bioresource Technology*, **98**(6), 1291-1297.

Karthikeyan, S., Balasubramanian, R., Iyer, C.S.P. 2007. Evaluation of the marine algae Ulva fasciata and Sargassum sp. for the biosorption of Cu(II) from aqueous solutions. *Bioresource Technology*, **98**(2), 452-455.

Kay, Y., Aksakal, Ö., Ucun, H. 2009. Biosorption of Lead(II) and Zinc(II) from Aqueous Solutions by Nordmann Fir (Abies nordmanniana (Stev.) Spach. subsp. nordmanniana) Cones. *Acta Chimica Slovenica*, **56**(2), 451-456.

Keith, L., Telliard, W. 1979. ES&T special report: priority pollutants: Ia perspective view. *Environmental Science & Technology*, **13**(4), 416-423.

Kelter, P.B., Grundman, J., Hage, D.S., Carr, J.D., Castro-Acu a, C.M. 1997. A discussion of water pollution in the United States and Mexico; with high school laboratory activities for the analysis of lead, atrazine, and nitrate. *Journal of Chemical Education*, **74**(12), 1413.

Kelter, P.B., Grundman, J., Hage, D.S., Carr, J.D., Castro-Acu a, C.M. 1997. A discussion of water pollution in the United States and Mexico; with high school laboratory activities for the analysis of lead, atrazine, and nitrate. *Journal of Chemical Education*, **74**(12), 1413.

Keskinkan, O., Goksu, M.Z.L., Basibuyuk, M., Forster, C.F. 2004. Heavy metal adsorption properties of a submerged aquatic plant (Ceratophyllum demersum). *Bioresource Technology*, **92**(2), 197-200.

Khan, A., Al-Waheab, I., Al-Haddad, A. 1996. A generalized equation for adsorption isotherms for multi-component organic pollutants in dilute aqueous solution. *Environmental Technology*, **17**(1), 13-23.

Khan, A.R., Ataullah, R., Al-Haddad, A. 1997. Equilibrium adsorption studies of some aromatic pollutants from dilute aqueous solutions on activated carbon at different temperatures. *Journal of Colloid and Interface Science*, **194**(1), 154-165.

Khan, M.A., Ngabura, M., Choong, T.S.Y., Masood, H., Chuah, L.A. 2012. Biosorption and desorption of Nickel on oil cake: Batch and column studies. *Bioresource Technology*, **103**(1), 35-42.

Khan, M.A., Ngabura, M., Choong, T.S.Y., Masood, H., Chuah, L.A. 2012. Biosorption and desorption of Nickel on oil cake: Batch and column studies. *Bioresource Technology*, **103**(1), 35-42.

Khan, N.A., Ibrahim, S., Subramaniam, P. 2004. Elimination of heavy metals from wastewater using agricultural wastes as adsorbents. *Malaysian Journal of Science*, **23**(43-51), 43.

Khlifi, R., Hamza-Chaffai, A. 2010. Head and neck cancer due to heavy metal exposure via tobacco smoking and professional exposure: A review. *Toxicology and Applied Pharmacology*, **248**(2), 71-88.

Khraisheh, M.A., Al-degs, Y.S., Mcminn, W.A. 2004. Remediation of wastewater containing heavy metals using raw and modified diatomite. *Chemical Engineering Journal*, **99**(2), 177-184.

Kicsi, A., Bilba, D., Macoveanu, M. 2010. Equilibrium and kinetic modeling of Zn(II) sorption from aqueous solutions by sphagnum moss peat. *Environmental Engineering and Management Journal*, **9**(3), 341-349.

Kim, T.Y., Jin, H.J., Park, S.S., Kim, S.J., Cho, S.Y. 2008. Adsorption equilibrium of copper ion and phenol by powdered activated carbon, alginate bead and alginate-activated carbon bead. *Journal of Industrial and Engineering Chemistry*, **14**(6), 714-719.

Kinniburgh, D., Jackson, M., Syers, J. 1976. Adsorption of alkaline earth, transition, and heavy metal cations by hydrous oxide gels of iron and aluminum. *Soil Science Society of America Journal*, **40**(5), 796-799.

Kiran, B., Kaushik, A., Kaushik, C.P. 2007. Response surface methodological approach for optimizing removal of Cr (VI) from aqueous solution using immobilized cyanobacterium. *Chemical Engineering Journal*, **126**(2–3), 147-153.

Kitagawa, T., Nishikawa, Y., Frankenfeld, J., Li, N. 1977. Wastewater treatment by liquid membrane process. *Environmental Science and Technology*, **11**(6), 602-605.

Kizilkaya, B., Akgul, R., Turker, G. 2013. Utilization on the Removal Cd(II) and Pb(II) Ions from Aqueous Solution Using Nonliving Rivularia bulata Algae. *Journal of Dispersion Science and Technology*, **34**(9), 1257-1264.

Ko, D.C.K., Porter, J.F., McKay, G. 2000. Optimized correlations for the fixed-bed adsorption of metal ions on bone char. *Chemical Engineering Science*, **55**(23), 5819-5829.

Koble, R.A., Corrigan, T.E. 1952. Adsorption isotherms for pure hydrocarbons. *Industrial and Engineering Chemistry*, **44**(2), 383-387.

Kobya, M., Demirbas, E., Senturk, E., Ince, M. 2005. Adsorption of heavy metal ions from aqueous solutions by activated carbon prepared from apricot stone. *Bioresource Technology*, **96**(13), 1518-1521.

Kolodynska, D., Hubicki, Z. 2008. Comparison of chelating ion exchange resins in sorption of copper(II) and zinc(II) complexes with ethylenediaminetetraacetic acid (EDTA) and nitrilotriacetic acid (NTA). *Canadian Journal of Chemistry-Revue Canadienne De Chimie*, **86**(10), 958-969.

Komy, Z.R., Abdelraheem, W.H., Ismail, N.M. 2013. Biosorption of $Cu^{2+}$ by Eichhornia crassipes: Physicochemical characterization, biosorption modeling and mechanism. *Journal of King Saud University - Science*, **25**(1), 47-56.

Kongsuwan, A., Patnukao, P., Pavasant, P. 2009. Binary component sorption of Cu(II) and Pb(II) with activated carbon from Eucalyptus camaldulensis Dehn bark. *Journal of Industrial and Engineering Chemistry*, **15**(4), 465-470.

Koopal, L., Van Riemsdijk, W., De Wit, J., Benedetti, M. 1994. Analytical isotherm equations for multicomponent adsorption to heterogeneous surfaces. *Journal of Colloid and Interface Science*, **166**(1), 51-60.

Kosasih, A.N., Febrianto, J., Sunarso, J., Ju, Y.H., Indraswati, N., Ismadji, S. 2010. Sequestering of Cu(II) from aqueous solution using cassava peel (Manihot esculenta). *Journal of Hazardous Materials*, **180**(1-3), 366-374.

Kosolapov, D.B., Kuschk, P., Vainshtein, M.B., Vatsourina, A.V., Wiebner, A., Kastner, M., Muller, R.A. 2004. Microbial processes of heavy metal removal from carbon-dericient effluents in constructed wetlands. *Engineering in Life Sciences*, **4**(5), 403-411.

Kratochvil, D., Fourest, E., Volesky, B. 1995. Biosorption of copper by Sargassum fluitans biomass in fixed-bed column. *Biotechnology Letters*, **17**(7), 777-782.

Kratochvil, D., Volesky, B. 1998. Advances in the biosorption of heavy metals. *Trends in Biotechnology*, **16**(7), 291-300.

Kumar, D., Pandey, L.K., Gaur, J.P. 2010. Evaluation of various isotherm models, and metal sorption potential of cyanobacterial mats in single and multi-metal systems. *Colloids and Surfaces B: Biointerfaces*, **81**(2), 476-485.

Kumar, D., Singh, A., Gaur, J.P. 2008. Mono-component versus binary isotherm models for Cu(II) and Pb(II) sorption from binary metal solution by the green alga Pithophora oedogonia. *Bioresource Technology*, **99**(17), 8280-8287.

Kumar, P.S., Ramakrishnan, K., Kirupha, S.D., Sivanesan, S. 2010. Thermodynamic and Kinetic Studies of Cadmium Adsorption from Aqueous Solution onto Rice Husk. *Brazilian Journal of Chemical Engineering*, **27**(2), 347-355.

Kundu, S., Gupta, A. 2006. Arsenic adsorption onto iron oxide-coated cement (IOCC): regression analysis of equilibrium data with several isotherm models and their optimization. *Chemical Engineering Journal*, **122**(1), 93-106.

Kurniawan, T.A., Chan, G., Lo, W. H., Babel, S. 2006. Physico–chemical treatment techniques for wastewater laden with heavy metals. *Chemical Engineering Journal*, **118**(1), 83-98.

Kusvuran, E., Yildirim, D., Samil, A., Gulnaz, O. 2012. A study: Removal of Cu(II), Cd(II), and Pb(II) Ions from Real Industrial Water and Contaminated Water Using Activated Sludge Biomass. *CLEAN–Soil, Air, Water*.

Kuyucak, N., Volesky, B. 1988. Biosorbents for recovery of metals from industrial solutions. *Biotechnology Letters*, **10**(2), 137-142.

Kuyucak, N., Volesky, B. 1989. The mechanism of cobalt biosorption. *Biotechnology and Bioengineering*, **33**(7), 823-831.

Kweon, D.-K., Choi, J.-K., Kim, E.-K., Lim, S.-T. 2001. Adsorption of divalent metal ions by succinylated and oxidized corn starches. *Carbohydrate Polymers*, **46**(2), 171-177.

Lafuente, A. 2013. The hypothalamic–pituitary–gonadal axis is target of cadmium toxicity. An update of recent studies and potential therapeutic approaches. *Food and Chemical Toxicology*, **59**(0), 395-404.

Lagergren, S. 1898. About the theory of so-called adsorption of soluble substances. *Kungliga Svenska Vetenskapsakademiens Handlingar*, **24**(4), 1-39.

Lake, D., Kirk, P., Lester, J. 1984. Fractionation, characterization, and speciation of heavy metals in sewage sludge and sludge-amended soils: a review. *Journal of Environmental Quality*, **13**(2), 175-183.

Langmuir, I. 1918. The adsorption of gases on plane surfaces of glass, mica and platinum. *Journal of the American Chemical Society*, **40**(9), 1361-1403.

Lasheen, M.R., Ammar, N.S., Ibrahim, H.S. 2012. Adsorption/desorption of Cd(II), Cu(II) and Pb(II) using chemically modified orange peel: Equilibrium and kinetic studies. *Solid State Sciences*, **14**(2), 202-210.

Lasheen, M.R., Ammar, N.S., Ibrahim, H.S. 2012. Adsorption/desorption of Cd (II), Cu (II) and Pb (II) using chemically modified orange peel: Equilibrium and kinetic studies. *Solid State Sciences*, **14**(2), 202-210.

Laus, R., de Fávere, V.T. 2011. Competitive adsorption of Cu(II) and Cd(II) ions by chitosan crosslinked with epichlorohydrin–triphosphate. *Bioresource Technology*, **102**(19), 8769-8776.

Leblanc, M., Achard, B., Othman, D.B., Luck, J.M., Bertrand-Sarfati, J., Personné, J.C. 1996. Accumulation of arsenic from acidic mine waters by ferruginous bacterial accretions (stromatolites). *Applied Geochemistry*, **11**(4), 541-554.

Lee, B., Kim, Y., Lee, H., Yi, J. 2001. Synthesis of functionalized porous silicas via templating method as heavy metal ion adsorbents: the introduction of surface hydrophilicity onto the surface of adsorbents. *Microporous and Mesoporous Materials*, **50**(1), 77-90.

Lester, M.L., Horst, R.L., Thatcher, R.W. 1986. Protective effects of zinc and calcium against heavy metal impairment of children's congestive function. *Nutrition and Behavior*, **3**(2), 145-161.

Leusch, A., Holan, Z.R., Volesky, B. 1995. Biosorption of heavy metals (Cd, Cu, Ni, Pb, Zn) by chemically reinforced biomass of marine algae. *Journal of Chemical Technology and Biotechnology*, **62**(3), 279-288.

Leyva-Ramos, R., Bernal-Jacome, L.A., Guerrero-Coronado, R.M., Fuentes-Rubio, L. 2001. Competitive adsorption of Cd(II) and Zn(II) from aqueous solution onto activated carbon. *Separation Science and Technology*, **36**(16), 3673-3687.

Li, D., Zhou, D. 2012. Toxicity and subcellular distribution of cadmium in wheat as affected by dissolved organic acids. *Journal of Environmental Sciences*, **24**(5), 903-911.

Li, G.X., Xue, P.Y., Yan, C.Z., Li, Q.Z. 2010. Copper biosorption by Myriophyllum spicatum: Effects of temperature and pH. *Korean Journal of Chemical Engineering*, **27**(4), 1239-1245.

Li, P., Wang, X., Allinson, G., Li, X., Xiong, X. 2009. Risk assessment of heavy metals in soil previously irrigated with industrial wastewater in Shenyang, China. *Journal of Hazardous Materials*, **161**(1), 516-521.

Li, Q., Zhai, J., Zhang, W., Wang, M., Zhou, J. 2007. Kinetic studies of adsorption of Pb(II), Cr(III) and Cu(II) from aqueous solution by sawdust and modified peanut husk. *Journal of Hazardous Materials*, **141**(1), 163-167.

Li, X., Tang, Y., Xuan, Z., Liu, Y., Luo, F. 2007. Study on the preparation of orange peel cellulose adsorbents and biosorption of $Cd^{2+}$ from aqueous solution. *Separation and Purification Technology*, **55**(1), 69-75.

Li, Y.S., Liu, C.C., Chiou, C.S. 2006. Kinetic studies of adsorption of lead(II) from aqueous solution by wine-processing waste sludge. *Water Environment Research*, **78**(3), 263-268.

Li, Z., Ma, Z., van der Kuijp, T.J., Yuan, Z., Huang, L. 2014. A review of soil heavy metal pollution from mines in China: Pollution and health risk assessment. *Science of the Total Environment*, **468–469**(0), 843-853.

Limousin, G., Gaudet, J.-P., Charlet, L., Szenknect, S., Barthes, V., Krimissa, M. 2007. Sorption isotherms: a review on physical bases, modeling and measurement. *Applied Geochemistry*, **22**(2), 249-275.

Lin, C.Y., Negev, I., Eshel, G., Banin, A. 2008. In situ accumulation of copper, chromium, nickel, and zinc in soils used for long-term waste water reclamation. *Journal of Environmental Quality*, **37**(4), 1477-1487.

Lin, S., Rayson, G.D. 1998. Impact of surface modification on binding affinity distributions of Datura innoxia biomass to metal ions. *Environmental Science and Technology*, **32**(10), 1488-1493.

Liu, Q., Cai, H., Xu, Y., Xiao, L., Yang, M., Wang, P. 2007. Detection of heavy metal toxicity using cardiac cell-based biosensor. *Biosensors and Bioelectronics*, **22**(12), 3224-3229.

Liu, Z.R., Zhou, L. M., Wei, P., Zeng, K., Wen, C.X., Lan, H.-h. 2008. Competitive adsorption of heavy metal ions on peat. *Journal of China University of Mining and Technology*, **18**(2), 255-260.

Liu, Z.S., Lin, C.L., Chou, J.D. 2010. Studies of Cd(II), Pb(II) and Cr(III) distribution characteristics in bottom ash following agglomeration/defluidization in a fluidized bed boiler incinerating artificial waste. *Fuel Processing Technology*, **91**(6), 591-599.

Lodeiro, P., Barriada, J., Herrero, R., Sastre de Vicente, M. 2006. The marine macroalga *Cystoseira baccata* as biosorbent for cadmium (II) and lead (II) removal: Kinetic and equilibrium studies. *Environmental Pollution*, **142**(2), 264-273.

Lonergan, D.J., Jenter, H.L., Coates, J.D., Phillips, E.J.P., Schmidt, T.M., Lovley, D.R. 1996. Phylogenetic analysis of dissimilatory Fe(III)-reducing bacteria. *Journal of Bacteriology*, **178**(8), 2402-2408.

Lopes, E.C.N., dos Anjos, F.S.C., Vieira, E.F.S., Cestari, A.R. 2003. An alternative Avrami equation to evaluate kinetic parameters of the interaction of Hg(II) with

thin chitosan membranes. *Journal of Colloid and Interface Science*, **263**(2), 542-547.

Lopes, M.H., Abelha, P., Oliveira, J.F.S., Cabrita, I., Gulyurtlu, I. 2005. Heavy metals behavior during monocombustion and co-combustion of sewage sludge. *Environmental Engineering Science*, **22**(2), 205-220.

Lovley, D. 1995. Bioremediation of organic and metal contaminants with dissimilatory metal reduction. *Journal of Industrial Microbiology*, **14**(2), 85-93.

Low, K.S., Lee, C.K., Liew, S.C. 2000. Sorption of cadmium and lead from aqueous solutions by spent grain. *Process Biochemistry*, **36**(1–2), 59-64.

Lu, S., Gibb, S.W. 2008. Copper removal from wastewater using spent-grain as biosorbent. *Bioresource Technology*, **99**(6), 1509-1517.

Lucaci, D., Duta, A. 2009. Adsorption of $Cu^{2+}$ on White Poplar and Oak Sawdust. *Environmental Engineering and Management Journal*, **8**(4), 871-876.

Lü, L., Lu, D., Chen, L., Luo, F. 2010. Removal of Cd(II) by modified lawny grass cellulose adsorbent. *Desalination*, **259**(1-3), 120-130.

Luo, S.L., Lin, Y., Chai, L.Y., Min, X.B., Wang, Y.Y., Yan, F., Pu, W. 2006. Biosorption behaviors of $Cu^{2+}$, $Zn^{2+}$, $Cd^{2+}$ and mixture by waste activated sludge. *Transactions of Nonferrous Metals Society of China*, **16**(6), 1431-1435.

Luo, X.D., Liu, Q.F., Zhang, Y., Sun, J., Wang, G.B., Fan, Z.P., Yi, Z.S., Ling, Y.W., Wei, Y.Q., Liu, X.L., Xu, B. 2011. Nephrotic syndrome after allogeneic hematopoietic stem cell transplantation: Etiology and pathogenesis. *Blood Cells, Molecules, and Diseases*, **46**(2), 182-187.

Lussier, S., Gentile, J., Walker, J. 1985. Acute and chronic effects of heavy metals and cyanide on *Mysidopsis bahia* (crustacea: mysidacea). *Aquatic Toxicology*, **7**(1), 25-35.

Macaskie, L.E., Lloyd, J.R., Thomas, R.A.P., Tolley, M.R. 1996. The use of micro-organisms for the remediation of solutions contaminated with actinide elements, other radionuclides, and organic contaminants generated by nuclear fuel cycle activities. *Nuclear Energy-Journal of the British Nuclear Energy Society*, **35**(4), 257-271.

MacBean, A. 2007. China's environment: problems and policies. *The World Economy*, **30**(2), 292-307.

Madhava Rao, M., Ramesh, A., Purna Chandra Rao, G., Seshaiah, K. 2006. Removal of copper and cadmium from the aqueous solutions by activated carbon derived from Ceiba pentandra hulls. *Journal of Hazardous Materials*, **129**(1-3), 123-129.

Mahboub, R., Mouzdahir, Y.E., Elmchaouri, A., Carvalho, A., Pinto, M., Pires, J. 2006. Characterization of a delaminated clay and pillared clays by adsorption of probe molecules. *Colloids and Surfaces A: Physicochemical and Engineering Aspects*, **280**(1–3), 81-87.

Mahvi, A.H. 2008. Application of agricultural fibers in pollution removal from aqueous solution. *International Journal of Environmental Science and Technology*, **5**(2), 275-285.

Maiti, A., DasGupta, S., Basu, J.K., De, S. 2008. Batch and column study: adsorption of arsenate using untreated laterite as adsorbent. *Industrial and Engineering Chemistry Research*, **47**(5), 1620-1629.

Maji, S.K., Pal, A., Pal, T., Adak, A. 2007. Modeling and fixed bed column adsorption of As (III) on laterite soil. *Separation and Purification Technology*, **56**(3), 284-290.

Malakootian, M., Almasi, A., Hossaini, H. 2008. Pb(II) and Co(II) removal from paint industries effluent using wood ash. *International Journal of Environmental Science and Technology*, **5**(2), 217-222.

Malakootian, M., Nouri, J., Hossaini, H. 2009. Removal of heavy metals from paint industry's wastewater using Leca as an available adsorbent. *International Journal of Environmental Science and Technology*, **6**(2), 183-190.

Malek, A., Farooq, S. 1996. Comparison of isotherm models for hydrocarbon adsorption on activated carbon. *Aiche Journal*, **42**(11), 3191-3201.

Malik, A. 2004. Metal bioremediation through growing cells. *Environment International*, **30**(2), 261-278.

Malkoc, E., Nuhoglu, Y. 2006. Fixed bed studies for the sorption of chromium (VI) onto tea factory waste. *Chemical Engineering Science*, **61**(13), 4363-4372.

Manousaki, E., Kalogerakis, N. 2009. Phytoextraction of Pb(II) and Cd(II) by the Mediterranean saltbush (*Atriplex halimus L.*): metal uptake in relation to salinity. *Environmental Science and Pollution Research*, **16**(7), 844-854.

Mansour, S.A., Gad, M.F. 2010. Risk assessment of pesticides and heavy metals contaminants in vegetables: A novel bioassay method using Daphnia magna Straus. *Food and Chemical Toxicology*, **48**(1), 377-389.

Manzoor, Q., Nadeem, R., Iqbal, M., Saeed, R., Ansari, T.M. 2013. Organic acids pretreatment effect on Rosa bourbonia phyto-biomass for removal of Pb(II) and Cu(II) from aqueous media. *Bioresource Technology*, **132**(0), 446-452.

Mao, J., Lee, S.Y., Won, S.W., Yun, Y.-S. 2010. Surface modified bacterial biosorbent with poly (allylamine hydrochloride): Development using response surface methodology and use for recovery of hexachloroplatinate (IV) from aqueous solution. *Water Research*, **44**(20), 5919-5928.

Marczewski, A.W. 2007. Kinetics and equilibrium of adsorption of organic solutes on mesoporous carbons. *Applied Surface Science*, **253**(13), 5818-5826.

Marder, L., Bernardes, A.M., Zoppas Ferreira, J. 2004. Cadmium electroplating wastewater treatment using a laboratory-scale electrodialysis system. *Separation and Purification Technology*, **37**(3), 247-255.

Marín, A.B.P., Ortuño, J.F., Aguilar, M.I., Meseguer, V.F., Sáez, J., Lloréns, M. 2010. Use of chemical modification to determine the binding of Cd(II), Zn(II) and Cr(III) ions by orange waste. *Biochemical Engineering Journal*, **53**(1), 2-6.

Marion, M., Denizeau, F. 1983. Rainbow trout and human cells in culture for the evaluation of the toxicity of aquatic pollutants: A study with cadmium. *Aquatic Toxicology*, **3**(4), 329-343.

Marques, P.A.S.S., Rosa, M.F., Pinheiro, H.M. 2000. pH effects on the removal of $Cu^{2+}$, $Cd^{2+}$ and $Pb^{2+}$ from aqueous solution by waste brewery biomass. *Bioprocess Engineering*, **23**(2), 135-141.

Martínez, M., Miralles, N., Hidalgo, S., Fiol, N., Villaescusa, I., Poch, J. 2006. Removal of lead(II) and cadmium(II) from aqueous solutions using grape stalk waste. *Journal of Hazardous Materials*, **133**(1–3), 203-211.

Martínez, M., Miralles, N., Hidalgo, S., Fiol, N., Villaescusa, I., Poch, J. 2006. Removal of lead (II) and cadmium (II) from aqueous solutions using grape stalk waste. *Journal of Hazardous Materials*, **133**(1), 203-211.

Martinez-Garcia, G., Bachmann, R.T., Williams, C.J., Burgoyne, A., Edyvean, R.G. 2006. Olive oil waste as a biosorbent for heavy metals. *International Biodeterioration and Biodegradation*, **58**(3), 231-238.

Martín-Lara, M.A., Blázquez, G., Ronda, A., Rodríguez, I.L., Calero, M. 2012. Multiple biosorption-desorption cycles in a fixed-bed column for Pb(II) removal by acid-treated olive stone. *Journal of Industrial and Engineering Chemistry*, **18**(3), 1006-1012.

Matheickal, J.T., Yu, Q. 1999. Biosorption of lead (II) and copper (II) from aqueous solutions by pre-treated biomass of Australian marine algae. *Bioresource Technology*, **69**(3), 223-229.

Mathialagan, T., Viraraghavan, T. 2002. Adsorption of cadmium from aqueous solutions by perlite. *Journal of Hazardous Materials*, **94**(3), 291-303.

Matlock, M.M., Howerton, B.S., Atwood, D.A. 2002. Chemical precipitation of heavy metals from acid mine drainage. *Water Research*, **36**(19), 4757-4764.

Mavrov, V., Erwe, T., Blöcher, C., Chmiel, H. 2003. Study of new integrated processes combining adsorption, membrane separation and flotation for heavy metal removal from wastewater. *Desalination*, **157**(1), 97-104.

McBride, M.B. 1995. Toxic metal accumulation from agricultural use of sludge: are USEPA regulations protective? *Journal of Environmental Quality*, **24**(1), 5-18.

McCann, M. 1996. Hazards in cottage industries in developing countries. *American Journal of Industrial Medicine*, **30**(2), 125-129.

McHale, A., McHale, S. 1994. Microbial biosorption of metals: potential in the treatment of metal pollution. *Biotechnology Advances*, **12**(4), 647-652.

McKay, G. 1982. Adsorption of dyestuffs from aqueous solutions with activated carbon I: Equilibrium and batch contact time studies. *Journal of Chemical Technology and Biotechnology*, **32**(7-12), 759-772.

Mckay, G., Blair, H., Gardner, J. 1982. Adsorption of dyes on chitin. I. Equilibrium studies. *Journal of Applied Polymer Science*, **27**(8), 3043-3057.

McKay, G., Ho, Y.S., Ng, J.C.Y. 1999. Biosorption of Copper from Waste Waters: A Review. *Separation and Purification Reviews*, **28**(1), 87-125.

Melo, J.S., D'Souza, S.F. 2004. Removal of chromium by mucilaginous seeds of Ocimum basilicum. *Bioresource Technology*, **92**(2), 151-155.

Memon, J.R., Memon, S.Q., Bhanger, M.I., Khuhawar, M.Y., Allen, G.C., Memon, G.Z., Pathan, A.G. 2008. Efficiency of Cd(II) removal from aqueous media using chemically modified polystyrene foam. *European Polymer Journal*, **44**(5), 1501-1511.

Memon, J.R., Memon, S.Q., Bhanger, M.I., Memon, G.Z., El-Turki, A., Allen, G.C. 2008. Characterization of banana peel by scanning electron microscopy and FT-IR spectroscopy and its use for cadmium removal. *Colloids and Surfaces B: Biointerfaces*, **66**(2), 260-265.

Meneghetti, E., Baroni, P., Vieira, R.S., da Silva, M.G.C., Beppu, M.M. 2010. Dynamic Adsorption of Chromium Ions onto Natural and Cross linked Chitosan Membranes for Wastewater Treatment. *Materials Research-Ibero-American Journal of Materials*, **13**(1), 89-94.

Michalak, I., Chojnacka, K. 2010. Interactions of metal cations with anionic groups on the cell wall of the macroalga Vaucheria sp. *Engineering in Life Sciences*, **10**(3), 209-217.

Mishra, S.P., Tiwari, D., Dubey, R., Mishra, M. 1998. Biosorptive behaviour of casein for $Zn^{2+}$, $Hg^{2+}$ and $Cr^{3+}$: effects of physico-chemical treatments. *Bioresource Technology*, **63**(1), 1-5.

Moghaddam, M.R., Fatemi, S., Keshtkar, A. 2013. Adsorption of lead ($Pb^{2+}$) and uranium cations by brown algae; experimental and thermodynamic modeling. *Chemical Engineering Journal*, **231**(0), 294-303.

Mohammadi, T., Moheb, A., Sadrzadeh, M., Razmi, A. 2005. Modeling of metal ion removal from wastewater by electrodialysis. *Separation and Purification Technology*, **41**(1), 73-82.

Mohammadi, T., Razmi, A., Sadrzadeh, M. 2004. Effect of operating parameters on $Pb^{2+}$ separation from wastewater using electrodialysis. *Desalination*, **167**, 379-385.

Mohan, D., Pittman, C.U. 2006. Activated carbons and low cost adsorbents for remediation of tri- and hexavalent chromium from water. *Journal of Hazardous Materials*, **137**(2), 762-811.

Mohan, S., Sreelakshmi, G. 2008. Fixed bed column study for heavy metal removal using phosphate treated rice husk. *Journal of Hazardous Materials*, **153**(1-2), 75-82.

Mohapatra, M., Khatun, S., Anand, S. 2009. Adsorption behaviour of Pb(II), Cd(II) and Zn(II) on NALCO plant sand. *Indian Journal of Chemical Technology*, **16**(4), 291-300.

Mondal, M.K. 2009. Removal of Pb(II) ions from aqueous solution using activated tea waste: Adsorption on a fixed-bed column. *Journal of Environmental Management*, **90**(11), 3266-3271.

Monser, L., Adhoum, N. 2002. Modified activated carbon for the removal of copper, zinc, chromium and cyanide from wastewater. *Separation and Purification Technology*, **26**(2-3), 137-146.

Montazer-Rahmati, M.M., Rabbani, P., Abdolali, A., Keshtkar, A.R. 2011. Kinetics and equilibrium studies on biosorption of cadmium, lead, and nickel ions from aqueous solutions by intact and chemically modified brown algae. *Journal of Hazardous Materials*, **185**(1), 401-407.

Mosavi, S.B., Karimi, S., Feiziasl, V. 2010. Biosorption of Lead and Nickel by Medicago sativa (alfalfa) and Datura from Contaminated Solution. *Asian Journal of Chemistry*, **22**(3), 1700-1704.

Mouni, L., Merabet, D., Bouzaza, A., Belkhiri, L. 2010. Removal of $Pb^{2+}$ and $Zn^{2+}$ from the aqueous solutions by activated carbon prepared from Dates stone. *Desalination and Water Treatment*, **16**(1-3), 66-73.

Muhamad, H., Doan, H., Lohi, A. 2010. Batch and continuous fixed-bed column biosorption of $Cd^{2+}$ and $Cu^{2+}$. *Chemical Engineering Journal*, **158**(3), 369-377.

Muhamad, H., Doan, H., Lohi, A. 2010. Batch and continuous fixed-bed column biosorption of $Cd^{2+}$ and $Cu^{2+}$. *Chemical Engineering Journal*, **158**(3), 369-377.

Munaf, E., Suhaili, R., Anwar, Y., Indrawati, Zein, R. 2009. Dynamic Removal of Toxic Metals from Wastewater using Perlite as Sorbent. *Asian Journal of Chemistry*, **21**(3), 2059-2066.

Munagapati, V.S., Yarramuthi, V., Nadavala, S.K., Alla, S.R., Abburi, K. 2010. Biosorption of Cu(II), Cd(II) and Pb(II) by Acacia leucocephala bark powder: Kinetics, equilibrium and thermodynamics. *Chemical Engineering Journal*, **157**(2-3), 357-365.

Munagapati, V.S., Yarramuthi, V., Nadavala, S.K., Alla, S.R., Abburi, K. 2010. Biosorption of Cu (II), Cd (II) and Pb (II) by *Acacia leucocephala* bark powder: Kinetics, equilibrium and thermodynamics. *Chemical Engineering Journal*, **157**(2), 357-365.

Muraleedharan, T., Iyengar, L., Venkobachar, C. 1991. Biosorption: an attractive alternative for metal removal and recovery. *Current Science*, **61**(6), 379-385.

Muraleedharan, T., Venkobachar, C. 1990. Mechanism of biosorption of Copper (Ii) by ganoderma iucidum. *Biotechnology and Bioengineering*, **35**(3), 320-325.

Muraleedharan, T., Venkobachar, L.I. 1994. Further insight into the mechanism of biosorption of heavy metals by Ganoderma lucidum. *Environmental Technology*, **15**(11), 1015-1027.

Murphy, J.M., Erkey, C. 1997. Thermodynamics of Extraction of Copper(II) from Aqueous Solutions by Chelation in Supercritical Carbon Dioxide. *Environmental Science and Technology*, **31**(6), 1674-1679.

Murphy, V., Hughes, H., McLoughlin, P. 2009. Enhancement strategies for Cu(II), Cr(III) and Cr(VI) remediation by a variety of seaweed species. *Journal of Hazardous Materials*, **166**(1), 318-326.

Murugesan, K., Kim, Y.M., Jeon, J.R., Chang, Y.S. 2009. Effect of metal ions on reactive dye decolorization by laccase from Ganoderma lucidum. *Journal of Hazardous Materials*, **168**(1), 523-529.

Mustafiz, S., Basu, A., Islam, M.R., Dewaidar, A., Chaalal, O. 2002. A novel method for heavy metal removal. *Energy Sources*, **24**(11), 1043-1051.

Myers, R.H. 1990. *Classical and Modern Regression with Applications*. PWS-KENT.

Nadeem, U., Kant, R., Tripathi, V.S., Chattopadhyaya, M.C. 2010. Biosorption of chromium(VI) by some algae. *Journal of the Indian Chemical Society*, **87**(4), 517-519.

Nagy, B., Măicăneanu, A., Indolean, C., Mânzatu, C., Silaghi-Dumitrescu, L., Majdik, C. 2013. Comparative study of Cd(II) biosorption on cultivated Agaricus bisporus and wild Lactarius piperatus based biocomposites. Linear and nonlinear equilibrium modelling and kinetics. *Journal of the Taiwan Institute of Chemical Engineers*(0).

Naiya, T., Bhattacharya, A., Das, S. 2008. Adsorption of Pb (II) by sawdust and neem bark from aqueous solutions. *Environmental Progress*, **27**(3), 313-328.

Naiya, T.K., Chowdhury, P., Bhattacharya, A.K., Das, S.K. 2009. Saw dust and neem bark as low-cost natural biosorbent for adsorptive removal of Zn(II) and Cd(II) ions from aqueous solutions. *Chemical Engineering Journal*, **148**(1), 68-79.

Naiya, T.K., Chowdhury, P., Bhattacharya, A.K., Das, S.K. 2009. Saw dust and neem bark as low-cost natural biosorbent for adsorptive removal of Zn (II) and Cd (II) ions from aqueous solutions. *Chemical Engineering Journal*, **148**(1), 68-79.

Namasivayam, C., Ranganathan, K. 1995a. Removal of Cd(II) from wastewater by adsorption on "waste" Fe (III) Cr (III) hydroxide. *Water Research*, **29**(7), 1737-1744.

Namasivayam, C., Ranganathan, K. 1995b. Removal of Pb(II), Cd(II), Ni(II) and Mixture of Metal-Ions by Adsorption onto Waste Fe(III)/Cr(III) Hydroxide and Fixed-Bed Studies. *Environmental Technology*, **16**(9), 851-860.

Namasivayam, C., Sangeetha, D. 2006. Recycling of agricultural solid waste, coir pith: Removal of anions, heavy metals, organics and dyes from water by adsorption onto $ZnCl_2$ activated coir pith carbon. *Journal of Hazardous Materials*, **135**(1), 449-452.

Namasivayam, C., Sangeetha, D., Gunasekaran, R. 2007. Removal of Anions, Heavy Metals, Organics and Dyes from Water by Adsorption onto a New Activated Carbon from Jatropha Husk, an Agro-industrial Solid Waste. *Process Safety and Environmental Protection: Transactions of the Institution of Chemical Engineers Part B*, **85**(2), 181-184.

Namasivayam, C., Sureshkumar, M. 2008. Removal of chromium (VI) from water and wastewater using surfactant modified coconut coir pith as a biosorbent. *Bioresource Technology*, **99**(7), 2218-2225.

Ncibi, M.C., Altenor, S., Seffen, M., Brouers, F., Gaspard, S. 2008a. Modelling single compound adsorption onto porous and non-porous sorbents using a deformed Weibull exponential isotherm. *Chemical Engineering Journal*, **145**(2), 196-202.

Ncibi, M.C., Mahjoub, B., Seffen, M. 2008b. Investigation of the sorption mechanisms of metal-complexed dye onto *Posidonia oceanica* (L.) fibres through kinetic modelling analysis. *Bioresource Technology*, **99**(13), 5582-5589.

Ngah, W., Hanafiah, M. 2008. Biosorption of copper ions from dilute aqueous solutions on base treatedrubber (*Hevea brasiliensis*) leaves powder: kinetics, isotherm, and biosorption mechanisms. *Journal of Environmental Sciences*, **20**(10), 1168-1176.

Ngah, W.S.W., Fatinathan, S. 2006. Chitosan flakes and chitosan–GLA beads for adsorption of p-nitrophenol in aqueous solution. *Colloids and Surfaces A: Physicochemical and Engineering Aspects*, **277**(1–3), 214-222.

Ngah, W.S.W., Fatinathan, S. 2008. Adsorption of Cu(II) ions in aqueous solution using chitosan beads, chitosan-GLA beads and chitosan-alginate beads. *Chemical Engineering Journal*, **143**(1-3), 62-72.

Ngu, I., Ledin, I. 2005. Effects of feeding wastes from Brassica species on growth of goats and pesticide/insecticide residues in goat meat. *Asian-Australian Journal of Animal Sciences*, **18**, 197-202.

Niu, H., Deng, W., Wu, Q., Chen, X. 2009. Potential toxic risk of heavy metals from sediment of the Pearl River in South China. *Journal of Environmental Sciences*, **21**(8), 1053-1058.

Niu, Y., Qu, R., Sun, C., Wang, C., Chen, H., Ji, C., Zhang, Y., Shao, X., Bu, F. 2013. Adsorption of Pb(II) from aqueous solution by silica-gel supported hyperbranched polyamidoamine dendrimers. *Journal of Hazardous Materials*, **244–245**(0), 276-286.

Norton, L., Baskaran, K., McKenzie, T. 2004. Biosorption of zinc from aqueous solutions using biosolids. *Advances in Environmental Research*, **8**(3-4), 629-635.

Nriagu, J. 2011. Zinc Toxicity in Humans. in: *Encyclopedia of Environmental Health*, (Ed.) O.N. Editor-in-Chief: Jerome, Elsevier. Burlington, pp. 801-807.

Nriagu, J.O. 1990. Global metal pollution: Poisoning the biosphere? *Environment: Science and Policy for Sustainable Development*, **32**(7), 7-33.

Nriagu, J.O. 1996. History of global metal pollution. *SCIENCE-NEW YORK THEN WASHINGTON*-, 223-223.

Nriagu, J.O., Kang, S.J., Murin, J.R., Wang, X.Q. 2004. Behavior of oxy-anions of As, Se, and Mo in full-scale wastewater treatment plants. *Geochemical Investigations in Earth and Space Science: A Tribute to Issac R. Kaplan*(9), 211-231.

Ochiai, E.-I. 1987. Toxicity of Heavy Metals. in: *General Principles of Biochemistry of the Elements*, Springer, pp. 361-395.

Oehme, F.W. 1978. *Toxicity of heavy metals in the environment. 1. 2*. Marcel Dekker, Inc.

Ofomaja, A.E. 2010. Equilibrium studies of copper ion adsorption onto palm kernel fibre. *Journal of Environmental Management*, **91**(7), 1491-1499.

Ofomaja, A.E., Ho, Y.S. 2007. Effect of pH on cadmium biosorption by coconut copra meal. *Journal of Hazardous Materials*, **139**(2), 356-362.

Oguz, E., Ersoy, M. 2010. Removal of $Cu^{2+}$ from aqueous solution by adsorption in a fixed bed column and Neural Network Modelling. *Chemical Engineering Journal*, **164**(1), 56-62.

Oliveira, R.C., Guibal, E., Garcia, O. 2012. Biosorption and desorption of lanthanum(III) and neodymium(III) in fixed-bed columns with Sargassum sp.: Perspectives for separation of rare earth metals. *Biotechnology Progress*, **28**(3), 715-722.

Omorogie, M.O., Babalola, J.O., Unuabonah, E.I., Gong, J.R. 2012. Kinetics and thermodynamics of heavy metal ions sequestration onto novel Nauclea diderrichii seed biomass. *Bioresource Technology*, **118**(0), 576-579.

Orth, J.D., Thiele, I., Palsson, B.Ø. 2010. What is flux balance analysis? *Nature Biotechnology*, **28**(3), 245-248.

Ozacar, M., Sengil, I.A., Turkmenler, H. 2008. Equilibrium and kinetic data, and adsorption mechanism for adsorption of lead onto valonia tannin resin. *Chemical Engineering Journal*, **143**(1-3), 32-42.

Ozcan, A., Ozcan, A.S., Tunali, S., Akar, T., Kiran, I. 2005. Determination of the equilibrium, kinetic and thermodynamic parameters of adsorption of copper(II) ions onto seeds of Capsicum annuum. *Journal of Hazardous Materials*, **124**(1-3), 200-208.

Özer, A., Özer, D. 2003. Comparative study of the biosorption of Pb(II), Ni(II) and Cr(VI) ions onto *S. cerevisiae*: determination of biosorption heats. *Journal of Hazardous Materials*, **100**(1), 219-229.

Ozer, A., Ozer, D., Ozer, A. 2004. The adsorption of copper(II) ions on to dehydrated wheat bran (DWB): determination of the equilibrium and thermodynamic parameters. *Process Biochemistry*, **39**(12), 2183-2191.

Öztürk, A., Artan, T., Ayar, A. 2004. Biosorption of nickel (II) and copper (II) ions from aqueous solution by *Streptomyces coelicolor* A3 (2). *Colloids and Surfaces B: Biointerfaces*, **34**(2), 105-111.

Öztürk, N., Kavak, D. 2005. Adsorption of boron from aqueous solutions using fly ash: batch and column studies. *Journal of Hazardous Materials*, **127**(1), 81-88.

Padilla-Ortega, E., Leyva-Ramos, R., Flores-Cano, J.V. 2013. Binary adsorption of heavy metals from aqueous solution onto natural clays. *Chemical Engineering Journal*, **225**(0), 535-546.

Padmavathiamma, P.K., Li, L.Y. 2009. Phytoremediation of Metal-Contaminated Soil in Temperate Humid Regions of British Columbia, Canada. *International Journal of Phytoremediation*, **11**(6), 575-590.

Padmesh, T.V.N., Vijayaraghavan, K., Sekaran, G., Velan, M. 2005. Batch and column studies on biosorption of acid dyes on fresh water macro alga Azolla filiculoides. *Journal of Hazardous Materials*, **125**(1–3), 121-129.

Pagnanelli, F., Petrangeli Papini, M., Toro, L., Trifoni, M., Veglio, F. 2000. Biosorption of metal ions on Arthrobacter sp.: biomass characterization and biosorption modeling. *Environmental Science and Technology*, **34**(13), 2773-2778.

Pagnanelli, F., Toro, L., Veglio, F. 2002. Olive mill solid residues as heavy metal sorbent material: a preliminary study. *Waste Management*, **22**(8), 901-907.

Påhlsson, A.-M.B. 1989. Toxicity of heavy metals (Zn, Cu, Cd, Pb) to vascular plants. *Water, Air, and Soil Pollution*, **47**(3-4), 287-319.

Pamukoglu, A.Y., Kargi, F. 2006. Batch kinetics and isotherms for biosorption of copper(II) ions onto pre-treated powdered waste sludge (PWS). *Journal of Hazardous Materials*, **138**(3), 479-484.

Pamukoglu, M.Y., Kargi, F. 2007. Cu(II) ion recovery by biosorption onto powdered waste sludge (PWS) in a fed-batch reactor: Particle size effects. *Separation Science and Technology*, **42**(2), 285-298.

Pan, J.Y., Wang, S., Zhang, R.F. 2006. A novel Pb(II)-imprinted IPN for selective preconcentration of lead from water and sediments. *International Journal of Environmental Analytical Chemistry*, **86**(11), 855-865.

Panday, K.K., Prasad, G., Singh, V.N. 1986. Use of wollastonite for the treatment of Cu(II) rich effluents. *Water, Air, andamp; Soil Pollution*, **27**(3), 287-296.

Papageorgiou, S., Katsaros, F., Kouvelos, E., Kanellopoulos, N. 2009. Prediction of binary adsorption isotherms of $Cu^{2+}$, $Cd^{2+}$ and $Pb^{2+}$ on calcium alginate beads from single adsorption data. *Journal of Hazardous Materials*, **162**(2), 1347-1354.

Parvathi, K., Nagendran, R. 2007. Biosorption of Chromium from Effluent Generated in Chrome-Electroplating Unit using *Saccharomyces cerevisiae*. *Separation Science and Technology*, **42**(3), 625 - 638.

Patil, S., Deshmukh, V., Renukdas, S., Pate, N. 2011. Kinetics of adsorption of crystal violet from aqueous solutions using different natural materials. *International Journal of Environmental Sciences*, **1**(6), 1116-1134.

Patterson, J.W., Allen, H.E., Scala, J.J. 1977. Carbonate precipitation for heavy metals pollutants. *Journal (Water Pollution Control Federation)*, 2397-2410.

Pavasant, P., Apiratikul, R., Sungkhum, V., Suthiparinyanont, P., Wattanachira, S., Marhaba, T.F. 2006. Biosorption of $Cu^{2+}$, $Cd^{2+}$, $Pb^{2+}$, and $Zn^{2+}$ using dried marine green macroalga Caulerpa lentillifera. *Bioresource Technology*, **97**(18), 2321-2329.

Pavia, D.L., Lampman, G.M., Kriz, G.S. 2001. Introduction to spectroscopy: A guide for for students of organic chemistry. *Thomson Learning, Inc, 2001, 3rd edition*, **14-24**, 353-358.

Peigney, A., Laurent, C., Flahaut, E., Bacsa, R., Rousset, A. 2001. Specific surface area of carbon nanotubes and bundles of carbon nanotubes. *Carbon*, **39**(4), 507-514.

Perez-Marin, A.B., Zapata, V.M., Ortuno, J.F., Aguilar, M., Saez, J., Llorens, M. 2007. Removal of cadmium from aqueous solutions by adsorption onto orange waste. *Journal of Hazardous Materials*, **139**(1), 122-131.

Peters, R.W., Ku, Y., Bhattacharyya, D. 1985. Evaluation of recent treatment techniques for removal of heavy metals from industrial wastewaters. *AICHE symposium series*. pp. 165-203.

Pierotti, R., Rouquerol, J. 1985. Reporting physisorption data for gas/solid systems with special reference to the determination of surface area and porosity. *Pure and Applied Chemistry*, **57**(4), 603-619.

Plaza Cazón, J., Viera, M., Donati, E., Guibal, E. 2013. Zinc and cadmium removal by biosorption on Undaria pinnatifida in batch and continuous processes. *Journal of Environmental Management*, **129**(0), 423-434.

Plazinski, W. 2012. Sorption of metal cations by alginate-based biosorbents. On the correct determination of the thermodynamic parameters. *Journal of Colloid and Interface Science*, **368**(1), 547-551.

Plazinski, W., Rudzinski, W. 2010. Binding stoichiometry in sorption of divalent metal ions: A theoretical analysis based on the ion-exchange model. *Journal of Colloid and Interface Science*, **344**(1), 165-170.

Pons, M.-N., Bonté, S.L., Potier, O. 2004. Spectral analysis and fingerprinting for biomedia characterisation. *Journal of Biotechnology*, **113**(1-3), 211-230.

Popuri, S.R., Vijaya, Y., Boddu, V.M., Abburi, K. 2009. Adsorptive removal of copper and nickel ions from water using chitosan coated PVC beads. *Bioresource Technology*, **100**(1), 194-199.

Poulson, S.R., Colberg, P.J., Drever, J.I. 1997. Toxicity of heavy metals (Ni, Zn) to Desulfovibrio desulfuricans. *Geomicrobiology Journal*, **14**(1), 41-49.

Prakash Williams, G., Gnanadesigan, M., Ravikumar, S. 2012. Biosorption and bio-kinetic studies of halobacterial strains against $Ni^{2+}$, $Al^{3+}$ and $Hg^{2+}$ metal ions. *Bioresource Technology*, **107**(0), 526-529.

Prasad, M., Saxena, S. 2008. Attenuation of divalent toxic metal ions using natural sericitic pyrophyllite. *Journal of Environmental Management*, **88**(4), 1273-1279.

Puranik, P., Paknikar, K. 1999. Biosorption of Lead, Cadmium, and Zinc by Citrobacter Strain MCM B-181: Characterization Studies. *Biotechnology Progress*, **15**(2), 228-237.

Puyen, Z.M., Villagrasa, E., Maldonado, J., Diestra, E., Esteve, I., Solé, A. 2012. Biosorption of lead and copper by heavy-metal tolerant *Micrococcus luteus* DE2008. *Bioresource Technology*, **126**(5), 233-237.

Qaiser, S., Saleemi, A.R., Mahmood Ahmad, M. 2007. Heavy metal uptake by agro based waste materials. *Electronic Journal of Biotechnology*, **10**(3), 409-416.

Qaiser, S., Saleemi, A.R., Umar, M. 2009. Biosorption of lead(III) and chromium(VI) on groundnut hull: Equilibrium, kinetics and thermodynamics study. *Electronic Journal of Biotechnology*, **12**(4), 1-17.

Qu, R., Wang, X., Liu, Z., Yan, Z., Wang, Z. 2013. Development of a model to predict the effect of water chemistry on the acute toxicity of cadmium to Photobacterium phosphoreum. *Journal of Hazardous Materials*, **262**(2), 288-296.

Qu, R.J., Wang, X.H., Feng, M.B., Li, Y., Liu, H.X., Wang, L.S., Wang, Z.Y. 2013. The toxicity of cadmium to three aquatic organisms (Photobacterium phosphoreum, Daphnia magna and Carassius auratus) under different pH levels. *Ecotoxicology and Environmental Safety*, **95**(0), 83-90.

Radjenović, J., Petrović, M., Ventura, F., Barceló, D. 2008. Rejection of pharmaceuticals in nanofiltration and reverse osmosis membrane drinking water treatment. *Water Research*, **42**(14), 3601-3610.

Radke, C.J., Prausnitz, J.M. 1972. Adsorption of Organic Solutes from Dilute Aqueous Solution of Activated Carbon. *Industrial and Engineering Chemistry Fundamentals*, **11**(4), 445-451.

Rafatullah, M., Sulaiman, O., Hashim, R., Ahmad, A. 2009. Adsorption of copper (II), chromium (III), nickel (II) and lead (II) ions from aqueous solutions by meranti sawdust. *Journal of Hazardous Materials*, **170**(2-3), 969-977.

Rafatullah, M., Sulaiman, O., Hashim, R., Ahmad, A. 2009. Adsorption of copper (II), chromium (III), nickel (II) and lead (II) ions from aqueous solutions by meranti sawdust. *Journal of Hazardous Materials*, **170**(2-3), 969-977.

Rahman, M.S., Islam, M.R. 2009. Effects of pH on isotherms modeling for Cu(II) ions adsorption using maple wood sawdust. *Chemical Engineering Journal*, **149**(1-3), 273-280.

Raize, O., Argaman, Y., Yannai, S. 2004. Mechanisms of biosorption of different heavy metals by brown marine macroalgae. *Biotechnology and Bioengineering*, **87**(4), 451-458.

Rajaei, G.E., Aghaie, H., Zare, K., Aghaie, M. 2013. Adsorption of Cu(II) and Zn(II) ions from aqueous solutions onto fine powder of Typha latifolia L. root: kinetics and isotherm studies. *Research on Chemical Intermediates*, **39**(8), 3579-3594.

Ramakul, P., Yanachawakul, Y., Leepipatpiboon, N., Sunsandee, N. 2012. Biosorption of palladium(II) and platinum(IV) from aqueous solution using tannin from Indian almond (Terminalia catappa L.) leaf biomass: Kinetic and equilibrium studies. *Chemical Engineering Journal*, **193–194**(0), 102-111.

Ramalho, R.S. 1977. Introduction to waste water treatment processes. *Academic Press, New York.* .

Raskin, I., Smith, R.D., Salt, D.E. 1997. Phytoremediation of metals: using plants to remove pollutants from the environment. *Current opinion in biotechnology*, **8**(2), 221-226.

Ratkowski, D.A. 1990. *Handbook of Nonlinear Regression Models*. Marcel Dekker, N. Y.2003.

Reddad, Z., Gerente, C., Andres, Y., Le Cloirec, P. 2002. Adsorption of several metal ions onto a low-cost biosorbent: kinetic and equilibrium studies. *Environmental Science and Technology*, **36**(9), 2067-2073.

Reddad, Z., Gerente, C., Andres, Y., Le Cloirec, P. 2002. Adsorption of several metal ions onto a low-cost biosorbent: kinetic and equilibrium studies. *Environmental Science & Technology*, **36**(9), 2067-2073.

Reddy, B.R., Das, R.P., Gaballah, I. 1999. Application of Indian modified Shorea robusta bark for removal and recovery of heavy metal ions from aqueous solutions. *Rewas'99 Global Symposium on Recycling, Waste Treatment and Clean Technology Volume I-Iii*, 2067-2076.

Reddy, D.H.K., Seshaiah, K., Reddy, A.V.R., Lee, S.M. 2012. Optimization of Cd(II), Cu(II) and Ni(II) biosorption by chemically modified Moringa oleifera leaves powder. *Carbohydrate Polymers*, **88**(3), 1077-1086.

Redlich, O., Peterson, D.L. 1959. A useful adsorption isotherm. *Journal of Physical Chemistry*, **63**(6), 1024-1024.

Remenárová, L., Pipíška, M., Horník, M., Rozložník, M., Augustín, J., Lesný, J. 2012. Biosorption of cadmium and zinc by activated sludge from single and binary solutions: Mechanism, equilibrium and experimental design study. *Journal of the Taiwan Institute of Chemical Engineers*, **43**(3), 433-443.

Ren, Y.M., Wei, X.Z., Zhang, M.L. 2008. Adsorption character for removal Cu(II) by magnetic Cu(II) ion imprinted composite adsorbent. *Journal of Hazardous Materials*, **158**(1), 14-22.

Repo, E., Warchol, J.K., Kurniawan, T.A., Sillanpaa, M.E.T. 2010. Adsorption of Co(II) and Ni(II) by EDTA- and/or DTPA-modified chitosan: Kinetic and equilibrium modeling. *Chemical Engineering Journal*, **161**(1-2), 73-82.

Rhazi, M., Desbrieres, J., Tolaimate, A., Rinaudo, M., Vottero, P., Alagui, A. 2002. Contribution to the study of the complexation of copper by chitosan and oligomers. *Polymer*, **43**(4), 1267-1276.

Riaz, M., Nadeem, R., Hanif, M.A., Ansari, T.M., Rehman, K.-u. 2009. Pb(II) biosorption from hazardous aqueous streams using Gossypium hirsutum (Cotton) waste biomass. *Journal of Hazardous Materials*, **161**(1), 88-94.

Ricordel, S., Taha, S., Cisse, I., Dorange, G. 2001. Heavy metals removal by adsorption onto peanut husks carbon: characterization, kinetic study and modeling. *Separation and Purification Technology*, **24**(3), 389-401.

Ridoutt, B.G., Pfister, S. 2010. A revised approach to water footprinting to make transparent the impacts of consumption and production on global freshwater scarcity. *Global Environmental Change*, **20**(1), 113-120.

Rijsberman, F.R. 2006. Water scarcity: Fact or fiction? *Agricultural water management*, **80**(1), 5-22.

Ringot, D., Lerzy, B., Chaplain, K., Bonhoure, J. P., Auclair, E., Larondelle, Y. 2007. In vitro biosorption of ochratoxin A on the yeast industry by-products: Comparison of isotherm models. *Bioresource Technology*, **98**(9), 1812-1821.

Robinson, J., Tarleton, E., Millington, C., Nijmeijer, A. 2004. Solvent flux through dense polymeric nanofiltration membranes. *Journal of Membrane Science*, **230**(1), 29-37.

Rodrigues, M.S., Ferreira, L.S., Carvalho, J.C.M.d., Lodi, A., Finocchio, E., Converti, A. 2012. Metal biosorption onto dry biomass of Arthrospira (Spirulina) platensis

and Chlorella vulgaris: Multi-metal systems. *Journal of Hazardous Materials*, **217–218**(0), 246-255.

Romera, E., Gonzalez, F., Ballester, A., Blazquez, M.L., Munoz, J.A. 2008. Biosorption of Cd, Ni, and Zn with mixtures of different types of algae. *Environmental Engineering Science*, **25**(7), 999-1008.

Ronda, A., Martín-Lara, M.A., Calero, M., Blázquez, G. 2013. Analysis of the kinetics of lead biosorption using native and chemically treated olive tree pruning. *Ecological Engineering*, **58**(0), 278-285.

Rowsell, J.L., Yaghi, O.M. 2006. Effects of functionalization, catenation, and variation of the metal oxide and organic linking units on the low-pressure hydrogen adsorption properties of metal-organic frameworks. *Journal of the American Chemical Society*, **128**(4), 1304-1315.

Rubio, J., Souza, M., Smith, R. 2002. Overview of flotation as a wastewater treatment technique. *Minerals Engineering*, **15**(3), 139-155.

Sadrzadeh, M., Razmi, A., Mohammadi, T. 2007. Separation of different ions from wastewater at various operating conditions using electrodialysis. *Separation and Purification Technology*, **54**(2), 147-156.

Saeed, A., Iqbal, M., Akhtar, M.W. 2005. Removal and recovery of lead(II) from single and multimetal (Cd, Cu, Ni, Zn) solutions by crop milling waste (black gram husk). *Journal of Hazardous Materials*, **117**(1), 65-73.

Saeed, A., Iqbal, M., Holl, W.H. 2009. Kinetics, equilibrium and mechanism of $Cd^{2+}$ removal from aqueous solution by mungbean husk. *Journal of Hazardous Materials*, **168**(2-3), 1467-1475.

Saha, P., Chowdhury, S., Gupta, S., Kumar, I. 2010. Insight into adsorption equilibrium, kinetics and thermodynamics of Malachite Green onto clayey soil of Indian origin. *Chemical Engineering Journal*, **165**(3), 874-882.

Saha, U., Taniguchi, S., Sakurai, K. 2001. Adsorption behavior of cadmium, zinc, and lead on hydroxyaluminum–and hydroxyaluminosilicate–montmorillonite complexes. *Soil Science Society of America Journal*, **65**(3), 694-703.

Saifuddin M, N., Kumaran, P. 2005. Removal of heavy metal from industrial wastewater using chitosan coated oil palm shell charcoal. *Electronic Journal of Biotechnology*, **8**(1), 43-53.

Salomons, W., Förstner, U. 1984. *Metals in the Hydrocycle*. Springer-Verlag.

Sampaio, R.M.M., Timmers, R.A., Xu, Y., Keesman, K.J., Lens, P.N.L. 2009. Selective precipitation of Cu from Zn in a pS controlled continuously stirred tank reactor. *Journal of Hazardous Materials*, **165**(1-3), 256-265.

Sanchez-Viveros, G., Gonzalez-Mendoza, D., Alarcon, A., Ferrera-Cerrato, R. 2010. Copper Effects on Photosynthetic Activity and Membrane Leakage of Azolla filiculoides and A. caroliniana. *International Journal of Agriculture and Biology*, **12**(3), 365-368.

Santorufo, L., Van Gestel, C.A.M., Maisto, G. 2012. Ecotoxicological assessment of metal-polluted urban soils using bioassays with three soil invertebrates. *Chemosphere*, **88**(4), 418-425.

Sari, A., Tuzen, M. 2008. Biosorption of cadmium(II) from aqueous solution by red algae (Ceramium virgatum): Equilibrium, kinetic and thermodynamic studies. *Journal of Hazardous Materials*, **157**(2-3), 448-454.

Sarı, A., Tuzen, M. 2008. Biosorption of Pb(II) and Cd(II) from aqueous solution using green alga (Ulva lactuca) biomass. *Journal of Hazardous Materials*, **152**(1), 302-308.

Sari, A., Tuzen, M. 2009. Kinetic and equilibrium studies of Pb(II) and Cd(II) removal from aqueous solution onto colemanite ore waste. *Desalination*, **249**(1), 260-266.

Sari, A., Tuzen, M., Citak, D., Soylak, M. 2007. Equilibrium, kinetic and thermodynamic studies of adsorption of Pb(II) from aqueous solution onto Turkish kaolinite clay. *Journal of Hazardous Materials*, **149**(2), 283-291.

Sarin, V., Singh, T.S., Pant, K.K. 2006. Thermodynamic and breakthrough column studies for the selective sorption of chromium from industrial effluent on activated eucalyptus bark. *Bioresource Technology*, **97**(16), 1986-1993.

Sathasivam, K., Haris, M.R.H.M. 2010. Banana Trunk Fibers as an Efficient Biosorbent for the Removal of Cd(II), Cu(II), Fe(II) and Zn(II) from Aqueous Solutions. *Journal of the Chilean Chemical Society*, **55**(2), 278-282.

Satiroglu, N., Kesenci, K., Bektas, S., Genc, O., Piskin, E. 1998. Competitive adsorption of heavy-metal ions on monodisperse polystyrene microspheres carrying dithiocarbamate groups. *Journal of Macromolecular Science-Pure and Applied Chemistry*, **A35**(1), 91-107.

SCECA (Senate Standing Committee on Environment Communications and the Arts, A. 2008. Management of australia's waste streams (including consideration of the Drink Container Recycling Bill 2008).

Schiermeier, Q., Balling, Y. 2010. Analysis lags on Hungarian sludge leak. *Nature*.

Schiewer, S., Volesky, B. 1995. Modeling of the proton-metal ion exchange in biosorption. *Environmental Science and Technology*, **29**(12), 3049-3058.

Schiewer, S., Volesky, B. 2000. Biosorption processes for heavy metal removal. *environmental microbe-metal interactions*, **14**, 329-362.

Schneider, I.A., Rubio, J., Smith, R.W. 2001. Biosorption of metals onto plant biomass: exchange adsorption or surface precipitation? *International Journal of Mineral Processing*, **62**(1), 111-120.

Šćiban, M., Radetić, B., Kevrešan, Ž., Klašnja, M. 2007. Adsorption of heavy metals from electroplating wastewater by wood sawdust. *Bioresource Technology*, **98**(2), 402-409.

Sekar, M., Sakthi, V., Rengaraj, S. 2004. Kinetics and equilibrium adsorption study of lead(II) onto activated carbon prepared from coconut shell. *Journal of Colloid and Interface Science*, **279**(2), 307-313.

Semerjian, L. 2010. Equilibrium and kinetics of cadmium adsorption from aqueous solutions using untreated Pinus halepensis sawdust. *Journal of Hazardous Materials*, **173**(1-3), 236-242.

Sen Gupta, B., Curran, M., Hasan, S., Ghosh, T.K. 2009. Adsorption characteristics of Cu and Ni on Irish peat moss. *Journal of Environmental Management*, **90**(2), 954-960.

Sen Gupta, B., Curran, M., Hasan, S., Ghosh, T.K. 2009. Adsorption characteristics of Cu and Ni on Irish peat moss. *Journal of Environmental Management*, **90**(2), 954-960.

Sengil, I.A., Özacar, M. 2008. Biosorption of Cu(II) from aqueous solutions by mimosa tannin gel. *Journal of Hazardous Materials*, **157**(2-3), 277-285.

Şengil, İ.A., Özacar, M. 2009. Competitive biosorption of $Pb^{2+}$, $Cu^{2+}$ and $Zn^{2+}$ ions from aqueous solutions onto valonia tannin resin. *Journal of Hazardous Materials*, **166**(2-3), 1488-1494.

Shaligram, S., Campbell, A. 2013. Toxicity of copper salts is dependent on solubility profile and cell type tested. *Toxicology in Vitro*, **27**(2), 844-851.

Sheng, P.X., Tan, L.H., Chen, J.P., Ting, Y.P. 2004a. Biosorption performance of two brown marine algae for removal of chromium and cadmium. *Journal of Dispersion Science and Technology*, **25**(5), 679-686.

Sheng, P.X., Ting, Y. P., Chen, J.P., Hong, L. 2004. Sorption of lead, copper, cadmium, zinc, and nickel by marine algal biomass: characterization of biosorptive capacity and investigation of mechanisms. *Journal of Colloid and Interface Science*, **275**(1), 131-141.

Shinde, N.R., Bankar, A.V., Kumar, A.R., Zinjarde, S.S. 2012. Removal of Ni (II) ions from aqueous solutions by biosorption onto two strains of Yarrowia lipolytica. *Journal of Environmental Management*, **102**(0), 115-124.

Shrestha, S., Son, G., Lee, S.H., Lee, T.G. 2013. Isotherm and thermodynamic studies of Zn(II) adsorption on lignite and coconut shell-based activated carbon fiber. *Chemosphere*, **92**(8), 1053-1061.

Simkiss, K., Taylor, M. 1995. Transport of metals across membranes. *Metal speciation and bioavailability in aquatic systems*, **3**, 1-44.

Simmons, P., Tobin, J.M., Singleton, I. 1995. Considerations on the use of commercially available yeast biomass for the treatment of metal-containing effluents. *Journal of Industrial Microbiology andamp; Biotechnology*, **14**(3), 240-246.

Sing, C., Yu, J. 1998. Copper adsorption and removal from water by living mycelium of white-rot fungus Phanerochaete chrysosporium. *Water Research*, **32**(9), 2746-2752.

Sing, K., Everett, D., Haul, R., Moscou, L., Pierotti, R., Rouquerol, J., Siemieniewska, T. 1982. Reporting physisorption data for gas/solid systems. *Pure and Appl Chem*, **54**(11), 2201.

Singh, A., Kumar, D., Gaur, J.P. 2008. Removal of Cu(II) and Pb(II) by Pithophora oedogonia: Sorption, desorption and repeated use of the biomass. *Journal of Hazardous Materials*, **152**(3), 1011-1019.

Singh, A., Mehta, S.K., Gaur, J.P. 2007. Removal of heavy metals from aqueous solution by common freshwater filamentous algae. *World Journal of Microbiology & Biotechnology*, **23**(8), 1115-1120.

Singh, S., Srivastava, V.C., Mall, I.D. 2009. Fixed-bed study for adsorptive removal of furfural by activated carbon. *Colloids and Surfaces A: Physicochemical and Engineering Aspects*, **332**(1), 50-56.

Singh, T.S., Pant, K.K. 2006. Experimental and modelling studies on fixed bed adsorption of As(III) ions from aqueous solution. *Separation and Purification Technology*, **48**(3), 288-296.

Singh, V., Sharma, A.K., Maurya, S. 2009. Efficient Cadmium(II) Removal from Aqueous Solution Using Microwave Synthesized Guar Gum-Graft-Poly(ethylacrylate). *Industrial and Engineering Chemistry Research*, **48**(10), 4688-4696.

Sips, R. 1948. Combined form of Langmuir and Freundlich equations. *J. Chem. Phys.*, **16**.

Solener, M., Tunali, S., Ozcan, A.S., Ozcan, A., Gedikbey, T. 2008. Adsorption characteristics of lead(II) ions onto the clay/poly(methoxyethyl)acrylamide (PMEA) composite from aqueous solutions. *Desalination*, **223**(1-3), 308-322.

Solisio, C., Lodi, A., Converti, A., Del Borghi, M. 2000. The effect of acid pre-treatment on the biosorption of chromium (III) by *Sphaerotilus natans* from industrial wastewater. *Water Research*, **34**(12), 3171-3178.

Solisio, C., Lodi, A., Torre, P., Converti, A., Del Borghi, M. 2006. Copper removal by dry and re-hydrated biomass of Spirulina platensis. *Bioresource Technology*, **97**(14), 1756-1760.

Song, J., Zou, W., Bian, Y., Su, F., Han, R. 2011. Adsorption characteristics of methylene blue by peanut husk in batch and column modes. *Desalination*, **265**(1–3), 119-125.

Sooksawat, N., Meetam, M., Kruatrachue, M., Pokethitiyook, P., Nathalang, K. 2013. Phytoremediation potential of charophytes: Bioaccumulation and toxicity studies of cadmium, lead and zinc. *Journal of Environmental Sciences*, **25**(3), 596-604.

Sörme, L., Lagerkvist, R. 2002. Sources of heavy metals in urban wastewater in Stockholm. *Science of the Total Environment*, **298**(1-3), 131-145.

Sourirajan, S. 1970. *Reverse osmosis*. London, UK: Logos Press Ltd.

Sousa, F.W., Oliveira, A.G., Ribeiro, J.P., Rosa, M.F., Keukeleire, D., Nascimento, R.F. 2010. Green coconut shells applied as adsorbent for removal of toxic metal ions using fixed-bed column technology. *Journal of Environmental Management*, **91**(8), 1634-1640.

Srihari, V., Das, A. 2008. The kinetic and thermodynamic studies of phenol-sorption onto three agro-based carbons. *Desalination*, **225**(1-3), 220-234.

Srinivasa Rao, P., Suresh Reddy, K.V.N., Kalyani, S., Krishnaiah, A. 2007. Comparative sorption of copper and nickel from aqueous solutions by natural neem (Azadirachta indica) sawdust and acid treated sawdust. *Wood Science and Technology*, **41**(5), 427-442.

Srivastava, N., Majumder, C. 2008. Novel biofiltration methods for the treatment of heavy metals from industrial wastewater. *Journal of Hazardous Materials*, **151**(1), 1-8.

Srivastava, S., Goyal, P. 2010. Novel Biomaterials, Environmental Science and Engineering, Springer-Verlag Berlin Heidelberg, Germany.

Srivastava, V.C., Mall, I.D., Mishra, I.M. 2006. Equilibrium modelling of single and binary adsorption of cadmium and nickel onto bagasse fly ash. *Chemical Engineering Journal*, **117**(1), 79-91.

Srivastava, V.C., Mall, I.D., Mishra, I.M. 2008. Removal of cadmium(II) and zinc(II) metal ions from binary aqueous solution by rice husk ash. *Colloids and Surfaces A: Physicochemical and Engineering Aspects*, **312**(2-3), 172-184.

Stark, J.S. 1998. Heavy metal pollution and macrobenthic assemblages in soft sediments in two Sydney estuaries, Australia. *Marine and Freshwater Research*, **49**(6), 533-540.

Stein, W. 1986. *Transport and diffusion across cell membranes*. Access Online via Elsevier.205-240.

Strathmann, H. 1992. Applications. in: *Membrane Handbook*, Springer, pp. 255-262.

Subhashini, S.S., Velan, M., Kaliappan, S. 2013. Biosorption of lead by Kluyveromyces marxianus immobilized in alginate beads. *Journal of Environmental Biology*, **34**(5), 831-835.

Sud, D., Mahajan, G., Kaur, M. 2008. Agricultural waste material as potential adsorbent for sequestering heavy metal ions from aqueous solutions–A review. *Bioresource Technology*, **99**(14), 6017-6027.

Suksabye, P., Thiravetyan, P., Nakbanpote, W. 2008. Column study of chromium (VI) adsorption from electroplating industry by coconut coir pith. *Journal of Hazardous Materials*, **160**(1), 56-62.

Summers, B., Gress, L., Philipp, W., Eastep, S. 1995. Peat-moss pellets for removal of metal-ion contaminants dissolved in dilute wastewater. US, 11 pp., Cont. *part of US Ser*(249), 733.

Summers, A.O., Sugarman, L.I. 1974. Cell-free mercury (II)-reducing activity in a plasmid-bearing strain of Escherichia-Coli. *Journal of Bacteriology*, **119**(1), 242-249.

Sun, G., Shi, W. 1998. Sunflower stalks as adsorbents for the removal of metal ions from wastewater. *Industrial & Engineering Chemistry Research*, **37**(4), 1324-1328.

Swain, A. 2001. Water wars: fact or fiction? *Futures*, **33**(8), 769-781.

Tan, I., Hameed, B., Ahmad, A. 2007. Equilibrium and kinetic studies on basic dye adsorption by oil palm fibre activated carbon. *Chemical Engineering Journal*, **127**(1), 111-119.

Tarley, C.R.T., Arruda, M.A.Z. 2004. Biosorption of heavy metals using rice milling by-products. Characterisation and application for removal of metals from aqueous effluents. *Chemosphere*, **54**(7), 987-995.

Tate Jr, D.J., Miceli, M.V., Newsome, D.A. 1999. Zinc protects against oxidative damage in cultured human retinal pigment epithelial cells. *Free Radical Biology and Medicine*, **26**(5–6), 704-713.

Taty-Costodes, V.C., Fauduet, H., Porte, C., Ho, Y.-S. 2005. Removal of lead (II) ions from synthetic and real effluents using immobilized *Pinus sylvestris* sawdust: Adsorption on a fixed-bed column. *Journal of Hazardous Materials*, **123**(1), 135-144.

Tchobanoglous, G., Burton, F.L. 2003. Wastewater engineering. *MANAGEMENT*, **7**, 1-4.

Tee, T.W., Khan, A.R.M. 1988. Removal of lead, cadmium and zinc by waste tea leaves. *Environmental Technology Letters*, **9**(11), 1223-1232.

Temkin, M., Pyzhev, V. 1940. Kinetics of ammonia synthesis on promoted iron catalysts. *Acta Physiochim. URSS*, **12**, 217-222.

Teng, H., Hsieh, C. T. 1998. Activation Energy for Oxygen Chemisorption on Carbon at Low Temperatures. *Industrial & Engineering Chemistry Research*, **38**(1), 292-297.

Texier, A., Andres, Y., Faur-Brasquet, C., Le Cloirec, P. 2002. Fixed-bed study for lanthanide (La, Eu, Yb) ions removal from aqueous solutions by immobilized *Pseudomonas aeruginosa*: experimental data and modelization. *Chemosphere*, **47**(3), 333-342.

Tharanitharan, V., Srinivasan, K. 2010. Kinetic and Equilibrium Studies of Removal of Pb(II) and Cd(II) Ions from Aqueous Solution by Modified Duolite XAD-761 Resins. *Asian Journal of Chemistry*, **22**(4), 3036-3046.

Thibodeaux, L.J., Valsaraj, K.T., John, V.T., Papadopoulos, K.D., Pratt, L.R., Pesika, N.S. 2011. Marine oil fate: Knowledge gaps, basic research, and development needs; A perspective based on the Deepwater Horizon spill. *Environmental Engineering Science*, **28**(2), 87-93.

Thiele, E. 1946. Material or Heat Transfer between a Granular Solid and Flowing, Fluid. *Industrial and Engineering Chemistry*, **38**(6), 646-650.

Thirumavalavan, M., Lai, Y.L., Lin, L.C., Lee, J.F. 2010. Cellulose-Based Native and Surface Modified Fruit Peels for the Adsorption of Heavy Metal Ions from Aqueous Solution: Langmuir Adsorption Isotherms. *Journal of Chemical and Engineering Data*, **55**(3), 1186-1192.

Thomas, H., Yong, R., Hashm, A. 1997. Numerical modelling of contaminant transport in Unsaturated soil. *Proc. Int. Conf on Geoenviromental Engineering, Cardiff. Thomas Telford, London*. pp. 278-283.

Thomas, H.C. 1944. Heterogeneous ion exchange in a flowing system. *Journal of the American Chemical Society*, **66**(10), 1664-1666.

Ting, Y., Teo, W. 1994. Uptake of cadmium and zinc by yeast: effects of co-metal ion and physical/chemical treatments. *Bioresource Technology*, **50**(2), 113-117.

Tiravanti, G., Petruzzelli, D., Passino, R. 1997. Pretreatment of tannery wastewaters by an ion exchange process for Cr (III) removal and recovery. *Water Science and Technology*, **36**(2), 197-207.

Tobin, J.M., Cooper, D.G., Neufeld, R.J. 1990. Investigation of the mechanism of metal uptake by dena¬tured Rhizopus arrhizus biomass. *Enzyme Microb. Technol.*, **12**, 591-595.

Tor, A., Danaoglu, N., Arslan, G., Cengeloglu, Y. 2009. Removal of fluoride from water by using granular red mud: batch and column studies. *Journal of Hazardous Materials*, **164**(1), 271-278.

Torab-Mostaedi, M., Asadollahzadeh, M., Hemmati, A., Khosravi, A. 2013. Equilibrium, kinetic, and thermodynamic studies for biosorption of cadmium and nickel on grapefruit peel. *Journal of the Taiwan Institute of Chemical Engineers*, **44**(2), 295-302.

Toth, J. 1971. State equations of the solid-gas interface layers. *Acta Chim Acad Sci Hungar*, **69**(3), 311-328.

Tóth, J. 2000. Calculation of the BET-Compatible Surface Area from Any Type I Isotherms Measured above the Critical Temperature. *Journal of Colloid and Interface Science*, **225**(2), 378-383.

Tran, H., Roddick, F. 1999. Comparison of chromatography and desiccant silica gels for the adsorption of metal ions. II. Fixed-bed study. *Water Research*, **33**(13), 3001-3011.

Treen-Sears, M.E., Volesky, B., Neufeld, R.J. 1984. Ion exchange/complexation of the uranyl ion by Rhizopus biosorbent. *Biotechnology and Bioengineering*, **26**(11), 1323-1329.

Trinelli, M.A., Areco, M.M., dos Santos Afonso, M. 2013. Co-biosorption of copper and glyphosate by Ulva lactuca. *Colloids and Surfaces B: Biointerfaces*, **105**(0), 251-258.

Tsai, L.J., Yu, K.C., Chen, S.F., Kung, P.Y. 2003. Effect of temperature on removal of heavy metals from contaminated river sediments via bioleaching. *Water Research*, **37**(10), 2449-2457.

Tsezos, M. 2007. Biological removal of ions: Principles and applications. *Biohydrometallury: From the Single Cell to the Environment*, **20-21**, 589-596.

Tsezos, M. 2009. Metal-microbes interactions: beyond environmental protection. *Biohydrometallurgy: A Meeting Point between Microbial Ecology, Metal Recovery Processes and Environmental Remediation*, **71-73**, 527-532.

Tsezos, M., Georgousis, Z. 1997. Mechanism of Aluminum Interference ön Uranium Biosorption by Rhizopus arrhizus.

Tsezos, M., Remoudaki, E., Angelatou, V. 1995. A systematic study on equilibrium and kinetics of biosorptive accumulation. The case of Ag and Ni. *International Biodeterioration and Biodegradation*, **35**(1), 129-153.

Tsezos, M., Remoudaki, E., Angelatou, V. 1996. A study of the effects of competing ions on the biosorption of metals. *International Biodeterioration and Biodegradation*, **38**(1), 19-29.

Tunali Akar, S., Arslan, D., Alp, T. 2012a. Ammonium pyrrolidine dithiocarbamate anchored Symphoricarpus albus biomass for lead(II) removal: Batch and column biosorption study. *Journal of Hazardous Materials*, **227/228**, 107-117.

Tunali Akar, S., Arslan, S., Alp, T., Arslan, D., Akar, T. 2012b. Biosorption potential of the waste biomaterial obtained from Cucumis melo for the removal of $Pb^{2+}$ ions from aqueous media: Equilibrium, kinetic, thermodynamic and mechanism analysis. *Chemical Engineering Journal*, **185–186**(0), 82-90.

Turgut, C. 2003. The contamination with organochlorine pesticides and heavy metals in surface water in Küçük Menderes River in Turkey, 2000–2002. *Environment International*, **29**(1), 29-32.

ul Islam, E., Yang, X.-e., He, Z.-l., Mahmood, Q. 2007. Assessing potential dietary toxicity of heavy metals in selected vegetables and food crops. *Journal of Zhejiang University Science B*, **8**(1), 1-13.

Ulmanu, M., Maranon, E., Fernandez, Y., Castrillon, L., Anger, I., Dumitriu, D. 2003. Removal of copper and cadmium ions from diluted aqueous solutions by low cost and waste material adsorbents. *Water Air and Soil Pollution*, **142**(1-4), 357-373.

Unal, D., Isik, N.O., Sukatar, A. 2010. Effects of Chromium VI stress on green alga Ulva lactuca (L.). *Turkish Journal of Biology*, **34**(2), 119-124.

Unnithan, M.R., Anirudhan, T. 2001. The kinetics and thermodynamics of sorption of chromium (VI) onto the iron (III) complex of a carboxylated polyacrylamide-grafted sawdust. *Industrial & Engineering Chemistry Research*, **40**(12), 2693-2701.

USEPA. 1979. Lead in water-related Environemental fate of 129 priority pollutants, vol 1. Introduction, technical background, Metals and inorganics, pesticides , Polychlorinated Biphenils. Office of water Planning and standards, U.S Environmental protection agency. *Washington, D.C.*, EPA-440/5-80-057.

USEPA. 1987. Meeting hazardous waste requirements for metal finisher in seminar publication, technology transfert. EPA 625/4-87/018.

USEPA. 1987. Meeting hazardous waste requirements for metal finisher in seminar publication, technology transfert. EPA 625/4-87/018.

USEPA. 1990. Innovative and alternative technology assesment manual, EPA, office of water Program Operations. EPA 625/7-90/007.

USEPA. 2002. Lead and Copper Monitoring and Reporting Guidance for Public Water Systems, . Ground Water and Drinking Water Division, US Environmental Protection Agency.

USEPA. 2002. Lead and Copper Monitoring and Reporting Guidance for Public Water Systems, Ground Water and Drinking Water Division, US Environmental Protection Agency, 245-789.

Valderrama, C., Arevalo, J.A., Casas, I., Martinez, M., Miralles, N., Florido, A. 2010. Modelling of the Ni(II) removal from aqueous solutions onto grape stalk wastes in fixed-bed column. *Journal of Hazardous Materials*, **174**(1-3), 144-150.

Van Genderen, E.J., Ryan, A.C., Tomasso, J.R., Klaine, S.J. 2005. Evaluation of acute copper toxicity to larval fathead minnows (Pimephales promelas) in soft surface waters. *Environmental Toxicology and Chemistry*, **24**(2), 408-414.

Van Hoof, S., Hashim, A., Kordes, A. 1999. The effect of ultrafiltration as pretreatment to reverse osmosis in wastewater reuse and seawater desalination applications. *Desalination*, **124**(1), 231-242.

Vargas, A.M.M., Cazetta, A.L., Kunita, M.H., Silva, T.L., Almeida, V.C. 2011. Adsorption of methylene blue on activated carbon produced from flamboyant pods (Delonix regia): Study of adsorption isotherms and kinetic models. *Chemical Engineering Journal*, **168**(2), 722-730.

Vaughan, T., Seo, C.W., Marshall, W.E. 2001. Removal of selected metal ions from aqueous solution using modified corncobs. *Bioresource Technology*, **78**(2), 133-139.

Vázquez, G., González-Álvarez, J., García, A.I., Freire, M.S., Antorrena, G. 2007. Adsorption of phenol on formaldehyde-pretreated Pinus pinaster bark: Equilibrium and kinetics. *Bioresource Technology*, **98**(8), 1535-1540.

Veglio, F., Beolchini, F. 1997. Removal of metals by biosorption: a review. *Hydrometallurgy*, **44**(3), 301-316.

Velmurugan, N., Hwang, G., Sathishkumar, M., Choi, T.K., Lee, K.J., Oh, B.T., Lee, Y.S. 2010. Isolation, identification, Pb(II) biosorption isotherms and kinetics of a lead adsorbing Penicillium sp MRF-1 from South Korean mine soil. *Journal of Environmental Sciences-China*, **22**(7), 1049-1056.

Venkata Mohan, S., Chandrasekhar Rao, N., Karthikeyan, J. 2002. Adsorptive removal of direct azo dye from aqueous phase onto coal based sorbents: a kinetic and mechanistic study. *Journal of Hazardous Materials*, **90**(2), 189-204.

Verma, V.K., Tewari, S., Rai, J.P.N. 2008. Ion exchange during heavy metal bio-sorption from aqueous solution by dried biomass of macrophytes. *Bioresource Technology*, **99**(6), 1932-1938.

Vidali, G., Ihm, G., Kim, H.-Y., Cole, M.W. 1991. Potentials of physical adsorption. *Surface Science Reports*, **12**(4), 135-181.

Vieira, A.P., Santana, S.A.A., Bezerra, C.W.B., Silva, H.A.S., de Melo, J.C.P., da Silva, E.C., Airoldi, C. 2010a. Copper sorption from aqueous solutions and sugar cane spirits by chemically modified babassu coconut (Orbignya speciosa) mesocarp. *Chemical Engineering Journal*, **161**(1-2), 99-105.

Vieira, M.G.A., Neto, A.F.A., Gimenes, M.L., da Silva, M.G.C. 2010b. Removal of nickel on Bofe bentonite calcined clay in porous bed. *Journal of Hazardous Materials*, **176**(1-3), 109-118.

Vieira, R.H., Volesky, B. 2010. Biosorption: a solution to pollution? *International Microbiology*, **3**(1), 17-24.

Vieth, W.R., Sladek, K.J. 1965. A model for diffusion in a glassy polymer. *Journal of Colloid Science*, **20**(9), 1014-1033.

Vijayaraghavan, K., Arun, M., Joshi, U.M., Balasubramanian, R. 2009. A Comparative Study of Seven Materials as Sorbents for Removal of Metal Ions from Real Storm Water Runoff. *Icheap-9: 9th International Conference on Chemical and Process Engineering, Pts 1-3*, **17**, 379-384.

Vijayaraghavan, K., Jegan, J., Palanivelu, K., Velan, M. 2004. Removal of nickel(II) ions from aqueous solution using crab shell particles in a packed bed up-flow column. *Journal of Hazardous Materials*, **113**(1-3), 223-230.

Vijayaraghavan, K., Padmesh, T., Palanivelu, K., Velan, M. 2006. Biosorption of nickel (II) ions onto *Sargassum wightii*: Application of two-parameter and three-parameter isotherm models. *Journal of Hazardous Materials*, **133**(1), 304-308.

Vijayaraghavan, K., Prabu, D. 2006. Potential of *Sargassum wightii* biomass for copper(II) removal from aqueous solutions: Application of different mathematical models to batch and continuous biosorption data. *Journal of Hazardous Materials*, **137**(1), 558-564.

Vijayaraghavan, K., Yun, Y.S. 2008. Polysulfone-immobilized Corynebacterium glutamicum: A biosorbent for Reactive black 5 from aqueous solution in an up-flow packed column. *Chemical Engineering Journal*, **145**(1), 44-49.

Vilar, V., Botelho, C., Boaventura, R. 2007a. Modeling equilibrium and kinetics of metal uptake by algal biomass in continuous stirred and packed bed adsorbers. *Adsorption-Journal of the International Adsorption Society*, **13**(5), 587-601.

Vilar, V.J., Botelho, C., Boaventura, R.A. 2007b. Methylene blue adsorption by algal biomass based materials: Biosorbents characterization and process behaviour. *Journal of Hazardous Materials*, **147**(1), 120-132.

Vilar, V.J., Botelho, C., Loureiro, J.M., Boaventura, R.A. 2008. Biosorption of copper by marine algae *Gelidium* and algal composite material in a packed bed column. *Bioresource Technology*, **99**(13), 5830-5838.

Vilar, V.J.P., Botelho, C.M.S., Pinheiro, J.P.S., Domingos, R.F., Boaventura, R.A.R. 2009. Copper removal by algal biomass: Biosorbents characterization and equilibrium modelling. *Journal of Hazardous Materials*, **163**(2-3), 1113-1122.

Villaescusa, I., Fiol, N., Martínez, M.a., Miralles, N., Poch, J., Serarols, J. 2004. Removal of copper and nickel ions from aqueous solutions by grape stalks wastes. *Water Research*, **38**(4), 992-1002.

Vinodhini, R., Narayanan, M. 2008. Bioaccumulation of heavy metals in organs of fresh water fish Cyprinus carpio (Common carp). *Int. J. Environ. Sci. Tech*, **5**(2), 179-182.

Volesky, B. 1994. Advances in Biosorption of Metals - Selection of Biomass Types. *Fems Microbiology Reviews*, **14**(4), 291-302.

Volesky, B. 1999. Biosorption for the Next Century. in: *Process Metallurgy*, (Eds.) R. Amils, A. Ballester, Vol. Volume 9, Elsevier, pp. 161-170.

Volesky, B. 2001. Detoxification of metal-bearing effluents: biosorption for the next century. *Hydrometallurgy*, **59**(2-3), 203-216.

Volesky, B. 2003. Biosorption process simulation tools. *Hydrometallurgy*, **71**(1–2), 179-190.

Volesky, B. 2007. Biosorption and me. *Water Research*, **41**(18), 4017-4029.

Volesky, B., Holan, Z. 1995. Biosorption of heavy metals. *Biotechnology Progress*, **11**(3), 235-250.

Volesky, B., Holan, Z.R. 1995. Biosorption of heavy metals. *Biotechnology Progress*, **11**(3), 235-250.

Waite, T., Davis, J., Payne, T., Waychunas, G., Xu, N. 1994. Uranium (VI) adsorption to ferrihydrite: Application of a surface complexation model. *Geochimica Et Cosmochimica Acta*, **58**(24), 5465-5478.

Walcarius, A., Mercier, L. 2010. Mesoporous organosilica adsorbents: nanoengineered materials for removal of organic and inorganic pollutants. *Journal of Materials Chemistry*, **20**(22), 4478-4511.

Wan, M.W., Kan, C.C., Rogel, B.D., Dalida, M.L.P. 2010. Adsorption of copper (II) and lead (II) ions from aqueous solution on chitosan-coated sand. *Carbohydrate Polymers*, **80**(3), 891-899.

Wang, J., Chen, C. 2006. Biosorption of heavy metals by *Saccharomyces cerevisiae*: A review. *Biotechnology Advances*, **24**(5), 427-451.

Wang, J.L., Chen, C. 2009. Biosorbents for heavy metals removal and their future. *Biotechnology Advances*, **27**(2), 195-226.

Wang, X. S., Qin, Y. 2005. Equilibrium sorption isotherms for of $Cu^{2+}$ on rice bran. *Process Biochemistry*, **40**(2), 677-680.

Wang, X. S., Tang, Y.P., Tao, S.R. 2008. Removal of Cr (VI) from aqueous solutions by the nonliving biomass of Alligator weed: kinetics and equilibrium. *Adsorption-Journal of the International Adsorption Society*, **14**(6), 823-830.

Wang, Y.T., Shen, H. 1995. Bacterial reduction of hexavalent chromium. *Journal of Industrial Microbiology*, **14**(2), 159-163.

Wankasi, D., Horsfall, M., Spiff, A.I. 2005. Retention of Pb(II) ion from aqueous solution by Nipah palm (Nypa fruticans Wurmb) petiole biomass. *Journal of the Chilean Chemical Society*, **50**(4), 691-696.

Ward, D., Young, T.P. 2002. Effects of large mammalian herbivores and ant symbionts on condensed tannins of Acacia drepanolobium in Kenya. *Journal of Chemical Ecology*, **28**(5), 921-937.

Warner, C.L., Addleman, R.S., Cinson, A.D., Droubay, T.C., Engelhard, M.H., Nash, M.A., Yantasee, W., Warner, M.G. 2010. High-Performance, Superparamagnetic, Nanoparticle-Based Heavy Metal Sorbents for Removal of Contaminants from Natural Waters. *Chemsuschem*, **3**(6), 749-757.

Weber, W., Morris, J. 1963. Kinetics of adsorption on carbon from solution. *J. Sanit. Eng. Div. Am. Soc. Civ. Eng*, **89**(17), 31-60.

Weber, W.J., Morris, T. 1963. Kinetics of adsorption on carbon from solution. *J. Sanit. Eng. Div. Proc.*, **89**, 31.

Wei, L.S., Yang, G., Wang, R., Ma, W. 2009. Selective adsorption and separation of chromium (VI) on the magnetic iron-nickel oxide from waste nickel liquid. *Journal of Hazardous Materials*, **164**(2-3), 1159-1163.

Whiston, C. 1987. *X-ray methods (Analytical chemistry by open learning)*. John Wiley and Sons, USA.

White, C., Wilkinson, S.C., Gadd, G.M. 1995. The role of microorganisms in biosorption of toxic metals and radionuclides. *International Biodeterioration and Biodegradation*, **35**(1-3), 17-40.

WHO. 1974. World Health Organization. Environmental Health Criteria for Cadmium.

Wickes, J.A. 1929. Ancient Documents and Hearsay. *Tex. L. Rev.*, **8**, 451.

Wilson, K., Yang, H., Seo, C.W., Marshall, W.E. 2006. Select metal adsorption by activated carbon made from peanut shells. *Bioresource Technology*, **97**(18), 2266-2270.

Witek, K., Anna, Harikishore, K., Reddy, D. 2013. Removal of microelemental Cr(III) and Cu(II) by using soybean meal waste – Unusual isotherms and insights of binding mechanism. *Bioresource Technology*, **127**(0), 350-357.

Witek-Krowiak, A. 2012. Analysis of temperature-dependent biosorption of $Cu^{2+}$ ions on sunflower hulls: Kinetics, equilibrium and mechanism of the process. *Chemical Engineering Journal*, **192**(0), 13-20.

Witek-Krowiak, A., Krysiak, M., Modelski, S., Eckert, K., Kloczkowski, P. 2010. Biosorption of cationic dyes from aqueous solutions with maple leaves. *Chemical and Process Engineering Selected full texts*, **31**(4), 825-837.

Witek-Krowiak, A., Szafran, R.G., Modelski, S. 2011. Biosorption of heavy metals from aqueous solutions onto peanut shell as a low-cost biosorbent. *Desalination*, **265**(1–3), 126-134.

Wolborska, A. 1989. Adsorption on activated carbon of p-nitrophenol from aqueous solution. *Water Research*, **23**(1), 85-91.

Wong, K.K., Lee, C.K., Low, K.S., Haron, M.J. 2003. Removal of Cu(II) and Pb(II) by tartaric acid modified rice husk from aqueous solutions. *Chemosphere*, **50**(1), 23-28.

Wright, R.J., Stuczynski, T., Sparks, D., Page, A., Helmke, P., Loeppert, R., Soltanpour, P., Tabatabai, M., Johnston, C., Sumner, M. 1996. Atomic absorption and flame emission spectrometry. *Methods of soil analysis. Part 3-chemical methods.*, 65-90.

Wu, S.J., Li, F.T., Xu, R., Wei, S.H., Li, G.T. 2010. Synthesis of thiol-functionalized MCM-41 mesoporous silicas and its application in Cu(II), Pb(II), Ag(I), and Cr(III) removal. *Journal of Nanoparticle Research*, **12**(6), 2111-2124.

Wu, W., Bromberg, P.A., Samet, J.M. 2013. Zinc ions as effectors of environmental oxidative lung injury. *Free Radical Biology and Medicine*, **65**(0), 57-69.

WWDR4. 2012. The 4th edition of the UN World Water Development Report (WWDR4). *The United Nations Educational, Scientific and Cultural Organization (UNESCO)*, **4**, 1-250.

Xiang, Z.Y., Lu, Y.C., Gong, X.C., Luo, G.S. 2010. Absorption and desorption of gaseous toluene by an absorbent microcapsules column. *Journal of Hazardous Materials*, **173**(1-3), 243-248.

Xiangliang, P., Jianlong, W., Daoyong, Z. 2005. Biosorption of Pb(II) by *Pleurotus ostreatus* immobilized in calcium alginate gel. *Process Biochemistry*, **40**(8), 2799-2803.

Xu, M., Zhang, Y., Zhang, Z., Shen, Y., Zhao, M., Pan, G. 2011. Study on the adsorption of $Ca^{2+}$, $Cd^{2+}$ and $Pb^{2+}$ by magnetic $Fe_3O_4$ yeast treated with EDTA dianhydride. *Chemical Engineering Journal*.

Xu, M., Zhang, Y., Zhang, Z., Shen, Y., Zhao, M., Pan, G. 2011. Study on the adsorption of $Ca^{2+}$, $Cd^{2+}$ and $Pb^{2+}$ by magnetic $Fe_3O_4$ yeast treated with EDTA dianhydride. *Chemical Engineering Journal*.

Xue, Y., Hou, H., Zhu, S. 2009. Competitive adsorption of copper(II), cadmium(II), lead(II) and zinc(II) onto basic oxygen furnace slag. *Journal of Hazardous Materials*, **162**(1), 391-401.

Yadav, S. 2010. Heavy metals toxicity in plants: an overview on the role of glutathione and phytochelatins in heavy metal stress tolerance of plants. *South African Journal of Botany*, **76**(2), 167-179.

Yahaya, N.E.M., Pakir, M.F., Latiff, M., Abustan, I., Bello, O.S., Ahmad, M.A. 2011. Fixed Bed Column Study for Cu(II) Removal from Aqueous Solutions Using Rice Husk Based Activated Carbon. *Int. J. Eng. Technol.*, **11**(1), 248-252.

Yalcin, E., Cavusoglu, K., Maras, M., Biyikoglu, M. 2008. Biosorption of lead(II) and copper(II) metal ions on Cladophora glomerata (L.) kutz. (Chlorophyta) algae: Effect of algal surface modification. *Acta Chimica Slovenica*, **55**(1), 228-232.

Yan, C.Z., Li, G.X., Xue, P.Y., Wei, Q.S., Li, Q.Z. 2010. Competitive effect of Cu(II) and Zn(II) on the biosorption of lead(II) by Myriophyllum spicatum. *Journal of Hazardous Materials*, **179**(1-3), 721-728.

Yan, G.Y., Viraraghavan, T. 2003. Heavy-metal removal from aqueous solution by fungus Mucor rouxii. *Water Research*, **37**(18), 4486-4496.

Yang, F., Pecina, D.A., Kelly, S.D., Kim, S.H., Kemner, K.M., Long, D.T., Marsh, T.L. 2010. Biosequestration via cooperative binding of copper by Ralstonia pickettii. *Environmental Technology*, **31**(8-9), 1045-1060.

Yang, H., Yan, R., Chen, H., Lee, D.H., Liang, D.T., Zheng, C. 2006a. Mechanism of palm oil waste pyrolysis in a packed bed. *Energy & Fuels*, **20**(3), 1321-1328.

Yang, H., Yan, R., Chen, H., Lee, D.H., Liang, D.T., Zheng, C. 2006b. Pyrolysis of palm oil wastes for enhanced production of hydrogen rich gases. *Fuel Processing Technology*, **87**(10), 935-942.

Yang, H.J., Kim, H., Guo, C.Y. 2010. Metal Ion Extraction with Bipyridine Derivatives as Chelating Ligands in Supercritical Carbon Dioxide. *Clean-Soil Air Water*, **38**(2), 159-166.

Yang, L., Chen, J.P. 2008. Biosorption of hexavalent chromium onto raw and chemically modified Sargassum sp. *Bioresource Technology*, **99**(2), 297-307.

Yang, S., Li, J., Shao, D., Hu, J., Wang, X. 2009. Adsorption of Ni (II) on oxidized multi-walled carbon nanotubes: effect of contact time, pH, foreign ions and PAA. *Journal of Hazardous Materials*, **166**(1), 109-116.

Yang, X., Al-Duri, B. 2005. Kinetic modeling of liquid-phase adsorption of reactive dyes on activated carbon. *Journal of Colloid and Interface Science*, **287**(1), 25-34.

Yao, Z.Y., Qi, J.H., Wang, L.H. 2010. Equilibrium, kinetic and thermodynamic studies on the biosorption of Cu(II) onto chestnut shell. *Journal of Hazardous Materials*, **174**(1-3), 137-143.

Yoon, Y.H., Nelson, J.H. 1984. Application of Gas Adsorption Kinetics I. A Theoretical Model for Respirator Cartridge Service Life. *American Industrial Hygiene Association Journal*, **45**(8), 509-516.

Yu, L.J., Shukla, S.S., Dorris, K.L., Shukla, A., Margrave, J.L. 2003. Adsorption of chromium from aqueous solutions by maple sawdust. *Journal of Hazardous Materials*, **100**(1-3), 53-63.

Yu, Q., Matheickal, J.T., Yin, P., Kaewsarn, P. 1999. Heavy metal uptake capacities of common marine macro algal biomass. *Water Research*, **33**(6), 1534-1537.

Yu, Q.M., Kaewsarn, P., Ma, W.D., Matheickal, J.T., Yin, P.H. 2001. Removal of heavy metal ions from wastewater by using biosorbents from marine algae - A cost effective new technology. *Chinese Journal of Chemical Engineering*, **9**(2), 133-136.

Yu, Y., Zhuang, Y.-Y., Wang, Z.-H. 2001. Adsorption of water-soluble dye onto functionalized resin. *Journal of Colloid and Interface Science*, **242**(2), 288-293.

Yuan, X.Z., Meng, Y.T., Zeng, G.M., Fang, Y.Y., Shi, J.G. 2008. Evaluation of tea-derived biosurfactant on removing heavy metal ions from dilute wastewater by ion flotation. *Colloids and Surfaces A: Physicochemical and Engineering Aspects*, **317**(1-3), 256-261.

Yun, C.H., Prasad, R., Guha, A.K., Sirkar, K.K. 1993. Hollow fiber solvent extraction removal of toxic heavy metals from aqueous waste streams. *Industrial and Engineering Chemistry Research*, **32**(6), 1186-1195.

Yurlova, L., Kryvoruchko, A., Kornilovich, B. 2002. Removal of Ni(II) ions from wastewater by micellar-enhanced ultrafiltration. *Desalination*, **144**(1-3), 255-260.

Yurtsever, M., Sengil, I.A. 2009. Biosorption of Pb(II) ions by modified quebracho tannin resin. *Journal of Hazardous Materials*, **163**(1), 58-64.

Zeroual, Y., Moutaouakkil, A., Zohra Dzairi, F., Talbi, M., Ung Chung, P., Lee, K., Blaghen, M. 2003. Biosorption of mercury from aqueous solution by *Ulva lactuca* biomass. *Bioresource Technology*, **90**(3), 349-351.

Zhang, H., Cao, H., Meng, Y., Jin, G., Zhu, M. 2012. The toxicity of cadmium ($Cd^{2+}$) towards embryos and pro-larva of soldatov's catfish (Silurus soldatovi). *Ecotoxicology and Environmental Safety*, **80**(0), 258-265.

Zhang, R., Zhou, L., Zhang, F., Ding, Y., Gao, J., Chen, J., Yan, H., Shao, W. 2013. Heavy metal pollution and assessment in the tidal flat sediments of Haizhou Bay, China. *Marine Pollution Bulletin*, **74**(1), 403-412.

Zhang, W., Li, C.Y., Mei, L.A., Geng, Y.M., Lu, C.H. 2010. Preparation of carboxylate-functionalized cellulose via solvent-free mechanochemistry and its characterization as a biosorbent for removal of $Pb^{2+}$ from aqueous solution. *Journal of Hazardous Materials*, **181**(1-3), 468-473.

Zhang, W., Liu, X., Cheng, H., Zeng, E.Y., Hu, Y. 2012b. Heavy metal pollution in sediments of a typical mariculture zone in South China. *Marine Pollution Bulletin*, **64**(4), 712-720.

Zhang, Y., Banks, C. 2006. A comparison of the properties of polyurethane immobilised *Sphagnum* moss, seaweed, sunflower waste and maize for the biosorption of Cu, Pb, Zn and Ni in continuous flow packed columns. *Water Research*, **40**(4), 788-798.

Zhang, Y., Liu, W., Xu, M., Zheng, F., Zhao, M. 2010. Study of the mechanisms of $Cu^{2+}$ biosorption by ethanol/caustic-pretreated baker's yeast biomass. *Journal of Hazardous Materials*, **178**(1–3), 1085-1093.

Zhang, Y., Liu, W., Xu, M., Zheng, F., Zhao, M. 2010. Study of the mechanisms of $Cu^{2+}$ biosorption by ethanol/caustic-pretreated baker's yeast biomass. *Journal of Hazardous Materials*, **178**(1–3), 1085-1093.

Zheng, L.C., Dang, Z., Yi, X.Y., Zhang, H. 2010. Equilibrium and kinetic studies of adsorption of Cd(II) from aqueous solution using modified corn stalk. *Journal of Hazardous Materials*, **176**(1-3), 650-656.

Zhong, L. X., Peng, X. W., Yang, D., Sun, R. C. 2012. Adsorption of heavy metals by a porous bioadsorbent from lignocellulosic biomass reconstructed in an ionic liquid. *Journal of Agricultural and Food Chemistry*, **60**(22), 5621-5628.

Zhou, Y., Chen, L., Lu, P., Tang, X., Lu, J. 2011. Removal of bisphenol A from aqueous solution using modified fibric peat as a novel biosorbent. *Separation and Purification Technology*, **81**(2), 184-190.

Zhu, Y., Hu, J., Wang, J. 2012. Competitive adsorption of Pb(II), Cu(II) and Zn(II) onto xanthate-modified magnetic chitosan. *Journal of Hazardous Materials*, **221–222**(0), 155-161.

Zou, W., Han, R., Chen, Z., Jinghua, Z., Shi, J. 2006. Kinetic study of adsorption of Cu(II) and Pb(II) from aqueous solutions using manganese oxide coated zeolite in batch mode. *Colloids and Surfaces A: Physicochemical and Engineering Aspects*, **279**(1–3), 238-246.

Zouboulis, A., Loukidou, M., Matis, K. 2004. Biosorption of toxic metals from aqueous solutions by bacteria strains isolated from metal-polluted soils. *Process Biochemistry*, **39**(8), 909-916.

Zouboulis, A.I., Lazaridis, I., Mlatis, K.A. 2008. The process of flotation: an efficient solid/liquid separation technique for biological materials. *International Journal of Environment and Pollution*, **32**(1), 29-42.

Zouboulis, A.I., Matis, K.A., Hancock, I.C. 1997. Biosorption of metals from dilute aqueous solutions. *Separation and Purification Methods*, **26**(2), 255-295.

Zouboulis, A.I., Matis, K.A., Lazaridis, N.K. 2001. Removal of metal ions from simulated wastewater by Saccharomyces yeast biomass: Combining biosorption and flotation processes. *Separation Science and Technology*, **36**(3), 349-365.

ZU, Y. G., ZHAO, X. H., HU, M. S., REN, Y., XIAO, P., ZHU, L., CAO, Y. J., ZHANG, Y. 2006. Biosorption effects of copper ions on *Candida utilis* under negative pressure cavitation. *Journal of Environmental Sciences*, **18**(6), 1254-1259.

Zuo, X., Balasubramanian, R., Fu, D., Li, H. 2012. Biosorption of copper, zinc and cadmium using sodium hydroxide immersed Cymbopogon schoenanthus L. Spreng (lemon grass). *Ecological Engineering*, **49**(0), 186-189.

Zvinowanda, C.M., Okonkwo, J.O., Agyei, N.M., Staden, M.V., Jordaan, W., Kharebe, B.V. 2010. Recovery of Lead(II) from Aqueous Solutions by Zea mays Tassel Biosorption. *American Journal of Biochemistry and Biotechnology*, **6**(1), 1-10.


**Faculty of Engineering and Information Technology**
**University of Technology, Sydney (UTS)**

# Appendices

# Appendix I

## MATLAB Programming for Isotherm

### M-file for object function

```
function [err, predY] = objfunction(p, varargin)
x = varargin{1};
y = varargin{2};
t = varargin{3};
switch t
   case 1
      % Langmuir Function
      qm = p(1);
      b = p(2);
      predY = (qm*b.*x)./(1+b.*x);

   case 2
      % Freundlich Function
      qm = p(1);
      n = p(2);
      predY = qm*x.^(1/n);

   case 3
      % Sips Function
      qm = p(1);
      b = p(2);
      n = p(3);
     predY =(qm*b*x.^(1/n))./(1+b*x.^(1/n));

   case 4
      % Toth Function
      qm = p(1);
      b = p(2);
      n = p(3);
      predY = (qm*x)./(b+x.^n).^(1/n);

   case 5
      % Unilan Function
      qm = p(1);
      b = p(2);
      s = p(3);
      predY = qm./(2*s).*log((1+b*exp(s)*x)./(1+b*exp(-s)*x));

   case 6
      % Langmuir-Sips Function
      qm = p(1);
      b1 = p(2);
```

```
        b2 = p(3);
        n = p(4);
        predY = (qm*b1*x./(1+b1*x)+(qm*b2*x.^(1/n))./(1+b2*x.^(1/n)));
     case 7
        % BET Function
        vm = p(1);
        c = p(2);
        cs = 300000;
        predY = (vm*c.*x)./((cs-x).*(1+(c-1).*x/cs));

    case 8
        % Ext - Langmuir
        n = length(p);
        s = 0;
        den = 1;
        for i = 1:n
            b = p{i}(2);
            den = den + (b.*x(:, i));
        end

        for i = 1:n
            qm = p{i}(1);
            b = p{i}(2);
            num = (qm*b.*x(:, i));
            s = s + (num./den);
        end
        predY = s;
    case 10
        % Ext - Sips
        n = length(p);
        s = 0;
        den = 1;
        for i = 1:n
            b = p{i}(2);
            n = p{i}(3);
            den = den + (b.*x(:, i)).^(1/n);
        end
        for i = 1:n
            qm = p{i}(1);
            b = p{i}(2);
            n = p{i}(3);
            num = (qm*b.*x(:, i).^(1/n));
            s = s + (num./den);
        end
        predY = s;
    otherwise
end
if length(x) == length(y)
    err = sum((y-predY).^2);
else
```

```
    err = 0;
end
```

## M-file Datafit

```
function varargout = datafit(varargin)
% DATAFIT MATLAB code for datafit.fig

gui_State = struct('gui_Name',       mfilename, ...
    'gui_Singleton',  gui_Singleton, ...
    'gui_OpeningFcn', @datafit_OpeningFcn, ...
    'gui_OutputFcn',  @datafit_OutputFcn, ...
    'gui_LayoutFcn',  [] , ...
    'gui_Callback',   []);
if nargin && ischar(varargin{1})
    gui_State.gui_Callback = str2func(varargin{1});
end
if nargout
    [varargout{1:nargout}] = gui_mainfcn(gui_State, varargin{:});
else
    gui_mainfcn(gui_State, varargin{:});
end
% End initialization code - DO NOT EDIT

% --- Executes just before datafit is made visible.
function datafit_OpeningFcn(hObject, eventdata, handles, varargin)
handles.output = hObject;
% Update handles structure
guidata(hObject, handles);
initialize_gui(hObject, eventdata, handles, false);
% UIWAIT makes datafit wait for user response (see UIRESUME)
% uiwait(handles.figure1);
 % --- Outputs from this function are returned to the command line.
function varargout = datafit_OutputFcn(hObject, eventdata, handles)
% varargout  cell array for returning output args (see VARARGOUT);
% hObject    handle to figure
% eventdata  reserved - to be defined in a future version of MATLAB
% handles    structure with handles and user data (see GUIDATA)
% Get default command line output from handles structure
varargout{1} = handles.output;

% GUI Initialization
% ---------------------------------------------------------------------
function initialize_gui(hObject, eventdata, handles, isreset)
% Check Reset
if ~isreset
    % Add directory to search path.
    if ~strncmp(path, pwd, length(pwd))
        addpath(genpath(pwd),'-end');
```

```
    end
    handles.data.pwd = pwd;

    handles.data.text2{1} = '-- Langmuir Isotherm --\n   qm b P\n     q = -----\n      1+b P';
    handles.data.text2{2} = '-- Freundlich Isotherm --\n     q = qm P^(1/n)';
    handles.data.text2{3} = '-- Sips Isotherm --\n       qm b P^(1/n) \n     q = ---\n 1+b
P^(1/n)';
    handles.data.text2{4} = '-- Toth Isotherm --\n       qm P  \n     q = ---\n  (b + P^n)^
(1/n)';
    handles.data.text2{5} = '-- Unlilan Isotherm --\n              qm          1 + b e(s) P  \n     q
= -------- ln ------------------\n              2 s          1 + b e(-s) P';
    handles.data.text2{6} = '-- Langmuir-Sips Isotherm --\n            qm bl P        qm bs
P^(1/n)  \n     q = ---------- + -----------------\n           1 + bl P        1 + bs P^(1/n)';
    handles.data.text2{7} = '-- BET Isotherm --\n                    vm c P  \n     q = ------------
--------------\n            (cs-P) (1+(c-1)P/cs)';
    handles.data.text3 = {char('qm', 'b'), char('qm', 'n'), char('qm', 'b', 'n'), char('qm', 'b',
'n'), ...
        char('qm', 'b', 's'), char('qm', 'b1', 'b2', 'n'), char('vm', 'c')};
    handles.data.xmin = 0;
    handles.data.xmax = 0;
    handles.data.ymin = 0;
    handles.data.ymax = 0;
end
cla(handles.ui_axes1, 'reset');
% data initialize
handles.data.list = 1;
handles.data.nlist = [];
handles.data.xlist = [];
handles.data.toggle = 0;
handles.data.method = 'Langmuir';
handles.data.ftype = 1;
handles.data.ident = 0;
handles.data.text1 = '';
handles.data.iv = {[10; 1], [10; .5], [10; .5; .5], [10; .5; .5], [10; .5; .5] ...
    , [10; .5; .5; 1], [10; 10000]};
handles.data.lb = {[0; 0], [0; 0], [0; 0; 0], [0; 0; 0], [0; 0; 0], [0; 0; 0; 0], [0; 0]};
handles.data.ub = {[1e10; 1e10], [1e10; 1e10], [1e10; 1e10; 1e10], [1e10; 1e10; 1e10]
...
    , [1e10; 1e10; 1e10], [1e10; 1e10; 1e10; 1e10], [1e10; 1e10]};

% GUI Obj initialize
set(handles.ui_sim, 'Enable', 'off');
set(handles.ui_toggle, 'Value', 0);
set(handles.ui_toggle, 'String', 'Current');
set(handles.ui_bt1, 'Value', 1);
set(handles.ui_list, 'Value', 1);
set(handles.ui_list, 'String', 'FileNames');
set(handles.ui_edit1, 'String', 'Data');
set(handles.ui_edit2, 'String', 'Result');
set(handles.ui_bt1, 'String', 'Langmuir');
```

```
set(handles.ui_bt2, 'String', 'Freundlich');
set(handles.ui_bt3, 'Visible', 'on');
set(handles.ui_bt4, 'Visible', 'on');
set(handles.ui_bt5, 'Visible', 'on');
set(handles.ui_bt6, 'Visible', 'on');
set(handles.ui_bt7, 'Visible', 'on');
set(handles.ui_iv, 'String', '[10; 1]');
set(handles.ui_lb, 'String', '[0; 0]');
set(handles.ui_ub, 'String', '[1e10; 1e10]');
set(handles.ui_xmin, 'Enable', 'off');
set(handles.ui_xmax, 'Enable', 'off');
set(handles.ui_ymin, 'Enable', 'off');
set(handles.ui_ymax, 'Enable', 'off');
% Update handles structure
guidata(hObject, handles);

% --------------------------------------------------------------------
function ui_reset_Callback(hObject, eventdata, handles)
initialize_gui(hObject, eventdata, handles, true);
function ui_end_Callback(hObject, eventdata, handles)
close(gcf);
function ui_sim_Callback(hObject, eventdata, handles)
set(handles.ui_sim, 'Enable', 'off');
h = handles.ui_axes1;
try
   % fmincon option
   fminopt = optimset('Display', 'off', 'FunValCheck', 'on', 'MaxFunEvals', 500);
   fminopt = optimset(fminopt, 'Algorithm', 'interior-point');
   fminopt = optimset(fminopt, 'OutputFcn', @outputfunction);
   fminopt = optimset(fminopt, 'UseParallel', 'always');
   %fminopt = optimset(fminopt, 'PlotFcns',{@optimplotx, @optimplotfval,
@optimplotfirstorderopt, @optimplotstepsize});
   c = '+o*xsdpn';
   str1 = handles.data.text1;
   if handles.data.toggle
      n = 1;
      m = 7;
   else
      n = handles.data.ftype;
      m = n;
   end
   s = 0;
   l = cell(2, length(handles.data.list));
   for i = n:m
      str1 = sprintf(sprintf('%s%s\n', str1, handles.data.text2{i}));
      str2 = '';
      for j = handles.data.list
         x = handles.sdata(j).data(:, 1);
         y = handles.sdata(j).data(:, end);
         plot(h, x, y, ['r' c(j)], 'MarkerSize', 6);
```

```
        xlabel(h, handles.sdata(j).label{1}, 'HorizontalAlignment', 'center', 'FontSize', 12);
        ylabel(h, handles.sdata(j).label{2}, 'HorizontalAlignment', 'center', 'FontSize', 12);
           title(h, 'Isotherm', 'HorizontalAlignment', 'center', 'FontSize', 14)
           hold(h, 'on');
           [p, fval] = fmincon(@objfunction, handles.data.iv{i}, [], [], [], [], ...
              handles.data.lb{i}, handles.data.ub{i}, [], fminopt, x, y, i, h);
           str2 = sprintf('%s- %d - %s\n', str2, j, handles.sdata(j).file);
           for k = 1:length(p)
              str2 = sprintf('%s%s = %g\n', str2, handles.data.text3{i}(k, :), p(k));
           end
           str2 = sprintf('%ssor = %g\n', str2, fval);
           handles.fdata(j).name{i} = handles.sdata(j).label{2};
           handles.fdata(j).param{i} = p;
           handles.fdata(j).error{i} = fval;
           s = s + 1;
           l{1, s} = handles.sdata(j).file;
           l{2, s} = handles.sdata(j).file;
        end
        if ~handles.data.toggle
           legend(h, l(:), 'Location', 'Best', 'Interpreter', 'none');
           hold(h, 'off');
        end
        str1 = sprintf('%s%s\n', str1, str2);
        set(handles.ui_edit2, 'String', str1);
        handles.data.text1 = str1;
     end
  catch me1
     msgbox({me1.identifier, me1.message}, 'error');
  end
  set(handles.ui_sim, 'Enable', 'on');
  hold(h, 'off');
  guidata(hObject, handles);
  % --------------------------------------------------------------------
  function ui_list_Callback(hObject, eventdata, handles)
  handles.data.list = get(hObject, 'Value');
  handles.data.xlist = setdiff(handles.data.nlist, handles.data.list);
  guidata(hObject, handles);
  function ui_list_CreateFcn(hObject, eventdata, handles)
  % Hint: listbox controls usually have a white background on Windows.
  %       See ISPC and COMPUTER.
  if ispc && isequal(get(hObject,'BackgroundColor'),
  get(0,'defaultUicontrolBackgroundColor'))
     set(hObject,'BackgroundColor','white');
  end
  function ui_edit1_Callback(hObject, eventdata, handles)
  function ui_edit1_CreateFcn(hObject, eventdata, handles)
  % Hint: edit controls usually have a white background on Windows.
  %       See ISPC and COMPUTER.
  if ispc && isequal(get(hObject,'BackgroundColor'),
  get(0,'defaultUicontrolBackgroundColor'))
```

```
   set(hObject,'BackgroundColor','white');
end
function ui_edit2_Callback(hObject, eventdata, handles)
function ui_edit2_CreateFcn(hObject, eventdata, handles)
% Hint: edit controls usually have a white background on Windows.
%       See ISPC and COMPUTER.
if ispc && isequal(get(hObject,'BackgroundColor'),
get(0,'defaultUicontrolBackgroundColor'))
   set(hObject,'BackgroundColor','white');
end
function ui_iv_Callback(hObject, eventdata, handles)
handles.data.iv{handles.data.ftype} = str2num(get(hObject, 'String'));
guidata(hObject, handles);
function ui_iv_CreateFcn(hObject, eventdata, handles)
% Hint: edit controls usually have a white background on Windows.
%       See ISPC and COMPUTER.
if ispc && isequal(get(hObject,'BackgroundColor'),
get(0,'defaultUicontrolBackgroundColor'))
   set(hObject,'BackgroundColor','white');
end
function ui_lb_Callback(hObject, eventdata, handles)
handles.data.lb{handles.data.ftype} = str2num(get(hObject, 'String'));
guidata(hObject, handles);
function ui_lb_CreateFcn(hObject, eventdata, handles)
% Hint: edit controls usually have a white background on Windows.
%       See ISPC and COMPUTER.
if ispc && isequal(get(hObject,'BackgroundColor'),
get(0,'defaultUicontrolBackgroundColor'))
   set(hObject,'BackgroundColor','white');
end
function ui_ub_Callback(hObject, eventdata, handles)
handles.data.ub{handles.data.ftype} = str2num(get(hObject, 'String'));
guidata(hObject, handles);
function ui_ub_CreateFcn(hObject, eventdata, handles)
% Hint: edit controls usually have a white background on Windows.
%       See ISPC and COMPUTER.
if ispc && isequal(get(hObject,'BackgroundColor'),
get(0,'defaultUicontrolBackgroundColor'))
   set(hObject,'BackgroundColor','white');
end
function handles = ui_panel2_SelectionChangeFcn(hObject, eventdata, handles)
handles.data.method = get(hObject, 'String');
switch handles.data.method
   case 'Langmuir'
      % Langmuir Function
      handles.data.ftype = 1;
   case 'Freundlich'
      % Freundlich Function
      handles.data.ftype = 2;
   case 'Sips'
```

```
        % Sips Function
        handles.data.ftype = 3;
    case 'Toth'
        % Toth Function
        handles.data.ftype = 4;
    case 'Unilan'
        % Unilan Function
        handles.data.ftype = 5;
    case 'Langmuir-Sips'
        % Langmuir-Sips Function
        handles.data.ftype = 6;
    case 'BET'
        % BET Function
        handles.data.ftype = 7;
    otherwise
        handles.data.ftype = 99;
end
if handles.data.ftype < 8
    set(handles.ui_iv, 'String', ['[', sprintf('%g;', handles.data.iv{handles.data.ftype}), ']']);
    set(handles.ui_lb, 'String', ['[', sprintf('%g;', handles.data.lb{handles.data.ftype}), ']']);
    set(handles.ui_ub, 'String', ['[', sprintf('%g;', handles.data.ub{handles.data.ftype}),
']']);
end
guidata(hObject, handles);
function ui_toggle_Callback(hObject, eventdata, handles)
handles.data.toggle = get(hObject, 'Value');
if handles.data.toggle
    set(hObject, 'String', 'All');
else
    set(hObject, 'String', 'Current');
end
guidata(hObject, handles);
% --------------------------------------------------------------------
function uipushtool1_ClickedCallback(hObject, eventdata, handles)
% Open dialogue
cd([handles.data.pwd '\data']);
[name, path] = uigetfile({'*.txt', 'Text-files (*.txt)'}, ...
    'MultiSelect', 'on');
cd(handles.data.pwd);
h = handles.ui_axes1;
n = 1;
m = ' +oxsdxph';
hold(h, 'on');
try
    if ischar(name)
        data = importdata([path, name]);

        cdata = {name(1:end-4), data.data, data.textdata};

        text0 = sprintf(' -- %s --', name(1:end-4));
```

```
        %text1 = sprintf('%s \t %s', data.textdata{1}, data.textdata{2});
        %text2 = char([num2str(data.data(:,1)) ones(length(data.data(:,1)),1)*9
num2str(data.data(:,2))]);
        [text1, text2] = textz(data);
        text3 = char(text0, text1, text2);
        plot(h, cdata{2}(:,1), cdata{2}(:,end), 'r.', 'MarkerSize', 15);
    elseif iscell(name)
        n = length(name);
        cdata = cell(n, 3);
        c = linspace(1, 0, 3*n);
        for i = 1:n
            data = importdata([path, name{i}]);
            cdata(i, :) = {name{i}(1:end-4), data.data, data.textdata};
            text0 = sprintf(' -- %s --', name{i}(1:end-4));
            %text1 = sprintf('%s \t %s', data.textdata{1}, data.textdata{2});
            %text2 = char([num2str(data.data(:,1)) ones(length(data.data(:,1)),1)*9
num2str(data.data(:,2))]);
            [text1, text2] = textz(data);
            if i == 1
                text3 = char(text0, text1, text2, '');
                plot(h, cdata{i, 2}(:, 1), cdata{i, 2}(:, end), 'r.', 'MarkerSize', 15);
            else
                text3 = char(text3, text0, text1, text2, '');
                p = plot(h, cdata{i, 2}(:, 1), cdata{i, 2}(:, end), 'r.', 'MarkerSize', 15);
                set(p, 'Color', [c(i), 0, 0]);
                set(p, 'Marker', m(i));
                set(p, 'MarkerSize', 7);
            end
        end
    else
        return
    end
    hold(h, 'off');
    %set(h, 'XTick', linspace(0, max(cdata{2}), 5));
    %set(h, 'XLim', [0, max(cdata{2})+max(cdata{2})*0.1]);
    %set(h, 'YLim', [0, max(cdata{3})+max(cdata{3})*0.1]);
    xlabel(h, cdata{1, 3}(1), 'HorizontalAlignment', 'center', 'FontSize', 12);
    ylabel(h, cdata{1, 3}(2),'HorizontalAlignment', 'center', 'FontSize', 12);
    title(h, 'Isotherm', 'HorizontalAlignment', 'center', 'FontSize', 14)
    legend(h, cdata(:, 1)', 'Location', 'Best', 'Interpreter', 'none');
    handles.data.nlist = 1:n;

    % cell to structure
    field = {'file', 'data', 'label'};
    handles.sdata = cell2struct(cdata, field, 2);
    handles.fdata = cell2struct(cell(n, 3), {'name', 'param', 'error'}, 2);
    % set gui
    ax = axis(h);
    handles.data.xmin = ax(1);
    handles.data.xmax = ax(2);
```

```
    handles.data.ymin = ax(3);
    handles.data.ymax = ax(4);
    set(handles.ui_xmin, 'Enable', 'on');
    set(handles.ui_xmax, 'Enable', 'on');
    set(handles.ui_ymin, 'Enable', 'on');
    set(handles.ui_ymax, 'Enable', 'on');
    set(handles.ui_xmin, 'String', handles.data.xmin);
    set(handles.ui_xmax, 'String', handles.data.xmax);
    set(handles.ui_ymin, 'String', handles.data.ymin);
    set(handles.ui_ymax, 'String', handles.data.ymax);
    set(handles.ui_list, 'Value', 1);
    set(handles.ui_list, 'String', {handles.sdata.file});
    set(handles.ui_edit1, 'String', text3);
    set(handles.ui_sim, 'Enable', 'on');

catch me1
    msgbox({me1.identifier, me1.message}, 'error');
end
guidata(hObject, handles);
function uipushtool2_ClickedCallback(hObject, eventdata, handles)
% Save dialogue
[name, path] = uiputfile('*.mat', 'Save As', 'Untitled.mat');
fdata = handles.fdata;
save(name, 'fdata');
% try
%     if ischar(name)
%         fid = fopen([path, name], 'w');
%         str = char(get(handles.ui_edit2, 'String'));
%         for i = 1:size(str, 1)
%             fprintf(fid, '%s\r\n', str(i, :));
%         end
%         fclose(fid);
%         winopen([path, name]);
%     end
% catch me1
%     msgbox({me1.identifier, me1.message}, 'error');
% end
function uipushtool3_ClickedCallback(hObject, eventdata, handles)
% new figure
f = figure();
h = copyobj(handles.ui_axes1, f);
set(h, 'Position', [0.13 0.11 0.775 0.815]);
function ui_xmin_Callback(hObject, eventdata, handles)
handles.data.xmin = str2num(get(hObject, 'String'));
axis(handles.ui_axes1, [handles.data.xmin, handles.data.xmax, handles.data.ymin,
handles.data.ymax]);
guidata(hObject, handles);
function ui_xmin_CreateFcn(hObject, eventdata, handles)
% Hint: edit controls usually have a white background on Windows.
%       See ISPC and COMPUTER.
```

```
if ispc && isequal(get(hObject,'BackgroundColor'),
get(0,'defaultUicontrolBackgroundColor'))
   set(hObject,'BackgroundColor','white');
end
function ui_xmax_Callback(hObject, eventdata, handles)
handles.data.xmax = str2num(get(hObject, 'String'));
axis(handles.ui_axes1, [handles.data.xmin, handles.data.xmax, handles.data.ymin,
handles.data.ymax]);
guidata(hObject, handles);
function ui_xmax_CreateFcn(hObject, eventdata, handles)
% Hint: edit controls usually have a white background on Windows.
%       See ISPC and COMPUTER.
if ispc && isequal(get(hObject,'BackgroundColor'),
get(0,'defaultUicontrolBackgroundColor'))
   set(hObject,'BackgroundColor','white');
end

function ui_ymin_Callback(hObject, eventdata, handles)
handles.data.ymin = str2num(get(hObject, 'String'));
axis(handles.ui_axes1, [handles.data.xmin, handles.data.xmax, handles.data.ymin,
handles.data.ymax]);
guidata(hObject, handles);

function ui_ymin_CreateFcn(hObject, eventdata, handles)

% Hint: edit controls usually have a white background on Windows.
%       See ISPC and COMPUTER.
if ispc && isequal(get(hObject,'BackgroundColor'),
get(0,'defaultUicontrolBackgroundColor'))
   set(hObject,'BackgroundColor','white');
end
function ui_ymax_Callback(hObject, eventdata, handles)
handles.data.ymax = str2num(get(hObject, 'String'));
axis(handles.ui_axes1, [handles.data.xmin, handles.data.xmax, handles.data.ymin,
handles.data.ymax]);
guidata(hObject, handles);
function ui_ymax_CreateFcn(hObject, eventdata, handles)
% Hint: edit controls usually have a white background on Windows.
%       See ISPC and COMPUTER.
if ispc && isequal(get(hObject,'BackgroundColor'),
get(0,'defaultUicontrolBackgroundColor'))
   set(hObject,'BackgroundColor','white');
end
% --------------------------------------------------------------------
% Subroutine
function [t1, t2] = textz(data)
l = size(data.data, 2);
for i = 1:l
   if i == 1
      t1 = sprintf('%s', data.textdata{i});
```

```
        t2 = char(num2str(data.data(:,i)));
    else
        t1 = sprintf('%s \t %s', t1, data.textdata{i});
        t2 = char([t2, ones(length(data.data(:,1)),1)*9, num2str(data.data(:,i))]);
        %t2 = char([num2str(data.data(:,1)) ones(length(data.data(:,1)),1)*9
num2str(data.data(:,2))]);
    end
end
```

## Output function

```
function stop = outputfunction(v, ~, flag, varargin)
persistent h p t c x y
stop = 0;
switch flag
    case 'init'
        x = varargin{1};
        y = varargin{2};
        t = varargin{3};
        h = varargin{4};
        c = t/7;
        p = plot(h, x, y, 'b-','LineWidth', 2);
        x = linspace(0, max(x), 1000);
        set(p, 'Color', [0 c 1]);
        set(p, 'XData', x);
    case 'iter'
        [~, predY] = objfunction(v, x, y, t);
        set(p, 'YData', predY);
        drawnow
    case 'done'
        %hold(h, 'off');
end
```

# Appendix II

## Excel Programming for Isotherm and Kinetics

### Algorithm and configuring the spreadsheet for non-linear models

| | A | B | C | D | E | F | G | H | I |
|---|---|---|---|---|---|---|---|---|---|
| 1 | **$C_e$** | **Exp. $q_e$** | **Langmuir, $q_e$** | **Upper CI** | **Lower CI** | | **$q_m$** | 59.3355258898998 | |
| 2 | 0.8613 | 0.059 | =($H$1*$H$2*A2)/(1+($H$2*A2)) | =C2+$H$8 | =C2-$H$8 | | **$K_L$** | 0.0192632647996077 | |
| 3 | 0.6411 | 0.451 | =($H$1*$H$2*A3)/(1+($H$2*A3)) | =C3+$H$8 | =C3-$H$8 | | **Mean of exp. $q_e$** | =AVERAGE(B2:B17) | |
| 4 | 1.3 | 0.899 | =($H$1*$H$2*A4)/(1+($H$2*A4)) | =C4+$H$8 | =C4-$H$8 | | **df** | =COUNT(B2:B17)-COUNT(H1:H2) | |
| 5 | 3.001 | 1.718 | =($H$1*$H$2*A5)/(1+($H$2*A5)) | =C5+$H$8 | =C5-$H$8 | | **SE of exp. $q_e$** | =SQRT(SUM((B2:B17-C2:C17)^2)/H4) | Array |
| 6 | 6.2225 | 4.551 | =($H$1*$H$2*A6)/(1+($H$2*A6)) | =C6+$H$8 | =C6-$H$8 | | **$R^2$** | =1-(SUM((B2:B17-C2:C17)^2)/SUM((B2:B17-H3)^2)) | Array |
| 7 | 13.4 | 8.91 | =($H$1*$H$2*A7)/(1+($H$2*A7)) | =C7+$H$8 | =C7-$H$8 | | **Crtical t** | =TINV(0.05,H4) | |
| 8 | 13.5825 | 12.669 | =($H$1*$H$2*A8)/(1+($H$2*A8)) | =C8+$H$8 | =C8-$H$8 | | **CI** | =H7*H5 | |
| 9 | 26.68 | 19.844 | =($H$1*$H$2*A9)/(1+($H$2*A9)) | =C9+$H$8 | =C9-$H$8 | | | | |
| 10 | 34.095 | 24.951 | =($H$1*$H$2*A10)/(1+($H$2*A10)) | =C10+$H$8 | =C10-$H$8 | | | | |
| 11 | 64.44 | 33.472 | =($H$1*$H$2*A11)/(1+($H$2*A11)) | =C11+$H$8 | =C11-$H$8 | | RMSE | =SQRT(SUM((B2:B17-C2:C17)^2)/(COUNT(B2:B17)-2)) | array |
| 12 | 94.65 | 39.02 | =($H$1*$H$2*A12)/(1+($H$2*A12)) | =C12+$H$8 | =C12-$H$8 | | $\chi^2$ | =SUM(((B2:B17-C2:C17)^2)/(C2:C17)) | array |
| 13 | 128.79 | 43.782 | =($H$1*$H$2*A13)/(1+($H$2*A13)) | =C13+$H$8 | =C13-$H$8 | | | | |
| 14 | 171.08 | 46.914 | =($H$1*$H$2*A14)/(1+($H$2*A14)) | =C14+$H$8 | =C14-$H$8 | | | | |
| 15 | 226 | 47.52 | =($H$1*$H$2*A15)/(1+($H$2*A15)) | =C15+$H$8 | =C15-$H$8 | | | | |
| 16 | 281.295 | 49.051 | =($H$1*$H$2*A16)/(1+($H$2*A16)) | =C16+$H$8 | =C16-$H$8 | | | | |
| 17 | 329.1 | 50.08 | =($H$1*$H$2*A17)/(1+($H$2*A17)) | =C17+$H$8 | =C17-$H$8 | | | | |
| 18 | | | | | | | | | |

**Figure 1** The experimental data are entered into Column A and B with all Excel functions into spreadsheet template for non-linear regression of Langmuir Isotherm

C24

| | A | B | C | D | E | F | G | H | I | J |
|---|---|---|---|---|---|---|---|---|---|---|
| 1 | **Time, t** | **Exp. qt** | **Pseudo 2nd Order** | **Upper CI** | **Lower CI** | | **$q_e$** | 142.546 | | |
| 2 | 0 | 0 | =($H$2*($H$1^2)*A2)/(1+$H$1*$H$2*A2) | =C2+$H$8 | =C2-$H$8 | | **$K_2$** | 0.0002 | | |
| 3 | 1 | 0.8 | =($H$2*($H$1^2)*A3)/(1+$H$1*$H$2*A3) | =C3+$H$8 | =C3-$H$8 | | **Mean of $q_t$** | 100.942 | | |
| 4 | 30 | 61.4 | =($H$2*($H$1^2)*A4)/(1+$H$1*$H$2*A4) | =C4+$H$8 | =C4-$H$8 | | **df** | =COUNT(B2:B15)-COUNT(H1:H2) | | |
| 5 | 60 | 83.84 | =($H$2*($H$1^2)*A5)/(1+$H$1*$H$2*A5) | =C5+$H$8 | =C5-$H$8 | | **SE of $q_t$** | =SQRT(SUM((B2:B15-C2:C15)^2)/H4) | Array | |
| 6 | 90 | 108.68 | =($H$2*($H$1^2)*A6)/(1+$H$1*$H$2*A6) | =C6+$H$8 | =C6-$H$8 | | **$R^2$** | =1-(SUM((B2:B15-C2:C15)^2)/SUM((B2:B15-H3)^2)) | Array | |
| 7 | 120 | 111.56 | =($H$2*($H$1^2)*A7)/(1+$H$1*$H$2*A7) | =C7+$H$8 | =C7-$H$8 | | **Crtical t** | =TINV(0.05,H4) | | |
| 8 | 180 | 120.428 | =($H$2*($H$1^2)*A8)/(1+$H$1*$H$2*A8) | =C8+$H$8 | =C8-$H$8 | | **CI** | =H7*H5 | | |
| 9 | 240 | 122.456 | =($H$2*($H$1^2)*A9)/(1+$H$1*$H$2*A9) | =C9+$H$8 | =C9-$H$8 | | | | | |
| 10 | 300 | 126.488 | =($H$2*($H$1^2)*A10)/(1+$H$1*$H$2*A10) | =C10+$H$8 | =C10-$H$8 | | | | | |
| 11 | 360 | 132.26 | =($H$2*($H$1^2)*A11)/(1+$H$1*$H$2*A11) | =C11+$H$8 | =C11-$H$8 | | NSD | =100*(SQRT(SUM(((B3:B15-C3:C15)/(B3:B15))^2)/(COUNT(B3:B15)-1))) | array | |
| 12 | 420 | 134.96 | =($H$2*($H$1^2)*A12)/(1+$H$1*$H$2*A12) | =C12+$H$8 | =C12-$H$8 | | ARE | =(100/(COUNT(B3:B15)-1))*(SUM((B3:B15-C3:C15)/(B3:B15))) | array | |
| 13 | 1440 | 137.624 | =($H$2*($H$1^2)*A13)/(1+$H$1*$H$2*A13) | =C13+$H$8 | =C13-$H$8 | | | | | |
| 14 | 1500 | 135.572 | =($H$2*($H$1^2)*A14)/(1+$H$1*$H$2*A14) | =C14+$H$8 | =C14-$H$8 | | | | | |
| 15 | 1560 | 137.12 | =($H$2*($H$1^2)*A15)/(1+$H$1*$H$2*A15) | =C15+$H$8 | =C15-$H$8 | | | | | |
| 16 | | | | | | | | | | |

**Figure 2** The experimental data are entered into Column A and B with all Excel functions into spreadsheet template for non-linear regression of Pseudo-2nd-order kinetics model

**Operation of SOLVER and controls**

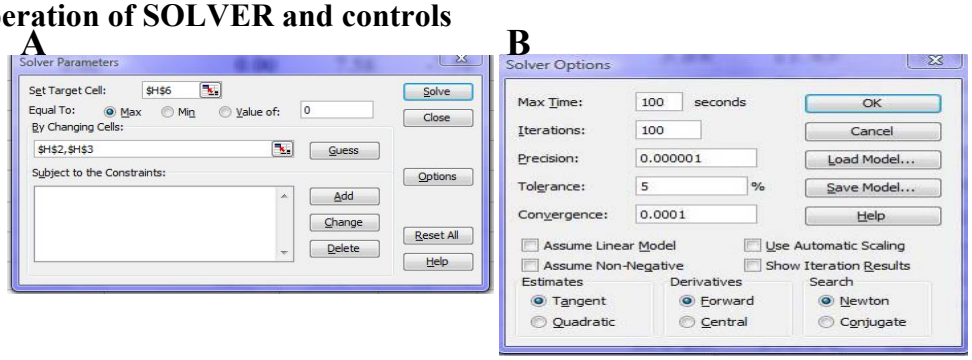


**Figure 3** The built-in 'Solver' functions for running the setup algorithm and advance option. **A:** The 'Solver' dialogue box used as an interface between the 'Solver' function and data on the spreadsheet. **B:** The control and fine tune of algorithms using the 'Solver Options' dialogue box.

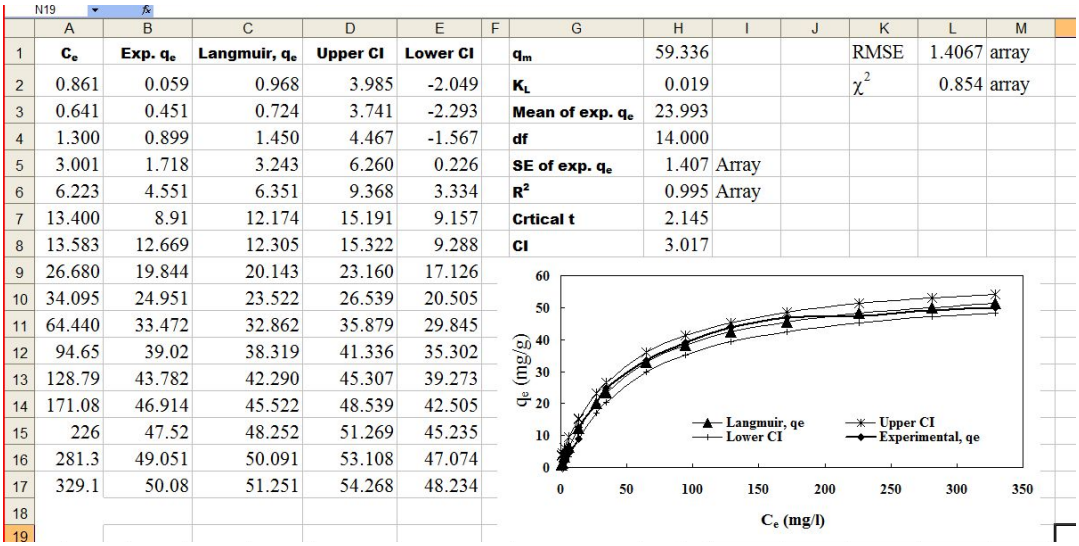


**Figure 4** The excel sheet after executed the algorithm for Langmuir isotherm model with predicted parameters and fitted data curve with experimental data curve.

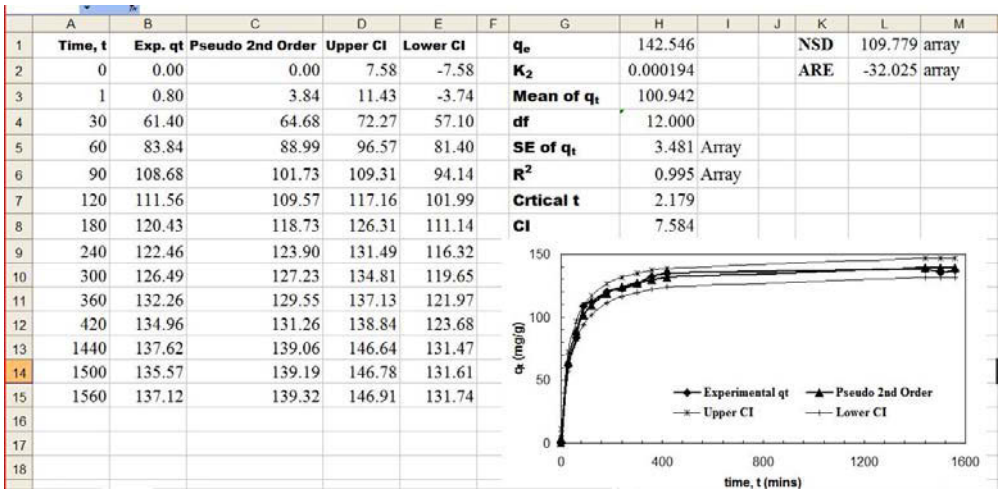


**Figure 5** The excel sheet after executed the pseudo-2nd-order kinetics model with predicted parameters and fitted data curve with experimental data curve.

# Appendix III

## Biosorbent preparation from Pal oil fruit shells

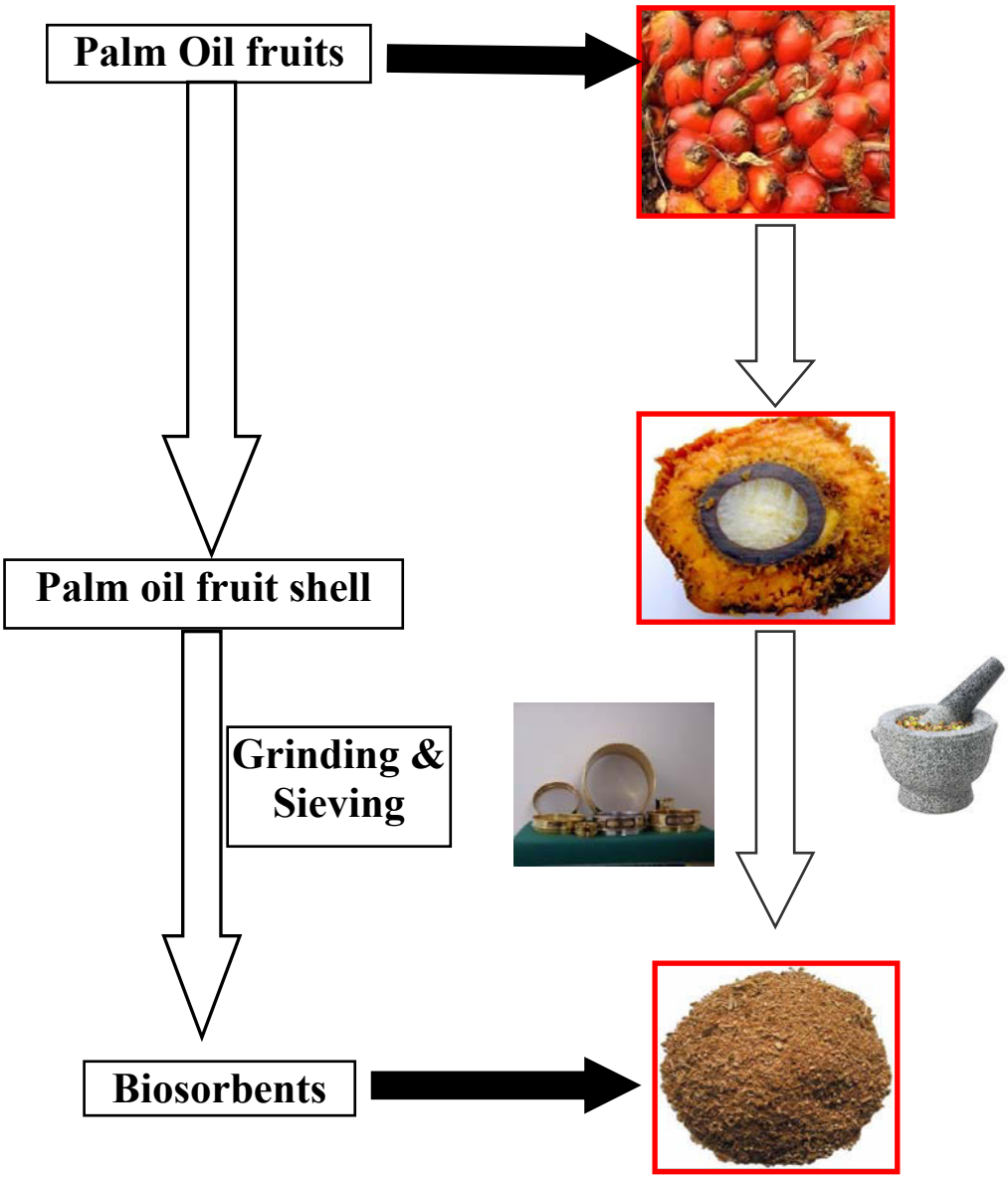

# Appendix IV

## Biosorbent preparation from Cabbage waste

# Appendix V

## Biosorbent preparation and experiment by Maple leaves

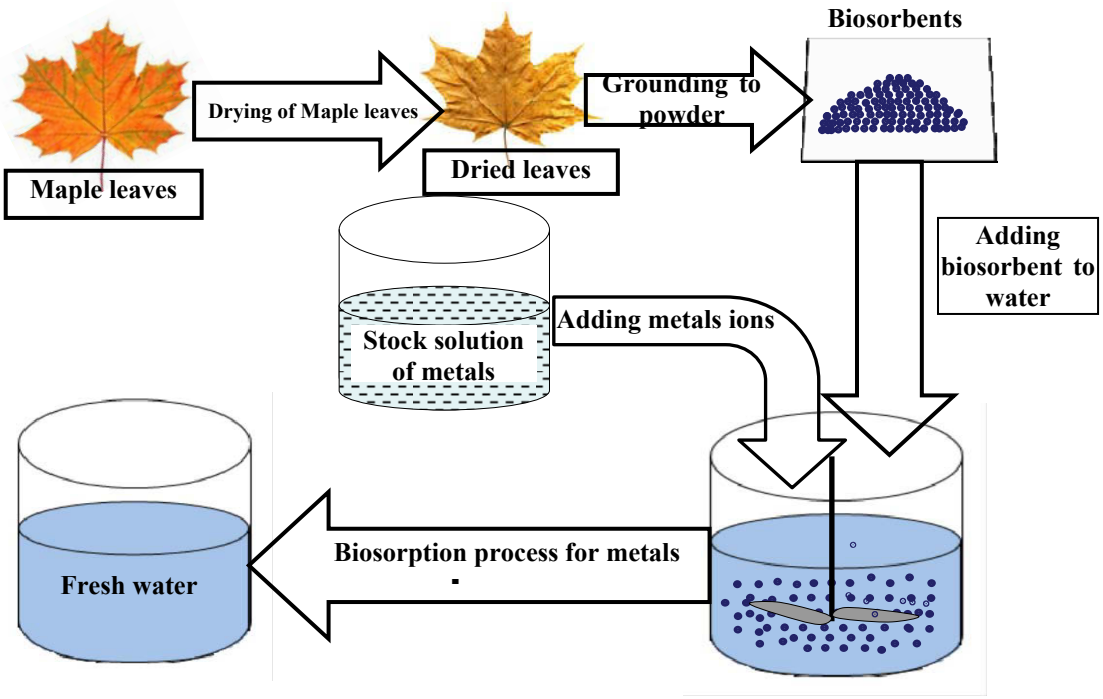

# Appendix VI

# Setup of biosorption column with CW

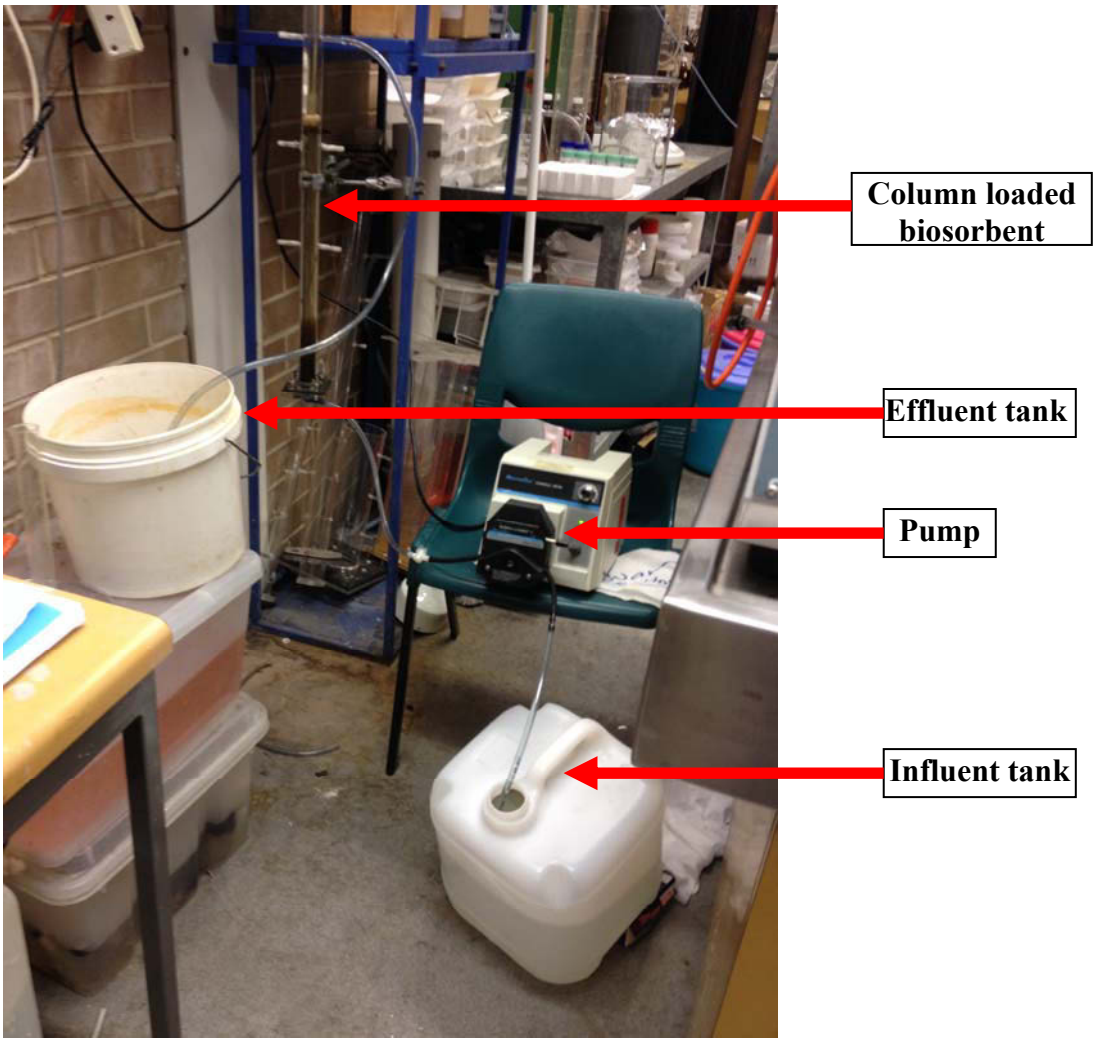


## The End